AD-A034 804 DAVID W TAYLOR NAVAL SHIP RESEARCH AND DEVELOPMENT CE--ETC F/G 13/10
EXPERIMENTAL UNSTEADY AND MEAN LOADS ON A CP PROPELLER BLADE ON--ETC(U)
OCT 76 R J BOSWELL, J J NELKA, S B DENNY

UNCLASSIFIED DTNSRDC-76-0125 NL

1 OF 4
AD
A034804

DAVID W. TAYLOR NAVAL SHIP
RESEARCH AND DEVELOPMENT CENTER

[illegible]

ADA034804

[illegible] UNSTEADY AND MEAN LOADS ON [illegible]
[illegible]

by

[illegible]

Report 76-0125

[illegible] UNSTEADY AND MEAN LOADS ON A CP PROPELLER BLADE ON A MODEL OF
[illegible] FOR SIMULATED MODES OF OPERATION

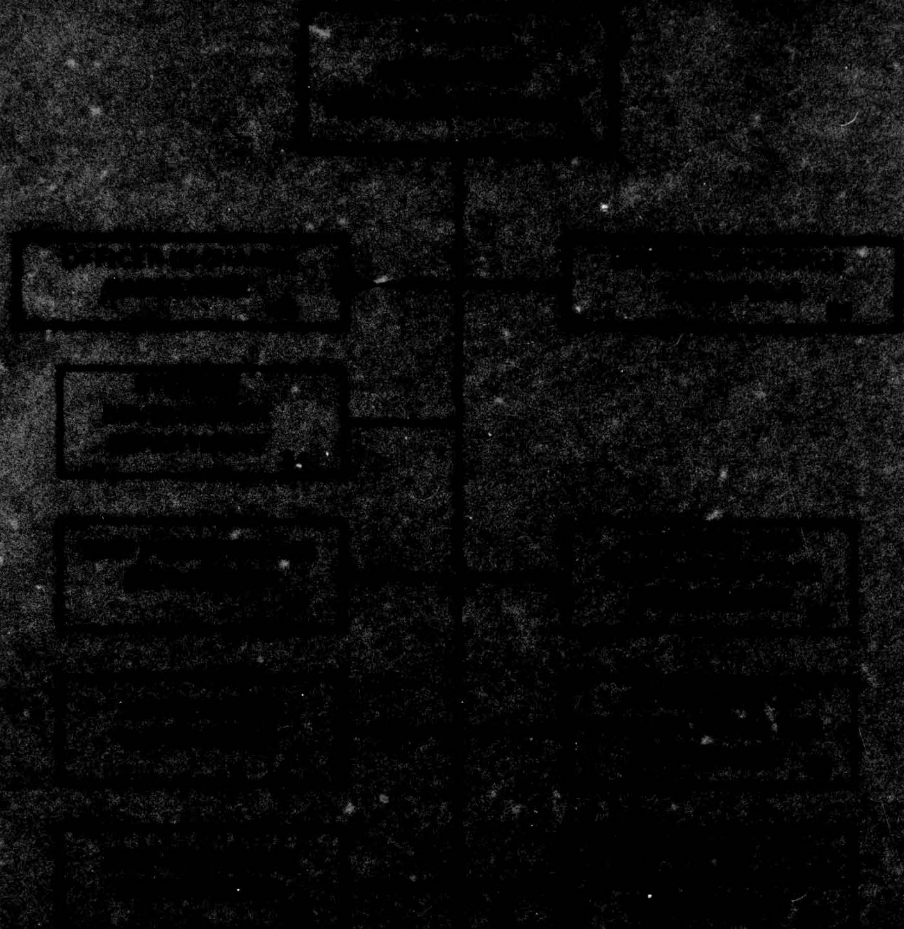

UNCLASSIFIED

SECURITY CLASSIFICATION OF THIS PAGE (When Data Entered)

REPORT DOCUMENTATION PAGE

READ INSTRUCTIONS BEFORE COMPLETING FORM

1. REPORT [redacted] — 14 DTNSRDC [redacted] 76-0125
2. GOVT ACCESSION NO.
3. RECIPIENT'S CATALOG NUMBER
4. TITLE (and Subtitle) — 6 EXPERIMENTAL UNSTEADY AND MEAN LOADS ON A CP PROPELLER BLADE ON A MODEL OF THE FF-1088 FOR SIMULATED MODES OF OPERATION.
5. TYPE OF REPORT & PERIOD COVERED — 9 Final rept.,
6. PERFORMING ORG. REPORT NUMBER
7. AUTHOR(s) — 10 Robert J. Boswell, John J. Nelka [redacted] Stephen B. Denny
8. CONTRACT OR GRANT NUMBER(s)
9. PERFORMING ORGANIZATION NAME AND ADDRESS — David W. Taylor Naval Ship Research and Development Center, Bethesda, Maryland 20084
10. PROGRAM ELEMENT, PROJECT, TASK AREA & WORK UNIT NUMBERS — (See reverse side)
11. CONTROLLING OFFICE NAME AND ADDRESS — Naval Sea Systems Command (0331G), Energy Conversion & Explosive Devices Div., Washington, D.C. 20362
12. REPORT DATE — 11 Oct [redacted] 76
13. NUMBER OF PAGES — 12 348p. 347
14. MONITORING AGENCY NAME & ADDRESS (if different from Controlling Office) — Naval Ship Engineering Center (6148), Propeller, Shafting & Bearing Branch, Prince Georges Plaza, Hyattsville, Maryland 20782
15. SECURITY CLASS. (of this report) — UNCLASSIFIED
15a. DECLASSIFICATION/DOWNGRADING SCHEDULE
16. DISTRIBUTION STATEMENT (of this Report)

APPROVED FOR PUBLIC RELEASE: DISTRIBUTION UNLIMITED

17. DISTRIBUTION STATEMENT (of the abstract entered in Block 20, if different from Report)

16 SL24001 17 19977

18. SUPPLEMENTARY NOTES

19. KEY WORDS (Continue on reverse side if necessary and identify by block number)

Marine Propeller
Controllable-Pitch Propeller
Loads
Maneuvering
Propulsion
Model Experiments
Propeller Strength
USS BARBEY (FF-1088)
Unsteady Loads

20. ABSTRACT (Continue on reverse side if necessary and identify by block number)

Experiments are described in which the mean and unsteady loads were measured on a single blade of a model of the controllable-pitch propeller on the FF-1088. The experiments were conducted behind a model of the FF-1088 hull under steady ahead operation, hull pitching motions, simulated crash ahead maneuvers, and simulated crash astern maneuvers. The

(Continued on reverse side)

DD FORM 1473, 1 JAN 73 — EDITION OF 1 NOV 65 IS OBSOLETE

S/N 0102-014-6601

UNCLASSIFIED

SECURITY CLASSIFICATION OF THIS PAGE (When Data Entered)

387682 XB

(Block 10)

Task Area SSL24001
Task 19977
Work Unit 1-1544-296

(Block 20 continued)

experimental techniques are outlined and the dynamometer and data analysis system described.

The results show that the circumferential variation of all measured components of blade loading is primarily a once-per-revolution variation, with maximum and minimum values occurring near the angular positions in which the spindle axis is horizontal.

For sinusoidal pitching of the model hull with amplitude of 2 deg and frequency of 0.8 Hz, the peak-to-peak circumferential variation of measured forces and moments increased by a minimum of 50 percent over the values without hull pitching.

For simulated operation during a crash ahead or crash astern maneuver, the circumferential variation of measured forces and moments varied approximately as the product of ship speed and propeller rotational speed, and was a function of propeller pitch. At no time during the simulated crash ahead or crash astern maneuvers were the circumferential variations of loads as large as during steady ahead operation.

For steady ahead operation, circumferential variation of loading determined from the model experiments agreed fairly well with full-scale data, but was substantially larger than the theoretically calculated values.

TABLE OF CONTENTS

LIST OF FIGURES

Page

Page

LIST OF TABLES

NOTATION

A_E	Expanded area, $Z\int_{r_h}^{R} c\,dr$
A_0	Propeller disc area, $\pi D^2/4$
A_r	Fourier cosine coefficients of radial component of wake velocity
A_t	Fourier cosine coefficient of tangential component of wake velocity
A_x	Fourier cosine coefficient of longitudinal component of wake velocity
B_r	Fourier sine coefficient of radial component of wake velocity
B_t	Fourier sine coefficients of tangential component of wake velocity
B_x	Fourier sine coefficients of longitudinal component of wake velocity
$C_{i,j}$	Elements of calibration matrix
C_{Th}	Thrust loading coefficient, $T/[(\rho/2)V_A{}^2 A_0]$
c	Blade section chord length
D	Propeller diameter
$(F)_n$	nth harmonic amplitude of F
$F_{x,y,z}$	Force components on blade in x,y,z directions
f_M	Camber of propeller blade section
J	Advance coefficient, $J=V_A/nD$
J_T	Effective advance coefficient based on thrust identity
J_Q	Effective advance coefficient based on torque identity
J_V	Ship speed advance coefficient, $J=V/nD$
$K_{F_{x,y,z}}$	Force coefficient, $F_{x,y,z}/(\rho n^2 D^4)$
$K_{M_{x,y,z}}$	Moment coefficient, $M_{x,y,z}/(\rho n^2 D^5)$

K_Q	Torque coefficient, $Q/(\rho n^2 D^5)$
K_{SC}	Centrifugal blade spindle torque coefficient, $M_{Z_C}/(\rho_p n^2 D^5)$
K_T	Thrust coefficient, $T/(\rho n^2 D^4)$
$M_{x,y,z}$	Moment components about x,y,z axes from loading on one blade
$(M)_n$	nth harmonic amplitude of M
n	Propeller revolutions per unit time
P	Propeller blade section pitch
Q	Time average propeller torque arising from loading on all blades, $-Z\bar{M}_x$
R	Radius of propeller
R_n	Reynolds number, $c_{0.7}V_R{}^*/\nu$
r	Radial coordinate from propeller axis
S	Skew back of propeller blade section measured from the spindle axis to the midchord point of the blade section, positive towards trailing edge
T	Time average thrust of propeller, positive forward, $Z\bar{F}_x$
t	Maximum thickness of propeller blade section
V	Model speed
V_A	Propeller speed of advance
$V_R{}^*$	Vector sum of speed of advance and rotational velocity at the 0.7 radius, $[V_A{}^2+(0.7\pi nD)^2]^{1/2}$
$V_r(r,\theta_W)$	Radial component of wake velocity, positive towards hub
$V_t(r,\theta_W)$	Tangential component of wake velocity, positive counterclockwise looking upstream

$V_x(r,\theta_W)$	Longitudinal component of wake velocity, positive forward
w_Q	Taylor wake fraction determined from torque identity
w_T	Taylor wake fraction determined from thrust identity
x,y,z	Coordinate axes
Z	Number of blades
Z_R	Rake of propeller blade section measured from the propeller plane to the generator line. Positive aft
β^*	Advance angle at 0.7 radius, $\tan^{-1} \dfrac{[V_x\ (r=0.7)]}{0.7\pi nD}$
θ	Angular coordinate used to define location of blade and variation of loads, from vertical upward positive clockwise looking upstream, $\theta = -\theta_W$
θ_S	Skew angle measured from spindle axis to projection of blade section midchord into propeller plane, positive toward trailing edge
θ_W	Angular coordinate of wake velocity, from upward vertical positive counterclockwise looking upstream, $\theta_W = -\theta$
λ	Ship to model linear scale ratio
ν	Kinematic viscosity of water
ρ	Mass density of water
ρ_P	Mass density of propeller blade
Φ	Pitch angle of propeller blade section, $\tan^{-1}$ [P/(πxD)]
$(\phi_{F,M})_n$	nth harmonic phase angles of F,M based on a cosine series, $(F,M)=(\bar{F},M) + \sum_{n=1}^{N} (F,M)_n \cos(n\theta-(\phi_{F,M})_n)$
ψ	Pitch angle of hull

Subscripts

A	Applied values of loads
C	Arising from centrifugal loading
CW	Value in calm water
h	Value at hub radius
I	Indicated values of loads before calibration matrix is applied
M	Model value
MAX	Maximum value at any blade angular position
MES	Value at model conditions derived from measurements on full-scale ship
n	Value of nth harmonic
S	Ship value
SP	Value at self-propulsion point
x,y,z	Component in x,y,z direction
0.4	Value at r=0.4R
0.7	Value at r=0.7R

Superscripts

$\bar{}$	Time average value per revolution
$\tilde{}$	Unsteady value
$\dot{}$	Rate of change with time

ABSTRACT

Experiments are described in which the mean and unsteady loads were measured on a single blade of a model of the controllable-pitch propeller on the FF-1088. The experiments were conducted behind a model of the FF-1088 hull under steady ahead operation, hull pitching motions, simulated crash ahead maneuvers, and simulated crash astern maneuvers. The experimental techniques are outlined and the dynamometer and data analysis system described.

The results show that the circumferential variation of all measured components of blade loading is primarily a once-per-revolution variation, with maximum and minimum values occurring near the angular positions in which the spindle axis is horizontal.

For sinusoidal pitching of the model hull with amplitude of 2 deg and frequency of 0.8 Hz, the peak-to-peak circumferential variation of measured forces and moments increased by a minimum of 50 percent over the values without hull pitching.

For simulated operation during a crash ahead or crash astern maneuver, the circumferential variation of measured forces and moments varied approximately as the product of ship speed and propeller rotational speed, and was a function of propeller pitch. At no time during the simulated crash ahead or crash astern maneuvers were the circumferential variations of loads as large as during steady ahead operation.

For steady ahead operation, circumferential variation of loading determined from the model experiments agreed fairly well with full-scale data, but was substantially larger than the theoretically calculated values.

ADMINISTRATIVE INFORMATION

The work reported herein was funded by the Naval Sea Systems Command (NAVSEA 033) Task Area SSL24001, Task 19977. The work was performed under David W. Taylor Naval Ship Research and Development Center (DTNSRDC), Work Unit 1-1544-296.

The International System (SI) of units is used in the present report. The equivalent English units are shown in parentheses following the SI units in cases in which this will facilitate understanding and allow direct comparison with previous reports.

INTRODUCTION

Major naval ships powered with marine gas turbines and using controllable-pitch (CP) propellers for thrust reversal are currently being added to the Fleet. Additional ships with gas turbine and CP propeller installations are planned for future Fleet application.

Accordingly, the Navy has been conducting a research and development (R&D) program to establish the technology for producing reliable CP propellers with delivered power in the range of 26,000 to 30,000 kW (35,000 to 40,000 hp). As part of this program, CP propellers were installed on the USS PATTERSON (FF-1061) and USS BARBEY (FF-1088) with delivered power of 26,100 kW (35,000 hp). These installations were intended to demonstrate that CP propellers in this range of power had adequate reliability for application to ships with gas turbine prime movers.

Because of the structural failure of the crank rings to which the blades of the CP propeller on the FF-1088 were bolted, R&D efforts were intensified. The program undertaken at DTNSRDC included:

1. Blade Loading of CP Propellers

    a. Model measurement and theoretical prediction of blade loading on CP propellers.

    b. Model and full-scale wake measurements and theoretical predictions of wake.

    c. Full-scale measurements of forces, pressures, and strains in CP propeller components.

2. Structural Design of CP Propeller Blade Attachments.

3. Development of Materials for CP Propeller Systems.

The current report presents the results of work conducted under Section 1a of the CP Propeller Research and Development Program, i.e., model measurement and theoretical prediction of blade loading of CP propellers. Work under the other sections of this program will be reported separately.

Most of the information contained in the current report has already been published.[1] The current report contains all that information as well as additional details on the experimental data and the pertinent full-scale conditions of the FF-1088.

BACKGROUND

Extreme care must be taken to design the blades and pitch-changing mechanisms of high power CP propellers so that they possess adequate strength including consideration of yield and fatigue stresses. This requires an accurate estimate of the maximum time-average and alternating loads under all operating conditions. High time-average and alternating loads occur at steady full-power ahead conditions and during high-speed maneuvers including full-power crash astern, full-power crash ahead, and full-power turns. In addition, the influence of the seaway may substantially increase the time-average and alternating loads. At present there appears to be no confirmed technique whereby the pertinent loads can be predicted to the desired accuracy. Schwanecke and Wereldsma[2] reviewed the factors affecting blade loading for propellers in general, and Rusetskiy[3] and Hawdon et al.[4] discussed some of the factors peculiar to blade loading CP propellers.

---

[1] Boswell, R.J. et al., "Experimental Determination of Mean and Unsteady Loads on a Model CP Propeller Blade for Various Simulated Loads of Ship Operation," Transactions of the Eleventh ONR Symposium on Naval Hydrodynamics, Government Printing Office (1976). A complete listing of references is given on pages 330--332.

[2] Schwanecke, H. and R. Wereldsma, "Strength of Propellers Considering Steady and Unsteady Shaft and Blade Forces, Stationary and Nonstationary Environmental Conditions," Proceedings of the Thirteenth International Towing Tank Conference, Report of the Propeller Committee, Appendix 2B, Vol. 2 (1972).

[3] Rusetskiy, A.A., "Hydrodynamics of Controllable Pitch Propellers," Shipbuilding Publishing House, Leningrad (1968).

[4] Hawdon, L. et al., "The Analysis of Controllable-Pitch Propeller Characteristics at Off-Design Conditions," Transactions of the Institute of Marine Engineers, Vol. 88 (1976).

Near the self-propulsion point in calm water, the time-average loads can probably be calculated with reasonable accuracy. However, even at these conditions, the variation of loads with blade angular position apparently cannot be calculated with high accuracy. Various techniques, including quasi-steady procedures, stripwise unsteady procedures, and methods based on unsteady lifting surface theory, have been proposed for calculating the unsteady loading arising from the circumferential variation in the inflow velocity.[5--8] However, all of these procedures require knowledge of the flow patterns (wake profile) in the propeller disk. In current practice, the wake profile is measured in the plane of the propeller behind the model hull with the propeller removed. For high-speed displacement ships of the type under consideration in this report, these results are usually extrapolated to full scale without making allowance for (1) the change in Reynolds number and the corresponding reduction in relative boundary layer thickness and (2) the effect of the propeller suction on the boundary layer and thereby the wake pattern in the propeller disk.

Existing measurements which give information on unsteady blade loading include:

1. Measurements of strain on the blades of the model propellers or full-scale propellers. However, some calculations and assumptions are

---

[5] Van Gent, W., "Unsteady Lifting Surface Theory for Ship Screws: Derivation and Numerical Treatment of Integral Equation," Journal of Ship Research, Vol. 19, No. 4, pp. 243--253 (Dec 1975).

[6] Schwanecke, H., "Comparative Calculations on Unsteady Propeller Blade Forces," Proceedings of the Fourteenth International Towing Tank Conference, Report of the Propeller Committee, Appendix 2c, vol. 2 (1972).

[7] Breslin, J.P., "Propeller Excitation Theory," Proceedings of the Fourteenth International Towing Tank Conference, Report of the Propeller Committee, Appendix 2c, Vol. 2 (1972).

[8] Boswell, R.J. and M.L. Miller, "Unsteady Propeller Loading-Measurement, Correlation with Theory, and Parametric Study," NSRDC Report 2625 (Oct 1968).

required to convert measured strains into loads. Published data of this have been summarized by Meyne.[9]

2. Measurement of bearing (shaft) forces and moments on model propellers operating in wakes generated by model hulls or wire grid screens. However, this gives information on only some components of blade loading and on only those harmonics of shaft rotational speed corresponding to nZ-1, nZ, and nZ+1, where n is an integer and Z is the number of blades. Measurements of this nature have been conducted by many investigators.[7,10]

3. Measurements of forces and moments on individual blades of model propellers operating in wakes generated by model hulls or wire grid screens. Measurements behind model hulls have been made by Huse[11] and Blaurock,[12] measurements behind screens have been made by Hawdon et al.,[4] measurements in inclined flow have been made by Albrecht and Suhrbier[13] and by Bednarzik,[14] and measurements on partially submerged propellers have been made by Dobay.[15]

---

[9] Meyne, K., "Propeller Manufacture-Propeller Materials-Propeller Strength," International Shipbuilding Progress, Vol. 2, No. 247, pp. 77--102 (Mar 1975).

[10] Wereldsma, R., "Comparative Tests on Vibratory Propeller Forces," Proceedings of the Thirteenth International Towing Tank Conference, Report of the Propeller Committee, Appendix 2a, Vol. 2 (1972).

[11] Huse, E., "An Experimental Investigation of the Dynamic Forces and Moments on One Blade of a Ship Propeller," Proceedings of the Symposium on Testing Techniques in Ship Cavitation Research, The Norwegian Ship Model Experimental Tank, Trondheim, Norway (May--Jun 1967).

[12] Blaurock, J., "Propeller Blade Loading in Nonuniform Flow," The Society of Naval Architects and Marine Engineers, Propellers 75 Symposium, (Jul 1975).

[13] Albrecht, K. and K.R. Suhbrier, "Investigation of the Fluctuating Blade Forces of a Cavitating Propeller in Oblique Flow," International Shipbuilding Progress, Vol. 22, No. 248, pp. 132--147 (Apr 1975).

[14] Bednarzik, R., "Untersuchung uber die Belastungs-schwankungen am Einzelflugel schrag angestromter Proper," Schiffbauforschung, Vol. 8, No. 1/2, pp. 57--80 (1968).

[15] Dobay, G.F., "Time-Dependent Blade-Load Measurements on a Screw-Propeller," presented to the Sixteenth American Towing Tank Conference, (Aug 1971).

Experiments in wakes generated by screens are advantageous for evaluating the ability of a procedure to calculate the loading for a given wake since for this case, the propeller apparently does not influence the wake pattern. Although some good correlation has apparently been obtained between analytical predictions and unsteady bearing forces measured behind wire grid screens,[7,8] correlation has been rather inconsistent between analytically predicted unsteady blade loads, or resulting strains, and measured blade loads, or strains.[10,16]

The mechanism by which the seaway influences the mean and unsteady blade loads is complex. Factors include the increased mean propeller loading due to increased hull resistance and the increased unsteady loading resulting from the influence of the free surface and modification of the flow patterns into the propeller disk. This flow pattern is influenced (1) by direct trochoidal velocities from the ocean waves, (2) by relative velocities of the propeller due to ship motions, and (3) by modification of the hull wake pattern due to the seaway and ship motions. Procedures for calculating the loads in a seaway are much less refined than for steady operation in calm water. Tasaki[17] gives a good review of the mechanisms and procedures for predicting the effect of the seaway on bearing forces which, in principle, also applies to unsteady loading on an individual blade. Keil et al.[18] and Watanabe et al.[19] present strain measurements on the blades of full-scale propellers in both calm and rough seas.

Apparently no rational analytical procedures are available for accurately calculating the time-average loads per revolution or the unsteady

---

[16] Wereldsma, R., "Last Remarks on the Comparative Model Tests on Vibratory Propeller Forces," Proceedings of the Fourteenth International Towing Tank Conference, Vol. 3, pp. 421--426 (1975).

[17] Tasaki, R., "Propulsion Factors and Fluctuating Propeller Loads in Waves," Proceedings of the Fourteenth International Towing Tank Conference, Vol. 4, pp. 224--236 (1975).

[18] Keil, H.G. et al., "Stresses in the Blades of a Cargo Ship Propeller," Journal of Hydronautics, Vol. 6, No. 1 (Jan 1972).

[19] Watanabe, K. et al., "Propeller Stress Measurements on the Container Ship HAKONE MARU," Shipbuilding Research Association of Japan (1973).

loads including variation with blade angular position during crash ahead or crash astern maneuvers. These loads may depend on many factors including the time rate of change of propeller pitch $\dot{P}$ (for CP propellers), time rate of change of rotational speed $\dot{n}$, time rate of change of ship speed $\dot{V}$, propeller blade section stall, cavitation, ventilation, flow separation from the hull, and large interactions between the propeller and the hull. Some of these factors are discussed and considered by Hawdon et al.[4] For crash astern maneuvers, a CP propeller has negative pitch P and develops negative thrust for forward speed, i.e., it decelerates the flow into the propeller, and this may tend to increase the time-average and time-dependent interaction between the propeller and the hull.

For turns, the factors affecting the time-average loads per revolution and the unsteady loads are somewhat the same as those affecting the loads under crash ahead and crash astern conditions except that for turns, there is a relatively large drift angle of the flow into the propeller. This drift angle tends to increase the circumferential nonuniformity of the flow into the propeller, thereby increasing the unsteady loading. However, this circumferential nonuniformity of the inflow tends to be offset by the lower values of ship speed and propeller rotational speed in turns compared to steady ahead operation.

The authors know of no experimental measurements of time-average loads and circumferential variation of loads with blade angular position on CP propellers behind a hull under a wide range of operating conditions. An experimental program was therefore undertaken to measure the six components of loading (Figure 1)* on a model CP propeller operating behind a model hull, namely, a model of the FF-1088. The experimental conditions included (1) steady ahead operation near the self-propulsion point, (2) steady ahead operation near the self-propulsion point with forced dynamic pitching of the model hull, (3) simulated crash ahead operation, and (4) simulated crash

---

*Main text figures are presented following the section on acknowledgments.

astern operation. Results for the steady ahead operation were correlated with predictions based on unsteady lifting surface theory as developed by Tsakonas et al.,[20] with the quasi-steady method of McCarthy,[21] and with strains measured on the full-scale propeller of the FF-1088.

The model propeller used in these experiments was DTNSRDC Propeller 4402; see Figure 2 and Table 1. Its geometry was nearly identical to that of the FF-1088 propeller; see Figure 3 and Table 2. The only differences between the two propeller designs are (1) the radial distributions of camber and pitch between the 70-percent radius and the tip and (2) the blade leading edge radii; see Tables 1 and 2. It was judged that these two propellers would have approximately the same loading under the same operating conditions. Therefore, no corrections were made for the difference in their geometries.

The hull of the FF-1088 was represented by DTNSRDC Model Hull 4989; see Figure 4.

---

[20]Tsakonas, S. et al., "An Exact Linear Lifting Surface Theory for Marine Propeller in a Nonuniform Flow Field," Journal of Ship Research, Vol. 17, No. 4 (Dec 1974).

[21]McCarthy, J.H. "On the Calculation of Thrust and Torque Fluctuations of Propellers in Nonuniform Wake Flow," David Taylor Model Basin Report 1533 (Oct 1961).

TABLE 1 - CHARACTERISTICS OF PROPELLER CORRESPONDING TO DTNSRDC MODEL PROPELLER 4402

Diameter: 4.572 m (15.0 ft)
Rotation: Right Hand
Number of Blades: 5
Maximum Rotational Speed (Rated):
25.13 rad/sec (240 rev/min)
Full Power (Rated):
26,100 kW (35,000 hp)
Speed at Full Power:
14.5 m/sec (28.1 knots)
Expanded Area Ratio: 0.83

Blade Thickness Fraction: 0.059
Section Meanline: NACA 65
Section Thickness Distribution:
NACA 16 (Modified)[1]
Design Advance Coefficient J: 0.767
Design Advance Angle β^*:
0.3356 rad (19.23 deg)
Design Thrust Loading Coefficient
C_{Th}: 0.706

x	c/D	P/D	S/D[3]	Z_R/D	t/D	f_M/c
0.30	0.1853	1.008	0.0185	0	0.0437	0.0243
0.40	0.2482	1.044	0.0248	0	0.0328	0.0302
0.50	0.3111	1.067	0.0311	0	0.0250	0.0280
0.60	0.3740	1.072	0.0374	0	0.0187	0.0240
0.70	0.4369	1.061[2]	0.0437	0	0.0131	0.0191[2]
0.80	0.4760	1.025[2]	0.0476	0	0.0089	0.0140[2]
0.90	0.4600	0.964[2]	0.0460	0	0.0061	0.0082[2]
0.95	0.4587	0.922[2]	0.0459	0	0.0051	0.0042[2]
1.00	0.3400	0.878[2]	0.0340	0	0.0040	0.0000

[1] Smaller leading edge radii than propeller on FF-1088.

[2] Different than for propeller on FF-1088.

[3] The spindle axis is the propeller reference line and passes through 40-percent chord for all radii.

TABLE 2 - CHARACTERISTICS OF PROPELLER ON FF-1088
(Corresponds to DTNSRDC Model Propeller 4402A)

Diameter: 4.572 m (15.0 ft)
Rotation: Right Hand
Number of Blades: 5
Maximum Rotational Speed (Rated):
25.13 rad/sec (240 rev/min)
Full Power (Rated):
26,100 kW (35,000 hp)
Speed at Full Power:
14.46 m/sec (28.1 knots)
Expanded Area Ratio: 0.83

Blade Thickness Fraction: 0.059
Section Meanline: NACA 65
Section Thickness Distribution:
NACA 16 (Modified)
Design Advance Coefficient J: 0.767
Design Advance Angle β^*:
0.3356 rad (19.23 deg)
Design Thrust Loading Coefficient
C_{Th}: 0.706

x	c/D	P/D	S/D[1]	Z_R/D	t/D	f_M/c
0.30	0.1853	1.008	0.0185	0	0.0437	0.0243
0.40	0.2482	1.044	0.0248	0	0.0328	0.0302
0.50	0.3111	1.067	0.0311	0	0.0250	0.0280
0.60	0.3740	1.072	0.0374	0	0.0187	0.0240
0.70	0.4369	1.056	0.0437	0	0.0131	0.0197
0.80	0.4760	1.018	0.0476	0	0.0089	0.0152
0.90	0.4600	0.956	0.0460	0	0.0061	0.0097
0.95	0.4587	0.911	0.0459	0	0.0051	0.0056
1.00	0.3400	0.861	0.0340	0	0.0040	0.0000

[1]The spindle axis is the propeller reference line and passes through 40-percent chord for all radii.

EXPERIMENTAL TECHNIQUE

FACILITY AND DYNAMOMETRY

All experiments were conducted on DTNSRDC Carriage I. The propeller was located in its proper position relative to the model hull but was isolated from the hull and driven from downstream (see Figure 5).

This downstream drive system was necessary in order to obtain the required characteristics of the system for measuring unsteady loading. The general criteria for the design of an unsteady force measuring system are:

1. The support structure of the force measuring system should be soft mounted and possess a large mass to eliminate transmission of extraneous vibration to the system.

2. The natural frequency of the system should be well above the highest frequency of the quantities to be measured (to avoid phase shift and amplification of the signal).

3. The system response in the force magnitude range should be sufficiently large to be measurable (sensitivity).

4. The system should be free of interaction, that is, each measuring element should respond only to that force or moment which it is intended to measure.

These four major aims are not complementary. The high natural frequency requires a stiff, rigid system whereas high sensitivity requires an elastic, soft system. The necessary compromise results in some interaction between the force-measuring elements.

Criterion 1 dictated that a massive flywheel be used, and Criterion 2 dictated that this flywheel be connected to the sensing elements (located inside the propeller hub) by a short thick shaft. Therefore, because of the geometry of the hull and shafting of the configuration under evaluation, it was not feasible to achieve both these criteria with an upstream drive system from inside the model hull. Criteria 1 and 2 controlled the the minimum allowable beam and draft of the downstream body and the maximum allowable clearance from the bow of the downstream body to the propeller.

Although the downstream body may exert some influence on the flow into the propeller, that location was considered necessary in order to meet these measuring criteria. The influence of the downstream body on the flow into the propeller is discussed in the section on experimental results.

The drive and mounting system was basically the same as that used in the DTNSRDC BASS dynamometer which has been described by Brandau.[22] Utilized from this dynamometer were the propeller (tail) shaft, drive shaft with flywheel, belt-type (quiet) transmission, and sliprings. Power to rotate the propeller was supplied by a d-c permanent-magnet servomotor capable of delivering up to 45 N-m of torque. This motor was selected for its ability to control and hold the shaft revolution rate over the wide range of propeller torque loadings required for some of the experimental conditions. Mounted on the propeller shaft was a digital encoder that generated electrical pulses as a function of shaft angular position. Two types of pulses were generated: a single pulse per revolution and a multipulse per revolution (90 equally spaced pulses for the current experiment). The single pulse was syncronized with the reference line of the instrumented propeller blade. The pulses generated by this encoder are accurate to within 0.01 deg.

The downstream body which housed the drive system was basically that used by Dobay[15] but modified to allow deeper submergence and an inclined shaft angle. Both the body housing the drive system (the drive system was soft mounted to this body) and the model hull were rigidly attached to a pitch-heave oscillator which, in turn, was rigidly mounted on the towing carriage. This arrangement enabled the model hull and the drive system to be dynamically pitched together while maintaining independent support from one another.

The sensing elements were flexures to which were bonded high-sensitivity, semiconductor strain-gage bridges. The design of these flexures has been described by Dobay.[15] There were three flexures, each

---

[22] Brandau, J.H., "Static and Dynamic Calibration of Propeller Model Fluctuating Force Balances," David Taylor Model Basin Report 2350 (Mar 1967); see also Technologia Naval, Vol. 1, pp. 48--74 (Jan 1968).

of which measured two components of blade loading. Flexure 1 measured components F_x and M_y, Flexure 2 measured components F_y and M_x, and Flexure 3 measured components F_z and M_z (Figures 1 and 6). An arrangement of three separate flexures rather than one to measure all components of blade loading was adopted because it appeared to result in higher natural frequencies (Criterion 1), higher sensitivities (Criterion 3) and lower interactions (Criterion 4) than would have resulted had a single flexure been used.

The flexures were mounted inside a propeller hub which was specifically designed for these experiments (Figure 7). Only one flexure could be mounted at a time, because of space limitations, and this necessitated duplicate runs, as discussed later in the section on experimental conditions and procedures.

The strain-gage bridges were excited by a common d-c voltage source, transmitted through the sliprings on the propeller shaft. The constant-current excitation used by Dobay[15] was not employed in the present experiment because it appeared to be too sensitive to temperature.

The voltage output from the flexures (due to blade loading) was transmitted through the sliprings to individual amplifiers (NEFF 119-121). These amplifiers utilized field effect transistors to produce an extremely high input-impedance (100 MΩ, minimum). This high impedance essentially eliminated slipring noise to the amplifier. The voltage signals were transferred across the sliprings in the presence of only a small amount of noise-producing current. The amplifiers used here had zero-phase shift qualities in the d-c-20 kHz range. They were chopper-stabilized to enable both the steady and unsteady signals to be recorded simultaneously. This signal-conditioning system was essentially the same as that used by Dobay.[15]

The signals were then digitized and analyzed by using a Model 70 Interdata Digital Computer, and were then stored in digital form on a nine-track magnetic tape. The on-line analysis of the data is discussed in the section on data acquisition and analysis.

CALIBRATION

Prior to the experiment, each flexure was statically calibrated in air to establish flexure sensitivities, interactions, and linearity over the loading range of interest. These calibrations were conducted with the flexures mounted in the propeller hub which was connected to the flywheel and drive assembly as in the experiment. Each flexure was subjected to independently controlled forces in the axial, transverse, and radial directions (i.e., F_x, F_y, and F_z, respectively) and to independently controlled moments about the axial, transverse, and radial directions (i.e., M_x, M_y, and M_z, respectively); see Figure 1.

The static calibration showed that all flexures had a linear response over the load range of interest. Table 3 shows the interaction matrix. These calibrations indicated that all flexures had good sensitivity except F_z whose sensitivity was lower than desirable. The interactions were small except for the effect of M_z on F_z. The rather poor characteristics of the F_z flexure is not considered a serious shortcoming since F_z arises primarily from centrifugal loading and can be analytically calculated. In addition, no significant variation of F_z with blade angular position is anticipated. Flexure 3, which measured F_z and M_z, was further evaluated by correlation of air-spin experiments with analytically calculated results, as discussed later. The interactions were taken into consideration during data analysis.

The flexures used in this experiment had been dynamically calibrated by Dobay[15] to determine the frequency range over which unsteady forces and moments could be reliably measured. In this procedure, an electromagnetic shaker in air was used to apply a relatively constant, maximum amplitude, variable-frequency force or moment-excitation in all six-component directions to all six flexure elements. The force or moment amplitude imposed by the shaker was monitored through an extremely lightweight, strain-gaged single flexure element. The measured lowest natural frequencies of the three flexures in air were as follows:

	Frequency (Hz)	Mode
Flexure 1	550	M_x
Flexure 2	450	M_y
Flexure 3	282	M_z

TABLE 3 - CALIBRATION MATRIX

$$\text{Calibration Matrix} = [C_{i,j}] = \begin{bmatrix} 0.0652 & 0.0017 & -0.0003 & 0.0292 & -0.0531 & -0.0212 \\ -0.0025 & 0.0680 & -0.0001 & 0.0398 & 0.0434 & 0.0363 \\ 0.0002 & 0.0018 & 0.0203 & 0.0319 & -0.0027 & -0.3363 \\ 0.0005 & 0.0009 & 0.0004 & 1.6853 & -0.0080 & 0.0920 \\ -0.0018 & -0.0026 & 0.0013 & -0.0460 & 1.6605 & 0.0478 \\ -0.0002 & 0.0002 & 0.0000 & 0.0035 & 0.0035 & 1.1666 \end{bmatrix}$$

where

$$\begin{bmatrix} F_{x_I} \\ F_{y_I} \\ F_{z_I} \\ M_{x_I} \\ M_{y_I} \\ M_{z_I} \end{bmatrix} = \begin{bmatrix} F_{x_A} \\ F_{y_A} \\ F_{z_A} \\ M_{x_A} \\ M_{y_A} \\ M_{z_A} \end{bmatrix} \cdot [C_{i,j}]$$

F_{x_I}, F_{y_I}, F_{z_I} are indicated forces in volts.

M_{x_I}, M_{y_I}, M_{z_I} are indicated moments in volts.

F_{x_A}, F_{y_A}, F_{z_A} are applied forces in Newtons.

M_{x_A}, M_{y_A}, M_{z_A} are applied moments in Newton-meters.

$C_{i,j}$ for j=1,2,3 are in volts/Newton.

$C_{i,j}$ for j=4,5,6 are in volts/Newton-meters.

The measured amplification factor (ratio of output amplitude to input amplitude) and phase shift for all three flexures was as follows:

Frequency Range (Hz)	0 to 60	60 to 120
Phase Shift (rad)	0 to 8.7×10^{-4}	8.7×10^{-4} to 2.6×10^{-3}
Phase Shift (deg)	0 to 0.05	0.05 to 0.15
Amplification Factor	1.00	1.00 to 1.05

After the experimental apparatus was completely assembled with propeller blades and attached in place under the towing carriage, the effect of submergence in water on flexure lowest natural frequency was checked. This check consisted of striking the blade a sharp, light blow and recording the response of Flexure 1 (the F_x, M_y flexure). The measured response indicated that the lowest natural frequency of the flexure was approximately 250 Hz or approximately 0.45 times its value in air. Similar measurements were not made for the other two flexures but it was assumed that their natural frequencies in water were also approximately 0.45 times the measured values in air. Based on this assumption, the natural frequencies in water are:

Flexure 1	250 Hz
Flexure 2	202 Hz
Flexure 3	127 Hz

The highest propeller rotational speed during the experiment was 110.9 rad/sec (17.65 rev/sec). Thus, the flexures had a "true" dynamic response (determined in air) up to at least the third harmonic of shaft rotation and no greater than 5 percent amplification up to the sixth harmonic of shaft rotation. Assuming that the lowest natural frequency of each flexure in water was 0.45 times its measured value in air, the lowest natural frequencies of Flexures 1, 2, and 3 were respectively greater than 14, 11, and 7 times the highest propeller rotational speed used during the experiments. As discussed in the section on experimental results, extraneous signals appeared in the unfiltered experimental data at frequencies close to the deduced natural frequency of each flexure in water.

The propeller shaft drive and soft-mount support system were dynamically loaded in the vertical, longitudinal, and transverse directions to obtain the systems lowest natural frequencies. The natural frequencies of the system in air were found to be:

Mode	Natural Frequency (Hz)
Vertical bending	12.25
Horizontal bending	6.0
Axial	4.6

The support system had a low resonant range; however, the soft-mount system was specifically designed to prevent towing-carriage oscillation (with the resonance at 100 to 200 Hz) from being transmitted to the blade flexures. Based on the measured resonance, it is concluded that the soft-mount system should successfully meet this objective. Although some resonances were close to the propeller rotational speed for some experimental conditions, it was considered more desirable to isolate the system from towing-carriage vibration. Therefore, the soft mount system was considered to be satisfactory.

EXPERIMENTAL CONDITIONS AND PROCEDURES

Experiments were conducted at several conditions including steady ahead operation, simulated pitching of the hull, simulated crash ahead (acceleration), and simulated crash astern (deceleration). All conditions were run with the model hull rigidly attached to its support, with no freedom to sink or trim.

The steady ahead condition is defined in Tables 4-7. The simulated full-scale speed for this condition was slightly higher than the speed at full power measured during standardization trials (see Table 4), but the propeller rotational speed was the same as that measured at full power during standardization trials. Model self-propulsion data (not corrected for wind drag at zero true wind) tend to agree with the standardization data; see Table 4. If the standardization data are correct, then the

TABLE 4 - PREDICTED FULL-SCALE STEADY AHEAD POWERING CONDITIONS FROM VARIOUS SOURCES

	V		n		$\overline{T}$		$\overline{Q}$		P_D	
	m/sec	(knots)	rad/sec	(rev/min)	$N \times 10^{-6}$	($lb \times 10^{-5}$)	N-m $\times 10^{-6}$	(ft-lb $\times 10^{-5}$)	$kw \times 10^{-4}$	($hp \times 10^{-4}$)
Model Experiments in Present Study[1]	14.7	(28.6)	25.1	240	1.14	(2.57)	0.97	(7.13)	2.44	(3.27)
Standardization Trials	14.4	(28.1)	25.1	(240)	1.13	(2.55)	1.04	(7.66)	2.61	(3.50)
Model Data[2]	14.5	(28.2)	25.1	(240)	1.19	(2.67)	1.04	(7.66)	2.61	(3.50)
Full-Scale Blade Stress Trials[3]	13.3	(25.8)	23.8	(227)	1.10	(2.48)	1.33	(9.80)	3.15	(4.23)

[1]Corrected for influence of dynamomenter boat.

[2]No correction for full-scale wind drag at zero true wind.

[3]Conducted by C.J. Noonan and G.P. Antonides, DTNSRDC Code 1962.

TABLE 5 - MODEL EXPERIMENTAL CONDITIONS

	Condition	V		n		J_V	P/D	$(\psi-\psi_{CW})$	$\dot{V}$		$t-t_0$
	No.	m/sec	(knots)	rad/sec	(rev/sec)			deg	m/sec^2	(knots/sec)	sec
Self-Propulsion	1	3.33	(6.50)	110.9	(17.65)	0.80	1.06	0	0	(0)	N/A
Quasi-Steady Hull Pitch	2	3.33	(6.50)	110.9	(17.65)	0.80	1.06	-2	0	(0)	N/A
	3	3.33	(6.50)	110.9	(17.65)	0.80	1.06	-1	0	(0)	N/A
	4	3.33	(6.50)	110.9	(17.65)	0.80	1.06	+1	0	(0)	N/A
	5	3.33	(6.50)	110.9	(17.65)	0.80	1.06	+2	0	(0)	N/A
Unsteady Hull Pitch	6	3.33	(6.50)	110.9	(17.65)	0.80	1.06	variable[2]	0	(0)	N/A
Quasi-Steady Crash Forward	7	0.33	(0.64)	39.3	(6.26)	0.22	1.39	0	0	(0)	N/A
	8	0.81	(1.59)	58.7	(9.35)	0.37	1.39	0	0	(0)	N/A
	9	1.46	(2.85)	70.3	(11.19)	0.56	1.39	0	0	(0)	N/A
	10	2.26	(4.41)	75.8	(12.07)	0.80	1.39	0	0	(0)	N/A
	11	3.10	(6.05)	84.2	(13.40)	0.99	1.39	0	0	(0)	N/A
Unsteady Crash Forward	12	0.33[1]	(0.64)[1]	39.3	(6.26)	0.22	1.39	0	+0.19[1]	(0.10)[1]	4.53
	13	0.81[1]	(1.59)[1]	58.7	(9.35)	0.37	1.39	0	+0.23[1]	(0.12)[1]	9.05
	14	1.46[1]	(2.85)[1]	70.3	(11.19)	0.56	1.39	0	+0.33[1]	(0.17)[1]	13.58
	15	2.26[1]	(4.41)[1]	75.8	(12.07)	0.80	1.39	0	+0.33[1]	(0.17)[1]	18.11
	16	3.10[1]	(6.05)[1]	84.2	(13.40)	0.99	1.39	0	+0.01	(0.01)[1]	31.69
Quasi-Steady Crash Astern	17	3.33	(6.50)	110.9	(17.65)	0.80	1.06	0	0	(0)	N/A
	18	2.57	(5.03)	109.5	(17.43)	0.63	0.61	0	0	(0)	N/A
	19	1.67	(3.26)	104.2	(16.59)	0.43	0.14	0	0	(0)	N/A
	20	0.74	(1.44)	42.5	(6.77)	0.46	-0.67	0	0	(0)	N/A
	21	0.17	(0.34)	48.0	(7.64)	0.10	-0.67	0	0	(0)	N/A
Unsteady Crash Astern	22	3.33[1]	(6.50)[1]	110.9	(17.65)	0.80	1.06	0	0.00[1]	(0.00)[1]	0
	23	2.57[1]	(5.03)[1]	109.5	(17.43)	0.63	0.61	0	-0.32[1]	(-0.16)[1]	9.05
	24	1.67[1]	(3.26)[1]	104.2	(16.59)	0.43	0.14	0	-0.43[1]	(-0.22)[1]	13.58
	25	0.74[1]	(1.44)[1]	42.5	(6.77)	0.46	-0.67	0	-0.32[1]	(-0.16)[1]	18.11
	26	0.17[1]	(0.34)[1]	48.0	(7.64)	0.10	-0.67	0	-0.18[1]	(-0.09)[1]	22.64

[1] Varies with time (Figure 8); value shown is at time of interest.

[2] Sinusoidal with amplitude equal to 2.0 deg, frequency equal to 0.8 Hz.

TABLE 6 - FULL-SCALE CONDITIONS SIMULATED BY MODEL EXPERIMENTS

	Condition No.	V m/sec	V (knots)	n rad/sec	n (rev/sec)	J_V	P/D	$(\psi-\psi_{CW})$ deg	$\dot{V}$ m/sec^2	$\dot{V}$ (knots/sec)	$t-t_o$ sec
Self-Propulsion	1	14.7	28.6	25.10	4.00	0.80	1.06	0	0	0	N/A
Quasi-Steady Hull Pitch	2	14.7	28.6	25.10	4.00	0.80	1.06	-2			
	3	14.7	28.6	25.10	4.00	0.80	1.06	-1			
	4	14.7	28.6	25.10	4.00	0.80	1.06	+1			
	5	14.7	28.6	25.10	4.00	0.80	1.06	+2			
Unsteady Hull Pitch	6	14.7	28.6	25.10	4.00	0.80	1.06	variable[2]			
Quasi-Steady Crash Forward	7	1.6	2.8	8.90	1.42	0.22	1.39	0			
	8	3.6	7.0	13.29	2.12	0.37	1.39	0			
	9	6.4	12.6	15.91	2.53	0.56	1.39	0			
	10	10.0	19.5	17.16	2.73	0.80	1.39	0			
	11	13.7	26.7	19.06	3.03	0.99	1.39	0	0	0	N/A
Unsteady Crash Forward	12	1.6[1]	2.8[1]	8.90	1.42	0.22	1.39	0	+0.19[1]	(0.10)[1]	20
	13	3.6[1]	7.0[1]	13.29	2.12	0.37	1.39	0	+0.23[1]	(0.12)[1]	40
	14	6.4[1]	12.6[1]	15.91	2.53	0.56	1.39	0	+0.33[1]	(0.17)[1]	60
	15	10.0[1]	19.5[1]	17.16	2.73	0.80	1.39	0	+0.33[1]	(0.17)[1]	80
	16	13.7[1]	26.7[1]	19.06	3.03	0.99	1.39	0	+0.01[1]	(0.01)[1]	140
Quasi-Steady Crash Astern	17	14.7	28.6	25.10	4.00	0.80	1.06	0	0	0	N/A
	18	11.4	22.2	24.78	3.94	0.63	0.61	0			
	19	7.4	14.4	23.59	3.76	0.43	0.14	0			
	20	3.3	6.4	9.62	1.53	0.46	-0.67	0			
	21	0.8	1.5	10.86	1.73	0.10	-0.67	0	0	0	N/A
Unsteady Crash Astern	22	14.7[1]	28.6[1]	25.10	4.00	0.80	1.06	0	0.00[1]	0.00[1]	0
	23	11.4[1]	22.2[1]	24.78	3.94	0.63	0.61	0	-0.32[1]	-0.16[1]	40
	24	7.4[1]	14.4[1]	23.59	3.76	0.43	0.14	0	-0.43[1]	-0.22[1]	60
	25	3.3[1]	6.4[1]	9.62	1.53	0.46	-0.67	0	-0.32[1]	-0.16[1]	80
	26	0.8[1]	1.5[1]	10.86	1.73	0.10	-0.67	0	-0.18[1]	-0.09[1]	100

[1]Varies with time (Figure 8); value shown is at time of interest.

[2]Sinusoidal with amplitude equal to 2.0 deg, frequency equal to 0.8 Hz.

TABLE 7 - TIME-AVERAGE LOADS FOR STEADY AHEAD OPERATION NEAR THE SELF-PROPULSION POINT

$V \approx 3.33$ m/sec = 10.92 ft/sec

$n = 110.9$ rad/sec = 17.65 rev/sec

$J_V = 0.80$

$P/D = 1.06$

$\overline{K}_{F_x}$	= 0.0321	$\overline{F}_x$	= 30.0 N = 6.74 lb
$\overline{K}_{F_y}$	= 0.0213	$\overline{F}_y$	= 19.9 N = 4.48 lb
$\overline{K}_{M_x}$	=-0.0059	$\overline{M}_x$	=-1.29 N-m =-11.42 in-lb
$\overline{K}_{M_y}$	= 0.0118	$\overline{M}_y$	= 2.59 N-m = 22.94 in-lb
$\overline{K}_{M_z}$	=-0.0006	$\overline{M}_z$	=-0.13 N-m = -1.15 in-lb
$\overline{K}_{M_h}$	= 0.0069	$\overline{M}_h$	= 1.51 N-m = 13.37 in-lb
$\overline{K}_{M_{0.4}}$	= 0.0050	$\overline{M}_{0.4}$	= 1.10 N-m = 9.74 in-lb

steady ahead condition run during the present study represents a slightly "overpropelled" condition. However, the thrust and propeller rotational speed determined from the present experiment were in good agreement with the standardization data; although the scaled torque and power were lower on the model experiment. This is not a serious shortcoming since the net bending moment on the blade at steady ahead operation is controlled predominantly by the bending moment arising from thrust.

The trim and draft at this speed was determined by setting the specified still water trim (even keel) and draft (4.65 m (15.27 ft) full-scale equivalent), attaching the model to the carriage so that it was free to trim and sink, running at the specified speed, and locking the model at this equilibrium trim and draft.

Runs simulating hull pitching were conducted at the same conditions as the steady ahead run, except that the hull pitch was varied. Two types of runs were conducted: (1) quasi-steady simulation in which the hull pitch angle ψ was set at various fixed position and (2) unsteady simulation in which ψ was varied sinusoidally with time. For the quasi-steady simulation, runs were conducted at five different values of ψ, from 2-deg bow up from the calm water equilibrium ψ ($\psi=\psi_{CW}$) to 2-deg bow down from ψ_{CW} (Tables 5 and 6). For the unsteady pitch simulation, the value of ψ was varied sinusoidally about ψ_{CW} with an amplitude of 2 deg and a frequency of 0.8 Hz. The selected scaled amplitude and frequency were within the predicted response characteristics of the FF-1088. All runs were conducted in calm water; therefore, the response of the hull to the seaway was simulated but the seaway was not simulated.

Crash ahead runs were conducted by using the still-in-the-water point as the initial condition. Trim and displacement were fixed at the values corresponding to the self-propulsion condition (Condition 1 of Table 5). Two types of runs were conducted: (1) quasi-steady runs in which all quantities including model speed V, rotational speed n, and propeller pitch P were held constant ($\dot{V}=\dot{n}=\dot{P}=0$) and (2) unsteady runs in which V was varied with time but n and P were held constant ($\dot{V}>0$, $\dot{n}=\dot{P}=0$). For the quasi-steady simulation,

runs were conducted at five different combinations of V, n, and P. The conditions for each run represent the conditions at one instant of time during a "true" crash ahead in which V, n, and P vary with time. Thus, one "true" crash ahead run is represented by five steady runs which do not simulate the time rate of change of V, n, and P. For the unsteady simulation, runs were conducted at the same five combinations of fixed n and P as used for the quaso-steady simulation, and V was varied with time (the same variation was used for each run) representing an acceleration of the model hull (Figure 8). For each of these runs, data are of interest only near that value of V which occurred concurrently with the fixed values of n and P during the "true" crash ahead ($\dot{V}\neq0$, $\dot{n}\neq0$, $\dot{P}\neq0$). Thus, one "true" crash ahead run is represented by five runs which simulate the proper time rate of change of V but not the proper time rate of change of n and P. The quasi-steady and unsteady crash ahead simulations were for the same conditions, the only difference being that $\dot{V}=0$ for the quasi-steady simulation whereas $\dot{V}>0$ for the unsteady simulation. In general, P varied with time during a "true" crash ahead run; however, for the crash ahead run under simulation here, P was constant throughout the portion of the run simulated.

Crash astern runs were conducted by using the self-propulsion condition (Condition 1 in Table 5) as the initial condition. Both quasi-steady ($\dot{V}=\dot{n}=\dot{P}=0$) and unsteady ($\dot{V}<0$, $\dot{n}=P=0$) runs were conducted (Table 5 and Figure 8) to simulate one "true" crash astern ($\dot{V}\neq0$, $\dot{n}\neq0$, $\dot{P}\neq0$) condition by procedures similar to those described for the crash ahead condition. Unlike the crash ahead simulation, the value of propeller pitch P varied through the portion of "true" crash astern under simulation.

For the unsteady crash ahead and crash astern runs, the carriage speed was manually varied with time in a carefully controlled manner. This was achieved with the aid of an inked pen on a two-dimensional Cartesian plotter. In one direction, the pen was controlled so that it moved linearly with time, and in the orthogonal direction, it was controlled so that it varied with the instantaneous carriage speed. When a crash ahead or crash astern maneuver was to be executed, the switch moving the pen with time was turned on and the carriage operator manually varied the carriage speed so that the inked pen followed a prescribed velocity versus time curve.

As discussed earlier, each of the three load-sensing flexures measured only two components of blade loading. Therefore, each of the experimental conditions described in Table 5 was run with each of the three blade loading flexures.

The blade pitch was set by using a template. In order to change either the blade pitch or the flexure, the propeller had to be removed from the drive system.

Supplemental experiments were conducted to assess the influence of the downstream dynamometer boat on the flow in the propeller plane. These supplemental experiments consisted of (1) wake surveys in the propeller plane at the self-propulsion point (Condition 1 in Table 5) with and without the downstream body, (2) measurement of time-average thrust and torque using a transmission dynamometer in the model hull near the self-propulsion point with and without the downstream body, and (3) measurement of the six components of blade loading at P/D=1.06 over a range of advance coefficient J with the downstream body at zero shaft angle but without the upstream ship model. The supplemental experiment on wake surveys yielded a direct measure of the change in volume mean velocity through the propeller disk attributable to the downstream body. The change in effective velocity through the propeller disk was deduced from Supplemental Experiments (2) and (3) by thrust and torque identity between similar conditions with and without the downstream body.

Some air spin experiments were conducted with the F_z, M_z flexure over a range of pitch settings in order (1) to isolate the centrifugal loading in the F_z and M_z directions and (2) to evaluate the reliability of the results with this flexure by correlation with analytically calculated centrifugal loading.

DATA ACQUISITION AND ANALYSIS

Data were collected, stored, and analyzed on-line by using a Model 70 Interdata Digital Computer. A special-purpose computer program was written with options for analyzing each of the three basic types of runs: (1) steady ahead, (2) dynamic hull pitching, and (3) unsteady crash-ahead or crash-astern. These types of runs have already been discussed in detail.

The program allowed the propeller blade force and moment data to be sampled and stored on magnetic tape as a function of shaft position. Sampling was triggered by external pulses generated by a digital encoder mounted on the propeller shaft, as discussed earlier. Pulses were generated as a function of shaft angular position; hence, the sampling of blade force and moment data was related to shaft position. There were two outputs from the shaft encoder; a single pulse per revolution and multipulse (90 pulses per revolution for the current experiments).

When the experimental condition was achieved, the computer operator initiated the data collection cycle. The program "waited" for the occurrence of the first following pulse of the 90 pulses; data were then sampled for all channels through an analog-to-digital converter and stored in computer memory. This process was repeated for 180 pulses, or two shaft revolutions. At the same time, the program "read" two frequency counters into core memory which measured model velocity V and propeller rotational speed n. V and n were measured by counting the pulses from geared wheels attached to the towing carriage drive system and to the propeller shaft, respectively. The V and n were averaged over two shaft revolutions. Thus, there was an average V and n corresponding to each pair of two consecutive revolutions.

After two revolutions of data were sampled and stored in core memory, the data were transmitted from core to a nine-track digital tape recorder. The transfer time was small and no pulses were missed during the transfer. The data collect cycle proceeded continuously until the operator disengaged the computer. The sampling procedure was the same for all types of experimental conditions, and at the completion of an experimental run, all data were stored on magnetic tape and were available for analysis immediately or at any later time. For that analysis, the computer operator selected the appropriate option of the program depending on the type of run, i.e., (1) steady ahead, (2) dynamic hull pitching, or (3) unsteady crash ahead or crash astern.

The appropriate calibration factors were stored in the computer and considered in the analysis. However, since only two of the six components of blade loading were measured during a given run, the interactions between

the various loading components could not be considered during the on-line analysis. The interactions were taken into account later after measurements were completed with all three flexures for a given condition.

For the steady ahead condition, blade force and moment data at each 4-deg increment of blade angular position were averaged over the number of cycles recorded (usually over more than 200 cycles). Spurious data not related to shaft position are averaged out by this method. A harmonic analysis was then performed on the average wave forms of the blade loading components. This gave the amplitude and phase of the first 16 harmonics.

For the dynamic pitch runs, the hull pitch angle ψ varied sinusoidally with a frequency of 0.8 Hz. A position potentiometer translated bow vertical displacement into hull pitch angle, and thus was read into the computer in the same manner as blade loading components. During dynamic pitching, the shaft rotated independent of the pitch oscillator. During a single propeller revolution, 90 pitch positions were measured. Thus, to correlate pitch angle position and revolution, an average pitch must be taken over each revolution.

The 16 dynamic pitch angle positions selected for analysis were characterized by pitch angle ψ and the sign of the time rate of change of pitch angle $\dot{\psi}$. The computer calculated an average ψ and sign of $\dot{\psi}$ corresponding to each propeller revolution. Based on these calculated average values of ψ and sign of $\dot{\psi}$, each propeller revolution was either placed in a suitable hull pitch angle category or discarded if its average ψ fell outside the tolerance band of all the 16 specified values of ψ. Several passes down the towing tank were required in order to obtain a sufficient number of samples. After all the data had been sorted based on (ψ, sign of $\dot{\psi}$), and tolerance, the cycles for each combination of (ψ, sign of $\dot{\psi}$) were analyzed in exactly the same manner as the data for the steady ahead condition at fixed ψ.

For unsteady crash ahead and crash astern runs, the model speed V varied with time t. During a crash ahead or crash astern run, data, including a measure of V, were sampled and stored in the same manner as for the steady ahead runs.

Five values of V were specified for analysis. For each crash ahead or crash astern run and for each specified V, the computer selected the propeller revolution which had the average value of measured V nearest to the specified V. However, because only one revolution at each specified velocity was obtained for a single crash ahead or crash astern run, each such run was repeated from three to five times. This yielded three to five revolutions at each specified velocity. All the cycles for each specified V were then analyzed in exactly the same manner as the data for the steady ahead conditions.

Thus the on-line analysis system yielded average wave forms and harmonic analysis of the average wave forms for steady ahead conditions, for specified conditions of (ψ, sign of $\dot{\psi}$) during the dynamic pitch cycle, and for specified velocities V during the crash ahead or crash astern operation. However, these on-line results are preliminary because:

1. They do not consider the interactions between the various load components. These interactions were determined during the static calibration of the flexures.

2. They include the complete measured signals with no filtering. As discussed in the section on experimental results, some extraneous signals near the natural frequency of the flexure being used appeared to be superimposed on the signals generated by blade loading.

Final analyses were conducted after completion of the experiment to consider interactions and to filter out extraneous high frequency noise. These analyses were conducted by using a CDC 6700 Computer. For each condition, the average wave form for each of the six loading components was multiplied by the inverse of the calibration matrix given in Table 2.

$$\begin{bmatrix} F_{xA} \\ F_{yA} \\ F_{zA} \\ M_{xA} \\ M_{yA} \\ M_{zA} \end{bmatrix} = \begin{bmatrix} F_{xI} \\ F_{yI} \\ F_{zI} \\ M_{xI} \\ M_{yI} \\ M_{zI} \end{bmatrix} \qquad \begin{bmatrix} C_{i,j} \end{bmatrix}^{-1}$$

This matrix multiplication was performed at 0.07-rad (4-deg) increments of blade angular position. A harmonic analysis was then performed on the signals corrected for the interactions. Based on a harmonic analysis of the wake in the propeller plane, it was judged that there should be no significant loading of hydrodynamic origin at frequencies above ten times shaft frequency. Therefore, the wave form was then reconstructed by using the first ten harmonics of shaft frequency, except for the spindle torque M_z which used the first five harmonics of shaft frequency. This reconstruction using only the first ten (or five) harmonics had the same effect as filtering out all frequencies above ten (or five) times shaft frequency.

From the known values of F_x, F_y, M_x and M_y, the values of the bending moment normal to the nose-tail line at the blade root (the 0.289 radius) and at the 0.4 radius were calculated. For the calculation about the 0.4 radius, it was assumed that the loading between the blade root and the 0.4 radius accounted for 3 percent of the moments about the shaft centerline. These bending moments were calculated at every 4 deg of blade angular position, harmonically analyzed, and the wave form reconstructed by using the first 10 harmonics of blade angular position in exactly the same manner as was used for the other components of blade loading.

Plots of the data were generated by the CDC computer system using a Calcomp Plotter.

ACCURACY

During experiments for steady ahead operation $\dot{V}=0$, the model speed V and rotational speed n could be controlled to within accuracies of ± 0.005 M/sec and +0.01 rev/sec, respectively. For the unsteady crash ahead and crash astern maneuvers ($\dot{V}\neq 0$), the average of the three to five values of V and n during the unsteady runs for which data are presented was generally within ± 0.01 M/sec and ± 0.05 rev/sec, respectively, of the target values.

For runs with fixed hull pitch angle ψ, ($\dot{\psi}=0$), the value of ψ could be controlled to within 0.005 deg. For dynamic pitch runs $\dot{\psi}\neq 0$, the selection of a propeller revolution at a specified ψ necessitated a tolerance of 0.1 deg to ψ; however, the average value of ψ during the unsteady runs for which data are presented was generally within 0.02 deg of the target ψ.

The forces F_x and F_y and moments M_x, M_y, and M_z were accurate to within (plus or minus) the following variations:

	F [N]	F_{MAX} [N]	$\overline{M}$ [N-m]	M_{MAX} [N-m]
Steady ahead $\dot{V}=0, \dot{\psi}=0$	1.0	1.5	0.04	0.06
Dynamic pitch $\dot{V}=0, \dot{\psi}\neq 0$	1.5	2.0	0.06	0.08
Crash ahead $\dot{V}>0, \dot{\psi}=0$	2.0	2.5	0.08	0.10
Crash astern $\dot{V}<0, \dot{\psi}=0$	2.0	2.5	0.08	0.10

The values are somewhat more accurate for the steady ahead runs than for the time-dependent runs, because the experimental conditions could be controlled more precisely for the steady runs and the measured forces and moments were averaged over many more revolutions of the propeller. The time-average values per revolution (based on 90 samples

per revolution) are slightly more accurate than the maximum values (based on one sample per revolution) which took into account the variation with blade angular position. Further, the peak values may have been slightly influenced by the dynamic response of the flexures, as discussed in the section on calibration.

The measured values of F_z were substantially less accurate than the other components of blade loading and these results are not presented as explained in the following section.

EXPERIMENTAL RESULTS

CENTRIFUGAL LOADS

The results of the air-spin experiments with the F_z, M_z flexure were compared with calculated values of F_z and M_z by using the method of Boswell.[23] Previous measurements of spindle torque by Boswell et al.[24] and by Hawdon et al.[4] have correlated well with values calculated by this procedure. Figures 9 and 10 show the correlation for M_z and F_z, respectively. M_z correlated fairly well except at P/D=-0.67, but the correlation for F_z was rather poor. This poor correlation for F_z, combined with the large interaction effect of M_z on F_z and the low natural frequency of this flexure, casts doubt on the reliability of the measured values of F_z. In addition, the experimental values of F_z in water were rather inconsistent. Since F_z arises primarily from centrifugal loading, no experimental results are presented for F_z in water.

INFLUENCE OF DYNAMOMETER BOAT

The results of the wake surveys with and without the downstream body (dynamometer boat) are presented in Figures 11 and 12, and in Appendix A.

---

[23] Boswell, R.J., "A Method of Calculating the Spindle Torque of a Controllable-Pitch Propeller at Design Conditions," David Taylor Model Basin Report 1529 (Aug 1961).

[24] Boswell, R.J. et al., "Experimental Spindle Torque and Open-Water Performance of Two Skewed Controllable-Pitch Propellers," DTNSRDC Report 4753 (Dec 1975).

These data indicate that the downstream body had only a small effect on the circumferential and radial variation in the flow and only a small effect on the harmonic content of the flow. However, they also indicate that the downstream body reduced the volume mean velocity through the propeller disk by approximately 12 percent. This reduction in mean flow due to the downstream body was confirmed by values deducted from thrust and torque identity between model experimental values with and without the downstream body in place. The values of reduction in effective velocity deduced in this manner are as follows:

1. A reduction of 10 to 14 percent from measurement of mean thrust and torque using a transmission dynamometer inside the model hull at the self-propulsion point (Condition 1 in Table 5) with and without the downstream body in place.

2. A reduction of 10 to 14 percent from mean thrust and torque deduced from the blade loading experiments at the self-propulsion point (condition 1 in Table 5) and thrust and torque measured during a previous self-propulsion model experiment.

3. A reduction of 9 to 12 percent from mean thrust and torque coefficients deduced from blade loading experiments at P/D=1.06 over a range of advance coefficient J with the downstream body at zero shaft angle with no upstream hull, and thrust and torque coefficient determined by previous open-water experiments (Figure 13).

Based on these results it was concluded that the downstream body reduced the mean velocity into the propeller by 12 percent at the self-propulsion condition. It was assumed that this 12-percent reduction occurred at all conditions at which experiments were conducted. Therefore, the time-average value per revolution of each loading component was corrected for the effect of the downstream body as follows: From the measured blade thrust ($\bar{F}_x$) and blade torque ($\bar{M}_x$), an effective advance coefficient J based on thrust identity (J_T) and torque identity (J_Q) was deduced from the open-water data (Figure 13). These

values were multiplied by (1/0.88) to obtain corrected values of J_T and J_Q, i.e., without the downstream body. The corrected values of $\overline{F}_x$ and $\overline{M}_x$ were obtained from the open-water data at the corrected advance coefficients J_T and J_Q, respectively. It is assumed that the downstream body did not affect the radial center of thrust $\overline{F}_x$ and tangential force $\overline{F}_y$. Therefore,

$$\overline{M}_y \text{ corrected} = (\overline{F}_x \text{ corrected}/\overline{F}_x \text{ measured})\ \overline{M}_y \text{ measured}$$

$$\overline{F}_y \text{ corrected} = (\overline{M}_x \text{ corrected}/\overline{M}_x \text{ measured})\ \overline{F}_y \text{ measured}$$

The spindle torque ($\overline{M}_z$) was corrected by the same procedure as used for $\overline{F}_x$ and $\overline{M}_x$, except that the centrifugal and hydrodynamic components of spindle torque were separated so that the correction was applied only to the hydrodynamic component. Centrifugal spindle torque was determined by air spin experiments, as discussed previously. The open-water hydrodynamic spindle torque data used for these corrections were those reported by Denny and Stevens[25] on DTNSRDC Model Propeller 4496. These data were presented over a range of pitch ratio P/D and advance coefficient J. The geometry of Propeller 4496 is nearly identical to that of the propeller on the FF-1088. The only differences between the two propeller designs are the chordwise distributions of camber and thickness, the radial distributions of camber and pitch, and the chord length and skewback between the 90-percent radius and the tip; see Tables 2 and 8. It was judged that these two propellers would have approximately the same spindle torque at the same advance coefficients and pitch ratios.

In addition to the correction to hydrodynamic spindle torque for mean advance coefficient, the centrifugal spindle torque was corrected for the difference in density between the aluminum model propeller and a nickel-aluminum-bronze full-scale propeller. Since centrifugal spindle

---

[25] Denny, S.B. and H.G. Stephens, "Blade Spindle Moment on Controllable-Pitch Propellers," NSRDC Departmental Report SPD-011-14 (Jul 1974).

TABLE 8 - CHARACTERISTICS OF PROPELLER CORRESPONDING TO DTNSRDC MODEL PROPELLER 4496

Diameter: 4.572 m (15.0 ft)
Rotation: Right hand
Number of Blades: 5
Maximum Rotational Speed (Rated):
25.13 rad/sec (240 rev/min)
Full Power (Rated):
26,100 kW (35,000 hp)
Speed at Full Power:
14.5 m/sec (28.1 knots)
Expanded Area Ratio: 0.83

Blade Thickness Fraction: 0.059
Section Meanline: NACA a=0.8[1]
Section Thickness Distribution:
NACA 66 (Modified)[1]
Design Advance Coefficient J: 0.767
Design Advance Angle β^*:
0.3356 rad (19.23 deg)
Design Thrust Loading Coefficient,
C_{Th}: 0.706

x	c/D	(P/D)[1]	S/D[2]	Z_R/D	t/D	(f_M/c)[1]
0.30	0.1853	0.998	0.0185	0	0.0437	0.0189
0.40	0.2482	1.070	0.0248	0	0.0328	0.0197
0.50	0.3111	1.104	0.0311	0	0.0250	0.0190
0.60	0.3740	1.102	0.0374	0	0.0187	0.0168
0.70	0.4369	1.078	0.0437	0	0.0131	0.0128
0.80	0.4760	1.035	0.0476	0	0.0089	0.0105
0.90	0.4600	0.979	0.0460	0	0.0061	0.0098
0.95	0.4228[1]	0.944	0.0423[1]	0	0.0051	0.0099
1.00	0.1500[1]	0.906	0.0150[1]	0	0.0040	0.0100

---

[1] Different than for propeller on FF-1088.

[2] The spindle axis is the propeller reference line and passes through the 40-percent chord for all radii.

torque is directly proportional to the density of the material, this correction factor is simply $(\rho_{NI-AL-BR})/(\rho_{AL})$. The time-average spindle torque per revolution presented in this report is the sum of the hydrodynamic spindle torque corrected for the downstream body and the centrifugal spindle torque which corresponds to nickel-aluminum-bronze propeller blades.

No correction for the effect of the downstream dynamometer boat was made to the measured circumferential variation of the loading components. Calculations made by the methods of Tsakonas et al.[20] and McCarthy[21] indicated that the influence of the downstream body may reduce the peak-to-peak circumferential variation of the loads by approximately 10 percent of the uncorrected unsteady loading. However, these methods did not agree well with the experimental results, as discussed in the section on correlation with full-scale data and theory.

STEADY AHEAD OPERATION

For operation near the self-propulsion point (Condition 1 in Table 5), Figure 14 presents the variation of the various components of blade loading with blade angular position and Figure 15 presents the amplitude of the first 25 harmonics of the various components of blade loading. For the harmonic amplitude and phases, the variation of F_x with blade angular position is represented as:

$$F_x(\theta)=\overline{F}_x + \sum_{n=1}^{N} (F_x)_n \cos\left(n\theta - (\phi_{Fx})_n\right)$$

where $\overline{F}_x$ = circumferential average value of F_x

$(F_x)_n$ = amplitude of the nth harmonic of F_x

θ = angular position in disk, positive clockwise from the vertical upward looking upstream

The reference line on the blade is the radial line through midchord at the hub radius. $(\phi_{Fx})_n$ = phase angle of nth harmonic of F_x. A similar representation is used for all components of blade loading.

Based on the dynamic calibration, as discussed in the section on calibration, it was judged that for all loading components the data are valid for the first 10 harmonics, except M_z which was judged to be valid for the first 5 harmonics. Therefore, all data and analysis except Figures 14 and 15 are based on reconstructed signals using 5 harmonics for M_z and 10 harmonics for other loading components. The circles shown on Figure 14 indicate unfiltered values determined from the experiment; each represents the average value at the indicated blade angular position for over 200 propeller revolutions. The lines are the signals reconstructed from the first 10 harmonics. Figure 14 indicates that the variation of the signal with blade angular position is adequately represented by the number of harmonics retained. Figures 14 and 15 show that there was a resonance in the F_x signal near the fourteenth harmonic. This corresponded to (14) x (17.65 Hz) = 247 Hz which is near the natural frequency of this flexure in water, as discussed in the section on calibration.

The variation of all measured loading components with blade angular position for Condition 1 in Table 5 is shown in Figure 16 and in Appendix B. Figure 17 and Appendix B present the amplitude and phases of the harmonics of these loading components. The values for each loading component are presented as decimal fractions of the time-average value of the corresponding loading component. These average values are presented in Table 7. These data indicate that the extreme values for all loading components occurred near θ=90 and 270 deg and that the variation was predominantly a once-per-revolution variation. This suggests that the tangential component of the wake is the primary driving force.

For F_x and M_y, the largest measured force and moment components, the maximum values were approximately 1.38 times the time-average values; the range of values with blade angular position, i.e., the maximum value minus the minimum value (double amplitude) was approximately 0.80 times the time-average value. For F_y and M_x, the maximum values and range of values with blade angular position were somewhat smaller fractions of

the respective time-average values. For M_z, the maximum value and range of values with blade angular position were much greater fractions of its time average. This large fractional variation in M_z occurs because M_z was very small at the self-propulsion point (the blade is designed with its area balanced forward and aft the spindle axis at the self-propulsion point).

HULL PITCH

Figure 18 presents the variation of the peak values and time-average values per revolution of the various components of blade loading with hull pitch angle ψ for both quasi-steady simulation (time rate of change of hull pitch angle $\dot{\psi}=0$) and unsteady simulation ($\dot{\psi}\neq 0$). These data show that except for spindle torque M_z, the time-average value per revolution of each loading component remains within 4 percent of its value corresponding to self-propulsion in calm water. This holds true for both quasi-steady simulation ($\dot{\psi}=0$) and unsteady simulation ($\dot{\psi}\neq 0$). The time-average spindle torque per revolution $\overline{M}_z$ varied as much as 20 percent from its calm-water value ($\psi=\psi_{CW}$). This large percentage variation occurred because $\overline{M}_z$ was very small at $\psi=\psi_{CW}$ as discussed earlier.

Data at each specified value of hull pitch angle ψ for the quasi-steady runs were recorded and averaged for a minimum of 200 propeller revolutions whereas data for the dynamic pitching runs at each specified ψ represented an average of from 10 to 35 propeller revolutions. As discussed earlier, the selection of a propeller revolution at a specified ψ during the dynamic pitch runs necessitated a tolerance of 0.1 deg to ψ; however, the average value of ψ during unsteady runs for which data are presented was generally within 0.02 deg of the target ψ. Therefore, the differences between the results for the quasi-steady and unsteady simulations, including the time-average values per revolution, was significantly larger than any errors which may have arisen from inaccuracies in setting the experimental conditions.

For quasi-steady simulation, the absolute value of the time-average value per revolution of all loading components, except spindle torque M_z, decreased slightly for stern down and increased slightly for stern up. This suggests that the effective speed of advance of the propeller increases slightly for the stern-down condition and decreases slightly for the stern-up condition. This appears reasonable since for stern-up the propeller tends to be further into the boundary layer of the hull.

For dynamic simulation, the absolute value of the time-average value per revolution of all loading components, except spindle torque M_z, increased slightly for stern-down and decreased slightly for stern-up. Comparison of the time or location during the cycle of hull pitch angle ψ at which the largest time average loads occurred for quasi-steady and unsteady simulations shows a lag of approximately 0.65 sec, or 0.5 cycles, between the motion of the hull and the flow into the propeller resulting from this motion. This time lag is the period required for a particle of fluid to move approximately one-third the length of the hull.

There was a significant difference between the peak values for the quasi-steady simulation and the unsteady simulation. For the quasi-steady simulation, the variation of the peak values with hull pitch angle ψ followed the same trend as the variation of time-average values per revolution. These quasi-steady results indicated that for $\psi-\psi_{CW}$ up to 2 deg, the maximum increase in the peak value of any loading component above the corresponding value for $\psi=\psi_{CW}$ was 4 percent. For the dynamic simulation, however, the maximum value of the peak loads increased as much as 20 percent above the corresponding value for steady ahead at a fixed hull pitch $\psi=\psi_{CW}$.

The dynamic simulation exhibited a dramatically different trend of peak load with ψ than indicated by the quasi-steady simulation. For the dynamic simulation, the largest value of the peak loading occurred near $\psi=\psi_{CW}$ as the hull passed from the stern-up to the

stern-down position of the cycle, and the smallest value of peak loading occurred near $\psi=\psi_{CW}$ as the hull passed from the stern-down to the stern-up position of the cycle.

This difference in the unsteady loading between the quasi-steady and unsteady simulations is apparently due to an additional relative velocity component arising from the motion of the hull during dynamic pitching. As the hull passes through $\psi=\psi_{CW}$, the vertical velocity of the hull (and propeller) is a maximum. As the hull goes from stern-up to stern-down through $\psi=\psi_{CW}$, the upward velocity component relative to the propeller in the plane of the propeller tends to increase above the values at fixed hull pitch at $\psi=\psi_{CW}$. This tends to increase the amplitude of the first harmonic of the tangential velocity, and thereby increase the unsteady loading (and increase the peak loading). The maximum vertical velocity of the propeller for sinusoidal pitching with $(\psi_{MAX}-\psi_{CW})=$ 2.0 deg and frequency = 0.8 Hz is approximately 0.086 m/sec. This is equivalent to an additional tangential velocity ratio (V_t/V) of 0.025. For ψ fixed at $\psi=\psi_{CW}$, $((V_t)_1/V) = 0.155$ (see Figure 12 and Appendix A). Therefore

$$\frac{((V_t)_1/V)_{MAX,\dot{\psi}\neq 0}}{((V_t)_1/V)_{\dot{\psi}=0,\psi=\psi_{CW}}} = \frac{0.155 + 0.025}{0.155} = 1.16$$

This maximum occurs at the same position during the dynamic pitch cycle as the maximum measured loads. The measured increase in unsteady loads arising from dynamic pitching was somewhat larger than this calculated increase in tangential velocity, for example:

$$\frac{(F_{x_{MAX}} - \bar{F}_x)_{\dot{\psi}\neq 0, \psi=\psi_{CW}}}{(F_{x_{MAX}} - \bar{F}_x)_{\dot{\psi}=0, \psi=\psi_{CW}}} = \frac{0.57}{0.38} = 1.50$$

However, on the basis of two-dimensional quasi-steady theory, the increase unsteady loading should be approximately proportional to the increase in tangential velocity.

The unsteady loading is important from consideration of fatigue of the propeller blades and hub mechanism. Since a ship may operate for an extended period in a seaway, the effect of the ship motions, such as dynamic hull pitching, on unsteady blade loads is significant. The difference between the peak load and the time-average load per revolution is a measure of the unsteady loading. With this difference as a measure of the unsteady loading, the quasi-steady simulation indicates that for hull pitch angles ψ up to 2 deg, each unsteady loading component increases by not more than 5 percent above its corresponding value for $\psi=\psi_{CW}$. By contrast, the dynamic simulation showed that unsteady loading components are increased by at least 50 percent above their corresponding values for $\psi=\psi_{CW}$. This indicates that the quasi-steady simulation is completely inadequate for estimating the effect of the seaway on unsteady loading. This also shows that the effect of the ship motions can dramatically increase the unsteady loading on the blades. Therefore, the effect of the ship motions due to operation in a seaway should be considered in any analysis of blade loading and in any fatigue analysis of the propeller blades or hub mechanism.

CRASH AHEAD AND CRASH ASTERN MANEUVERS

Figures 19 and 20 and Appendix B present the variation of components of blade loading with blade angular position along with the corresponding harmonic amplitudes and phases for the quasi-steady simulated crash-ahead

condition $\dot{V}=\dot{P}=\dot{n}=0$. Figures 21 and 22 and Appendix B present similar results for the quasi-steady simulated crash-astern conditions $\dot{V}=\dot{n}=\dot{P}=0$. The values for each loading component are presented as decimal fractions of the time-average values of the corresponding loading component at the self-propulsion condition (Condition 1 of Table 5). These time-average values are presented in Table 7.

Figure 23 presents the Taylor wake fraction based on thrust $1-w_T$ and the Taylor wake fraction based on torque $1-w_Q$ as derived from the measured values of $\overline{F}_x$ and $\overline{M}_x$ and the open-water characteristics of the propeller (Figure 13). These data indicate a substantial variation in $1-w_T$ and $1-w_Q$ during the simulated crash ahead and crash astern maneuvers. During the crash-ahead maneuver, $1-w_T$ and $1-w_Q$ were respectively larger and smaller than their values near the self-propulsion point. For the crash astern maneuver, both $1-w_T$ and $1-w_Q$ initially decreased with decreasing speed and then increased dramatically as speed was further reduced. At the lowest experimental speed during simulated crash astern (V=0.17 m/sec), both $1-w_T$ and $1-w_Q$ were greater than 2.5.

These indicated values of $1-w_T$ and $1-w_Q$ are subject to significant inaccuracies in the initial portion of the simulated crash forward and in the final portion of the crash astern (dashed lines in Figure 23). These inaccuracies arise because the thrust and torque, which are measured on only one blade, are small in these regions, ($\overline{F}_x \leq 15N, \overline{M}_x \leq 0.5N\text{-m}$).

Figure 19 shows that for almost all measured loading components, the maximum time-average values per revolution and the peak values, including variation with blade angular position, occurred at the third experimental condition (V=1.46 m/sec, n=11.19 rev/sec, P/D=1.39) during the crash-ahead maneuver. For M_y, which is the largest moment component, the peak value and the maximum time-average value per revolution were respectively 1.51 and 1.35 times the time-average value at the self-propulsion point. For the other loading components, except spindle torque M_z, the peak

value and the maximum time-average value per revolution were respectively in the range 1.35--1.60 and 1.20--1.45 times the corresponding time-average value at the self-propulsion point. For spindle torque M_z, the peak value and the maximum time-average value per revolution were respectively 5.6 and 4.8 times the time-average value at the self-propulsion point. These represent large increases for M_z because $\overline{M}_z$ was quite small at the self-propulsion point, as already discussed.

Results for the crash astern maneuver show that, except for spindle torque, the maximum time-average load per revolution and the peak load, including variation with blade angular position, occurred at the initial (steady ahead) condition.

Higher loads than those shown in Figures 19 and 21 could, of course, be developed during crash ahead or crash astern maneuvers, depending on values of $\dot{V}$, $\dot{n}$, and $\dot{P}$.

For all loading components, the variation with blade angular position tended to be dominated by the first harmonic for all conditions throughout the simulated crash ahead and crash astern maneuvers. For all conditions at which there was significant variation in loading with blade angular position, the maximum and minimum values occurred near θ=90 or 270 deg. This suggests that the variation in loading with blade angular position is produced primarily by the circumferential variation of the tangential velocity in the propeller plane (see Figures 11 and 12). For the crash ahead simulation, in which pitch P was constant throughout, the angular variation of each loading component retained basically the same shape independent of speed and advance coefficient. By contrast, for the crash astern simulation, in which P/D changed from +1.06 to -0.67 for the different simulated conditions, the circumferential variation of each loading component changed shape substantially for different simulated combinations of speed, advance coefficient, and pitch ratio.

For both crash ahead and crash astern simulations, there was a dramatic reduction in the circumferential variation of all measured

loading components with decreasing speed V and decreasing rotational speed n. Previous data have shown that for a given propeller in a given flow field, the circumferential variation in the loading varies approximately as the product of ship speed V and rotational speed n; see Wereldsma.[26] Figure 24 presents some "typical" results in a form which allows evaluation of how closely the measured unsteady loading varies with nV. The ordinate is $(F_x)_1 \sin \phi$ which is the portion of the first harmonic in phase with the tangential velocity. This measure of the unsteady loading was selected because it may be positive or negative depending on ϕ. The abscissa is $nV \sin \Phi_{0.7}$. The term $\sin \Phi_{0.7}$ is intended to correct for the difference in pitch for the various runs, since the tangential component of the first harmonic of the wake $(V_t)_1$ is the primary forcing function, and the component of $(V_t)_1$ normal to the blade is $(V_t)_1 \sin \Phi_{0.7}$; see Wereldsma.[26]

The data shown in Figure 24 indicate that the unsteady loading $(F_x)_1 \sin \phi$ was approximately proportional to $nV \sin \Phi_{0.7}$. The results for the crash ahead simulation, with P/D=1.39, were consistently somewhat higher than those for the crash astern simulation, and they followed a linear variation with $nV \sin \Phi_{0.7}$ somewhat more closely than did the results for the crash astern simulation.

The reason for the systematic difference between the crash ahead data and crash astern data in Figure 24 is not clear; however, it may have resulted from one or more of the following:

1. The difference in the time-average loading between the crash ahead and crash astern conditions. Thrust loading coefficient $\overline{C}_{Th}$ is a measure of this time-average loading. For crash ahead simulation, the algebraic value of $\overline{C}_{Th}$ is much larger than it is for crash astern. This tends to increase the axial induced velocities and increase the spacing of the downstream vortex sheets for a given value of $nV \sin \Phi_{0.7}$. This would tend to reduce the influence of the shed vorticity and thereby increase the net unsteady loading.

---

[26] Wereldsma, T., "Tendencies of Marine Propeller Shaft Excitations," International Shipbuilding Progress, Vol. 19, No. 218 (Oct 1972).

2. The effect of the action of the propeller on the wake pattern in the propeller disk. During a portion of the crash astern maneuver, the propeller generates negative thrust so that the time-average induced velocity is upstream. This may interact with the flow over the hull and thereby influence the circumferential mean and circumferential variation of the flow pattern. As discussed previously, the time-average loading indicated that $1-w_T$ and $1-w_Q$ varied substantially over the simulated crash ahead and crash astern maneuvers (see Figure 23). However, if $V(1-w_T)$ rather than V is used as the reference velocity, the trends shown in Figure 24 would not change substantially.

3. Failure of the factor sin $\Phi_{0.7}$ to properly account for the difference in propeller pitch over the range of $(P/D)_{0.7}$ from +1.39 to -0.67. As nominal pitch is changed over this range, the radial distribution of pitch changes dramatically.

4. Experimental accuracy. For nV sin $\Phi_{0.7}$<2.0 m/sec^2, the measured unsteady loading is quite small; therefore, these results are not nearly as accurate as the results for higher values of nV sin $\Phi_{0.7}$.

The trends shown in Figure 24 for $(F_x)_1$ are typical of the trends of all measured loading components when plotted versus nV times the appropriate function of pitch as presented by Wereldsma.[26] Even though there is some scatter, the data follow the nV law quite well considering the wide range of advance coefficient J and pitch ratio P/D covered.

Figure 25 presents the variation of the time-average values per revolution and peak values of the various components of blade loading for both quasi-steady simulated crash ahead ($\dot{V}=\dot{n}=\dot{P}=0$) and unsteady simulated crash ahead ($\dot{V}>0$, $\dot{n}=\dot{P}=0$). Figure 26 gives similar data for quasi-steady and unsteady simulated crash astern runs.

There was only a small variation in the measured loading components between the quasi-steady simulated crash ahead and the unsteady simulated crash ahead. Except for spindle torque, the largest variation between the results from two types of simulation expressed on a decimal fraction

of the corresponding time-average value at the self-propulsion point was 0.05 for the peak values and 0.03 for the time-average value per revolution. For most cases, the variation was much smaller. In fact, the variation in the results between the two types of simulation appeared to be almost random. This suggests that these deviations are some measure of the experimental accuracy and do not represent any systematic trends arising from the difference in $\dot{V}$ between the two types of simulation.

For the crash astern runs, the variation in loads between the quasi-steady simulation and the unsteady simulation was not great, but it was somewhat larger than the variation for the crash ahead simulations. Except for spindle torque, the largest variation between the results for the two types of simulation was approximately 0.20 times the time-average steady-ahead value for the peak load and 0.15 times the time-average steady-ahead value for the mean load. For most cases, the variation was much smaller. The magnitude of most loading components was larger for the unsteady simulation for time $t \geq 13.6$ sec ($V \leq 1.67$ m/sec) and larger for the quasi-steady simulation for $t=9.05$ sec ($V=2.57$ m/sec).

Data for the quasi-steady simulation were recorded and averaged for a minimum of 200 propeller revolutions whereas data presented for the unsteady runs represent an average of only three revolutions for crash ahead simulation and five revolutions for crash astern simulation. Further, the steady experimental conditions which were set during the quasi-steady simulation allow the values of V and n to be controlled more precisely than during the unsteady runs; however, the average of the three to five values of V and n during the unsteady runs for which data are presented was generally within 1 percent of the target values.

Therefore, for crash astern the differences between the results for the quasi-steady simulation and the unsteady simulation was significantly greater than the errors arising from inaccuracies in setting the experimental results. It is concluded that there was a small

influence of $\dot{V}$ on the measured loads at a given combination of V, n, and P. However, this difference did not affect the peak loads that occurred during a crash astern maneuver.

CORRELATION WITH FULL-SCALE DATA AND THEORY

For operation near the self-propulsion point (Condition 1 in Table 5), correlation was made between the model experimental results obtained in the present investigation, bending moments deduced from strains measured on the corresponding full-scale propeller, and analytical calculations.

From the experimental values of F_x, F_y, M_x, and M_y, the bending moment can be calculated about any radial station $r_o \leq r_h$ and about any axis normal to the radial direction. However, in calculating bending moments about $r_o > r_h$, an adjustment must be made to allow for the contribution of the loading in the region $r_o > r > r_h$. In calculating the bending moment about the 0.4 radius $M_{0.4}$ from experimental values of F_x, F_y, M_x, and M_y, it was estimated that for all harmonics including the time-average values, 3 percent of M_x and M_y was contributed by the loading in the region $0.4R > r > r_h$.

The full-scale strains used for correlation were measured* at the midchord position of the 40-percent radius on the face of the propeller under steady ahead operation. The full-scale operating condition corresponds approximately, but not precisely, to the Froude scaled steady ahead condition on the model; see Table 4.

The correlation is based on the bending moment vector parallel to the nose-tail line at the 40-percent radius at conditions corresponding to Condition 1 in Table 5. Radial stresses for the trial data were deducted from strains by using the appropriate values of Young's modulus and Poisson's ratio. The bending moment vector parallel to the nose-tail line was deduced from the stress by assuming that the blade behaves structurally as a cantilever beam.

---

*The full-scale measurements were conducted by C.J. Noonan and G.P. Antonides of DTNSRDC Code 1962. The details of this full scale trial will be reported in a future DTNSRDC report.

The time-average bending moment deduced from the full-scale data was corrected for the difference between the scaled thrust and torque measured during the full-scale trial and the thrust and torque measured on the model. With this correction, the time-average bending moment determined from the full-scale data is 1.02 times the value determined from the model experiment.

The unsteady bending moment determined from the full-scale data was adjusted to the model conditions by using

$$M_{MES} = (M_S/\lambda^4)[V_M n_M \rho_M/(V_S n_S \rho_S)]$$

Here subscripts M refer to model values, subscript S refers to ship values, M_{MES} is the equivalent bending moment at the model conditions as deduced from the ship data, and λ is the linear scale ratio L_S/L_M. This adjustment assumes that the unsteady loading varies linearly with nV; see Wereldsma.[26] Since the ship conditions are near the Froude scaled model conditions, this adjustment is small except for the factor λ^4.

The time-average bending moment from the full-scale data was determined* from analysis of records of many propeller revolutions. The variation of the full-scale bending moment with blade angular position was determined from analysis of 37 consecutive propeller revolutions. Six of these revolutions were selected for detailed analysis: the two with the largest peak-to-peak variation, the two with the smallest peak-to-peak variation, and the two with the mean peak-to-peak variation. These six revolutions were harmonically analyzed and reconstructed by using the first ten harmonics; see Figures 27 and 28. The results from these six revolutions were averaged to obtain an effective variation of full-scale blade bending moment with blade angular position for comparison with model data.

Figures 29 and 30 present the variation with blade angular position and the first ten harmonics, respectively, of $M_{0.4}$ from the model data and from the full-scale ship data. All data are nondimensionalized

---

*By C.J. Noonan, DTNSRDC Code 1962.

on the same quantity, i.e., the time-average bending moment determined from the model experiments. This comparison indicated reasonable agreement of model and full-scale results for peak-to-peak values and for the first harmonic.

Theoretical calculations were made by using the method of Tsakonas, Jacobs, and Ali[20] (which is based on unsteady lifting surface theory) and the method of McCarthy,[21] a quasi-steady technique which utilizes the open-water characteristics of the propeller. These calculations were made for Condition 1 in Table 5 using the symmetric part* of the wake measured in the plane of the propeller both with and without the downstream dynamometer boat in place (Figures 11 and 12 and Appendix A). The difference in the calculated results with and without the dynamometer boat is a measure of the effect of the dynamometer boat on the circumferential variation of the unsteady loads.

For the method of Tsakonas et al.,[20] calculations were conducted for the first ten harmonics of the wake. These calculations were made by using the computer program developed by Davidson Laboratory including refinements made in December 1975. The "normal" components of wake harmonics, as required by this method, were defined as the wake harmonics normal to the chord line of the blade section at the local radius rather than normal to the advance angle at the local radius as recommended by Tsakonas, Breslin, and Miller.[27]. With the wake harmonics resolved normal to the blade chord, this method apparently considers both the unsteady flow parallel to the resultant inflow and the unsteady flow normal to the resultant inflow.

---

*Although the model hull and dynamometer boat were intended to be symmetric about a vertical plane containing the propeller axis, the measured wakes were not perfectly symmetrical; see Appendix A. The measured asymmetrical part of the wake apparently arises from inaccuracies in construction of the model hull, alignment of the model in the towing basin, and in the wake measurements. Calculations (unreported) were in slightly worse agreement with experimental results when the complete wake was used rather than only the symmetric part of the wake.

[27] Tsakonas, S. et al., "Correlation and Application of an Unsteady Flow Theory for Propeller Forces," Transactions of the Society of Naval Architects and Marine Engineers, Vol. 75, pp. 158-193 (1967).

The quasi-steady calculations are based on the circumferential variation of the wakes measured at the 0.71 radial station except that the narrow velocity defects behind the struts at approximately $\theta_w=25$ and 335 deg are not considered. Since these defects are narrow relative to the blade width, it is judged that they should have only a slight influence on the circumferential variation of blade loading. It is assumed that the radial centers of the unsteady thrust and tangential force are the same as the radial centers of the respective mean values.

Figures 30-32 present the variation with blade angular position and the first ten harmonics of $M_{0.4}$ from the model experiment and analytical calculations. All data are nondimensionalized on the same quantity, i.e., the time-average bending moment determined from the model experiments. This comparison indicated that the experimental results were considerably higher than the calculated results. For other components of blade loading F_x, F_y, M_x, and M_y, the circumferential variation in the model experimental results was larger than the values calculated by the two indicated procedures by approximately the same ratio as shown for $M_{0.4}$. These comparisons are not shown.

In previous investigations, experimentally determined unsteady forces and moments on a single blade of various propellers in inclined flow have been compared with forces and moments calculated by a quasi-steady procedure similar to that described by McCarthy.[21] These experimental loads were obtained by direct measurement of unsteady forces and moments on a single blade (References 13 and 14) or were deduced from measured steady transverse forces and moments along axes fixed relative to the flow, i.e., not rotating with the propeller (Reference 28). References 13, 14, and 28 all show that for noncavitating conditions, the experimental unsteady blade loading was from 1.7 to 2.0 times as large as the values calculated by the quasi-steady method. This agrees with the results of the present investigation; see Figure 31.

---

[28] Gutsche, F., "Untersuchung von Schiffsschrauben in schrager Anstromung," Schiffbauforschung, Vol. 3, No. 3/4 (1964).

The reason for the large discrepancy between the experimental and calculated results is not clear. Some possibilities are as follows:

1. Inaccuracies in theoretical results. The unsteady lifting surface procedure of Tsakonas et al.[20] is based on linearized theory which considers the harmonic content of the longitudinal and tangential components of the wake. It is possible that nonlinear effects or the significant radial component of the wake may influence the circumferential variation of the loading. In addition, there may be inaccuracies in the numerical evaluation of the theory. The quasi-steady procedure of McCarthy[21] is exceedingly simple and should give reasonable results, especially for the first harmonic which has a low reduced frequency. However, this method does not consider any possible effects of the circumferential variation of the radial component of inflow velocity.

2. Interaction between the propeller and the hull may increase the circumferential nonuniformity of the flow into the propeller from the values measured without the propeller in place. (Both sets of calculations are based on the wake measured in the plane of the propeller with propeller removed.) The experimental data show that the maximum and minimum loading occurs near θ=90 and 270 deg. This implies that the dominant influence of the wake is the tangential velocity. Therefore, if the effect of the propeller on the wake pattern is the reason for the large discrepancy between theory and experiment, the propeller must increase the upsweep angle between the flow and the propeller shaft from approximately 10 deg without the propeller to approximately 20 deg with it.

3. Other interactions between the propeller and the nearby surfaces which are not considered in the calculations based on the measured wake distribution.

4. Inaccuracies in the measured wake. This is unlikely since the tangential component of the wake indicates that the flow is approximately parallel to the stern.

5. Error in the experimental results. This appears unlikely in view of the reasonably good agreement between model experiments and full-scale experiments conducted entirely independently. In addition, previous experimental results in which the dominant component of wake was the tangential yielded results which were substantially larger than calculated by quasi-steady procedures.[13,14,28]

SUMMARY AND CONCLUSIONS

Experiments were described in which the mean and unsteady loads were measured on a single blade of a model of the CP propeller on the FF-1088. The experiments were conducted behind a model of the FF-1088 hull under steady ahead operation, hull pitching motions, simulated crash ahead maneuvers, and simulated crash astern maneuvers. The discussion of experimental techniques included a description of the dynamometer and data analysis system. The results are summarized as follows:

1. The circumferential variation of all measured components of blade loading is primarily a first harmonic, with maximum and minimum values occurring near the blade angular position at which the blade spindle axis is horizontal.

2. For steady ahead operation:

   a. The maximum values and the peak-to-peak circumferential variations for measured forces and bending moments were up to approximately 1.38 and 0.80, respectively, the time average values.

   b. The model results for circumferential variation of bending moments about the nose-tail line of the 0.4 radius agreed fairly well with loads deduced from strain measurements on the full-scale propeller, but they were larger than theoretically calculated values.

3. For simulated hull pitch (maximum pitch angle of 2 deg):

   a. The maximum value of measured forces and bending moments increased over the corresponding values without hull pitch by 4 percent for quasi-steady simulation and by 20 percent for unsteady simulation with pitching frequency equal to 0.8 Hz.

b. The peak-to-peak circumferential variation of the measured forces and bending moments increased over the corresponding values without hull pitch by approximately 5 percent for quasi-steady simulation and by 50 percent or more for unsteady simulation with pitching frequency equal to 0.8 Hz. Therefore, any quasi-steady simulation of ship motions is completely inadequate for estimating the effect of ship motions on unsteady propeller blade loading.

4. For the simulated crash ahead maneuver:

a. The dominant first harmonic of the measured forces and bending moments varied in a nearly linear manner with the product of ship speed and propeller rotational speed.

b. The acceleration of the hull did not have a significant effect on the measured loads. Therefore, propeller blade loading during a crash ahead maneuver can be adequately estimated by quasi-steady experiments.

c. The maximum time-average values of measured forces and bending moments per revolution were in the range of 1.20 to 1.45 of the time-average values at the self-propulsion point.

d. The peak values of measured forces and bending moments were in the range of 1.35 to 1.60 of the time-average values at the self-propulsion point.

e. The Taylor wake fractions deduced from the time-average thrust and torque per revolution varied substantially from the values at the self-propulsion point.

5. For the simulated crash astern maneuver:

a. The first harmonic of the measured forces and bending moments varied approximately linearly with the product of ship speed and propeller rotational speed and was a function of propeller pitch.

b. The deceleration of the hull altered the peak value of a given component of loading at a given condition by up to 20 percent of the

time-average value at the self-propulsion point; however, this did not alter the peak load occurring at any time during the maneuver. Therefore, propeller blade loading during a crash astern maneuver can be adequately estimated from quasi-steady experiments.

c. The largest time-average loads per revolution and the peak loads including circumferential variation occurred at the initiation of the maneuver; i.e., loads during the crash astern maneuver did not exceed the loads at the self-propulsion point.

d. The Taylor wake fractions deduced from the time-average thrust and torque per revolution varied substantially from the values at the self-propulsion point.

ACKNOWLEDGMENTS

The authors are indebted to many members of the staff of the David W. Taylor Naval Ship Research and Development Center. Special appreciation is extended to Mr. Stephen Callanen for adaptation and design of the experimental apparatus, to Mr. Arthur Block for development of the on-line data analysis system, to Mr. John Gordon for development of electronic and mechanical systems for the experiment, to Mr. Robert Roddy for conducting the wake surveys, to Mr. Kenneth Remmers for conducting supporting self-propulsion experiments, to Mr. Richard Kader for assistance in conducting the experiments and data analysis, and to Messrs. Charles Crockett and Jack Diskin for assistance in data analysis and analytical calculations.

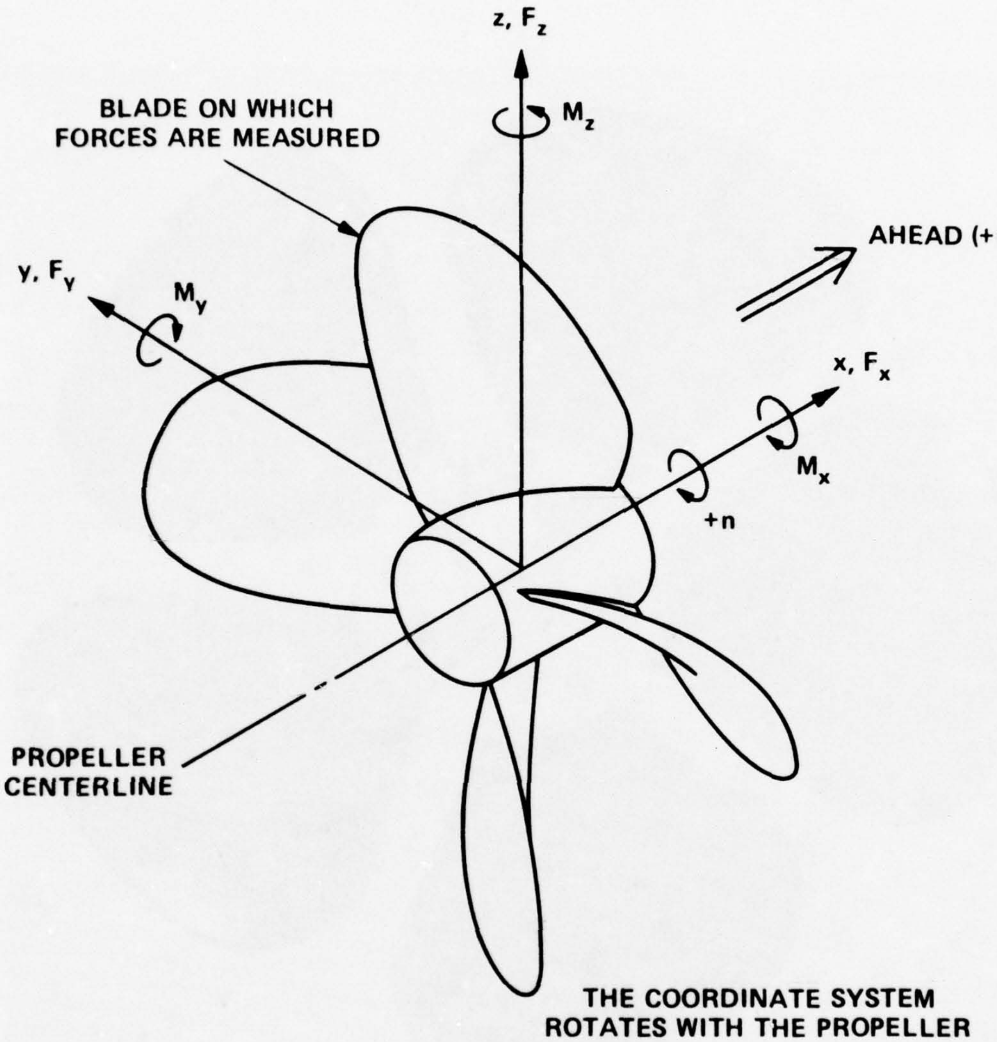

Figure 1- Components of Blade Loading

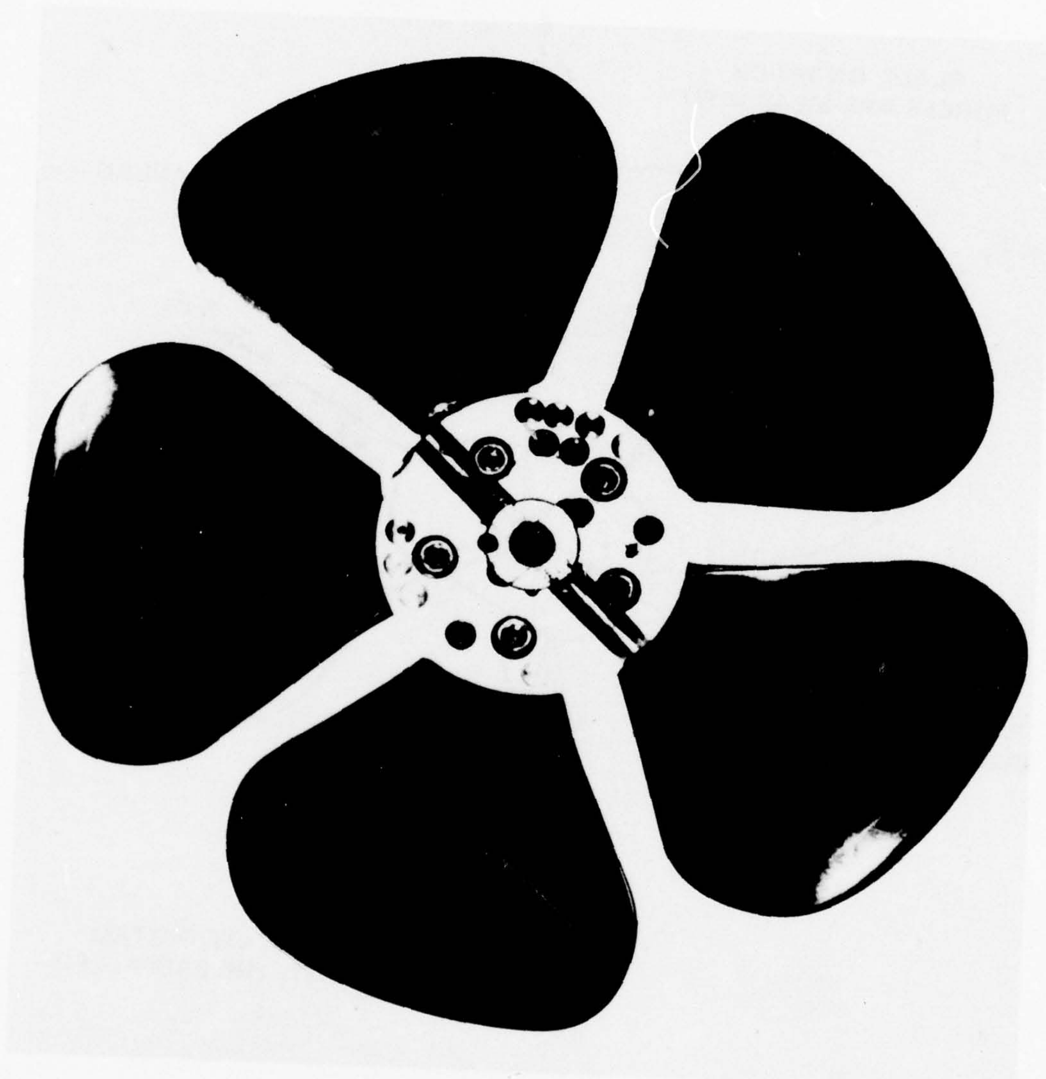

Figure 2- DTNSRDC Model Propeller 4402A

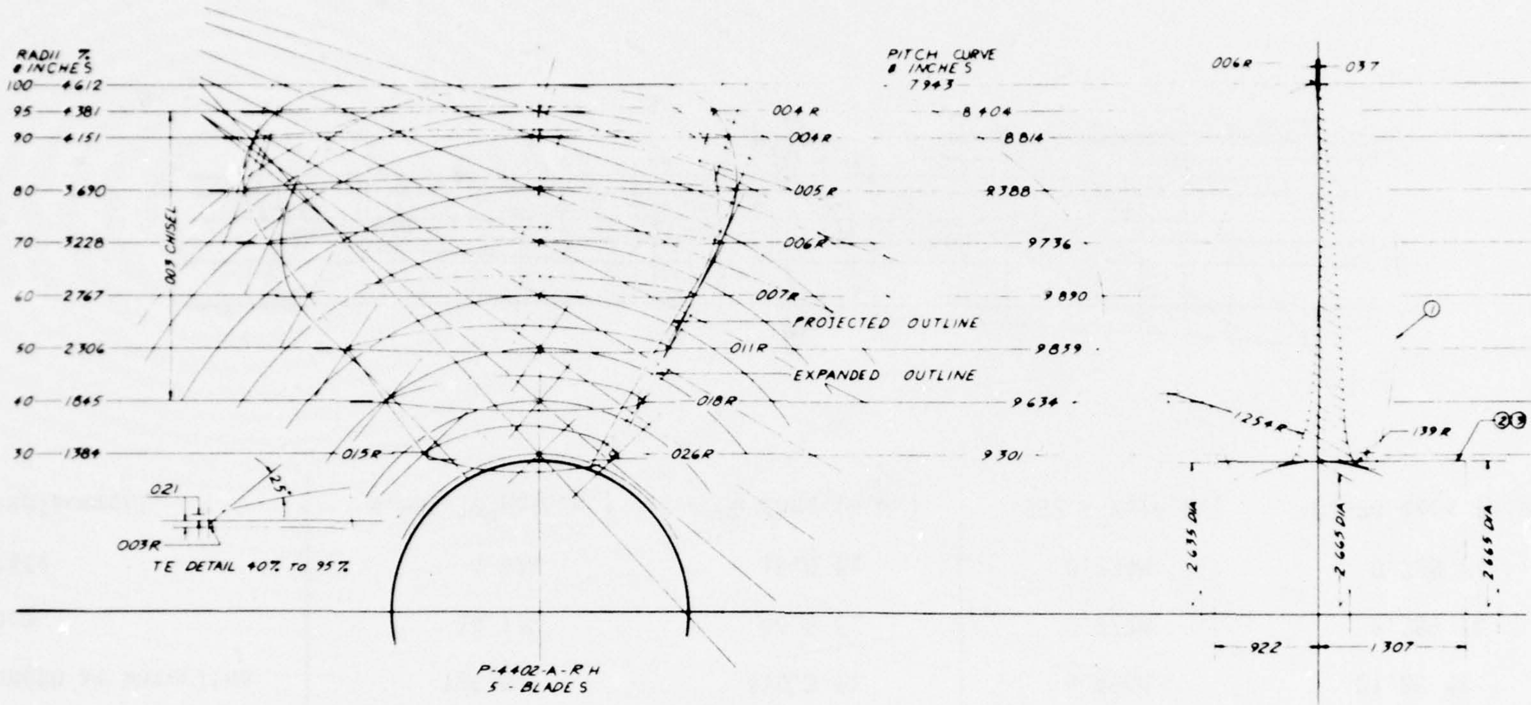

Figure 3- Geometries of Model of Propeller on FF-1088; DTNSRDC Model Propeller 4402A

	Ship		Model	
Length at Waterline	126.6M	415.3 ft	6.486M	21.28 ft
Beam	14.17M	46.5 ft	0.727M	2.385 ft
Draft	4.57M	15.0 ft	0.234M	0.769 ft
Displacement	4.064×10^6 Kg(S.W.)	4000 tons (S.W.)	532.4 Kg(F.W.)	0.524 tons (F.W.)

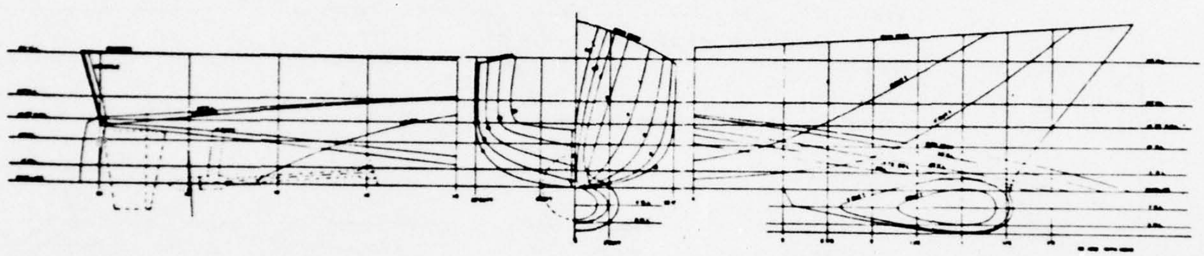

Figure 4 - Ship and Model Particulars

Figure 5- Experimental Arrangement of Hull and Dynamometer Boat

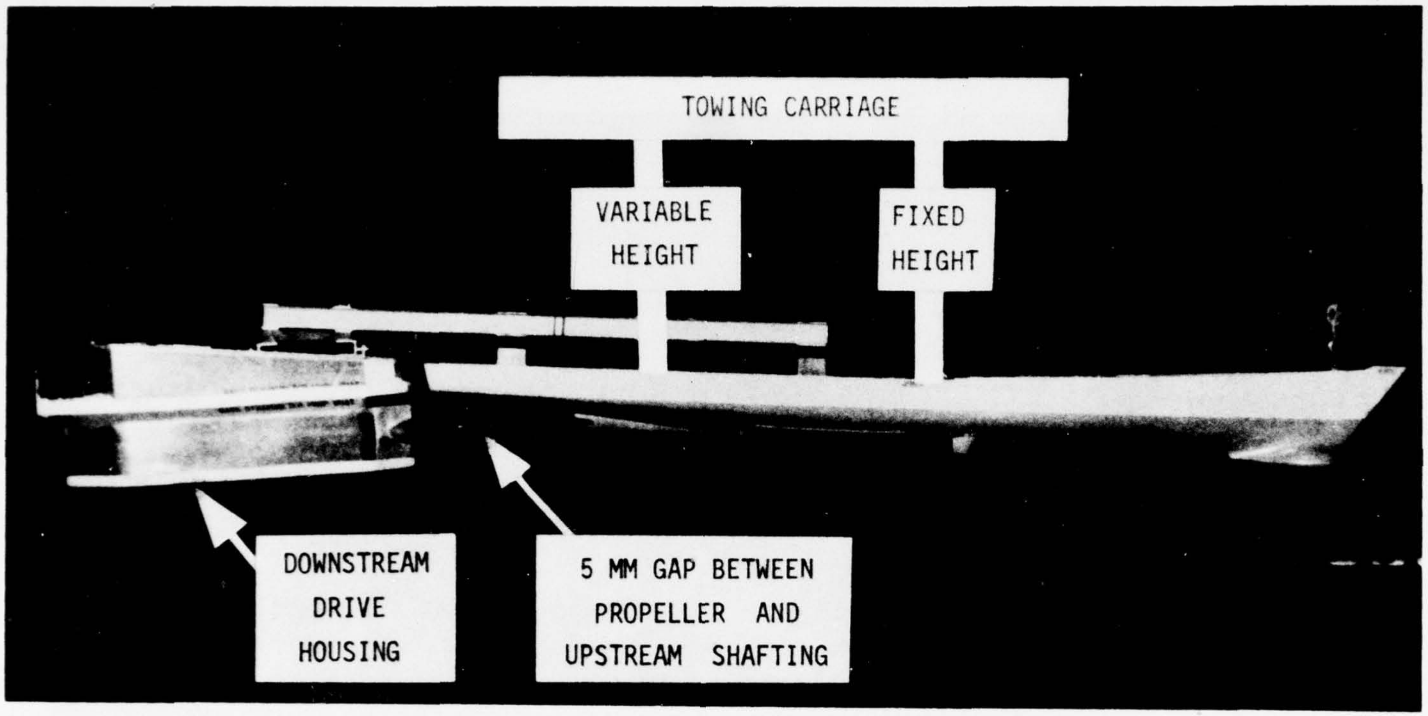

Figure 5a- Overall View

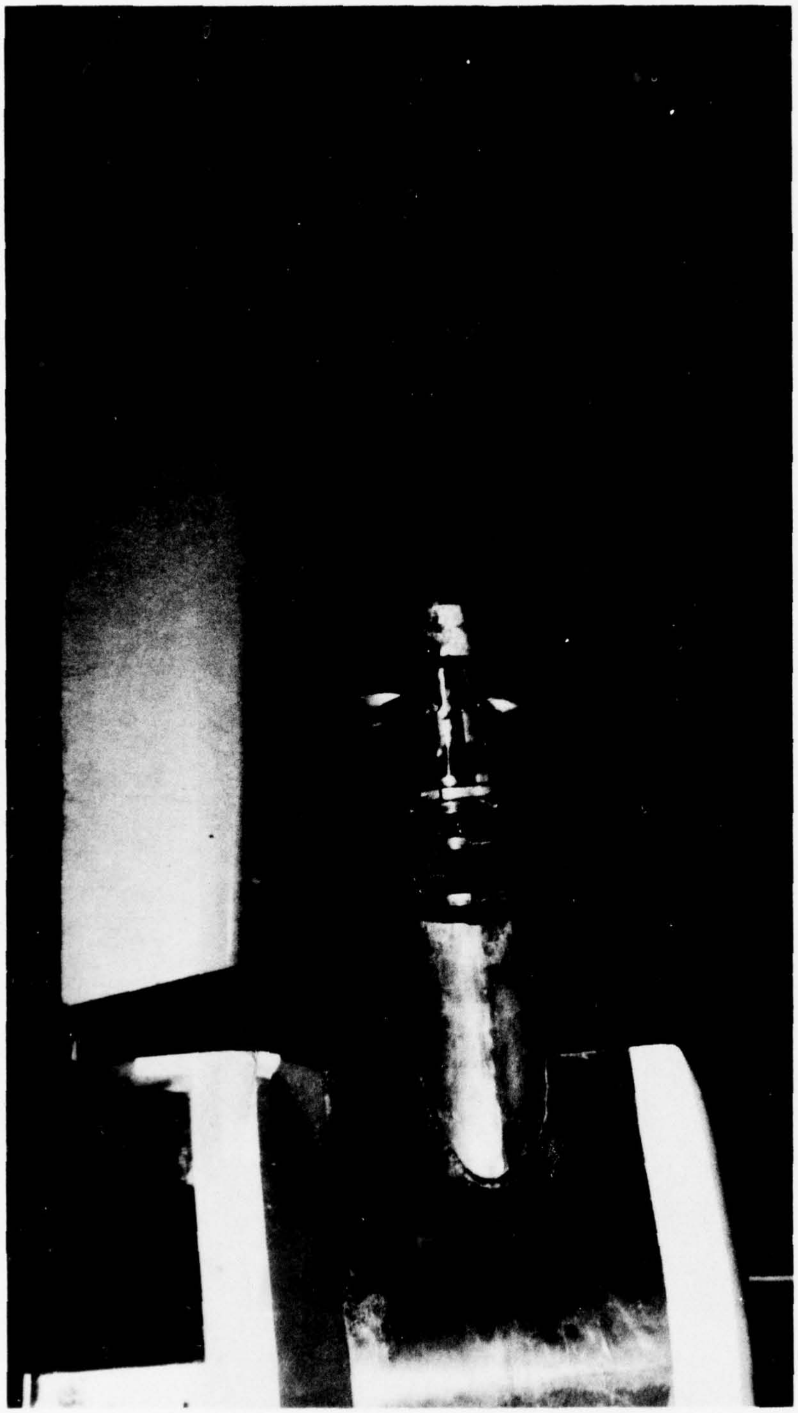

Figure 5b- Closeup of Propeller

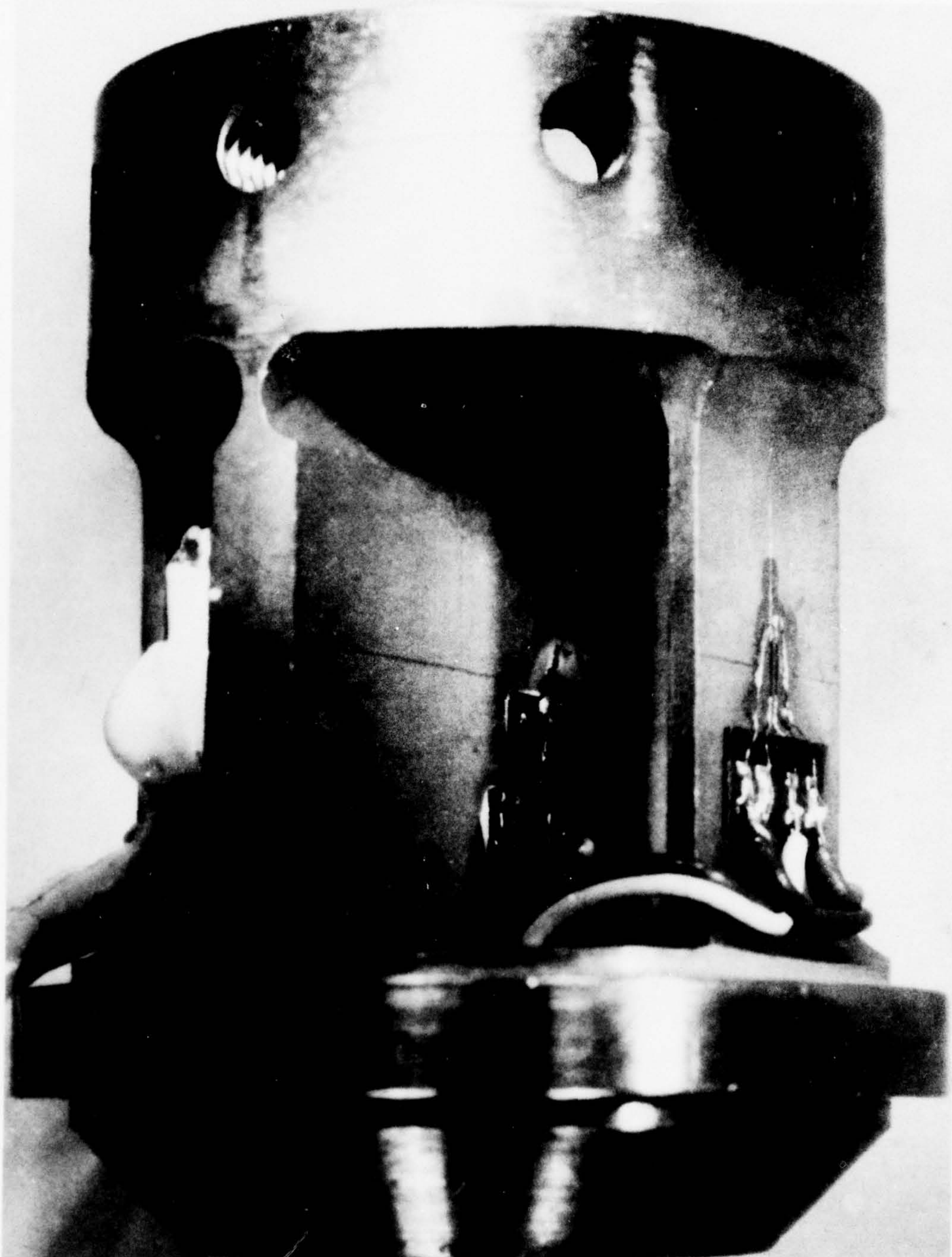

Figure 6- Strain-Gaged Blade Flexures in Hub

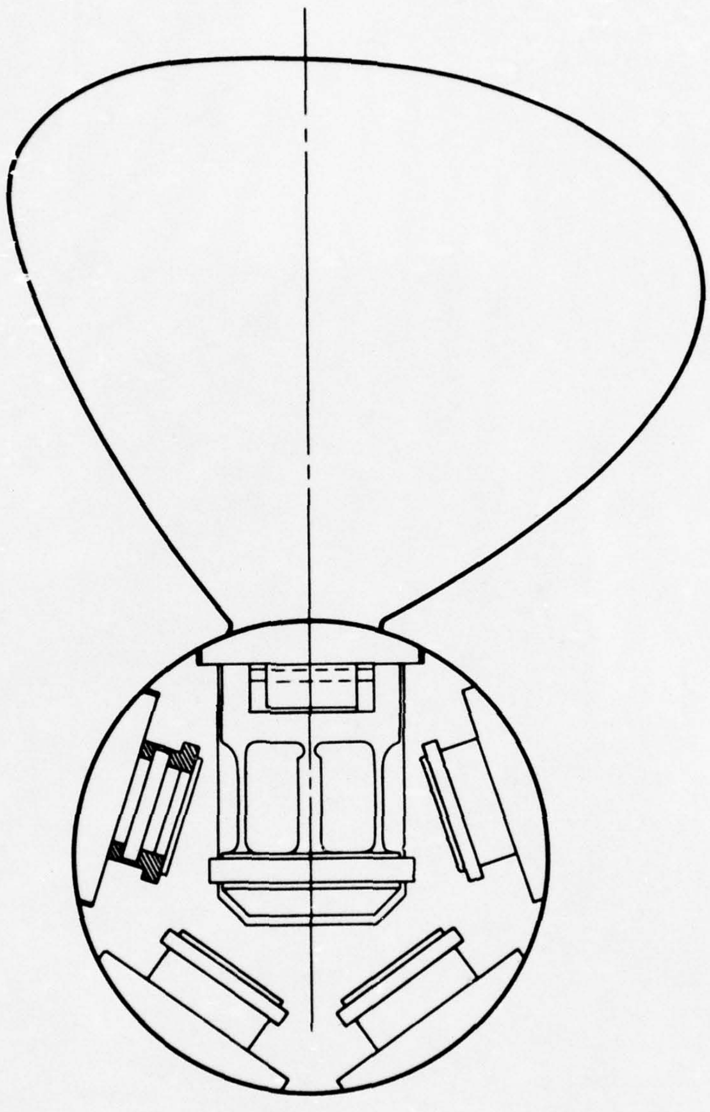

Figure 7- Arrangement of Flexures in Hub

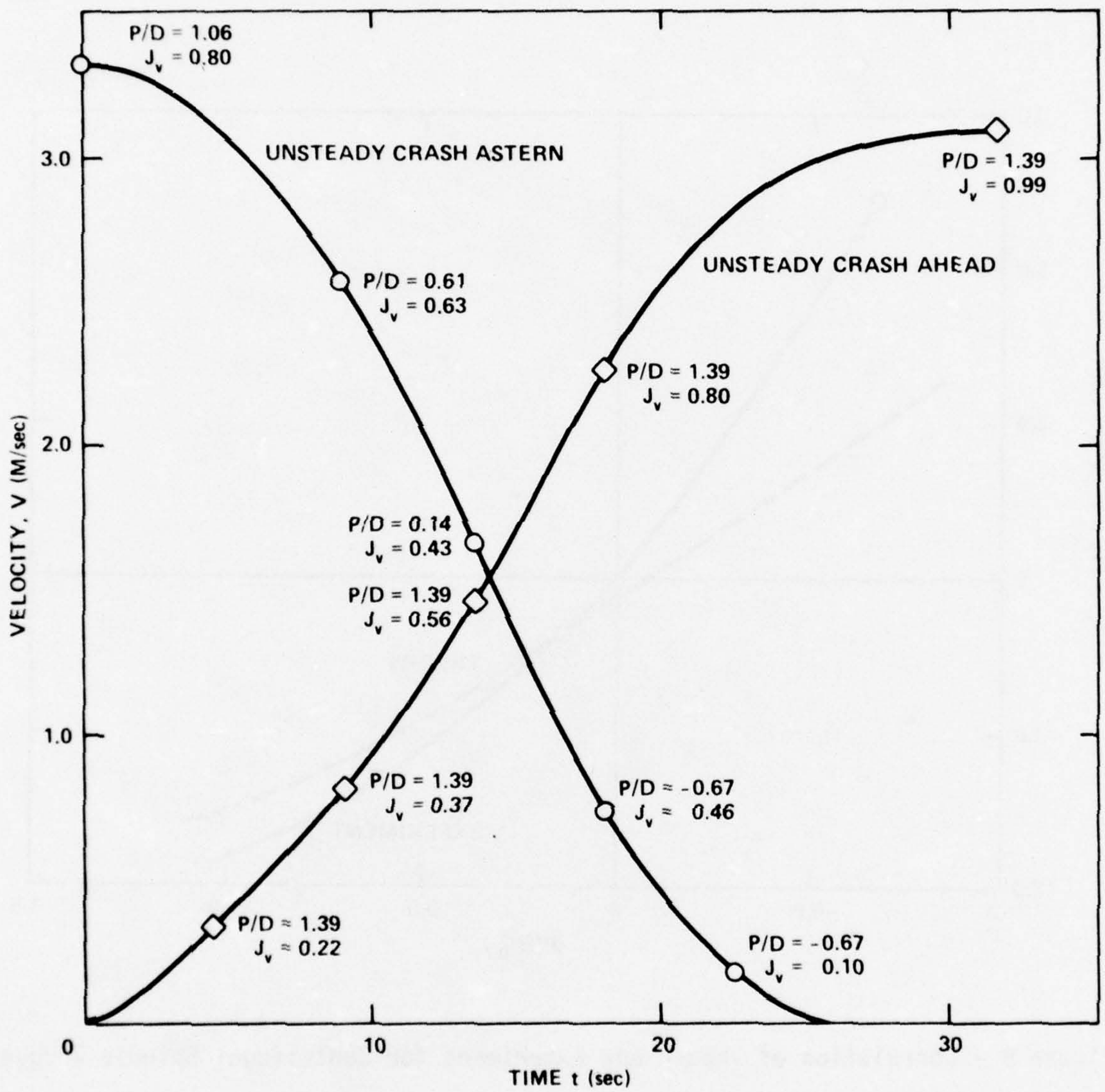

Figure 8 - Experimental Deceleration and Acceleration Conditions

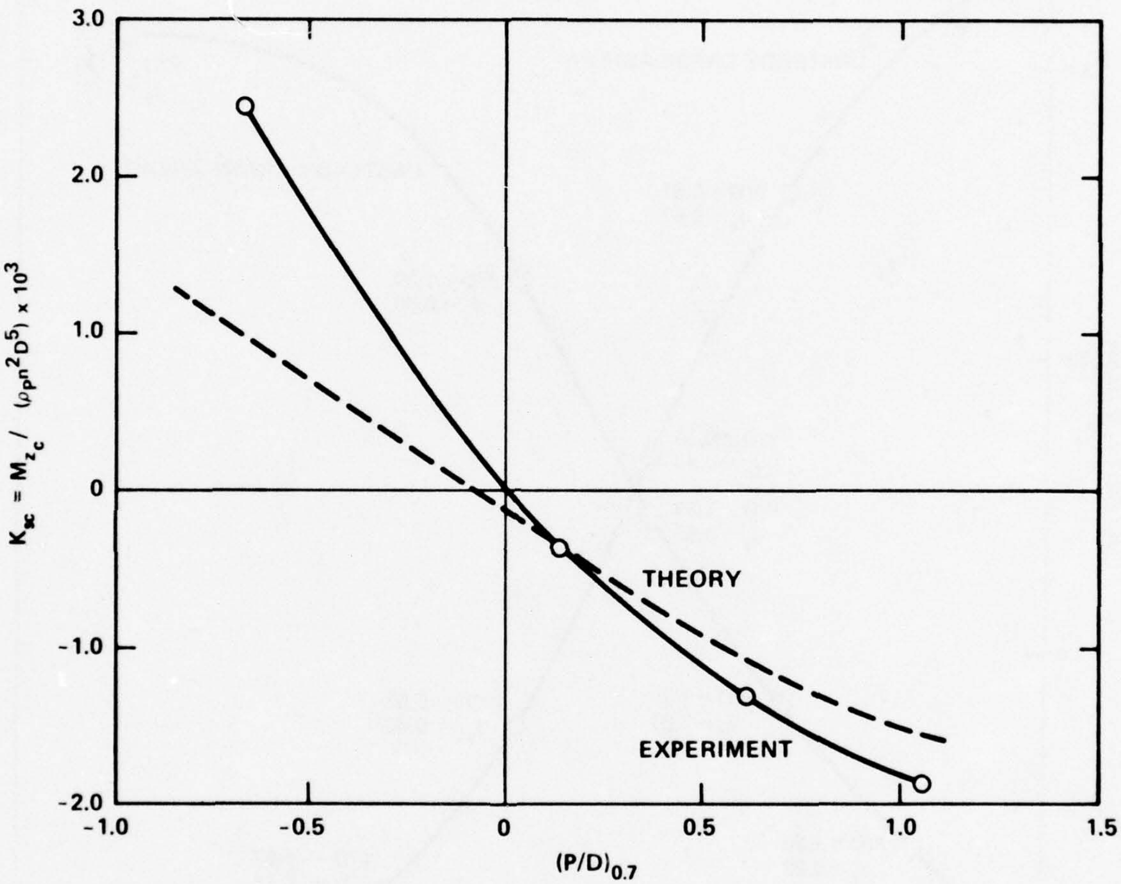

Figure 9 - Correlation of Theory and Experiment for Centrifugal Spindle Torque

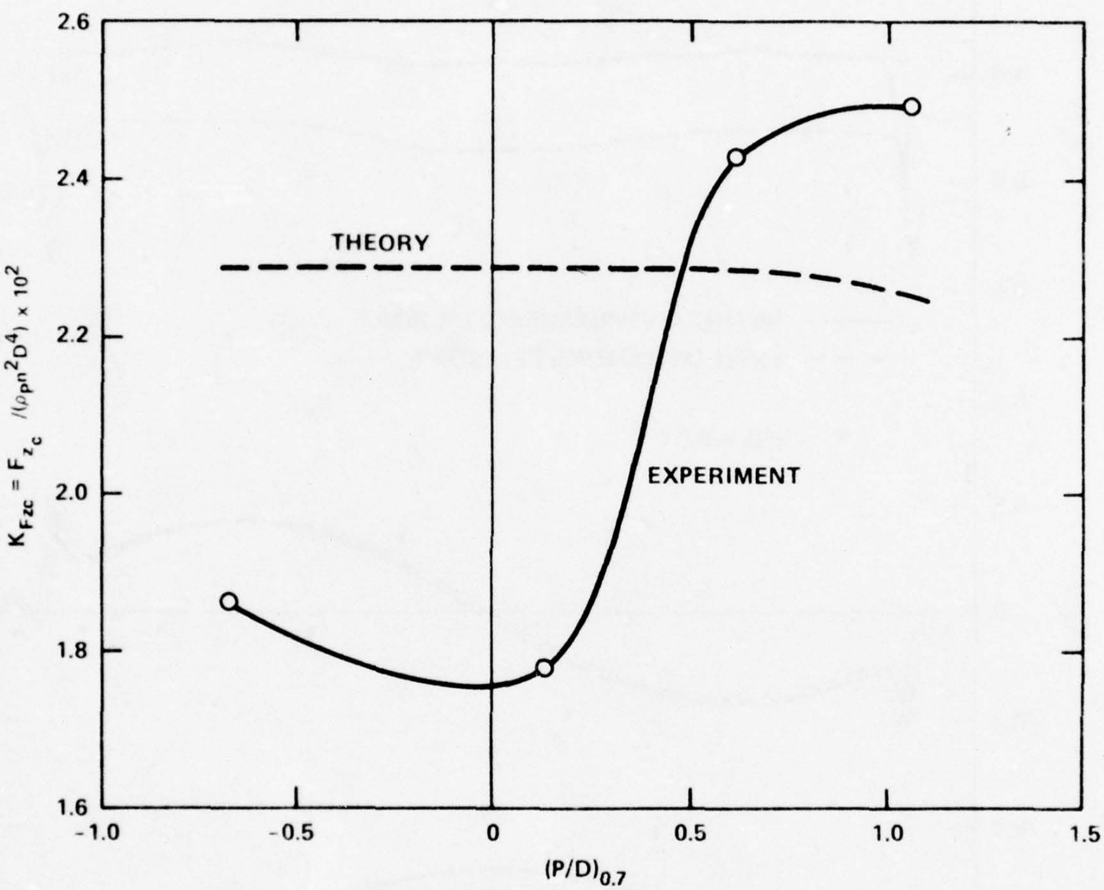

Figure 10 - Correlation of Theory and Experiment for Centrifugal Force

Figure 11- Circumferential Distribution of Wake in Propeller Disk

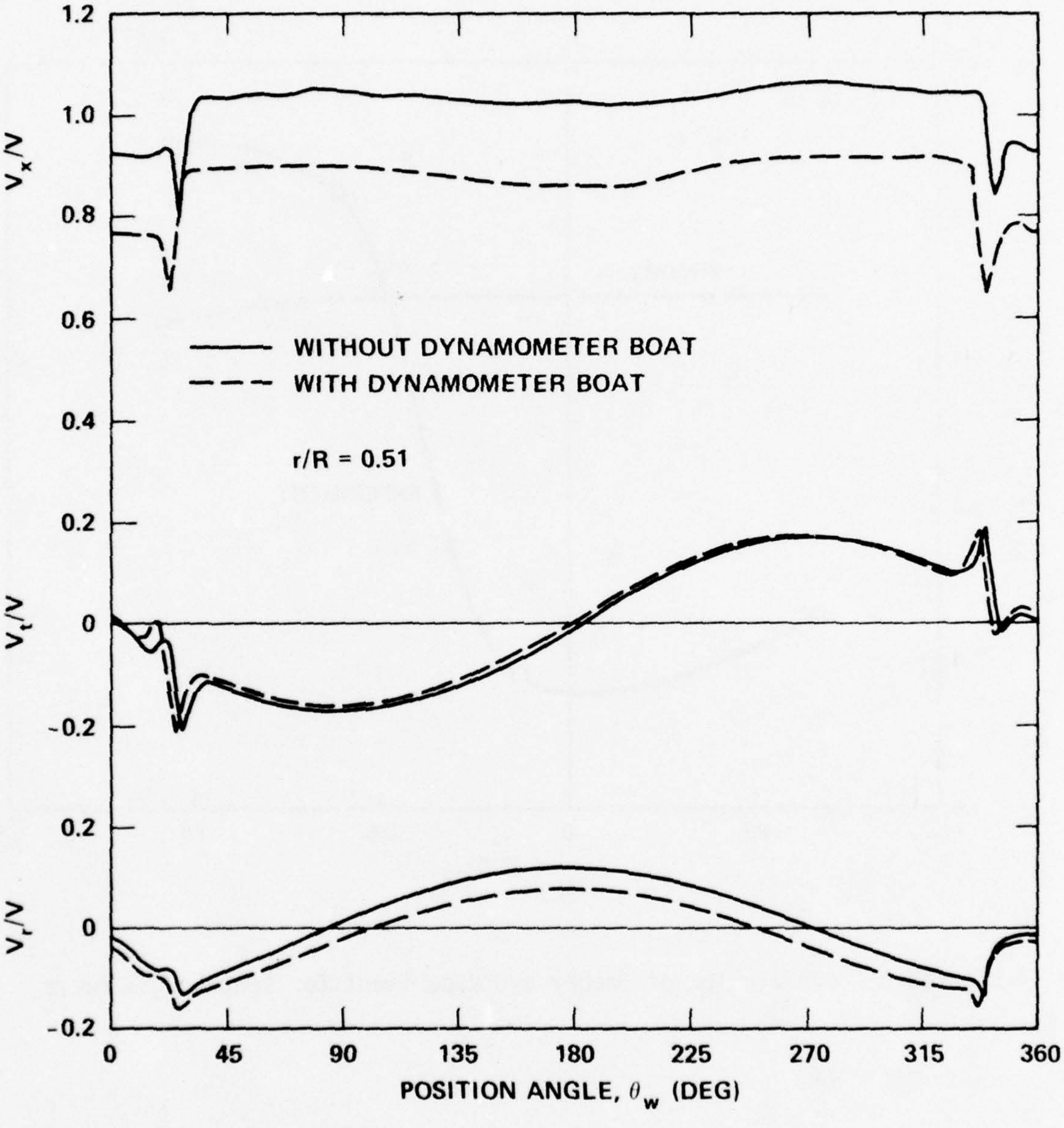

Figure 11a- 51 Percent Radius

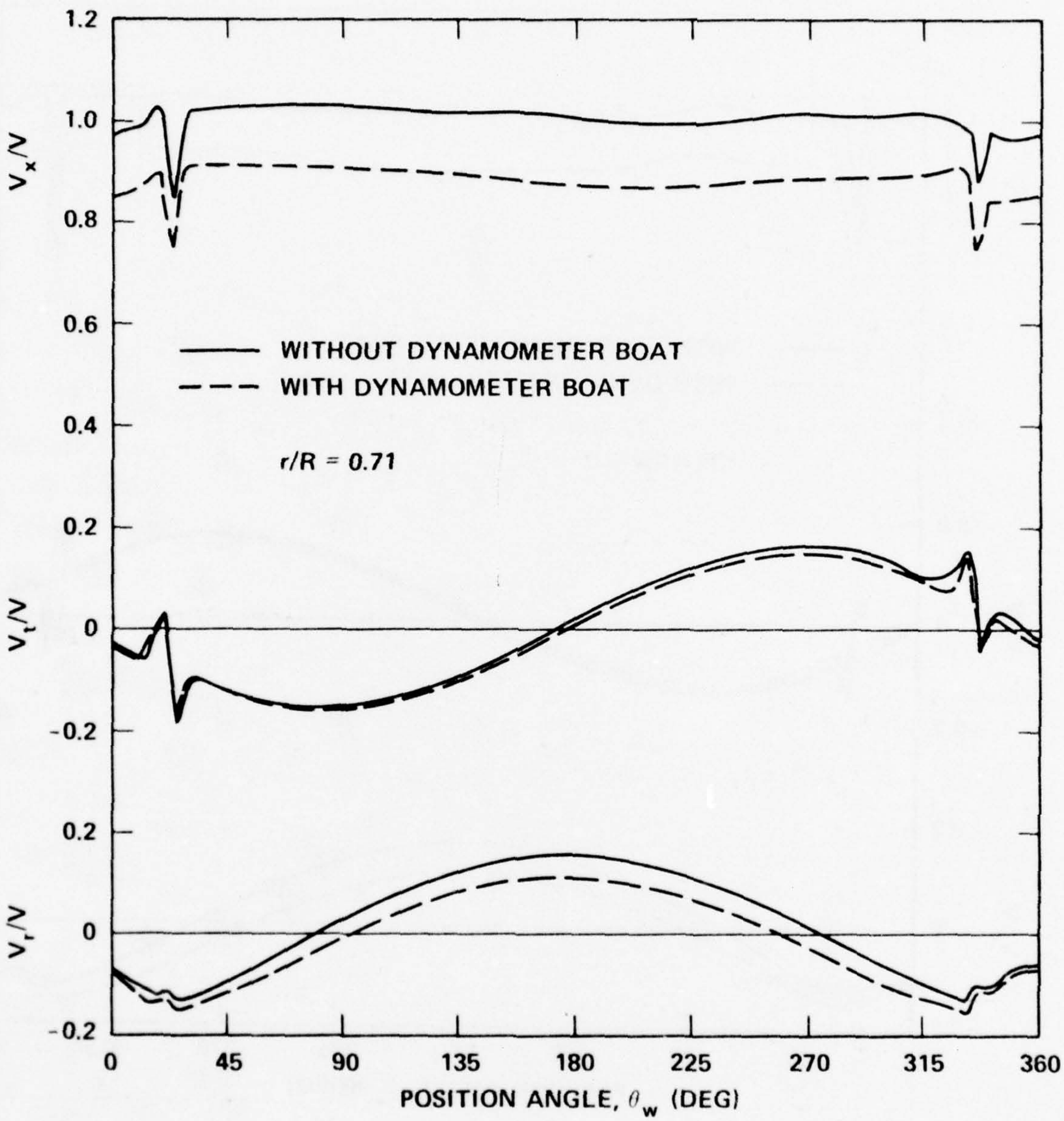

Figure 11b- 71 Percent Radius

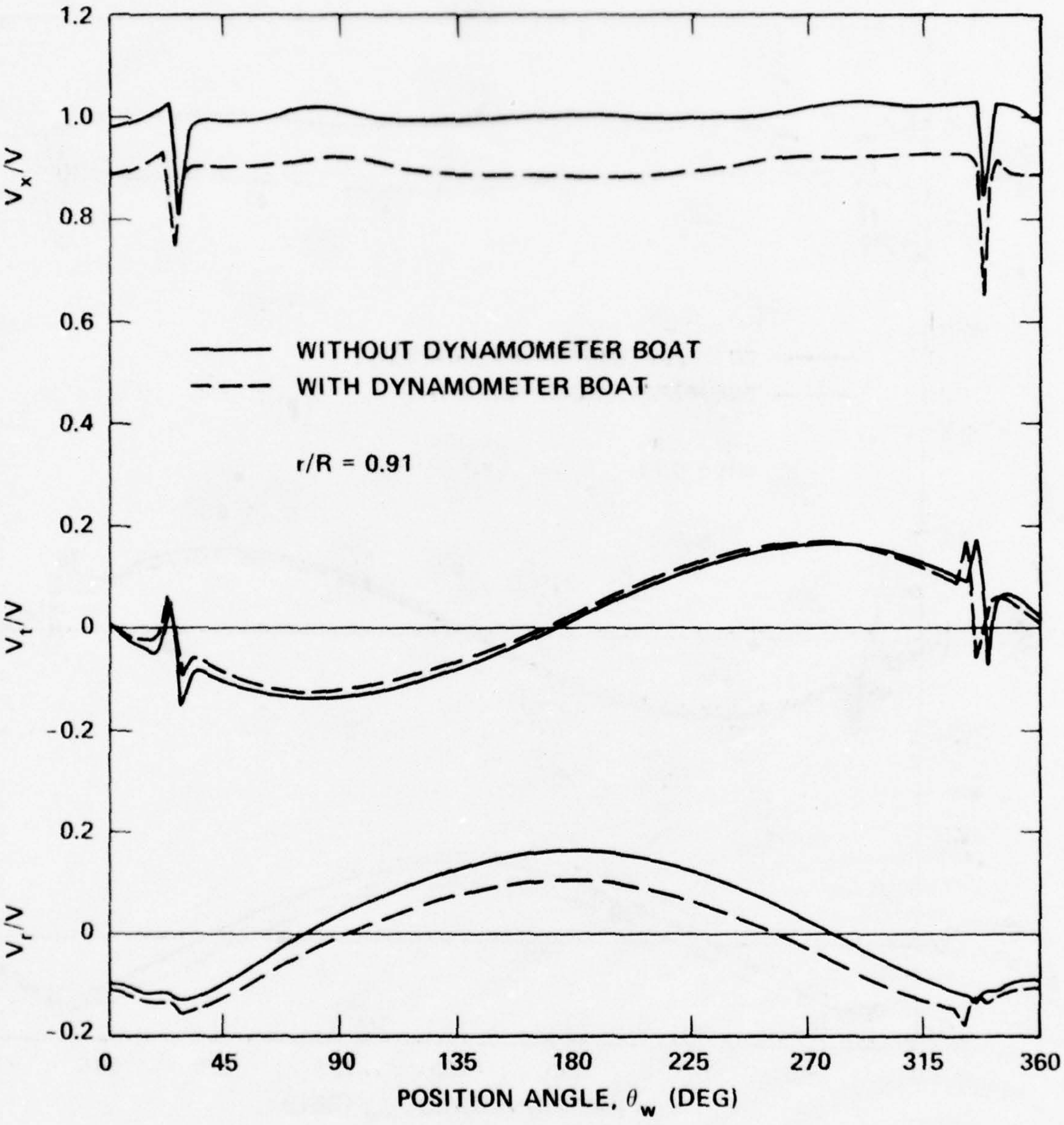

Figure 11c- 91 Percent Radius

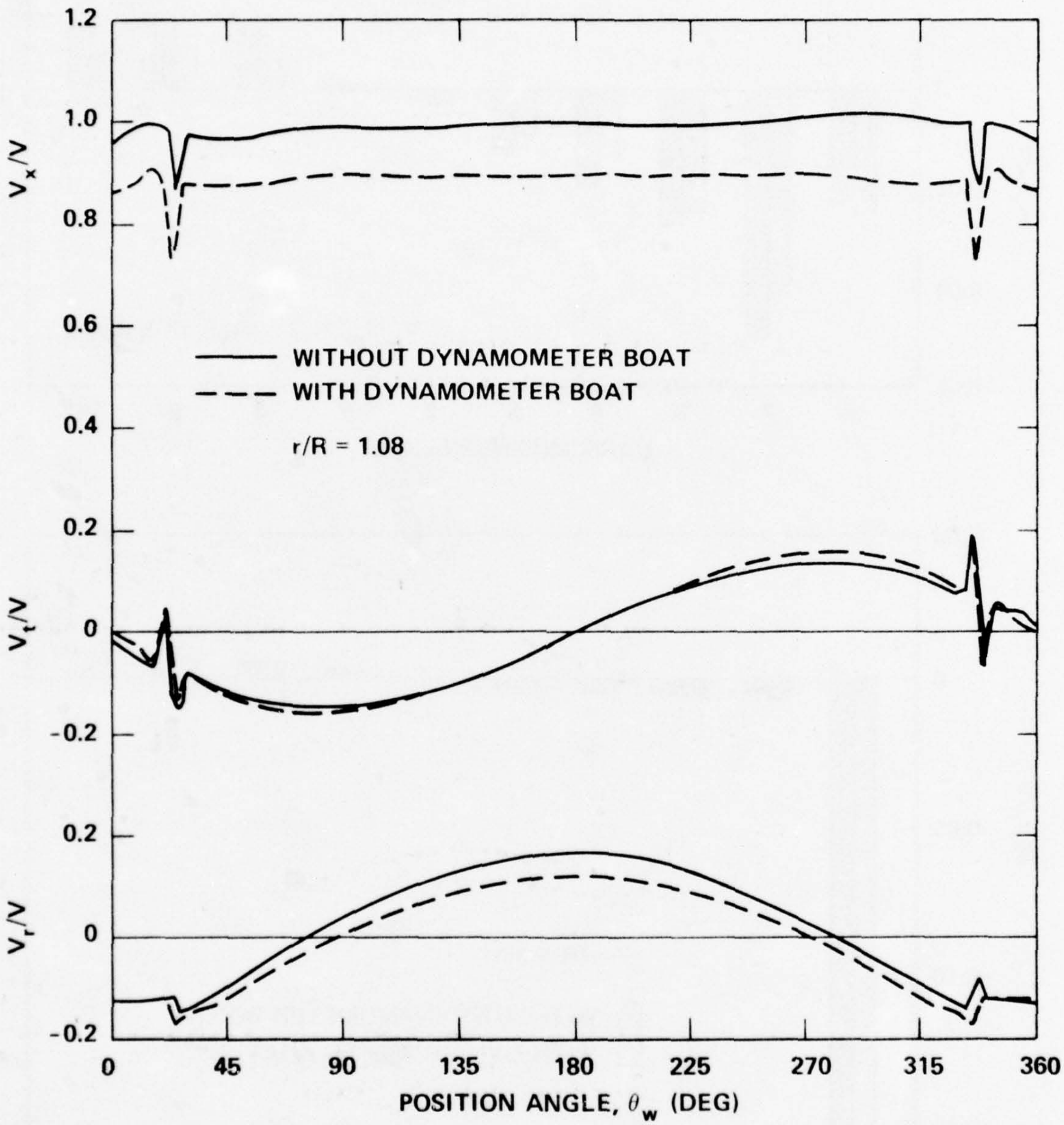

Figure 11d- 108 Percent Radius

Figure 12- Harmonic Amplitudes of Wake Velocities

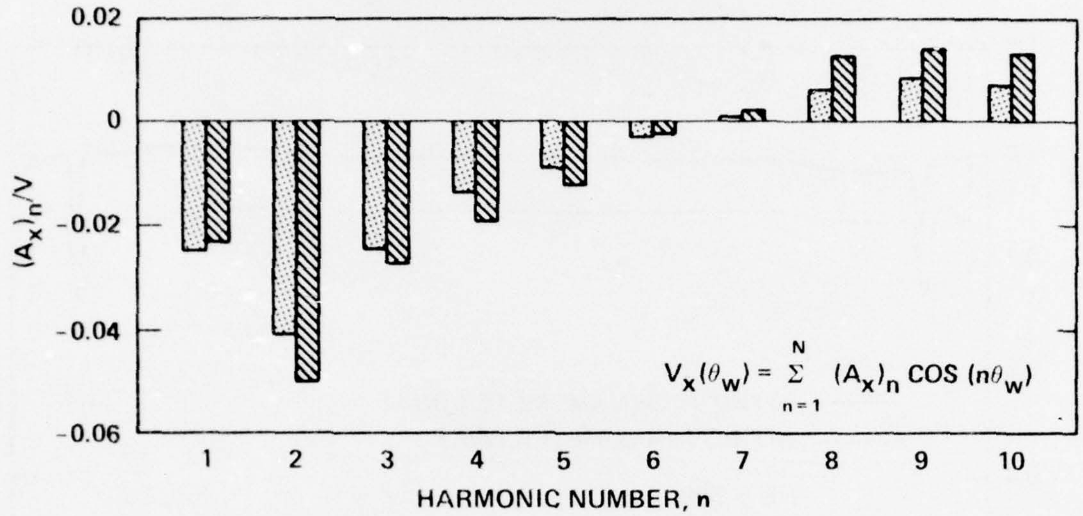

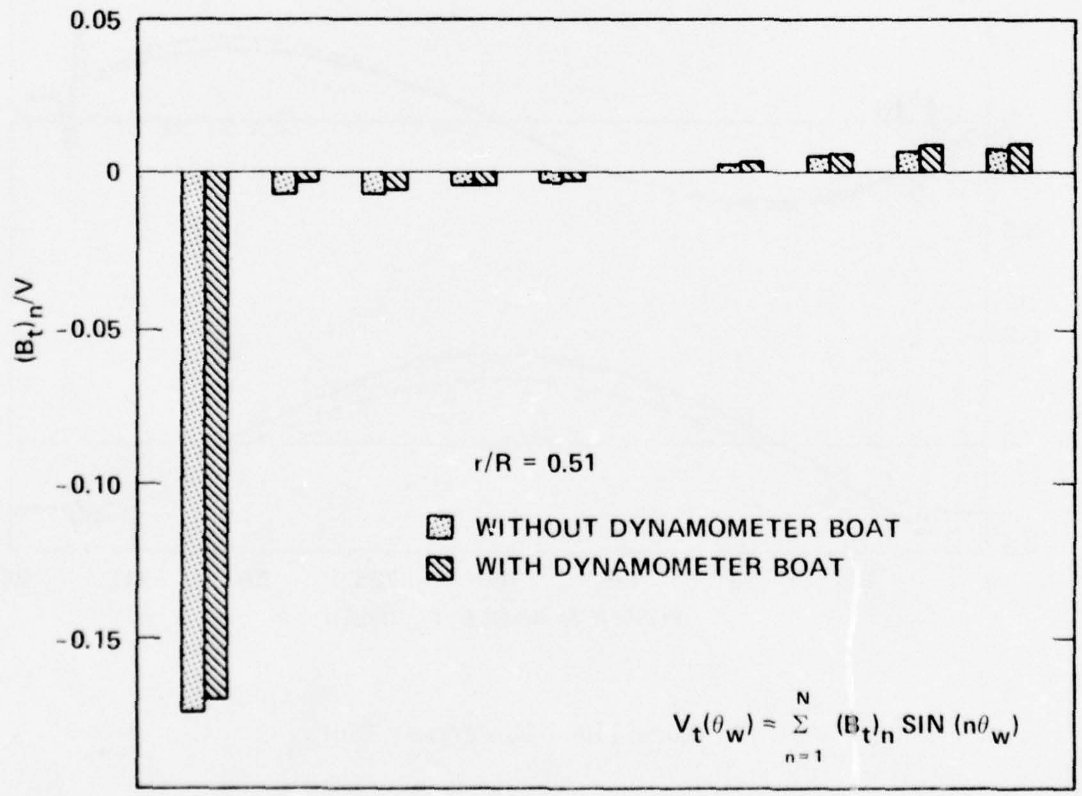

Figure 12a- 51 Percent Radius

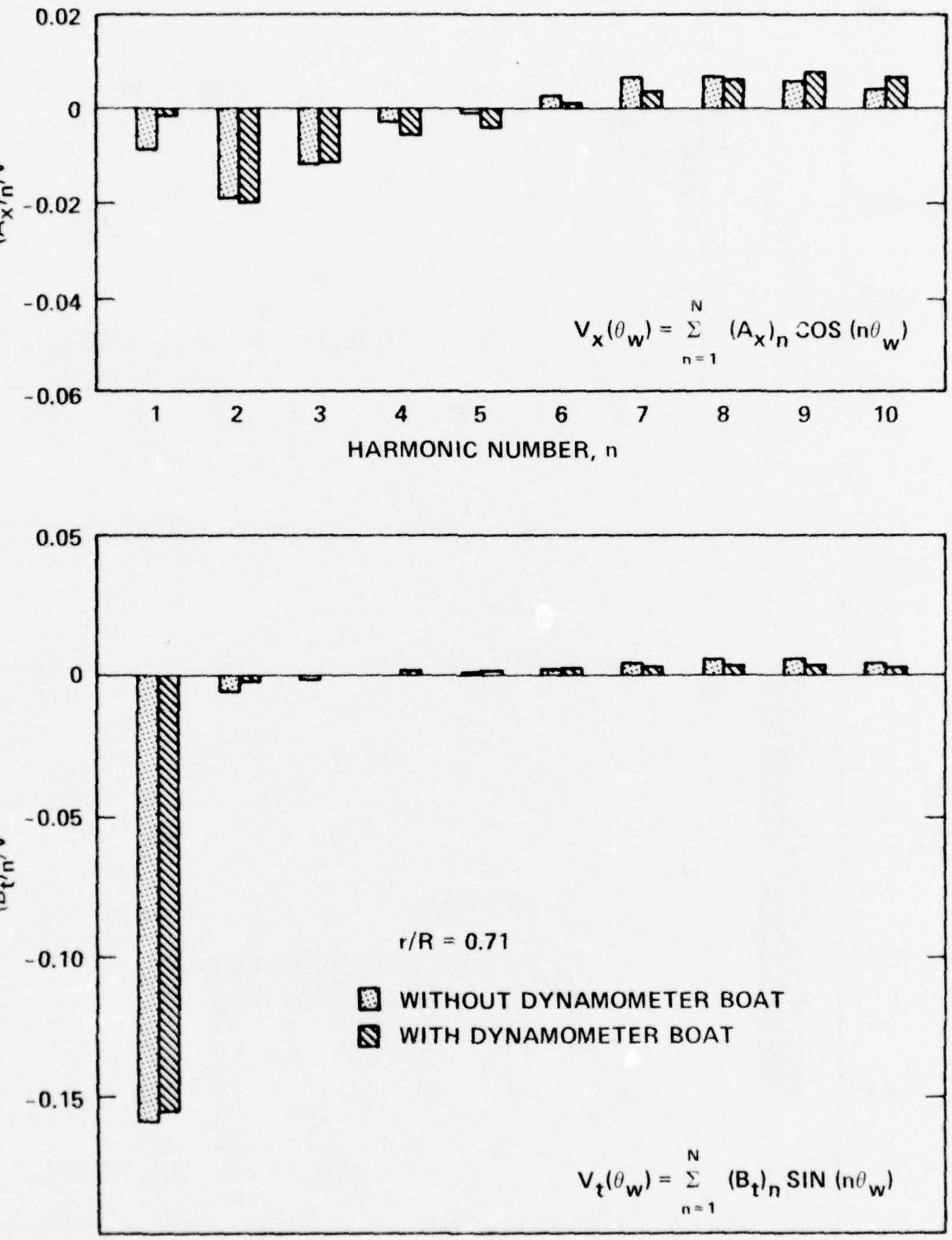

Figure 12b- 71 Percent Radius

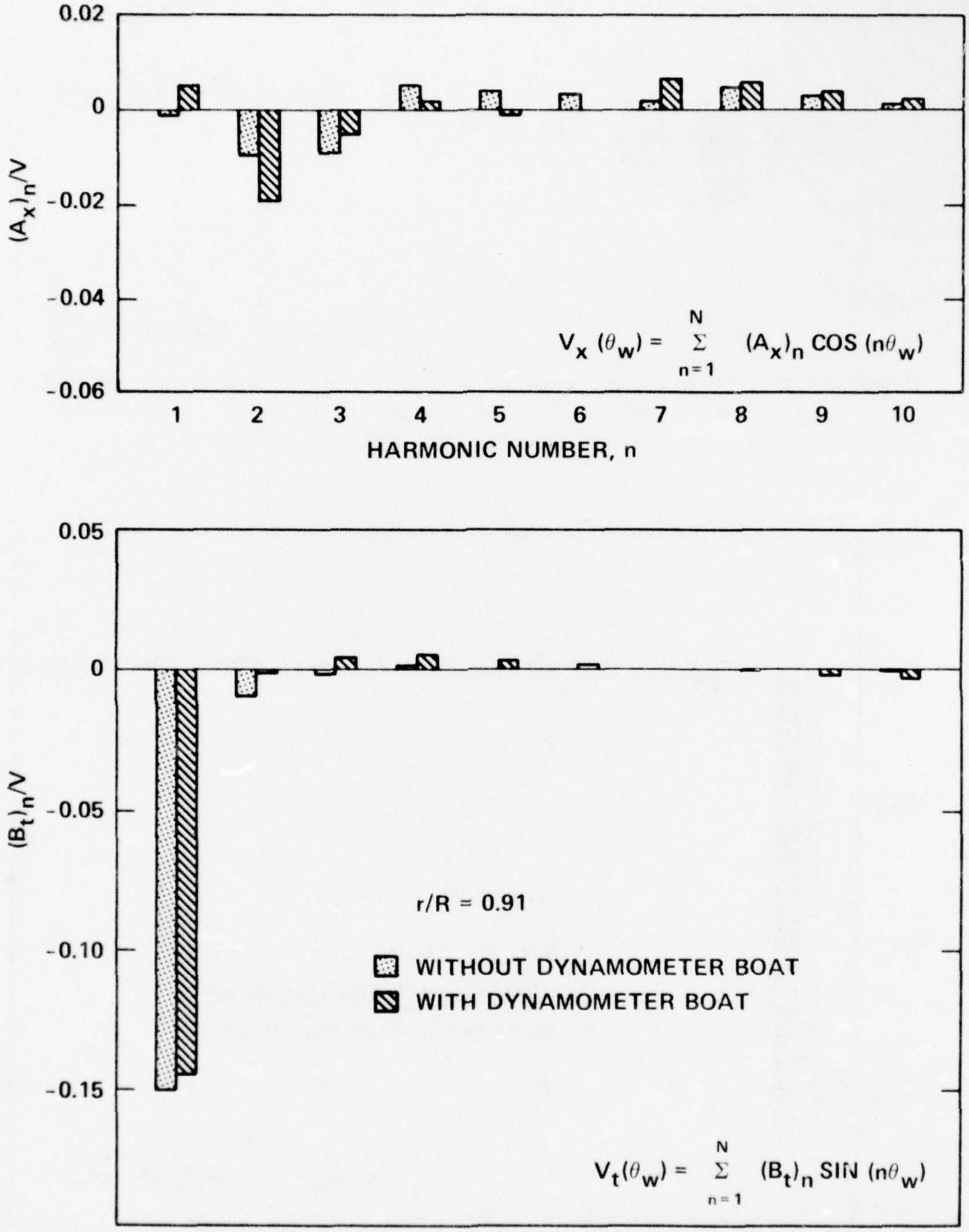

Figure 12c- 91 Percent Radius

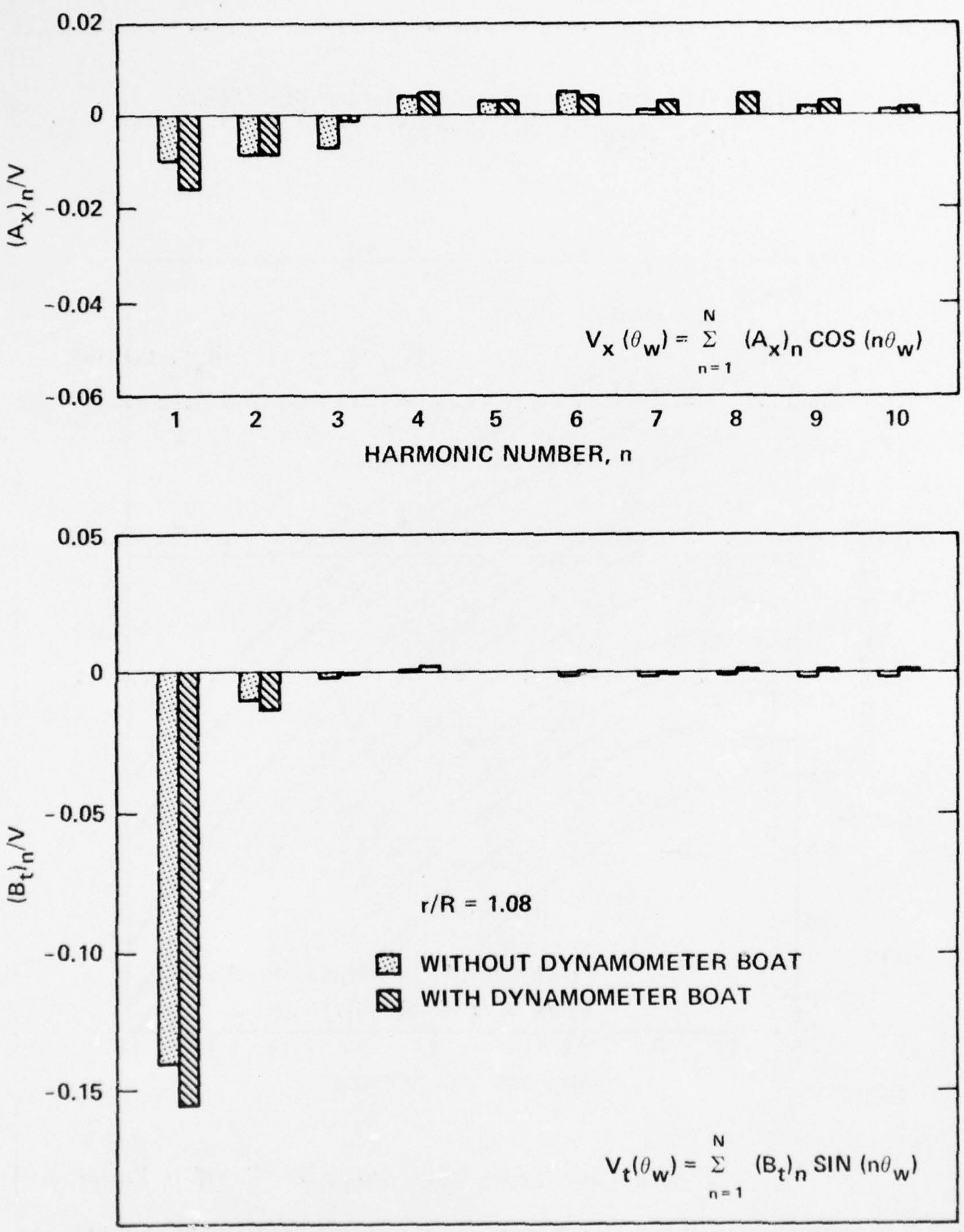

Figure 12d- 108 Percent Radius

Figure 13- Open Water Characteristics of DTNSRDC Model Propeller 4402

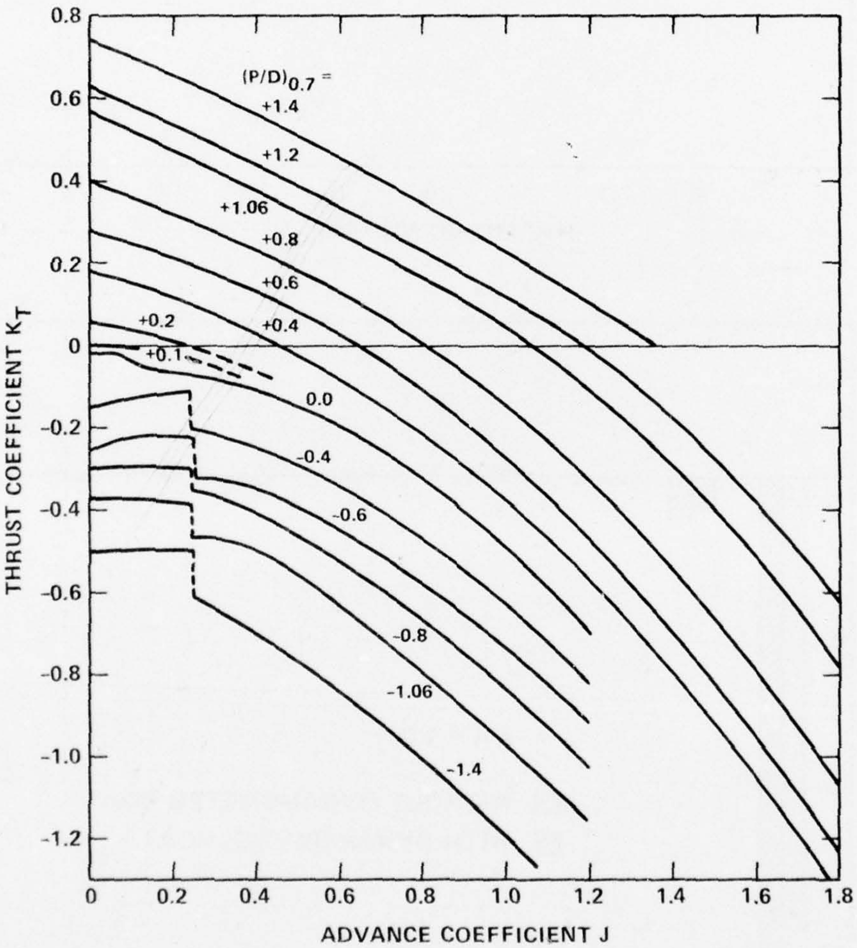

Figure 13a- Thrust Coefficient

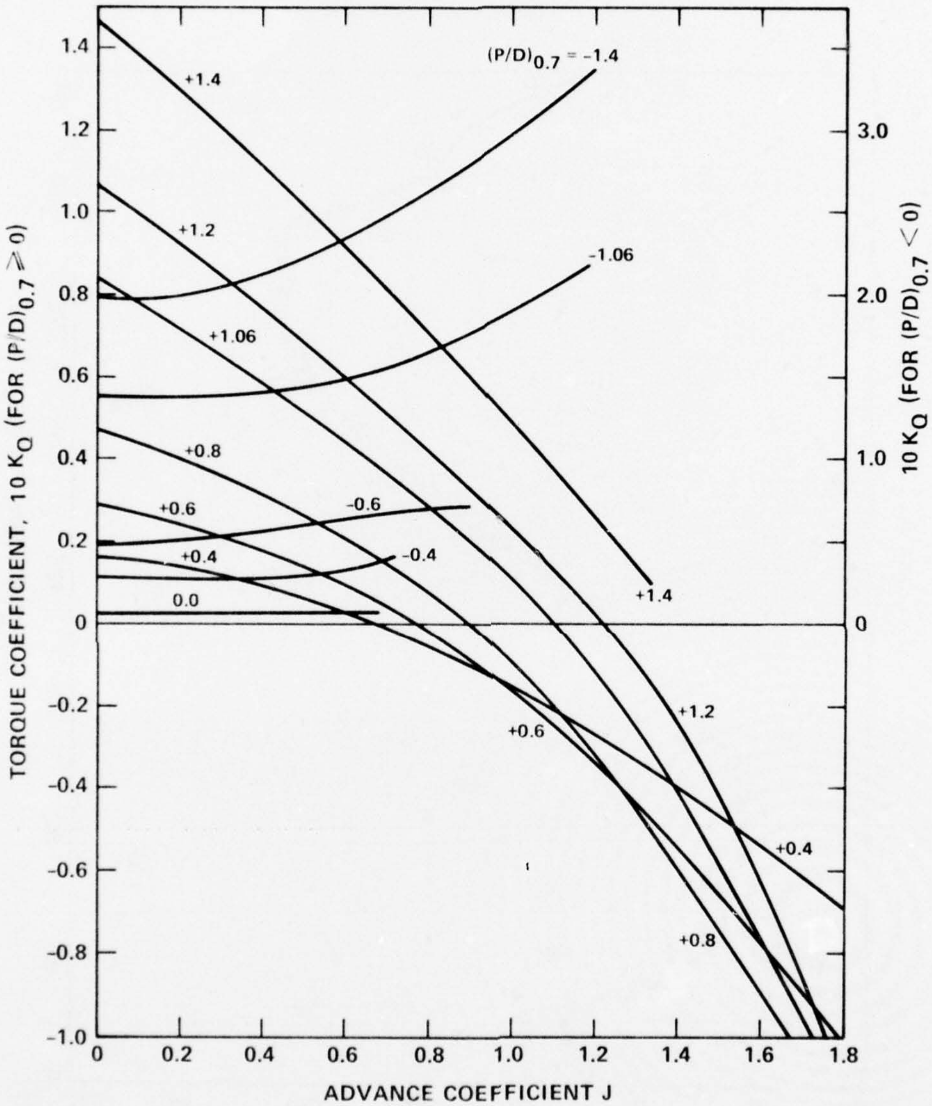

Figure 13b- Torque Coefficient

Figure 14- Influence of Extraneous Signals on Measured Loads

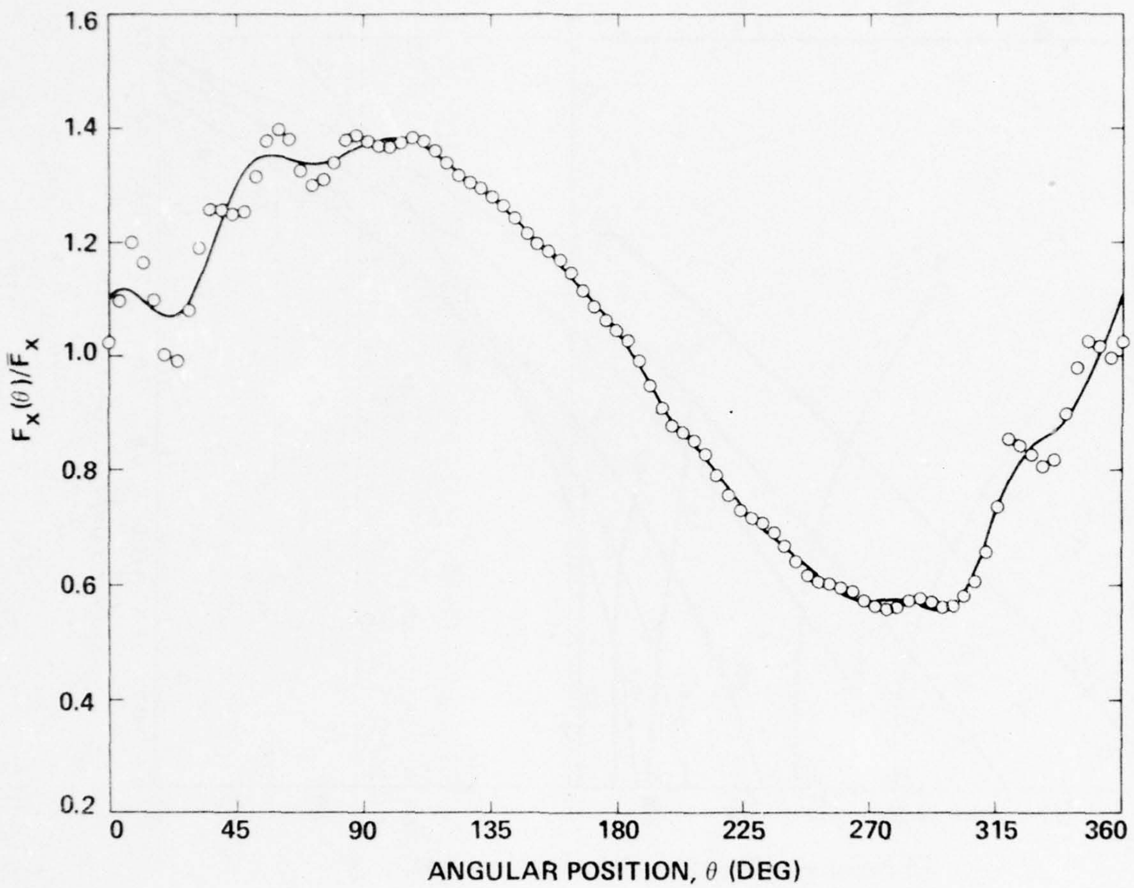

Figure 14a- F_X

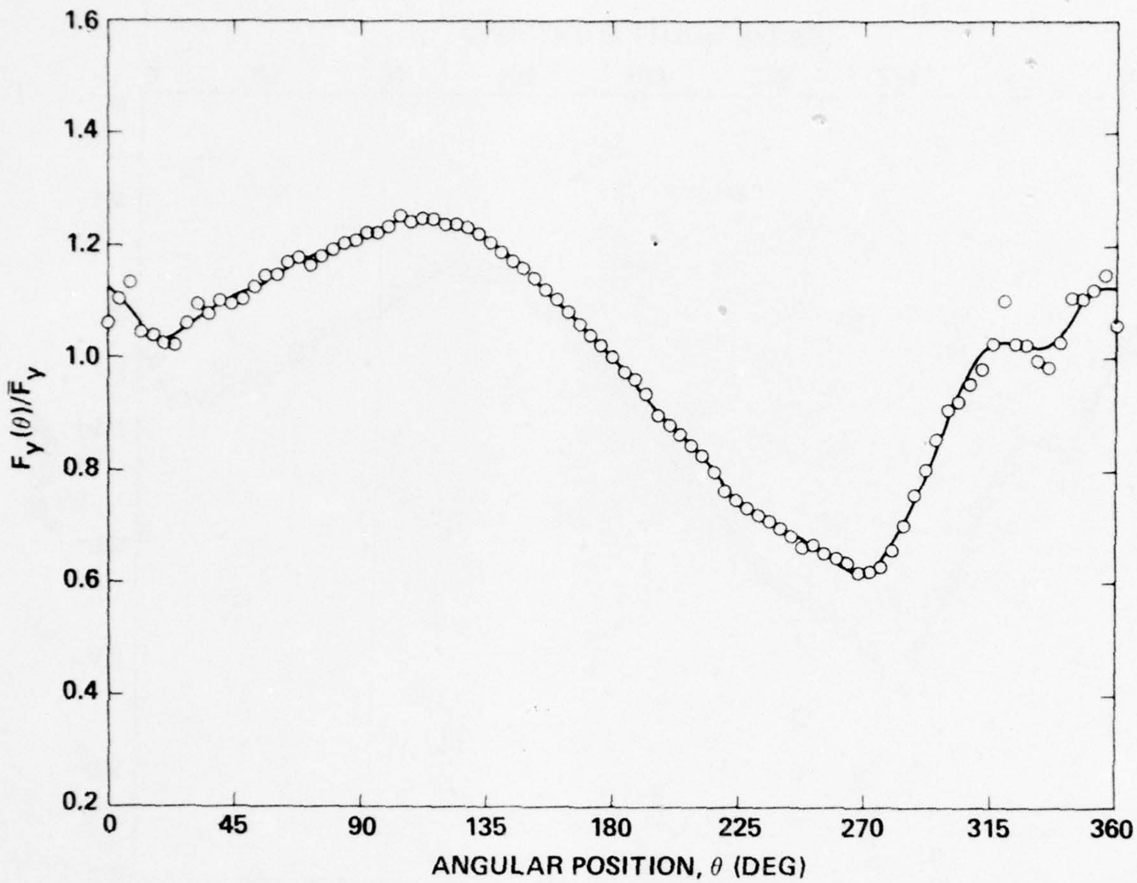

Figure 14b- F_y

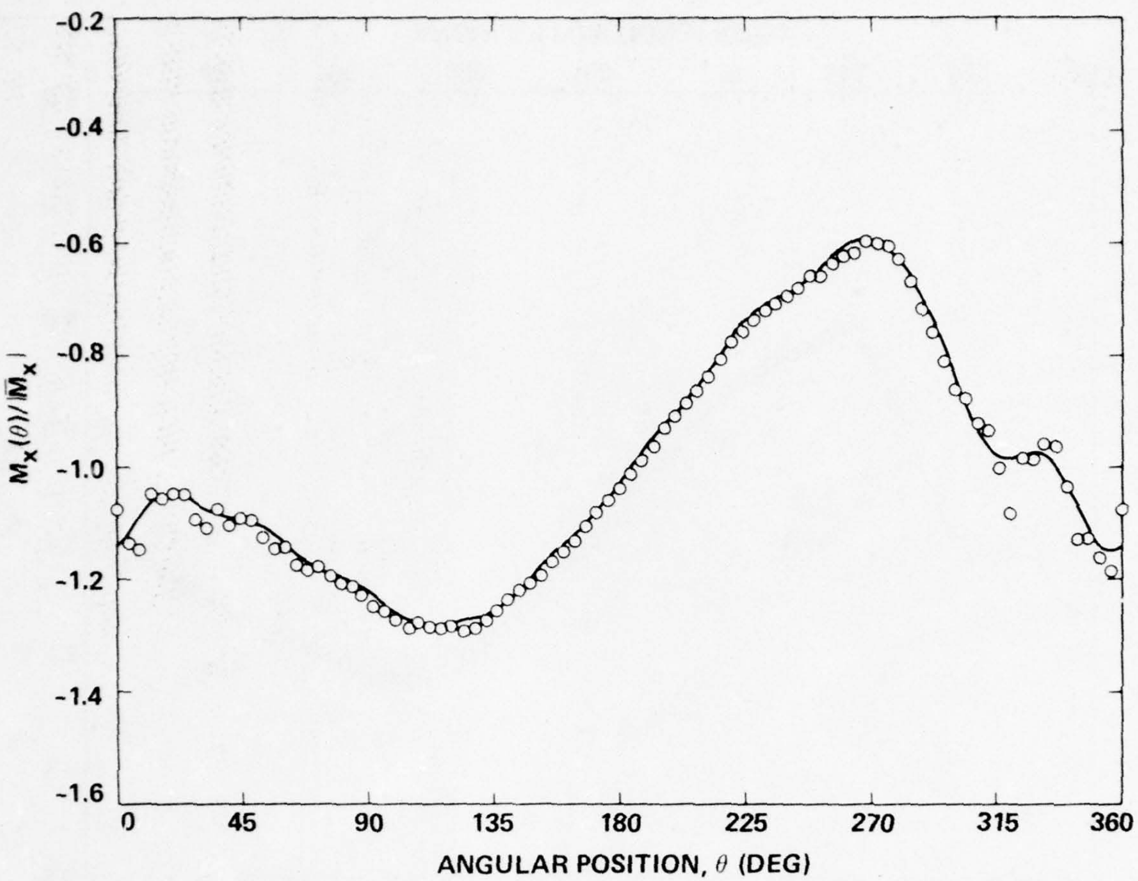

Figure 14c- M_x

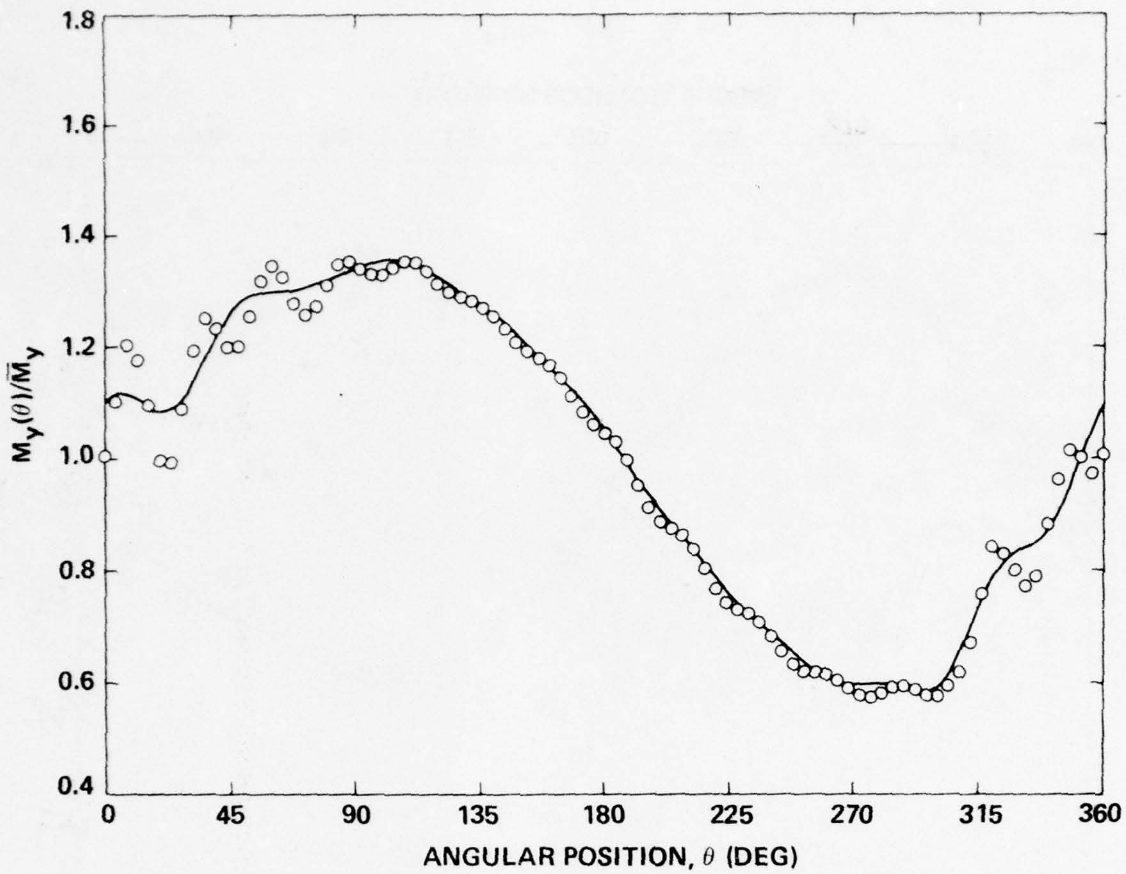

Figure 14d- M_y

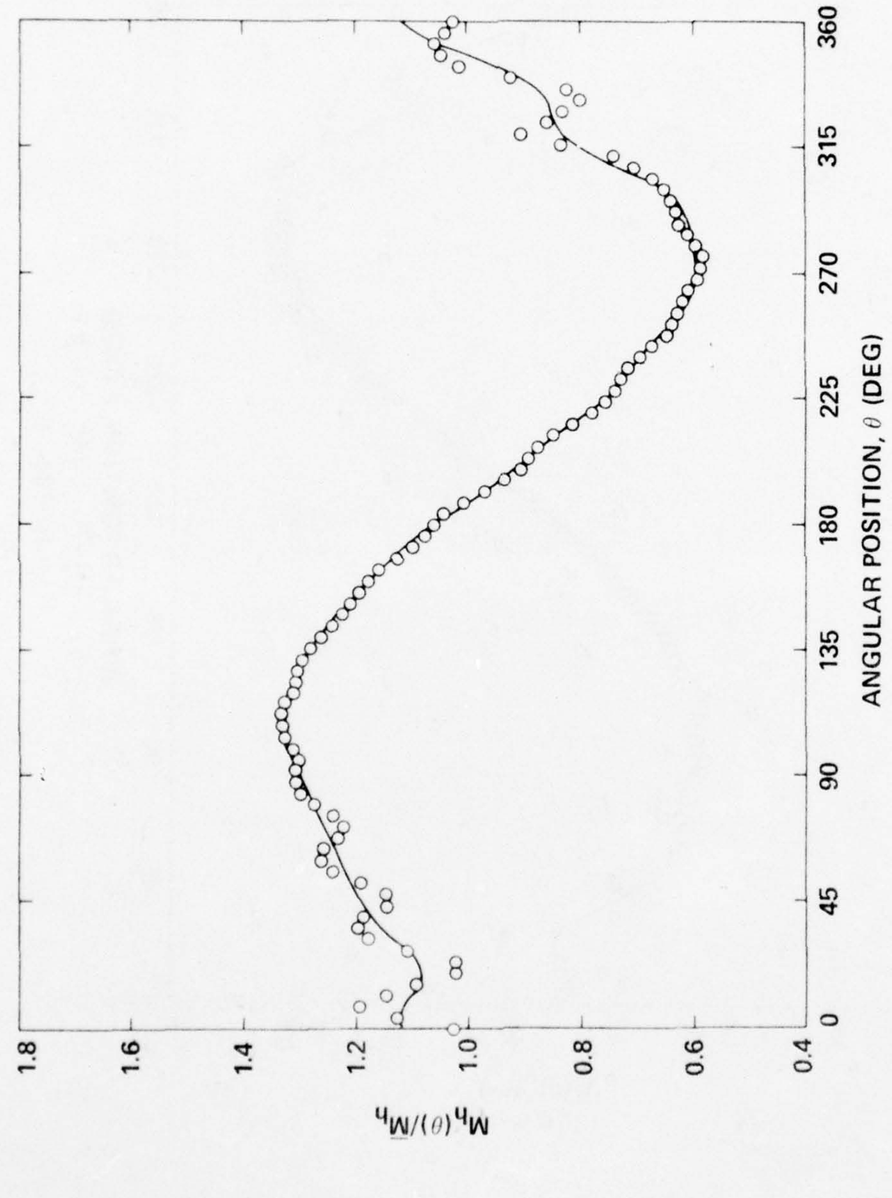

Figure 14e- M_h

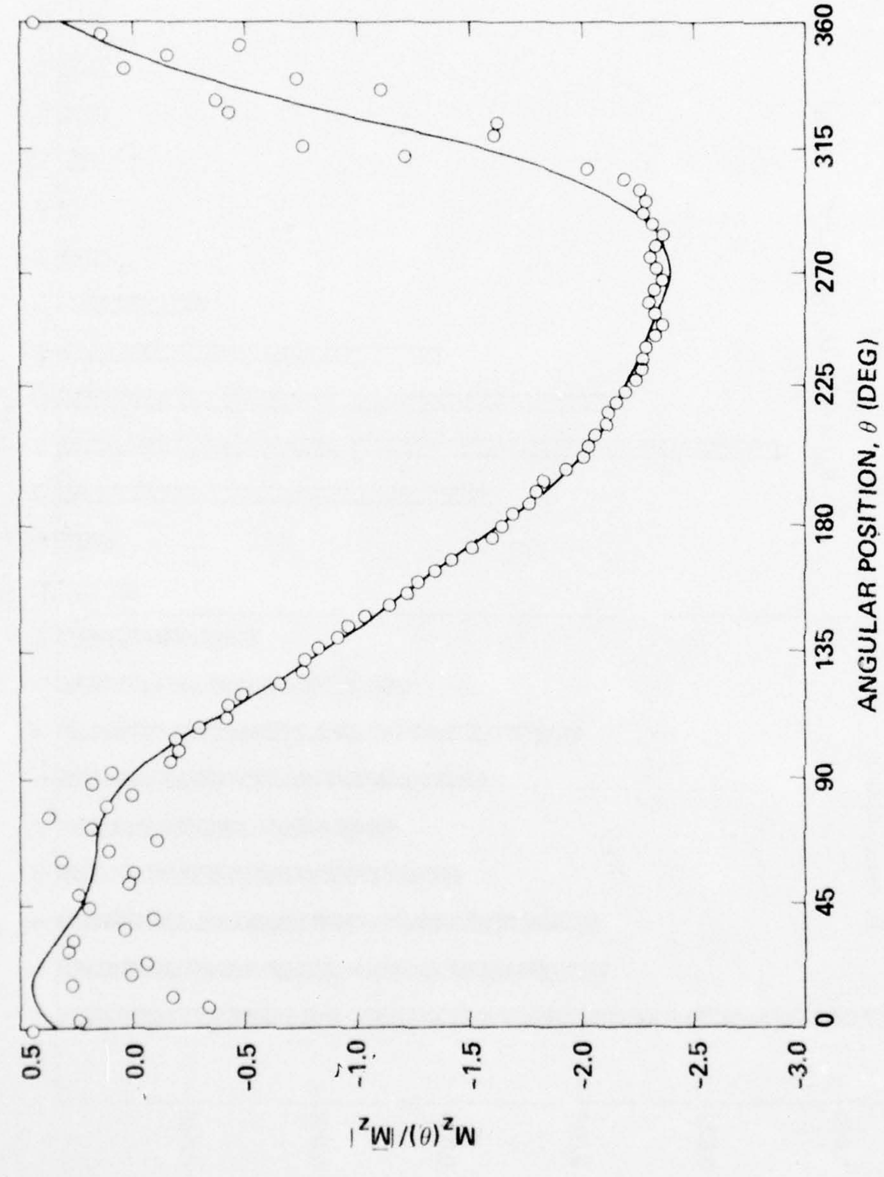

Figure 14f- M_z

Figure 15 - Experimental Data Showing Extraneous Higher Harmonics

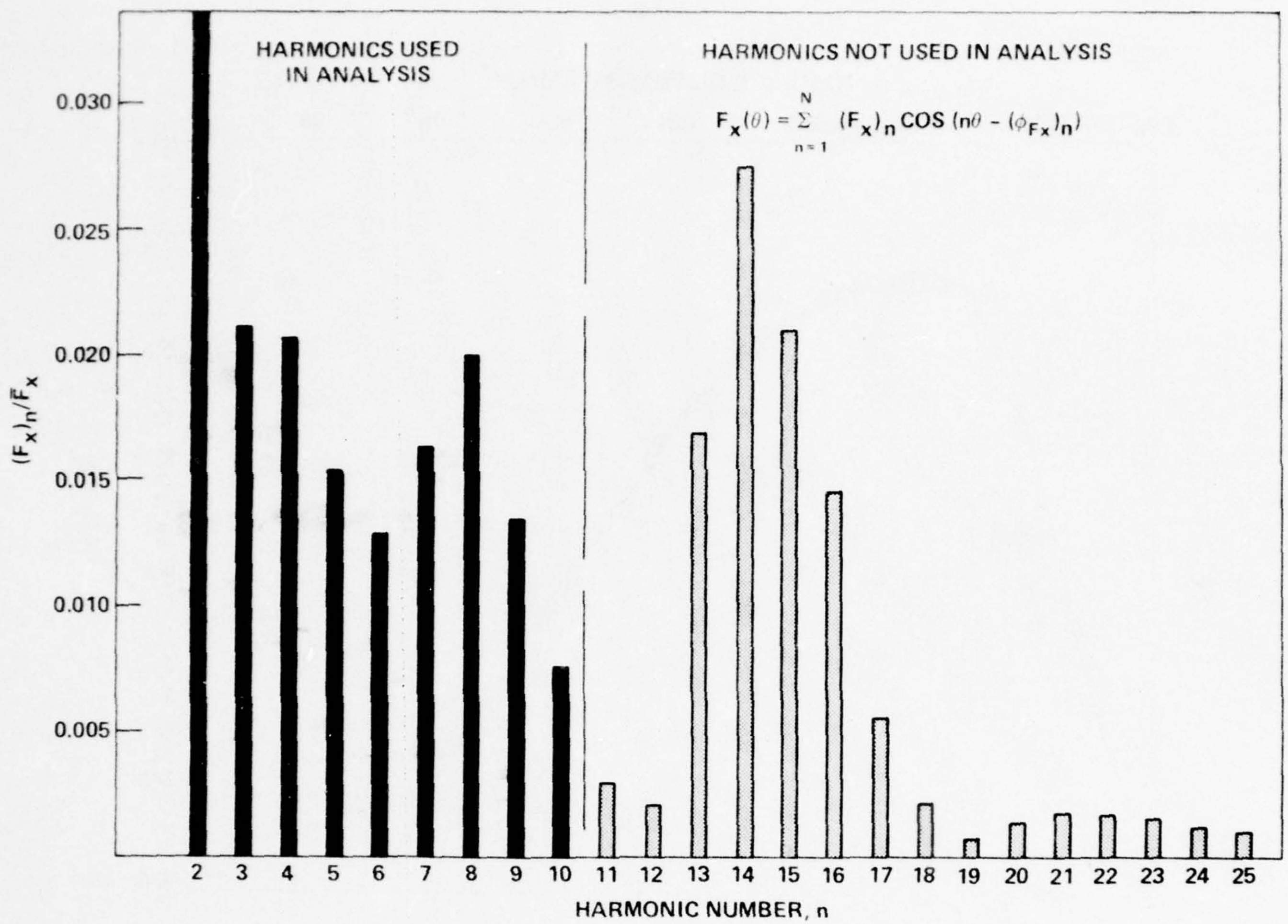

Figure 15a - F_x

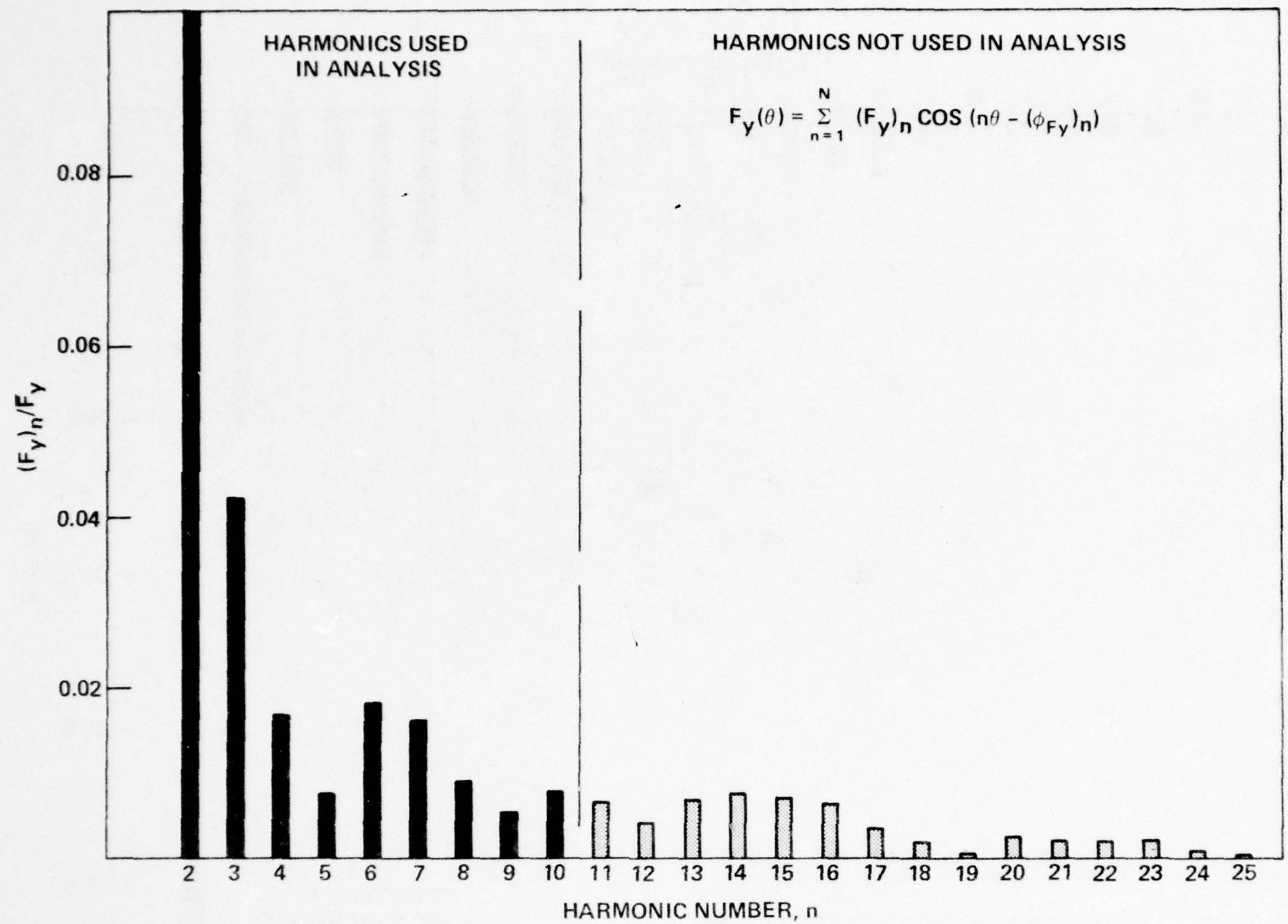

Figure 15b- F_y

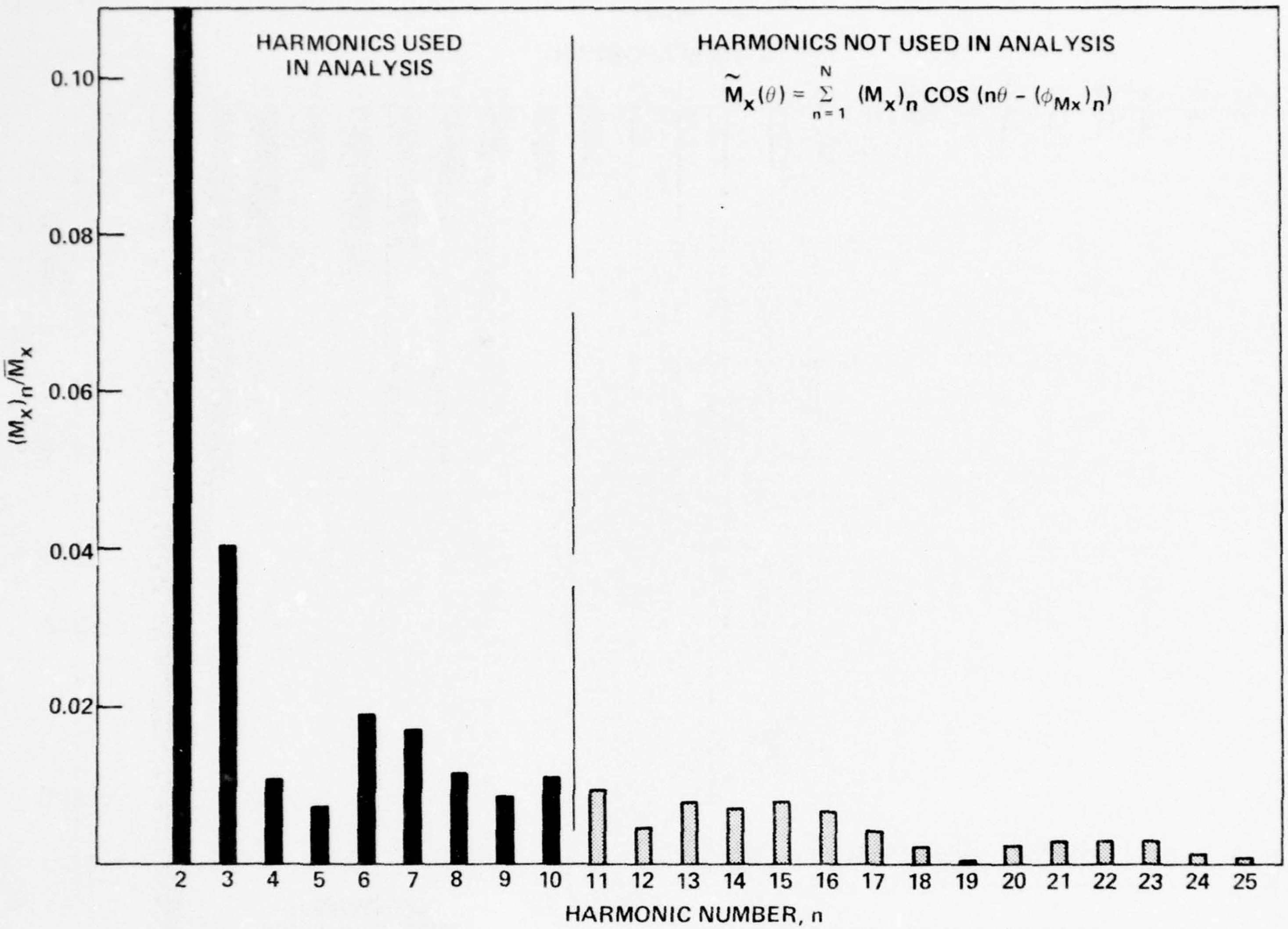

Figure 15c- M_x

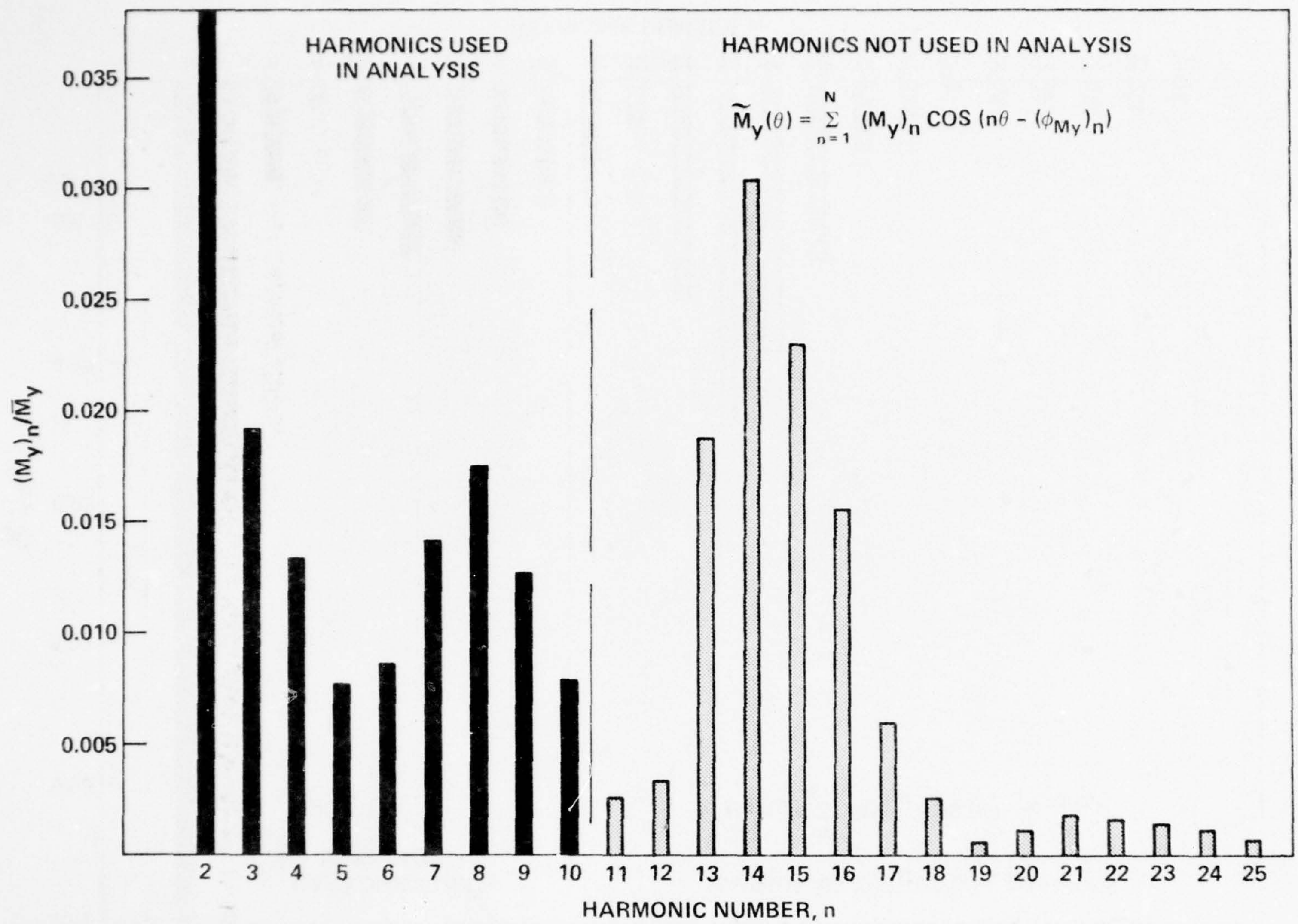

Figure 15d- M_y

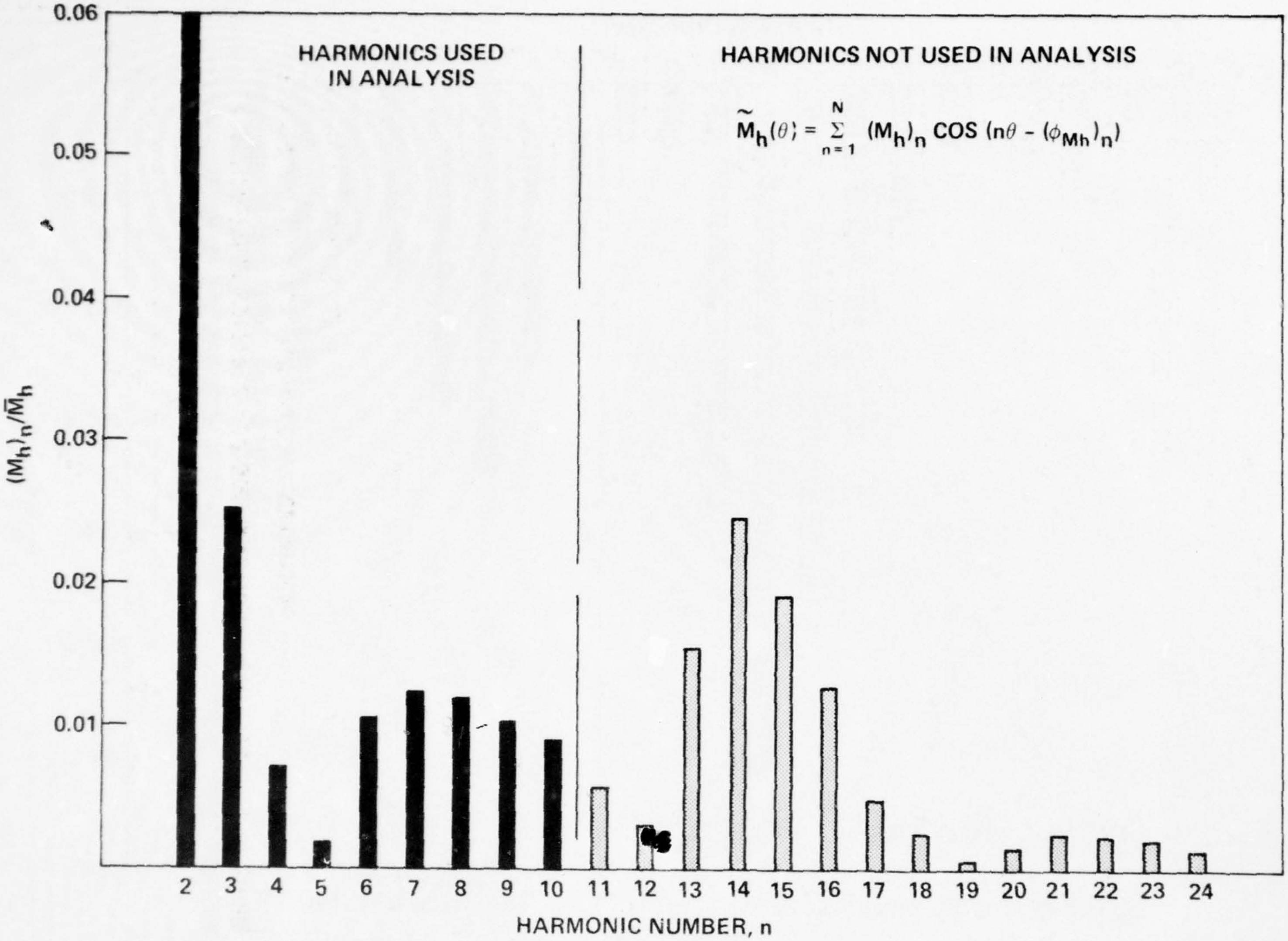

Figure 15e- M_h

AD-A034 804 DAVID W TAYLOR NAVAL SHIP RESEARCH AND DEVELOPMENT CE--ETC F/G 13/10
EXPERIMENTAL UNSTEADY AND MEAN LOADS ON A CP PROPELLER BLADE ON--ETC(U)
OCT 76 R J BOSWELL, J J NELKA, S B DENNY

UNCLASSIFIED DTNSRDC-76-0125 NL

2 OF 4
AD
A034804

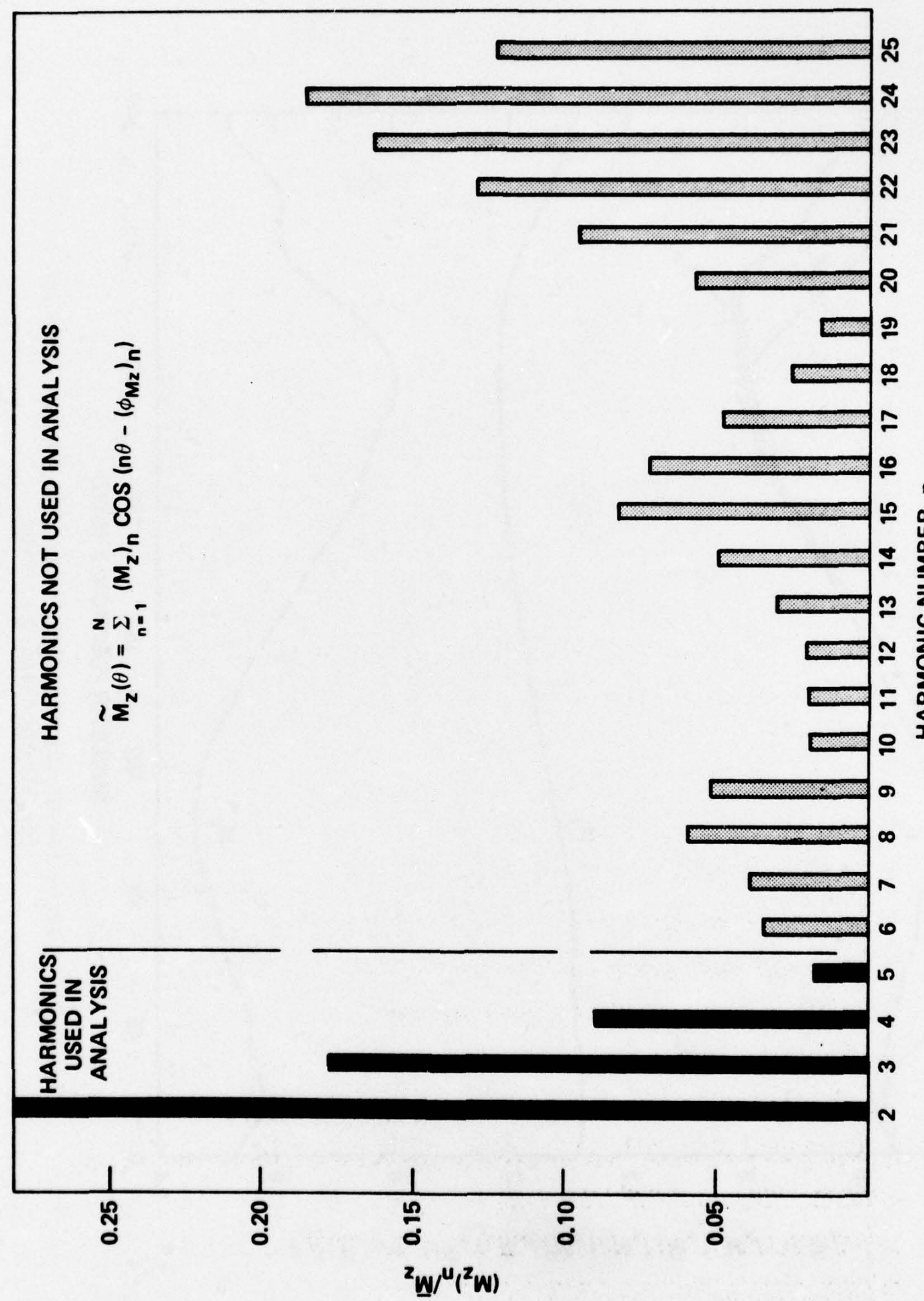

Figure 15f- M_z

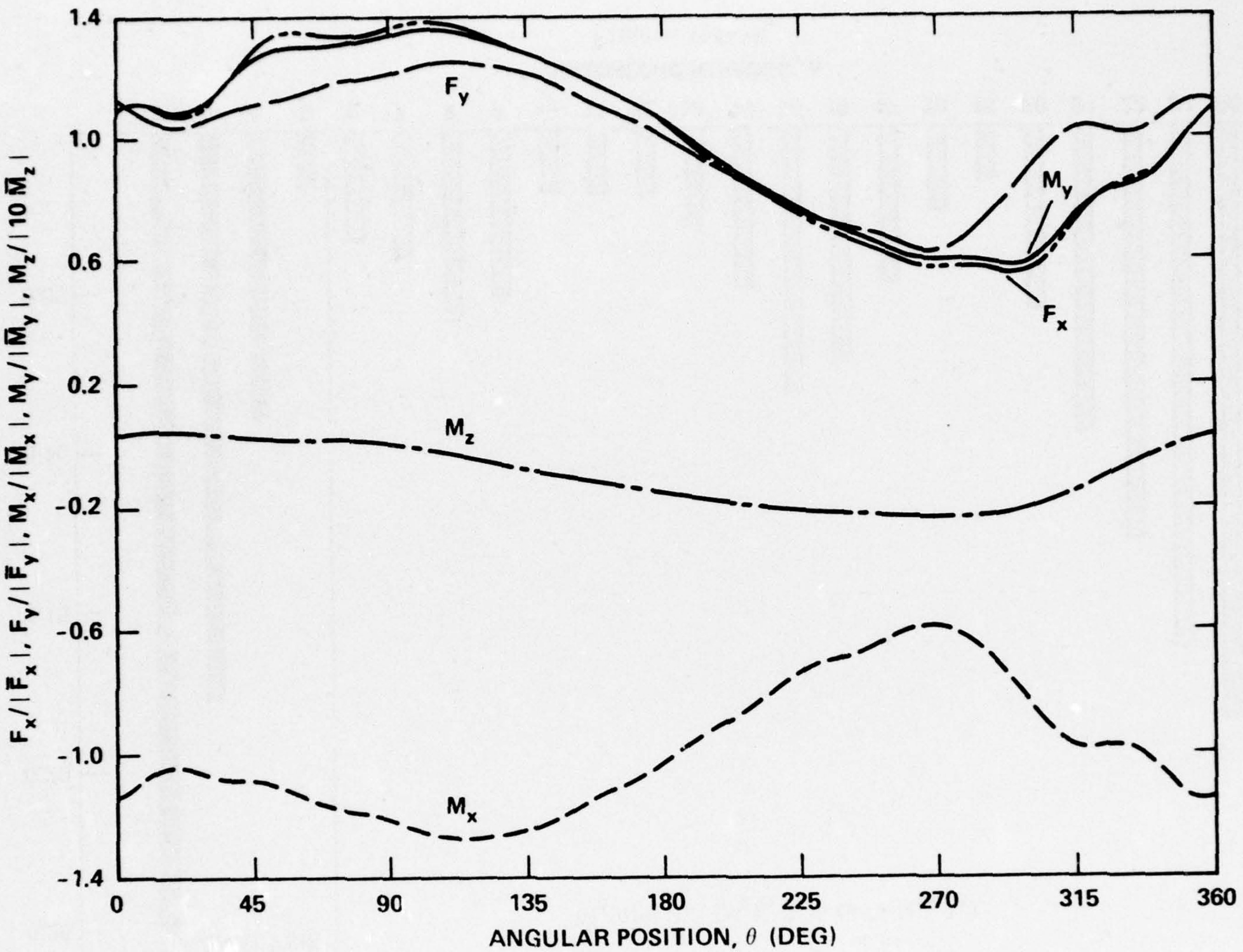

Figure 16 - Variation of Experimental Loads with Angular Position
for Steady Ahead Operation

Figure 17 - Harmonic Content of Experimental Loads for Steady Ahead Operation

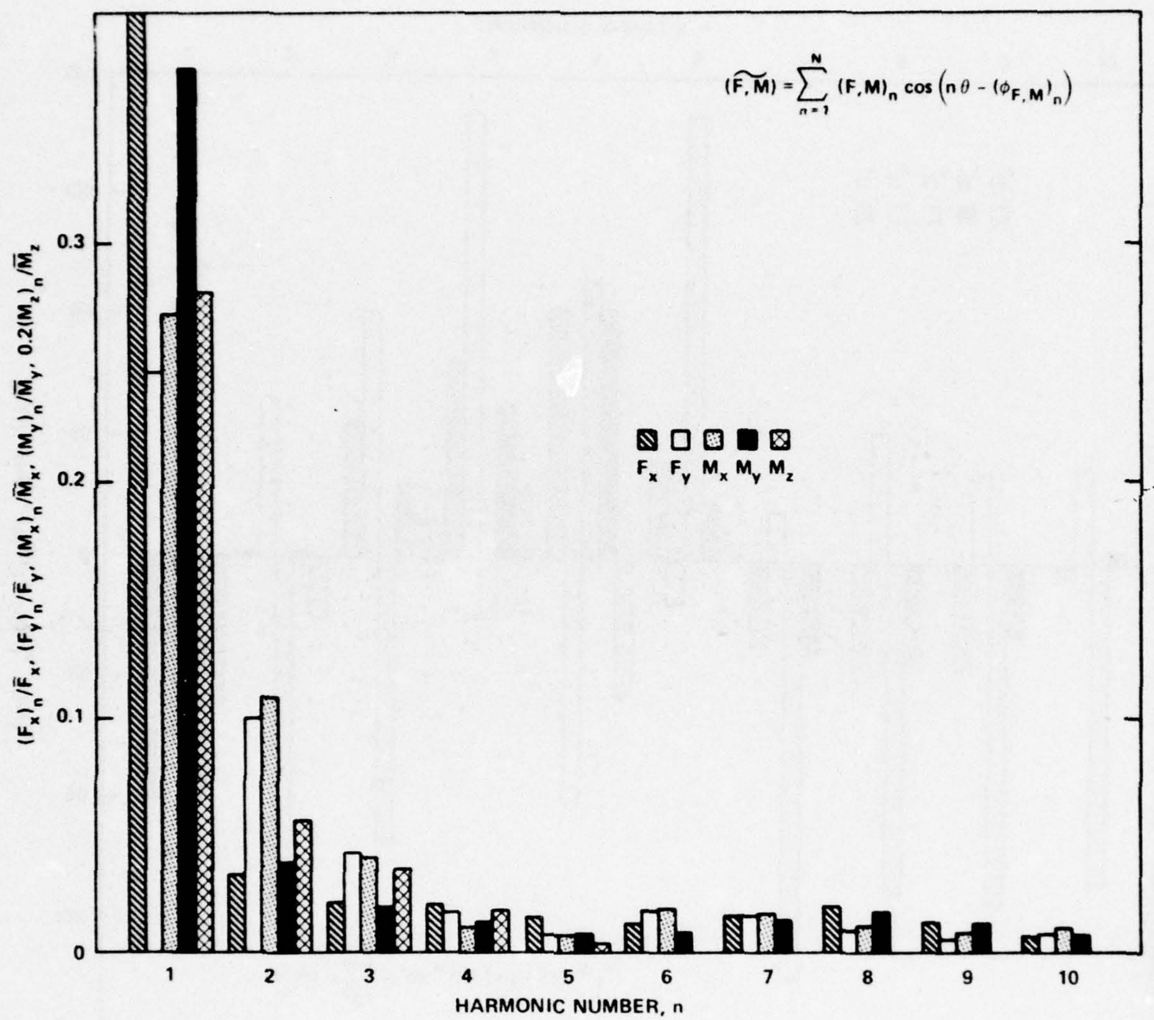

Figure 17a - Amplitudes

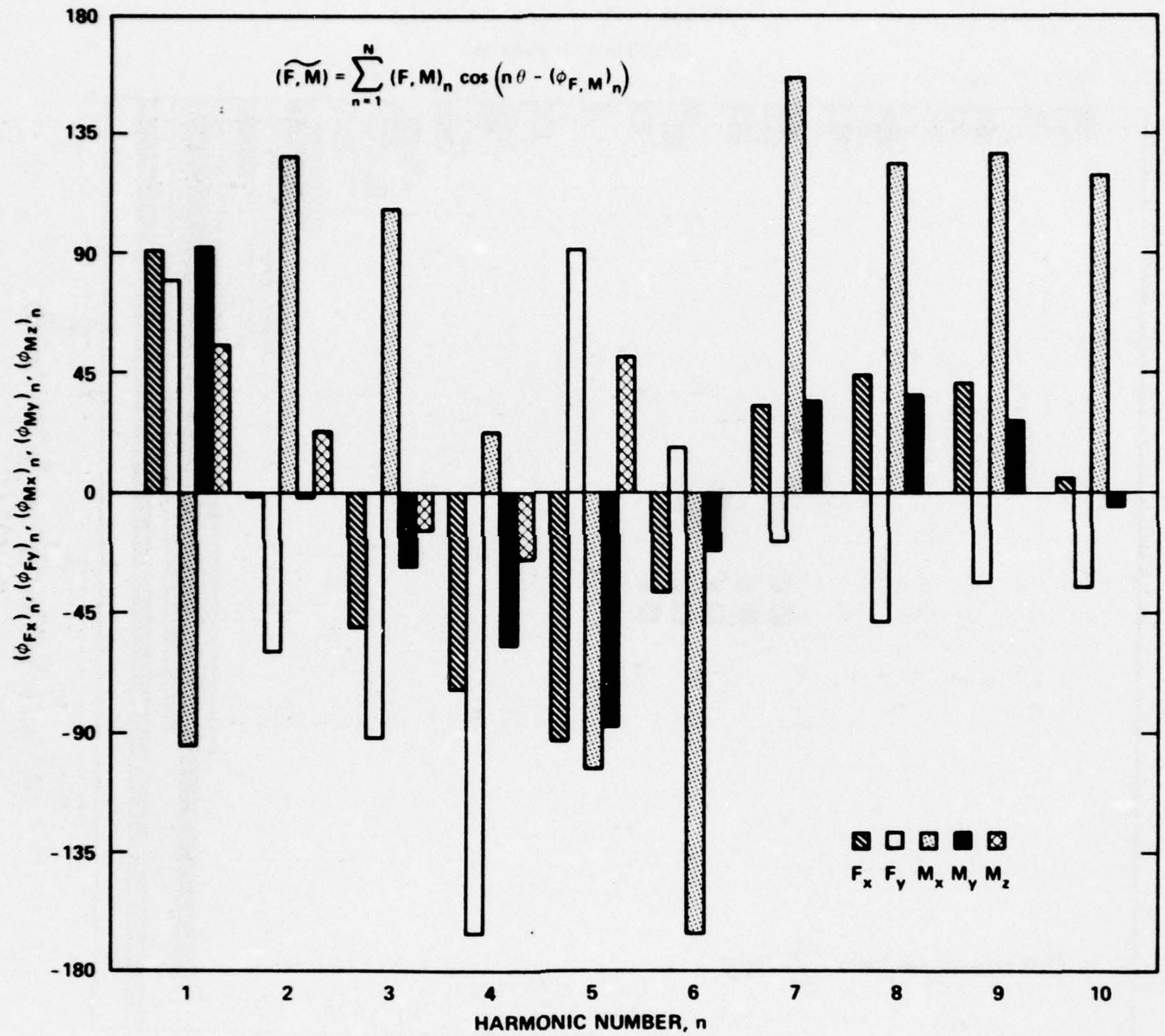

Figure 17b - Phases

Figure 18 - Variation of Components of Blade Loading with Hull Pitch Angle ψ

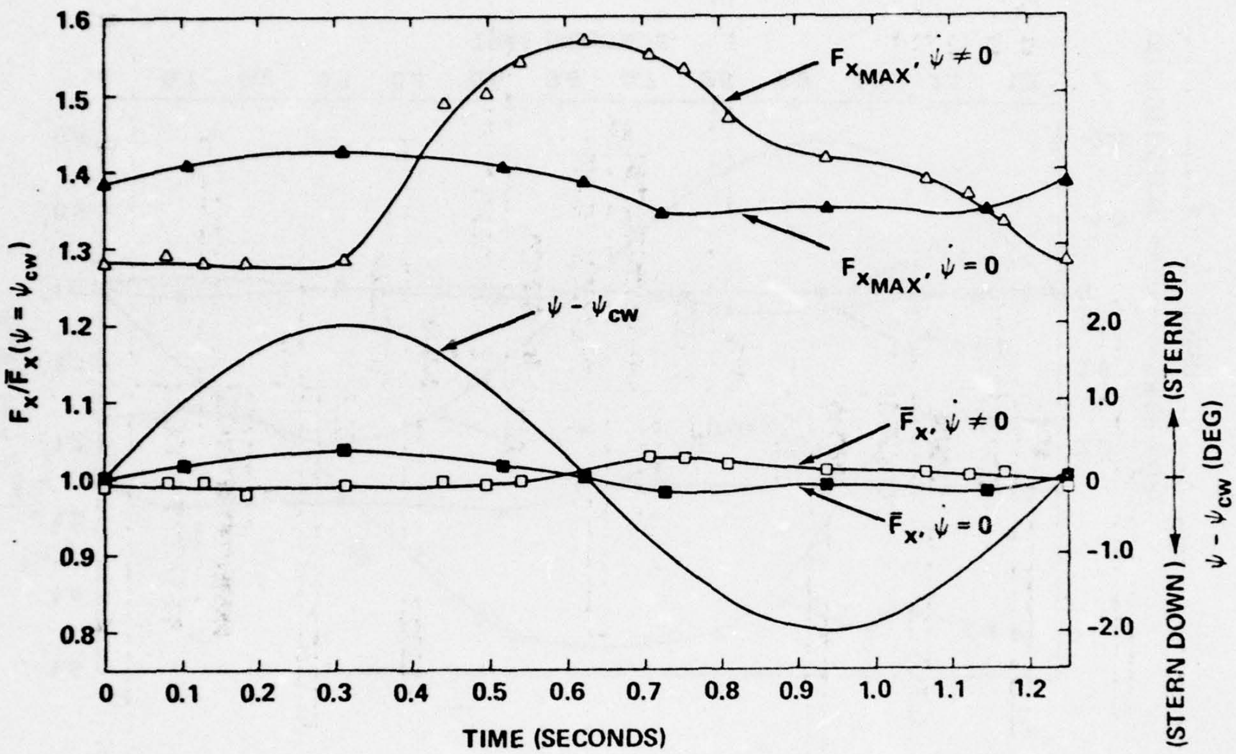

Figure 18a - F_x

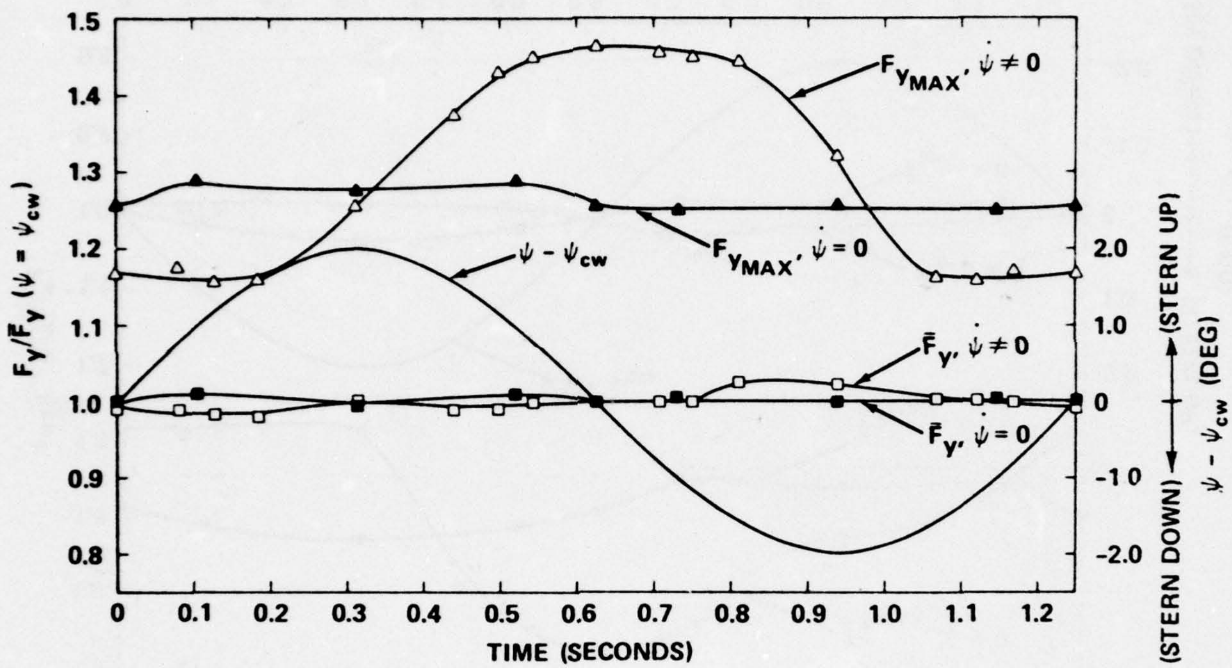

Figure 18b - F_y

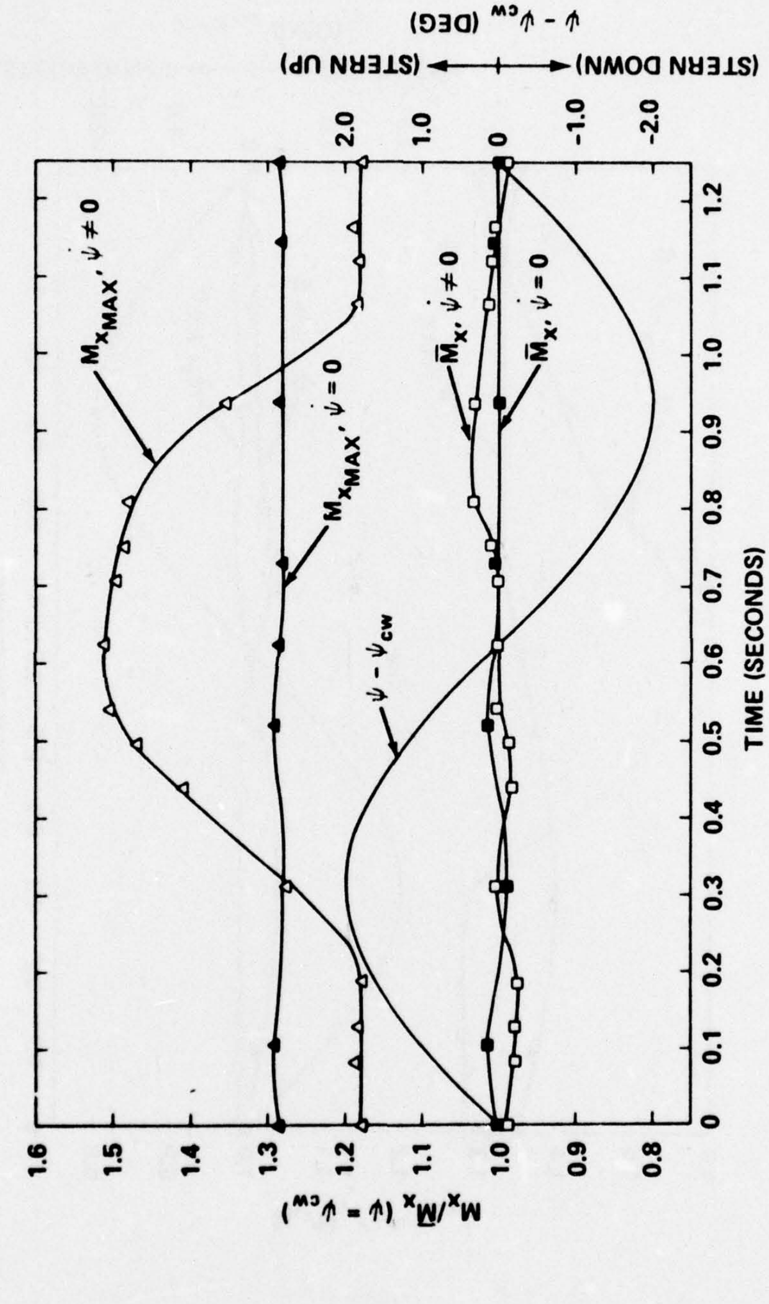

Figure 18c - M_X

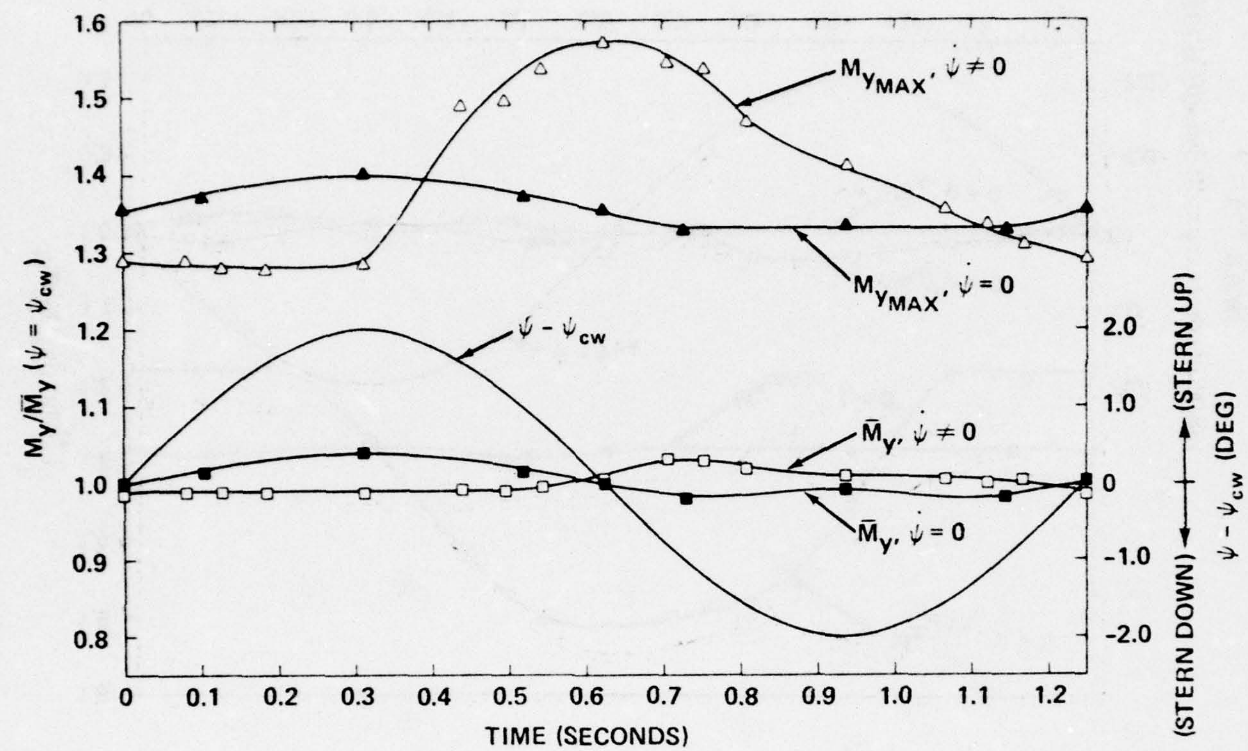

Figure 18d - M_y

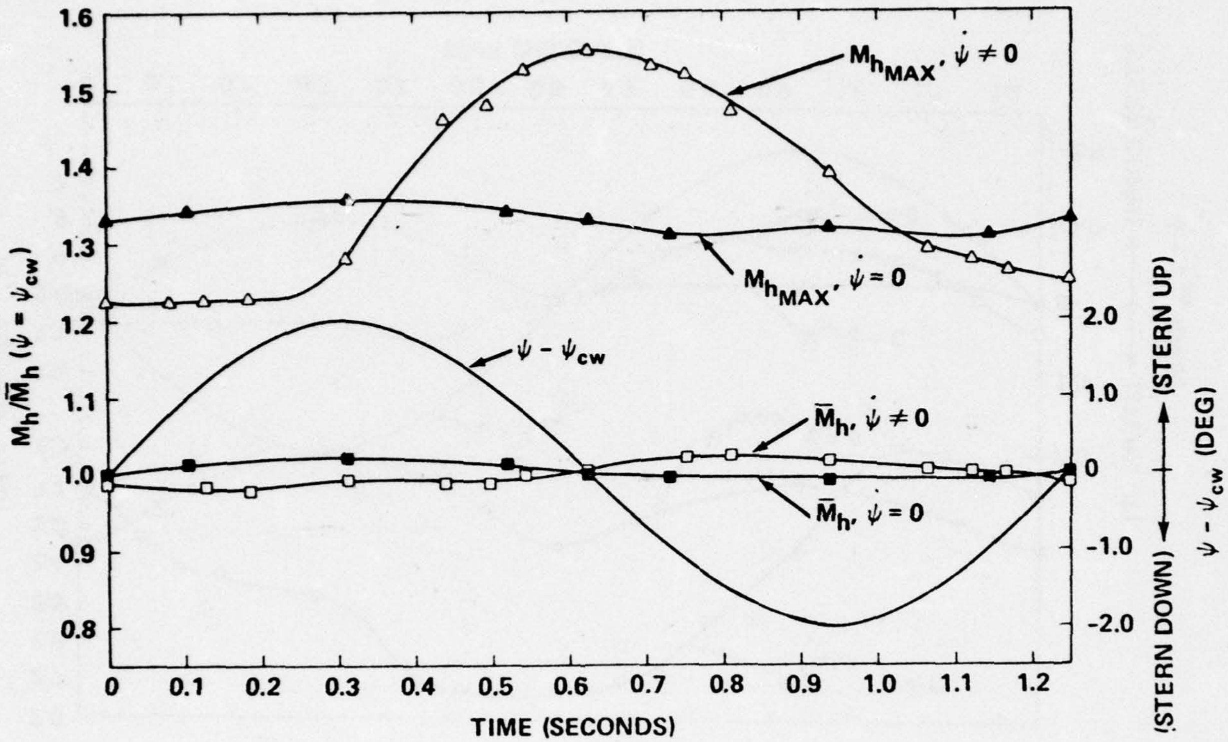

Figure 18e - M_h

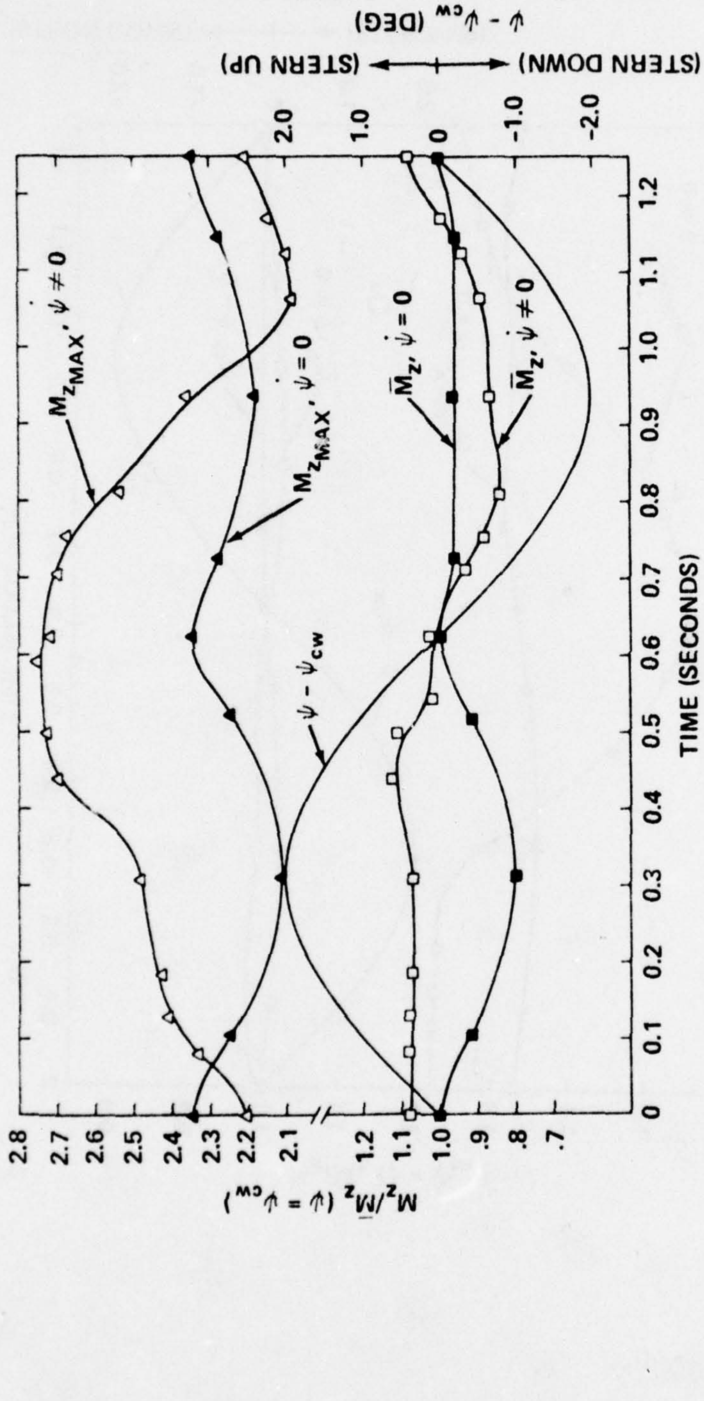

Figure 18f - M_Z

Figure 19 - Variation of Loads with Angular Position for Quasi-Steady Crash Ahead

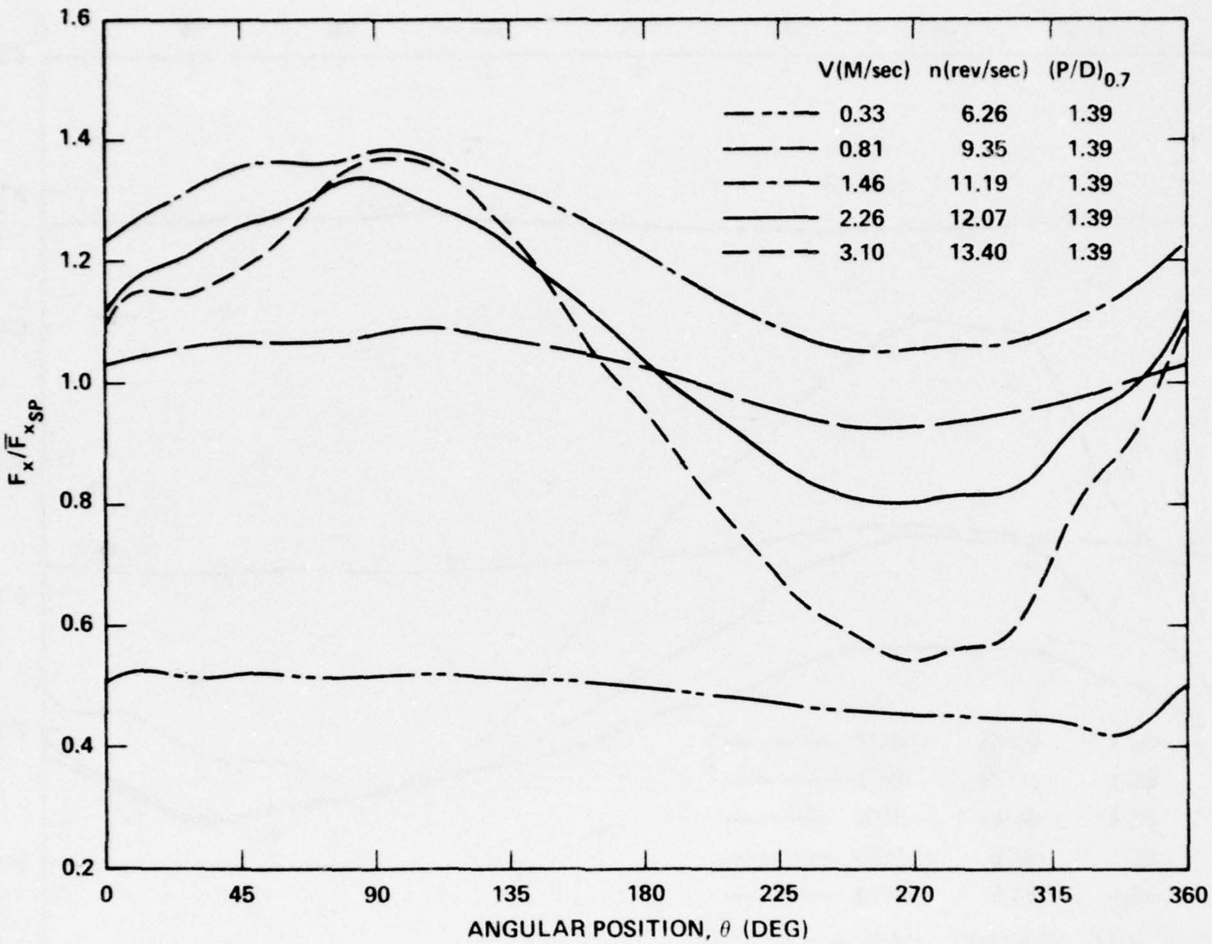

Figure 19a - F_x

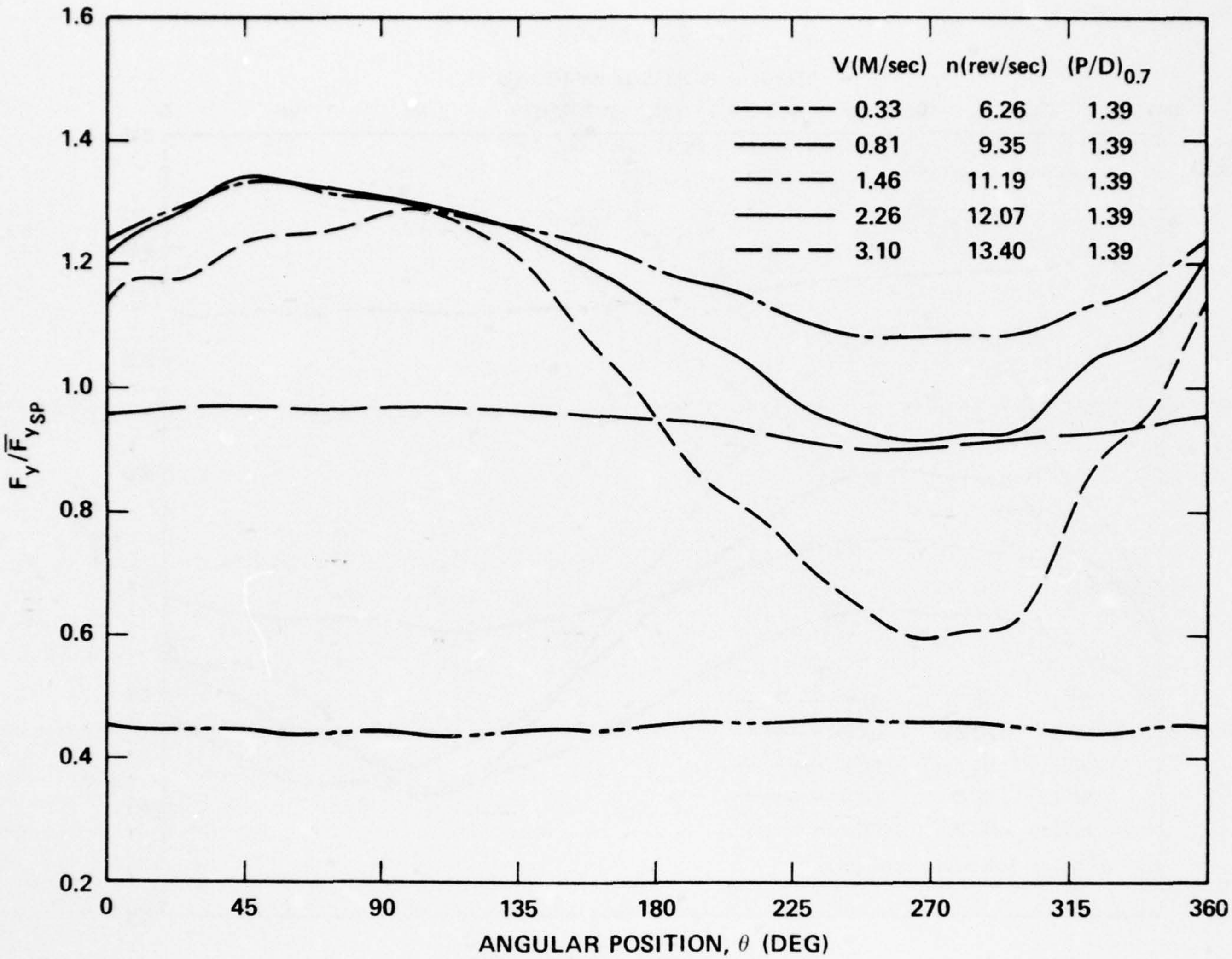

Figure 19b- F_y

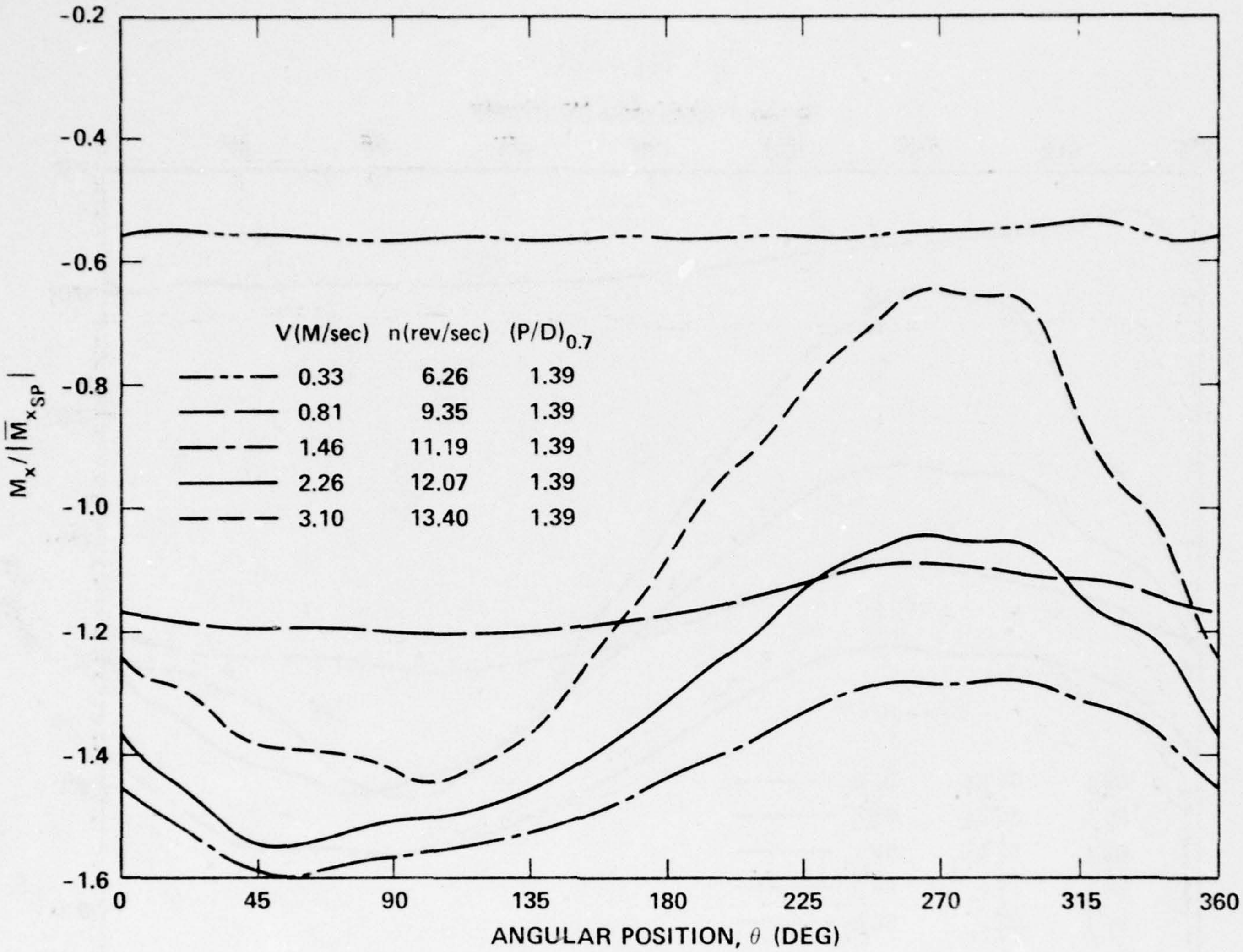

Figure 19c- M_X

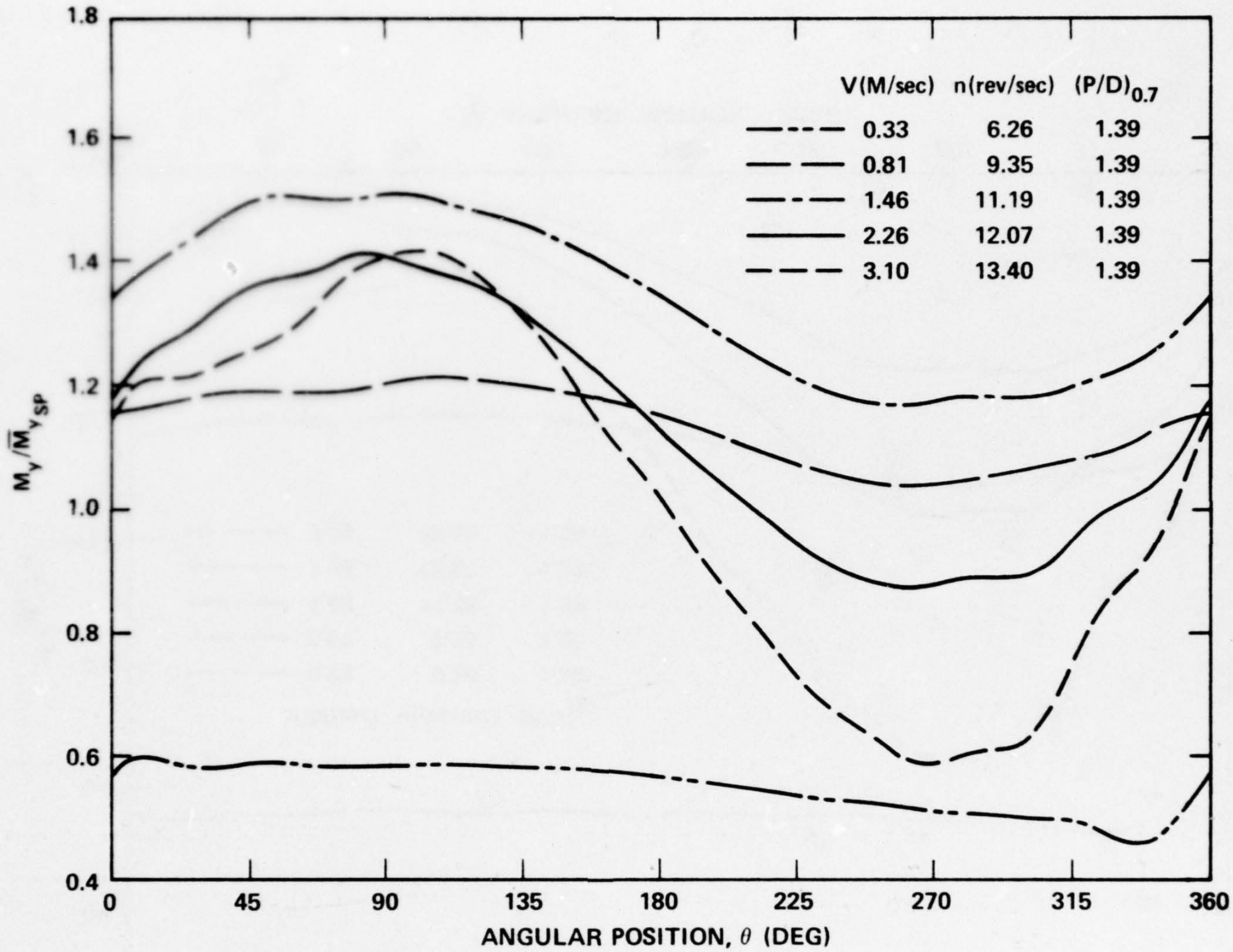

Figure 19d - M_y

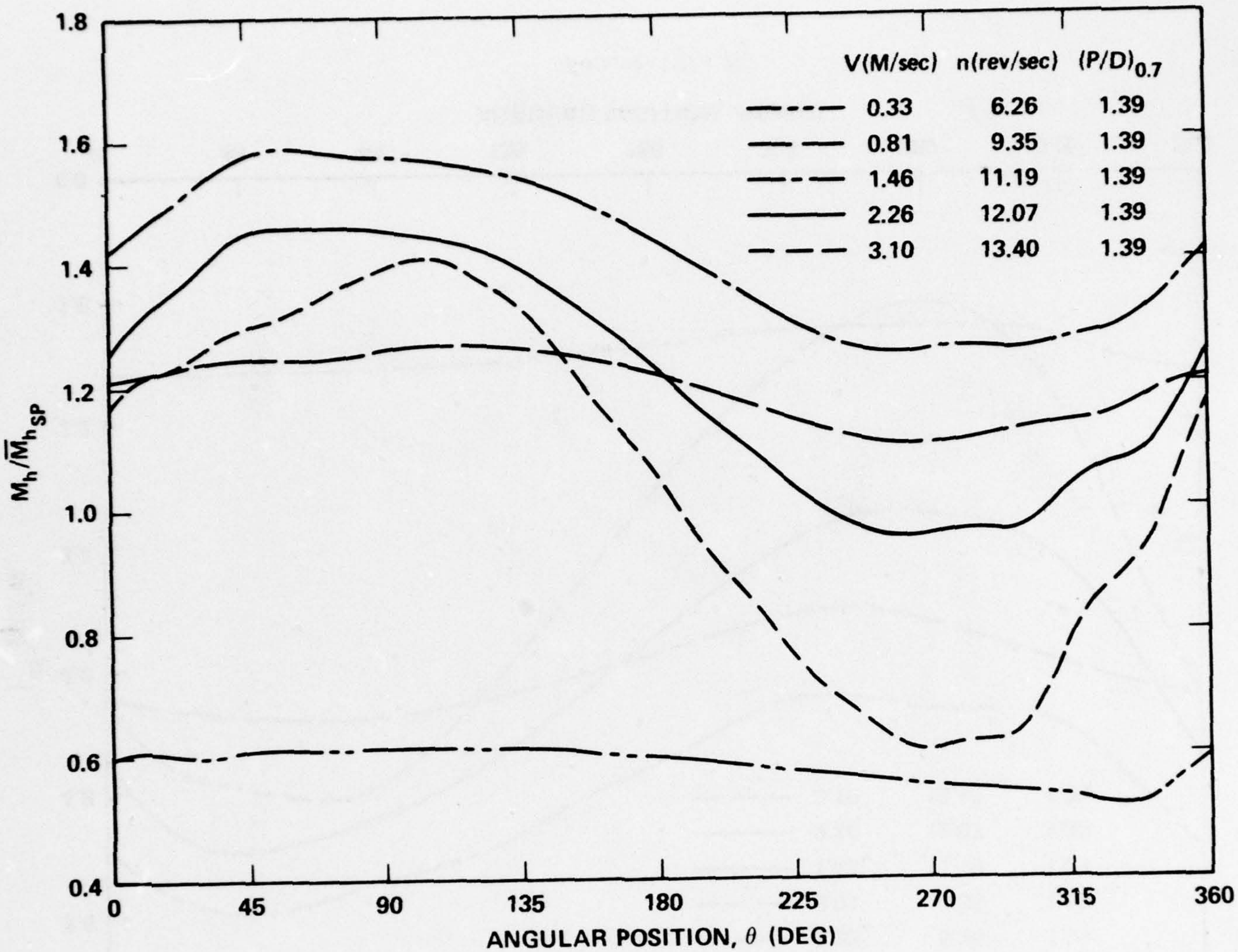

Figure 19e- M_h

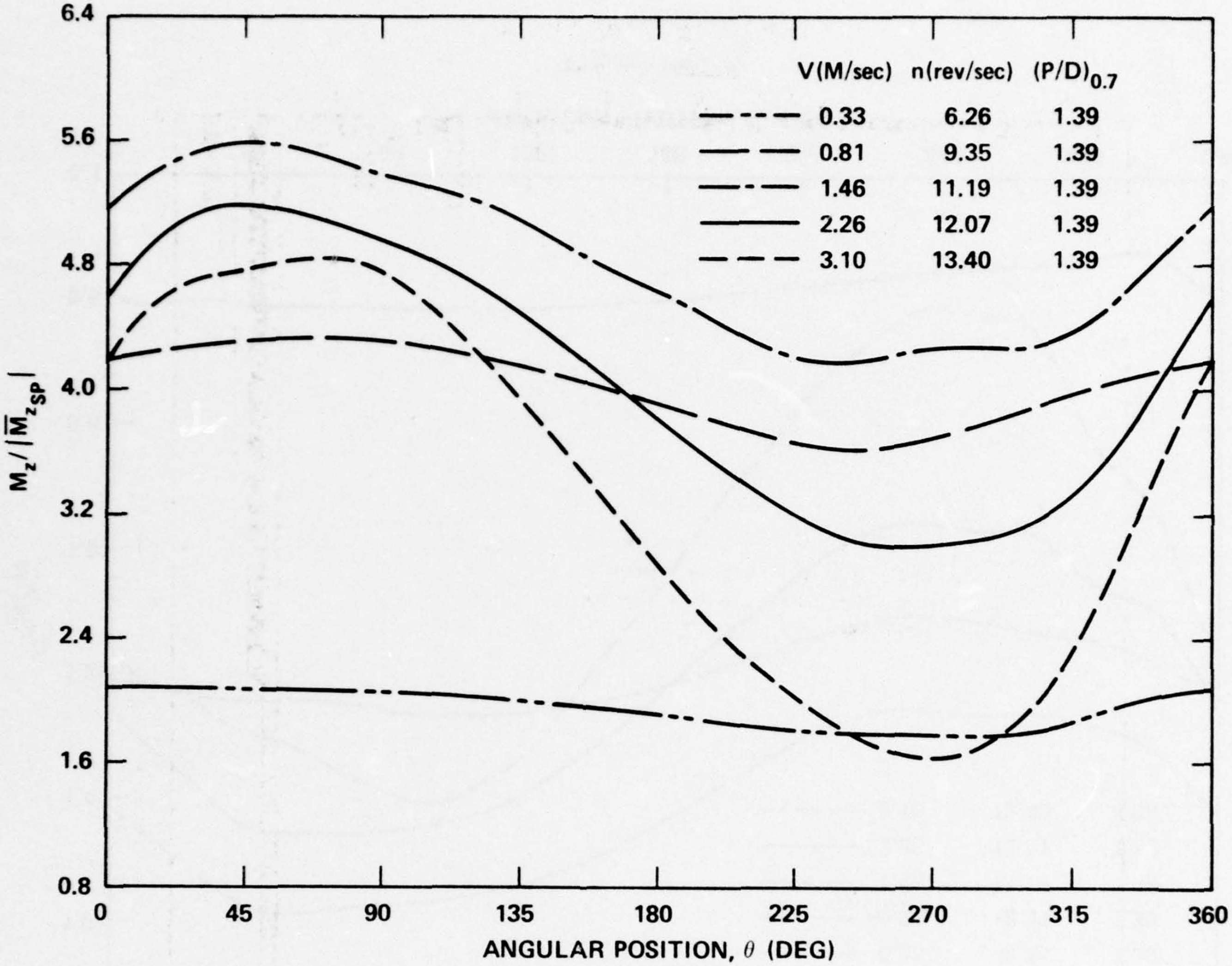

Figure 19f- M_Z

Figure 20 - Harmonic Content of F_x for Quasi-Steady Crash Ahead

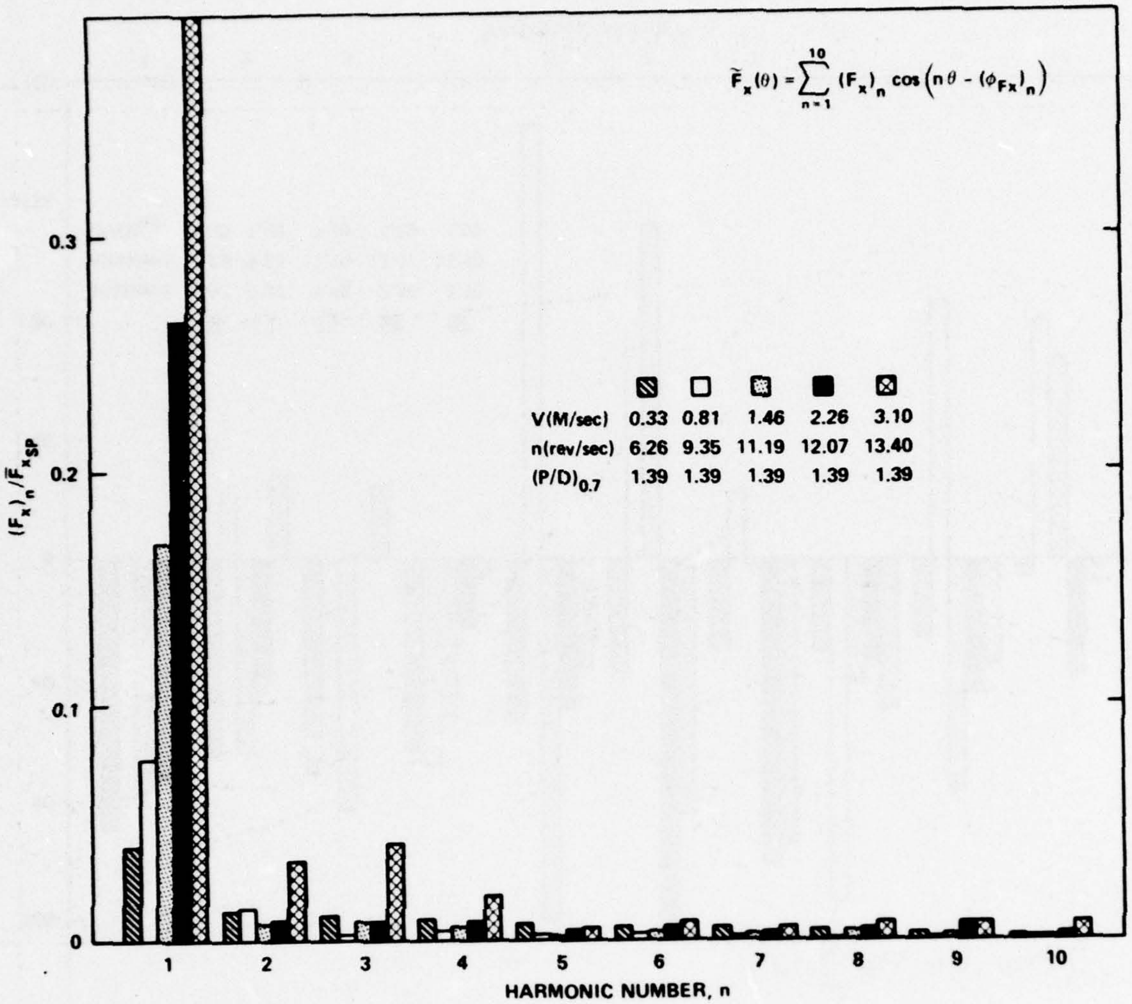

Figure 20a - Amplitudes

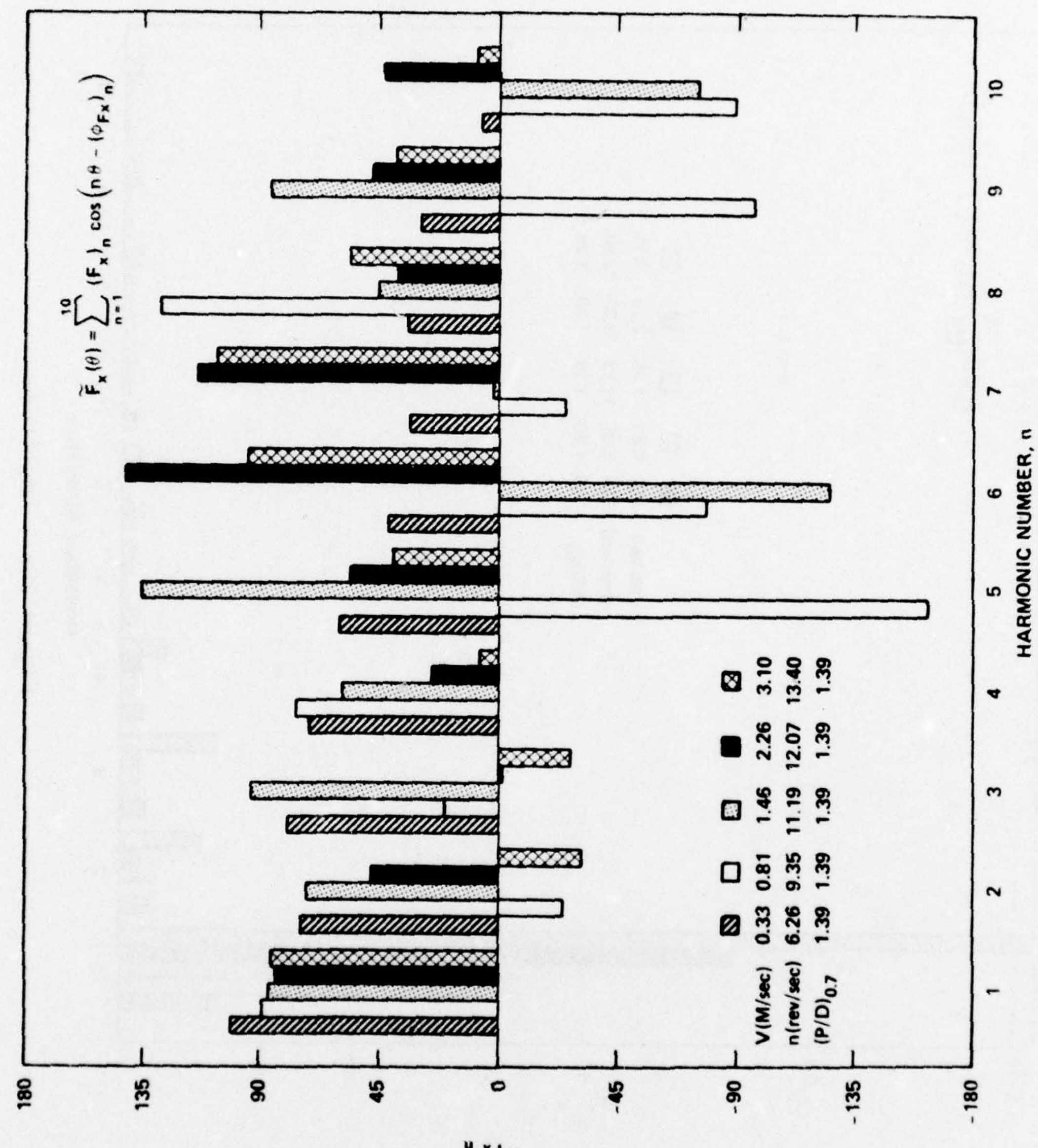

Figure 20b - Phases

Figure 21 - Variation of Loads with Angular Position for Quasi-Steady Crash Astern

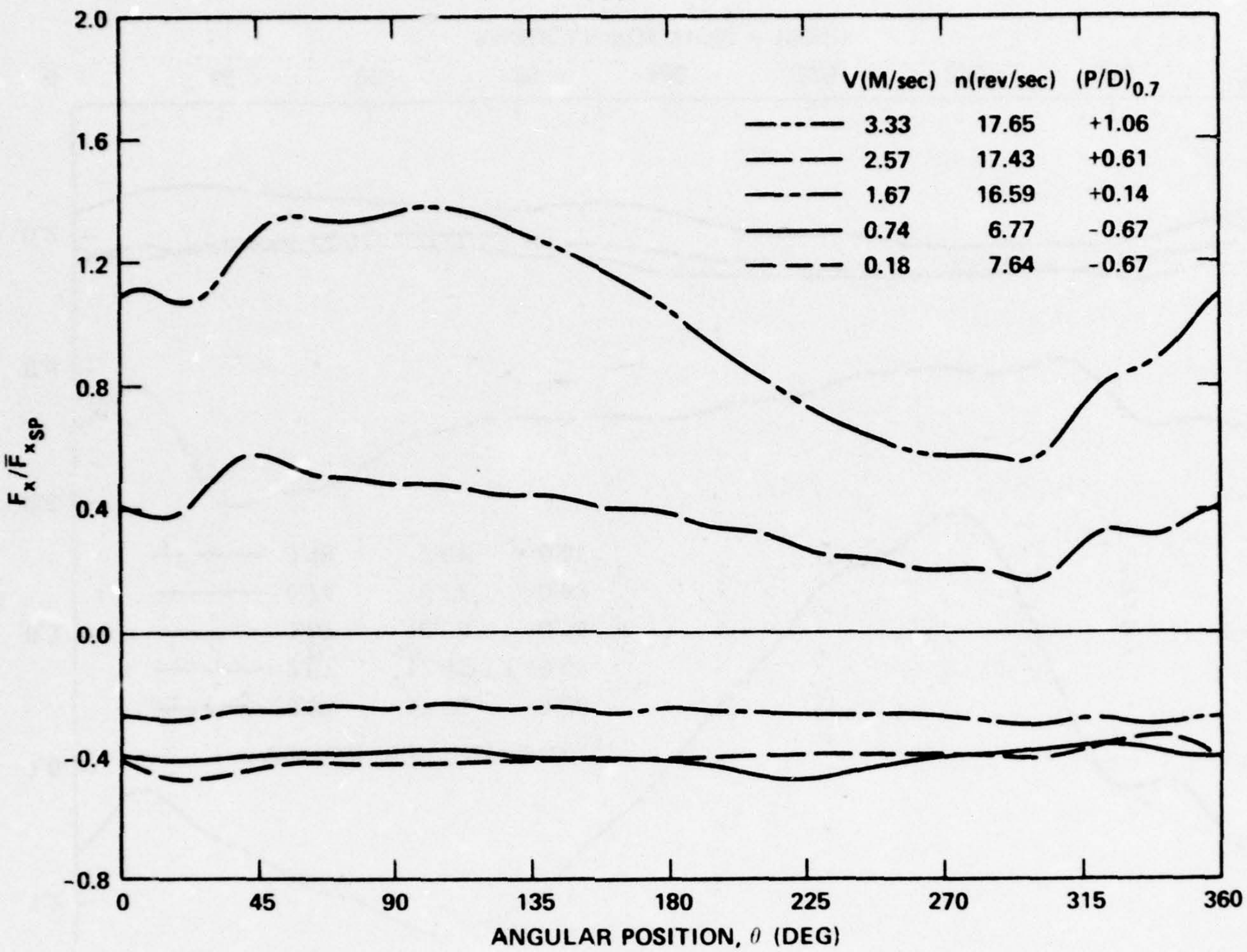

Figure 21a - F_x

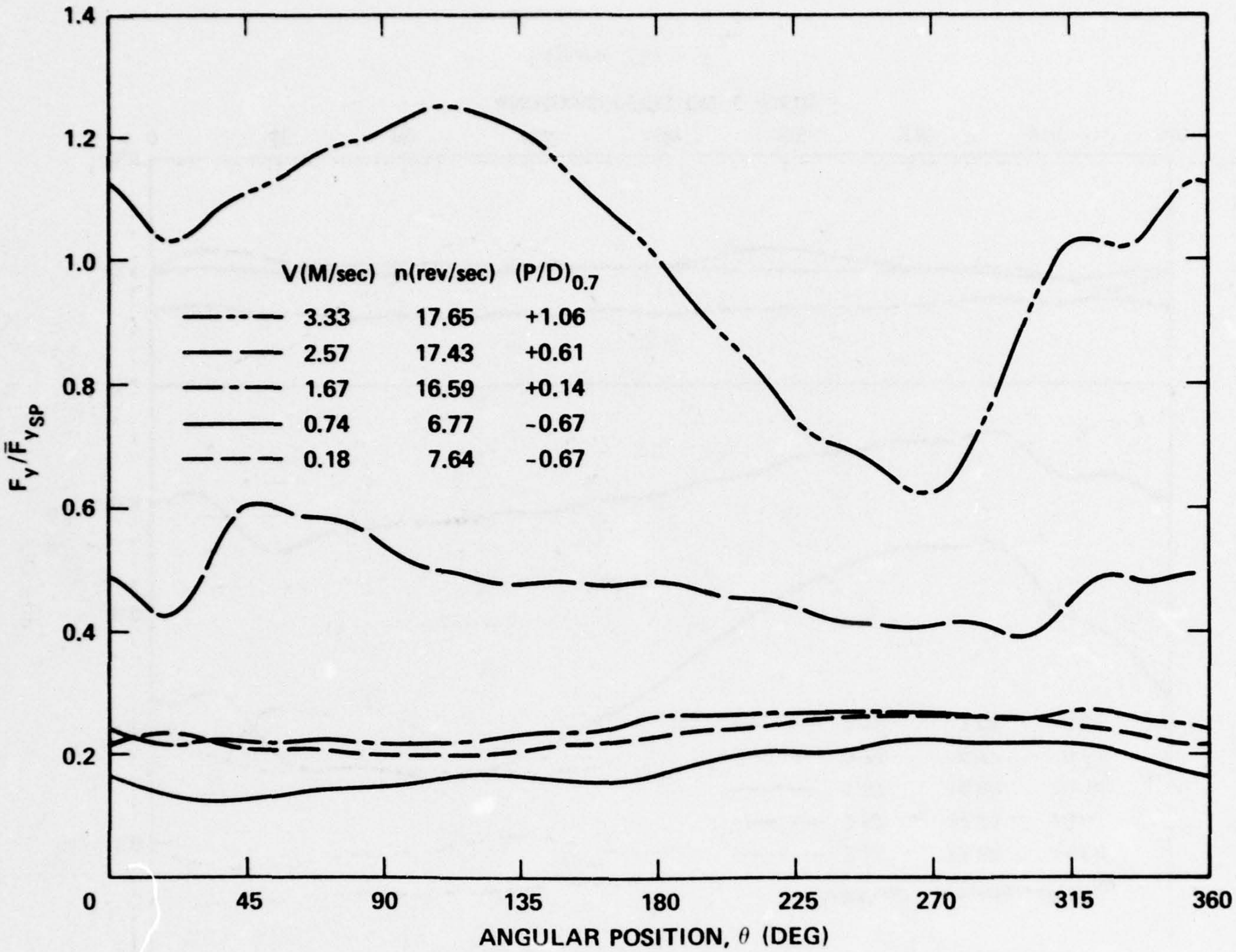

Figure 21b- F_y

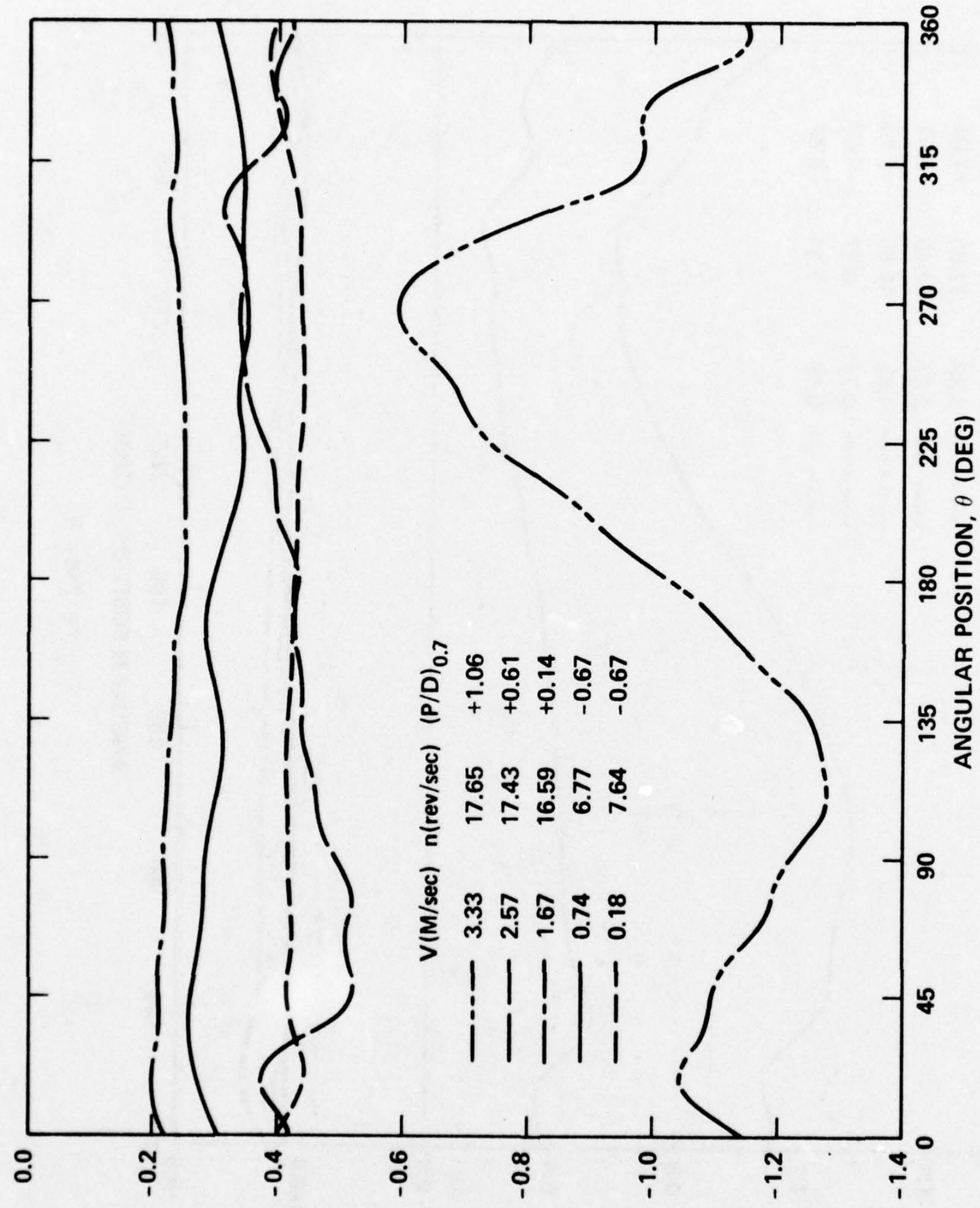

Figure 21c- M_x

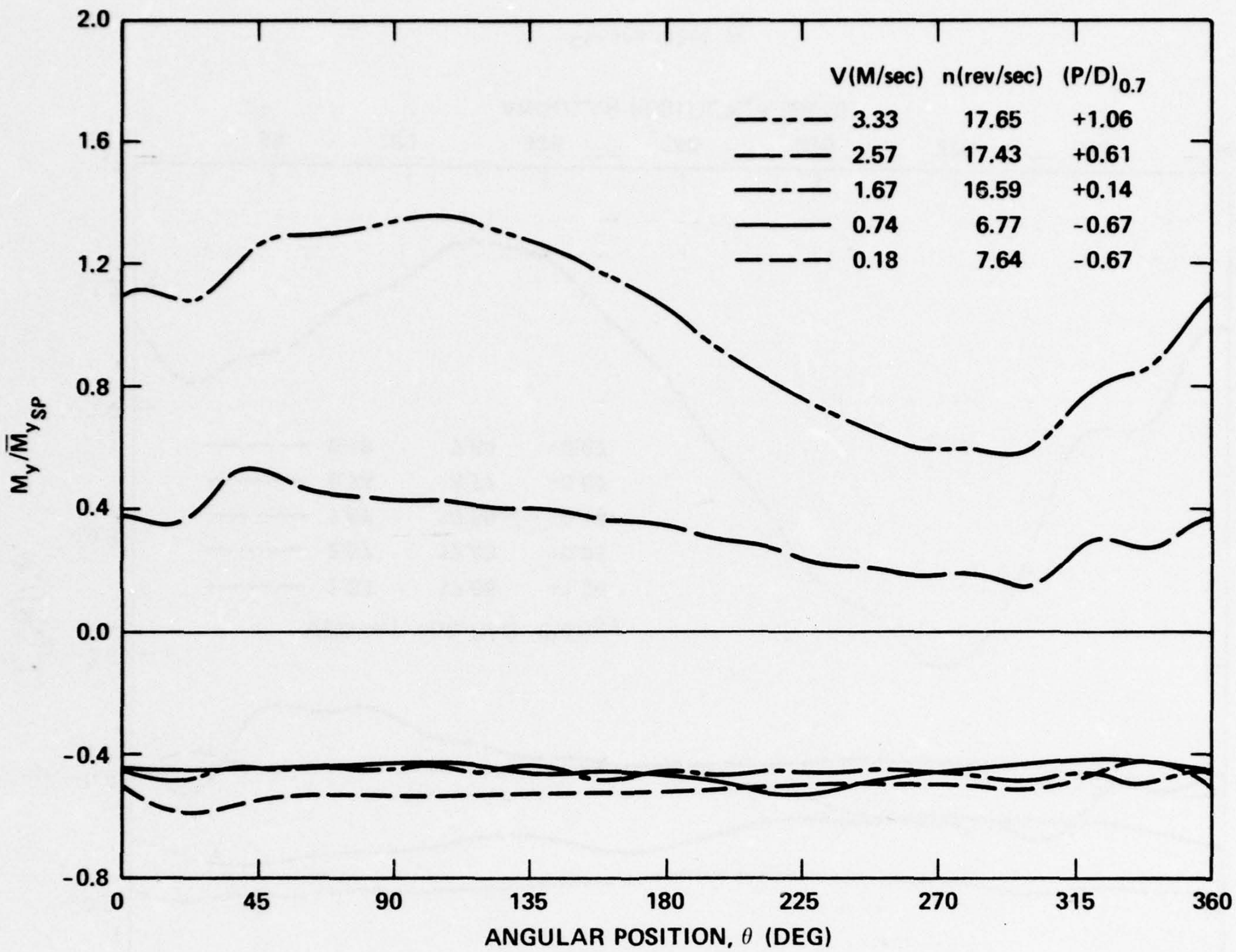

Figure 21d- M_y

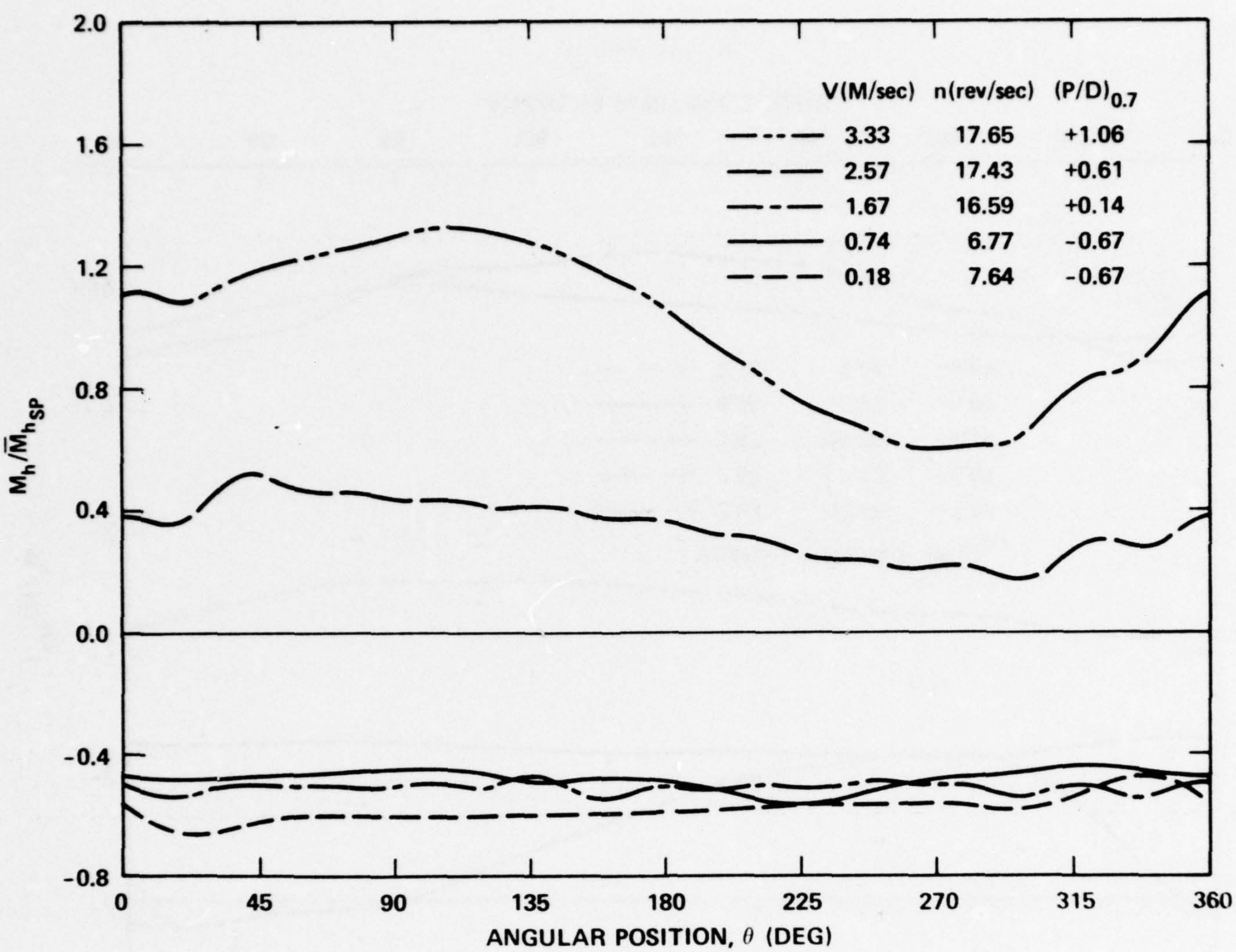

Figure 21e- M_h

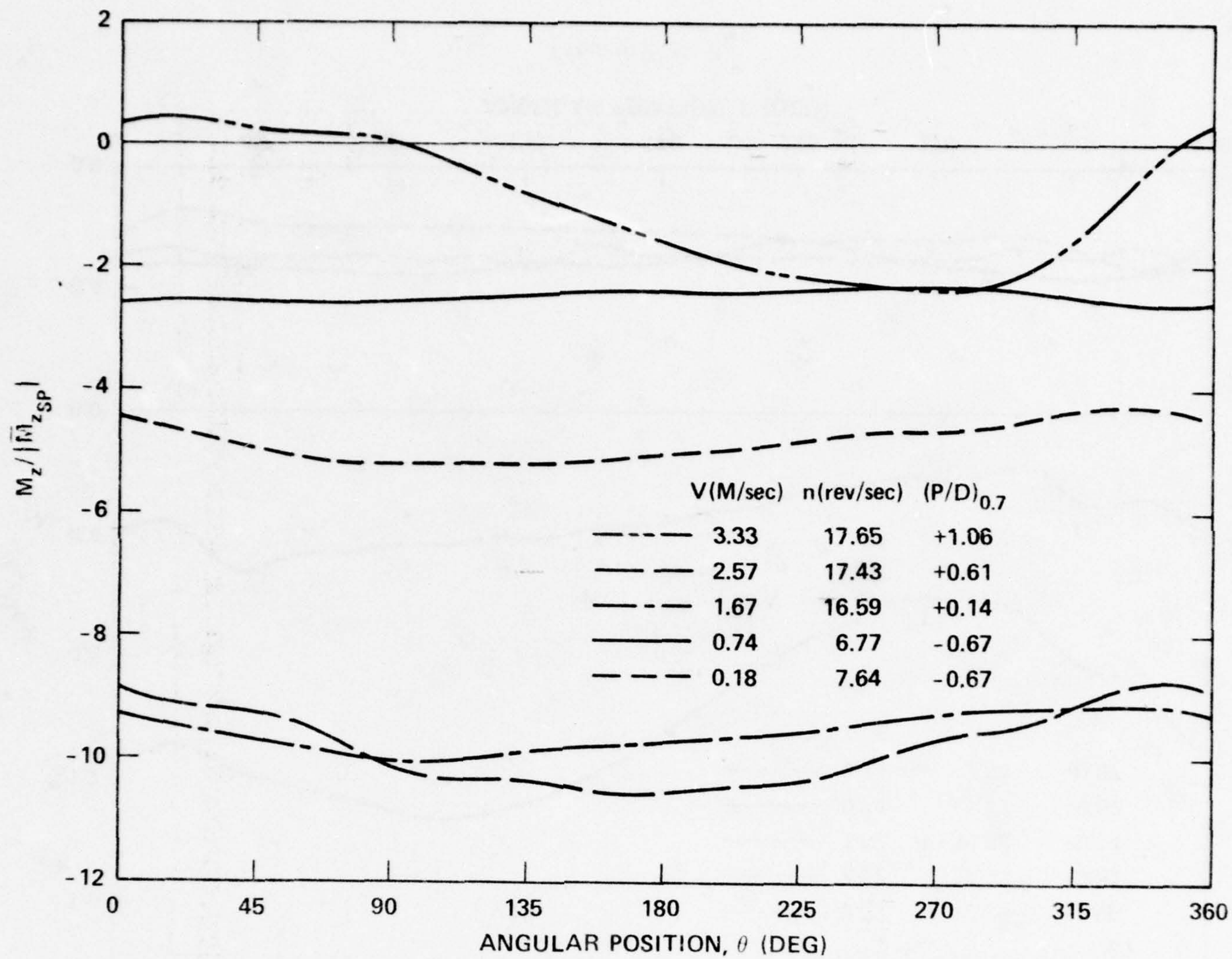

Figure 21f- M_Z

Figure 22 - Harmonic Content of F_X for Quasi-Steady Crash Astern

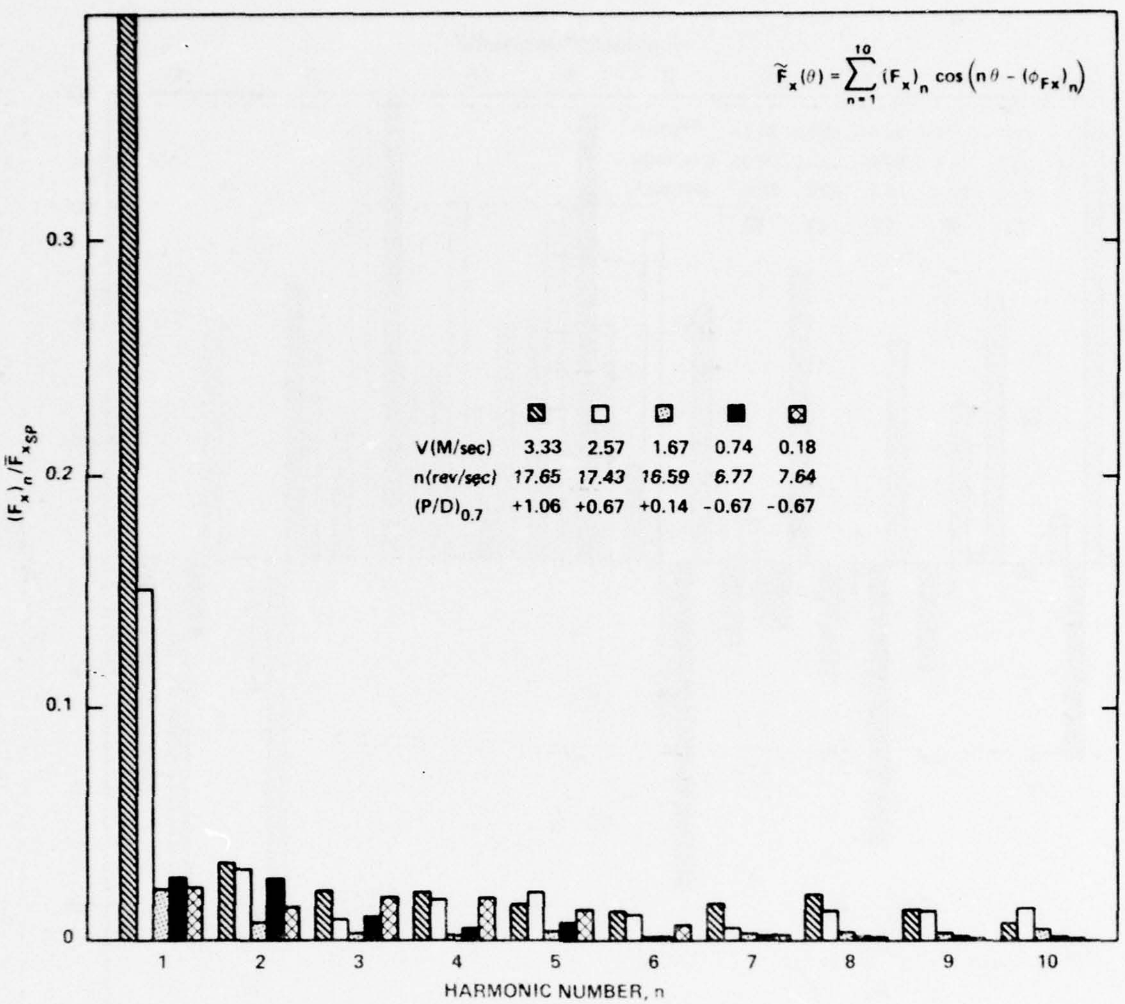

Figure 22a - Amplitudes

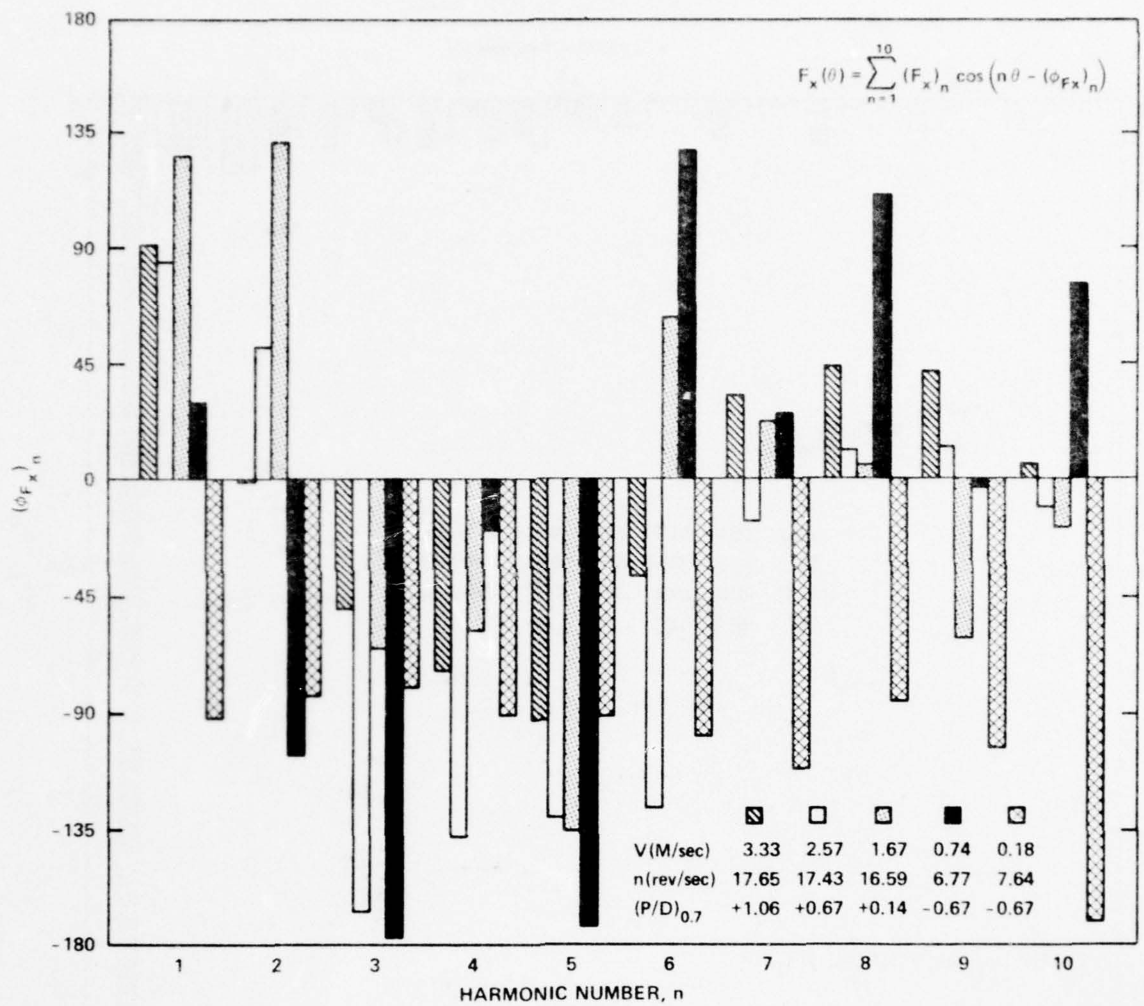

Figure 22b - Phases

Figure 23 - Taylor Wake Fractions during Simulated Crash Ahead and Crash Astern Maneuvers

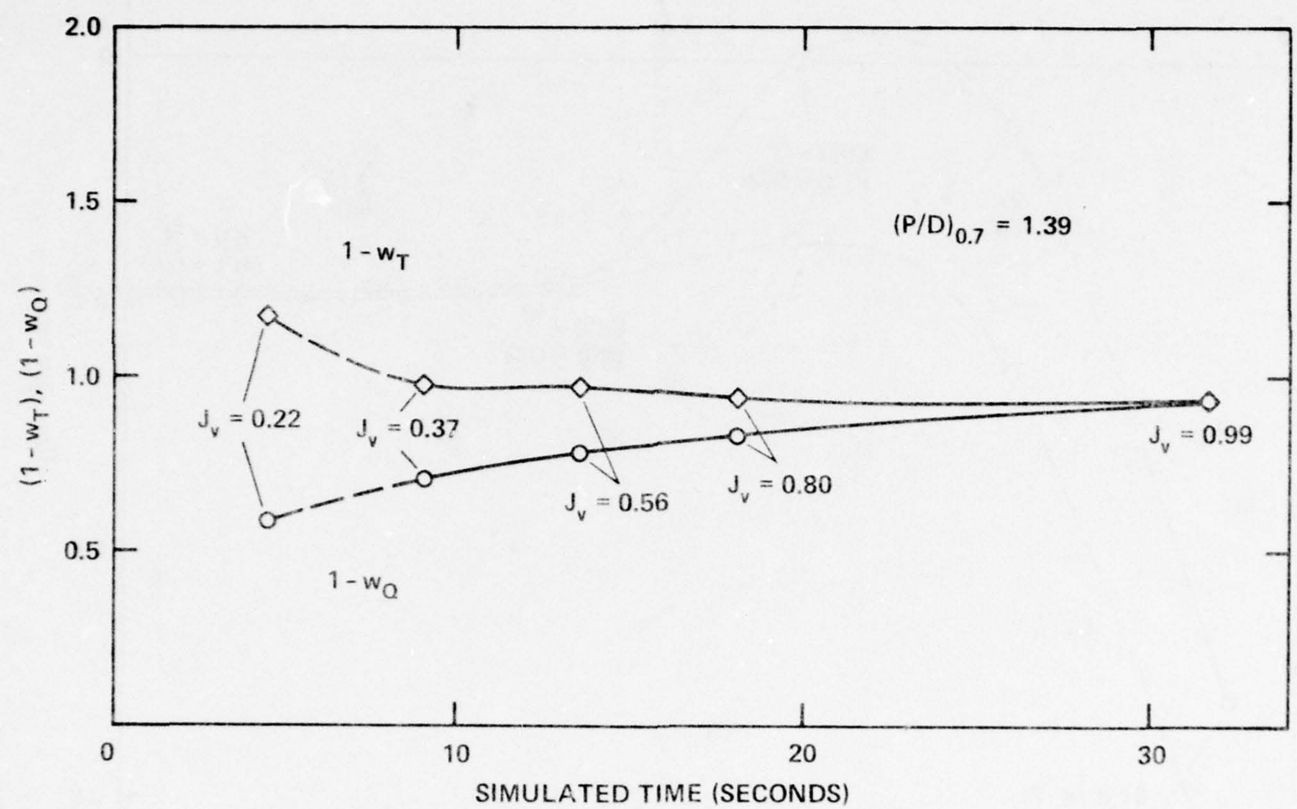

Figure 23a - Crash Ahead

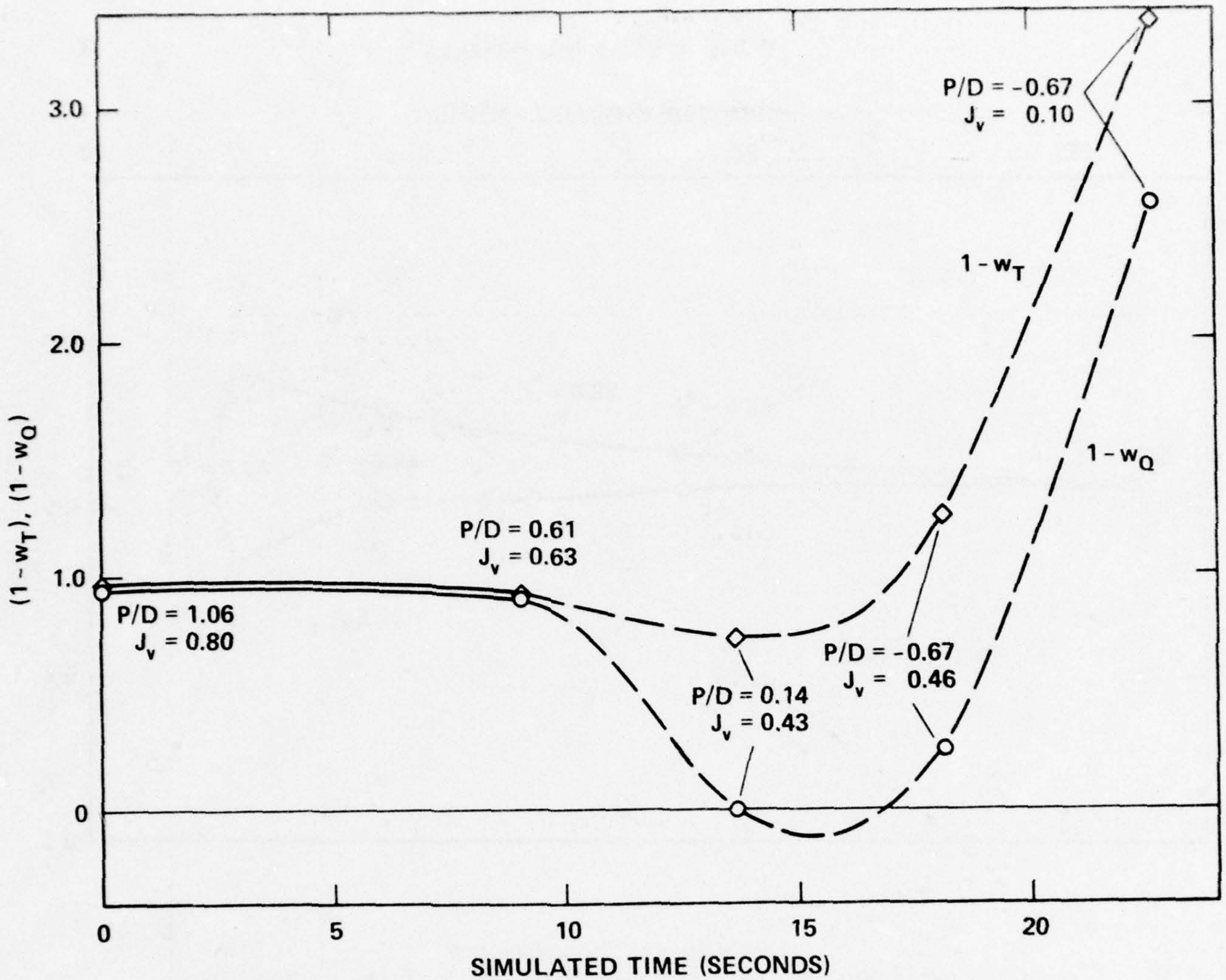

Figure 23b - Crash Astern

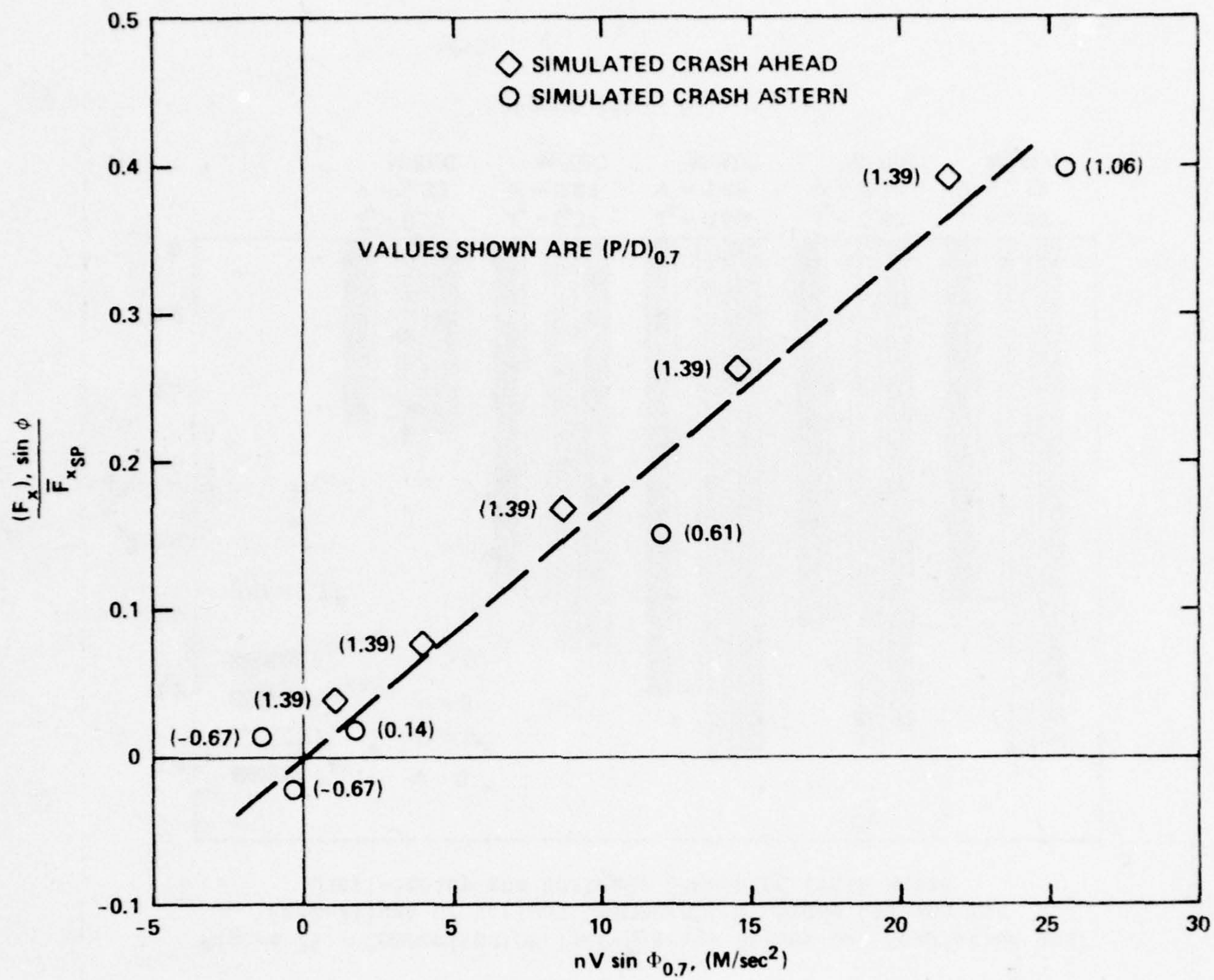

Figure 24- Variation of $(F_x)_1 \sin\phi/\overline{F}_{xSP}$ with $nV \sin\phi$ for Quasi-Steady Crash Ahead and Crash Astern

Figure 25 - Comparison of Time-Average Values per Revolution and Peak Values of Various Components of Blade Loading for Quasi-Steady and Unsteady Simulated Crash Ahead

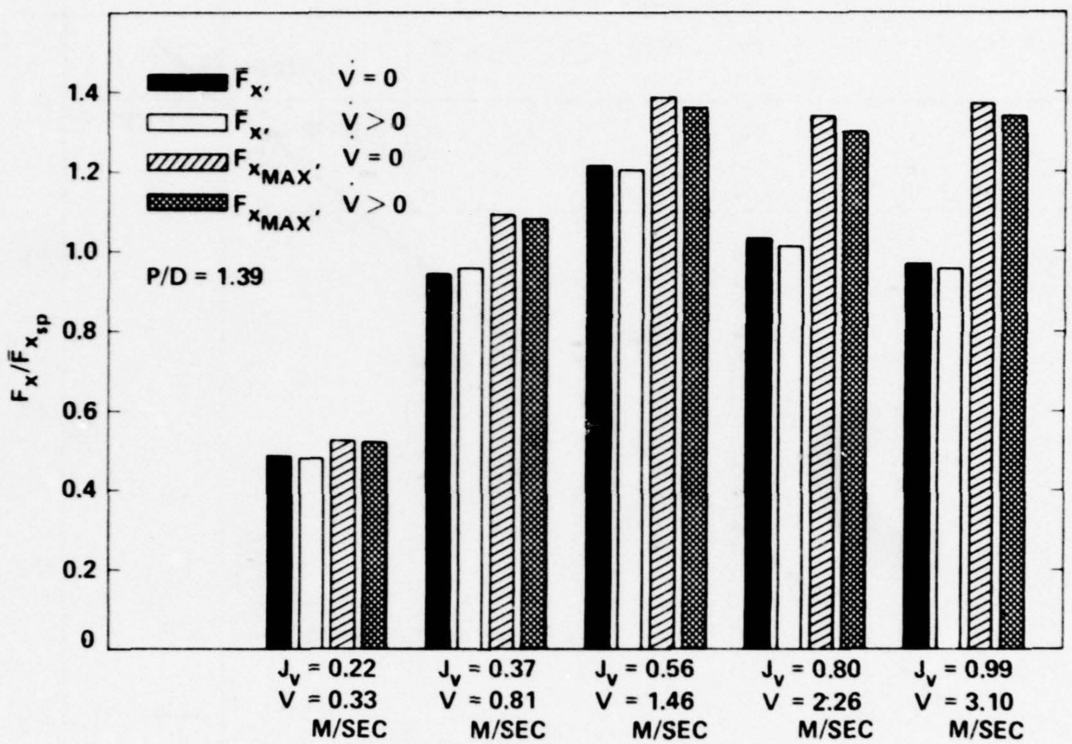

Figure 25a - F_x

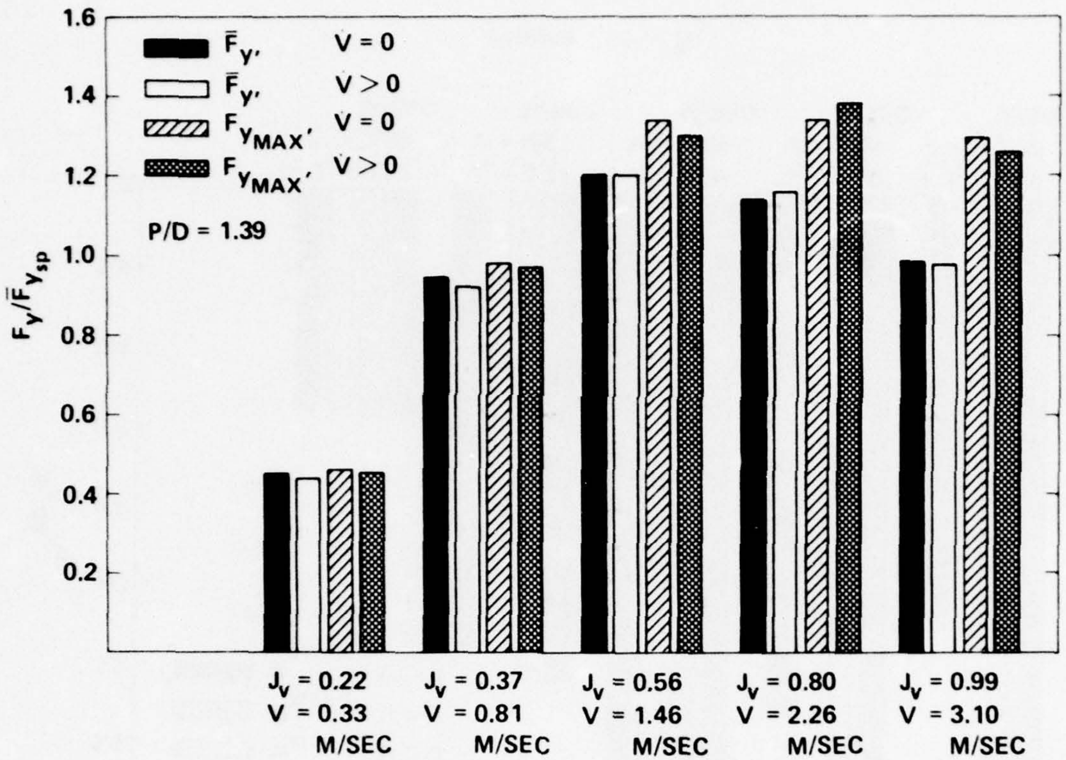

Figure 25b - F_y

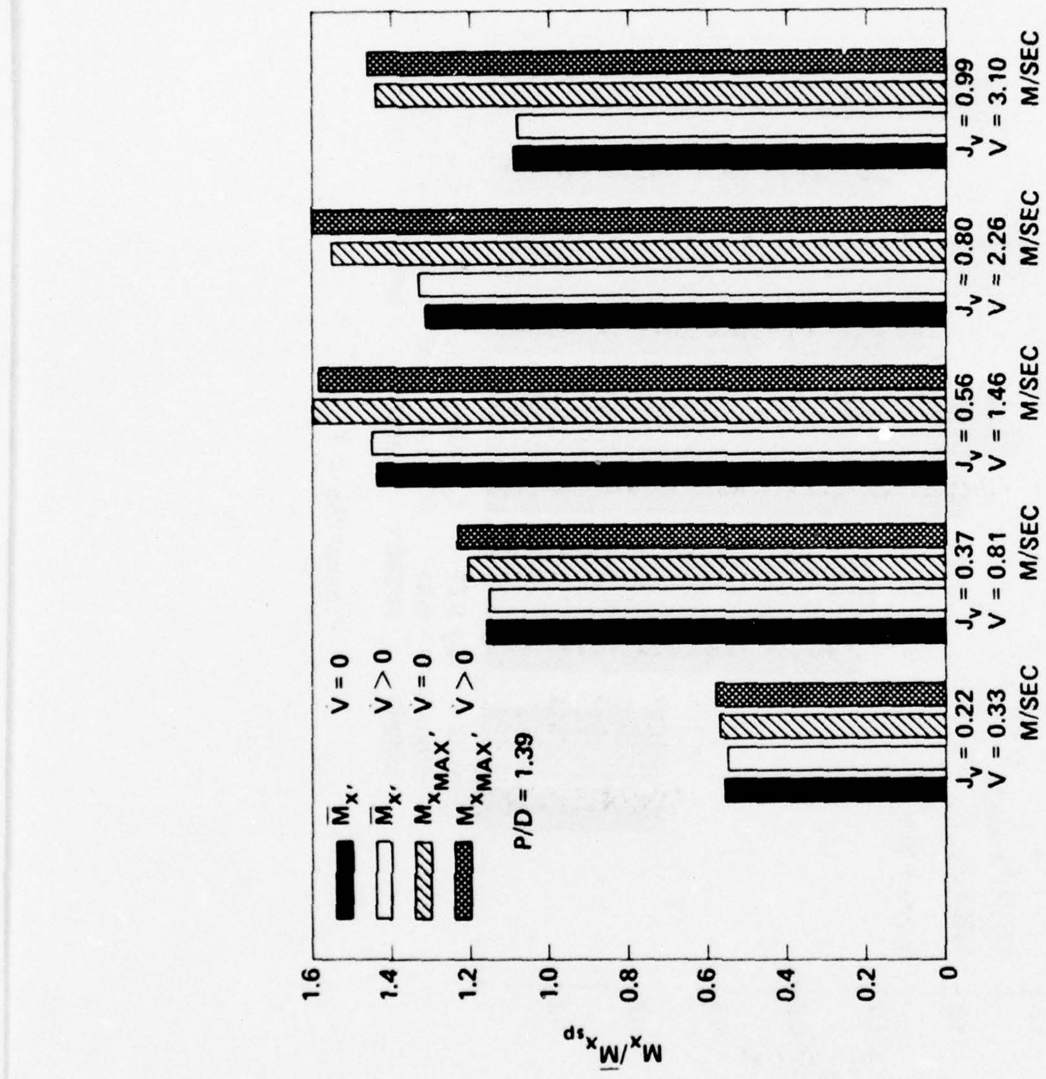

Figure 25c - M_x

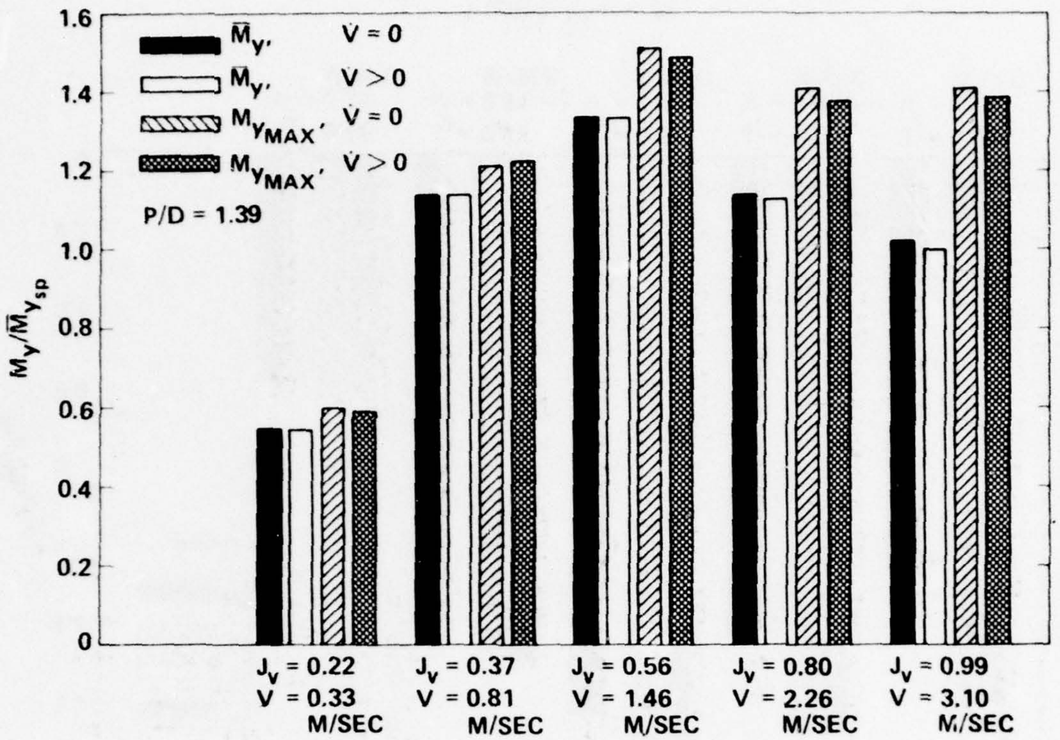

Figure 25d - M_y

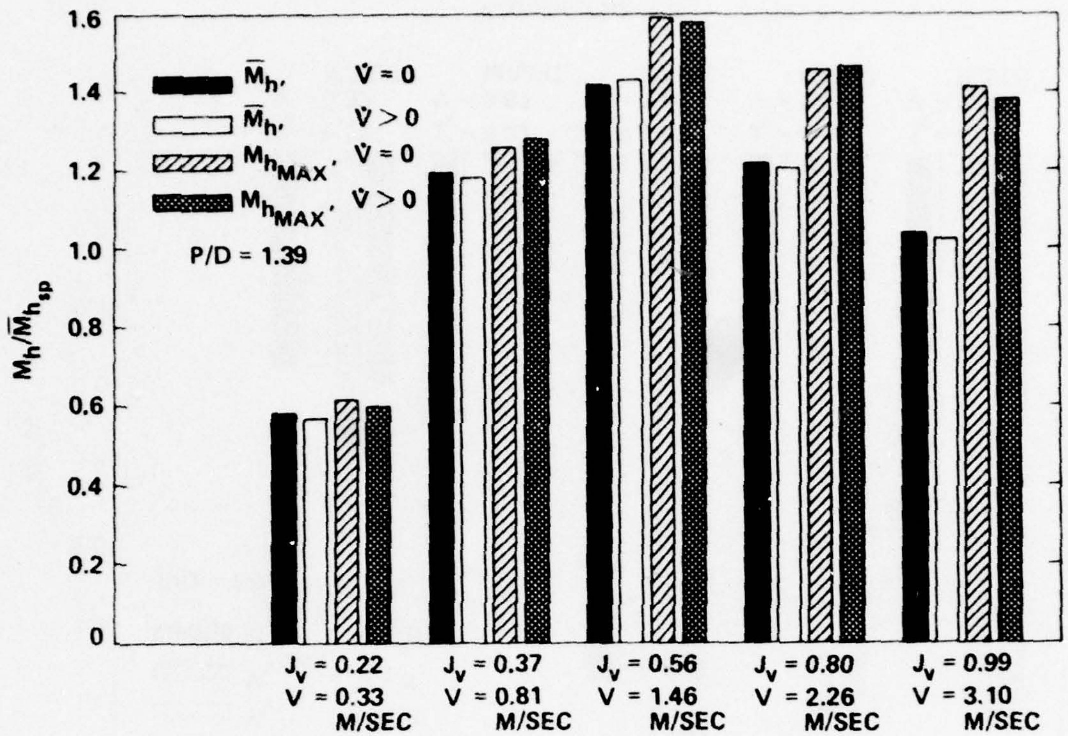

Figure 25e - M_h

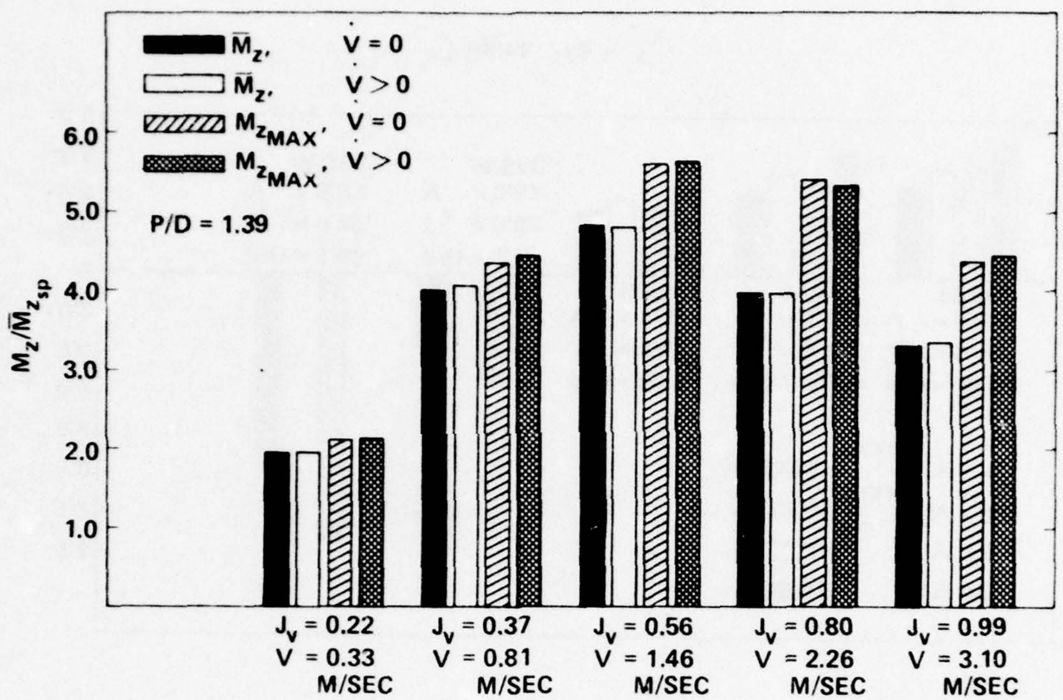

Figure 25f - M_z

Figure 26 - Comparison of Time-Average Values per Revolution and Peak Values of Various Components of Blade Loading for Quasi-Steady and Unsteady Simulated Crash Astern

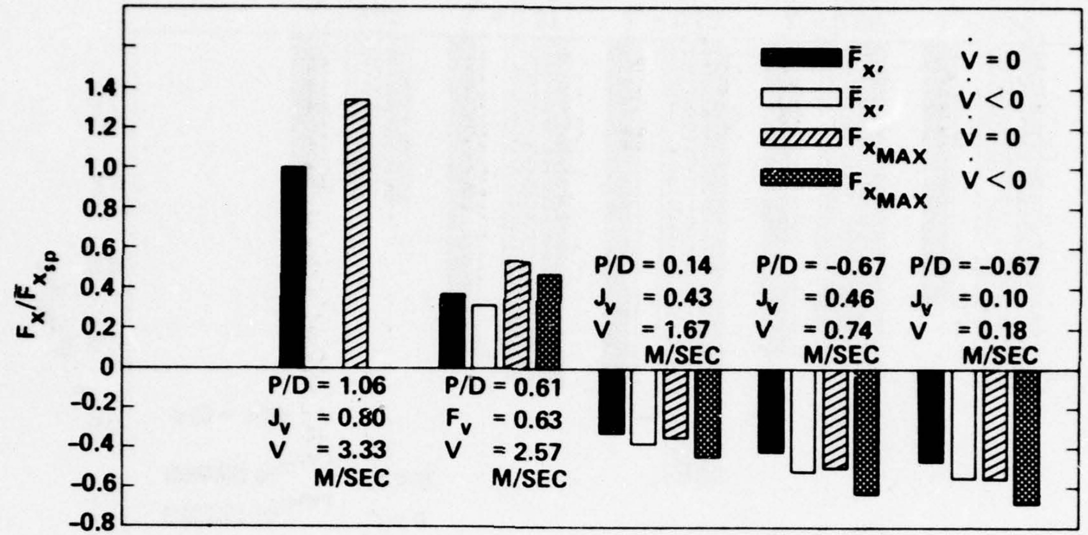

Figure 26a - F_x

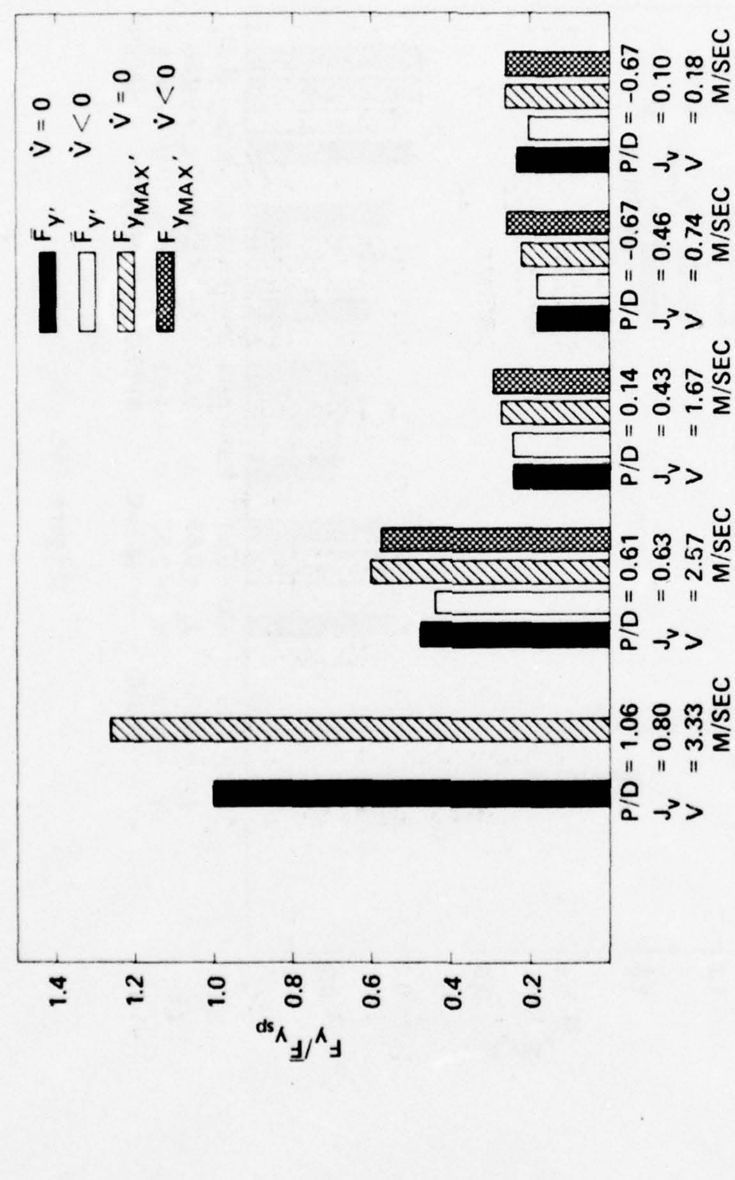

Figure 26b - F_y

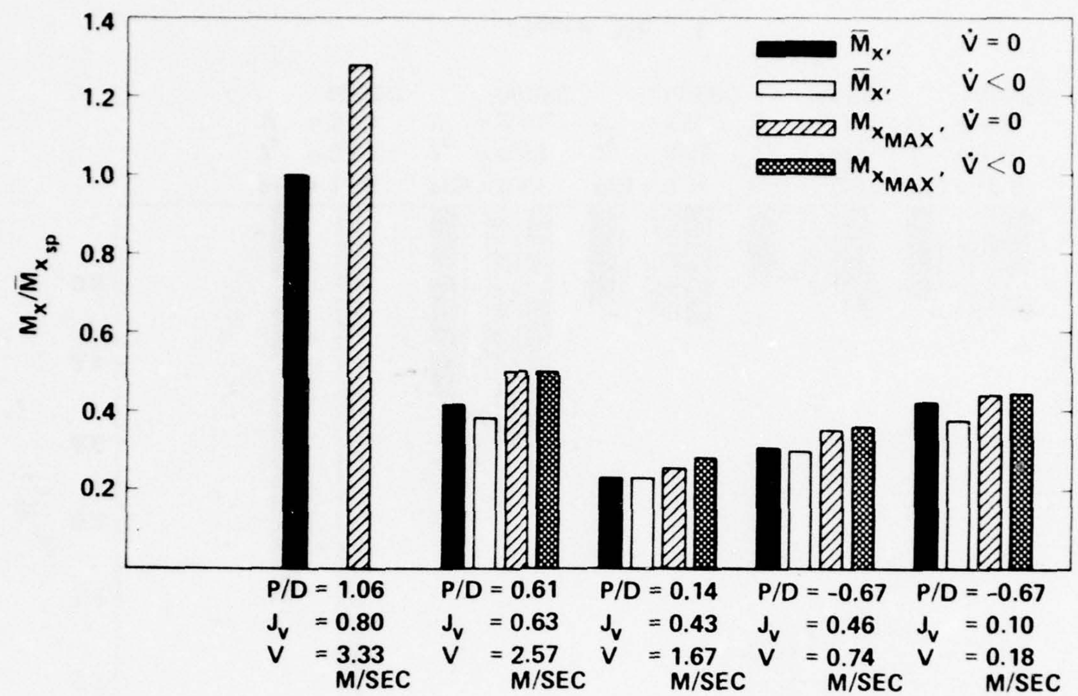

Figure 26c - M_X

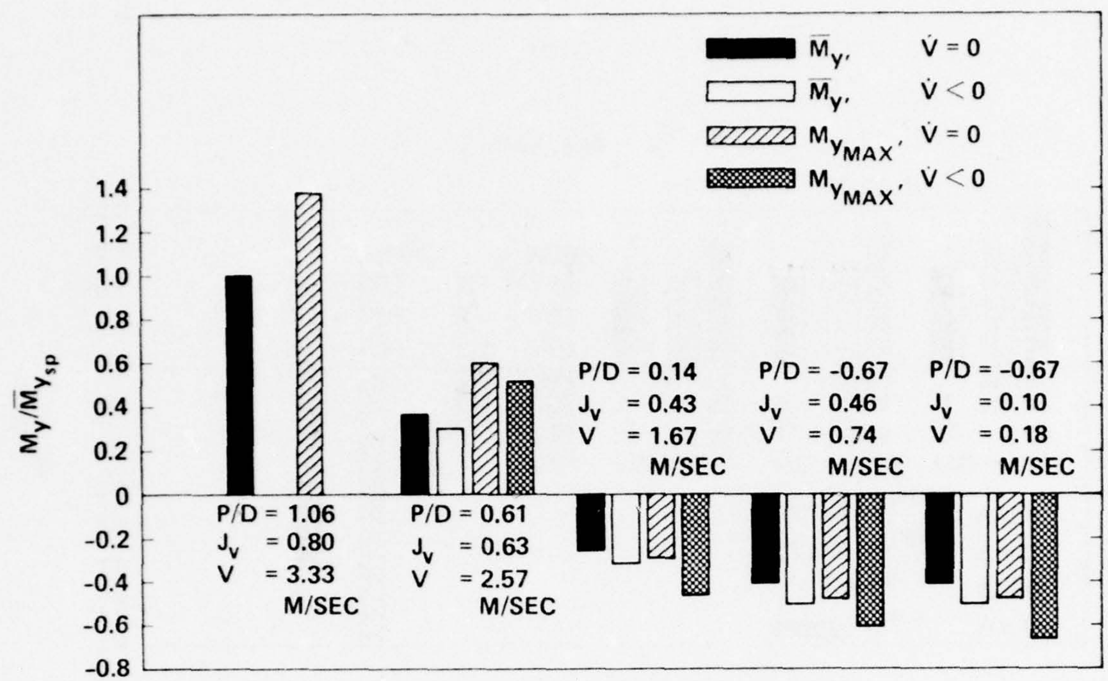

Figure 26d - M_y

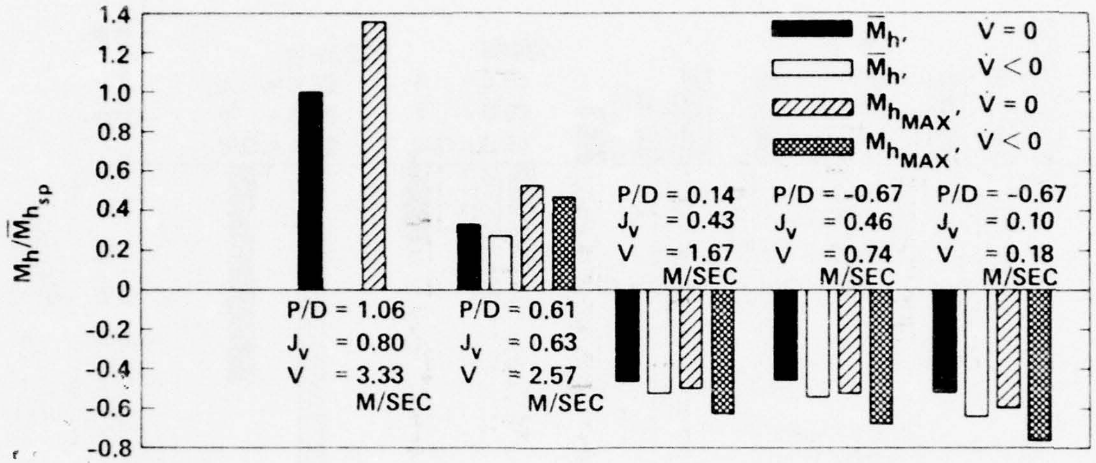

Figure 26e - M_h

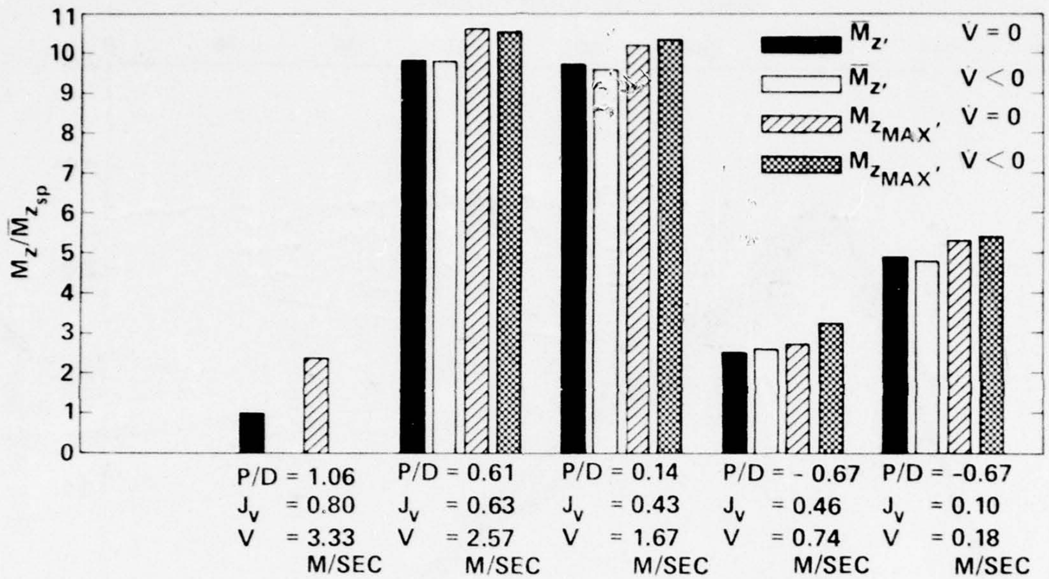

Figure 26f - M_z

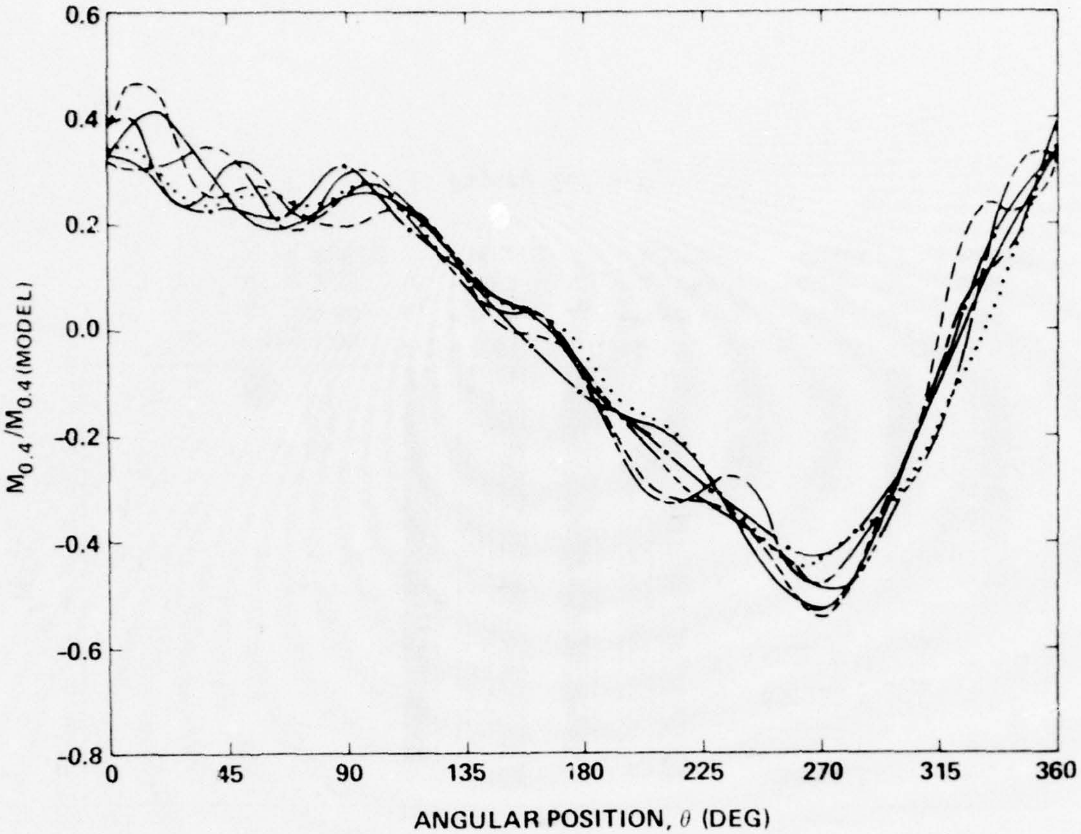

Figure 27 - Variation of Bending Moment with Blade Angular Position Measured on the Full-Scale Propeller for Six Individual Revolutions

Figure 28 - Harmonic Content of Blade Bending Moment on the Full-Scale Propeller for Six Individual Revolutions

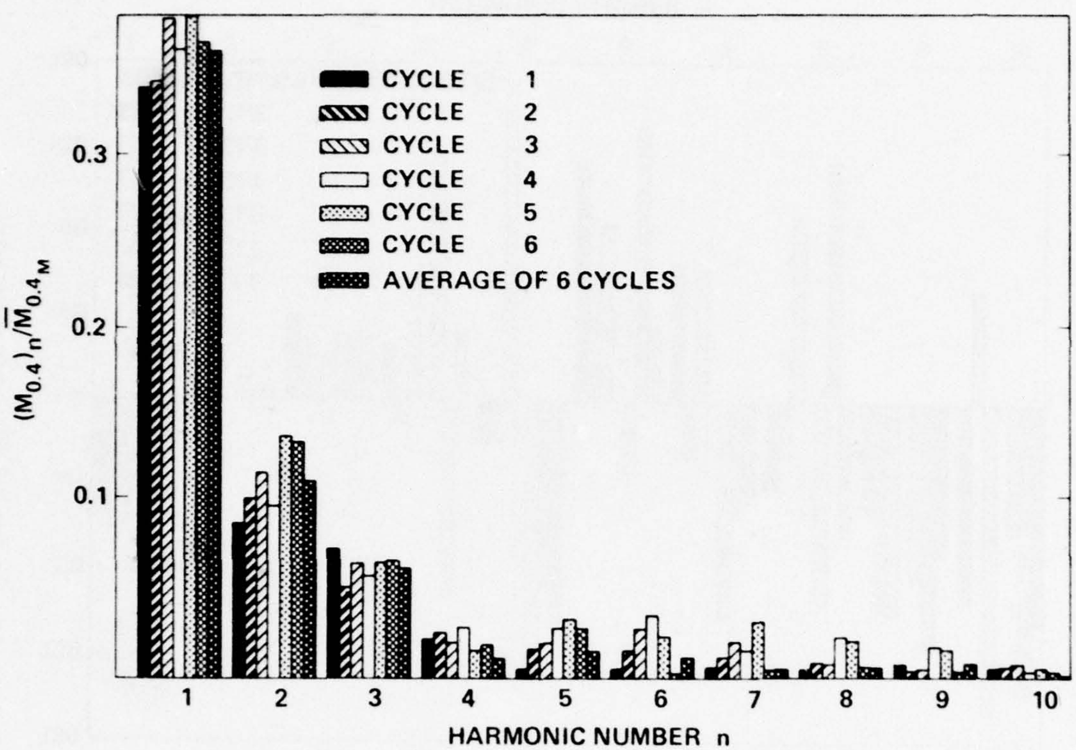

Figure 28a - Amplitudes

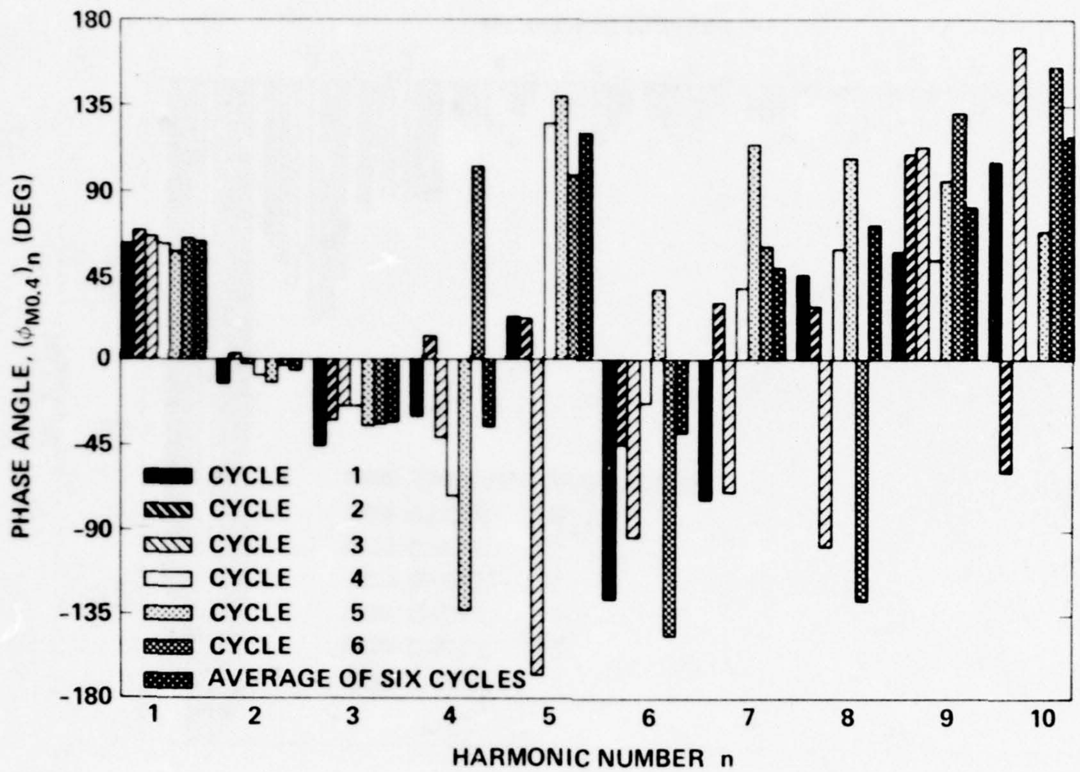

Figure 28b - Phases

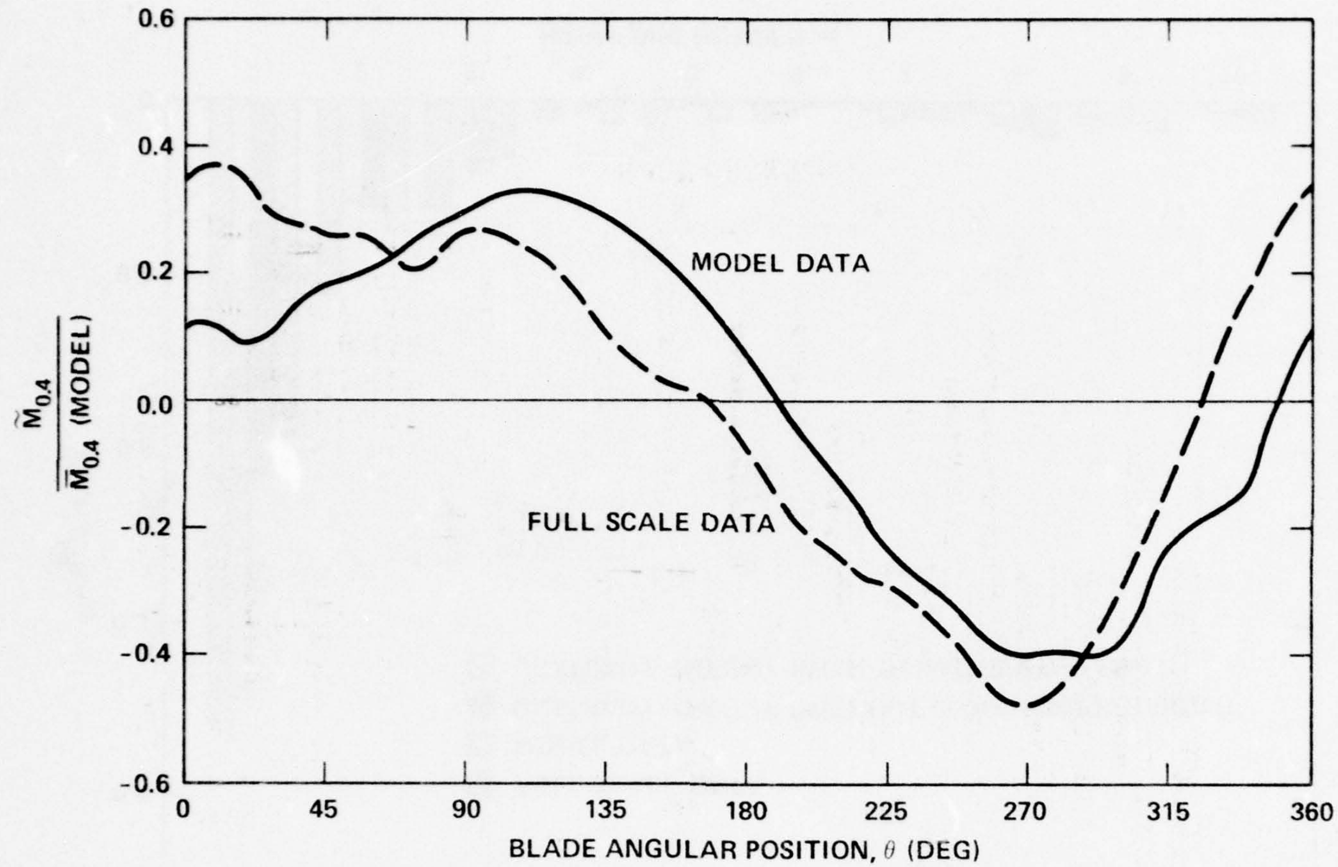

Figure 29- Variation of Bending Moment at 40 Percent Radius with Blade Angular Position, Comparison of Model Data and Scale Data

Figure 30- Harmonic Content of Bending Moment at 40 Percent Radius-Comparison of Model Data, Full Scale Data and Theory

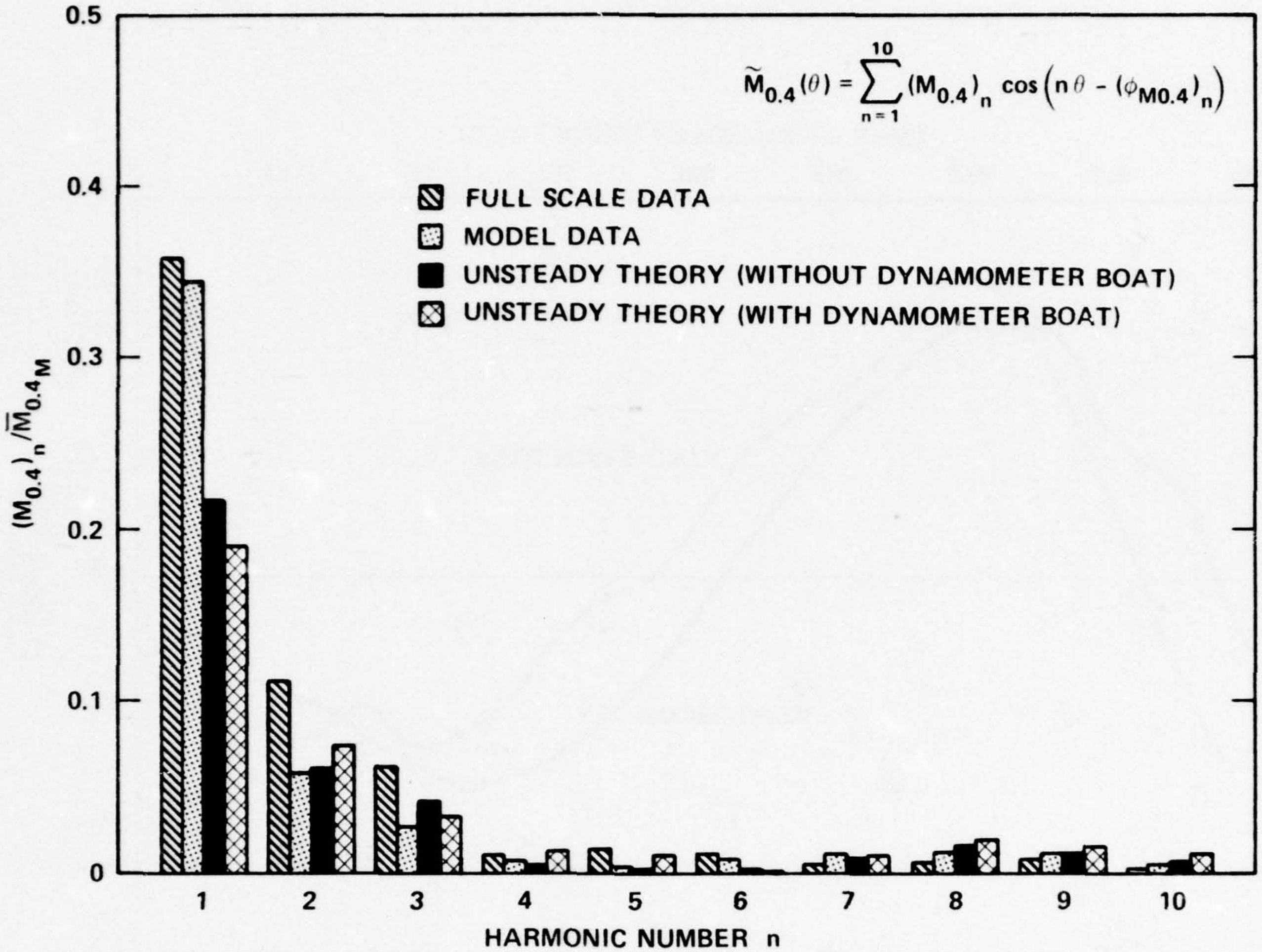

Figure 30a- Amplitudes

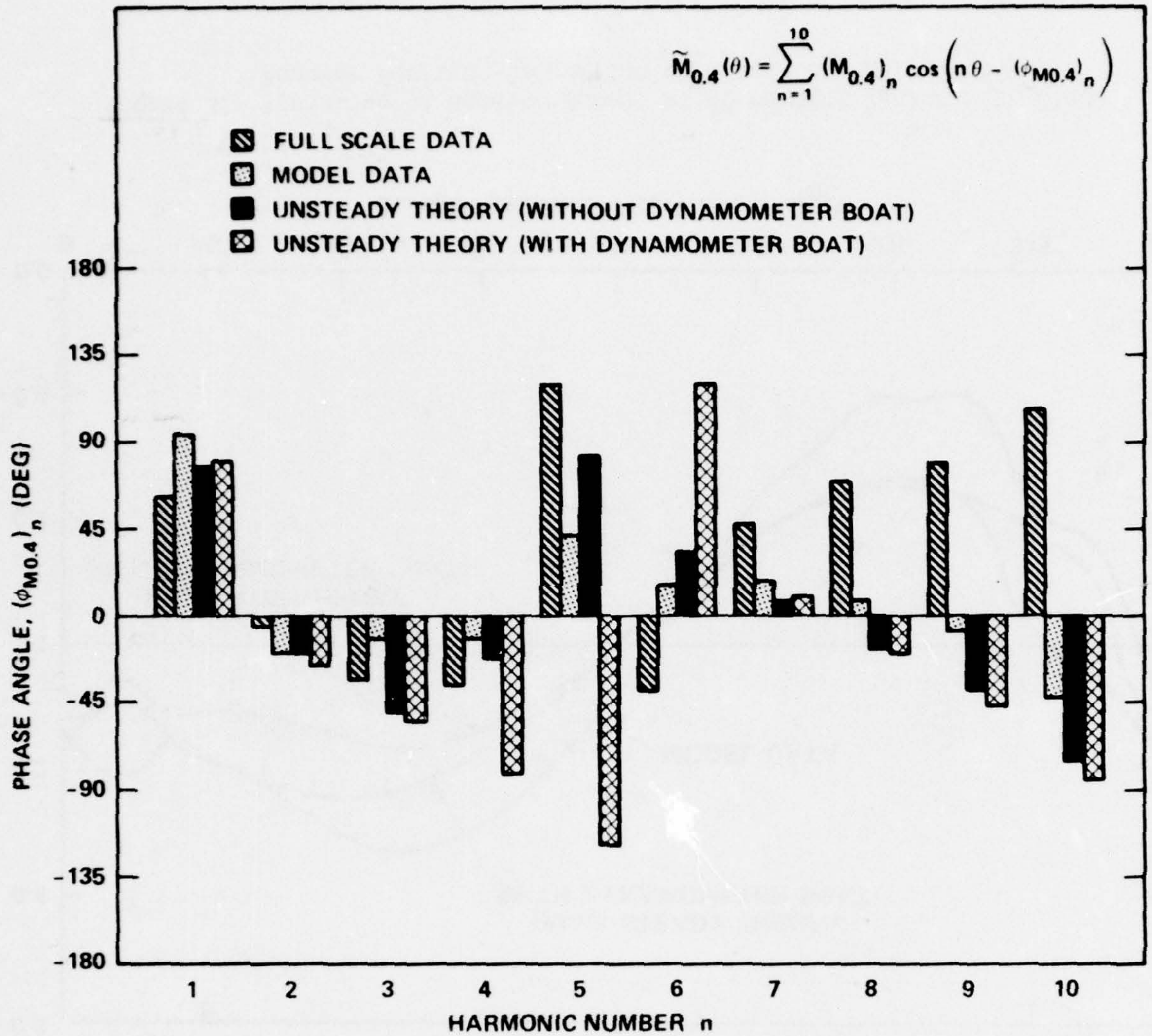

Figure 30b - Phases

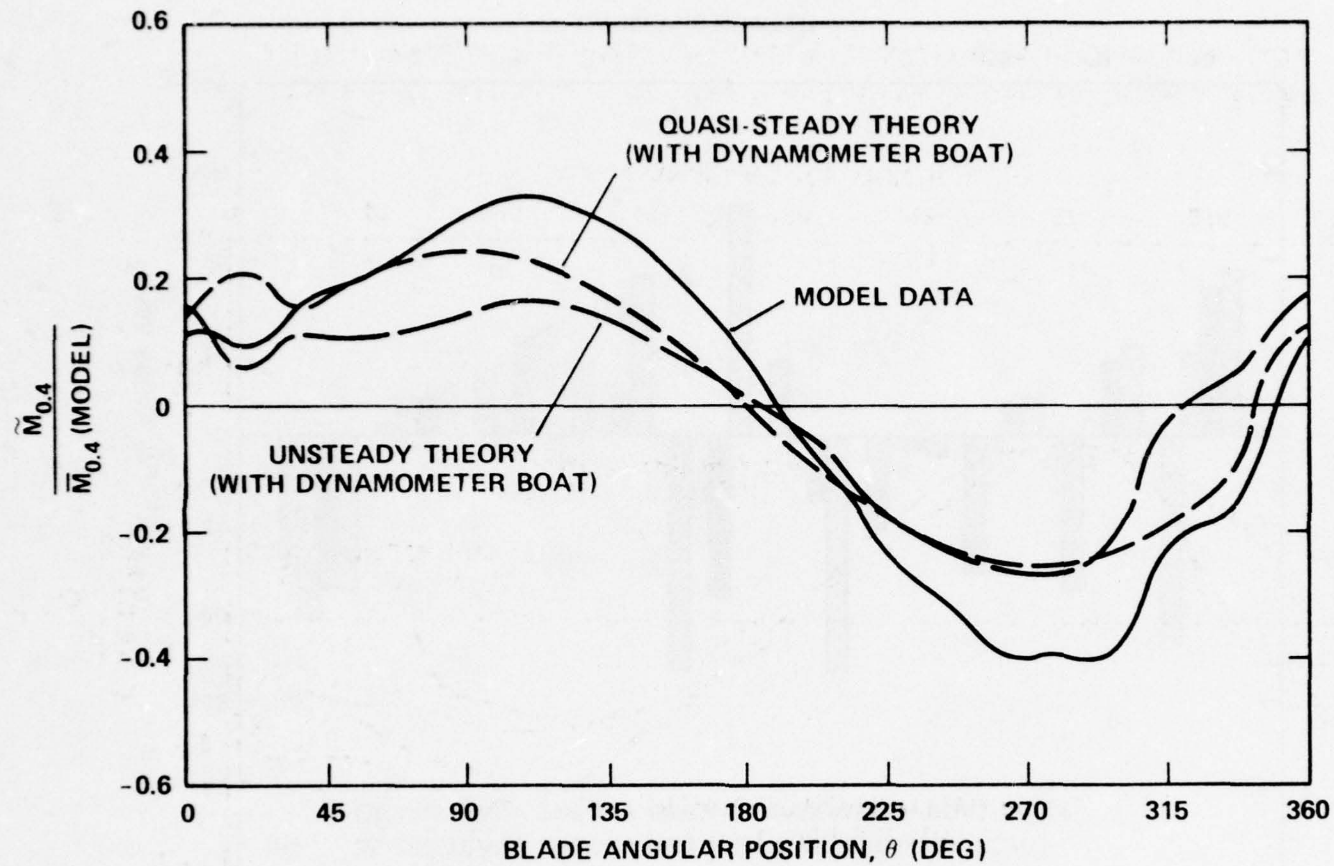

Figure 31- Variation of Bending Moment at 40 Percent Radius With Blade Angular Position-Comparison of Model Data with Theory

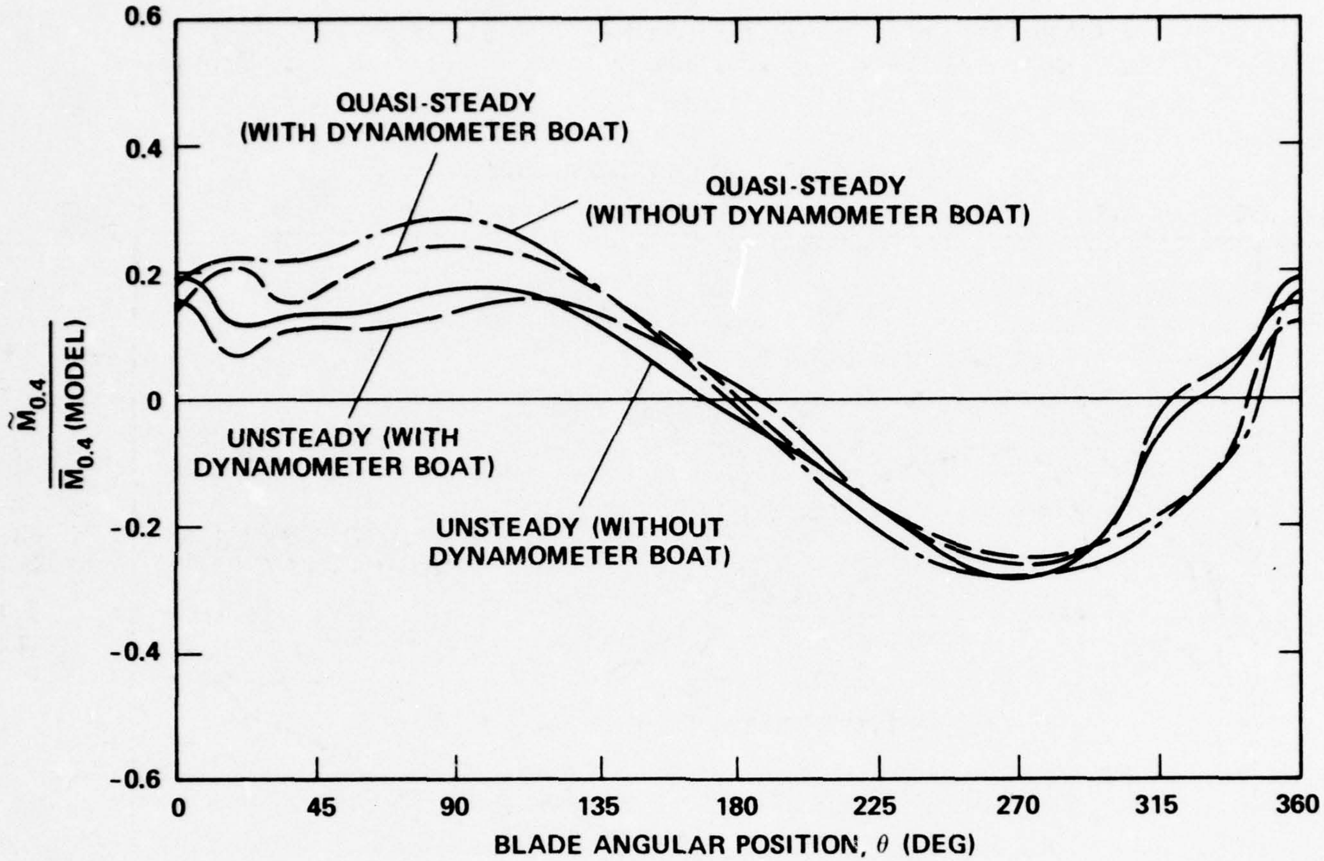

Figure 32 - Variation of Bending Moment at 40 Percent Radius With Blade Angular Position-Theoretical Prediction With and Without Downstream Body

APPENDIX A

DETAILS OF WAKES

Figure 33 and Tables 9 and 10 present the wake data measured in the plane of the propeller, both with and without the downstream dynamometer boat. The data presented in Figure 33 are similar to those in Figure 12 except that here wake harmonics are given at even radial stations whereas the data of Figure 12 are only for the radial stations at which the wake was measured. The data at even radial stations were obtained by extrapolation and interpolation of the measured data.[29] The wake data presented in Tables 9 and 10 are tabulated values of the data presented graphically in Figures 11, 12, and 33.

---

[29]Cheng, H.M., "Analysis of Wake Survey of Ship Models - Computer Program AML Problem No. 840-219F," David Taylor Model Basin Report 1804 (Mar 1964).

Figure 33 - Wake Harmonics

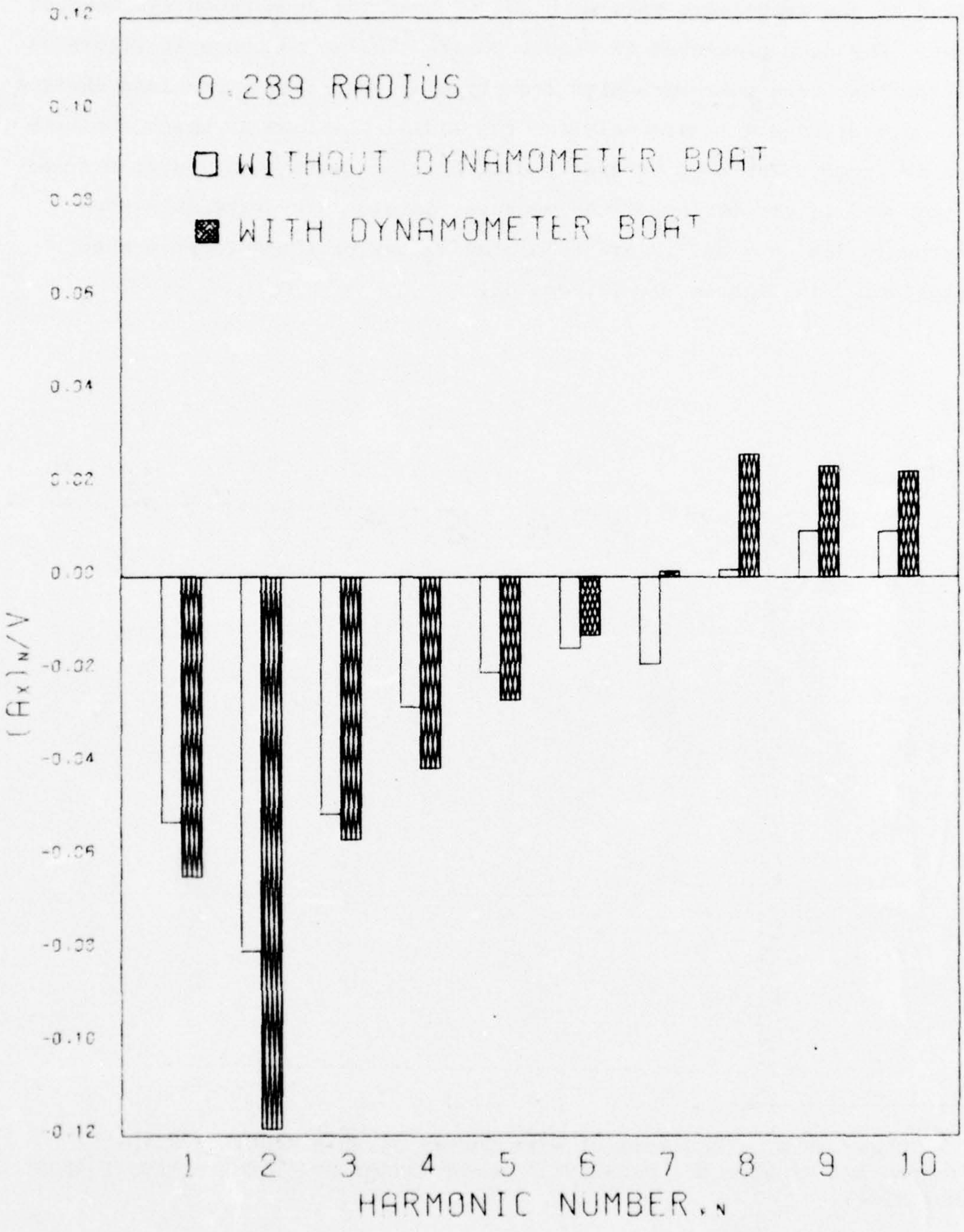

Figure 33 (Continued)

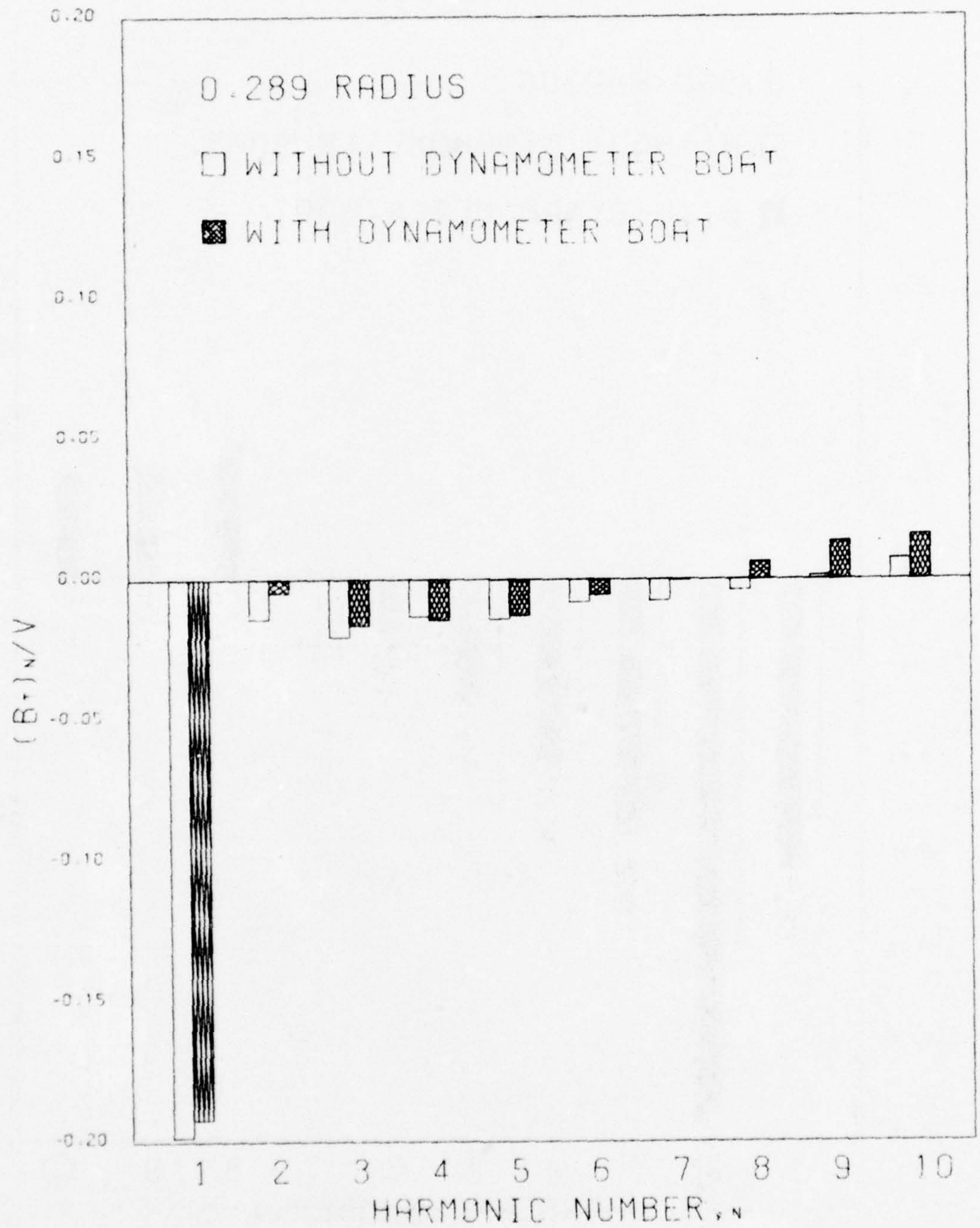

Figure 33 (Continued)

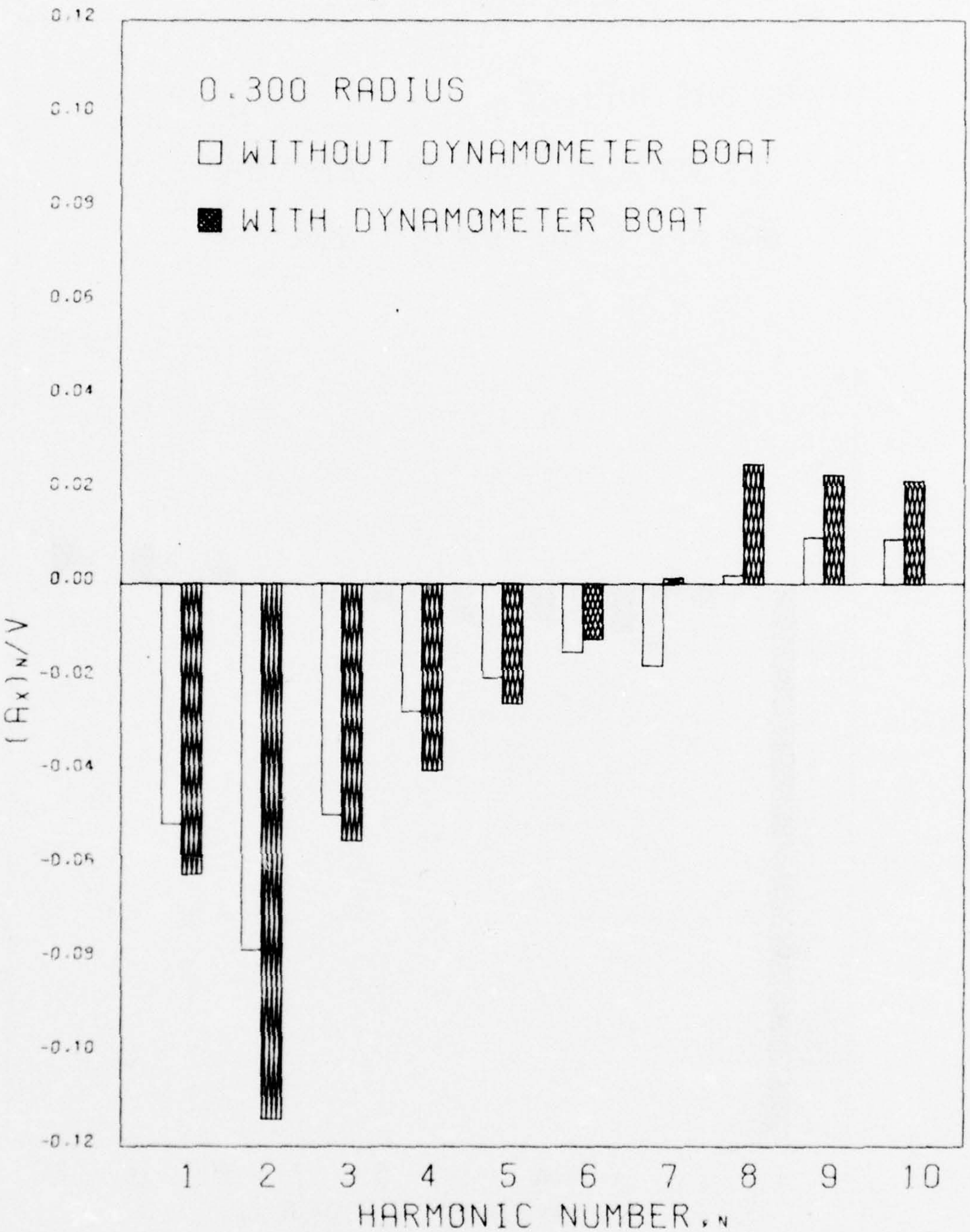

Figure 33 (Continued)

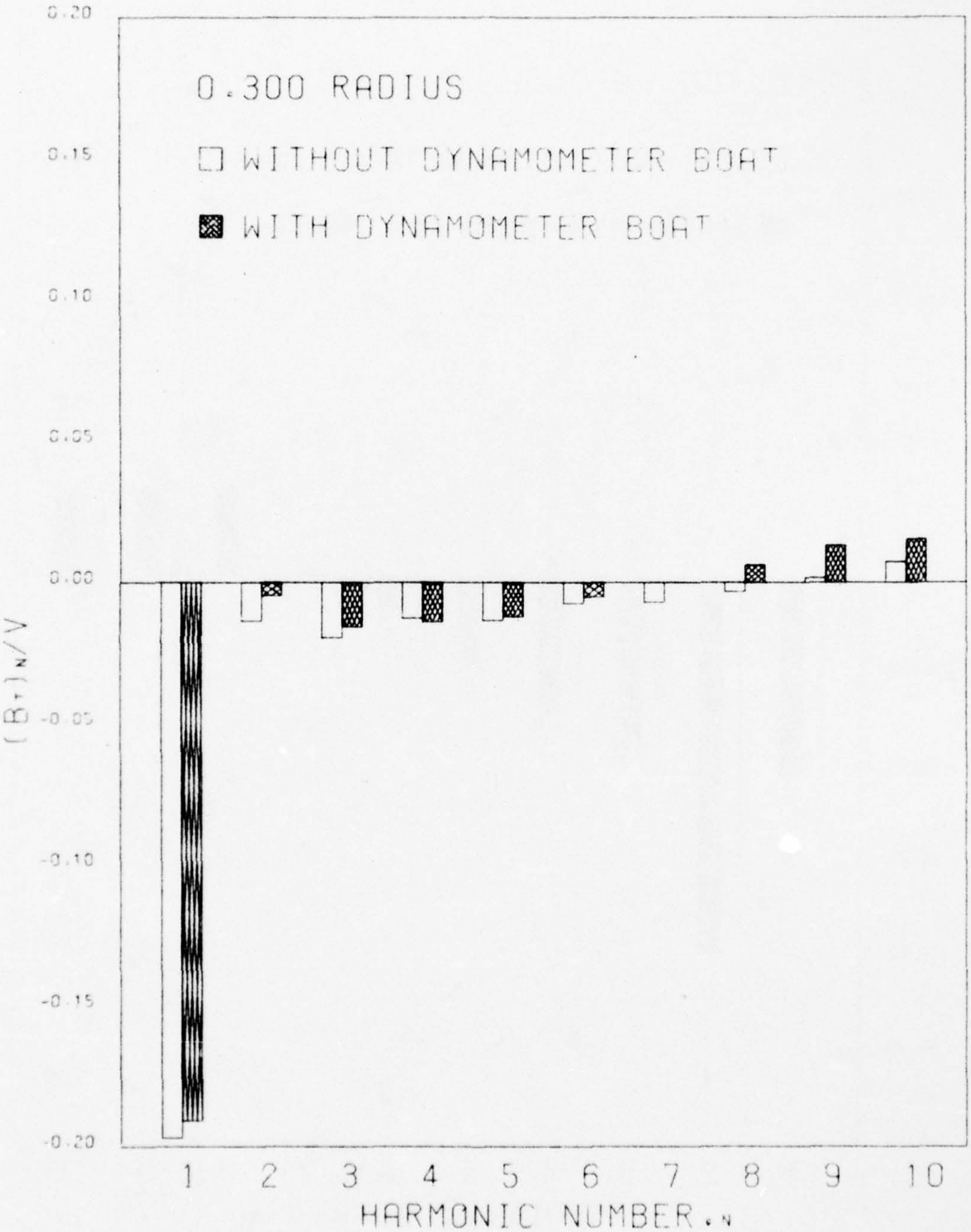

FIGURE 33 - WAKE HARMONICS(CONTINUED)

Figure 33 (Continued)

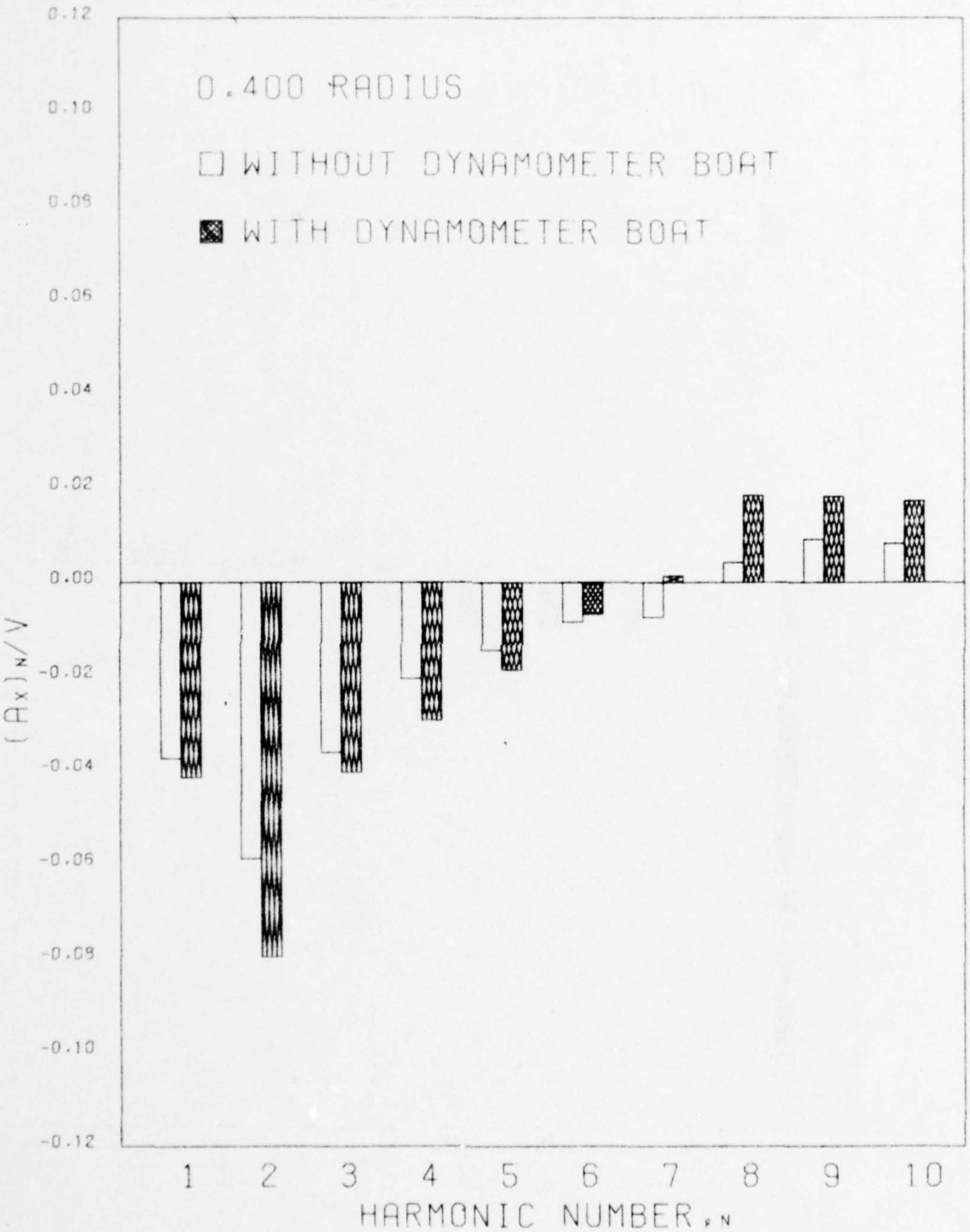

Figure 33 (Continued)

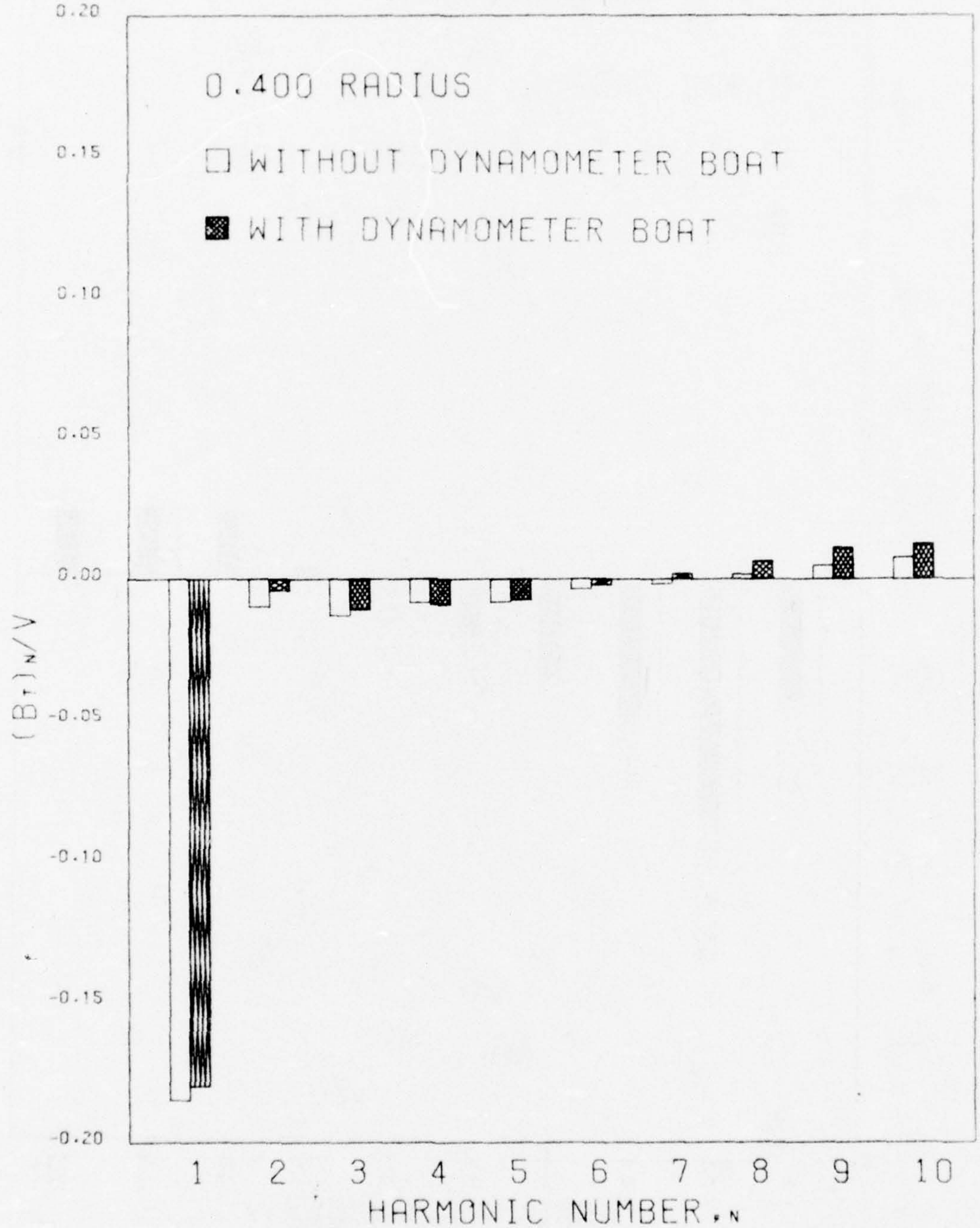

Figure 33 (Continued)

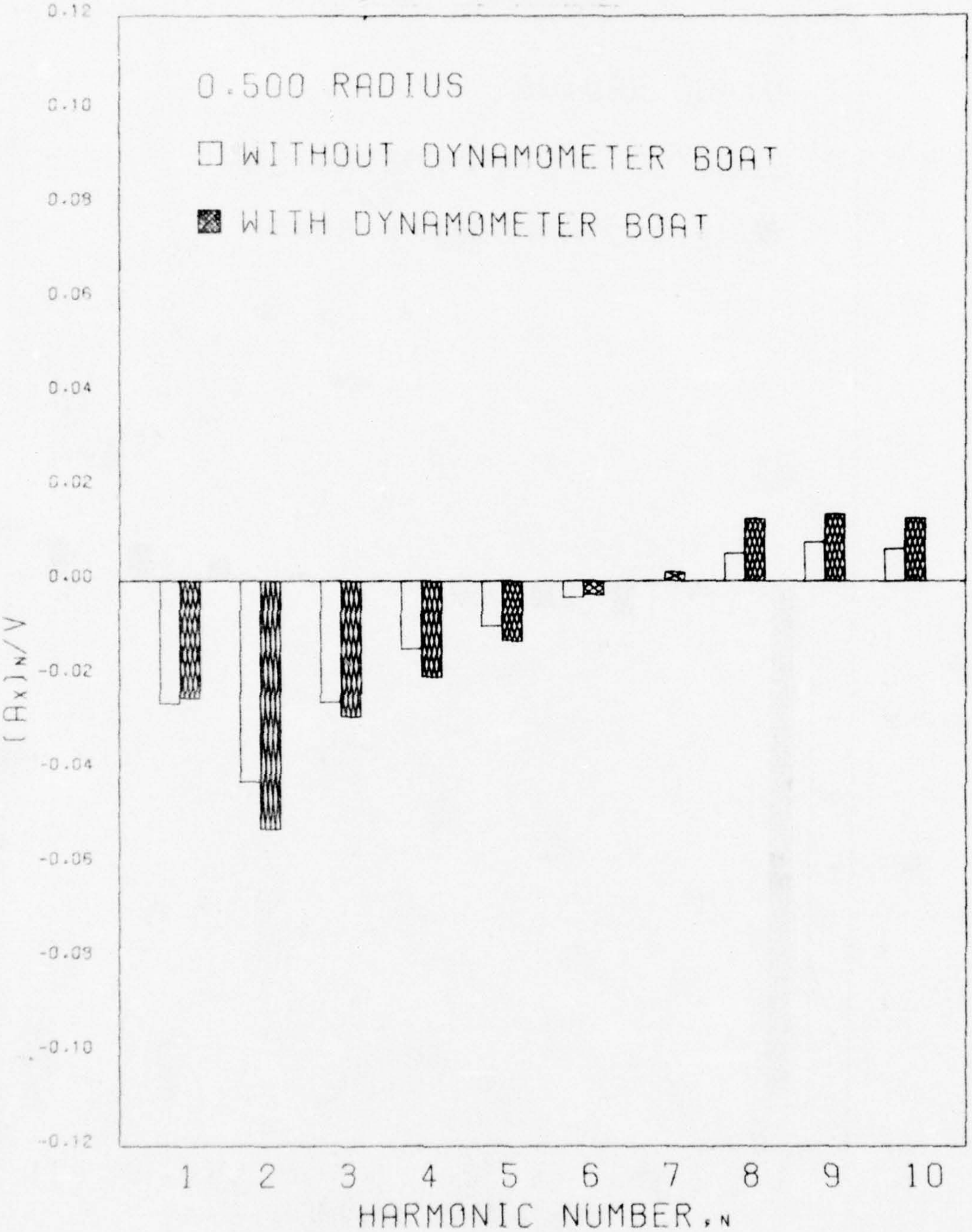

Figure 33 (Continued)

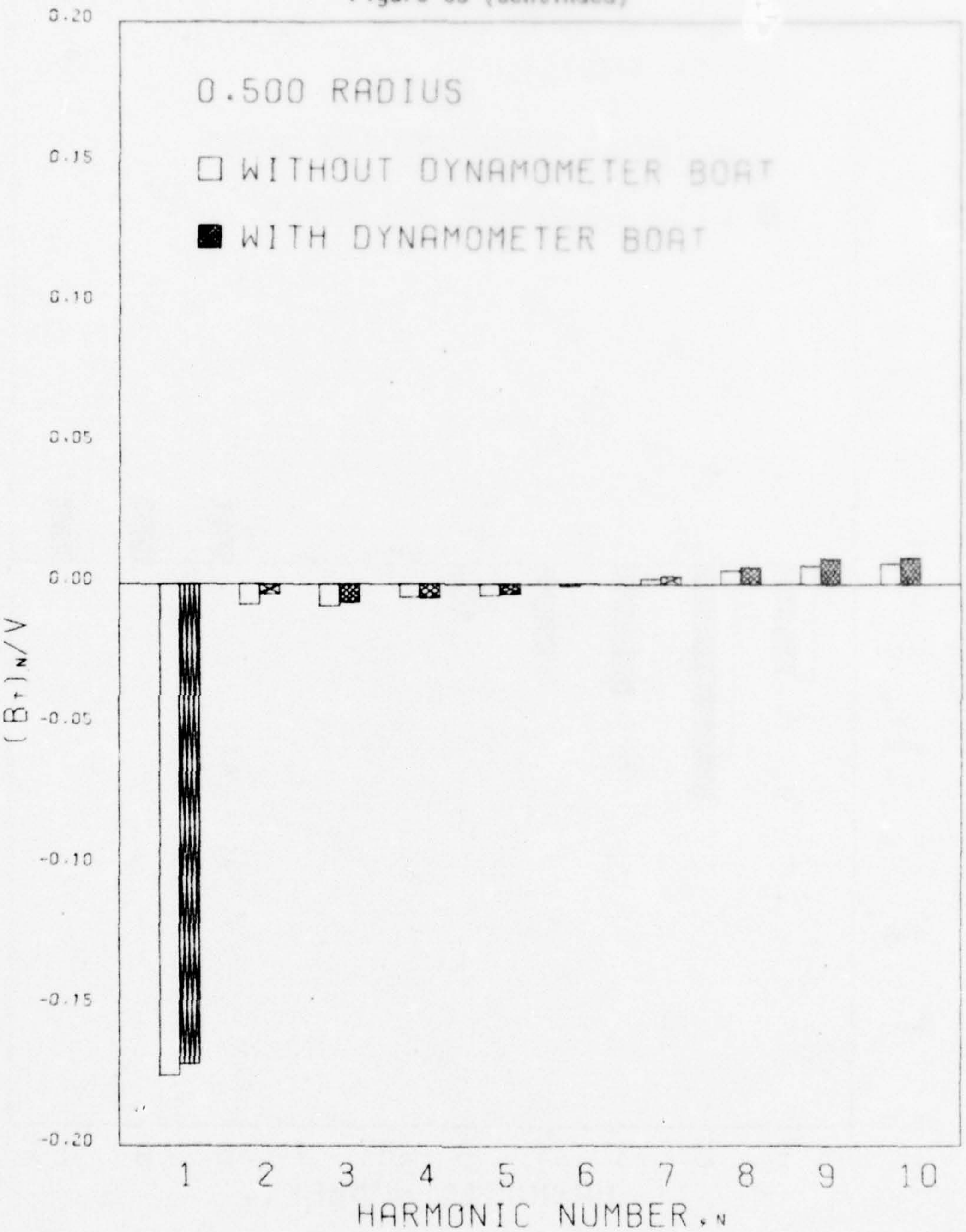

Figure 33 (Continued)

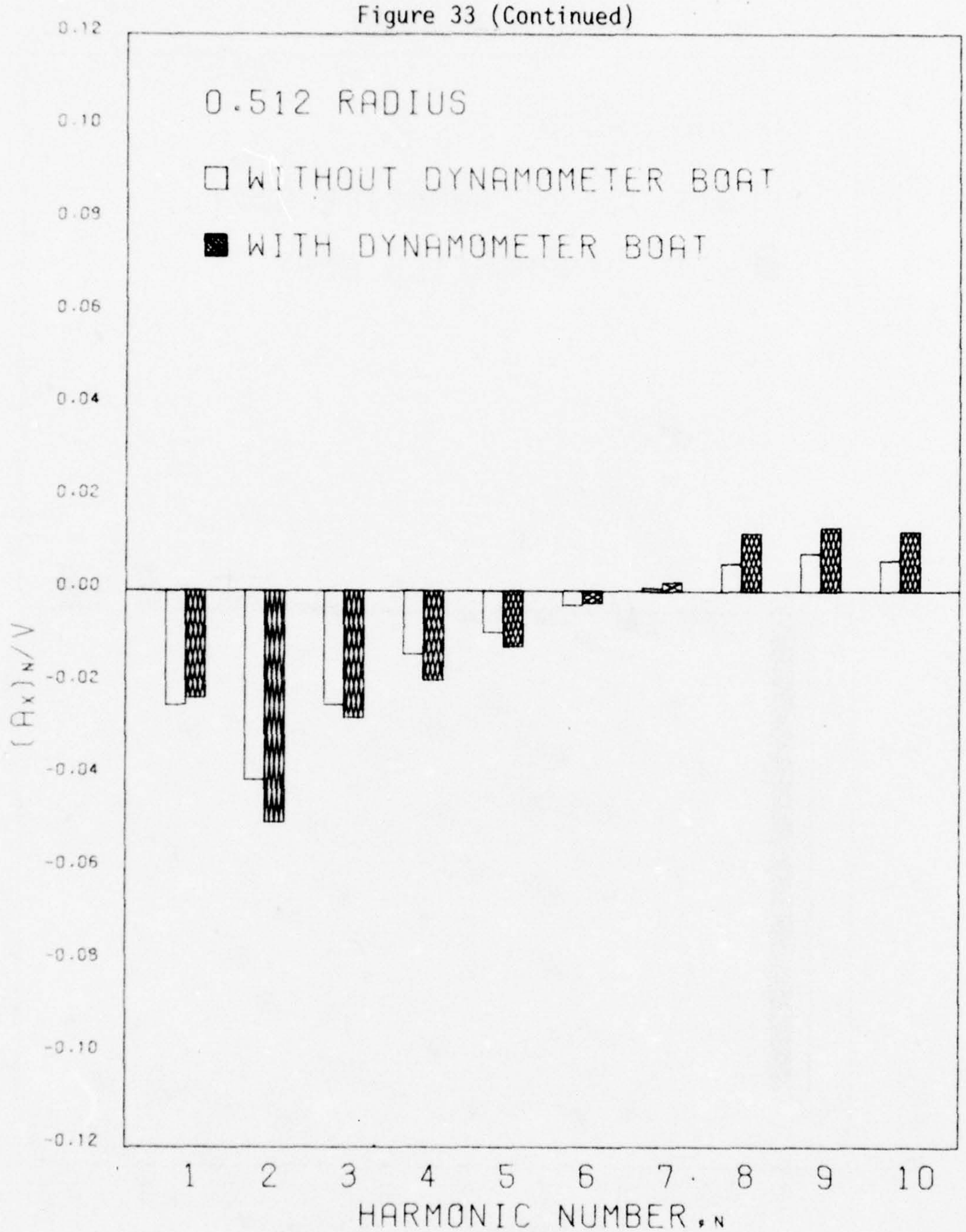

Figure 33 (Continued)

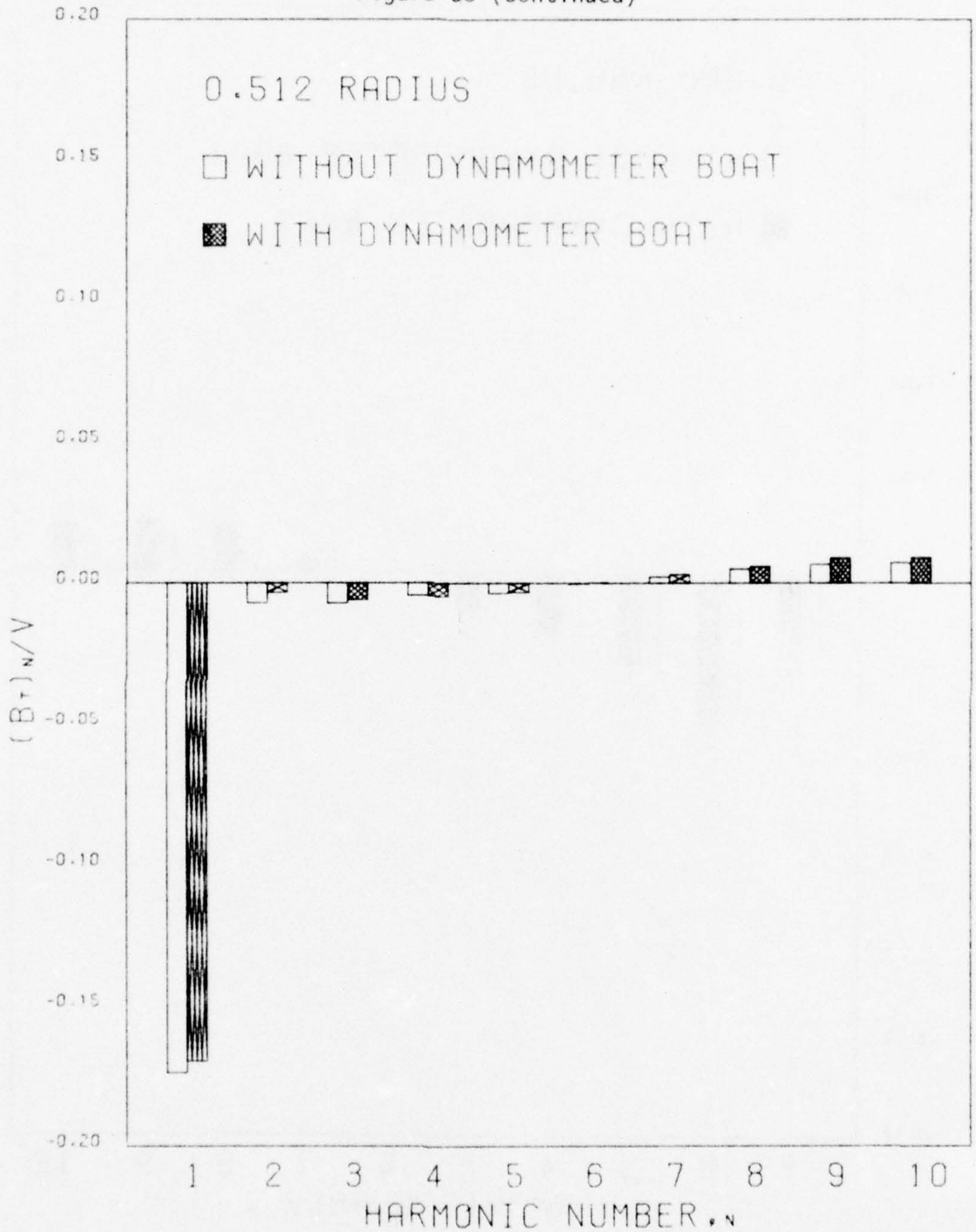

Figure 33 (Continued)

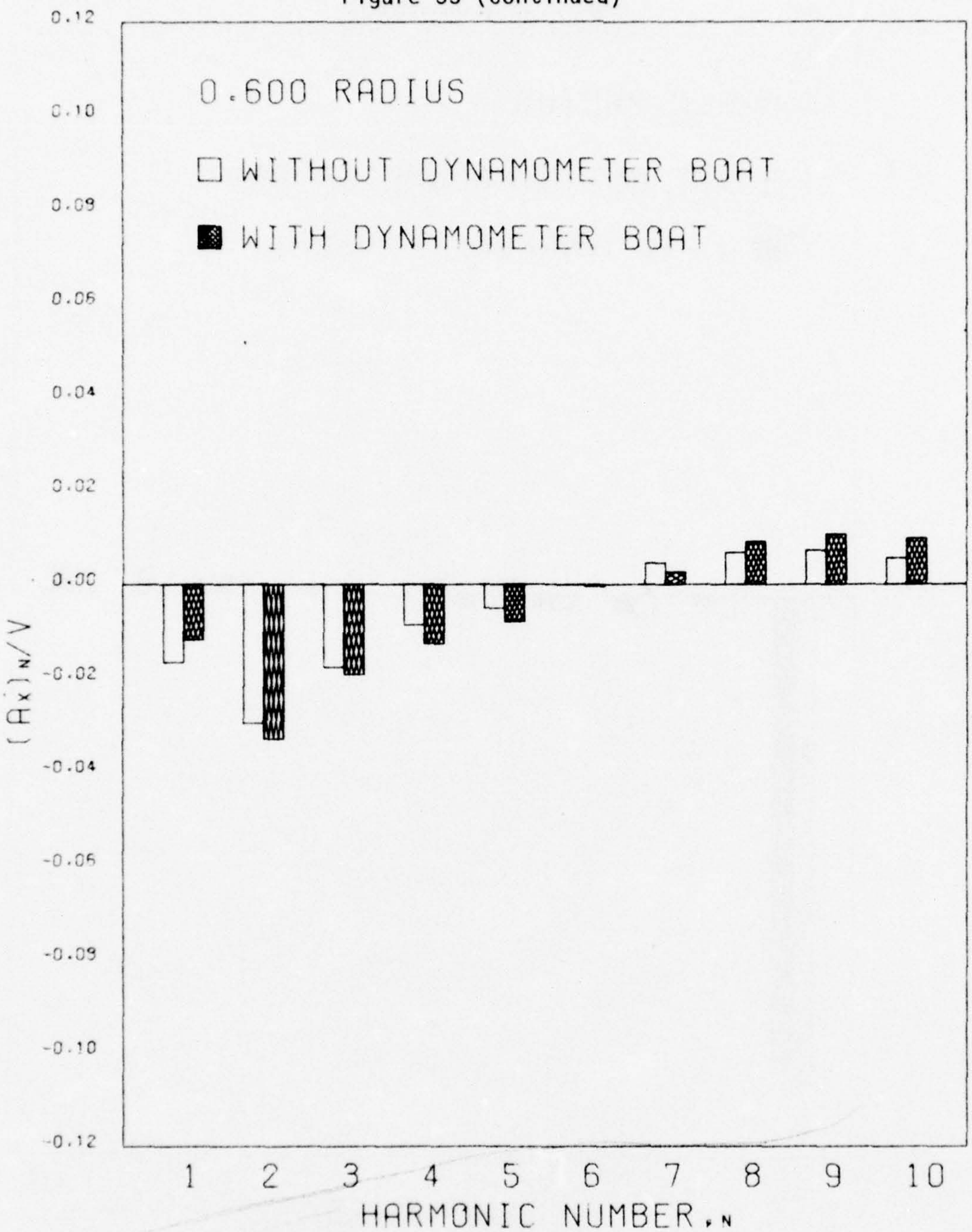

Figure 33 (Continued)

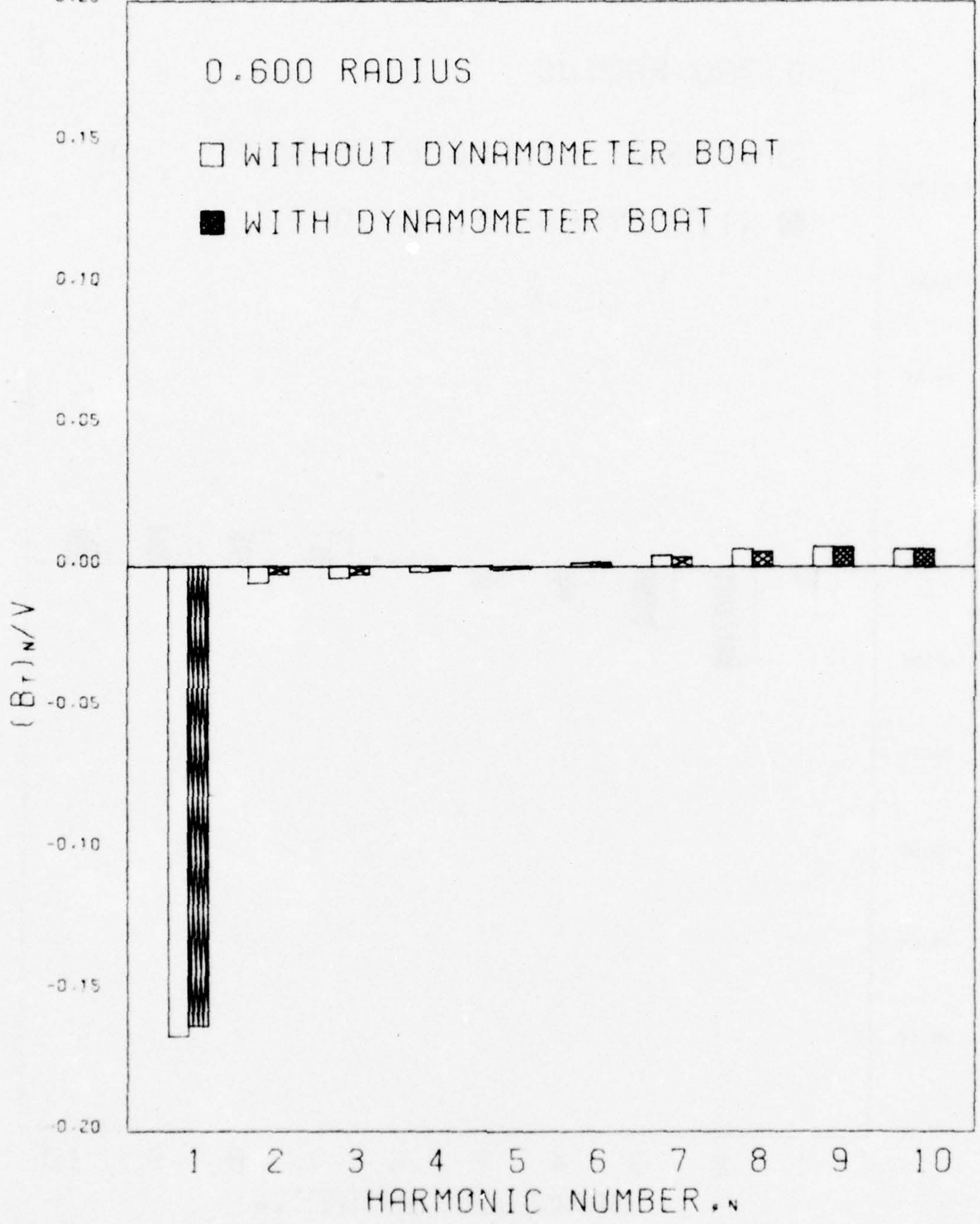

Figure 33 (Continued)

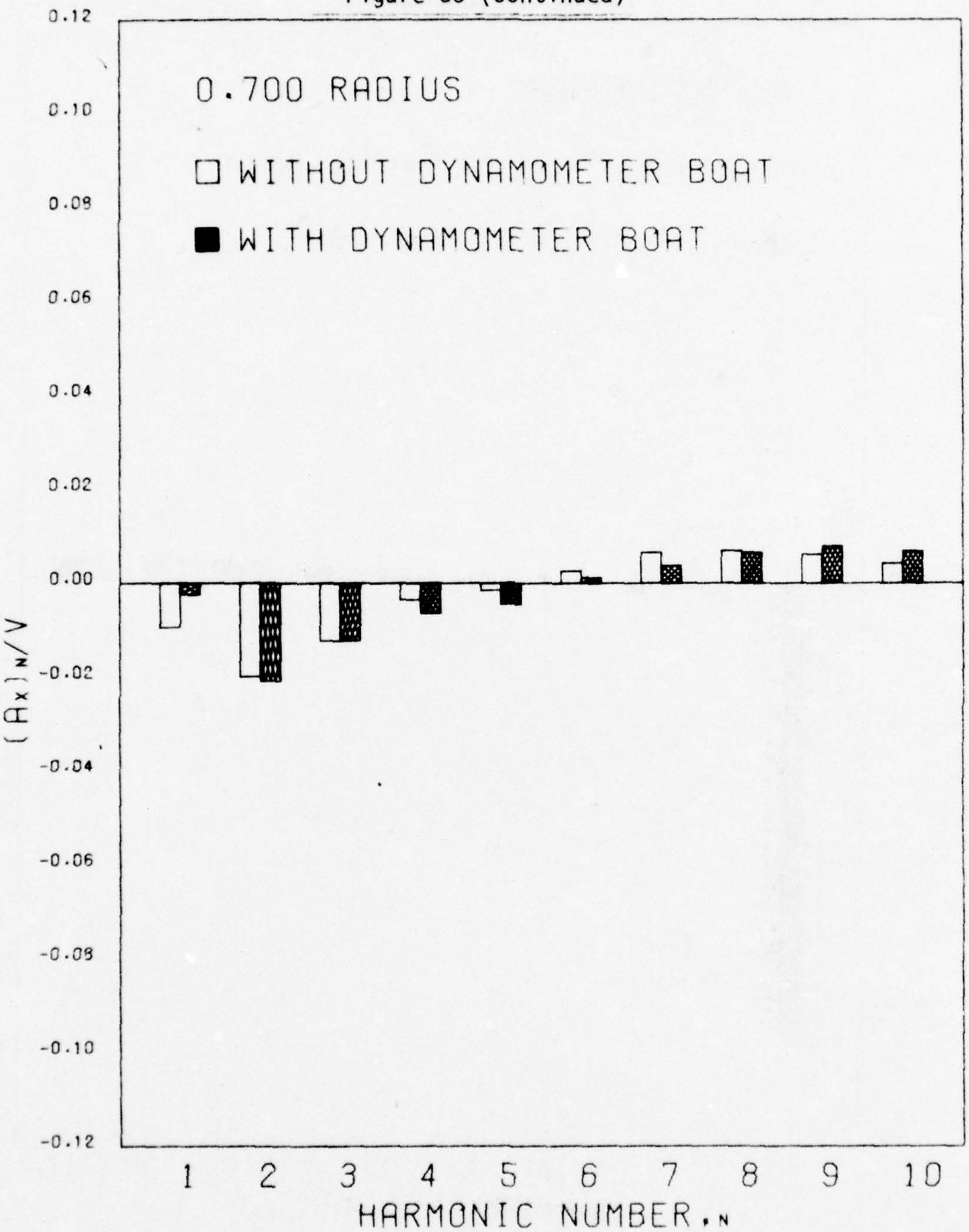

Figure 33 (Continued)

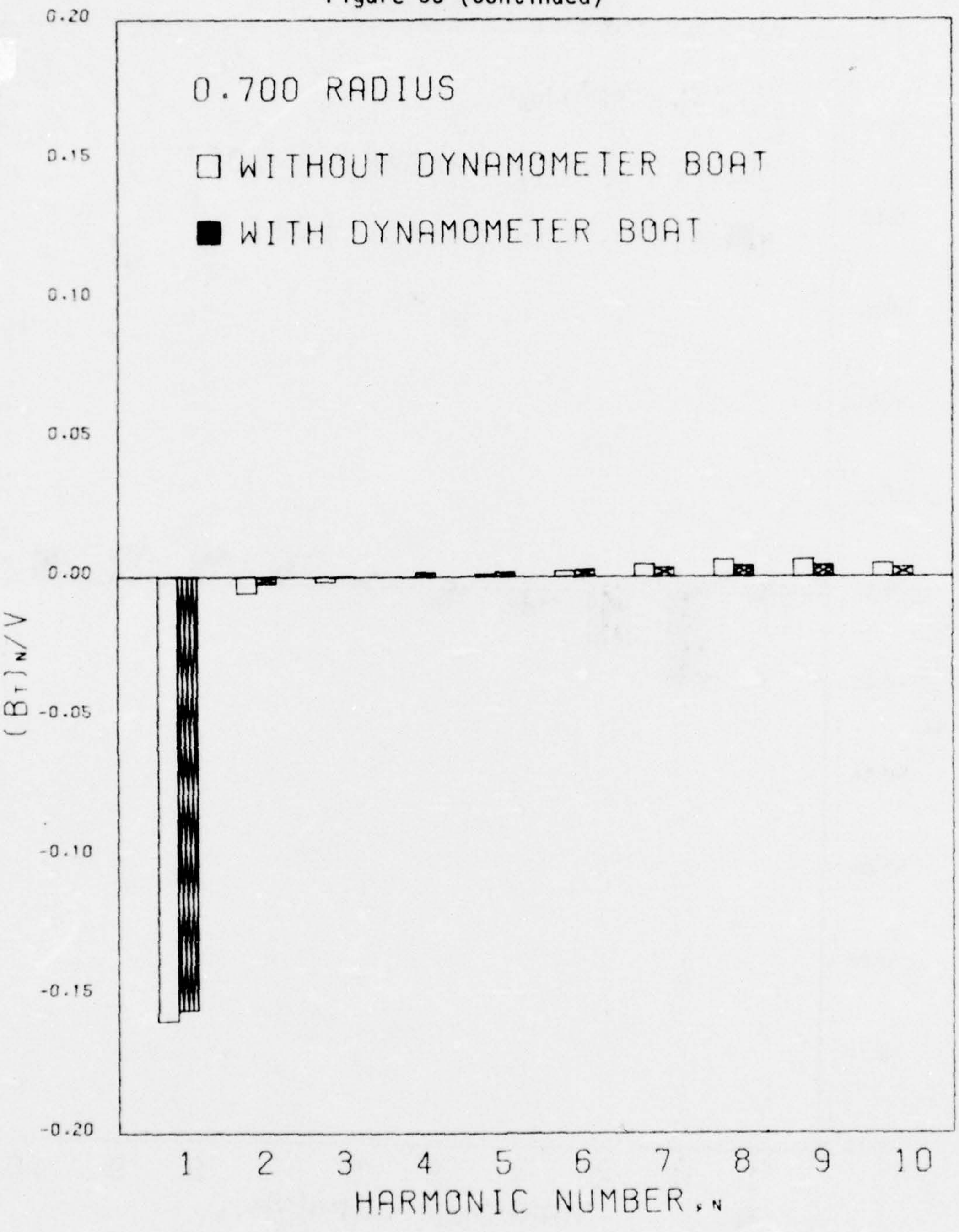

Figure 33 (Continued)

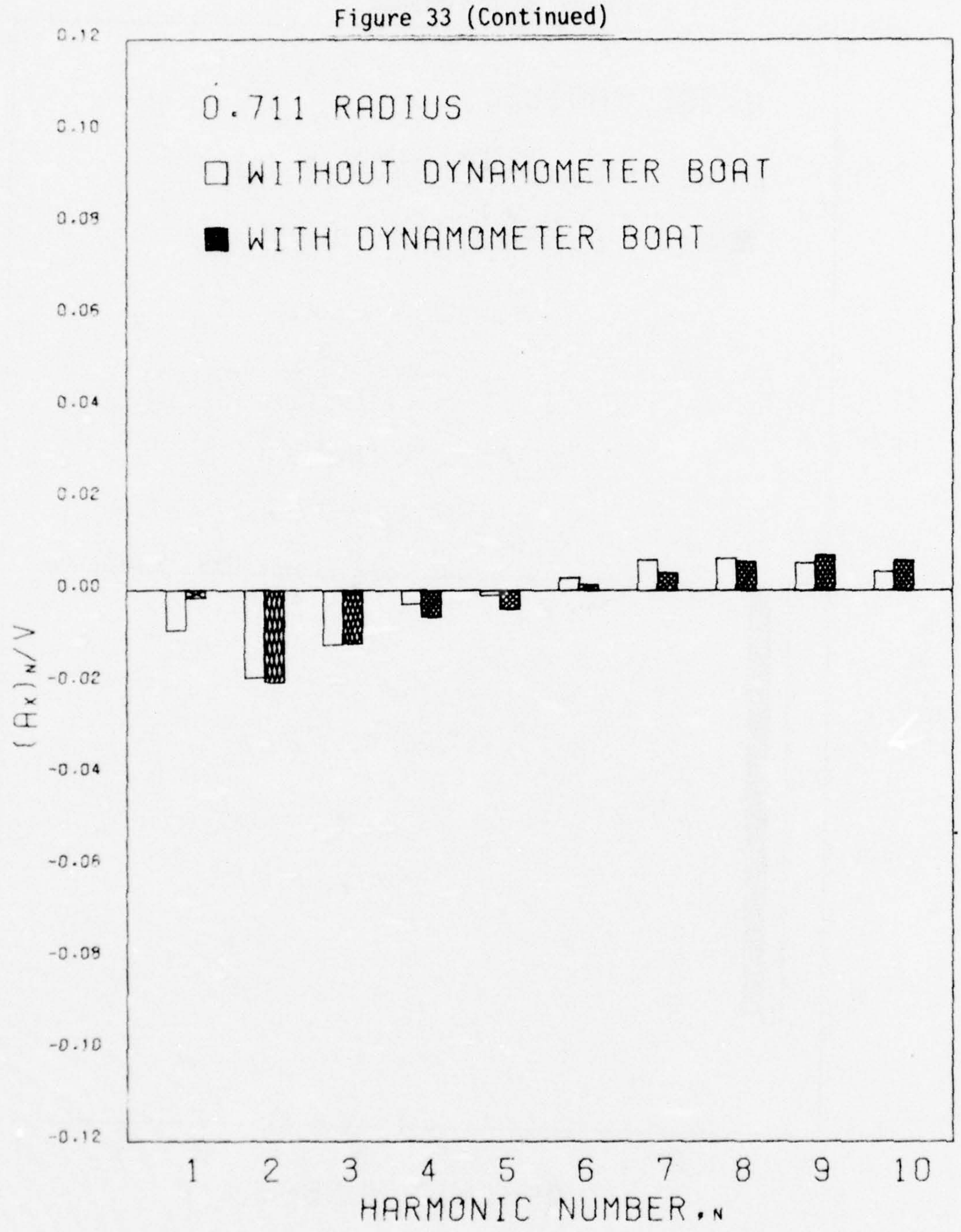

Figure 33 (Continued)

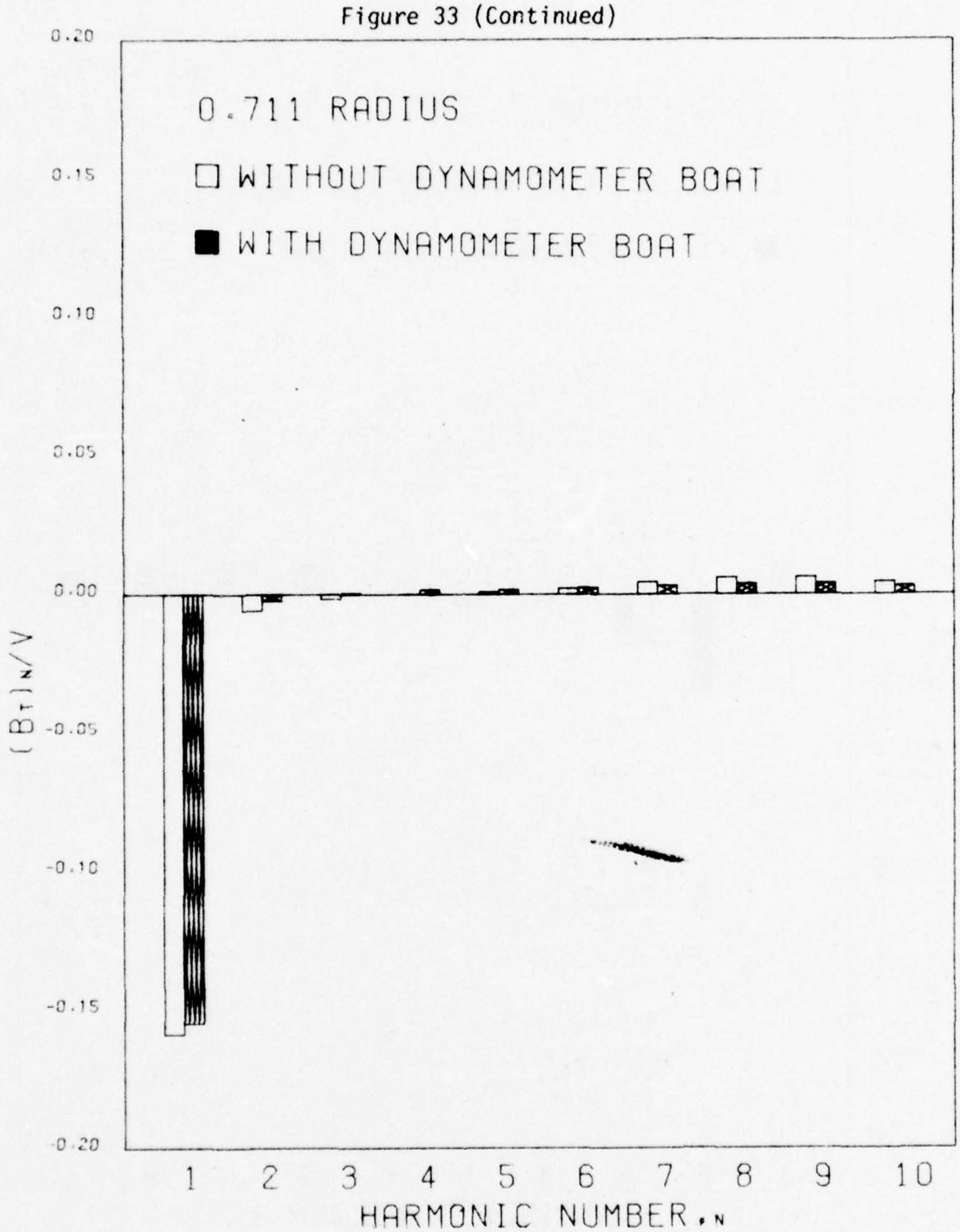

Figure 33 (Continued)

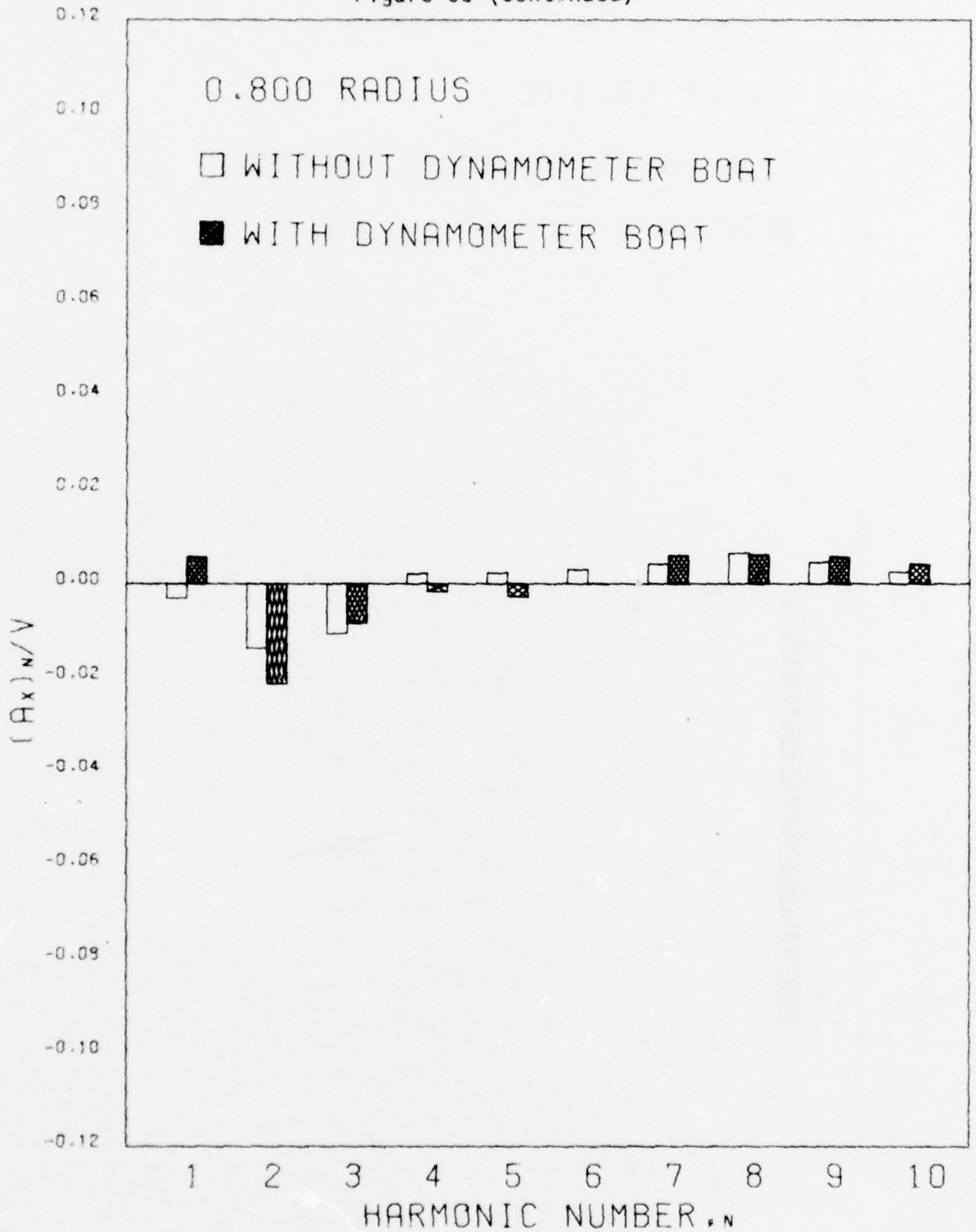

Figure 33 (Continued)

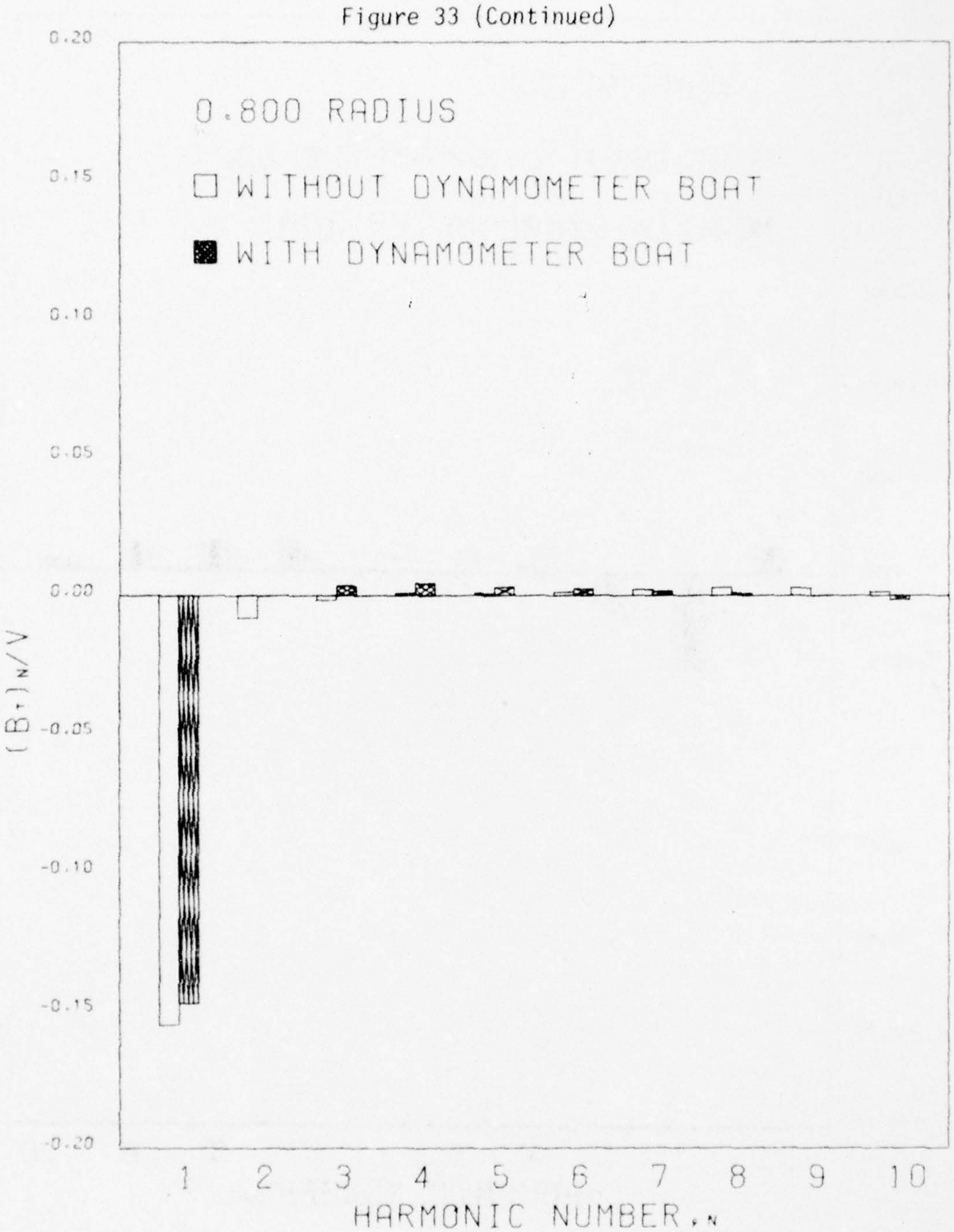

Figure 33 (Continued)

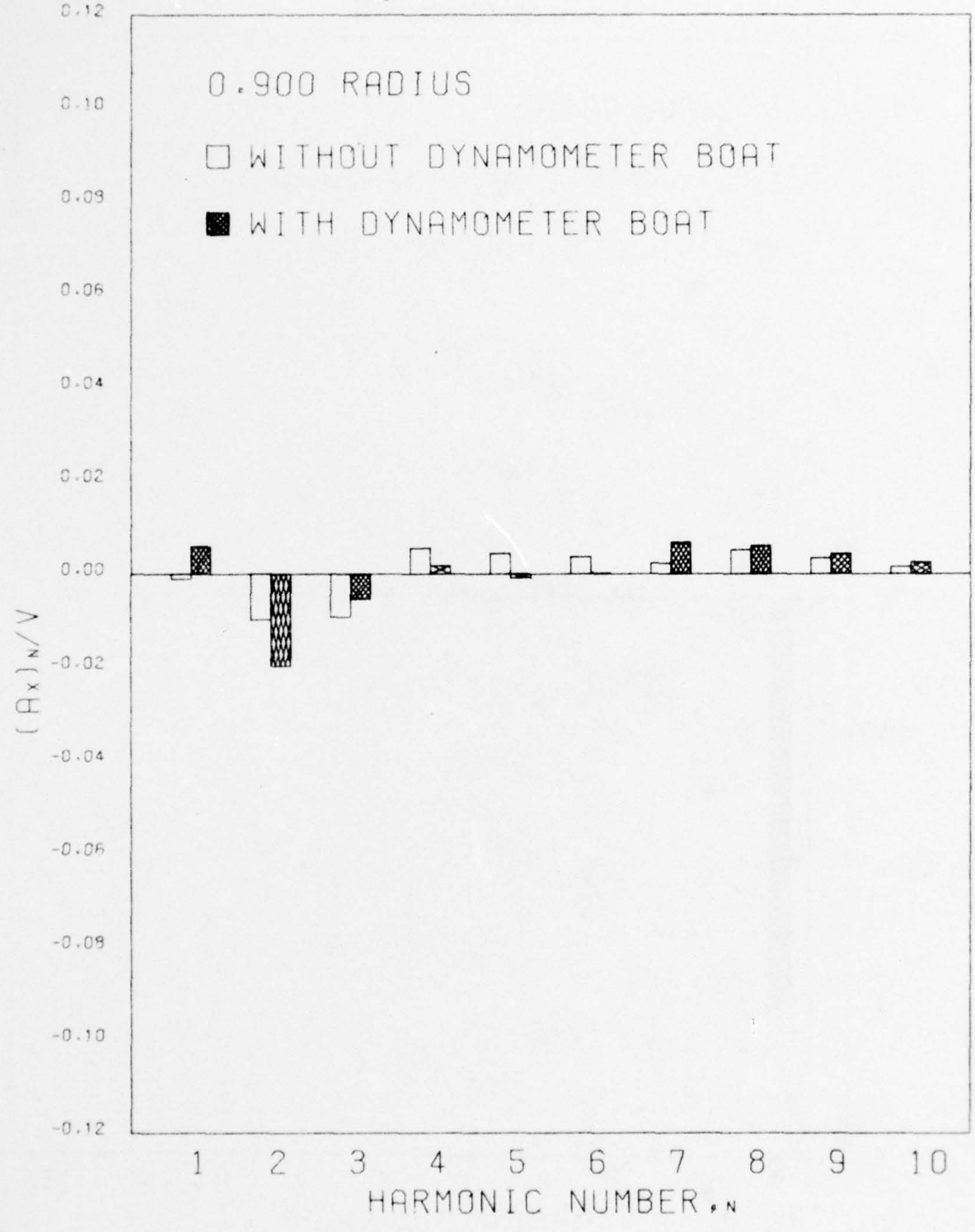

Figure 33 (Continued)

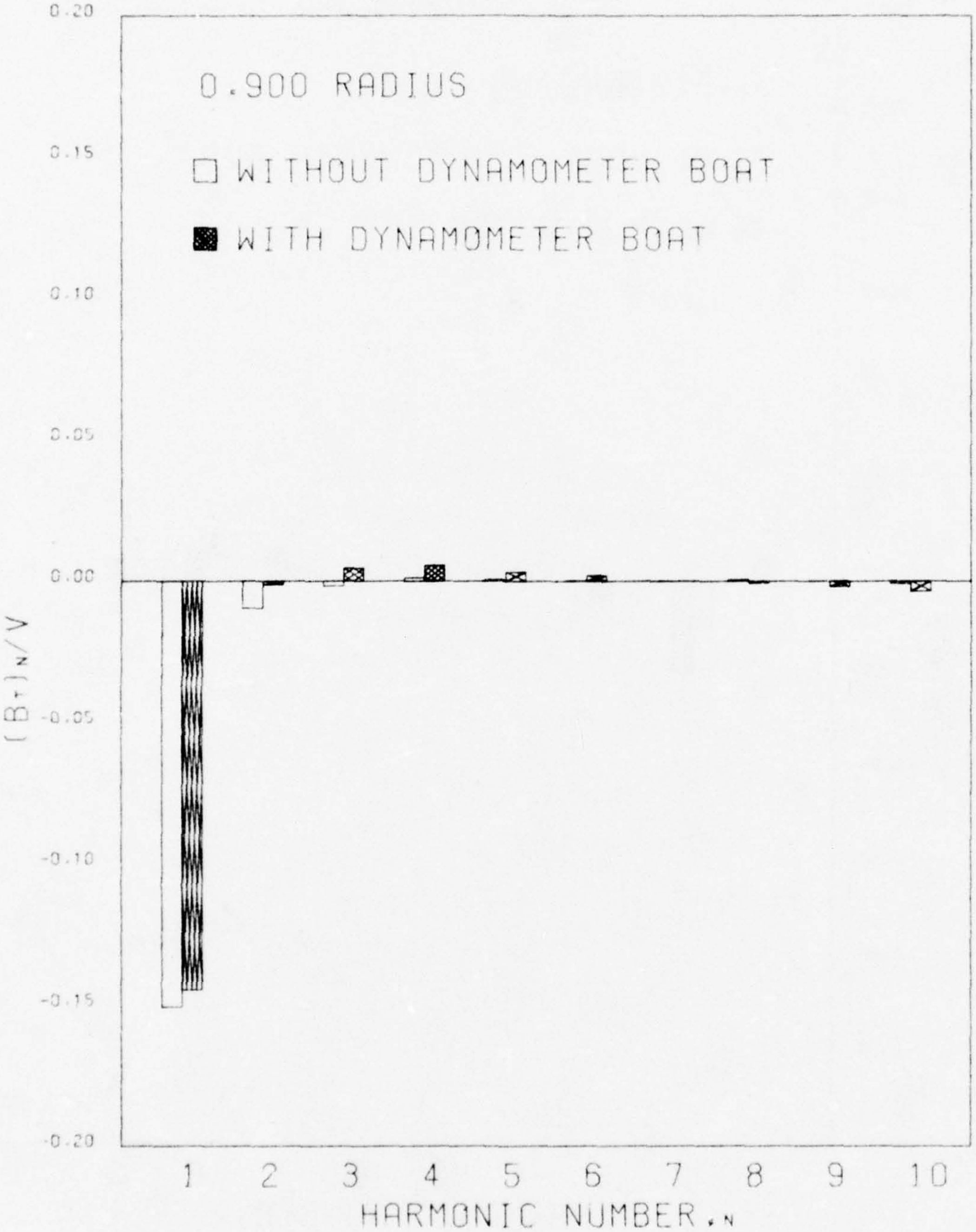

Figure 33 (Continued)

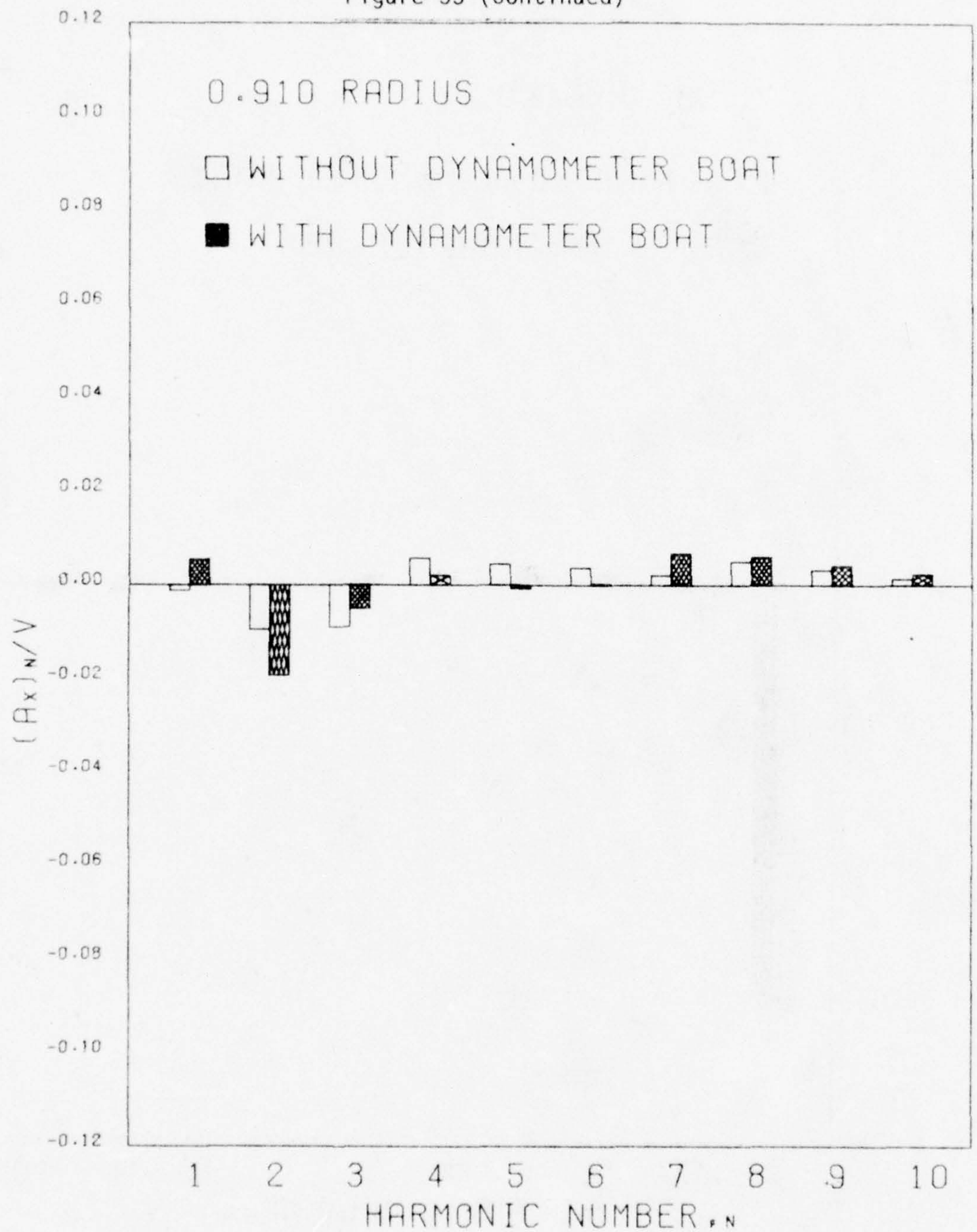

Figure 33 (Continued)

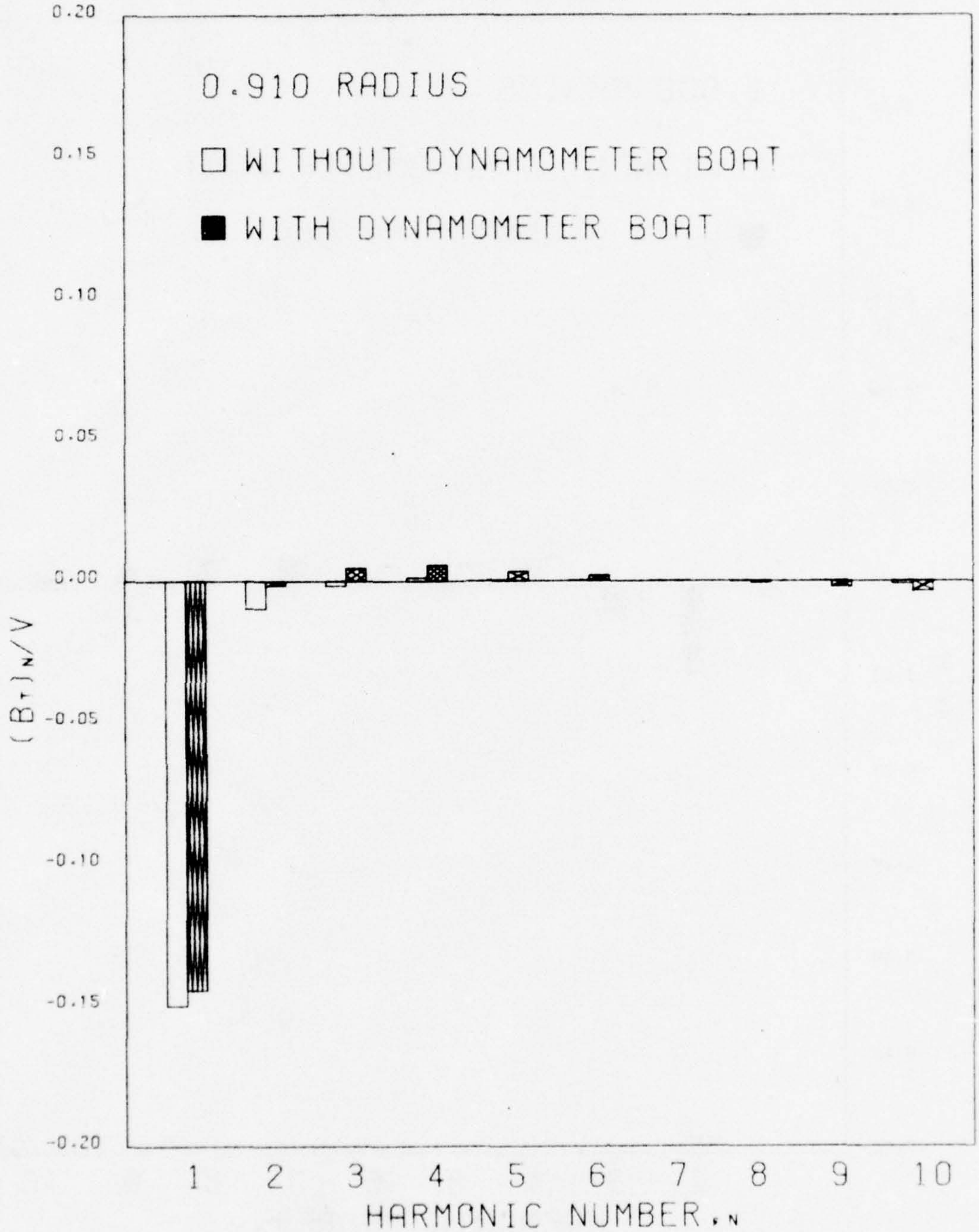

Figure 33 (Continued)

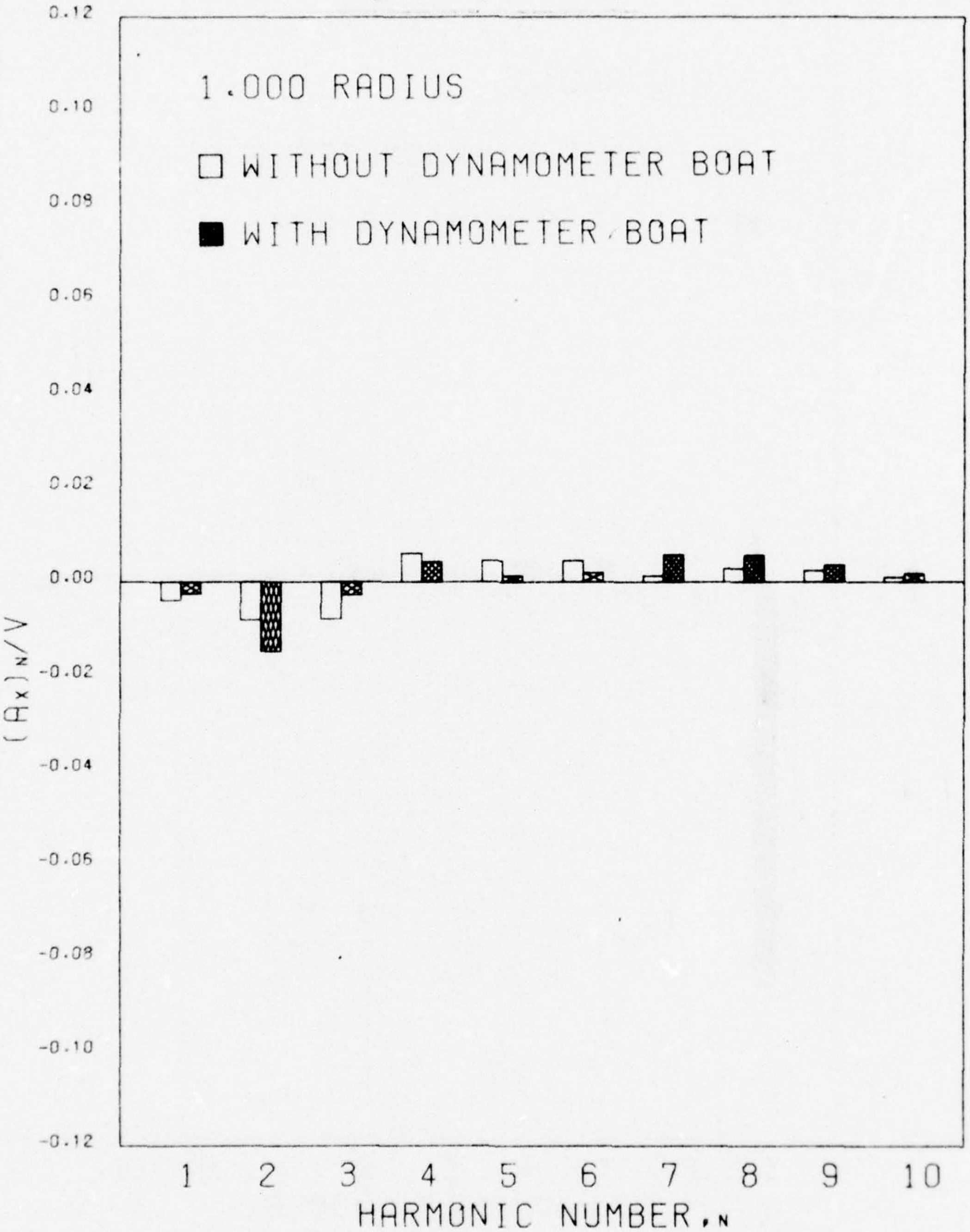

Figure 33 (Continued)

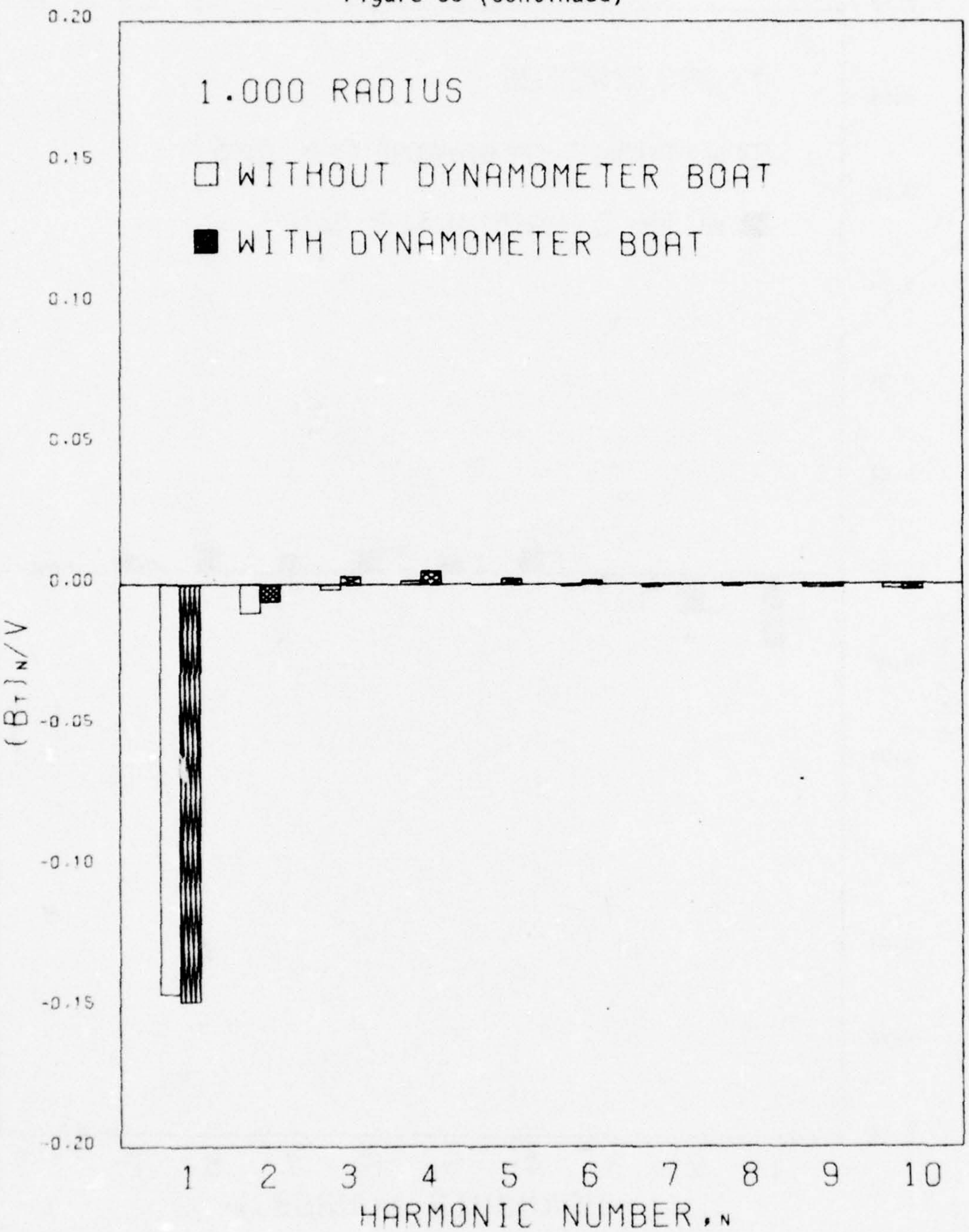

Figure 33 (Continued)

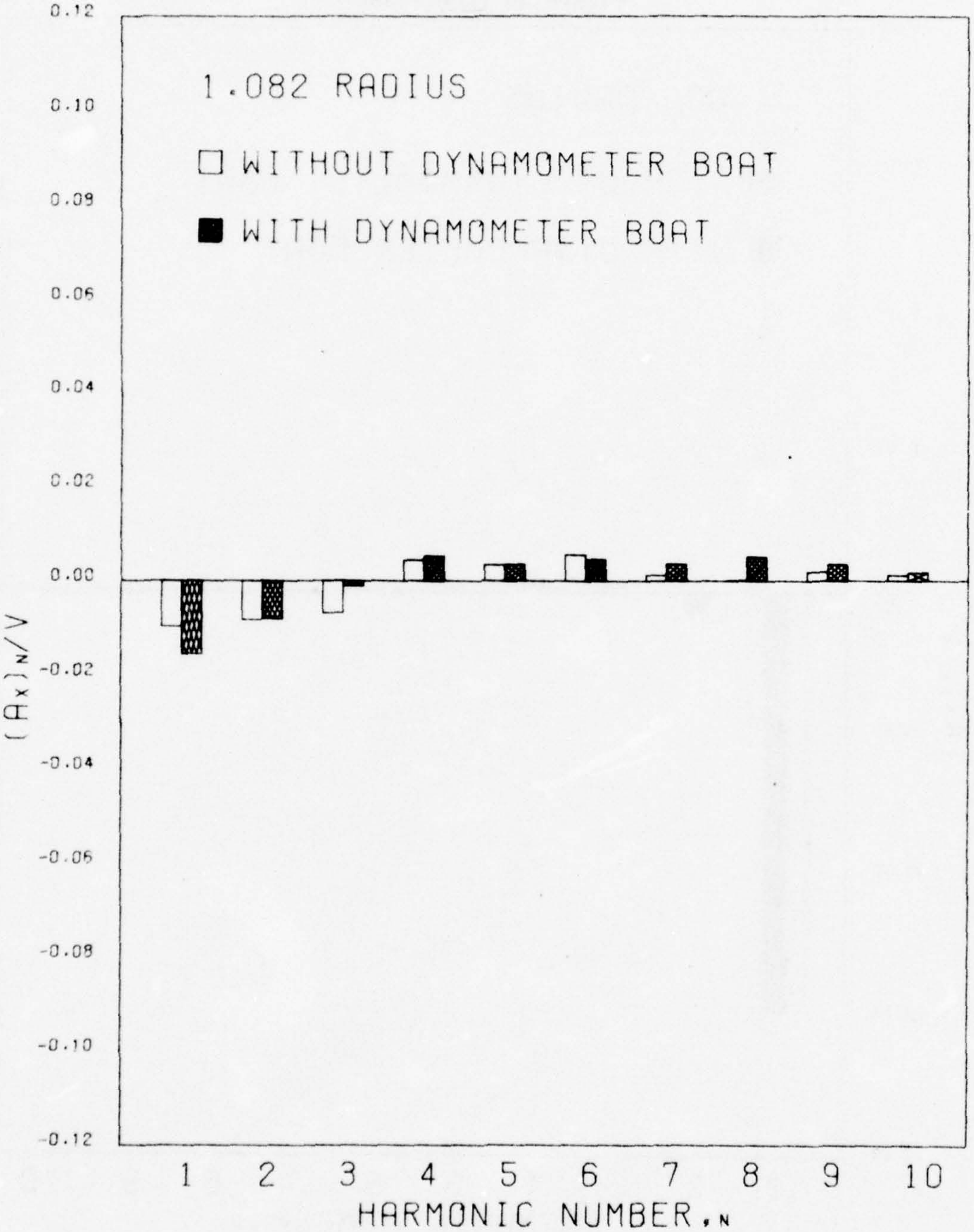

Figure 33 (Continued)

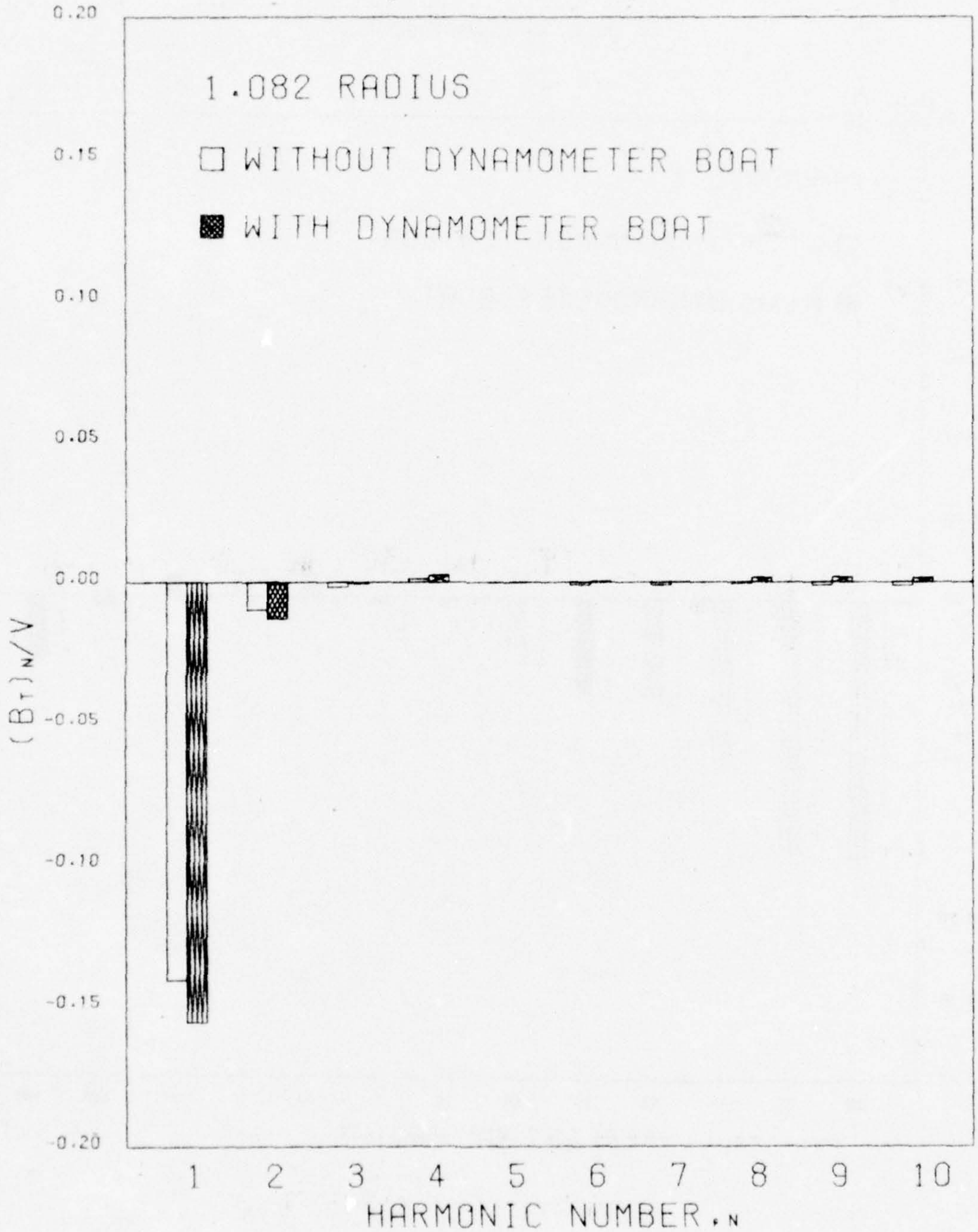

Figure 33 (Continued)

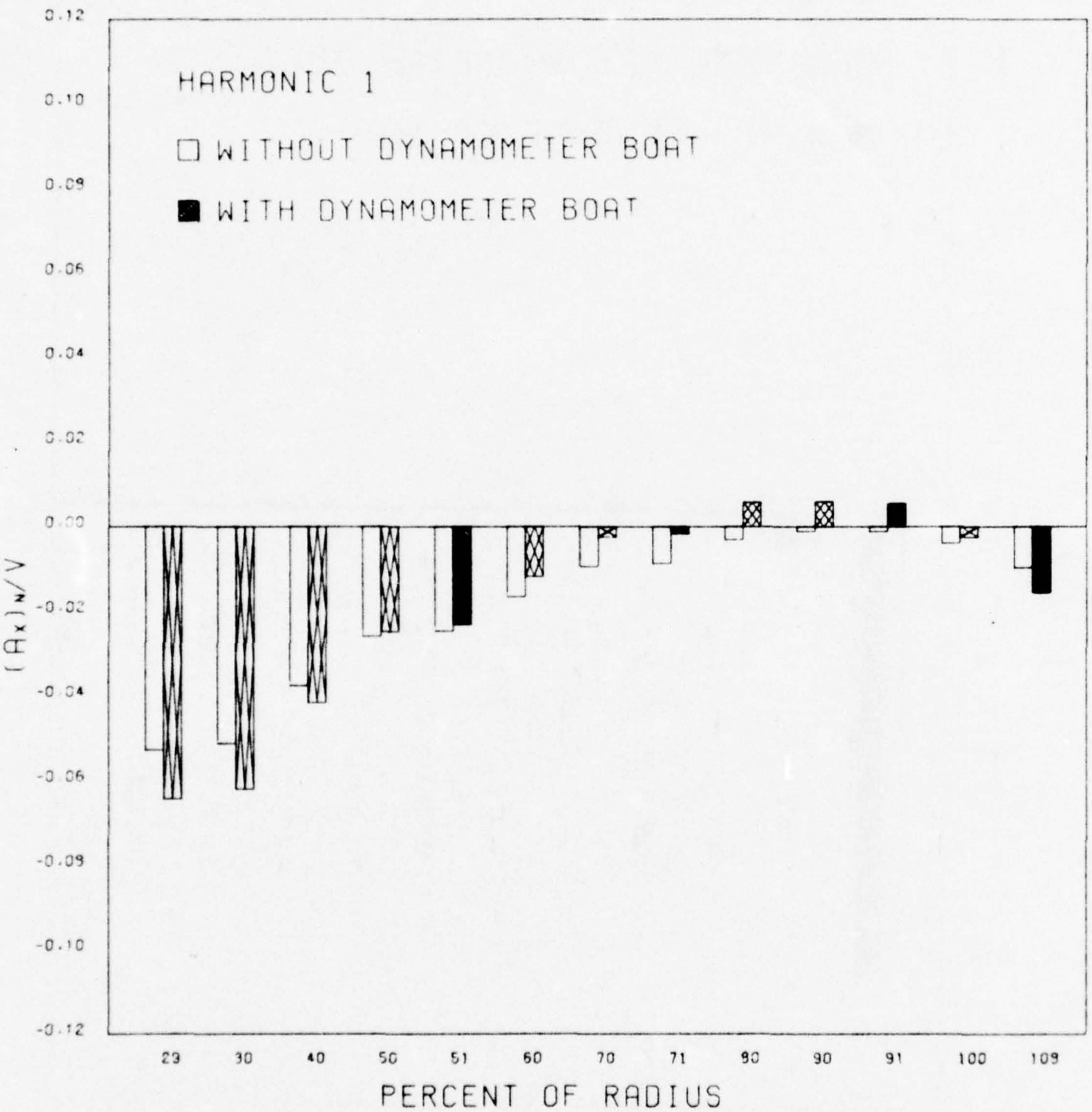

Figure 33 (Continued)

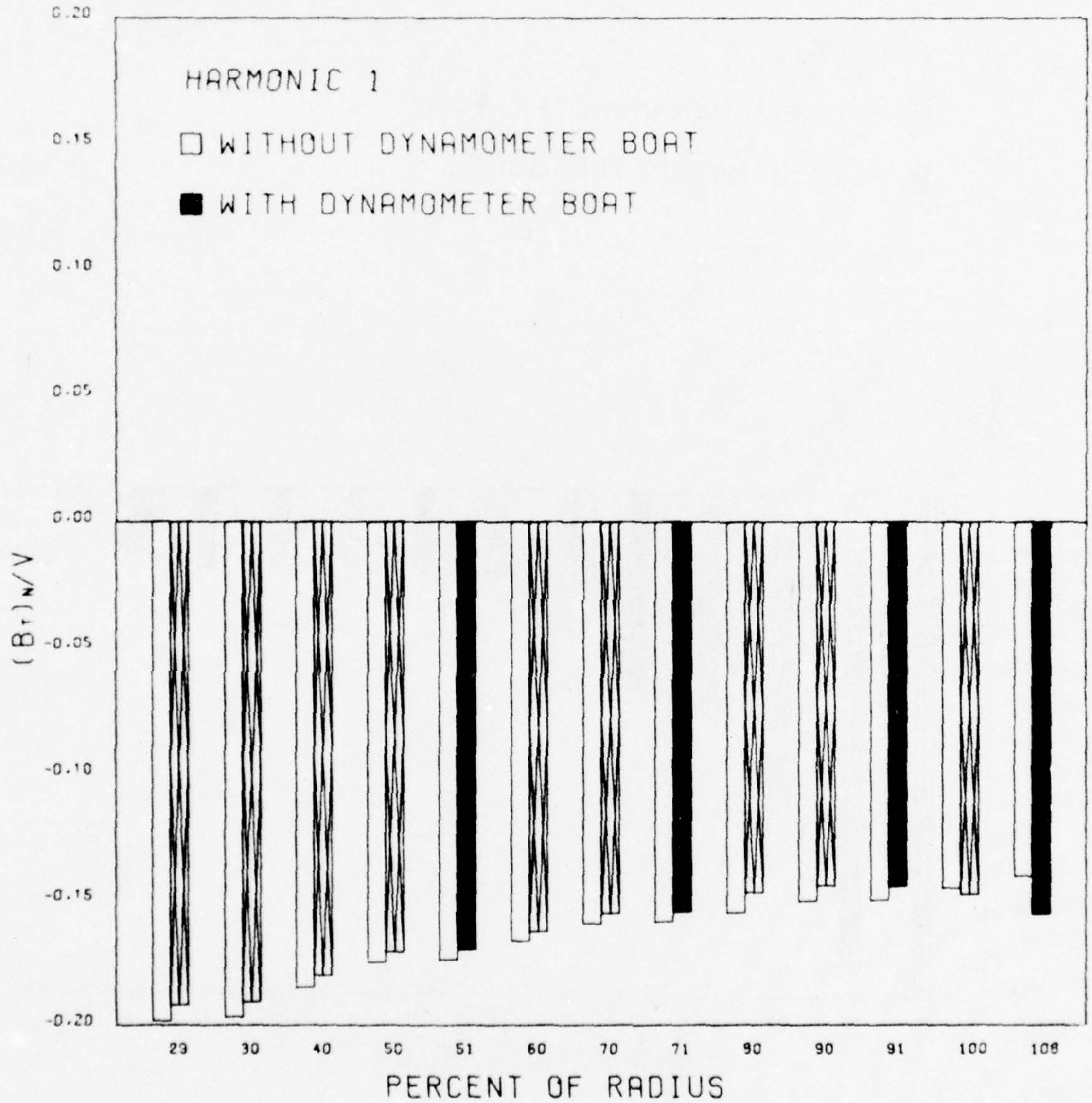

Figure 33 (Continued)

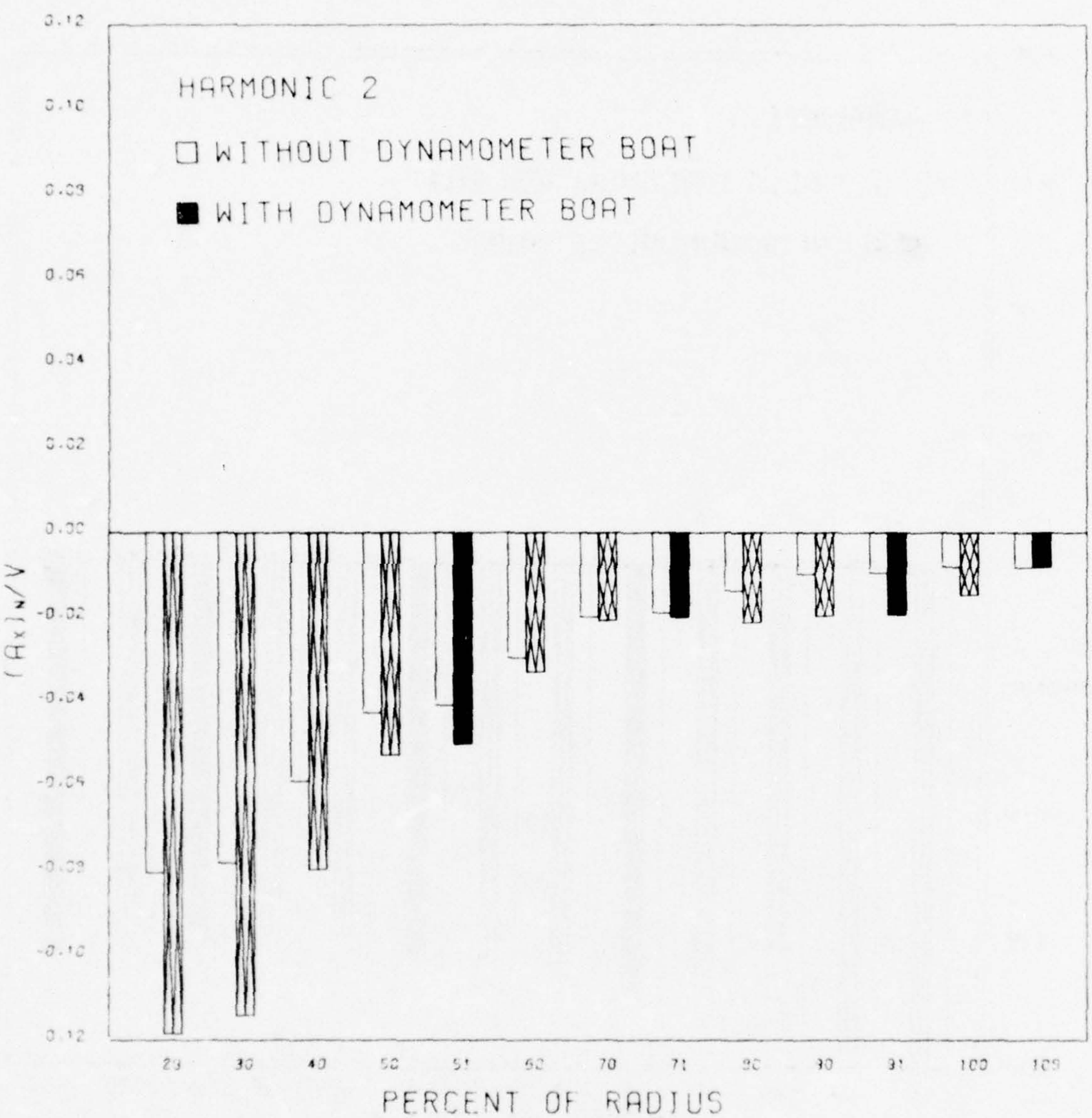

Figure 33 (Continued)

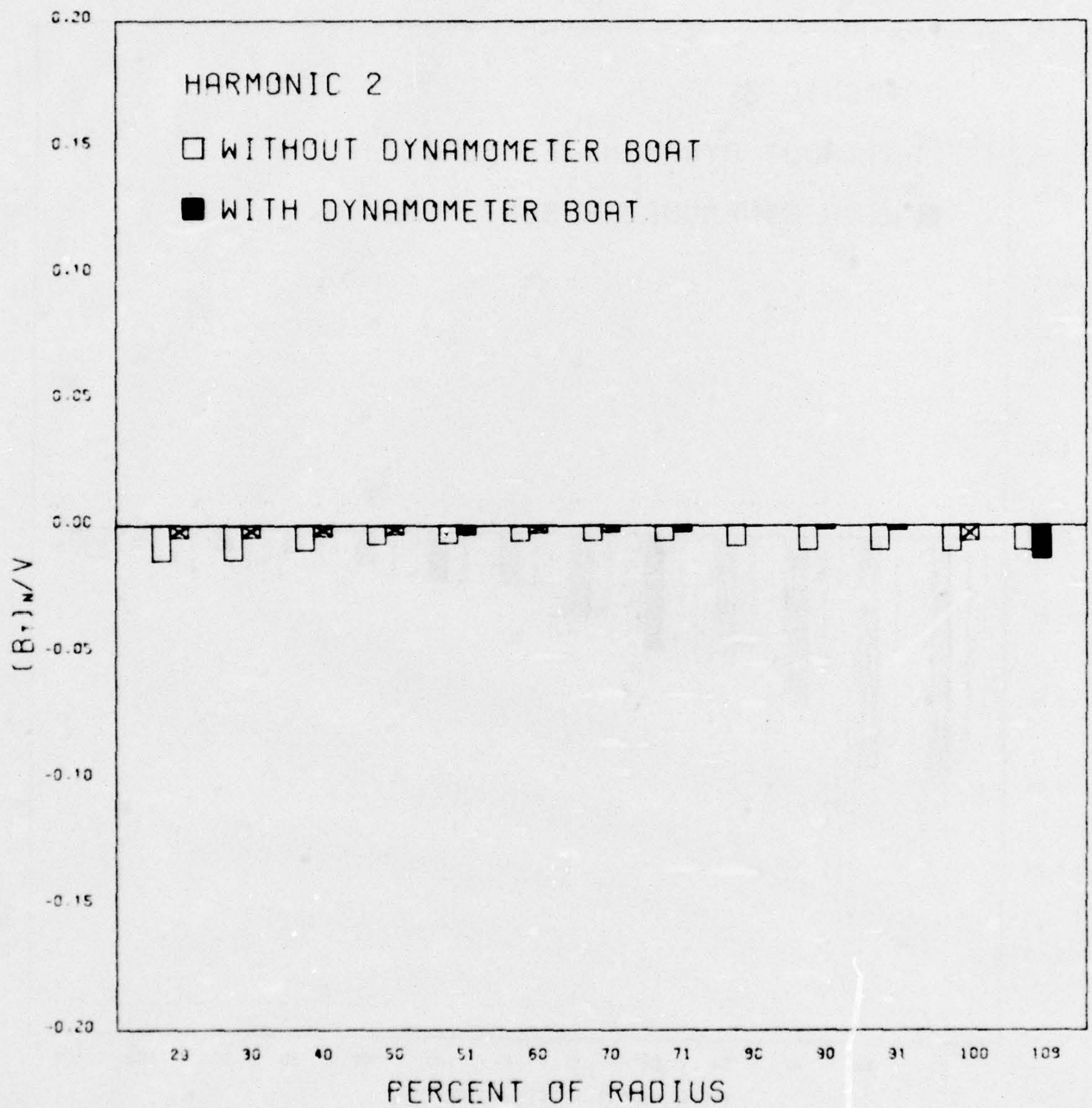

Figure 33 (Continued)

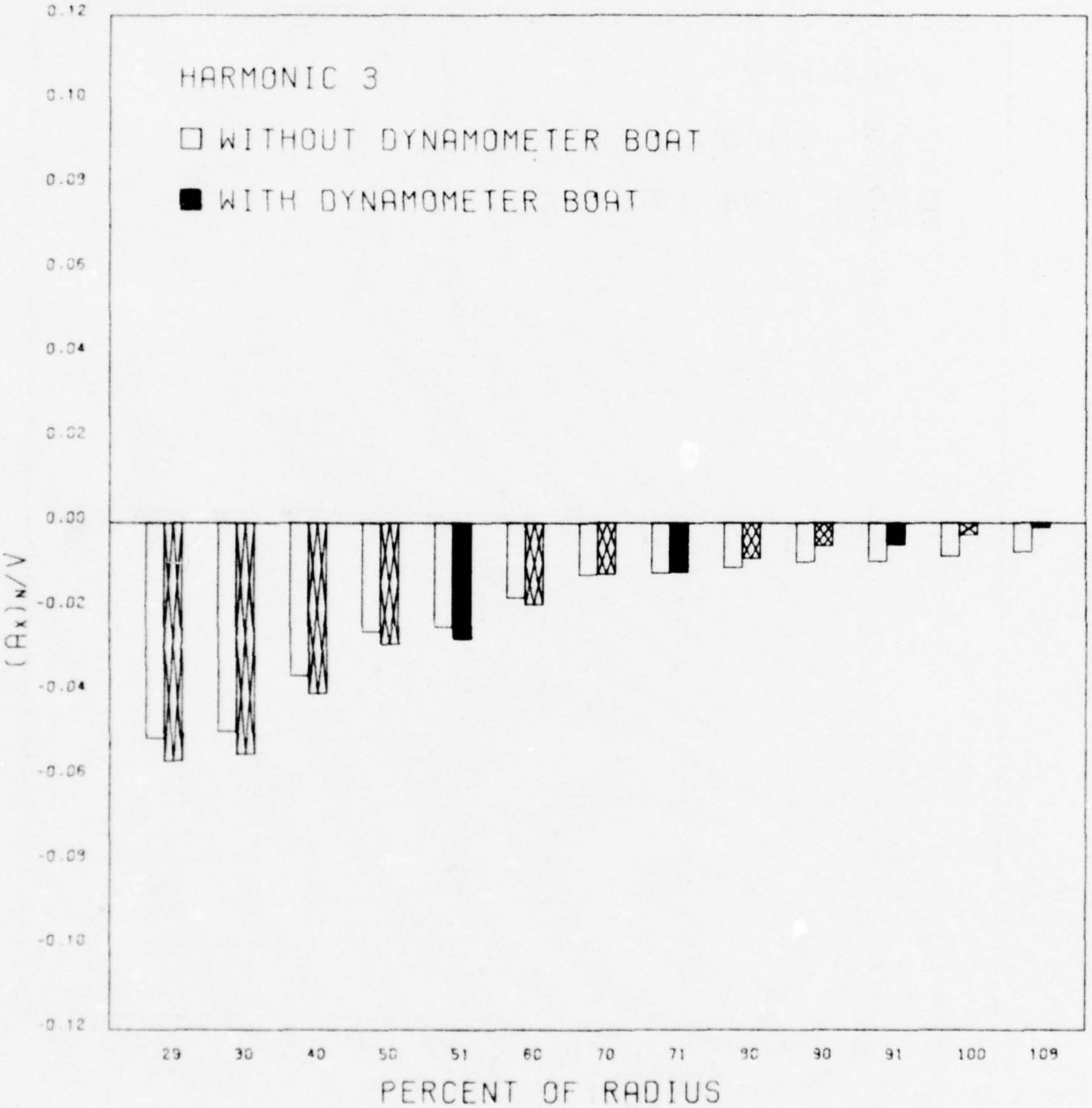

Figure 33 (Continued)

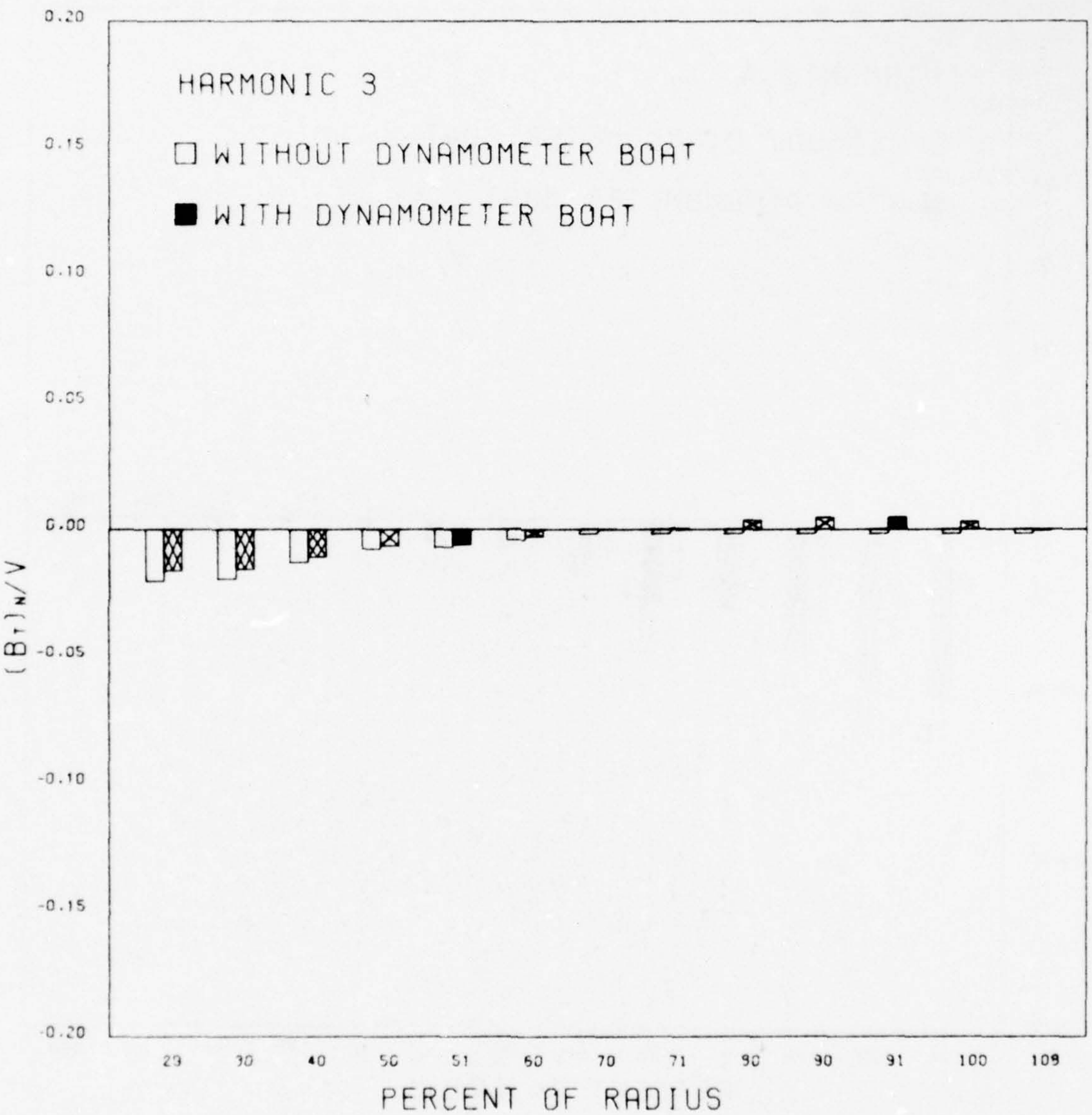

Figure 33 (Continued)

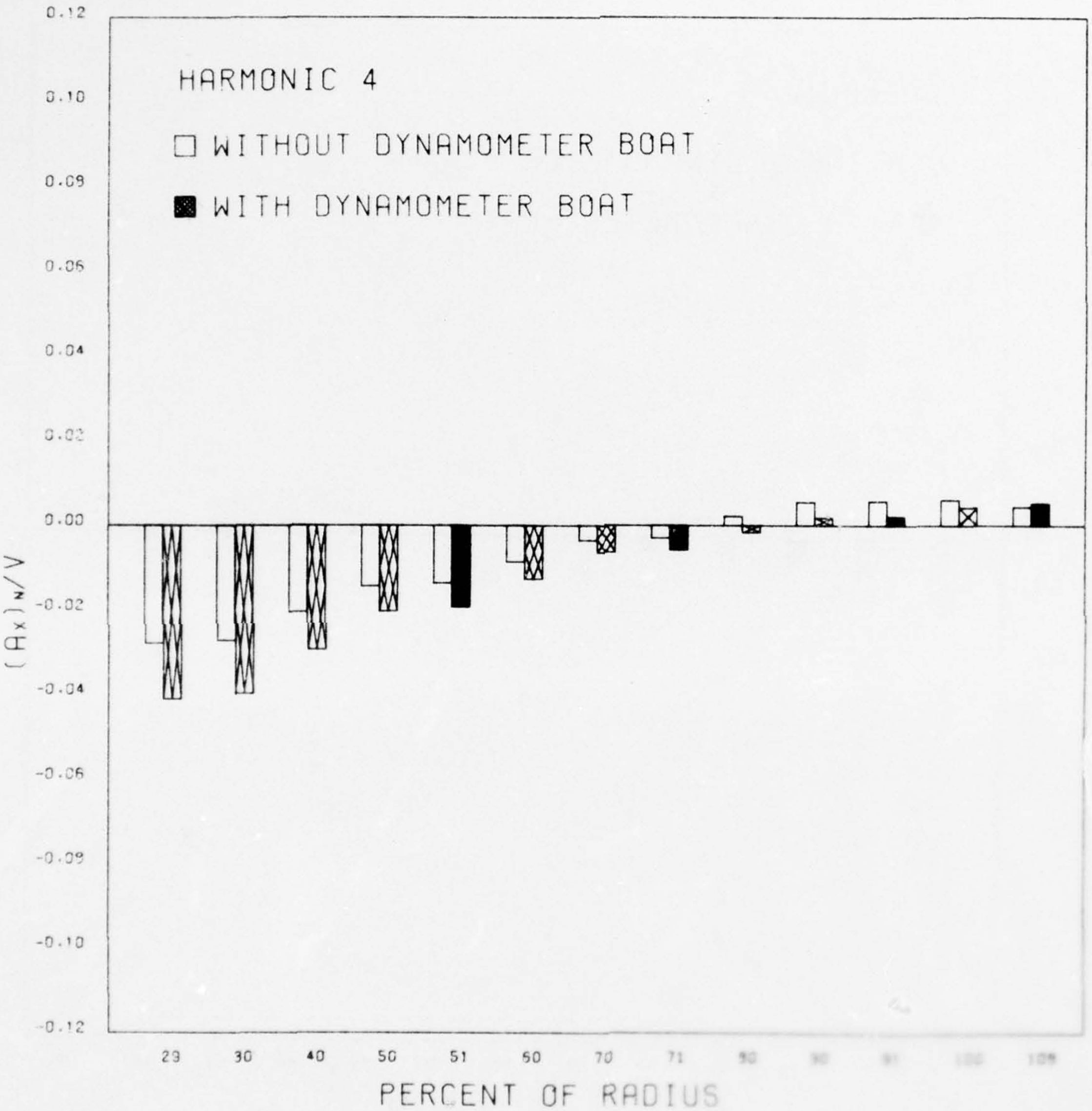

Figure 33 (Continued)

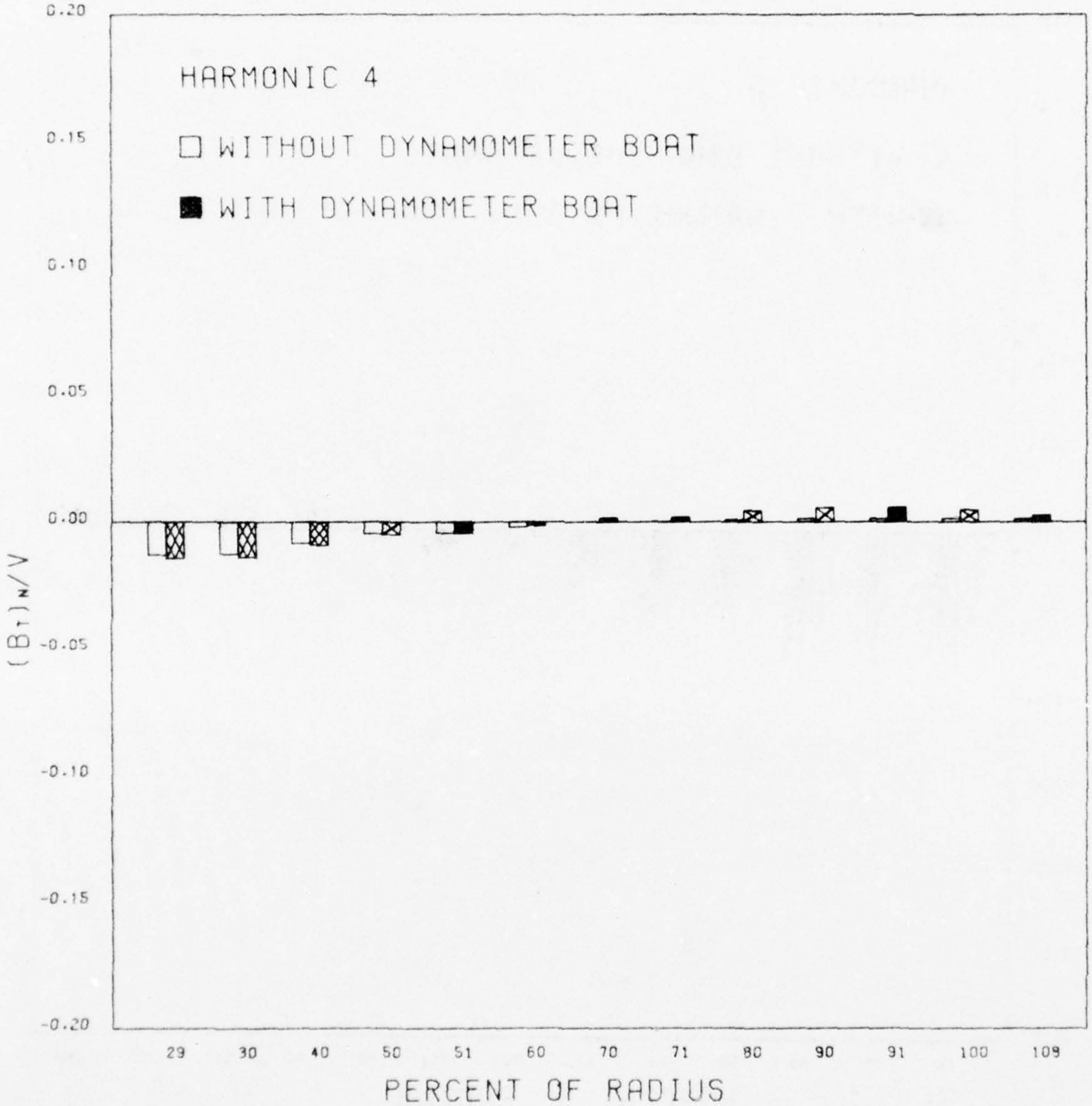

Figure 33 (Continued)

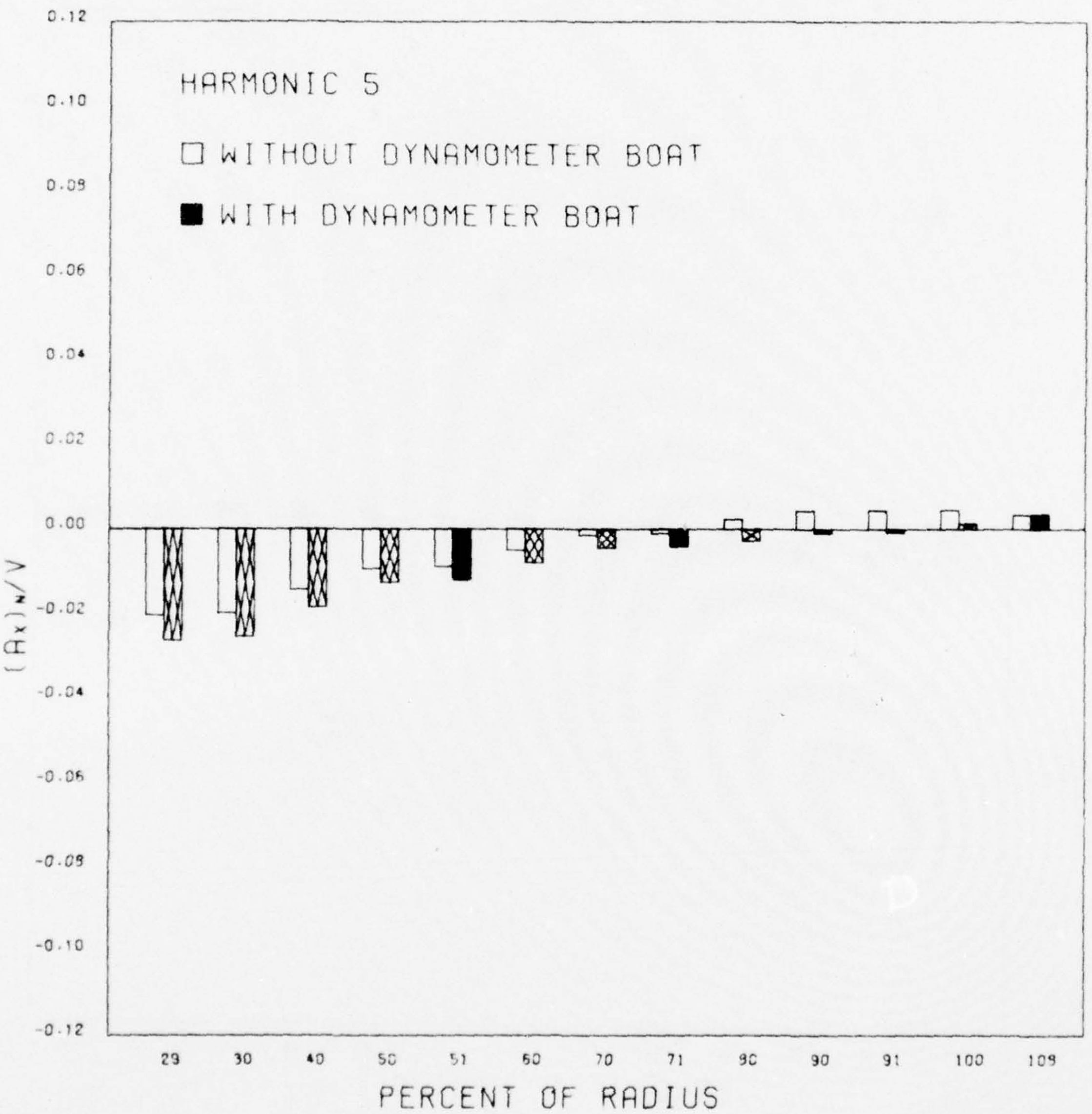

Figure 33 (Continued)

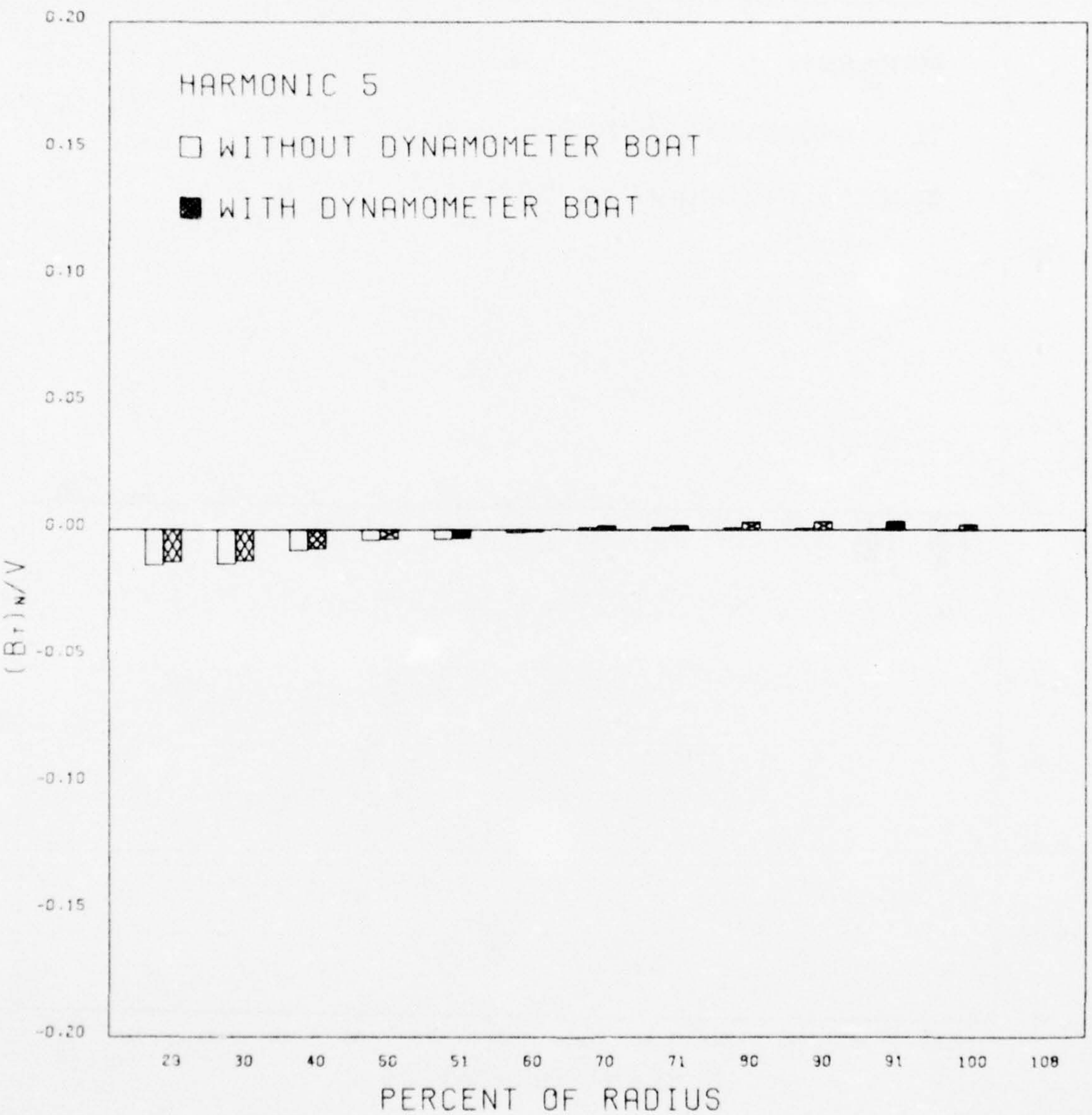

Figure 33 (Continued)

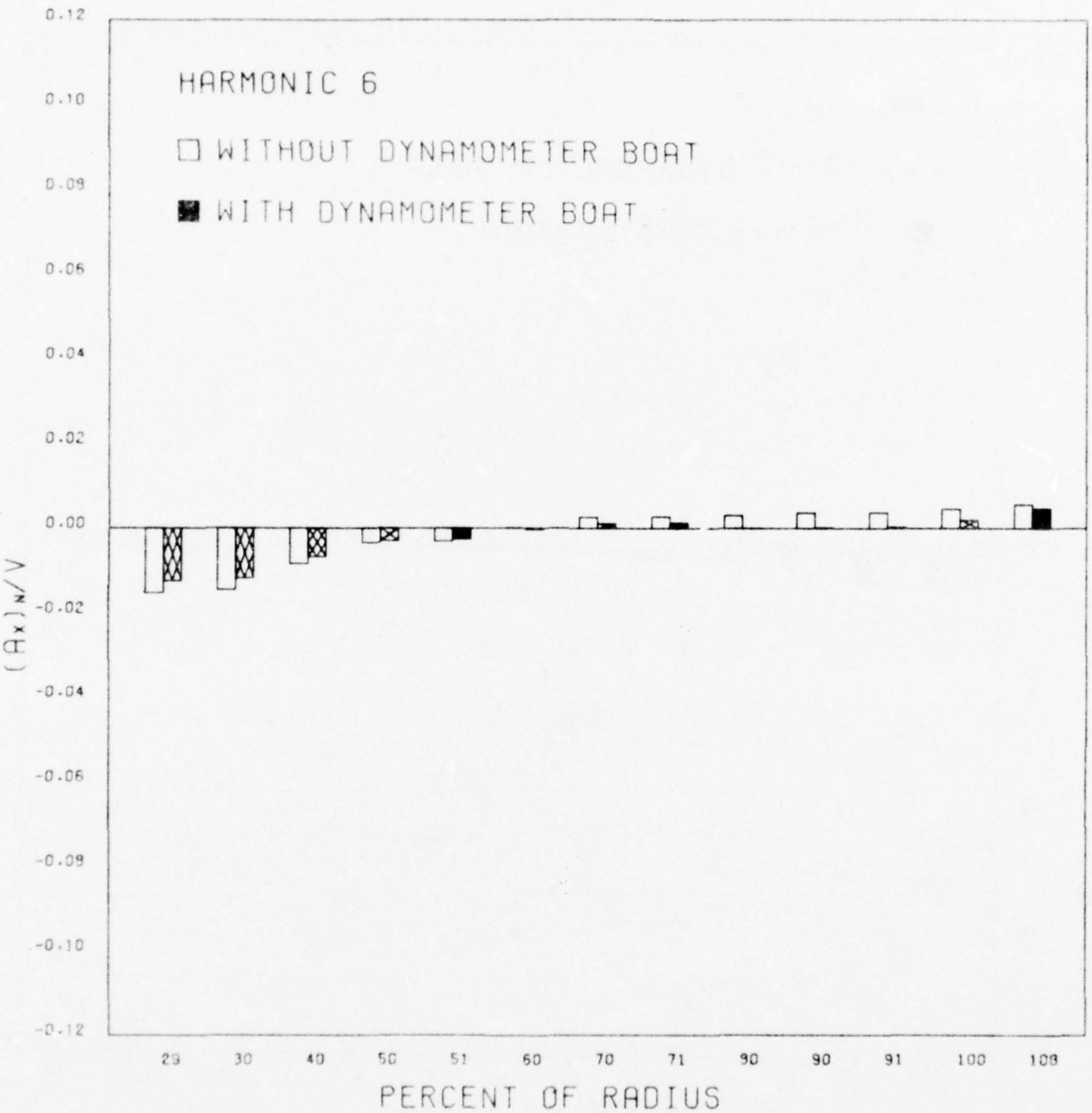

Figure 33 (Continued)

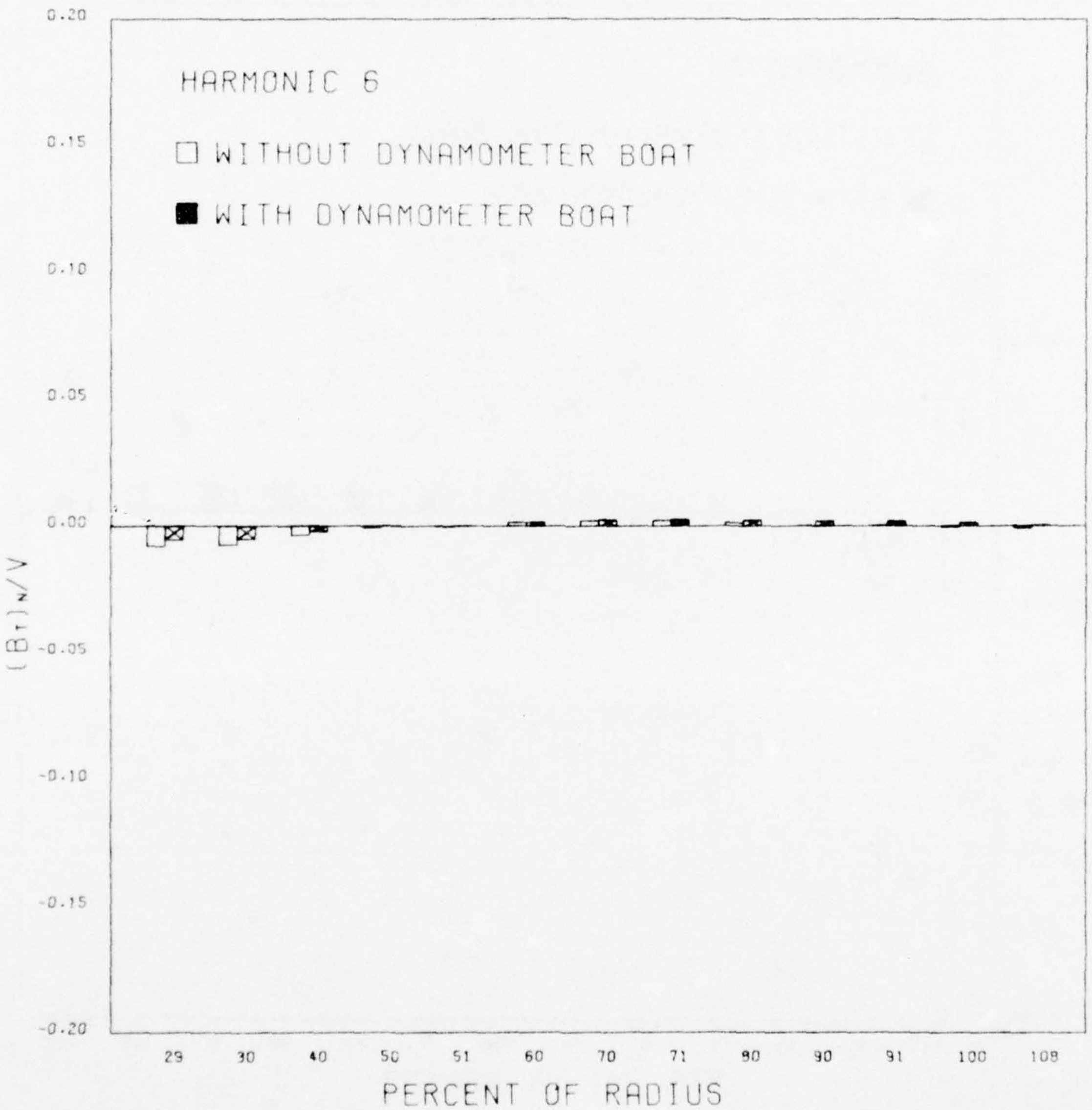

Figure 33 (Continued)

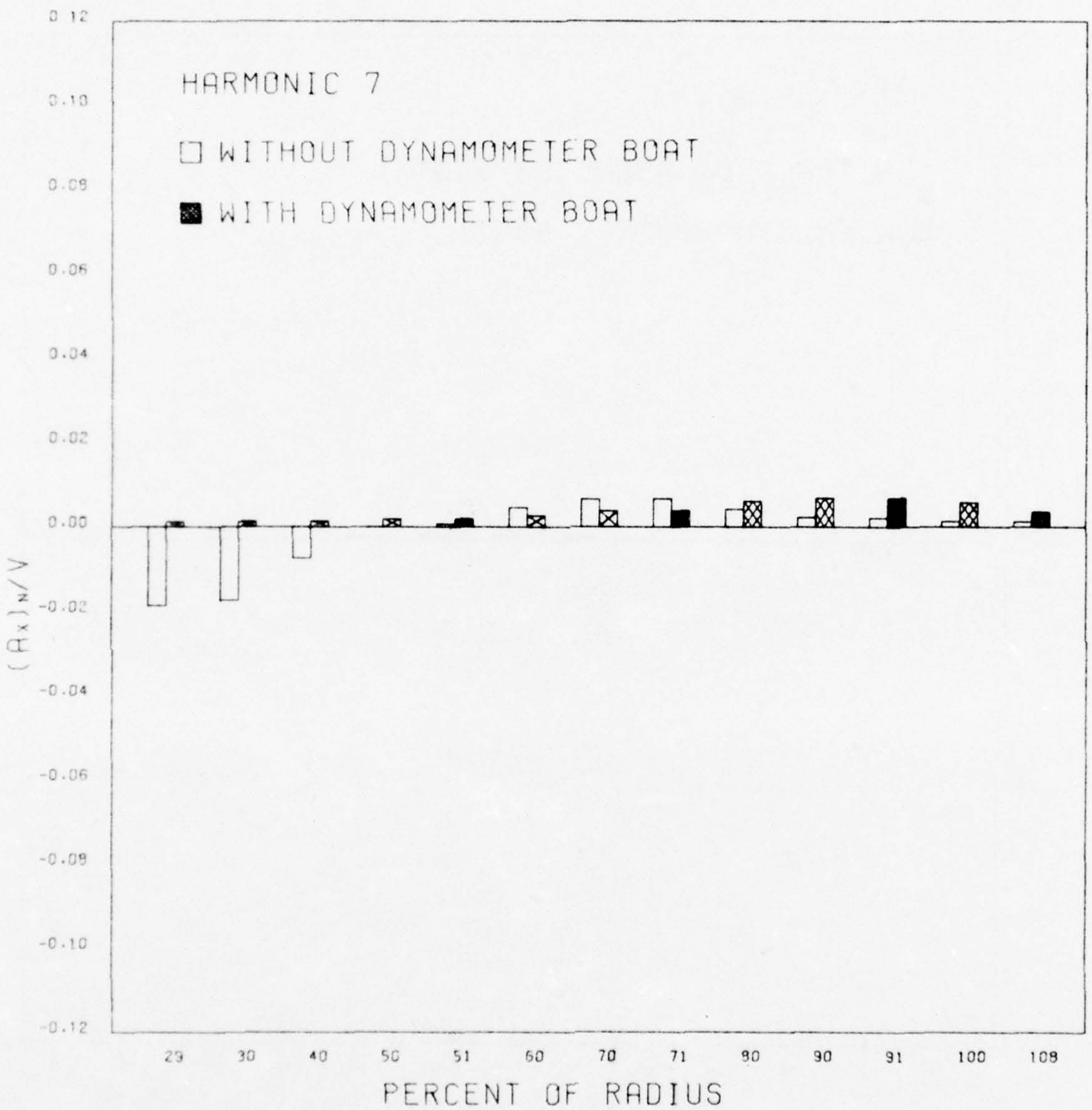

Figure 33 (Continued)

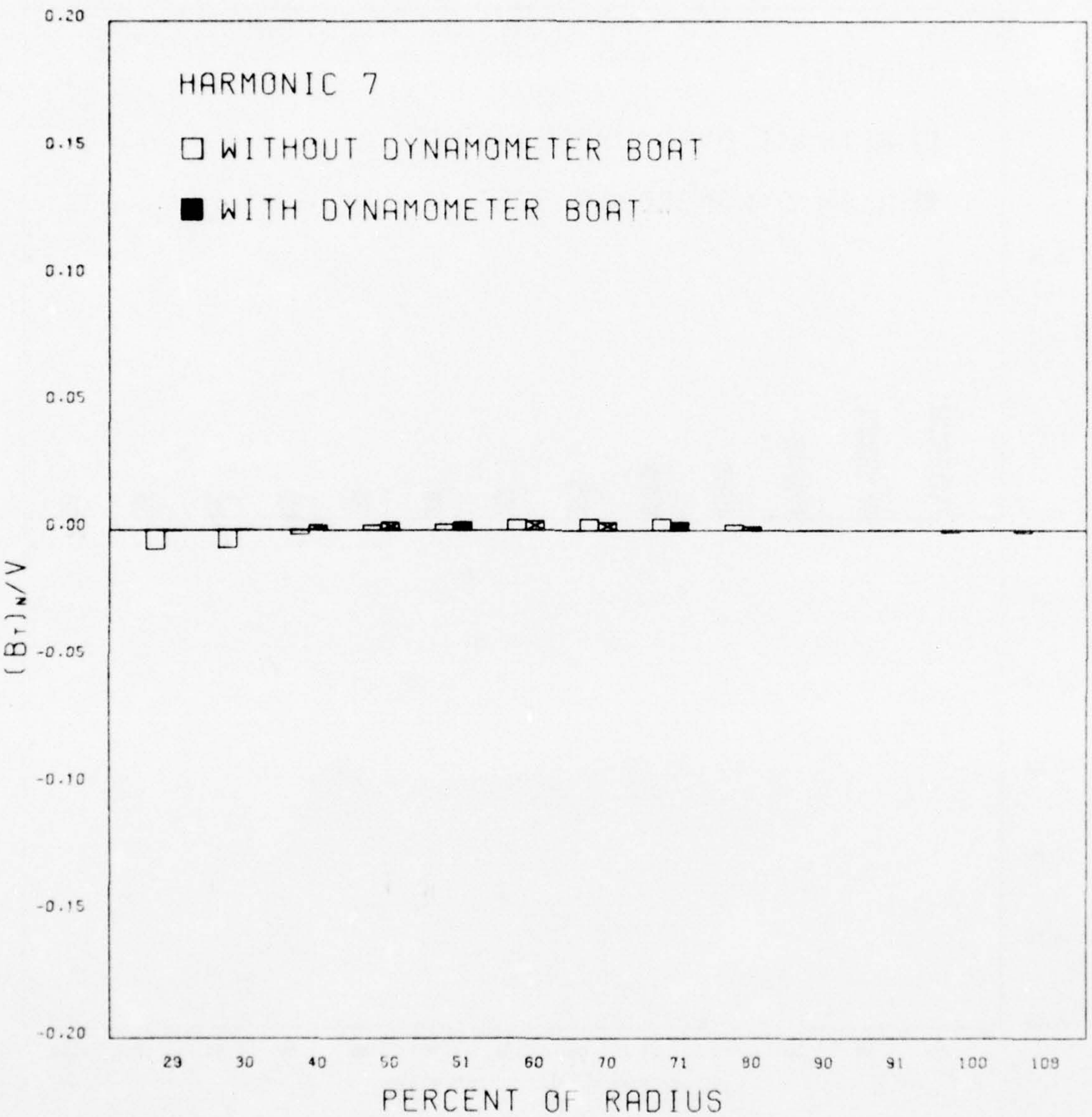

Figure 33 (Continued)

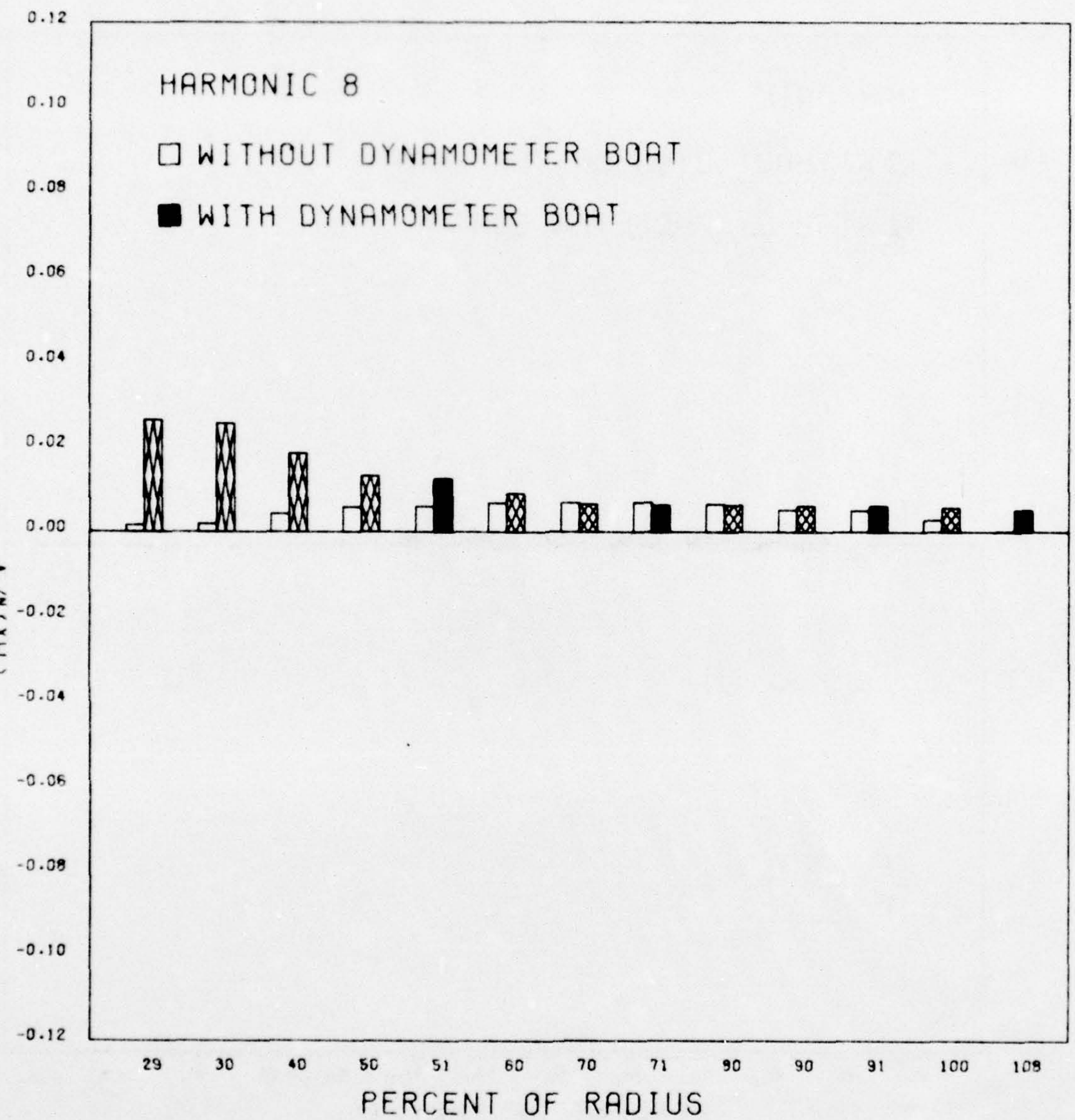

Figure 33 (Continued)

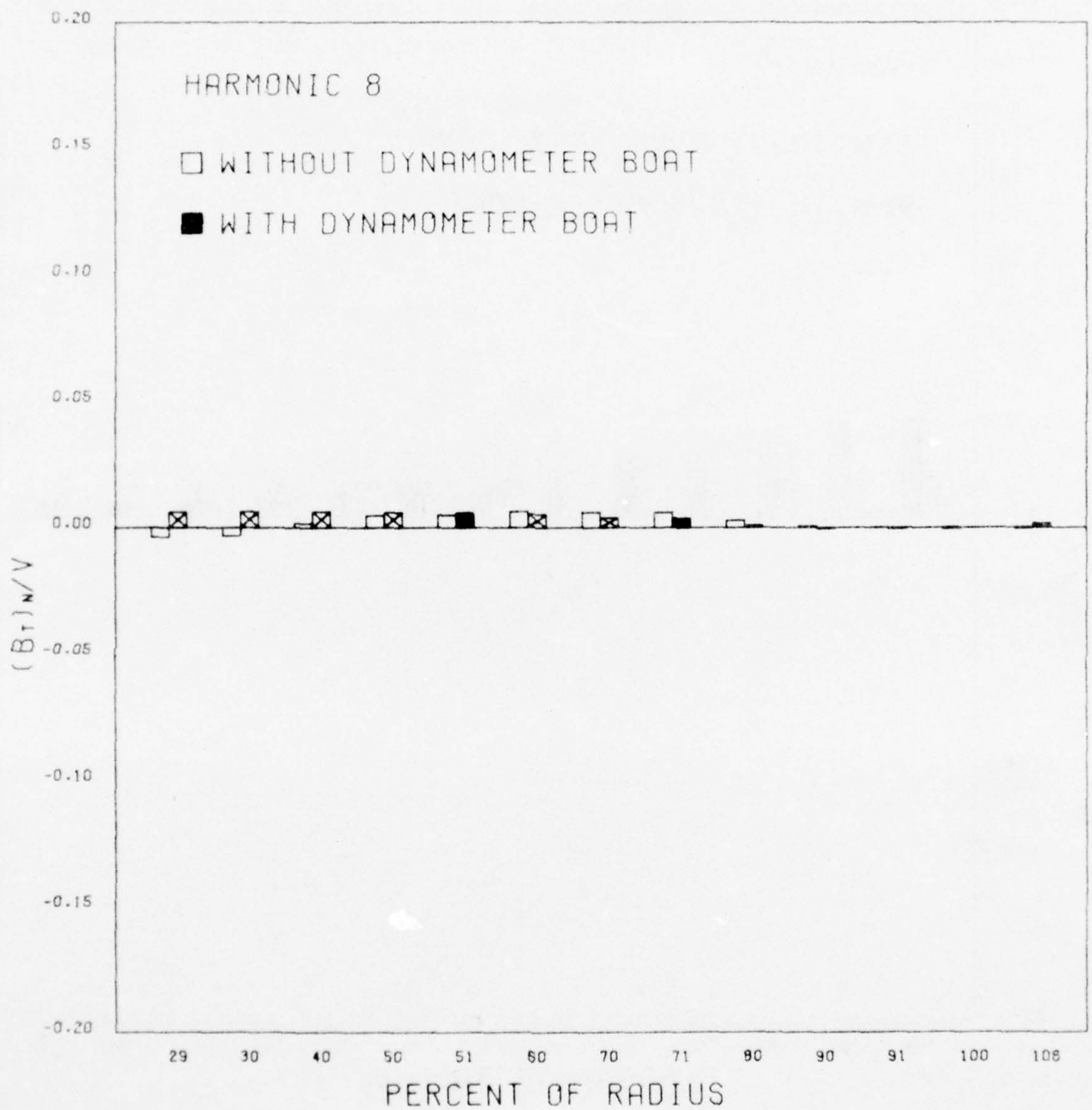

Figure 33 (Continued)

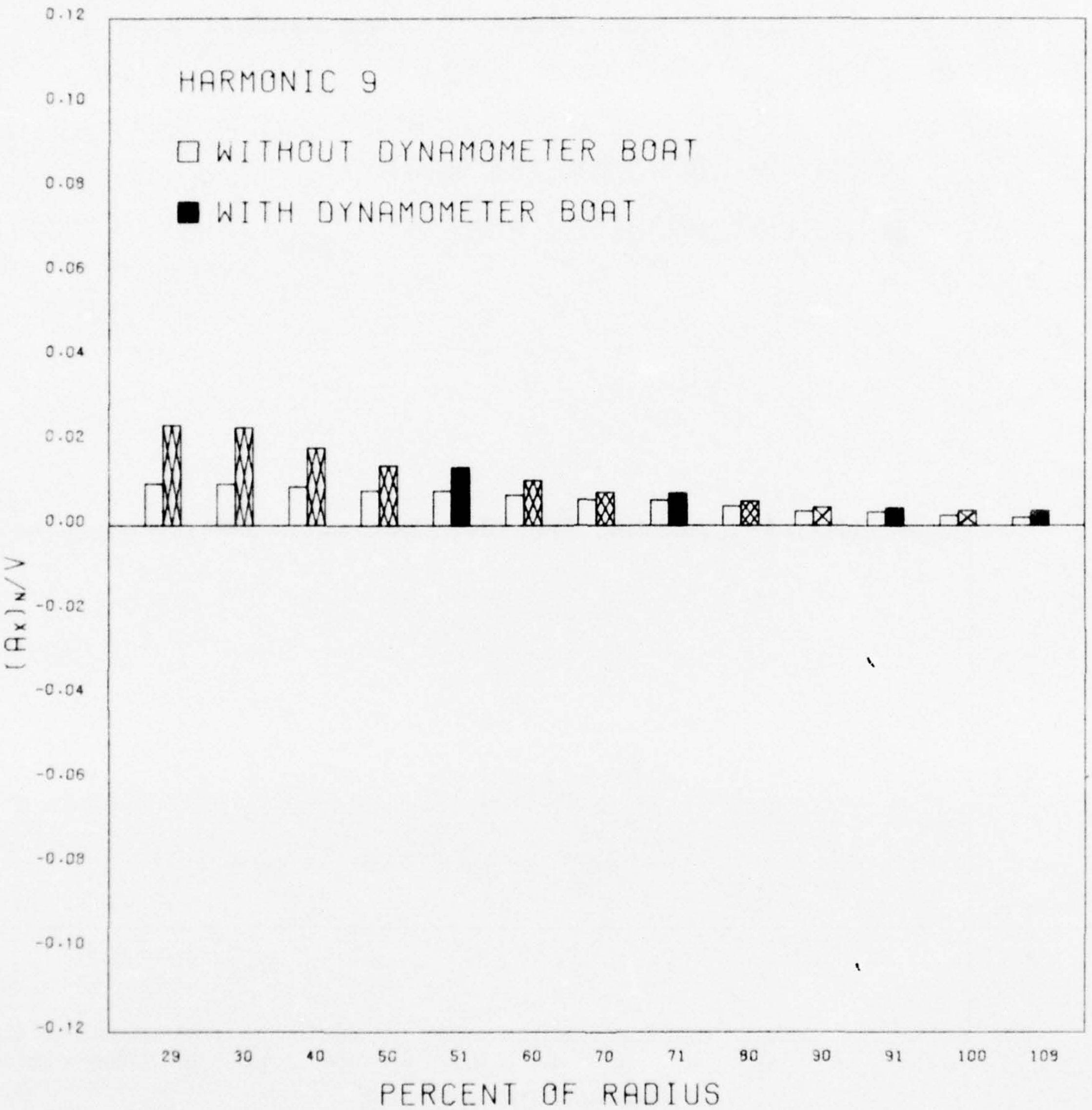

Figure 33 (Continued)

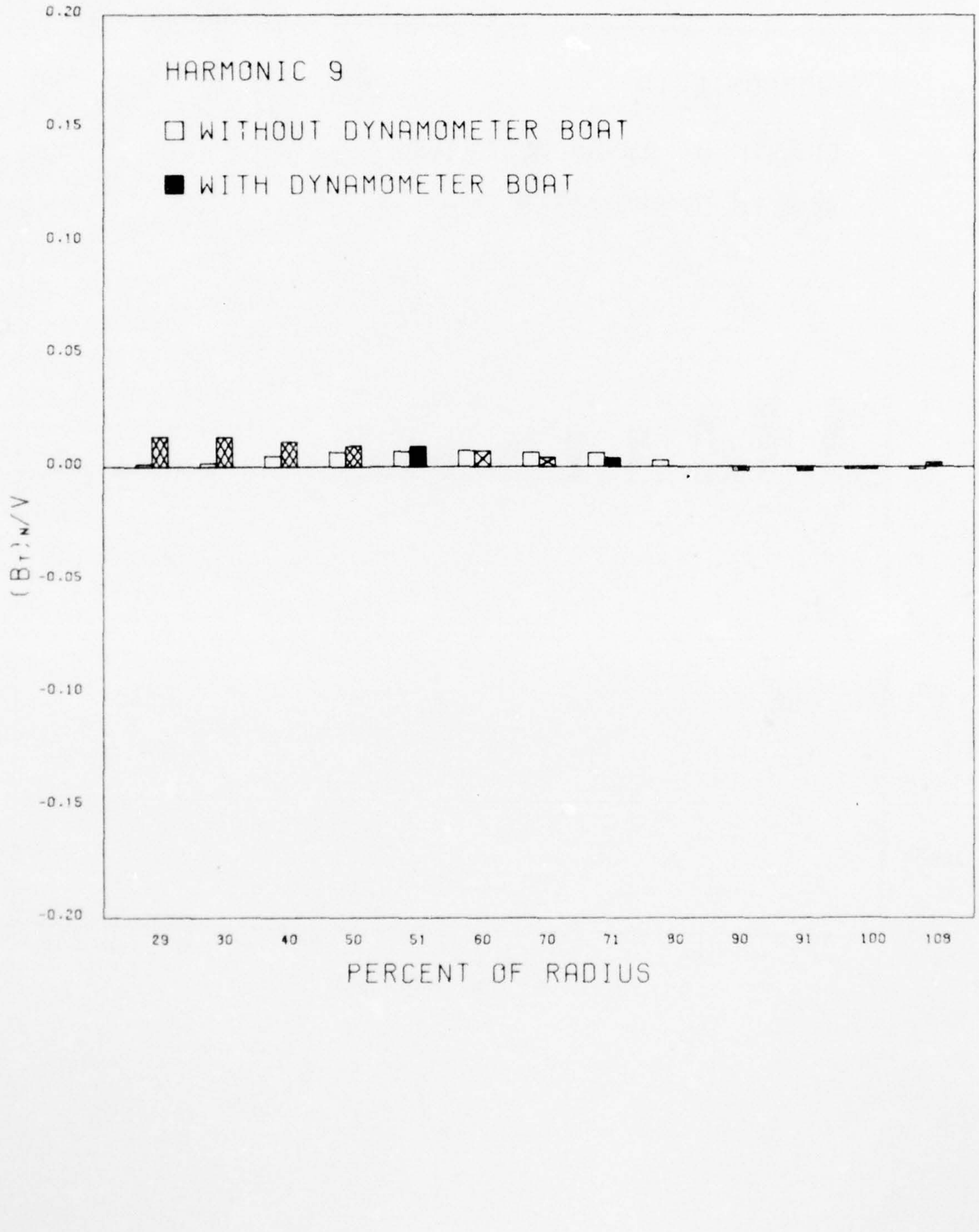

Figure 33 (Continued)

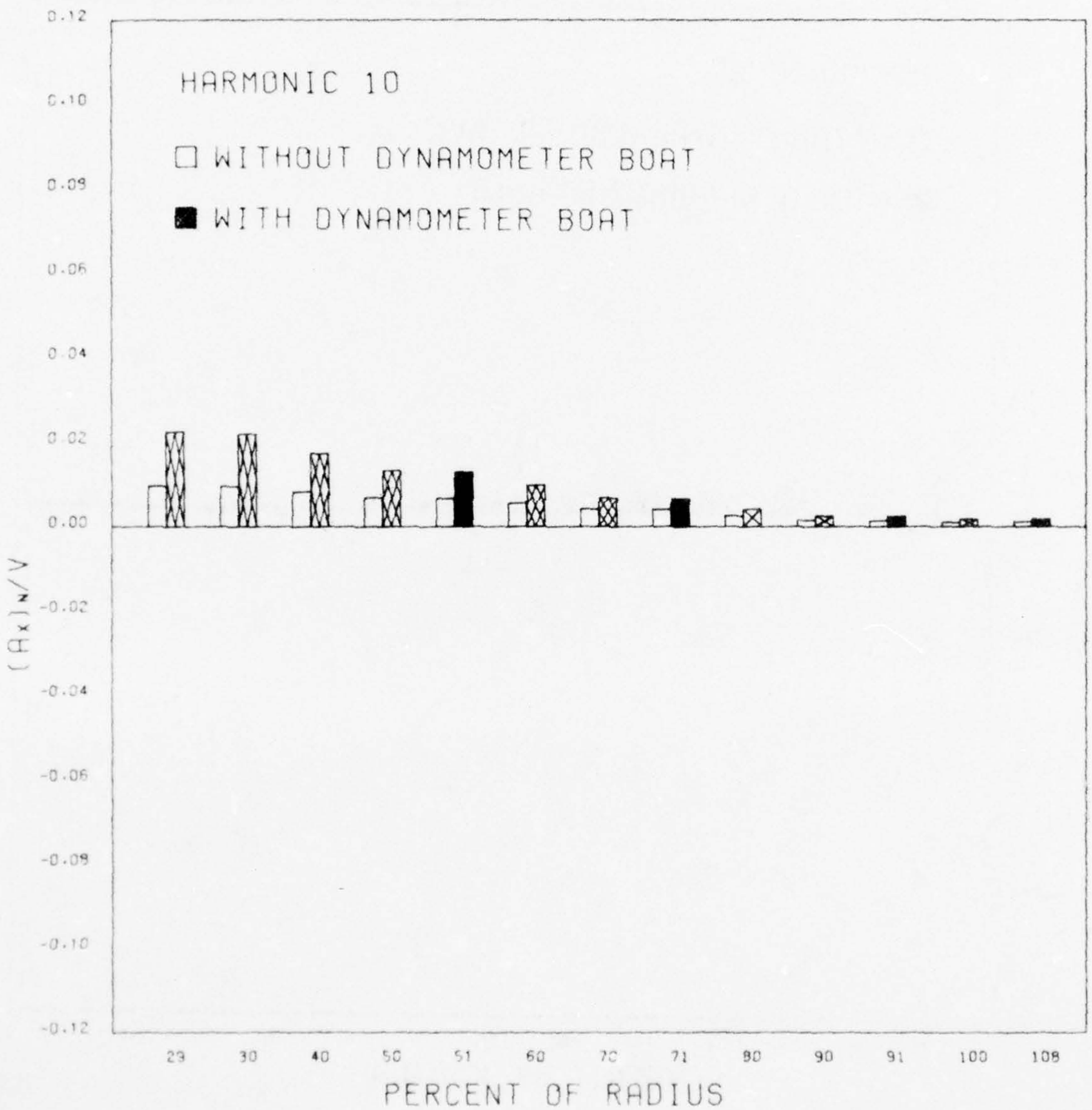

Figure 33 (Continued)

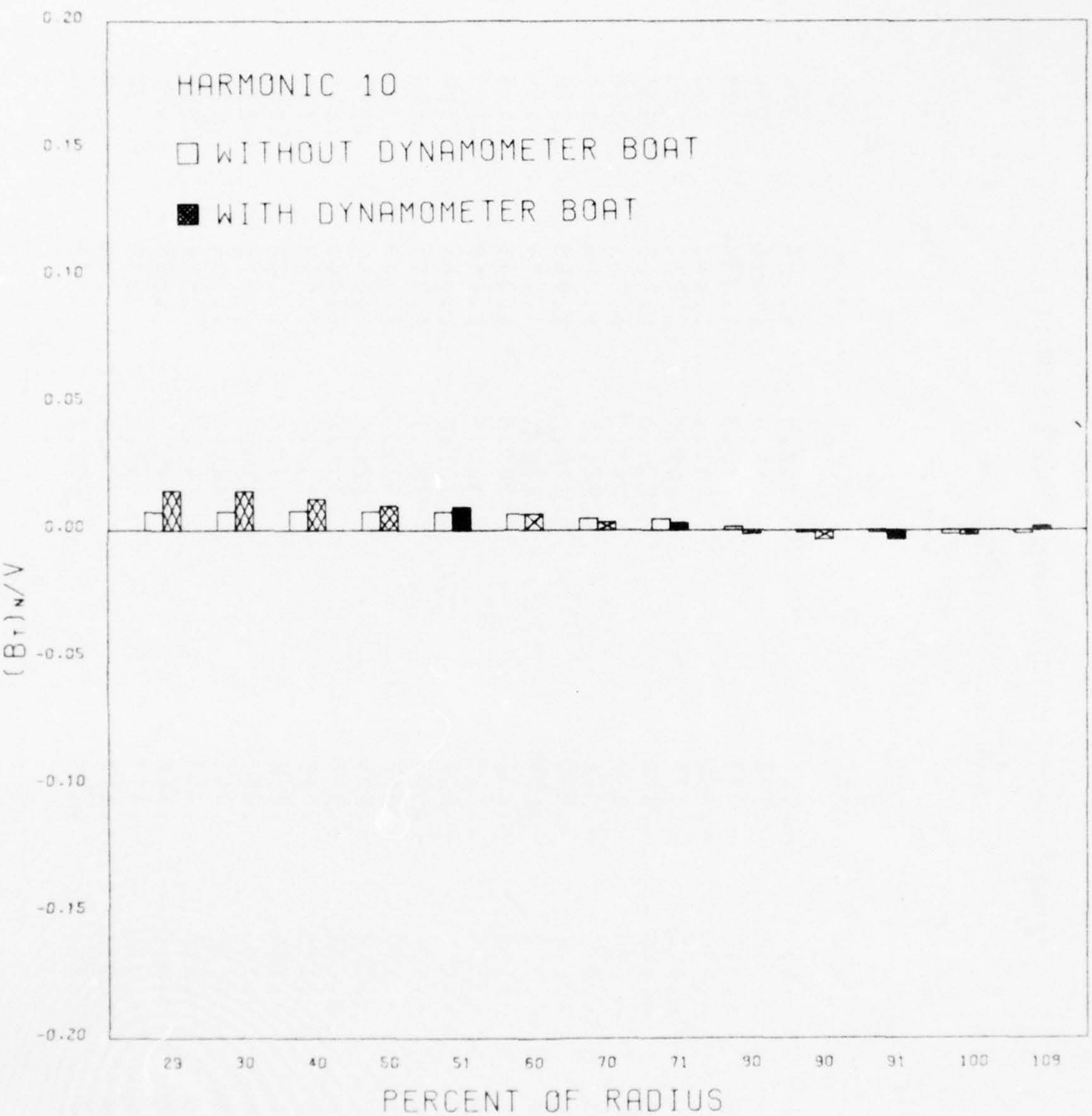

AD-A034 804 DAVID W TAYLOR NAVAL SHIP RESEARCH AND DEVELOPMENT CE--ETC F/G 13/10
EXPERIMENTAL UNSTEADY AND MEAN LOADS ON A CP PROPELLER BLADE ON--ETC(U)
OCT 76 R J BOSWELL, J J NELKA, S B DENNY

UNCLASSIFIED DTNSRDC-76-0125 NL

3 OF 4
AD
A034804

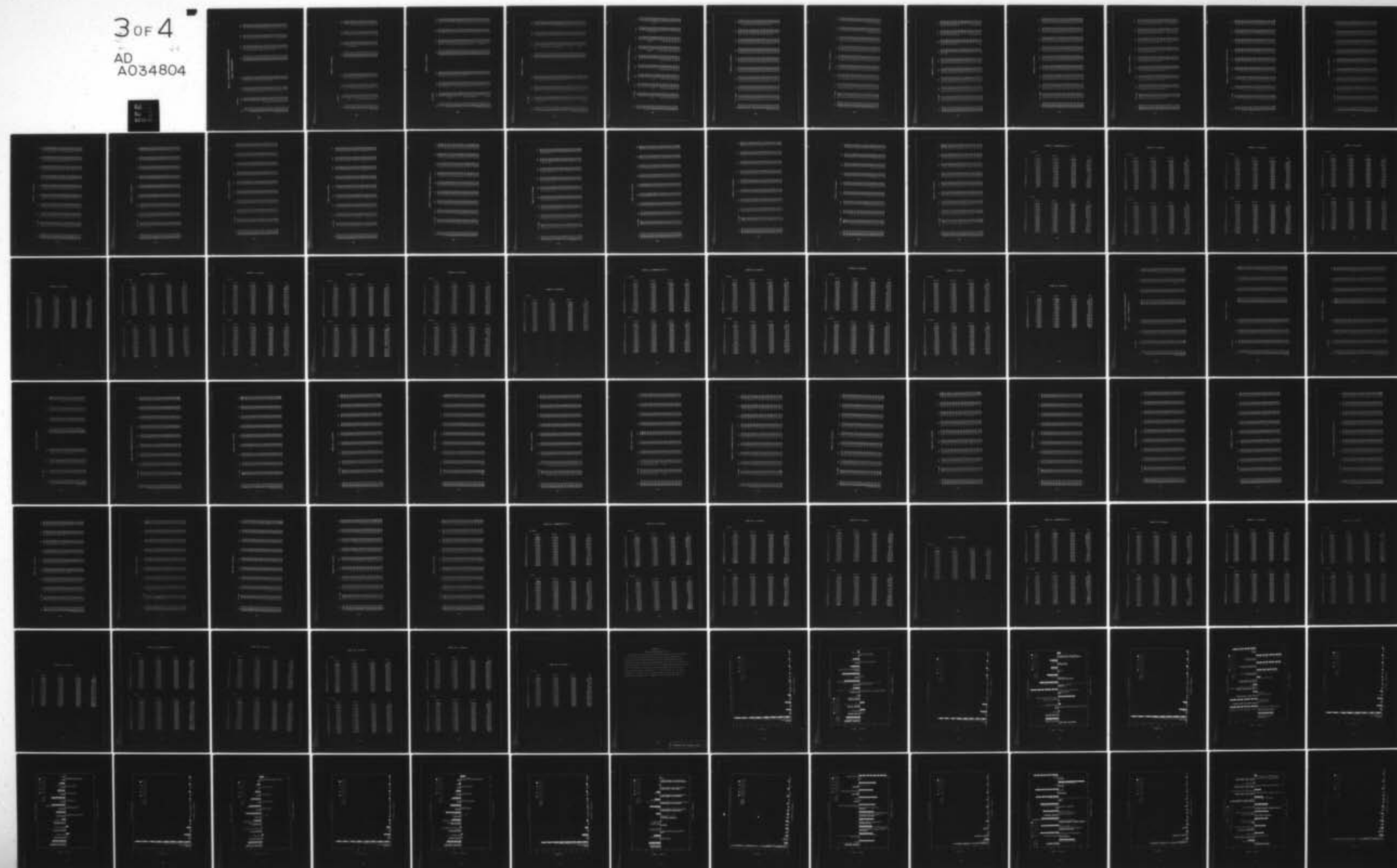

TABLE 9 – WAKE WITHOUT DYNAMOMETER BOAT

TABLE 9a – MEASURED DATA

r/R = 0.512

θ_w	V_x/V	V_t/V	V_r/V	θ_w	V_x/V	V_t/V	V_r/V
1.0	.926	.011	-.013	207.0	1.025	.074	.106
4.8	.925	-.008	-.023	214.9	1.026	.094	.098
6.8	.924	-.012	-.033	230.9	1.033	.128	.076
14.8	.921	-.054	-.071	239.1	1.041	.142	.062
16.9	.924	-.054	-.077	247.0	1.051	.152	.047
18.8	.936	-.043	-.079	255.0	1.040	.163	.032
20.8	.939	-.029	-.077	263.1	1.053	.166	.017
22.8	.913	-.033	-.071	271.1	1.064	.168	.001
24.8	.811	-.101	-.090	279.2	1.063	.166	-.015
26.6	.857	-.202	-.124	295.4	1.054	.154	-.047
28.8	.963	-.198	-.131	303.5	1.051	.143	-.061
31.0	1.040	-.155	-.119	311.5	1.048	.128	-.075
32.5	1.039	-.135	-.112	321.6	1.041	.107	-.091
42.7	1.034	-.126	-.085	323.7	1.044	.103	-.094
54.6	1.045	-.145	-.062	325.6	1.045	.100	-.097
66.9	1.041	-.163	-.035	329.5	1.040	.097	-.101
78.7	1.053	-.170	-.008	331.6	1.042	.100	-.101
90.7	1.048	-.171	.015	333.5	1.043	.110	-.103
102.8	1.041	-.166	.040	337.5	1.040	.149	-.112
114.8	1.040	-.154	.061	339.5	.975	.178	-.124
126.9	1.033	-.137	.081	341.5	.845	.107	-.090
138.8	1.028	-.115	.097	343.7	.844	-.002	-.050
166.8	1.022	-.045	.118	345.5	.893	-.021	-.030
174.9	1.026	-.021	.119	347.4	.935	-.006	-.021
191.0	1.020	.030	.118	349.6	.945	.012	-.019
199.0	1.022	.052	.113	353.8	.932	.018	-.016

TABLE 9a – (Continued)

r/R = 0.711

θ_w	V_x/V	V_t/V	V_r/V	θ_w	V_x/V	V_t/V	V_r/V
5.9	.988	-.040	-.088	202.0	.995	.075	.145
10.6	.992	-.051	-.098	226.0	.993	.123	.115
17.8	1.007	.017	-.121	237.9	1.000	.140	.092
18.5	1.006	.015	-.122	249.9	1.008	.153	.065
21.9	.851	-.018	-.107	273.9	1.015	.162	.003
23.8	.872	-.179	-.122	285.9	1.011	.157	-.029
25.8	.986	-.167	-.138	298.0	1.011	.145	-.060
27.8	1.021	-.127	-.129	322.0	1.010	.102	-.111
28.4	1.022	-.126	-.128	330.0	.993	.135	-.129
30.0	1.022	-.106	-.125	332.3	.991	.155	-.134
38.3	1.025	-.110	-.110	333.9	.931	.184	-.113
48.2	1.028	-.130	-.087	334.0	.905	.184	-.113
58.2	1.031	-.143	-.060	336.0	.864	.022	-.082
82.1	1.032	-.155	.008	338.0	.930	-.039	-.101
94.2	1.030	-.150	.040	340.2	.979	.001	-.111
106.2	1.024	-.140	.069	342.0	.973	.026	-.110
130.4	1.016	-.104	.116	344.1	.962	.033	-.098
142.4	1.018	-.078	.133	346.0	.960	.032	-.087
178.0	1.007	.017	.155	358.1	.972	-.023	-.064
190.1	.999	.048	.154	358.8	.968	-.020	-.063

TABLE 9a – (Continued)

r/R = 0.910

θ_w	V_x/V	V_t/V	V_r/V	θ_w	V_x/V	V_t/V	V_r/V
2.5	.982	-.004	-.094	186.6	1.008	.034	.160
3.3	.990	-.004	-.092	194.7	1.007	.052	.156
6.5	.988	-.021	-.099	202.7	1.003	.071	.150
7.5	.988	-.024	-.101	210.9	.995	.089	.142
10.6	.999	-.033	-.109	218.6	.999	.104	.131
13.5	1.001	-.037	-.112	226.7	1.001	.118	.119
20.5	1.026	-.026	-.114	234.8	1.002	.130	.105
22.5	1.029	.026	-.112	250.9	1.005	.150	.070
24.7	.887	.048	-.115	258.9	1.013	.157	.051
26.4	.812	-.128	-.110	266.9	1.019	.161	.031
28.5	.914	-.155	-.140	274.9	1.024	.165	.010
30.4	.985	-.095	-.125	283.1	1.031	.163	-.010
32.7	.990	-.083	-.124	291.1	1.031	.159	-.030
38.4	.997	-.089	-.111	307.3	1.023	.142	-.073
42.4	.995	-.098	-.100	315.3	1.022	.128	-.093
58.5	1.000	-.127	-.054	323.3	1.024	.108	-.110
66.4	1.011	-.134	-.028	327.2	1.022	.097	-.117
74.4	1.023	-.136	-.004	329.3	1.024	.094	-.118
82.5	1.021	-.137	.016	331.3	1.030	.098	-.121
90.4	1.012	-.132	.035	333.5	1.026	.121	-.132
98.5	1.007	-.127	.054	335.2	1.024	.183	-.152
106.5	1.005	-.121	.072	337.2	.837	.116	-.115
114.7	.986	-.113	.092	339.2	.878	-.077	-.113
122.6	.996	-.101	.105	341.5	1.036	.005	-.116
130.6	.996	-.088	.120	343.2	1.031	.049	-.117
138.6	.997	-.074	.131	345.2	1.024	.064	-.112
154.5	.997	-.042	.151	347.2	1.023	.065	-.106
162.6	1.003	-.025	.156	355.3	1.005	.042	-.091
170.7	1.009	-.005	.160	359.1	.976	.020	-.091
178.6	1.010	.015	.163	359.3	.998	.027	-.090

TABLE 9a – (Continued)

r/R = 1.082

θ_w	V_x/V	V_t/V	V_r/V
7.9	.987	-.045	-.128
12.0	1.000	-.050	-.129
19.7	.993	-.052	-.119
20.0	1.000	-.050	-.118
21.7	1.012	-.019	-.118
23.6	.960	.050	-.111
24.0	.916	.066	-.113
25.5	.875	-.123	-.116
25.9	.807	-.185	-.125
28.0	.983	-.136	-.143
29.9	.983	-.097	-.139
31.9	.980	-.089	-.135
39.9	.969	-.104	-.114
45.9	.967	-.117	-.093
53.8	.971	-.133	-.068
53.8	.969	-.131	-.070
61.9	.988	-.142	-.044
69.8	1.008	-.148	-.018
77.8	.980	-.152	.007
77.9	1.024	-.149	.007
85.7	.993	-.149	.027
93.9	.995	-.145	.046
101.9	.995	-.139	.065
118.3	.994	-.121	.101
126.2	.993	-.110	.117
134.4	.999	-.098	.129
142.5	.987	-.082	.145
158.4	1.005	-.050	.160
166.3	1.011	-.033	.165
174.5	1.010	-.014	.170
182.5	1.006	.004	.169

θ_w	V_x/V	V_t/V	V_r/V
190.6	1.002	.023	.166
198.4	1.002	.039	.161
214.5	.995	.069	.146
222.5	.995	.082	.135
230.6	1.001	.094	.120
238.9	1.001	.106	.105
246.7	1.003	.114	.090
254.8	1.009	.120	.072
263.0	1.010	.126	.051
271.3	.997	.134	.027
271.3	1.009	.132	.027
279.2	1.011	.133	.008
287.3	1.034	.131	-.016
295.4	1.016	.128	-.040
303.5	1.020	.121	-.062
311.6	1.017	.109	-.087
319.7	1.008	.093	-.110
323.7	.997	.084	-.121
325.6	.998	.080	-.126
329.7	.989	.069	-.135
331.6	1.001	.075	-.138
333.6	1.015	.113	-.135
335.6	.844	.194	-.100
337.8	.887	-.109	-.082
339.6	.983	-.011	-.130
341.6	1.004	.036	-.130
343.7	1.008	.043	-.131
347.7	.999	.040	-.131
355.7	.980	.029	-.124
359.7	.961	.004	-.119

TABLE 9b – INTERPOLATED VALUES OF V_x/V

θ_w	r/R = 0.289	0.3	0.4	0.5	0.6	0.7	0.8	0.9	1.0
0.0	.830	.836	.883	.922	.952	.972	.985	.986	.977
2.5	.805	.812	.873	.921	.956	.979	.987	.986	.977
5.0	.783	.792	.863	.919	.960	.985	.988	.986	.981
7.5	.771	.780	.857	.917	.961	.988	.990	.990	.988
10.0	.767	.776	.854	.915	.960	.989	.995	.997	.997
12.5	.695	.709	.823	.911	.974	1.010	1.006	1.001	.999
15.0	.639	.657	.801	.910	.986	1.028	1.018	1.006	.998
17.5	.717	.731	.837	.919	.979	1.015	1.020	1.016	1.005
20.0	1.145	1.130	1.020	.947	.909	.908	.980	1.023	1.026
22.5	1.299	1.273	1.071	.933	.858	.847	.959	1.026	1.032
25.0	.431	.456	.652	.797	.893	.938	.898	.870	.860
27.5	.424	.456	.705	.882	.987	1.019	.908	.854	.876
30.0	.935	.941	.983	1.011	1.024	1.023	.993	.975	.973
32.5	1.039	1.040	1.042	1.039	1.034	1.024	1.007	.993	.983
35.0	1.033	1.034	1.038	1.038	1.033	1.025	1.009	.995	.983
37.5	1.028	1.029	1.035	1.036	1.033	1.026	1.012	.998	.984
40.0	1.021	1.023	1.031	1.035	1.033	1.027	1.013	.998	.982
42.5	1.015	1.016	1.028	1.034	1.034	1.027	1.012	.997	.981
45.0	1.017	1.018	1.030	1.035	1.035	1.028	1.012	.996	.980
47.5	1.022	1.023	1.033	1.038	1.036	1.029	1.013	.996	.980
50.0	1.028	1.029	1.038	1.041	1.038	1.030	1.013	.996	.980
52.5	1.035	1.036	1.042	1.043	1.040	1.031	1.014	.997	.981
55.0	1.040	1.041	1.045	1.045	1.041	1.031	1.015	.999	.984
57.5	1.038	1.038	1.044	1.044	1.041	1.032	1.016	1.000	.987

TABLE 9b – (Continued)

θ_w	r/R = 0.289	0.3	0.4	0.5	0.6	0.7	0.8	0.9	1.0
60.0	1.036	1.037	1.042	1.043	1.040	1.032	1.017	1.003	.991
62.5	1.035	1.036	1.041	1.042	1.040	1.033	1.019	1.006	.996
65.0	1.035	1.036	1.040	1.041	1.039	1.033	1.020	1.010	1.002
67.5	1.040	1.040	1.042	1.042	1.039	1.033	1.023	1.014	1.007
70.0	1.052	1.052	1.049	1.045	1.039	1.033	1.025	1.018	1.012
72.5	1.066	1.065	1.056	1.048	1.040	1.033	1.028	1.022	1.014
75.0	1.078	1.076	1.063	1.051	1.041	1.033	1.030	1.024	1.015
77.5	1.087	1.085	1.068	1.054	1.042	1.033	1.030	1.024	1.014
80.0	1.090	1.088	1.070	1.055	1.042	1.033	1.030	1.024	1.012
82.5	1.087	1.085	1.068	1.054	1.042	1.033	1.029	1.022	1.010
85.0	1.081	1.080	1.065	1.053	1.042	1.033	1.028	1.019	1.007
87.5	1.074	1.073	1.062	1.051	1.042	1.032	1.026	1.016	1.005
90.0	1.067	1.066	1.058	1.050	1.041	1.032	1.023	1.013	1.003
92.5	1.061	1.060	1.054	1.048	1.040	1.031	1.021	1.011	1.002
95.0	1.057	1.056	1.052	1.046	1.039	1.031	1.020	1.010	1.001
97.5	1.054	1.053	1.050	1.045	1.038	1.030	1.018	1.008	1.000
100.0	1.053	1.052	1.048	1.043	1.036	1.028	1.017	1.008	1.000
102.5	1.053	1.053	1.048	1.042	1.035	1.027	1.017	1.008	1.000
105.0	1.056	1.055	1.049	1.042	1.034	1.026	1.015	1.007	1.000
107.5	1.056	1.055	1.049	1.041	1.033	1.024	1.012	1.003	.998
110.0	1.052	1.052	1.047	1.041	1.033	1.023	1.007	.997	.993
112.5	1.048	1.048	1.046	1.041	1.033	1.022	1.002	.991	.989
115.0	1.046	1.046	1.045	1.041	1.033	1.021	.999	.987	.986
117.5	1.048	1.048	1.045	1.040	1.031	1.020	1.000	.989	.988

TABLE 9b – (Continued)

θ_w	r/R = 0.289	0.3	0.4	0.5	0.6	0.7	0.8	0.9	1.0
120.0	1.051	1.050	1.045	1.038	1.030	1.019	1.003	.993	.990
122.5	1.053	1.052	1.045	1.037	1.028	1.018	1.005	.996	.993
125.0	1.051	1.050	1.043	1.035	1.027	1.018	1.006	.997	.993
127.5	1.047	1.047	1.040	1.034	1.026	1.017	1.005	.997	.994
130.0	1.044	1.043	1.038	1.032	1.025	1.017	1.004	.997	.994
132.5	1.039	1.039	1.036	1.031	1.025	1.017	1.004	.997	.995
135.0	1.035	1.035	1.033	1.030	1.025	1.018	1.005	.997	.995
137.5	1.031	1.031	1.031	1.029	1.025	1.018	1.006	.997	.994
140.0	1.026	1.026	1.028	1.028	1.024	1.018	1.006	.998	.992
142.5	1.020	1.021	1.025	1.026	1.024	1.019	1.007	.997	.991
145.0	1.016	1.017	1.023	1.025	1.024	1.019	1.007	.997	.991
147.5	1.013	1.014	1.021	1.024	1.023	1.019	1.006	.997	.991
150.0	1.011	1.012	1.020	1.023	1.023	1.018	1.006	.997	.993
152.5	1.010	1.011	1.019	1.022	1.022	1.018	1.005	.997	.994
155.0	1.011	1.012	1.019	1.022	1.021	1.017	1.005	.998	.996
157.5	1.014	1.015	1.019	1.021	1.021	1.017	1.005	.999	.999
160.0	1.018	1.018	1.021	1.021	1.020	1.016	1.006	1.001	1.002
162.5	1.023	1.023	1.023	1.022	1.019	1.015	1.007	1.003	1.004
165.0	1.030	1.030	1.026	1.022	1.018	1.014	1.008	1.005	1.006
167.5	1.039	1.038	1.030	1.023	1.017	1.013	1.009	1.007	1.008
170.0	1.049	1.048	1.035	1.025	1.017	1.012	1.009	1.009	1.009
172.5	1.059	1.057	1.040	1.026	1.017	1.010	1.010	1.010	1.010
175.0	1.067	1.065	1.044	1.028	1.016	1.009	1.010	1.010	1.010
177.5	1.071	1.068	1.045	1.027	1.015	1.008	1.009	1.010	1.010

TABLE 9b – (Continued)

θ_w	r/R = 0.289	0.3	0.4	0.5	0.6	0.7	0.8	0.9	1.0
180.0	1.074	1.071	1.046	1.027	1.013	1.006	1.008	1.010	1.009
182.5	1.075	1.072	1.046	1.026	1.012	1.004	1.007	1.009	1.008
185.0	1.076	1.073	1.045	1.024	1.010	1.003	1.006	1.008	1.008
187.5	1.078	1.074	1.045	1.023	1.009	1.001	1.006	1.008	1.007
190.0	1.079	1.076	1.045	1.022	1.007	.999	1.005	1.008	1.006
192.5	1.083	1.079	1.047	1.023	1.006	.998	1.004	1.007	1.006
195.0	1.088	1.083	1.049	1.023	1.006	.997	1.004	1.007	1.006
197.5	1.092	1.087	1.051	1.024	1.006	.997	1.002	1.006	1.005
200.0	1.096	1.091	1.053	1.025	1.006	.996	1.001	1.005	1.004
202.5	1.099	1.094	1.056	1.026	1.006	.995	1.000	1.003	1.003
205.0	1.102	1.097	1.057	1.027	1.006	.995	.998	1.000	1.001
207.5	1.103	1.098	1.059	1.028	1.007	.994	.996	.998	.998
210.0	1.104	1.099	1.059	1.029	1.007	.994	.994	.995	.996
212.5	1.106	1.101	1.061	1.029	1.006	.993	.994	.995	.996
215.0	1.110	1.105	1.062	1.029	1.006	.993	.995	.997	.996
217.5	1.114	1.109	1.064	1.030	1.006	.993	.996	.998	.997
220.0	1.118	1.112	1.066	1.031	1.006	.993	.997	.999	.998
222.5	1.121	1.115	1.068	1.032	1.007	.993	.998	1.000	.999
225.0	1.123	1.117	1.070	1.033	1.008	.994	.998	1.001	1.000
227.5	1.125	1.119	1.071	1.034	1.009	.995	.998	1.001	1.001
230.0	1.126	1.120	1.073	1.036	1.010	.996	.999	1.001	1.002
232.5	1.128	1.122	1.075	1.038	1.012	.997	1.000	1.002	1.002
235.0	1.130	1.125	1.077	1.040	1.014	.999	1.000	1.002	1.002
237.5	1.133	1.127	1.080	1.043	1.017	1.001	1.001	1.002	1.002

TABLE 9b – (Continued)

θ_w	r/R = 0.289	0.3	0.4	0.5	0.6	0.7	0.8	0.9	1.0
240.0	1.138	1.132	1.084	1.046	1.019	1.003	1.002	1.002	1.002
242.5	1.145	1.139	1.089	1.050	1.022	1.004	1.003	1.002	1.002
245.0	1.150	1.144	1.093	1.054	1.024	1.006	1.004	1.003	1.002
247.5	1.148	1.142	1.093	1.054	1.026	1.008	1.005	1.003	1.003
250.0	1.133	1.127	1.084	1.050	1.025	1.009	1.006	1.005	1.005
252.5	1.117	1.113	1.075	1.046	1.024	1.011	1.008	1.007	1.007
255.0	1.106	1.102	1.069	1.043	1.024	1.012	1.010	1.009	1.009
257.5	1.113	1.109	1.073	1.045	1.025	1.013	1.012	1.012	1.011
260.0	1.127	1.122	1.081	1.050	1.027	1.014	1.014	1.014	1.013
262.5	1.142	1.137	1.091	1.055	1.030	1.015	1.016	1.016	1.014
265.0	1.157	1.150	1.100	1.060	1.032	1.015	1.018	1.018	1.014
267.5	1.170	1.163	1.107	1.064	1.034	1.016	1.020	1.020	1.014
270.0	1.181	1.173	1.114	1.068	1.035	1.016	1.021	1.021	1.014
272.5	1.187	1.180	1.117	1.069	1.036	1.016	1.022	1.023	1.015
275.0	1.191	1.183	1.119	1.069	1.035	1.016	1.023	1.024	1.017
277.5	1.195	1.186	1.120	1.069	1.034	1.015	1.024	1.027	1.020
280.0	1.196	1.188	1.120	1.068	1.033	1.014	1.024	1.029	1.024
282.5	1.198	1.189	1.119	1.067	1.031	1.013	1.024	1.030	1.029
285.0	1.197	1.188	1.118	1.065	1.030	1.012	1.023	1.031	1.033
287.5	1.194	1.185	1.116	1.064	1.029	1.012	1.023	1.031	1.035
290.0	1.189	1.180	1.113	1.062	1.028	1.012	1.023	1.031	1.033
292.5	1.183	1.175	1.109	1.060	1.028	1.012	1.023	1.030	1.030
295.0	1.177	1.169	1.106	1.059	1.027	1.012	1.024	1.029	1.026
297.5	1.171	1.163	1.103	1.058	1.027	1.012	1.023	1.028	1.025

TABLE 9b – (Continued)

θ_w	r/R = 0.289	0.3	0.4	0.5	0.6	0.7	0.8	0.9	1.0
300.0	1.163	1.156	1.099	1.056	1.028	1.013	1.022	1.027	1.024
302.5	1.154	1.148	1.095	1.055	1.028	1.014	1.021	1.025	1.024
305.0	1.146	1.140	1.091	1.054	1.029	1.015	1.020	1.024	1.023
307.5	1.139	1.133	1.088	1.053	1.029	1.016	1.020	1.023	1.022
310.0	1.133	1.127	1.085	1.052	1.029	1.016	1.020	1.022	1.021
312.5	1.125	1.120	1.080	1.050	1.028	1.017	1.020	1.022	1.020
315.0	1.116	1.111	1.074	1.046	1.027	1.016	1.020	1.022	1.020
317.5	1.113	1.108	1.072	1.044	1.025	1.015	1.021	1.023	1.019
320.0	1.118	1.113	1.073	1.043	1.023	1.013	1.021	1.024	1.018
322.5	1.139	1.132	1.083	1.046	1.021	1.009	1.021	1.024	1.015
325.0	1.167	1.159	1.096	1.049	1.018	1.003	1.018	1.023	1.014
327.5	1.177	1.169	1.099	1.047	1.014	.998	1.016	1.022	1.012
330.0	1.189	1.180	1.103	1.046	1.009	.994	1.018	1.027	1.015
332.5	1.233	1.220	1.122	1.050	1.004	.984	1.011	1.028	1.029
335.0	1.621	1.583	1.287	1.071	.936	.881	.987	1.029	.988
337.5	1.248	1.236	1.136	1.050	.976	.916	.858	.833	.841
340.0	.812	.821	.888	.937	.966	.977	.944	.935	.955
342.5	.591	.605	.722	.821	.901	.964	1.015	1.038	1.033
345.0	.765	.771	.824	.873	.917	.956	1.000	1.023	1.024
347.5	.959	.956	.941	.936	.941	.957	1.000	1.022	1.020
350.0	.984	.981	.957	.946	.946	.957	.998	1.019	1.015
352.5	.950	.948	.939	.938	.945	.959	.995	1.013	1.009
355.0	.901	.903	.914	.928	.944	.962	.992	1.006	1.001
357.5	.863	.867	.898	.924	.947	.966	.987	.994	.987

TABLE 9c – INTERPOLATED VALUES OF V_T/V

θ_w	r/R = 0.289	0.3	0.4	0.5	0.6	0.7	0.8	0.9	1.0
0.0	.157	.148	.073	.019	-.014	-.026	.002	.017	.016
2.5	.120	.112	.051	.007	-.021	-.032	-.012	-.001	-.004
5.0	.087	.081	.031	-.005	-.028	-.038	-.022	-.015	-.019
7.5	.082	.076	.025	-.011	-.035	-.046	-.030	-.024	-.030
10.0	.043	.038	.001	-.027	-.044	-.051	-.037	-.032	-.037
12.5	-.076	-.074	-.058	-.046	-.038	-.033	-.032	-.036	-.043
15.0	-.216	-.205	-.121	-.060	-.022	-.005	-.025	-.043	-.057
17.5	-.280	-.265	-.146	-.059	-.006	.014	-.021	-.049	-.064
20.0	-.272	-.256	-.132	-.042	.013	.034	-.003	-.032	-.047
22.5	.195	.179	.060	-.022	-.067	-.076	-.016	.024	.036
25.0	.295	.267	.049	-.100	-.178	-.188	-.052	.018	.002
27.5	-.413	-.401	-.298	-.220	-.167	-.139	-.153	-.161	-.160
30.0	-.340	-.329	-.246	-.182	-.136	-.108	-.110	-.109	-.104
32.5	-.214	-.210	-.170	-.138	-.114	-.096	-.087	-.083	-.084
35.0	-.143	-.141	-.128	-.117	-.106	-.097	-.086	-.081	-.083
37.5	-.095	-.097	-.105	-.109	-.110	-.106	-.093	-.086	-.088
40.0	-.093	-.094	-.106	-.114	-.116	-.113	-.099	-.092	-.095
42.5	-.118	-.119	-.124	-.125	-.123	-.118	-.105	-.098	-.101
45.0	-.117	-.118	-.125	-.128	-.128	-.124	-.110	-.104	-.106
47.5	-.115	-.116	-.126	-.131	-.132	-.129	-.115	-.109	-.111
50.0	-.120	-.121	-.131	-.136	-.137	-.133	-.120	-.114	-.116
52.5	-.129	-.130	-.137	-.141	-.141	-.137	-.124	-.118	-.121
55.0	-.139	-.140	-.144	-.146	-.144	-.140	-.128	-.122	-.125
57.5	-.147	-.148	-.150	-.150	-.148	-.143	-.131	-.126	-.129

TABLE 9c – (Continued)

θ_w	r/R = 0.289	0.3	0.4	0.5	0.6	0.7	0.8	0.9	1.0
60.0	-.155	-.155	-.155	-.154	-.151	-.146	-.134	-.129	-.132
62.5	-.162	-.162	-.160	-.158	-.154	-.148	-.136	-.131	-.134
65.0	-.168	-.168	-.165	-.161	-.156	-.150	-.138	-.133	-.136
67.5	-.173	-.173	-.169	-.164	-.158	-.152	-.140	-.135	-.138
70.0	-.176	-.175	-.171	-.166	-.160	-.153	-.141	-.135	-.139
72.5	-.178	-.178	-.173	-.168	-.162	-.154	-.141	-.136	-.139
75.0	-.180	-.180	-.175	-.169	-.163	-.155	-.142	-.136	-.140
77.5	-.182	-.182	-.176	-.170	-.164	-.156	-.142	-.137	-.141
80.0	-.184	-.184	-.178	-.171	-.164	-.156	-.143	-.137	-.141
82.5	-.187	-.186	-.179	-.172	-.164	-.156	-.143	-.137	-.140
85.0	-.188	-.187	-.180	-.172	-.164	-.155	-.142	-.136	-.139
87.5	-.189	-.189	-.181	-.172	-.164	-.155	-.140	-.134	-.138
90.0	-.190	-.189	-.181	-.172	-.163	-.153	-.138	-.132	-.136
92.5	-.192	-.191	-.181	-.172	-.162	-.152	-.137	-.131	-.135
95.0	-.193	-.192	-.182	-.171	-.161	-.151	-.135	-.129	-.133
97.5	-.194	-.193	-.181	-.170	-.159	-.149	-.134	-.128	-.132
100.0	-.195	-.193	-.181	-.169	-.158	-.147	-.132	-.126	-.130
102.5	-.195	-.194	-.180	-.168	-.156	-.145	-.130	-.124	-.128
105.0	-.195	-.193	-.179	-.166	-.154	-.142	-.128	-.122	-.126
107.5	-.194	-.192	-.177	-.164	-.151	-.140	-.126	-.120	-.124
110.0	-.193	-.191	-.175	-.161	-.148	-.137	-.123	-.118	-.122
112.5	-.192	-.190	-.173	-.158	-.145	-.134	-.121	-.116	-.119
115.0	-.190	-.188	-.171	-.155	-.142	-.131	-.118	-.113	-.116
117.5	-.188	-.186	-.168	-.152	-.139	-.127	-.114	-.109	-.113

TABLE 9c – (Continued)

θ_w	r/R = 0.289	0.3	0.4	0.5	0.6	0.7	0.8	0.9	1.0
120.0	-.185	-.183	-.165	-.149	-.135	-.123	-.110	-.105	-.109
122.5	-.183	-.181	-.162	-.146	-.131	-.119	-.106	-.101	-.105
125.0	-.180	-.178	-.159	-.142	-.127	-.115	-.102	-.097	-.101
127.5	-.178	-.176	-.155	-.138	-.123	-.111	-.098	-.093	-.098
130.0	-.175	-.173	-.152	-.134	-.118	-.106	-.093	-.089	-.094
132.5	-.173	-.170	-.148	-.129	-.114	-.101	-.089	-.085	-.090
135.0	-.170	-.168	-.144	-.125	-.108	-.096	-.084	-.080	-.086
137.5	-.168	-.165	-.140	-.120	-.103	-.090	-.079	-.076	-.081
140.0	-.165	-.162	-.136	-.115	-.098	-.085	-.074	-.071	-.077
142.5	-.162	-.158	-.132	-.109	-.092	-.079	-.069	-.066	-.072
145.0	-.158	-.155	-.127	-.104	-.086	-.073	-.063	-.061	-.067
147.5	-.155	-.151	-.122	-.098	-.080	-.067	-.058	-.056	-.062
150.0	-.151	-.148	-.117	-.092	-.073	-.060	-.052	-.051	-.057
152.5	-.148	-.144	-.112	-.086	-.067	-.054	-.046	-.046	-.052
155.0	-.144	-.140	-.106	-.080	-.060	-.047	-.041	-.041	-.047
157.5	-.140	-.135	-.101	-.074	-.053	-.040	-.035	-.036	-.042
160.0	-.135	-.131	-.095	-.067	-.046	-.033	-.029	-.030	-.037
162.5	-.130	-.125	-.089	-.060	-.039	-.026	-.023	-.025	-.032
165.0	-.124	-.119	-.082	-.053	-.032	-.020	-.016	-.019	-.026
167.5	-.117	-.112	-.075	-.046	-.025	-.013	-.010	-.013	-.020
170.0	-.109	-.105	-.068	-.039	-.018	-.006	-.003	-.006	-.014
172.5	-.101	-.097	-.060	-.031	-.011	.001	.003	.000	-.008
175.0	-.093	-.088	-.052	-.024	-.004	.008	.010	.007	-.002
177.5	-.082	-.078	-.043	-.015	.004	.015	.017	.013	.004

TABLE 9c – (Continued)

θ_w	r/R = 0.289	0.3	0.4	0.5	0.6	0.7	0.8	0.9	1.0
180.0	-.072	-.068	-.034	-.007	.011	.022	.023	.019	.010
182.5	-.061	-.057	-.024	.001	.018	.028	.029	.025	.016
185.0	-.050	-.046	-.015	.009	.025	.035	.036	.031	.022
187.5	-.039	-.035	-.006	.017	.033	.041	.041	.037	.027
190.0	-.028	-.025	.003	.025	.039	.047	.047	.042	.033
192.5	-.019	-.015	.012	.032	.046	.053	.053	.048	.038
195.0	-.009	-.006	.020	.039	.052	.059	.059	.053	.044
197.5	.000	.004	.028	.046	.058	.065	.065	.059	.049
200.0	.011	.014	.036	.053	.065	.070	.071	.065	.055
202.5	.022	.024	.045	.060	.071	.076	.076	.071	.060
205.0	.032	.034	.053	.067	.077	.081	.082	.077	.066
207.5	.042	.044	.061	.074	.083	.087	.088	.083	.071
210.0	.051	.053	.069	.081	.088	.092	.093	.088	.076
212.5	.060	.062	.076	.087	.094	.097	.099	.093	.081
215.0	.068	.070	.083	.093	.100	.103	.104	.098	.086
217.5	.076	.078	.090	.099	.105	.108	.109	.103	.090
220.0	.084	.085	.097	.105	.110	.112	.113	.108	.094
222.5	.091	.092	.103	.111	.115	.117	.118	.112	.099
225.0	.098	.099	.109	.116	.120	.121	.122	.116	.103
227.5	.105	.106	.115	.121	.124	.125	.126	.120	.107
230.0	.112	.113	.121	.126	.129	.129	.130	.124	.110
232.5	.120	.120	.126	.131	.133	.133	.134	.128	.114
235.0	.126	.127	.132	.135	.137	.136	.137	.131	.118
237.5	.133	.133	.137	.139	.140	.140	.141	.135	.121

TABLE 9c – (Continued)

θ_w	r/R = 0.289	0.3	0.4	0.5	0.6	0.7	0.8	0.9	1.0
240.0	.138	.139	.141	.143	.144	.143	.144	.138	.124
242.5	.142	.143	.145	.146	.147	.146	.147	.141	.127
245.0	.147	.147	.149	.150	.149	.148	.150	.144	.130
247.5	.152	.152	.153	.153	.152	.151	.153	.147	.133
250.0	.160	.159	.158	.157	.155	.153	.156	.150	.135
252.5	.167	.167	.163	.160	.158	.155	.158	.153	.138
255.0	.174	.173	.168	.163	.160	.157	.160	.155	.140
257.5	.176	.175	.169	.165	.161	.159	.162	.157	.142
260.0	.176	.175	.170	.166	.162	.160	.164	.159	.144
262.5	.176	.175	.170	.166	.163	.161	.165	.160	.145
265.0	.177	.175	.171	.167	.164	.162	.166	.161	.147
267.5	.179	.179	.173	.168	.164	.162	.166	.162	.149
270.0	.182	.181	.174	.168	.165	.162	.167	.164	.150
272.5	.184	.183	.175	.169	.164	.162	.168	.165	.152
275.0	.184	.183	.175	.168	.164	.162	.168	.166	.152
277.5	.184	.183	.174	.167	.163	.161	.168	.166	.152
280.0	.183	.182	.173	.166	.162	.160	.167	.165	.152
282.5	.182	.181	.172	.165	.161	.159	.166	.164	.151
285.0	.181	.180	.171	.164	.159	.158	.165	.163	.150
287.5	.180	.179	.169	.162	.158	.156	.163	.162	.149
290.0	.180	.178	.168	.160	.155	.154	.162	.160	.148
292.5	.178	.177	.166	.158	.153	.151	.160	.159	.147
295.0	.177	.175	.164	.155	.150	.149	.157	.157	.145
297.5	.175	.173	.161	.152	.147	.146	.155	.154	.144

TABLE 9c – (Continued)

θ_w	r/R = 0.289	0.3	0.4	0.5	0.6	0.7	0.8	0.9	1.0
300.0	.183	.180	.162	.149	.142	.139	.150	.152	.142
302.5	.193	.190	.164	.146	.135	.132	.146	.149	.139
305.0	.202	.198	.166	.143	.129	.124	.141	.146	.137
307.5	.209	.204	.166	.138	.122	.117	.135	.142	.134
310.0	.211	.206	.164	.134	.116	.110	.130	.138	.130
312.5	.209	.203	.160	.129	.110	.105	.125	.134	.126
315.0	.199	.194	.153	.123	.106	.101	.121	.129	.121
317.5	.182	.177	.142	.118	.103	.099	.117	.123	.115
320.0	.155	.152	.128	.112	.102	.099	.113	.117	.109
322.5	.120	.113	.111	.106	.103	.103	.111	.111	.101
325.0	.076	.078	.091	.100	.106	.108	.108	.103	.093
327.5	.021	.026	.066	.095	.113	.119	.109	.098	.085
330.0	-.039	-.030	.041	.092	.124	.135	.115	.096	.080
332.5	-.095	-.082	.022	.097	.143	.161	.131	.107	.092
335.0	.232	.224	.164	.125	.106	.108	.148	.177	.189
337.5	.710	.673	.383	.170	.032	-.030	.062	.088	.032
340.0	.486	.467	.310	.181	.078	.003	-.051	-.067	-.045
342.5	.115	.111	.080	.056	.039	.030	.030	.033	.038
345.0	-.108	-.103	-.061	-.024	.006	.031	.054	.063	.059
347.5	-.041	-.040	-.024	-.007	.010	.027	.054	.065	.059
350.0	.047	.044	.025	.015	.013	.019	.047	.061	.056
352.5	.095	.090	.049	.021	.008	.008	.037	.053	.051
355.0	.128	.120	.062	.022	.000	-.005	.025	.043	.043
357.5	.158	.149	.075	.023	-.008	-.017	.014	.032	.032

TABLE 9d – INTERPOLATED VALUES OF V_r/V

θ_w	r/R = 0.289	0.3	0.4	0.5	0.6	0.7	0.8	0.9	1.0
0.0	.090	.084	.034	-.008	-.041	-.066	-.077	-.089	-.105
2.5	.106	.098	.038	-.011	-.048	-.074	-.081	-.091	-.106
5.0	.104	.097	.033	-.019	-.057	-.083	-.087	-.095	-.109
7.5	.078	.071	.014	-.032	-.066	-.090	-.093	-.100	-.113
10.0	.046	.040	-.007	-.046	-.075	-.095	-.100	-.107	-.117
12.5	.035	.029	-.020	-.058	-.086	-.105	-.106	-.111	-.119
15.0	.034	.027	-.026	-.068	-.097	-.115	-.113	-.113	-.118
17.5	.030	.023	-.032	-.074	-.103	-.120	-.116	-.114	-.117
20.0	-.011	-.015	-.049	-.076	-.096	-.109	-.112	-.114	-.116
22.5	.020	.015	-.031	-.067	-.094	-.110	-.111	-.112	-.113
25.0	.020	.012	-.046	-.090	-.118	-.132	-.121	-.114	-.113
27.5	-.121	-.121	-.127	-.130	-.132	-.132	-.127	-.126	-.131
30.0	-.131	-.130	-.127	-.125	-.125	-.125	-.126	-.129	-.133
32.5	-.096	-.097	-.105	-.111	-.116	-.120	-.121	-.123	-.128
35.0	-.076	-.077	-.091	-.101	-.110	-.116	-.117	-.120	-.124
37.5	-.060	-.062	-.080	-.094	-.104	-.111	-.112	-.113	-.117
40.0	-.052	-.054	-.073	-.088	-.099	-.106	-.106	-.107	-.110
42.5	-.048	-.051	-.069	-.084	-.094	-.100	-.099	-.100	-.102
45.0	-.044	-.046	-.064	-.079	-.089	-.095	-.093	-.093	-.094
47.5	-.041	-.043	-.060	-.074	-.083	-.088	-.087	-.086	-.086
50.0	-.039	-.041	-.057	-.069	-.078	-.082	-.080	-.079	-.079
52.5	-.039	-.040	-.054	-.065	-.072	-.076	-.073	-.072	-.072
55.0	-.038	-.040	-.051	-.060	-.066	-.069	-.066	-.065	-.064
57.5	-.036	-.037	-.048	-.055	-.060	-.062	-.059	-.057	-.057

TABLE 9d – (Continued)

θ_w	r/R = 0.289	0.3	0.4	0.5	0.6	0.7	0.8	0.9	1.0
60.0	-.033	-.034	-.043	-.050	-.054	-.055	-.051	-.049	-.049
62.5	-.030	-.031	-.039	-.044	-.047	-.048	-.044	-.041	-.041
65.0	-.026	-.027	-.034	-.039	-.041	-.041	-.036	-.033	-.032
67.5	-.023	-.024	-.030	-.033	-.035	-.034	-.028	-.025	-.024
70.0	-.020	-.020	-.025	-.028	-.028	-.027	-.021	-.017	-.016
72.5	-.017	-.017	-.020	-.022	-.022	-.020	-.014	-.010	-.008
75.0	-.015	-.015	-.016	-.016	-.015	-.012	-.007	-.003	-.001
77.5	-.013	-.013	-.012	-.011	-.008	-.005	-.000	.004	.006
80.0	-.013	-.013	-.009	-.006	-.002	.002	.006	.010	.012
82.5	-.015	-.014	-.007	-.001	.004	.009	.013	.016	.018
85.0	-.015	-.014	-.005	.003	.010	.015	.019	.022	.024
87.5	-.016	-.014	-.002	.008	.016	.022	.025	.028	.030
90.0	-.016	-.015	.000	.012	.022	.029	.032	.034	.036
92.5	-.015	-.013	.004	.017	.028	.035	.038	.040	.042
95.0	-.013	-.011	.008	.022	.034	.041	.044	.046	.047
97.5	-.011	-.008	.012	.028	.040	.048	.050	.052	.053
100.0	-.008	-.005	.016	.033	.045	.054	.056	.057	.059
102.5	-.006	-.003	.019	.038	.051	.060	.061	.063	.065
105.0	-.004	-.001	.023	.042	.056	.066	.067	.068	.070
107.5	-.002	.001	.026	.046	.061	.071	.073	.074	.076
110.0	.000	.003	.030	.051	.066	.077	.079	.081	.082
112.5	.003	.006	.033	.055	.071	.082	.085	.087	.088
115.0	.005	.009	.037	.059	.076	.087	.090	.092	.094
117.5	.007	.011	.040	.063	.081	.092	.095	.097	.098

TABLE 9d – (Continued)

θ_w	r/R = 0.289	0.3	0.4	0.5	0.6	0.7	0.8	0.9	1.0
120.0	.009	.013	.043	.067	.085	.097	.099	.101	.103
122.5	.011	.015	.047	.071	.090	.102	.103	.105	.107
125.0	.014	.018	.050	.075	.094	.106	.108	.109	.112
127.5	.018	.022	.054	.079	.098	.110	.112	.114	.117
130.0	.021	.025	.057	.083	.102	.114	.117	.119	.121
132.5	.023	.027	.060	.086	.106	.118	.121	.123	.125
135.0	.025	.029	.063	.090	.109	.122	.124	.126	.128
137.5	.027	.031	.066	.093	.113	.126	.128	.129	.132
140.0	.029	.033	.068	.096	.116	.129	.131	.133	.136
142.5	.031	.036	.071	.098	.119	.132	.134	.136	.140
145.0	.034	.038	.073	.101	.122	.135	.137	.140	.144
147.5	.036	.040	.075	.103	.124	.138	.140	.143	.147
150.0	.038	.042	.077	.106	.126	.140	.143	.146	.150
152.5	.040	.044	.079	.108	.129	.143	.146	.149	.152
155.0	.041	.045	.081	.109	.131	.145	.148	.151	.155
157.5	.042	.046	.082	.111	.132	.147	.150	.153	.156
160.0	.042	.046	.083	.112	.134	.148	.152	.154	.158
162.5	.042	.047	.084	.113	.136	.150	.153	.156	.159
165.0	.042	.047	.084	.114	.137	.151	.154	.157	.161
167.5	.042	.047	.085	.115	.138	.152	.155	.158	.162
170.0	.042	.046	.085	.115	.138	.153	.156	.159	.163
172.5	.042	.046	.085	.116	.139	.154	.157	.161	.165
175.0	.042	.047	.085	.116	.139	.154	.158	.162	.166
177.5	.043	.047	.086	.116	.139	.155	.159	.162	.166

TABLE 9d – (Continued)

θ_w	r/R = 0.289	0.3	0.4	0.5	0.6	0.7	0.8	0.9	1.0
180.0	.043	.047	.086	.116	.139	.155	.159	.162	.166
182.5	.042	.047	.086	.116	.139	.155	.158	.162	.165
185.0	.042	.047	.085	.116	.139	.154	.158	.160	.164
187.5	.041	.046	.085	.116	.139	.154	.156	.159	.163
190.0	.041	.046	.085	.115	.138	.153	.155	.158	.162
192.5	.041	.046	.084	.114	.137	.152	.154	.157	.161
195.0	.040	.045	.083	.113	.135	.150	.153	.155	.159
197.5	.039	.044	.081	.111	.133	.148	.151	.154	.158
200.0	.038	.043	.080	.109	.131	.146	.149	.152	.156
202.5	.037	.042	.078	.107	.129	.143	.147	.150	.154
205.0	.036	.040	.076	.105	.127	.141	.144	.148	.152
207.5	.034	.038	.074	.103	.124	.139	.142	.145	.149
210.0	.032	.036	.072	.100	.122	.136	.139	.143	.147
212.5	.030	.034	.069	.098	.119	.133	.136	.140	.144
215.0	.027	.032	.067	.095	.116	.130	.133	.136	.141
217.5	.025	.029	.064	.092	.113	.127	.129	.132	.137
220.0	.022	.026	.061	.089	.110	.123	.126	.129	.133
222.5	.020	.024	.058	.086	.106	.120	.122	.125	.130
225.0	.018	.022	.055	.082	.102	.116	.118	.121	.126
227.5	.016	.020	.052	.079	.098	.111	.114	.117	.122
230.0	.014	.018	.050	.075	.094	.107	.110	.113	.117
232.5	.013	.016	.046	.071	.089	.102	.105	.109	.113
235.0	.011	.014	.043	.067	.085	.097	.101	.104	.108
237.5	.008	.012	.040	.062	.080	.092	.096	.099	.104

TABLE 9d – (Continued)

θ_w	r/R = 0.289	0.3	0.4	0.5	0.6	0.7	0.8	0.9	1.0
240.0	.006	.009	.036	.058	.075	.087	.090	.094	.099
242.5	.003	.006	.032	.053	.070	.081	.085	.089	.094
245.0	.000	.003	.028	.049	.064	.075	.079	.083	.088
247.5	-.002	.001	.025	.044	.059	.070	.073	.077	.083
250.0	-.004	-.001	.021	.039	.054	.064	.067	.072	.077
252.5	-.005	-.003	.018	.035	.048	.058	.061	.066	.072
255.0	-.006	-.004	.015	.030	.043	.052	.055	.060	.066
257.5	-.006	-.004	.012	.026	.037	.045	.049	.054	.060
260.0	-.006	-.004	.010	.022	.031	.039	.043	.048	.054
262.5	-.006	-.005	.007	.017	.026	.033	.037	.042	.047
265.0	-.007	-.006	.004	.012	.020	.026	.031	.035	.041
267.5	-.008	-.007	.000	.007	.014	.020	.024	.029	.034
270.0	-.009	-.009	-.003	.003	.008	.013	.018	.022	.027
272.5	-.010	-.010	-.006	-.002	.002	.006	.011	.016	.020
275.0	-.011	-.011	-.009	-.007	-.004	-.000	.004	.009	.014
277.5	-.011	-.011	-.012	-.012	-.010	-.007	-.002	.003	.008
280.0	-.011	-.012	-.015	-.017	-.016	-.014	-.008	-.003	.002
282.5	-.012	-.013	-.018	-.021	-.022	-.020	-.014	-.009	-.005
285.0	-.013	-.014	-.022	-.026	-.028	-.027	-.021	-.015	-.011
287.5	-.014	-.015	-.025	-.031	-.034	-.033	-.027	-.021	-.018
290.0	-.015	-.016	-.028	-.036	-.040	-.040	-.033	-.028	-.025
292.5	-.016	-.018	-.031	-.041	-.046	-.046	-.039	-.034	-.032
295.0	-.017	-.019	-.035	-.045	-.051	-.053	-.046	-.041	-.038
297.5	-.018	-.020	-.037	-.050	-.057	-.059	-.052	-.047	-.045

TABLE 9d ~ (Continued)

θ_w	r/R = 0.289	0.3	0.4	0.5	0.6	0.7	0.8	0.9	1.0
300.0	-.020	-.022	-.041	-.054	-.062	-.065	-.058	-.054	-.052
302.5	-.023	-.025	-.044	-.058	-.067	-.070	-.065	-.061	-.059
305.0	-.026	-.029	-.048	-.062	-.071	-.075	-.071	-.067	-.066
307.5	-.030	-.033	-.052	-.067	-.076	-.081	-.076	-.074	-.073
310.0	-.034	-.036	-.056	-.071	-.081	-.086	-.082	-.080	-.080
312.5	-.037	-.040	-.060	-.075	-.085	-.091	-.088	-.086	-.087
315.0	-.040	-.043	-.063	-.079	-.090	-.096	-.093	-.092	-.094
317.5	-.042	-.045	-.067	-.083	-.095	-.101	-.099	-.098	-.100
320.0	-.043	-.046	-.069	-.087	-.099	-.106	-.104	-.103	-.106
322.5	-.042	-.045	-.071	-.090	-.104	-.112	-.109	-.108	-.112
325.0	-.041	-.044	-.072	-.094	-.109	-.117	-.114	-.113	-.118
327.5	-.037	-.041	-.073	-.097	-.114	-.123	-.118	-.117	-.122
330.0	-.024	-.029	-.068	-.098	-.118	-.128	-.120	-.118	-.125
332.5	-.023	-.028	-.068	-.099	-.120	-.131	-.126	-.125	-.130
335.0	-.196	-.190	-.140	-.108	-.092	-.093	-.133	-.151	-.140
337.5	-.174	-.170	-.137	-.114	-.100	-.095	-.110	-.114	-.102
340.0	-.139	-.138	-.127	-.119	-.113	-.111	-.110	-.113	-.122
342.5	.003	-.001	-.038	-.068	-.091	-.106	-.111	-.116	-.123
345.0	.077	.070	.015	-.030	-.065	-.091	-.101	-.112	-.122
347.5	.085	.079	.027	-.016	-.051	-.077	-.091	-.104	-.118
350.0	.067	.062	.021	-.015	-.044	-.068	-.082	-.097	-.114
352.5	.058	.053	.018	-.013	-.040	-.062	-.077	-.093	-.111
355.0	.059	.055	.020	-.011	-.038	-.060	-.074	-.090	-.108
357.5	.070	.065	.025	-.009	-.037	-.060	-.074	-.089	-.106

TABLE 9e – HARMONICS OF V_x/V

$r/R = 0.289$

n	$(A_x)_n/V$	$(B_x)_n/V$	$(V_x)_n/V$	$(\phi_x^*)_n$
0	1.0555	0.0000	0.0000	0.0
1	-.0527	-.0725	.0896	216.0
2	-.0805	-.0259	.0845	252.2
3	-.0509	-.0374	.0632	233.7
4	-.0279	-.0173	.0328	238.1
5	-.0205	-.0215	.0297	223.7
6	-.0153	-.0127	.0199	230.2
7	-.0187	-.0010	.0187	267.0
8	.0015	.0099	.0100	8.7
9	.0099	.0166	.0193	30.8
10	.0097	.0141	.0171	34.4
11	.0092	.0132	.0161	35.0
12	.0144	.0012	.0145	85.4
13	.0139	-.0111	.0178	128.6
14	.0103	-.0186	.0213	151.0
15	.0083	-.0231	.0246	160.2
16	.0076	-.0318	.0327	166.6

$r/R = 0.3$

n	$(A_x)_n/V$	$(B_x)_n/V$	$(V_x)_n/V$	$(\phi_x^*)_n$
0	1.0534	0.0000	0.0000	0.0
1	-.0511	-.0681	.0852	216.9
2	-.0781	-.0246	.0819	252.5
3	-.0493	-.0353	.0606	234.4
4	-.0271	-.0165	.0318	238.6
5	-.0199	-.0204	.0285	224.3
6	-.0145	-.0121	.0189	230.3
7	-.0174	-.0009	.0174	267.2
8	.0018	.0095	.0096	10.9
9	.0098	.0159	.0187	31.7
10	.0095	.0136	.0166	35.0
11	.0090	.0128	.0156	35.0
12	.0139	.0014	.0140	84.2
13	.0132	-.0102	.0167	127.8
14	.0096	-.0175	.0199	151.1
15	.0077	-.0218	.0231	160.5
16	.0070	-.0301	.0309	167.0

TABLE 9e – (Continued)

r/R = 0.4

n	$(A_x)_n/V$	$(B_x)_n/V$	$(V_x)_n/V$	$(\phi_x^*)_n$
0	1.0364	0.0000	0.0000	0.0
1	-.0375	-.0338	.0504	228.0
2	-.0588	-.0143	.0605	256.3
3	-.0362	-.0183	.0405	243.2
4	-.0205	-.0104	.0229	243.1
5	-.0144	-.0117	.0185	230.8
6	-.0084	-.0068	.0108	231.1
7	-.0074	.0001	.0074	270.8
8	.0042	.0062	.0075	33.8
9	.0091	.0103	.0138	41.4
10	.0082	.0093	.0124	41.5
11	.0067	.0095	.0116	35.3
12	.0095	.0031	.0100	72.1
13	.0076	-.0037	.0085	115.9
14	.0042	-.0083	.0093	153.0
15	.0025	-.0115	.0118	167.6
16	.0019	-.0171	.0172	173.6

r/R = 0.5

n	$(A_x)_n/V$	$(B_x)_n/V$	$(V_x)_n/V$	$(\phi_x^*)_n$
0	1.0229	0.0000	0.0000	0.0
1	-.0259	-.0090	.0275	250.8
2	-.0426	-.0069	.0432	260.8
3	-.0257	-.0059	.0263	257.0
4	-.0143	-.0057	.0154	248.5
5	-.0094	-.0051	.0107	241.9
6	-.0036	-.0027	.0044	233.2
7	-.0001	.0008	.0008	353.3
8	.0058	.0038	.0069	56.9
9	.0082	.0060	.0102	53.8
10	.0068	.0058	.0090	49.7
11	.0047	.0067	.0082	35.4
12	.0056	.0038	.0068	55.5
13	.0030	.0007	.0031	77.6
14	-.0001	-.0019	.0019	182.6
15	-.0015	-.0042	.0044	200.0
16	-.0019	-.0075	.0079	194.3

TABLE 9e – (Continued)

r/R = 0.6

n	$(A_x)_n/V$	$(B_x)_n/V$	$(V_x)_n/V$	$(\phi_x^*)_n$
0	1.0129	0.0000	0.0000	0.0
1	-.0166	.0061	.0177	290.1
2	-.0296	-.0023	.0297	265.6
3	-.0177	.0017	.0177	275.6
4	-.0087	-.0024	.0090	254.4
5	-.0051	-.0004	.0051	265.9
6	.0001	.0003	.0003	16.4
7	.0046	.0013	.0047	74.2
8	.0067	.0021	.0071	72.4
9	.0072	.0030	.0078	67.4
10	.0055	.0032	.0064	59.5
11	.0030	.0043	.0053	34.8
12	.0022	.0037	.0043	30.3
13	-.0007	.0028	.0029	346.4
14	-.0033	.0017	.0037	296.9
15	-.0044	.0003	.0044	273.5
16	-.0046	-.0017	.0049	250.3

r/R = 0.7

n	$(A_x)_n/V$	$(B_x)_n/V$	$(V_x)_n/V$	$(\phi_x^*)_n$
0	1.0065	0.0000	0.0000	0.0
1	-.0094	.0116	.0149	321.0
2	-.0198	-.0006	.0198	268.3
3	-.0122	.0047	.0131	291.2
4	-.0035	-.0007	.0036	259.2
5	-.0014	.0023	.0027	328.3
6	.0025	.0021	.0033	50.1
7	.0065	.0015	.0067	76.8
8	.0069	.0013	.0070	79.7
9	.0061	.0013	.0062	78.2
10	.0042	.0015	.0044	69.7
11	.0015	.0025	.0029	31.8
12	-.0008	.0027	.0028	344.2
13	-.0034	.0028	.0044	309.8
14	-.0053	.0024	.0058	294.2
15	-.0062	.0017	.0064	285.7
16	-.0061	.0008	.0062	277.6

TABLE 9e – (Continued)

r/R = 0.8

n	$(A_x)_n/V$	$(B_x)_n/V$	$(V_x)_n/V$	$(\phi_x^*)_n$
0	1.0064	0.0000	0.0000	0.0
1	-.0030	.0004	.0031	276.8
2	-.0137	-.0038	.0142	254.6
3	-.0105	-.0009	.0106	264.9
4	.0022	-.0018	.0028	129.8
5	.0023	.0013	.0026	59.5
6	.0029	.0020	.0036	55.6
7	.0041	.0013	.0043	72.7
8	.0065	.0022	.0069	71.3
9	.0045	.0019	.0049	67.5
10	.0025	.0015	.0029	58.4
11	.0001	.0012	.0012	4.5
12	-.0034	-.0006	.0034	260.5
13	-.0049	-.0019	.0053	249.0
14	-.0059	-.0028	.0065	244.4
15	-.0064	-.0024	.0069	249.3
16	-.0059	-.0034	.0068	240.2

r/R = 0.9

n	$(A_x)_n/V$	$(B_x)_n/V$	$(V_x)_n/V$	$(\phi_x^*)_n$
0	1.0047	0.0000	0.0000	0.0
1	-.0011	-.0077	.0078	188.3
2	-.0098	-.0061	.0115	238.2
3	-.0092	-.0041	.0101	246.2
4	.0054	-.0019	.0057	109.2
5	.0043	.0013	.0045	72.7
6	.0035	.0021	.0041	59.6
7	.0022	.0012	.0025	60.3
8	.0051	.0021	.0055	68.1
9	.0033	.0018	.0038	61.0
10	.0014	.0009	.0017	56.3
11	-.0007	.0002	.0007	289.1
12	-.0051	-.0023	.0056	245.5
13	-.0059	-.0042	.0072	234.5
14	-.0059	-.0052	.0079	228.5
15	-.0062	-.0047	.0078	233.2
16	-.0055	-.0054	.0076	225.6

TABLE 9e – (Continued)

r/R = 1.0

n	$(A_x)_n/V$	$(B_x)_n/V$	$(V_x)_n/V$	$(\phi_x^*)_n$
0	1.0007	0.0000	0.0000	0.0
1	-.0039	-.0109	.0115	199.7
2	-.0080	-.0070	.0106	229.1
3	-.0079	-.0036	.0087	245.2
4	.0059	-.0006	.0060	95.4
5	.0045	.0027	.0052	59.0
6	.0044	.0024	.0051	61.4
7	.0012	.0015	.0019	39.2
8	.0028	.0006	.0028	78.2
9	.0024	.0008	.0025	70.7
10	.0010	-.0005	.0011	115.9
11	-.0007	-.0006	.0009	231.3
12	-.0060	-.0023	.0064	248.8
13	-.0063	-.0035	.0072	241.0
14	-.0055	-.0042	.0069	232.8
15	-.0057	-.0043	.0072	233.1
16	-.0050	-.0044	.0066	228.9

TABLE 9f – HARMONICS OF V_t/V

$r/R = 0.289$

n	$(A_t)_n/V$	$(B_t)_n/V$	$(V_t)_n/V$	$(\phi_t^*)_n$
0	-.0089	0.0000	0.0000	0.0
1	.0484	-.1984	.2042	166.3
2	-.0035	-.0141	.0145	194.0
3	.0109	-.0203	.0231	151.7
4	.0055	-.0132	.0143	157.2
5	.0113	-.0140	.0180	141.0
6	.0120	-.0080	.0144	123.6
7	.0112	-.0077	.0136	124.4
8	.0051	-.0038	.0063	126.9
9	-.0031	.0011	.0033	290.1
10	-.0078	.0071	.0106	312.3
11	-.0073	.0117	.0138	328.1
12	-.0003	.0158	.0158	358.8
13	.0102	.0165	.0194	31.6
14	.0215	.0147	.0260	55.7
15	.0291	.0109	.0311	69.5
16	.0327	.0077	.0336	76.8

$r/R = 0.3$

n	$(A_t)_n/V$	$(B_t)_n/V$	$(V_t)_n/V$	$(\phi_t^*)_n$
0	-.0086	0.0000	0.0000	0.0
1	.0453	-.1970	.2021	167.0
2	-.0033	-.0136	.0140	193.6
3	.0103	-.0195	.0221	152.0
4	.0053	-.0127	.0137	157.3
5	.0107	-.0134	.0171	141.3
6	.0113	-.0075	.0135	123.5
7	.0105	-.0070	.0126	123.7
8	.0047	-.0032	.0056	124.2
9	-.0030	.0016	.0034	297.1
10	-.0075	.0072	.0104	313.9
11	-.0070	.0114	.0133	328.4
12	-.0004	.0150	.0150	358.4
13	.0095	.0156	.0182	31.4
14	.0202	.0137	.0244	55.9
15	.0275	.0100	.0292	70.0
16	.0309	.0069	.0317	77.4

TABLE 9f – (Continued)

r/R = 0.4

n	$(A_t)_n/V$	$(B_t)_n/V$	$(V_t)_n/V$	$(\phi_t^*)_n$
0	-.0061	0.0000	0.0000	0.0
1	.0207	-.1852	.1863	173.6
2	-.0016	-.0099	.0100	189.1
3	.0057	-.0129	.0141	156.1
4	.0034	-.0083	.0090	157.6
5	.0055	-.0081	.0098	145.5
6	.0057	-.0035	.0067	121.8
7	.0049	-.0018	.0052	109.9
8	.0016	.0016	.0022	45.3
9	-.0025	.0047	.0053	331.8
10	-.0048	.0075	.0089	327.5
11	-.0045	.0085	.0096	332.3
12	-.0011	.0091	.0091	353.2
13	.0043	.0079	.0090	28.5
14	.0102	.0057	.0116	60.8
15	.0145	.0028	.0148	79.0
16	.0170	.0009	.0170	86.9

r/R = 0.5

n	$(A_t)_n/V$	$(B_t)_n/V$	$(V_t)_n/V$	$(\phi_t^*)_n$
0	-.0031	0.0000	0.0000	0.0
1	.0026	-.1750	.1750	179.1
2	-.0003	-.0073	.0073	182.3
3	.0023	-.0078	.0081	163.6
4	.0019	-.0047	.0051	157.7
5	.0017	-.0040	.0043	156.5
6	.0015	-.0006	.0017	112.2
7	.0008	.0019	.0020	22.5
8	-.0006	.0047	.0047	353.3
9	-.0020	.0064	.0067	342.8
10	-.0026	.0072	.0077	339.8
11	-.0025	.0059	.0064	337.3
12	-.0014	.0043	.0045	342.2
13	.0006	.0019	.0020	17.5
14	.0029	-.0004	.0029	97.9
15	.0050	-.0025	.0056	116.5
16	.0067	-.0035	.0075	117.5

TABLE 9f – (Continued)

r/R = 0.6

n	$(A_t)_n/V$	$(B_t)_n/V$	$(V_t)_n/V$	$(\phi_t^*)_n$
0	.0004	0.0000	0.0000	0.0
1	-.0090	-.1664	.1667	183.1
2	.0005	-.0060	.0060	174.9
3	.0001	-.0041	.0041	179.2
4	.0009	-.0020	.0022	156.0
5	-.0007	-.0011	.0013	215.3
6	-.0012	.0012	.0017	316.5
7	-.0018	.0039	.0043	335.6
8	-.0018	.0062	.0064	344.0
9	-.0015	.0069	.0071	347.7
10	-.0011	.0062	.0063	350.4
11	-.0010	.0036	.0037	344.8
12	-.0013	.0007	.0015	297.1
13	-.0015	-.0023	.0028	214.0
14	-.0016	-.0046	.0048	199.0
15	-.0010	-.0060	.0061	189.6
16	-.0001	-.0062	.0062	180.6

r/R = 0.7

n	$(A_t)_n/V$	$(B_t)_n/V$	$(V_t)_n/V$	$(\phi_t^*)_n$
0	.0044	0.0000	0.0000	0.0
1	-.0140	-.1595	.1601	185.0
2	.0009	-.0059	.0060	171.1
3	-.0010	-.0018	.0021	208.4
4	.0003	-.0001	.0003	112.2
5	-.0019	.0007	.0020	289.7
6	-.0024	.0020	.0031	310.0
7	-.0028	.0044	.0052	327.4
8	-.0020	.0060	.0063	341.3
9	-.0010	.0061	.0061	350.4
10	-.0000	.0046	.0046	359.7
11	.0000	.0015	.0015	.6
12	-.0009	-.0017	.0020	207.4
13	-.0022	-.0048	.0052	204.4
14	-.0033	-.0068	.0075	205.6
15	-.0036	-.0077	.0085	205.2
16	-.0032	-.0074	.0080	203.4

TABLE 9f – (Continued)

r/R = 0.8

n	$(A_t)_n/V$	$(B_t)_n/V$	$(V_t)_n/V$	$(\phi_t^*)_n$
0	.0136	0.0000	0.0000	0.0
1	-.0081	-.1553	.1555	183.0
2	.0002	-.0081	.0081	178.6
3	.0001	-.0017	.0017	176.6
4	.0003	.0007	.0008	25.5
5	-.0008	.0007	.0010	312.8
6	-.0013	.0011	.0017	312.1
7	-.0012	.0020	.0024	328.6
8	-.0006	.0027	.0028	347.0
9	-.0006	.0026	.0027	346.5
10	.0001	.0013	.0013	6.3
11	.0003	-.0006	.0006	155.4
12	.0003	-.0026	.0026	173.5
13	.0000	-.0047	.0047	179.4
14	.0001	-.0061	.0061	178.8
15	-.0001	-.0064	.0064	180.6
16	-.0000	-.0058	.0058	180.4

r/R = 0.9

n	$(A_t)_n/V$	$(B_t)_n/V$	$(V_t)_n/V$	$(\phi_t^*)_n$
0	.0149	0.0000	0.0000	0.0
1	-.0036	-.1507	.1507	181.4
2	.0002	-.0096	.0096	178.6
3	.0007	-.0018	.0019	158.3
4	.0004	.0011	.0012	18.0
5	.0000	.0005	.0005	6.1
6	-.0003	.0003	.0004	314.3
7	-.0000	.0002	.0002	356.1
8	.0004	.0004	.0006	41.5
9	-.0001	.0002	.0002	318.8
10	.0003	-.0008	.0009	160.5
11	.0004	-.0018	.0019	166.7
12	.0011	-.0030	.0031	160.1
13	.0014	-.0044	.0046	162.2
14	.0021	-.0054	.0058	158.5
15	.0021	-.0053	.0057	158.4
16	.0019	-.0046	.0049	157.5

TABLE 9f – (Continued)

r/R = 1.0

n	$(A_t)_n/V$	$(B_t)_n/V$	$(V_t)_n/V$	$(\phi_t^*)_n$
0	.0072	0.0000	0.0000	0.0
1	-.0015	-.1455	.1455	180.6
2	.0012	-.0101	.0102	173.4
3	.0006	-.0017	.0018	161.4
4	.0003	.0012	.0013	14.0
5	.0003	.0001	.0003	74.2
6	.0003	-.0004	.0005	144.0
7	.0006	-.0007	.0010	138.4
8	.0009	-.0006	.0011	126.1
9	.0005	-.0011	.0011	156.4
10	.0005	-.0016	.0017	163.2
11	.0006	-.0022	.0023	164.7
12	.0013	-.0030	.0032	155.9
13	.0016	-.0041	.0044	158.4
14	.0021	-.0048	.0052	156.0
15	.0022	-.0046	.0051	154.0
16	.0020	-.0039	.0044	153.5

TABLE 9g – HARMONICS OF V_r/V

$r/R = 0.289$

n	$(A_r)_n/V$	$(B_r)_n/V$	$(V_r)_n/V$	$(\phi_r^*)_n$
0	.0012	0.0000	0.0000	0.0
1	-.0264	-.0002	.0264	269.6
2	.0225	-.0016	.0225	94.0
3	.0155	.0035	.0159	77.1
4	.0209	.0041	.0213	78.8
5	.0225	.0045	.0230	78.6
6	.0175	.0052	.0183	73.3
7	.0136	.0041	.0142	73.2
8	.0094	.0023	.0097	76.2
9	.0064	-.0002	.0064	92.0
10	.0023	-.0019	.0030	130.0
11	-.0011	-.0044	.0046	194.1
12	-.0037	-.0072	.0081	207.6
13	-.0052	-.0080	.0096	213.0
14	-.0050	-.0063	.0080	218.1
15	-.0049	-.0037	.0062	232.9
16	-.0041	-.0001	.0041	268.6

$r/R = 0.3$

n	$(A_r)_n/V$	$(B_r)_n/V$	$(V_r)_n/V$	$(\phi_r^*)_n$
0	.0019	0.0000	0.0000	0.0
1	-.0311	.0001	.0311	270.1
2	.0219	-.0016	.0220	94.3
3	.0155	.0032	.0158	78.5
4	.0205	.0038	.0208	79.5
5	.0219	.0042	.0223	79.2
6	.0171	.0049	.0177	74.1
7	.0132	.0038	.0138	74.1
8	.0092	.0021	.0094	77.1
9	.0062	-.0003	.0062	92.8
10	.0022	-.0019	.0029	130.6
11	-.0010	-.0043	.0044	193.8
12	-.0036	-.0069	.0077	207.7
13	-.0050	-.0077	.0092	212.9
14	-.0047	-.0061	.0077	218.0
15	-.0047	-.0036	.0059	232.5
16	-.0039	-.0001	.0039	267.9

TABLE 9g – (Continued)

r/R = 0.4

n	$(A_r)_n/V$	$(B_r)_n/V$	$(V_r)_n/V$	$(\phi_r^*)_n$
0	.0075	0.0000	0.0000	0.0
1	-.0691	.0023	.0691	271.9
2	.0171	-.0021	.0172	96.9
3	.0155	.0001	.0155	89.6
4	.0173	.0010	.0173	86.6
5	.0171	.0014	.0172	85.4
6	.0134	.0018	.0135	82.3
7	.0103	.0012	.0104	83.1
8	.0072	.0004	.0072	86.5
9	.0045	-.0010	.0046	101.8
10	.0016	-.0016	.0023	135.8
11	-.0006	-.0030	.0030	191.3
12	-.0023	-.0043	.0049	208.3
13	-.0030	-.0048	.0057	211.7
14	-.0028	-.0039	.0048	216.0
15	-.0026	-.0025	.0036	226.7
16	-.0021	-.0005	.0022	256.8

r/R = 0.5

n	$(A_r)_n/V$	$(B_r)_n/V$	$(V_r)_n/V$	$(\phi_r^*)_n$
0	.0123	0.0000	0.0000	0.0
1	-.0995	.0038	.0996	272.2
2	.0126	-.0023	.0128	100.2
3	.0149	-.0021	.0150	97.8
4	.0146	-.0009	.0146	93.6
5	.0133	-.0006	.0133	92.4
6	.0104	-.0003	.0104	91.6
7	.0079	-.0005	.0079	93.8
8	.0055	-.0007	.0056	97.5
9	.0032	-.0014	.0035	113.0
10	.0011	-.0014	.0018	141.6
11	-.0003	-.0020	.0020	187.5
12	-.0013	-.0024	.0027	209.0
13	-.0015	-.0027	.0030	209.0
14	-.0013	-.0022	.0026	211.5
15	-.0011	-.0016	.0019	213.9
16	-.0008	-.0007	.0011	228.1

TABLE 9g – (Continued)

r/R = 0.6

n	$(A_r)_n/V$	$(B_r)_n/V$	$(V_r)_n/V$	$(\phi_r^*)_n$
0	.0161	0.0000	0.0000	0.0
1	-.1222	.0048	.1223	272.2
2	.0084	-.0023	.0087	105.0
3	.0137	-.0033	.0141	103.6
4	.0123	-.0021	.0125	103.6
5	.0104	-.0016	.0105	99.5
6	.0081	-.0015	.0082	98.9
7	.0059	-.0015	.0061	100.4
8	.0041	-.0014	.0043	104.5
9	.0022	-.0016	.0027	108.8
10	.0008	-.0012	.0014	125.2
11	-.0001	-.0012	.0012	147.2
12	-.0006	-.0011	.0012	182.6
13	-.0005	-.0012	.0013	208.8
14	-.0003	-.0010	.0011	201.2
15	.0000	-.0009	.0009	196.5
16	.0002	-.0007	.0008	179.4
				166.9

r/R = 0.7

n	$(A_r)_n/V$	$(B_r)_n/V$	$(V_r)_n/V$	$(\phi_r^*)_n$
0	.0190	0.0000	0.0000	0.0
1	-.1373	.0051	.1374	272.1
2	.0045	-.0020	.0050	114.0
3	.0120	-.0037	.0125	107.2
4	.0105	-.0024	.0108	102.8
5	.0084	-.0018	.0086	102.1
6	.0065	-.0018	.0067	105.2
7	.0044	-.0018	.0048	111.8
8	.0030	-.0016	.0034	118.0
9	.0015	-.0015	.0021	135.4
10	.0006	-.0010	.0011	151.3
11	.0000	-.0008	.0008	178.7
12	-.0002	-.0004	.0005	200.8
13	.0001	-.0004	.0004	167.8
14	.0003	-.0004	.0005	139.8
15	.0006	-.0005	.0008	129.5
16	.0007	-.0006	.0010	131.1

TABLE 9g – (Continued)

r/R = 0.8

n	$(A_r)_n/V$	$(B_r)_n/V$	$(V_r)_n/V$	$(\phi_r^*)_n$
0	.0208	0.0000	0.0000	0.0
1	-.1400	.0047	.1401	271.9
2	.0012	-.0014	.0018	139.6
3	.0091	-.0026	.0094	105.9
4	.0094	-.0012	.0095	97.0
5	.0079	-.0003	.0079	92.1
6	.0062	-.0004	.0062	93.2
7	.0038	-.0006	.0038	99.3
8	.0024	-.0010	.0026	111.7
9	.0015	-.0012	.0019	127.3
10	.0008	-.0010	.0012	141.7
11	.0001	-.0010	.0010	173.9
12	-.0001	-.0010	.0010	185.2
13	-.0003	-.0008	.0009	201.2
14	.0000	-.0005	.0005	177.9
15	.0001	-.0004	.0004	161.8
16	.0005	-.0001	.0005	105.5

r/R = 0.9

n	$(A_r)_n/V$	$(B_r)_n/V$	$(V_r)_n/V$	$(\phi_r^*)_n$
0	.0220	0.0000	0.0000	0.0
1	-.1435	.0039	.1436	271.6
2	-.0021	-.0009	.0023	247.5
3	.0066	-.0017	.0068	104.2
4	.0084	-.0005	.0084	93.4
5	.0073	.0006	.0073	85.0
6	.0055	.0006	.0055	83.8
7	.0029	.0002	.0029	86.7
8	.0016	-.0004	.0017	104.8
9	.0010	-.0007	.0012	123.9
10	.0005	-.0007	.0008	141.9
11	-.0002	-.0009	.0009	192.4
12	-.0001	-.0011	.0011	187.5
13	-.0004	-.0009	.0010	204.1
14	.0001	-.0006	.0006	170.2
15	.0002	-.0003	.0004	149.3
16	.0006	.0001	.0006	79.7

TABLE 9g – (Continued)

$r/R = 1.0$

n	$(A_r)_n/V$	$(B_r)_n/V$	$(V_r)_n/V$	$(\phi_r^*)_n$
0	.0227	0.0000	0.0000	0.0
1	-.1488	.0027	.1488	271.0
2	-.0054	-.0005	.0054	265.0
3	.0046	-.0011	.0048	103.5
4	.0073	-.0005	.0073	94.3
5	.0062	.0008	.0063	82.7
6	.0041	.0009	.0042	77.6
7	.0018	.0005	.0018	75.5
8	.0004	-.0000	.0004	94.7
9	-.0002	-.0001	.0002	242.6
10	-.0003	-.0000	.0003	260.3
11	-.0009	-.0004	.0010	246.1
12	-.0003	-.0007	.0007	205.3
13	-.0001	-.0005	.0005	189.9
14	.0007	-.0005	.0009	129.3
15	.0009	-.0002	.0009	103.5
16	.0011	-.0000	.0011	90.3

TABLE 10 – WAKE WITH DYNAMOMETER BOAT

TABLE 10a – MEASURED DATA

$r/R = 0.512$

θ_w	V_x/V	V_t/V	V_r/V	θ_w	V_x/V	V_t/V	V_r/V
.3	.769	.013	-.032	180.8	.868	.013	.081
4.2	.778	.006	-.044	186.7	.865	.031	.080
8.3	.769	-.011	-.059	192.7	.867	.049	.077
12.2	.768	-.027	-.080	204.6	.861	.085	.070
16.3	.766	-.007	-.084	216.4	.880	.113	.057
18.2	.765	.003	-.083	228.1	.893	.137	.041
20.4	.730	-.016	-.087	240.0	.905	.156	.022
22.3	.655	-.105	-.100	252.1	.908	.172	.001
24.2	.701	-.214	-.136	263.8	.920	.175	-.020
26.3	.826	-.184	-.153	275.9	.919	.173	-.043
28.3	.888	-.138	-.142	288.0	.918	.165	-.066
32.3	.896	-.102	-.126	312.0	.915	.127	-.105
36.2	.899	-.098	-.119	324.0	.920	.103	-.119
40.3	.897	-.105	-.112	332.0	.905	.123	-.121
44.3	.898	-.112	-.107	333.9	.902	.149	-.125
56.5	.892	-.135	-.086	335.8	.887	.177	-.134
68.5	.904	-.149	-.062	335.9	.857	.180	-.136
80.5	.907	-.156	-.036	338.1	.655	.179	-.147
92.5	.909	-.157	-.013	339.8	.645	.074	-.101
104.6	.884	-.153	.009	341.8	.686	-.010	-.060
116.5	.893	-.138	.028	343.8	.736	-.017	-.042
128.5	.886	-.120	.046	346.0	.772	-0.000	-.036
140.6	.877	-.096	.060	347.8	.784	.017	-.035
160.8	.865	-.045	.077	349.8	.788	.024	-.034
164.7	.866	-.034	.078	353.9	.782	.030	-.028
168.8	.869	-.022	.079	358.1	.772	.023	-.028

TABLE 10a – (Continued)

r/R = 0.711

θ_w	V_x/V	V_t/V	V_r/V	θ_w	V_x/V	V_t/V	V_r/V
.5	.849	-.037	-.076	138.3	.877	-.098	.088
1.8	.853	-.036	-.078	146.3	.879	-.079	.096
2.6	.858	-.041	-.077	154.2	.884	-.058	.102
3.8	.856	-.045	-.088	162.2	.875	-.039	.107
6.6	.862	-.045	-.091	170.2	.878	-.015	.109
7.8	.861	-.052	-.103	178.3	.877	.007	.108
10.0	.868	-.052	-.113	194.3	.864	.047	.105
10.5	.875	-.055	-.112	202.4	.867	.066	.098
12.0	.876	-.060	-.121	218.3	.868	.098	.081
13.9	.883	-.052	-.131	226.4	.874	.111	.069
16.0	.903	-.025	-.130	234.3	.870	.125	.056
18.1	.885	.014	-.126	242.3	.881	.133	.039
20.0	.799	.031	-.123	258.0	.878	.148	.003
22.0	.737	-.046	-.124	268.1	.888	.148	-.021
24.0	.797	-.183	-.148	278.0	.892	.146	-.047
26.0	.902	-.144	-.152	288.1	.892	.139	-.071
28.0	.911	-.113	-.149	306.1	.890	.114	-.112
30.0	.916	-.101	-.145	314.1	.892	.097	-.126
32.0	.913	-.098	-.140	322.2	.899	.082	-.136
42.1	.910	-.120	-.125	330.2	.903	.101	-.152
48.0	.909	-.131	-.112	332.3	.888	.142	-.158
60.1	.907	-.151	-.084	334.3	.760	.139	-.135
66.0	.908	-.157	-.069	336.2	.737	-.010	-.112
72.1	.908	-.160	-.054	338.2	.797	-.047	-.112
78.1	.907	-.163	-.037	340.3	.844	-.011	-.118
84.0	.908	-.162	-.022	342.5	.841	.014	-.113
96.0	.904	-.158	.008	346.4	.839	.014	-.094
102.2	.907	-.153	.022	350.5	.842	0.000	-.077
122.4	.892	-.128	.063	354.5	.848	-.016	-.069
130.4	.892	-.113	.075				

TABLE 10a – (Continued)

r/R = 0.910

θ_w	V_x/V	V_t/V	V_r/V	θ_w	V_x/V	V_t/V	V_r/V
4.3	.892	-.007	-.109	168.5	.894	-0.000	.104
8.2	.897	-.016	-.120	180.6	.879	.031	.107
12.3	.904	-.024	-.127	192.5	.884	.060	.103
16.0	.911	-.026	-.133	204.4	.890	.086	.093
17.8	.917	-.022	-.133	216.1	.892	.109	.080
20.2	.939	.007	-.133	239.9	.906	.148	.040
20.3	.939	.008	-.136	246.1	.909	.156	.027
21.8	.898	.066	-.134	251.7	.919	.161	.015
24.4	.742	.027	-.132	257.9	.936	.165	.003
28.4	.905	-.091	-.158	263.6	.930	.167	-.009
32.3	.901	-.058	-.153	269.9	.934	.169	-.024
36.3	.904	-.067	-.146	282.3	.923	.168	-.058
40.3	.906	-.076	-.138	287.8	.923	.164	-.071
44.1	.905	-.087	-.131	294.2	.928	.157	-.086
48.4	.899	-.096	-.120	299.9	.928	.150	-.101
52.2	.906	-.104	-.109	306.2	.928	.140	-.114
56.3	.907	-.111	-.099	311.9	.931	.128	-.127
60.3	.907	-.116	-.085	316.4	.926	.118	-.135
66.1	.908	-.123	-.069	320.0	.932	.107	-.140
78.0	.921	-.126	-.035	324.0	.935	.096	-.143
84.3	.915	-.126	-.020	328.2	.930	.094	-.148
90.1	.926	-.124	-.007	332.0	.923	.174	-.180
96.2	.926	-.120	.006	335.6	.884	-.056	-.121
102.1	.918	-.115	.016	337.5	.655	-.033	-.122
108.2	.909	-.110	.030	340.0	.884	.048	-.134
114.3	.897	-.104	.043	343.7	.910	.063	-.119
120.2	.900	-.094	.052	348.1	.891	.057	-.105
126.1	.895	-.086	.064	352.2	.890	.046	-.104
132.6	.883	-.076	.074	356.2	.890	.032	-.102
138.2	.894	-.065	.080	359.8	.892	.010	-.103
144.4	.887	-.053	.088	359.9	.900	.017	-.103
156.4	.888	-.028	.098				

TABLE 10a – (Continued)

r/R = 1.082

θ_w	V_x/V	V_t/V	V_r/V
0.0	.866	0.000	-.124
10.0	.879	-.026	-.127
17.8	.898	-.042	-.124
21.2	.835	.047	-.123
23.1	.696	-.181	-.150
25.1	.766	-.137	-.176
27.0	.882	-.089	-.156
29.1	.885	-.084	-.154
29.4	.881	-.083	-.151
31.1	.881	-.087	-.149
32.9	.879	-.092	-.147
44.9	.873	-.121	-.119
50.8	.876	-.135	-.103
56.9	.881	-.143	-.085
62.6	.886	-.152	-.069
92.4	.898	-.152	.012
104.8	.897	-.142	.038
116.4	.894	-.128	.061
128.6	.896	-.108	.080
160.5	.893	-.047	.115
172.6	.902	-.019	.118
184.6	.897	.009	.117

θ_w	V_x/V	V_t/V	V_r/V
187.4	.902	.019	.118
199.5	.893	.047	.115
231.4	.896	.108	.080
243.6	.894	.128	.061
255.2	.897	.142	.038
267.6	.898	.152	.012
297.4	.886	.152	-.069
303.1	.881	.143	-.085
309.2	.876	.135	-.103
315.1	.873	.121	-.119
327.1	.879	.092	-.147
328.9	.881	.087	-.149
330.6	.881	.083	-.151
330.9	.885	.084	-.154
333.0	.882	.089	-.156
334.9	.766	.137	-.176
336.9	.696	.181	-.150
338.8	.835	-.047	-.123
342.2	.898	.042	-.124
350.0	.879	.026	-.127
360.0	.866	0.000	-.124

TABLE 10b – INTERPOLATED VALUES OF V_x/V

θ_w	r/R = 0.289	0.3	0.4	0.5	0.6	0.7	0.8	0.9	1.0
0.0	.640	.647	.709	.763	.809	.846	.881	.896	.888
2.5	.632	.640	.709	.767	.815	.852	.881	.894	.887
5.0	.626	.635	.709	.770	.819	.856	.882	.892	.887
7.5	.599	.610	.694	.764	.819	.859	.885	.896	.890
10.0	.566	.578	.678	.760	.823	.867	.891	.900	.894
12.5	.547	.561	.670	.759	.826	.873	.894	.904	.905
15.0	.487	.504	.644	.755	.838	.891	.903	.908	.910
17.5	.492	.509	.646	.756	.838	.892	.910	.916	.911
20.0	.771	.767	.743	.739	.756	.794	.890	.938	.929
22.5	.587	.590	.617	.651	.691	.738	.830	.859	.817
25.0	.378	.403	.595	.734	.820	.852	.790	.750	.742
27.5	.702	.713	.801	.863	.901	.913	.875	.857	.865
30.0	.871	.873	.890	.902	.911	.916	.919	.914	.900
32.5	.845	.849	.875	.894	.907	.912	.909	.902	.891
35.0	.862	.864	.883	.897	.906	.910	.910	.904	.891
37.5	.867	.869	.885	.897	.906	.910	.911	.906	.892
40.0	.863	.865	.883	.896	.905	.910	.913	.907	.892
42.5	.864	.866	.883	.896	.905	.910	.913	.907	.892
45.0	.864	.866	.884	.897	.905	.909	.911	.905	.890
47.5	.858	.860	.881	.896	.905	.909	.908	.901	.888
50.0	.857	.860	.879	.894	.904	.908	.909	.903	.890
52.5	.859	.862	.879	.893	.902	.908	.911	.907	.894
55.0	.858	.860	.877	.891	.901	.907	.911	.908	.896
57.5	.859	.861	.878	.891	.901	.907	.911	.908	.897

TABLE 10b – (Continued)

θ_w	r/R = 0.289	0.3	0.4	0.5	0.6	0.7	0.8	0.9	1.0
60.0	.867	.869	.883	.894	.902	.907	.911	.908	.898
62.5	.874	.876	.887	.897	.903	.907	.911	.908	.898
65.0	.882	.884	.893	.900	.905	.908	.911	.908	.900
67.5	.893	.893	.898	.903	.906	.908	.912	.910	.902
70.0	.902	.902	.903	.905	.906	.908	.914	.913	.904
72.5	.910	.910	.907	.906	.906	.908	.916	.917	.907
75.0	.917	.916	.910	.906	.905	.907	.918	.919	.910
77.5	.922	.921	.912	.907	.905	.907	.919	.921	.912
80.0	.919	.918	.912	.907	.906	.907	.917	.919	.910
82.5	.918	.918	.912	.908	.907	.908	.915	.916	.909
85.0	.923	.922	.914	.910	.907	.908	.915	.916	.909
87.5	.934	.932	.919	.911	.906	.907	.919	.921	.913
90.0	.944	.941	.923	.911	.905	.905	.922	.926	.916
92.5	.946	.943	.923	.910	.904	.904	.922	.928	.918
95.0	.931	.929	.914	.905	.901	.903	.922	.927	.917
97.5	.908	.907	.901	.899	.899	.904	.920	.925	.916
100.0	.881	.881	.886	.892	.898	.905	.918	.922	.913
102.5	.855	.857	.873	.886	.897	.906	.916	.918	.910
105.0	.842	.844	.865	.882	.896	.905	.913	.914	.908
107.5	.846	.848	.868	.883	.896	.904	.910	.910	.905
110.0	.853	.855	.872	.886	.896	.902	.906	.905	.901
112.5	.862	.864	.878	.888	.896	.900	.901	.900	.898
115.0	.876	.877	.885	.891	.895	.898	.898	.897	.896
117.5	.889	.889	.891	.893	.894	.896	.898	.898	.897

TABLE 10b – (Continued)

θ_w	r/R = 0.289	0.3	0.4	0.5	0.6	0.7	0.8	0.9	1.0
120.0	.896	.895	.893	.892	.892	.893	.898	.900	.898
122.5	.895	.895	.892	.891	.891	.892	.897	.899	.898
125.0	.884	.884	.886	.889	.891	.893	.895	.896	.896
127.5	.871	.872	.880	.886	.891	.893	.892	.892	.893
130.0	.861	.863	.875	.884	.890	.892	.887	.886	.890
132.5	.865	.867	.876	.882	.887	.888	.883	.883	.888
135.0	.882	.882	.881	.881	.882	.883	.884	.887	.891
137.5	.899	.898	.887	.880	.877	.878	.886	.892	.895
140.0	.900	.898	.886	.878	.875	.876	.886	.893	.895
142.5	.888	.887	.880	.876	.874	.876	.884	.890	.893
145.0	.872	.872	.872	.873	.875	.878	.882	.886	.890
147.5	.857	.858	.865	.870	.875	.880	.882	.886	.889
150.0	.844	.845	.858	.868	.876	.882	.883	.885	.889
152.5	.834	.836	.853	.866	.876	.883	.884	.886	.889
155.0	.831	.833	.851	.865	.875	.883	.885	.887	.890
157.5	.840	.841	.854	.864	.873	.880	.885	.888	.891
160.0	.852	.852	.858	.864	.870	.877	.885	.890	.893
162.5	.863	.863	.863	.865	.869	.874	.884	.892	.895
165.0	.866	.866	.865	.866	.869	.875	.885	.893	.897
167.5	.869	.868	.867	.868	.871	.876	.886	.893	.898
170.0	.867	.867	.867	.869	.872	.877	.885	.892	.897
172.5	.864	.865	.867	.870	.873	.878	.883	.889	.896
175.0	.861	.861	.865	.869	.873	.877	.880	.885	.892
177.5	.857	.858	.864	.869	.873	.877	.878	.882	.889

TABLE 10b – (Continued)

θ_w	r/R = 0.289	0.3	0.4	0.5	0.6	0.7	0.8	0.9	1.0
180.0	.856	.857	.863	.868	.872	.875	.876	.879	.887
182.5	.858	.859	.863	.866	.870	.873	.874	.878	.886
185.0	.863	.863	.864	.865	.868	.871	.873	.879	.888
187.5	.871	.871	.867	.865	.866	.868	.872	.880	.891
190.0	.883	.882	.872	.866	.864	.866	.872	.881	.893
192.5	.895	.893	.877	.868	.863	.864	.873	.883	.894
195.0	.896	.893	.877	.867	.862	.864	.874	.884	.894
197.5	.889	.883	.874	.865	.862	.864	.876	.886	.893
200.0	.882	.881	.869	.863	.862	.865	.878	.887	.892
202.5	.875	.874	.866	.862	.862	.866	.879	.889	.893
205.0	.876	.874	.866	.862	.862	.866	.880	.890	.893
207.5	.887	.885	.872	.865	.863	.866	.881	.890	.894
210.0	.900	.898	.881	.869	.865	.866	.881	.890	.894
212.5	.915	.912	.889	.874	.867	.867	.881	.891	.894
215.0	.930	.927	.899	.879	.869	.867	.881	.891	.895
217.5	.942	.938	.906	.883	.871	.867	.882	.892	.895
220.0	.947	.943	.910	.887	.873	.869	.884	.893	.896
222.5	.951	.947	.913	.889	.876	.872	.885	.895	.897
225.0	.956	.951	.917	.892	.878	.873	.887	.896	.898
227.5	.966	.961	.922	.895	.879	.873	.888	.898	.900
230.0	.982	.976	.931	.898	.879	.872	.889	.899	.901
232.5	.998	.992	.939	.902	.879	.870	.889	.901	.902
235.0	1.008	1.001	.945	.904	.880	.871	.891	.902	.903
237.5	1.008	1.001	.946	.907	.883	.874	.893	.904	.904

TABLE 10b – (Continued)

θ_w	r/R = 0.289	0.3	0.4	0.5	0.6	0.7	0.8	0.9	1.0
240.0	1.003	.995	.945	.908	.886	.877	.896	.906	.904
242.5	.993	.987	.942	.909	.889	.881	.898	.906	.904
245.0	.995	.989	.943	.909	.889	.882	.899	.908	.905
247.5	1.001	.995	.945	.910	.889	.881	.901	.911	.907
250.0	1.011	1.004	.950	.911	.888	.880	.904	.915	.911
252.5	1.025	1.018	.956	.912	.887	.879	.908	.921	.915
255.0	1.046	1.037	.966	.916	.886	.878	.913	.929	.921
257.5	1.064	1.054	.975	.919	.886	.878	.917	.935	.926
260.0	1.066	1.056	.977	.922	.889	.879	.917	.934	.925
262.5	1.061	1.052	.977	.924	.892	.882	.916	.931	.923
265.0	1.056	1.047	.976	.925	.895	.885	.916	.930	.922
267.5	1.050	1.041	.973	.925	.896	.887	.918	.932	.923
270.0	1.046	1.037	.971	.925	.897	.889	.921	.934	.924
272.5	1.038	1.030	.968	.924	.898	.890	.920	.933	.922
275.0	1.030	1.023	.964	.923	.899	.891	.919	.930	.921
277.5	1.023	1.016	.962	.922	.899	.892	.917	.928	.918
280.0	1.018	1.012	.960	.922	.900	.892	.916	.925	.916
282.5	1.015	1.009	.958	.922	.900	.892	.914	.923	.915
285.0	1.014	1.008	.958	.922	.900	.892	.914	.923	.914
287.5	1.015	1.008	.958	.921	.900	.892	.915	.923	.914
290.0	1.016	1.010	.958	.921	.899	.892	.916	.925	.914
292.5	1.019	1.012	.958	.921	.898	.891	.918	.927	.915
295.0	1.020	1.013	.959	.920	.897	.891	.919	.928	.915
297.5	1.020	1.013	.958	.920	.897	.890	.919	.929	.915

TABLE 10b – (Continued)

θ_w	r/R = 0.289	0.3	0.4	0.5	0.6	0.7	0.8	0.9	1.0
300.0	1.019	1.012	.958	.919	.897	.890	.919	.928	.914
302.5	1.018	1.011	.957	.919	.896	.890	.919	.928	.913
305.0	1.017	1.010	.956	.918	.896	.890	.919	.928	.912
307.5	1.018	1.011	.957	.918	.896	.890	.921	.930	.912
310.0	1.019	1.011	.957	.918	.896	.890	.922	.931	.912
312.5	1.018	1.011	.957	.919	.897	.891	.922	.931	.911
315.0	1.017	1.010	.958	.921	.899	.893	.921	.928	.908
317.5	1.017	1.010	.959	.923	.902	.895	.922	.928	.909
320.0	1.017	1.011	.960	.924	.903	.897	.926	.933	.912
322.5	1.010	1.004	.957	.924	.905	.900	.929	.935	.914
325.0	.977	.973	.942	.920	.909	.907	.932	.935	.914
327.5	.948	.946	.927	.915	.909	.909	.930	.932	.912
330.0	.950	.947	.925	.910	.903	.903	.926	.930	.913
332.5	1.041	1.032	.960	.911	.882	.876	.916	.933	.921
335.0	1.461	1.424	1.128	.916	.787	.741	.868	.918	.871
337.5	.415	.435	.589	.697	.758	.773	.693	.656	.673
340.0	.256	.280	.474	.631	.750	.833	.866	.883	.886
342.5	.487	.499	.603	.694	.771	.835	.894	.924	.924
345.0	.652	.658	.707	.753	.796	.835	.878	.905	.915
347.5	.717	.720	.750	.779	.808	.836	.870	.893	.902
350.0	.722	.725	.756	.785	.812	.839	.871	.889	.890
352.5	.701	.705	.745	.781	.814	.842	.876	.890	.881
355.0	.670	.675	.729	.774	.813	.845	.879	.890	.874
357.5	.653	.660	.718	.768	.810	.845	.881	.893	.876

TABLE 10c – INTERPOLATED VALUES OF V_t/V

θ_w	r/R = 0.289	0.3	0.4	0.5	0.6	0.7	0.8	0.9	1.0
0.0	.178	.167	.082	.020	-.018	-.033	-.005	.012	.012
2.5	.172	.161	.076	.014	-.025	-.041	-.016	-.000	.002
5.0	.161	.151	.069	.009	-.029	-.046	-.024	-.010	-.007
7.5	.129	.120	.049	-.002	-.035	-.048	-.028	-.015	-.013
10.0	.095	.087	.027	-.016	-.043	-.053	-.033	-.021	-.019
12.5	.092	.084	.022	-.022	-.049	-.059	-.035	-.024	-.032
15.0	.059	.054	.016	-.012	-.031	-.039	-.027	-.026	-.039
17.5	-.037	-.034	-.013	.000	.006	.004	-.009	-.022	-.035
20.0	-.131	-.123	-.059	-.012	.018	.031	.004	.000	.026
22.5	-.016	-.024	-.085	-.116	-.117	-.089	.033	.070	.007
25.0	-.088	-.098	-.173	-.212	-.214	-.180	-.044	.009	-.034
27.5	-.183	-.182	-.172	-.159	-.142	-.122	-.088	-.070	-.070
30.0	-.129	-.129	-.123	-.116	-.109	-.102	-.091	-.085	-.083
32.5	-.061	-.064	-.087	-.100	-.104	-.099	-.070	-.058	-.067
35.0	-.046	-.049	-.078	-.096	-.103	-.101	-.072	-.062	-.073
37.5	-.042	-.046	-.077	-.098	-.107	-.106	-.080	-.069	-.080
40.0	-.038	-.043	-.079	-.102	-.114	-.114	-.086	-.075	-.085
42.5	-.036	-.041	-.080	-.106	-.120	-.121	-.093	-.082	-.092
45.0	-.042	-.047	-.085	-.111	-.125	-.126	-.099	-.089	-.099
47.5	-.048	-.053	-.090	-.116	-.129	-.131	-.104	-.094	-.104
50.0	-.054	-.059	-.096	-.121	-.134	-.135	-.109	-.099	-.110
52.5	-.060	-.065	-.101	-.126	-.138	-.140	-.114	-.104	-.115
55.0	-.066	-.070	-.106	-.130	-.143	-.144	-.119	-.109	-.118
57.5	-.070	-.075	-.110	-.134	-.147	-.148	-.122	-.113	-.122

TABLE 10c – (Continued)

θ_w	r/R = 0.289	0.3	0.4	0.5	0.6	0.7	0.8	0.9	1.0
60.0	-.073	-.077	-.113	-.138	-.150	-.151	-.126	-.116	-.125
62.5	-.076	-.081	-.117	-.141	-.153	-.154	-.128	-.119	-.129
65.0	-.081	-.085	-.120	-.144	-.156	-.157	-.131	-.122	-.132
67.5	-.085	-.090	-.123	-.146	-.158	-.159	-.133	-.124	-.134
70.0	-.089	-.094	-.126	-.148	-.159	-.160	-.134	-.125	-.135
72.5	-.092	-.096	-.129	-.150	-.161	-.161	-.135	-.126	-.136
75.0	-.093	-.097	-.130	-.152	-.163	-.162	-.136	-.126	-.136
77.5	-.093	-.097	-.131	-.153	-.164	-.164	-.136	-.126	-.136
80.0	-.096	-.100	-.132	-.154	-.164	-.164	-.137	-.126	-.136
82.5	-.100	-.104	-.135	-.155	-.164	-.163	-.137	-.126	-.136
85.0	-.103	-.107	-.136	-.155	-.164	-.163	-.136	-.126	-.135
87.5	-.105	-.109	-.137	-.156	-.164	-.162	-.136	-.125	-.134
90.0	-.106	-.110	-.138	-.156	-.164	-.161	-.135	-.124	-.133
92.5	-.107	-.110	-.138	-.156	-.163	-.161	-.134	-.123	-.131
95.0	-.108	-.112	-.138	-.155	-.162	-.159	-.132	-.121	-.129
97.5	-.110	-.113	-.139	-.155	-.161	-.158	-.130	-.119	-.127
100.0	-.111	-.115	-.139	-.154	-.160	-.156	-.128	-.117	-.125
102.5	-.113	-.116	-.139	-.153	-.158	-.154	-.126	-.115	-.123
105.0	-.113	-.116	-.138	-.152	-.156	-.151	-.124	-.113	-.121
107.5	-.111	-.114	-.136	-.149	-.153	-.149	-.122	-.111	-.119
110.0	-.108	-.111	-.133	-.146	-.151	-.146	-.120	-.109	-.116
112.5	-.104	-.107	-.129	-.143	-.147	-.143	-.117	-.106	-.114
115.0	-.100	-.103	-.126	-.139	-.144	-.140	-.114	-.103	-.110
117.5	-.095	-.098	-.121	-.136	-.141	-.137	-.110	-.099	-.106

TABLE 10c – (Continued)

θ_w	r/R = 0.289	0.3	0.4	0.5	0.6	0.7	0.8	0.9	1.0
120.0	-.092	-.095	-.118	-.132	-.137	-.133	-.106	-.094	-.102
122.5	-.090	-.093	-.115	-.129	-.133	-.129	-.102	-.091	-.098
125.0	-.089	-.092	-.112	-.125	-.129	-.124	-.098	-.088	-.095
127.5	-.088	-.090	-.110	-.121	-.124	-.120	-.095	-.084	-.091
130.0	-.086	-.088	-.106	-.117	-.119	-.115	-.090	-.080	-.087
132.5	-.082	-.084	-.102	-.112	-.115	-.110	-.086	-.076	-.083
135.0	-.076	-.078	-.097	-.107	-.110	-.105	-.081	-.071	-.079
137.5	-.070	-.073	-.091	-.102	-.105	-.101	-.076	-.066	-.074
140.0	-.066	-.068	-.086	-.097	-.100	-.095	-.071	-.062	-.069
142.5	-.062	-.064	-.081	-.091	-.094	-.089	-.066	-.057	-.064
145.0	-.058	-.060	-.076	-.085	-.088	-.083	-.061	-.052	-.060
147.5	-.055	-.057	-.071	-.079	-.081	-.077	-.055	-.047	-.055
150.0	-.051	-.053	-.066	-.073	-.075	-.070	-.049	-.042	-.050
152.5	-.047	-.049	-.061	-.067	-.068	-.063	-.043	-.036	-.045
155.0	-.042	-.043	-.054	-.060	-.061	-.057	-.037	-.031	-.040
157.5	-.033	-.035	-.047	-.054	-.055	-.051	-.032	-.025	-.034
160.0	-.025	-.026	-.039	-.047	-.049	-.045	-.026	-.020	-.029
162.5	-.017	-.019	-.032	-.040	-.042	-.039	-.020	-.014	-.023
165.0	-.012	-.014	-.026	-.033	-.035	-.031	-.013	-.008	-.018
167.5	-.007	-.009	-.019	-.025	-.027	-.024	-.007	-.002	-.012
170.0	-.002	-.004	-.013	-.018	-.019	-.016	.000	.004	-.006
172.5	.005	.003	-.006	-.011	-.012	-.009	.007	.011	.000
175.0	.012	.011	.002	-.004	-.005	-.002	.014	.017	.006
177.5	.021	.020	.010	.004	.002	.004	.020	.024	.012

TABLE 10c – (Continued)

θ_w	r/R = 0.289	0.3	0.4	0.5	0.6	0.7	0.8	0.9	1.0
180.0	.030	.029	.018	.011	.009	.011	.027	.030	.018
182.5	.040	.038	.026	.019	.016	.017	.033	.036	.024
185.0	.051	.049	.035	.027	.023	.024	.039	.042	.031
187.5	.061	.059	.044	.034	.030	.030	.045	.049	.038
190.0	.072	.069	.053	.042	.036	.036	.051	.054	.045
192.5	.082	.080	.062	.049	.043	.042	.057	.060	.051
195.0	.093	.091	.071	.057	.050	.048	.063	.066	.056
197.5	.105	.102	.080	.065	.057	.054	.069	.072	.062
200.0	.116	.113	.090	.073	.063	.060	.074	.077	.067
202.5	.127	.124	.099	.081	.070	.066	.080	.082	.072
205.0	.137	.134	.107	.088	.076	.072	.085	.088	.077
207.5	.146	.142	.115	.094	.082	.077	.090	.093	.082
210.0	.154	.150	.121	.101	.087	.082	.095	.098	.087
212.5	.162	.158	.128	.106	.093	.087	.100	.103	.092
215.0	.169	.165	.134	.112	.098	.092	.105	.107	.097
217.5	.177	.173	.141	.118	.103	.097	.110	.112	.102
220.0	.186	.181	.148	.123	.108	.101	.114	.117	.106
222.5	.194	.190	.154	.129	.112	.105	.118	.121	.111
225.0	.202	.197	.161	.134	.116	.109	.122	.125	.115
227.5	.208	.203	.166	.139	.121	.113	.127	.130	.119
230.0	.211	.207	.170	.143	.126	.118	.131	.134	.124
232.5	.214	.210	.174	.147	.130	.122	.135	.138	.128
235.0	.219	.214	.178	.151	.134	.126	.139	.141	.132
237.5	.226	.221	.183	.155	.137	.129	.142	.145	.136

TABLE 10c – (Continued)

θ_w	r/R = 0.289	0.3	0.4	0.5	0.6	0.7	0.8	0.9	1.0
240.0	.234	.229	.188	.159	.140	.131	.145	.148	.139
242.5	.243	.238	.195	.163	.143	.134	.148	.152	.143
245.0	.249	.244	.199	.167	.146	.136	.151	.155	.147
247.5	.254	.248	.203	.170	.149	.139	.153	.158	.149
250.0	.257	.251	.206	.173	.152	.142	.156	.160	.152
252.5	.259	.253	.208	.175	.154	.144	.158	.162	.154
255.0	.258	.252	.209	.177	.156	.146	.159	.164	.156
257.5	.256	.251	.209	.177	.157	.148	.161	.165	.158
260.0	.257	.252	.209	.178	.158	.149	.161	.166	.160
262.5	.258	.252	.210	.178	.158	.149	.162	.167	.161
265.0	.259	.254	.210	.178	.158	.149	.162	.168	.162
267.5	.261	.255	.211	.178	.157	.148	.162	.168	.164
270.0	.262	.256	.211	.178	.157	.148	.162	.169	.165
272.5	.262	.256	.210	.177	.156	.148	.162	.169	.166
275.0	.261	.255	.210	.177	.156	.147	.162	.169	.167
277.5	.260	.254	.209	.175	.155	.146	.161	.169	.167
280.0	.259	.254	.208	.174	.153	.145	.160	.169	.167
282.5	.258	.252	.206	.173	.152	.144	.159	.168	.167
285.0	.257	.251	.204	.171	.150	.142	.157	.166	.166
287.5	.255	.249	.202	.169	.148	.140	.155	.164	.165
290.0	.251	.245	.199	.166	.145	.137	.152	.161	.163
292.5	.247	.241	.196	.163	.142	.135	.149	.158	.161
295.0	.243	.237	.192	.159	.139	.132	.146	.156	.158
297.5	.239	.233	.188	.156	.136	.128	.143	.153	.155

TABLE 10c – (Continued)

θ_w	r/R = 0.289	0.3	0.4	0.5	0.6	0.7	0.8	0.9	1.0
300.0	.235	.229	.184	.152	.132	.124	.139	.149	.152
302.5	.231	.225	.180	.148	.128	.120	.136	.146	.148
305.0	.227	.221	.176	.143	.123	.116	.131	.142	.144
307.5	.223	.218	.172	.139	.118	.111	.126	.137	.140
310.0	.220	.214	.168	.134	.113	.106	.121	.131	.135
312.5	.214	.208	.162	.128	.108	.100	.116	.126	.130
315.0	.202	.195	.152	.120	.101	.095	.110	.121	.124
317.5	.193	.188	.144	.114	.095	.089	.104	.114	.118
320.0	.184	.178	.138	.109	.091	.084	.097	.106	.110
322.5	.178	.173	.134	.106	.088	.081	.091	.099	.103
325.0	.187	.182	.136	.103	.082	.073	.082	.091	.096
327.5	.167	.162	.127	.101	.084	.076	.084	.090	.092
330.0	.185	.180	.137	.109	.096	.097	.137	.149	.127
332.5	.088	.090	.112	.128	.139	.145	.152	.144	.118
335.0	.212	.211	.196	.171	.136	.093	-.007	-.032	.028
337.5	.745	.711	.430	.212	.056	-.038	-.061	-.038	.030
340.0	.327	.310	.173	.073	.009	-.017	.038	.050	.007
342.5	-.031	-.031	-.028	-.020	-.007	.012	.047	.066	.063
345.0	-.020	-.020	-.018	-.011	.001	.016	.044	.062	.067
347.5	.079	.074	.039	.016	.007	.010	.040	.058	.060
350.0	.136	.129	.069	.028	.006	.001	.035	.052	.047
352.5	.178	.168	.090	.034	.002	-.008	.030	.045	.031
355.0	.203	.192	.101	.036	-.004	-.018	.023	.037	.018
357.5	.203	.191	.098	.031	-.010	-.025	.012	.026	.009

TABLE 10d – INTERPOLATED VALUES OF V_r/V

θ_w	r/R = 0.289	0.3	0.4	0.5	0.6	0.7	0.8	0.9	1.0
0.0	.034	.030	-.001	-.028	-.052	-.072	-.088	-.102	-.114
2.5	.029	.025	-.007	-.035	-.059	-.079	-.092	-.105	-.116
5.0	.023	.019	-.015	-.043	-.067	-.087	-.099	-.110	-.119
7.5	.020	.015	-.021	-.052	-.077	-.097	-.109	-.117	-.123
10.0	.015	.010	-.031	-.065	-.091	-.110	-.118	-.123	-.126
12.5	.015	.009	-.039	-.077	-.105	-.123	-.126	-.127	-.127
15.0	.025	.018	-.037	-.080	-.111	-.130	-.133	-.132	-.129
17.5	.012	.006	-.041	-.079	-.107	-.126	-.132	-.133	-.130
20.0	-.013	-.017	-.053	-.082	-.105	-.122	-.132	-.135	-.129
22.5	-.047	-.051	-.079	-.101	-.118	-.129	-.130	-.133	-.137
25.0	-.112	-.114	-.132	-.144	-.151	-.152	-.136	-.134	-.150
27.5	-.146	-.146	-.147	-.148	-.149	-.150	-.151	-.152	-.153
30.0	-.125	-.125	-.129	-.134	-.139	-.144	-.154	-.158	-.156
32.5	-.111	-.112	-.118	-.125	-.131	-.138	-.148	-.153	-.152
35.0	-.105	-.106	-.113	-.120	-.127	-.134	-.143	-.148	-.148
37.5	-.098	-.099	-.108	-.116	-.123	-.130	-.139	-.143	-.143
40.0	-.090	-.091	-.102	-.111	-.120	-.127	-.135	-.139	-.137
42.5	-.086	-.087	-.098	-.108	-.116	-.123	-.131	-.134	-.132
45.0	-.088	-.089	-.098	-.105	-.112	-.118	-.126	-.129	-.126
47.5	-.088	-.089	-.095	-.101	-.107	-.113	-.120	-.123	-.119
50.0	-.085	-.086	-.092	-.097	-.102	-.107	-.114	-.115	-.112
52.5	-.082	-.083	-.088	-.093	-.097	-.101	-.107	-.108	-.105
55.0	-.080	-.080	-.084	-.088	-.092	-.096	-.102	-.103	-.098
57.5	-.075	-.076	-.080	-.084	-.087	-.090	-.095	-.095	-.091

TABLE 10d – (Continued)

θ_w	r/R = 0.289	0.3	0.4	0.5	0.6	0.7	0.8	0.9	1.0
60.0	-.070	-.071	-.075	-.079	-.082	-.084	-.087	-.086	-.082
62.5	-.067	-.067	-.071	-.074	-.076	-.078	-.080	-.079	-.075
65.0	-.064	-.065	-.067	-.069	-.071	-.071	-.073	-.072	-.068
67.5	-.061	-.061	-.063	-.064	-.065	-.065	-.067	-.065	-.061
70.0	-.056	-.056	-.058	-.059	-.059	-.059	-.060	-.058	-.054
72.5	-.051	-.051	-.053	-.053	-.053	-.053	-.053	-.051	-.046
75.0	-.049	-.049	-.049	-.048	-.047	-.046	-.046	-.044	-.039
77.5	-.048	-.048	-.045	-.043	-.041	-.039	-.039	-.037	-.032
80.0	-.046	-.046	-.041	-.037	-.034	-.032	-.032	-.030	-.026
82.5	-.045	-.044	-.038	-.033	-.029	-.026	-.027	-.025	-.020
85.0	-.044	-.043	-.034	-.028	-.023	-.020	-.021	-.019	-.013
87.5	-.043	-.042	-.032	-.023	-.017	-.013	-.015	-.013	-.008
90.0	-.043	-.042	-.029	-.019	-.011	-.007	-.009	-.008	-.002
92.5	-.043	-.041	-.026	-.014	-.006	-.001	-.003	-.002	.004
95.0	-.043	-.041	-.023	-.010	-.000	.005	.002	.003	.009
97.5	-.043	-.040	-.020	-.005	.005	.011	.007	.008	.014
100.0	-.042	-.040	-.018	-.001	.011	.017	.012	.012	.018
102.5	-.042	-.039	-.015	.004	.016	.022	.017	.017	.023
105.0	-.040	-.037	-.011	.008	.021	.028	.022	.022	.028
107.5	-.038	-.035	-.008	.012	.026	.033	.028	.028	.034
110.0	-.037	-.034	-.006	.016	.030	.039	.034	.034	.040
112.5	-.036	-.032	-.003	.020	.035	.044	.039	.039	.045
115.0	-.035	-.031	-.000	.023	.040	.049	.044	.044	.049
117.5	-.035	-.031	.002	.027	.044	.054	.048	.048	.053

TABLE 10d – (Continued)

θ_w	r/R = 0.289	0.3	0.4	0.5	0.6	0.7	0.8	0.9	1.0
120.0	-.033	-.029	.005	.031	.049	.058	.052	.051	.057
122.5	-.030	-.026	.009	.035	.053	.063	.057	.056	.062
125.0	-.025	-.021	.013	.038	.056	.066	.062	.062	.067
127.5	-.020	-.016	.017	.042	.060	.070	.066	.066	.071
130.0	-.018	-.014	.020	.045	.063	.074	.070	.070	.075
132.5	-.018	-.014	.021	.048	.067	.078	.074	.074	.078
135.0	-.020	-.015	.022	.051	.071	.082	.077	.076	.081
137.5	-.022	-.017	.023	.054	.075	.086	.080	.079	.084
140.0	-.021	-.015	.025	.056	.078	.089	.083	.082	.087
142.5	-.017	-.012	.028	.059	.080	.092	.086	.085	.090
145.0	-.012	-.007	.032	.062	.083	.094	.089	.088	.093
147.5	-.008	-.003	.035	.064	.085	.096	.092	.091	.096
150.0	-.004	.000	.038	.067	.087	.098	.094	.093	.098
152.5	-.001	.003	.041	.069	.089	.100	.096	.095	.101
155.0	.001	.006	.043	.071	.091	.102	.097	.097	.102
157.5	.002	.007	.044	.073	.092	.104	.099	.098	.104
160.0	.003	.007	.045	.074	.094	.105	.100	.100	.106
162.5	.002	.007	.045	.075	.095	.106	.102	.101	.107
165.0	.002	.007	.046	.075	.096	.107	.103	.102	.108
167.5	.004	.008	.046	.076	.096	.108	.104	.103	.109
170.0	.006	.010	.048	.076	.097	.108	.104	.104	.110
172.5	.009	.013	.049	.077	.097	.108	.105	.105	.110
175.0	.012	.017	.051	.078	.097	.108	.106	.106	.111
177.5	.016	.020	.053	.078	.096	.107	.106	.106	.111

TABLE 10d – (Continued)

θ_w	r/R = 0.289	0.3	0.4	0.5	0.6	0.7	0.8	0.9	1.0
180.0	.018	.022	.054	.078	.096	.107	.106	.107	.111
182.5	.017	.021	.053	.078	.096	.107	.106	.107	.111
185.0	.016	.020	.053	.078	.096	.107	.105	.106	.111
187.5	.014	.018	.051	.077	.096	.107	.104	.105	.110
190.0	.011	.015	.049	.076	.095	.106	.103	.104	.110
192.5	.007	.012	.047	.074	.094	.105	.102	.103	.109
195.0	.006	.010	.046	.073	.092	.104	.100	.101	.108
197.5	.006	.010	.045	.072	.091	.102	.098	.099	.106
200.0	.007	.011	.045	.071	.089	.100	.096	.097	.104
202.5	.007	.011	.044	.069	.087	.097	.093	.094	.102
205.0	.006	.010	.042	.067	.085	.095	.091	.092	.100
207.5	.003	.007	.040	.065	.082	.093	.088	.089	.097
210.0	.000	.004	.037	.062	.080	.090	.086	.087	.095
212.5	-.003	.001	.034	.059	.077	.087	.083	.084	.092
215.0	-.007	-.002	.031	.056	.074	.084	.080	.081	.089
217.5	-.010	-.006	.027	.053	.071	.081	.077	.078	.086
220.0	-.013	-.009	.024	.050	.068	.078	.073	.074	.083
222.5	-.016	-.012	.021	.046	.064	.074	.069	.070	.079
225.0	-.019	-.015	.018	.043	.061	.071	.065	.066	.076
227.5	-.022	-.018	.014	.039	.057	.067	.061	.062	.072
230.0	-.026	-.022	.011	.036	.053	.063	.057	.058	.068
232.5	-.029	-.025	.007	.032	.049	.059	.053	.054	.064
235.0	-.032	-.028	.004	.028	.045	.054	.048	.049	.059
237.5	-.033	-.030	.001	.024	.040	.049	.043	.044	.055

TABLE 10d – (Continued)

θ_w	r/R = 0.289	0.3	0.4	0.5	0.6	0.7	0.8	0.9	1.0
240.0	-.034	-.031	-.002	.020	.035	.044	.037	.039	.050
242.5	-.035	-.032	-.005	.016	.030	.038	.032	.034	.046
245.0	-.036	-.033	-.008	.012	.025	.033	.026	.029	.041
247.5	-.037	-.034	-.011	.007	.020	.027	.021	.023	.036
250.0	-.038	-.035	-.014	.003	.015	.021	.015	.018	.031
252.5	-.039	-.036	-.016	-.001	.009	.016	.010	.013	.025
255.0	-.039	-.036	-.019	-.005	.004	.010	.005	.008	.021
257.5	-.038	-.037	-.022	-.010	-.001	.004	-.001	.003	.016
260.0	-.039	-.037	-.024	-.014	-.007	-.002	-.006	-.002	.011
262.5	-.040	-.039	-.027	-.019	-.012	-.008	-.012	-.007	.006
265.0	-.041	-.040	-.031	-.023	-.017	-.014	-.017	-.013	.000
267.5	-.042	-.041	-.034	-.028	-.023	-.020	-.023	-.019	-.006
270.0	-.043	-.042	-.037	-.032	-.029	-.026	-.030	-.025	-.012
272.5	-.044	-.043	-.040	-.037	-.034	-.033	-.036	-.032	-.018
275.0	-.045	-.045	-.043	-.041	-.040	-.039	-.043	-.039	-.025
277.5	-.046	-.046	-.046	-.046	-.046	-.046	-.050	-.046	-.032
280.0	-.048	-.049	-.050	-.051	-.051	-.052	-.057	-.053	-.039
282.5	-.051	-.051	-.054	-.055	-.057	-.058	-.063	-.059	-.046
285.0	-.053	-.054	-.057	-.060	-.062	-.064	-.069	-.065	-.052
287.5	-.055	-.056	-.061	-.065	-.068	-.069	-.075	-.071	-.058
290.0	-.056	-.057	-.064	-.069	-.073	-.075	-.080	-.077	-.065
292.5	-.057	-.058	-.067	-.073	-.078	-.081	-.086	-.083	-.071
295.0	-.058	-.059	-.070	-.078	-.084	-.087	-.092	-.089	-.078
297.5	-.060	-.061	-.073	-.082	-.089	-.093	-.098	-.096	-.085

TABLE 10d – (Continued)

θ_w	r/R = 0.289	0.3	0.4	0.5	0.6	0.7	0.8	0.9	1.0
300.0	-.061	-.063	-.076	-.086	-.094	-.099	-.104	-.102	-.091
302.5	-.062	-.064	-.078	-.090	-.098	-.104	-.109	-.107	-.097
305.0	-.063	-.065	-.081	-.094	-.103	-.109	-.114	-.112	-.103
307.5	-.064	-.066	-.084	-.097	-.107	-.114	-.119	-.118	-.110
310.0	-.067	-.069	-.087	-.101	-.111	-.119	-.124	-.123	-.116
312.5	-.070	-.073	-.090	-.104	-.115	-.123	-.129	-.129	-.122
315.0	-.075	-.077	-.094	-.108	-.119	-.126	-.133	-.133	-.128
317.5	-.080	-.082	-.098	-.111	-.122	-.129	-.136	-.137	-.133
320.0	-.083	-.085	-.101	-.114	-.125	-.132	-.138	-.140	-.138
322.5	-.081	-.084	-.102	-.116	-.128	-.136	-.140	-.142	-.141
325.0	-.071	-.074	-.098	-.117	-.131	-.140	-.142	-.143	-.143
327.5	-.055	-.059	-.090	-.115	-.134	-.145	-.145	-.146	-.146
330.0	-.063	-.066	-.093	-.116	-.135	-.150	-.164	-.168	-.163
332.5	-.060	-.064	-.094	-.119	-.139	-.155	-.169	-.173	-.167
335.0	-.145	-.144	-.136	-.131	-.127	-.125	-.120	-.127	-.148
337.5	-.251	-.245	-.192	-.153	-.126	-.111	-.114	-.121	-.131
340.0	-.067	-.068	-.082	-.095	-.106	-.116	-.129	-.134	-.129
342.5	.075	.067	.004	-.046	-.085	-.111	-.121	-.126	-.127
345.0	.095	.087	.021	-.032	-.072	-.099	-.107	-.113	-.120
347.5	.069	.062	.011	-.031	-.063	-.087	-.096	-.105	-.116
350.0	.040	.036	.000	-.030	-.056	-.077	-.090	-.103	-.116
352.5	.029	.025	-.002	-.027	-.050	-.070	-.087	-.102	-.117
355.0	.029	.026	-.000	-.024	-.047	-.067	-.085	-.101	-.116
357.5	.033	.030	.001	-.025	-.048	-.068	-.085	-.101	-.115

TABLE 10e – HARMONICS OF V_x/V

r/R = 0.289

n	$(A_x)_n/V$	$(B_x)_n/V$	$(V_x)_n/V$	$(\phi_x^*)_n$
0	.8831	0.0000	0.0000	0.0
1	-.0644	-.0778	.1010	219.6
2	-.1185	-.0177	.1198	261.5
3	-.0563	-.0143	.0581	255.8
4	-.0410	-.0179	.0448	246.4
5	-.0263	-.0011	.0264	267.7
6	-.0124	.0072	.0144	300.1
7	.0012	-.0010	.0016	129.4
8	.0263	-.0014	.0263	93.1
9	.0237	.0062	.0245	75.3
10	.0225	.0081	.0239	70.1
11	.0283	.0017	.0284	86.6
12	.0194	-.0039	.0197	101.5
13	.0118	-.0022	.0120	100.8
14	-.0011	-.0122	.0122	185.0
15	.0044	-.0198	.0203	167.5
16	-.0116	-.0136	.0179	220.4

r/R = 0.3

n	$(A_x)_n/V$	$(B_x)_n/V$	$(V_x)_n/V$	$(\phi_x^*)_n$
0	.8823	0.0000	0.0000	0.0
1	-.0619	-.0732	.0959	220.2
2	-.1142	-.0167	.1154	261.7
3	-.0546	-.0134	.0563	256.2
4	-.0398	-.0169	.0432	247.0
5	-.0255	-.0009	.0255	267.9
6	-.0118	.0068	.0136	300.1
7	.0012	-.0009	.0015	125.4
8	.0254	-.0013	.0255	92.9
9	.0231	.0059	.0239	75.6
10	.0219	.0078	.0233	70.5
11	.0273	.0016	.0273	86.6
12	.0187	-.0037	.0190	101.1
13	.0112	-.0021	.0114	100.6
14	-.0012	-.0115	.0116	185.8
15	.0038	-.0187	.0191	168.5
16	-.0114	-.0129	.0172	221.2

TABLE 10e – (Continued)

r/R = 0.4

n	$(A_x)_n/V$	$(B_x)_n/V$	$(V_x)_n/V$	$(\phi_x^*)_n$
0	.8766	0.0000	0.0000	0.0
1	-.0416	-.0375	.0560	227.9
2	-.0797	-.0091	.0802	263.5
3	-.0404	-.0064	.0409	261.0
4	-.0293	-.0091	.0307	252.8
5	-.0185	.0002	.0185	270.7
6	-.0068	.0040	.0079	300.3
7	.0014	.0003	.0014	79.7
8	.0185	-.0002	.0185	90.7
9	.0183	.0038	.0187	78.3
10	.0173	.0048	.0180	74.6
11	.0187	.0010	.0187	87.1
12	.0131	-.0015	.0132	96.7
13	.0065	-.0011	.0066	99.7
14	-.0020	-.0064	.0067	197.7
15	-.0008	-.0100	.0101	184.8
16	-.0096	-.0078	.0123	230.9

r/R = 0.5

n	$(A_x)_n/V$	$(B_x)_n/V$	$(V_x)_n/V$	$(\phi_x^*)_n$
0	.8746	0.0000	0.0000	0.0
1	-.0249	-.0116	.0274	245.1
2	-.0526	-.0037	.0527	266.0
3	-.0286	-.0013	.0287	267.3
4	-.0202	-.0033	.0205	260.9
5	-.0126	.0013	.0127	275.6
6	-.0030	.0020	.0036	303.8
7	.0019	.0012	.0022	56.6
8	.0131	.0006	.0131	87.2
9	.0141	.0023	.0143	80.9
10	.0133	.0025	.0135	79.3
11	.0119	.0005	.0119	87.7
12	.0084	-.0001	.0084	90.9
13	.0027	-.0005	.0027	100.6
14	-.0029	-.0027	.0040	226.5
15	-.0043	-.0037	.0057	229.0
16	-.0082	-.0039	.0091	244.5

TABLE 10e – (Continued)

$r/R = 0.6$

n	$(A_x)_n/V$	$(B_x)_n/V$	$(V_x)_n/V$	$(\phi_x^*)_n$
0	.8761	0.0000	0.0000	0.0
1	-.0118	.0046	.0127	291.4
2	-.0330	-.0003	.0330	269.4
3	-.0192	.0018	.0193	275.2
4	-.0126	.0006	.0126	272.7
5	-.0080	.0021	.0082	285.0
6	-.0003	.0009	.0009	339.8
7	.0026	.0020	.0033	51.9
8	.0091	.0012	.0091	82.3
9	.0107	.0014	.0107	82.7
10	.0097	.0010	.0098	84.3
11	.0068	.0002	.0069	88.4
12	.0045	.0006	.0045	82.8
13	-.0003	-.0003	.0004	231.2
14	-.0037	-.0006	.0037	260.9
15	-.0065	.0001	.0065	271.3
16	-.0072	-.0013	.0073	259.6

$r/R = 0.7$

n	$(A_x)_n/V$	$(B_x)_n/V$	$(V_x)_n/V$	$(\phi_x^*)_n$
0	.8812	0.0000	0.0000	0.0
1	-.0024	.0110	.0113	347.6
2	-.0208	.0009	.0208	272.4
3	-.0121	.0029	.0125	283.3
4	-.0063	.0024	.0068	290.9
5	-.0044	.0029	.0053	303.0
6	.0011	.0006	.0013	60.2
7	.0037	.0027	.0046	53.3
8	.0065	.0016	.0067	76.5
9	.0078	.0011	.0079	82.2
10	.0068	.0002	.0068	88.6
11	.0036	.0001	.0036	88.7
12	.0014	.0006	.0016	68.7
13	-.0025	-.0004	.0026	261.1
14	-.0045	.0000	.0045	270.5
15	-.0075	.0016	.0077	282.3
16	-.0067	-.0001	.0067	269.6

TABLE 10e – (Continued)

$r/R = 0.8$

n	$(A_x)_n/V$	$(B_x)_n/V$	$(V_x)_n/V$	$(\phi_x^*)_n$
0	.8971	0.0000	0.0000	0.0
1	.0058	-.0007	.0058	96.5
2	-.0211	-.0023	.0212	263.9
3	-.0083	.0004	.0083	272.4
4	-.0015	.0008	.0017	299.3
5	-.0027	.0041	.0049	326.9
6	.0002	.0024	.0024	3.7
7	.0062	.0038	.0072	58.3
8	.0064	.0016	.0066	75.6
9	.0058	.0022	.0062	69.4
10	.0042	.0006	.0043	82.5
11	.0032	.0002	.0032	85.6
12	-.0004	-.0012	.0013	200.9
13	-.0035	-.0017	.0039	244.3
14	-.0050	-.0027	.0057	241.7
15	-.0061	-.0017	.0063	254.7
16	-.0065	-.0013	.0066	258.8

$r/R = 0.9$

n	$(A_x)_n/V$	$(B_x)_n/V$	$(V_x)_n/V$	$(\phi_x^*)_n$
0	.9034	0.0000	0.0000	0.0
1	.0059	-.0070	.0092	140.2
2	-.0196	-.0035	.0199	259.8
3	-.0053	-.0011	.0054	258.5
4	.0019	-.0001	.0019	94.4
5	-.0009	.0040	.0041	346.9
6	.0002	.0031	.0031	3.9
7	.0068	.0038	.0078	61.2
8	.0061	.0015	.0062	76.1
9	.0043	.0025	.0049	59.7
10	.0024	.0008	.0026	71.1
11	.0025	.0004	.0025	80.6
12	-.0021	-.0018	.0027	229.5
13	-.0044	-.0019	.0048	246.2
14	-.0060	-.0036	.0070	238.9
15	-.0057	-.0030	.0065	242.0
16	-.0068	-.0016	.0070	256.6

TABLE 10e – (Continued)

r/R = 1.0

n	$(A_x)_n/V$	$(B_x)_n/V$	$(V_x)_n/V$	$(\phi_x^*)_n$
0	.8984	0.0000	0.0000	0.0
1	-.0029	-.0061	.0068	205.0
2	-.0151	-.0024	.0153	260.8
3	-.0032	-.0010	.0034	252.2
4	.0038	-.0002	.0038	93.1
5	.0009	.0025	.0027	19.7
6	.0016	.0023	.0028	34.4
7	.0054	.0024	.0059	65.9
8	.0053	.0012	.0054	77.6
9	.0032	.0018	.0037	60.5
10	.0014	.0009	.0017	57.4
11	.0012	.0006	.0013	64.2
12	-.0034	-.0009	.0036	254.8
13	-.0052	-.0009	.0053	259.9
14	-.0073	-.0022	.0076	253.5
15	-.0067	-.0019	.0070	254.2
16	-.0077	-.0008	.0077	264.0

TABLE 10f – HARMONICS OF V_t/V

$r/R = 0.289$

n	$(A_t)_n/V$	$(B_t)_n/V$	$(V_t)_n/V$	$(\phi_t^*)_n$
0	.0730	0.0000	0.0000	0.0
1	.0254	-.1921	.1938	172.5
2	-.0020	-.0048	.0052	202.4
3	.0137	-.0163	.0213	139.8
4	.0086	-.0145	.0168	149.3
5	.0129	-.0127	.0181	134.4
6	.0098	-.0054	.0112	119.0
7	.0088	-.0003	.0088	91.9
8	.0052	.0061	.0080	40.3
9	.0048	.0133	.0142	19.9
10	.0024	.0157	.0158	8.6
11	.0017	.0160	.0161	6.1
12	.0032	.0150	.0153	12.1
13	.0065	.0110	.0128	30.6
14	.0077	.0048	.0090	58.1
15	.0106	-.0004	.0106	92.3
16	.0119	-.0051	.0130	113.1

$r/R = 0.3$

n	$(A_t)_n/V$	$(B_t)_n/V$	$(V_t)_n/V$	$(\phi_t^*)_n$
0	.0685	0.0000	0.0000	0.0
1	.0234	-.1909	.1923	173.0
2	-.0019	-.0047	.0050	201.7
3	.0130	-.0157	.0203	140.4
4	.0081	-.0139	.0161	149.7
5	.0122	-.0121	.0172	134.8
6	.0093	-.0051	.0106	118.7
7	.0083	-.0000	.0083	90.3
8	.0049	.0062	.0079	38.4
9	.0046	.0131	.0139	19.2
10	.0022	.0153	.0155	8.3
11	.0016	.0156	.0156	5.9
12	.0030	.0144	.0147	11.8
13	.0061	.0105	.0121	30.2
14	.0072	.0043	.0084	59.0
15	.0100	-.0008	.0100	94.4
16	.0113	-.0053	.0125	115.2

TABLE 10f – (Continued)

r/R = 0.4

n	$(A_t)_n/V$	$(B_t)_n/V$	$(V_t)_n/V$	$(\phi_t^*)_n$
0	.0340	0.0000	0.0000	0.0
1	.0076	-.1803	.1804	177.6
2	-.0010	-.0040	.0041	194.2
3	.0068	-.0108	.0128	147.7
4	.0045	-.0092	.0102	153.8
5	.0065	-.0074	.0098	138.8
6	.0050	-.0022	.0054	113.9
7	.0045	.0019	.0049	67.8
8	.0025	.0063	.0068	21.9
9	.0024	.0112	.0114	12.2
10	.0011	.0124	.0124	5.3
11	.0007	.0117	.0117	3.5
12	.0015	.0098	.0099	8.6
13	.0031	.0061	.0068	26.7
14	.0038	.0009	.0039	76.9
15	.0053	-.0034	.0063	123.1
16	.0062	-.0069	.0092	138.1

r/R = 0.5

n	$(A_t)_n/V$	$(B_t)_n/V$	$(V_t)_n/V$	$(\phi_t^*)_n$
0	.0100	0.0000	0.0000	0.0
1	-.0039	-.1708	.1709	181.3
2	-.0004	-.0034	.0034	186.1
3	.0023	-.0065	.0069	160.4
4	.0018	-.0050	.0053	160.3
5	.0022	-.0036	.0042	148.9
6	.0017	.0000	.0017	89.8
7	.0017	.0030	.0034	29.0
8	.0008	.0060	.0060	7.3
9	.0008	.0090	.0091	5.0
10	.0003	.0093	.0094	2.0
11	.0001	.0081	.0081	.5
12	.0003	.0057	.0057	3.5
13	.0008	.0024	.0025	18.8
14	.0013	-.0018	.0022	145.3
15	.0017	-.0052	.0055	161.6
16	.0023	-.0076	.0079	163.3

TABLE 10f – (Continued)

r/R = 0.6

n	$(A_t)_n/V$	$(B_t)_n/V$	$(V_t)_n/V$	$(\phi_t^*)_n$
0	-.0034	0.0000	0.0000	0.0
1	-.0112	-.1626	.1630	183.9
2	.0001	-.0028	.0028	178.0
3	-.0006	-.0028	.0029	191.4
4	.0000	-.0015	.0015	179.5
5	-.0008	-.0006	.0010	230.8
6	-.0005	.0015	.0016	341.0
7	-.0003	.0034	.0034	354.8
8	-.0004	.0051	.0052	355.0
9	-.0003	.0066	.0067	357.5
10	-.0002	.0063	.0063	358.1
11	-.0003	.0047	.0047	355.8
12	-.0004	.0021	.0021	350.2
13	-.0006	-.0007	.0009	223.4
14	-.0004	-.0038	.0039	186.0
15	-.0006	-.0062	.0062	185.5
16	-.0004	-.0075	.0075	182.9

r/R = 0.7

n	$(A_t)_n/V$	$(B_t)_n/V$	$(V_t)_n/V$	$(\phi_t^*)_n$
0	-.0062	0.0000	0.0000	0.0
1	-.0142	-.1556	.1562	185.2
2	.0004	-.0024	.0024	171.3
3	-.0018	.0002	.0018	276.5
4	-.0009	.0014	.0017	328.7
5	-.0023	.0015	.0027	303.5
6	-.0017	.0024	.0029	324.2
7	-.0014	.0031	.0034	335.7
8	-.0011	.0038	.0039	344.0
9	-.0009	.0041	.0041	348.2
10	-.0005	.0032	.0032	351.5
11	-.0005	.0014	.0015	339.4
12	-.0007	-.0009	.0011	216.7
13	-.0013	-.0030	.0033	202.6
14	-.0012	-.0051	.0052	193.2
15	-.0018	-.0063	.0066	195.5
16	-.0018	-.0065	.0067	195.4

TABLE 10f – (Continued)

r/R = 0.8

n	$(A_t)_n/V$	$(B_t)_n/V$	$(V_t)_n/V$	$(\phi_t^*)_n$
0	.0141	0.0000	0.0000	0.0
1	-.0107	-.1473	.1477	184.2
2	.0006	-.0002	.0006	109.3
3	.0001	.0036	.0036	.8
4	.0001	.0043	.0043	.7
5	-.0015	.0029	.0032	333.1
6	-.0011	.0022	.0025	333.4
7	-.0011	.0012	.0016	318.5
8	-.0007	.0007	.0010	315.1
9	-.0005	-.0003	.0006	236.2
10	-.0001	-.0017	.0017	184.7
11	-.0003	-.0033	.0033	185.0
12	-.0001	-.0046	.0046	181.4
13	-.0004	-.0056	.0057	184.6
14	-.0004	-.0060	.0060	184.0
15	-.0010	-.0052	.0053	190.6
16	-.0012	-.0037	.0039	198.5

r/R = 0.9

n	$(A_t)_n/V$	$(B_t)_n/V$	$(V_t)_n/V$	$(\phi_t^*)_n$
0	.0224	0.0000	0.0000	0.0
1	-.0070	-.1446	.1448	182.8
2	.0003	-.0013	.0013	165.7
3	.0009	.0046	.0047	10.9
4	.0003	.0055	.0055	3.4
5	-.0009	.0032	.0033	344.1
6	-.0008	.0019	.0021	337.7
7	-.0008	.0001	.0008	276.0
8	-.0006	-.0006	.0008	223.2
9	-.0003	-.0020	.0021	188.1
10	-.0001	-.0035	.0035	181.9
11	-.0002	-.0048	.0048	182.2
12	.0000	-.0055	.0055	179.5
13	.0000	-.0059	.0059	179.7
14	-.0000	-.0055	.0055	180.3
15	-.0004	-.0040	.0040	185.4
16	-.0007	-.0019	.0020	201.2

TABLE 10f – (Continued)

r/R = 1.0

n	$(A_t)_n/V$	$(B_t)_n/V$	$(V_t)_n/V$	$(\phi_t^*)_n$
0	.0158	0.0000	0.0000	0.0
1	-.0037	-.1481	.1482	181.4
2	-.0004	-.0060	.0061	183.9
3	.0003	.0030	.0030	6.5
4	-.0002	.0048	.0049	357.1
5	-.0008	.0023	.0024	341.1
6	-.0009	.0015	.0017	329.3
7	-.0007	-.0000	.0007	267.7
8	-.0008	.0002	.0008	281.4
9	-.0004	-.0007	.0008	207.6
10	-.0005	-.0017	.0018	195.5
11	-.0003	-.0027	.0027	186.0
12	-.0003	-.0031	.0031	185.1
13	.0000	-.0036	.0036	179.5
14	-.0002	-.0035	.0035	183.0
15	-.0001	-.0027	.0027	182.5
16	-.0005	-.0015	.0016	198.2

TABLE 10g – HARMONICS OF V_r/V

$r/R = 0.289$

n	$(A_r)_n/V$	$(B_r)_n/V$	$(V_r)_n/V$	$(\phi_r^*)_n$
0	-.0333	0.0000	0.0000	0.0
1	-.0231	-.0026	.0233	263.7
2	.0258	-.0030	.0260	96.6
3	.0159	-.0033	.0163	101.7
4	.0244	.0001	.0244	89.7
5	.0189	.0000	.0189	90.0
6	.0133	.0020	.0134	81.5
7	.0093	.0008	.0094	85.3
8	.0057	-.0014	.0059	103.7
9	.0013	-.0013	.0018	135.0
10	-.0021	-.0020	.0029	227.0
11	-.0058	-.0036	.0068	238.3
12	-.0069	-.0037	.0078	241.4
13	-.0094	-.0053	.0108	240.6
14	-.0078	-.0044	.0089	240.5
15	-.0089	-.0027	.0093	253.0
16	-.0058	-.0009	.0058	260.8

$r/R = 0.3$

n	$(A_r)_n/V$	$(B_r)_n/V$	$(V_r)_n/V$	$(\phi_r^*)_n$
0	-.0323	0.0000	0.0000	0.0
1	-.0273	-.0021	.0274	265.6
2	.0253	-.0030	.0254	96.8
3	.0160	-.0033	.0164	101.7
4	.0238	-.0000	.0238	90.1
5	.0186	-.0001	.0186	90.5
6	.0131	.0017	.0132	82.6
7	.0092	.0006	.0092	86.4
8	.0056	-.0014	.0058	104.2
9	.0013	-.0013	.0019	133.8
10	-.0019	-.0019	.0027	225.0
11	-.0055	-.0035	.0065	237.8
12	-.0066	-.0036	.0075	241.2
13	-.0089	-.0051	.0103	240.6
14	-.0074	-.0042	.0085	240.6
15	-.0085	-.0026	.0089	252.8
16	-.0055	-.0009	.0056	260.5

TABLE 10g – (Continued)

$r/R = 0.4$

n	$(A_r)_n/V$	$(B_r)_n/V$	$(V_r)_n/V$	$(\phi_r^*)_n$
0	-.0244	0.0000	0.0000	0.0
1	-.0616	.0017	.0616	271.6
2	.0207	-.0028	.0209	97.8
3	.0168	-.0033	.0171	101.3
4	.0194	-.0013	.0195	93.8
5	.0154	-.0013	.0155	94.8
6	.0112	-.0004	.0112	92.1
7	.0082	-.0009	.0082	96.1
8	.0051	-.0017	.0054	107.9
9	.0020	-.0015	.0025	128.0
10	-.0007	-.0017	.0019	201.8
11	-.0032	-.0025	.0040	232.0
12	-.0042	-.0025	.0049	238.8
13	-.0056	-.0032	.0064	239.9
14	-.0047	-.0027	.0054	240.7
15	-.0051	-.0018	.0054	250.7
16	-.0032	-.0007	.0033	257.7

$r/R = 0.5$

n	$(A_r)_n/V$	$(B_r)_n/V$	$(V_r)_n/V$	$(\phi_r^*)_n$
0	-.0188	0.0000	0.0000	0.0
1	-.0888	.0046	.0889	273.0
2	.0165	-.0026	.0168	99.1
3	.0169	-.0033	.0172	101.2
4	.0159	-.0022	.0161	97.9
5	.0129	-.0021	.0131	99.1
6	.0095	-.0018	.0097	100.8
7	.0071	-.0019	.0074	104.6
8	.0046	-.0018	.0049	111.5
9	.0022	-.0017	.0028	126.9
10	.0001	-.0015	.0015	175.0
11	-.0015	-.0017	.0023	220.2
12	-.0023	-.0017	.0029	234.1
13	-.0030	-.0018	.0035	238.5
14	-.0026	-.0015	.0030	241.1
15	-.0024	-.0011	.0027	246.1
16	-.0015	-.0005	.0015	250.9

TABLE 10g – (Continued)

r/R = 0.6

n	$(A_r)_n/V$	$(B_r)_n/V$	$(V_r)_n/V$	$(\phi_r^*)_n$
0	-.0155	0.0000	0.0000	0.0
1	-.1090	.0066	.1092	273.5
2	.0129	-.0024	.0131	100.4
3	.0165	-.0033	.0168	101.3
4	.0134	-.0027	.0136	101.5
5	.0109	-.0024	.0112	102.7
6	.0081	-.0025	.0085	107.3
7	.0060	-.0023	.0065	111.2
8	.0039	-.0018	.0043	115.1
9	.0022	-.0017	.0028	128.6
10	.0006	-.0014	.0015	157.9
11	-.0004	-.0012	.0013	197.0
12	-.0011	-.0011	.0015	224.1
13	-.0012	-.0008	.0015	234.6
14	-.0011	-.0006	.0013	242.9
15	-.0006	-.0005	.0008	227.1
16	-.0002	-.0003	.0003	206.9

r/R = 0.7

n	$(A_r)_n/V$	$(B_r)_n/V$	$(V_r)_n/V$	$(\phi_r^*)_n$
0	-.0145	0.0000	0.0000	0.0
1	-.1221	.0077	.1224	273.6
2	.0097	-.0020	.0099	102.0
3	.0154	-.0032	.0158	101.7
4	.0117	-.0028	.0121	103.6
5	.0095	-.0024	.0098	104.4
6	.0068	-.0025	.0073	110.1
7	.0049	-.0024	.0054	115.6
8	.0032	-.0018	.0036	119.1
9	.0018	-.0017	.0025	133.7
10	.0006	-.0012	.0013	154.9
11	.0001	-.0009	.0009	172.6
12	-.0004	-.0008	.0008	205.7
13	-.0002	-.0003	.0004	214.6
14	-.0002	-.0000	.0002	260.2
15	.0005	-.0001	.0005	106.2
16	.0007	-.0001	.0007	100.3

TABLE 10g – (Continued)

r/R = 0.8

n	$(A_r)_n/V$	$(B_r)_n/V$	$(V_r)_n/V$	$(\phi_r^*)_n$
0	-.0195	0.0000	0.0000	0.0
1	-.1238	.0084	.1241	273.9
2	.0082	-.0017	.0084	101.7
3	.0136	-.0034	.0140	104.2
4	.0118	-.0025	.0121	102.4
5	.0089	-.0019	.0091	101.8
6	.0058	-.0012	.0059	101.2
7	.0033	-.0016	.0037	115.1
8	.0023	-.0017	.0028	126.7
9	.0007	-.0017	.0019	156.9
10	-.0000	-.0011	.0011	182.2
11	-.0003	-.0011	.0011	193.5
12	-.0003	-.0009	.0010	200.3
13	-.0003	-.0005	.0006	213.0
14	-.0000	.0000	.0000	326.9
15	.0006	.0001	.0006	81.4
16	.0010	.0001	.0010	81.7

r/R = 0.9

n	$(A_r)_n/V$	$(B_r)_n/V$	$(V_r)_n/V$	$(\phi_r^*)_n$
0	-.0201	0.0000	0.0000	0.0
1	-.1265	.0073	.1267	273.3
2	.0049	-.0012	.0050	104.2
3	.0116	-.0030	.0120	104.3
4	.0115	-.0020	.0117	99.8
5	.0084	-.0012	.0085	98.3
6	.0050	-.0002	.0050	92.5
7	.0024	-.0009	.0026	109.4
8	.0015	-.0014	.0020	132.4
9	-.0000	-.0014	.0014	181.2
10	-.0007	-.0009	.0011	219.7
11	-.0008	-.0010	.0013	219.1
12	-.0007	-.0009	.0011	218.2
13	-.0007	-.0005	.0009	232.6
14	-.0002	.0000	.0002	276.1
15	.0003	.0002	.0004	60.8
16	.0009	.0003	.0009	74.1

TABLE 10g – (Continued)

r/R = 1.0

n	$(A_r)_n/V$	$(B_r)_n/V$	$(V_r)_n/V$	$(\phi_r^*)_n$
0	-.0153	0.0000	0.0000	0.0
1	-.1312	.0041	.1312	271.8
2	-.0007	-.0006	.0009	229.3
3	.0096	-.0017	.0097	99.9
4	.0105	-.0010	.0106	95.5
5	.0079	-.0006	.0079	94.1
6	.0044	.0002	.0044	87.9
7	.0023	-.0003	.0023	97.8
8	.0008	-.0007	.0011	130.5
9	-.0004	-.0008	.0009	209.1
10	-.0014	-.0004	.0015	253.0
11	-.0015	-.0006	.0016	248.8
12	-.0014	-.0005	.0015	249.9
13	-.0013	-.0003	.0013	255.8
14	-.0009	.0000	.0009	272.0
15	-.0001	.0002	.0002	320.8
16	.0004	.0002	.0005	66.5

APPENDIX B

DETAILED EXPERIMENTAL RESULTS

Figures 34 and 35 and Tables 11-20 present the measured experimental loads, including variation with blade angular position and harmonic analyses, for steady ahead operation near the self-propulsion point, quasi-steady crash forward, and quasi-steady crash astern. The data presented in Figures 34 and 35 are similar to those presented earlier, except that here all measured components of blade loading are given whereas Figures 22 and 24 were restricted to the one component F_x. The loads presented in Tables 11-20 are tabulated values of the data presented graphically in Figures 14-17, Figures 19-22, and Figures 34 and 35.

Figure 34 - Harmonics of Loads for Quasi-Steady Crash Ahead

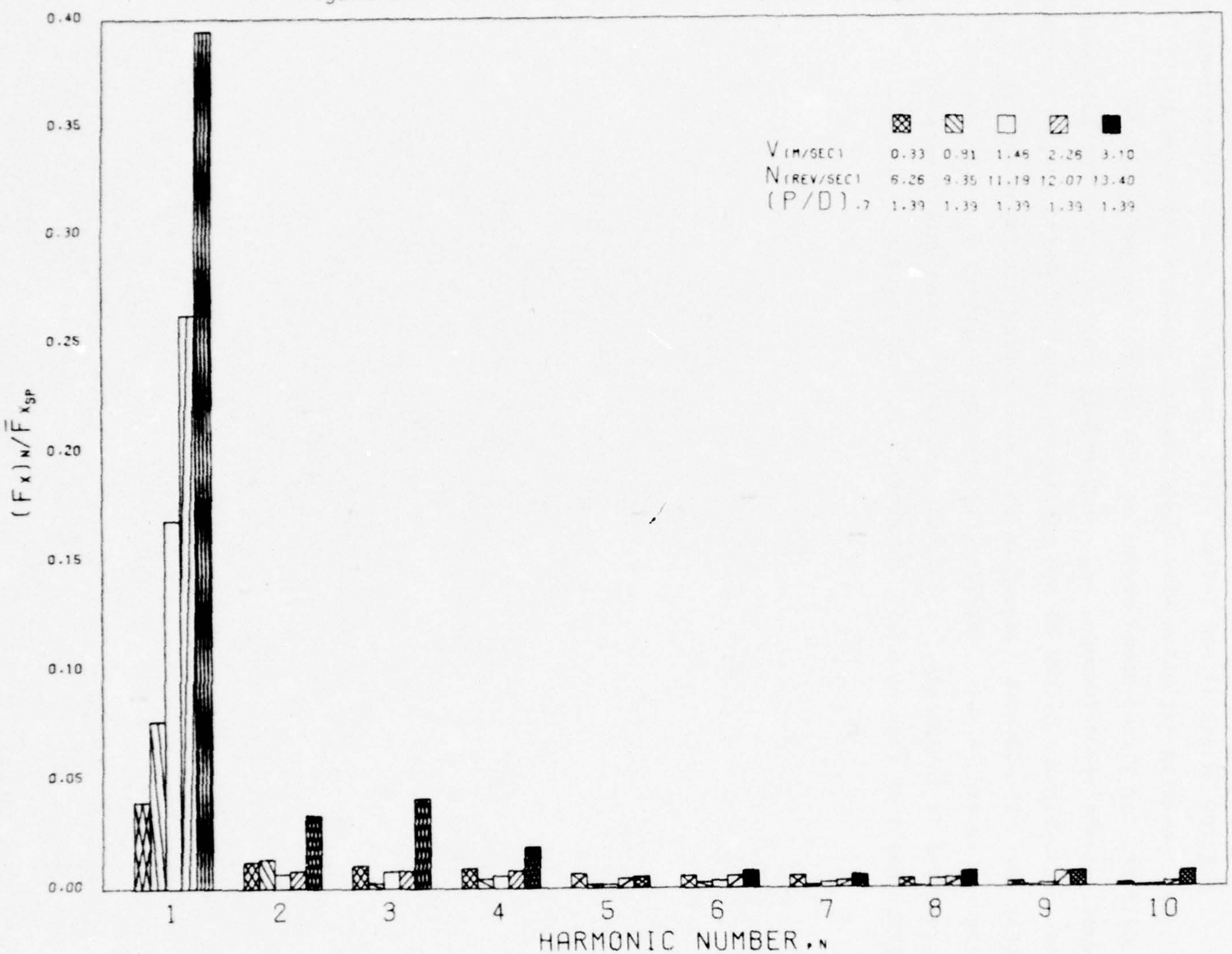

Figure 34 (Continued)

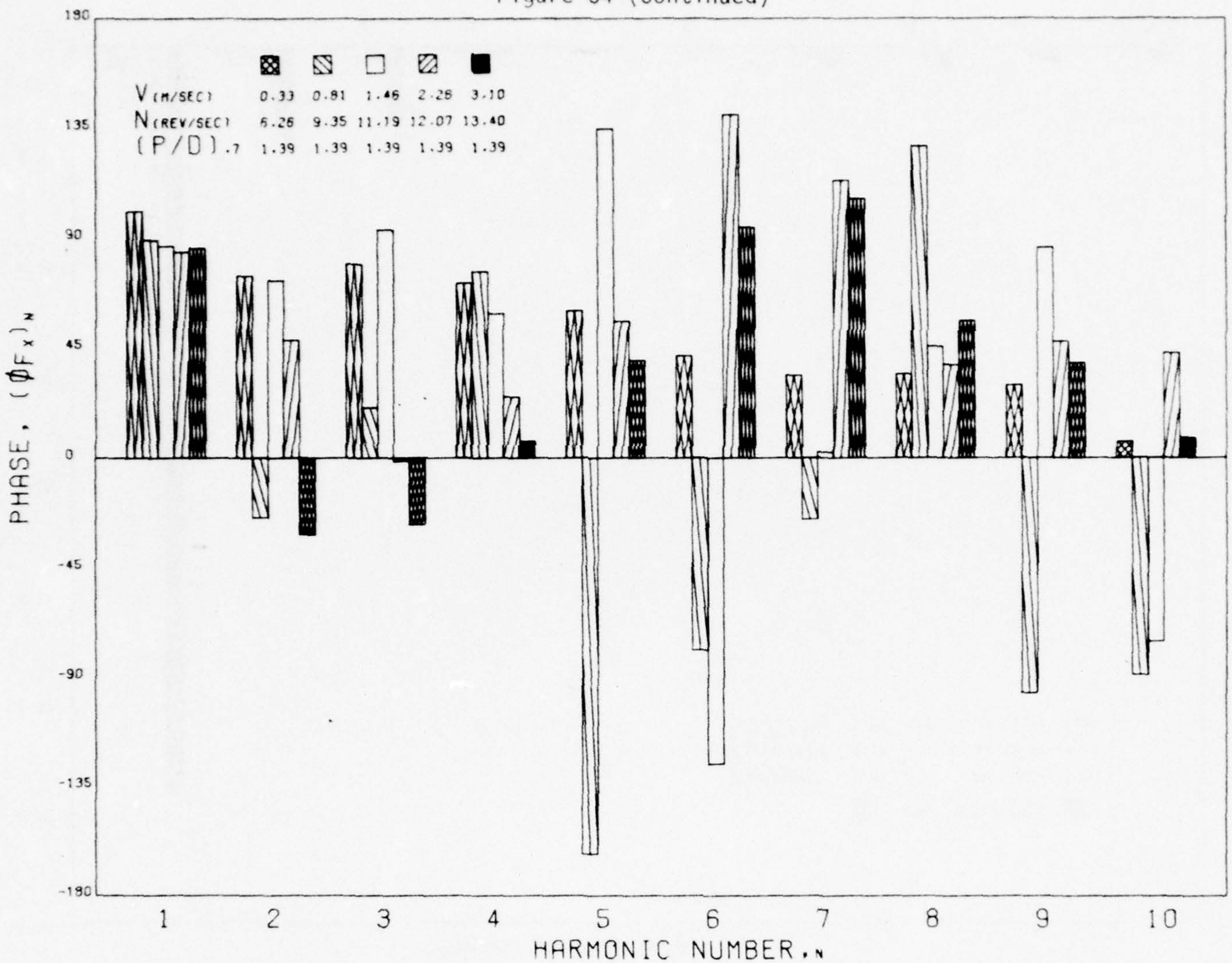

Figure 34 (Continued)

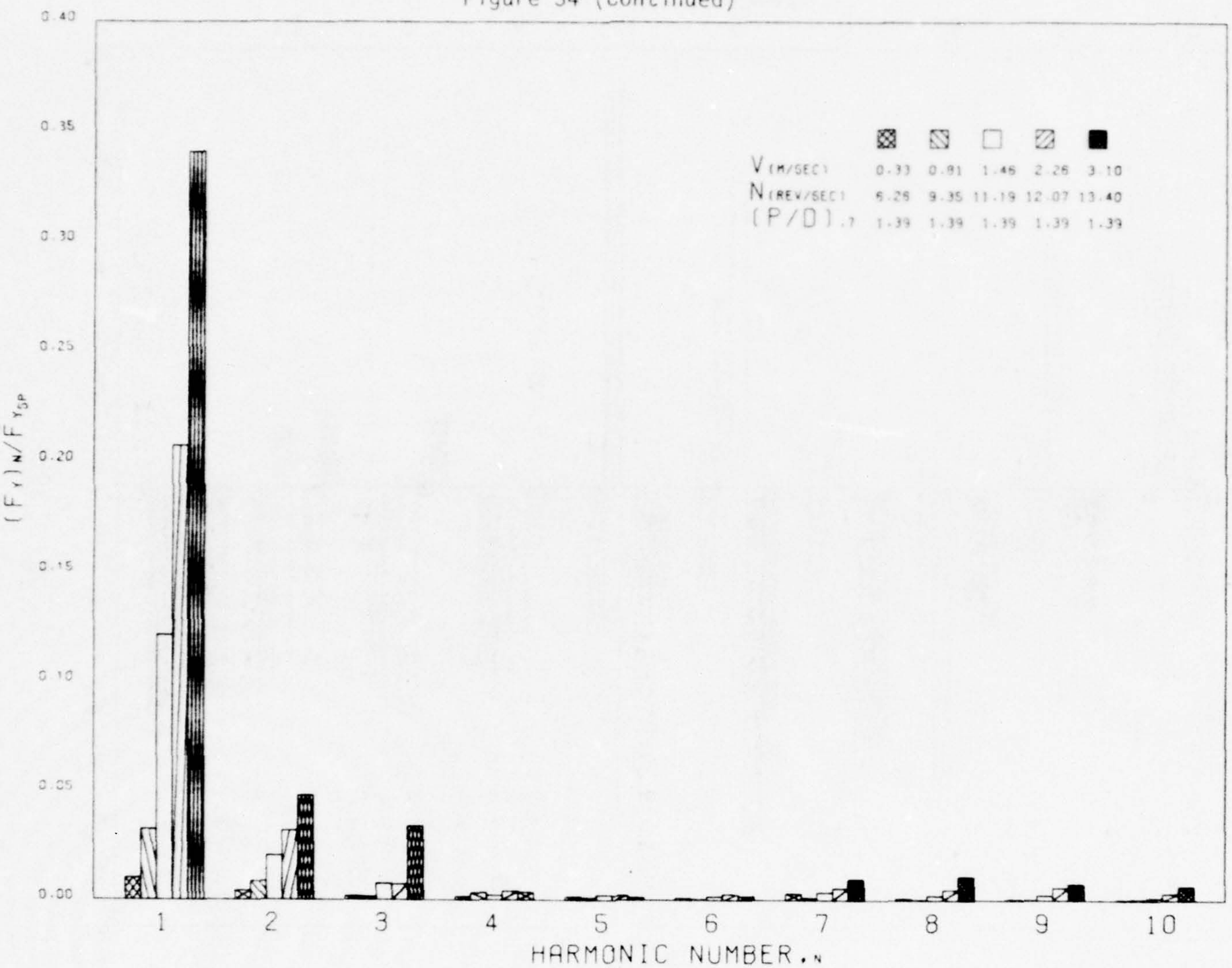

Figure 34 (Continued)

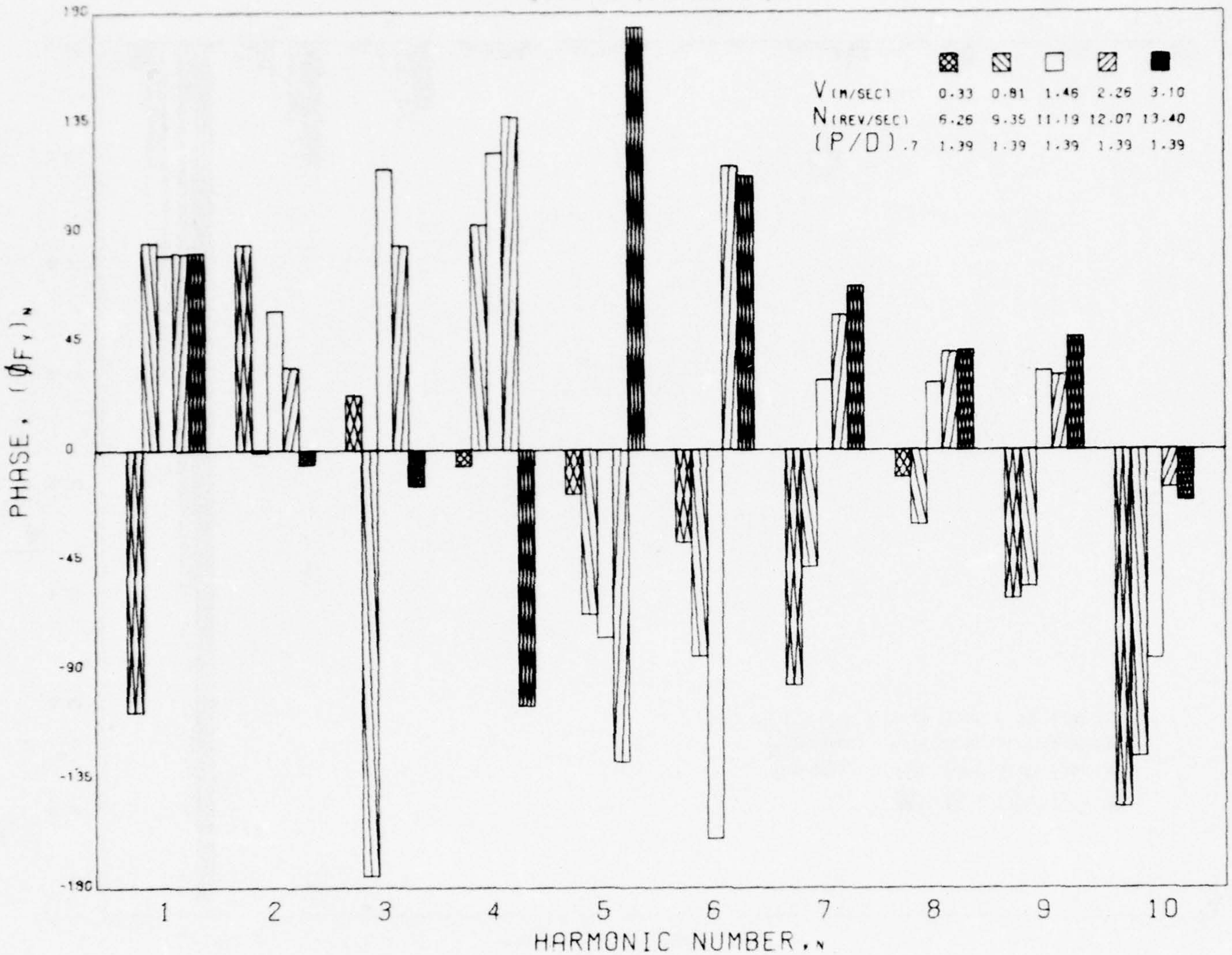

Figure 34 (Continued)

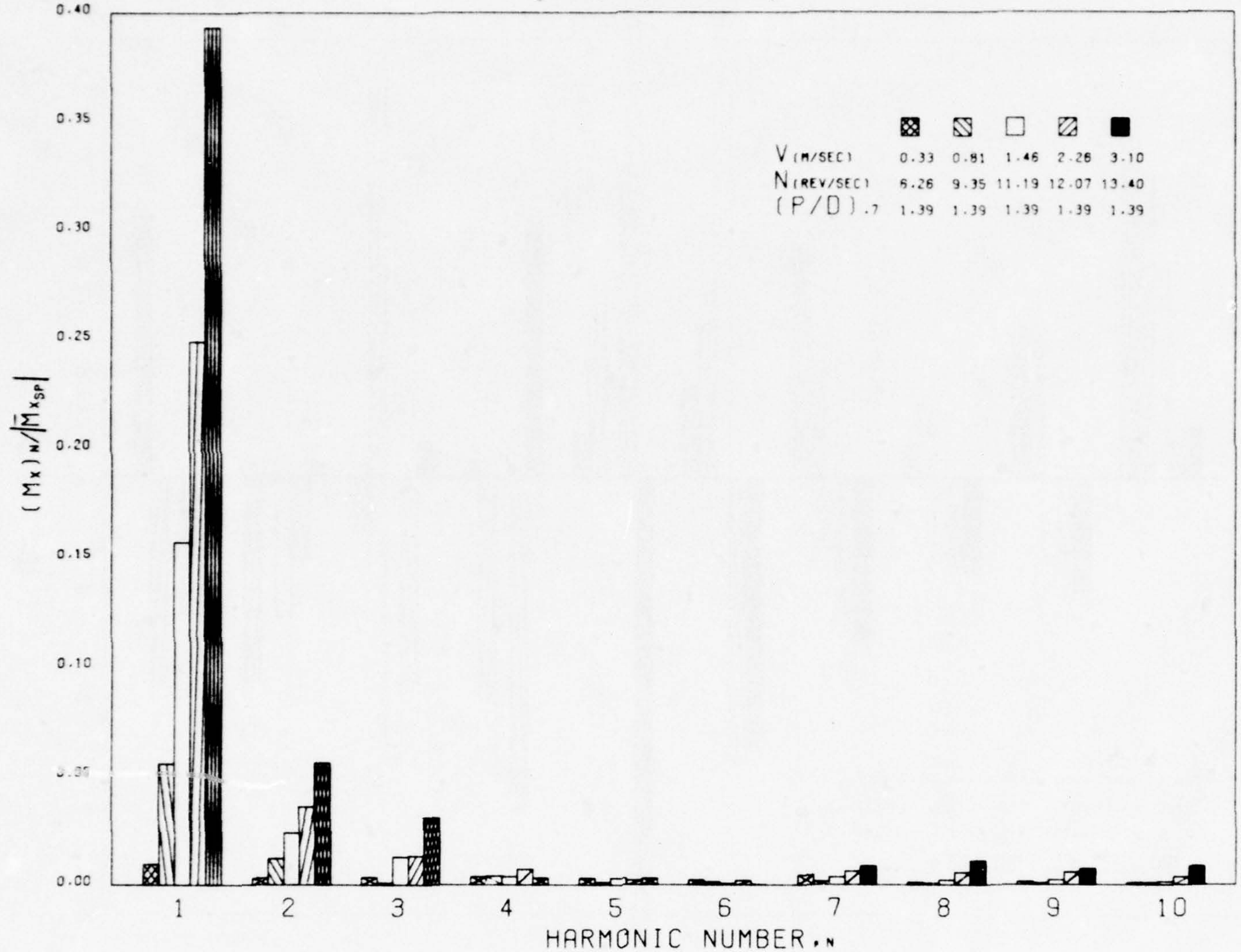

Figure 34 (Continued)

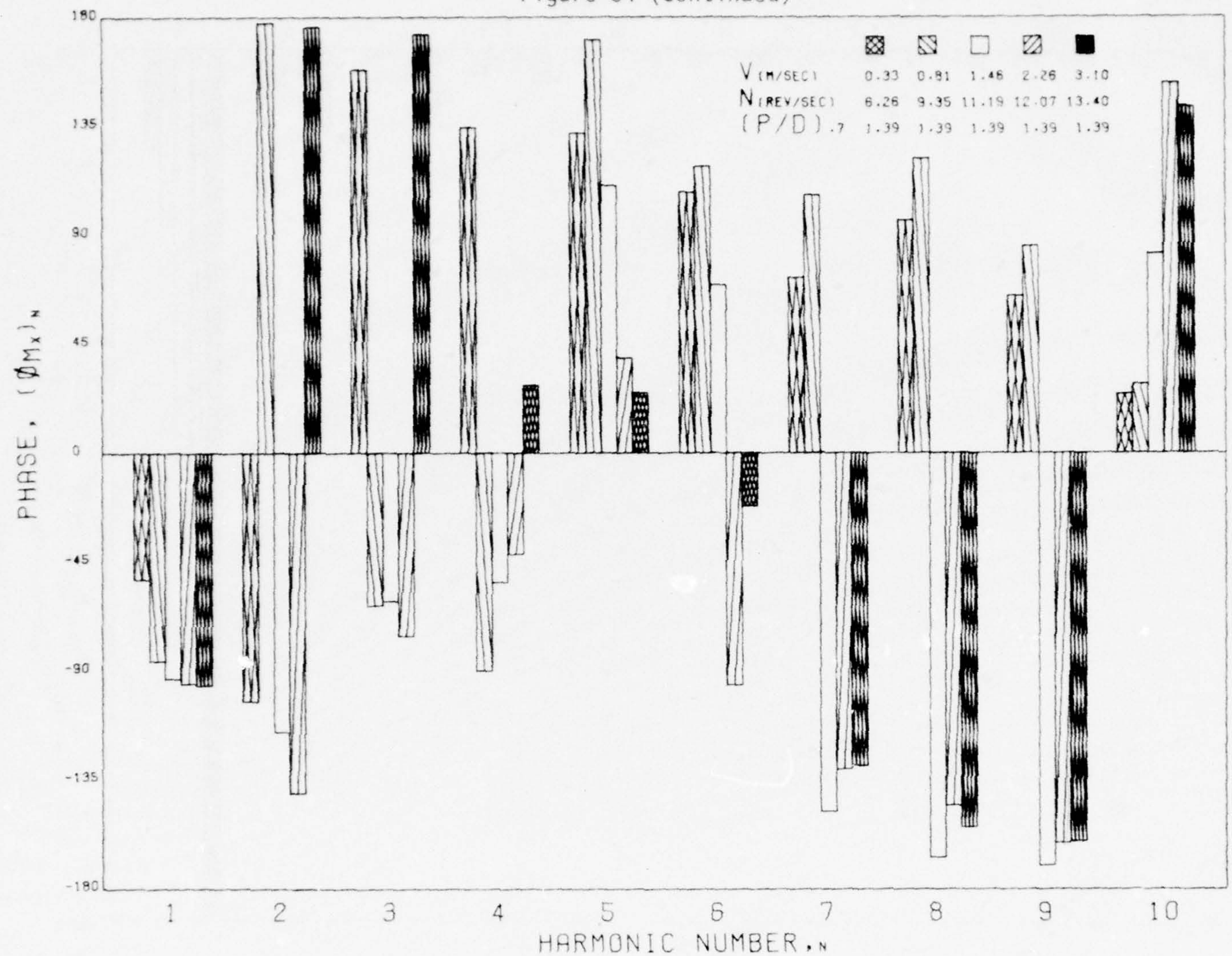

Figure 34 (Continued)

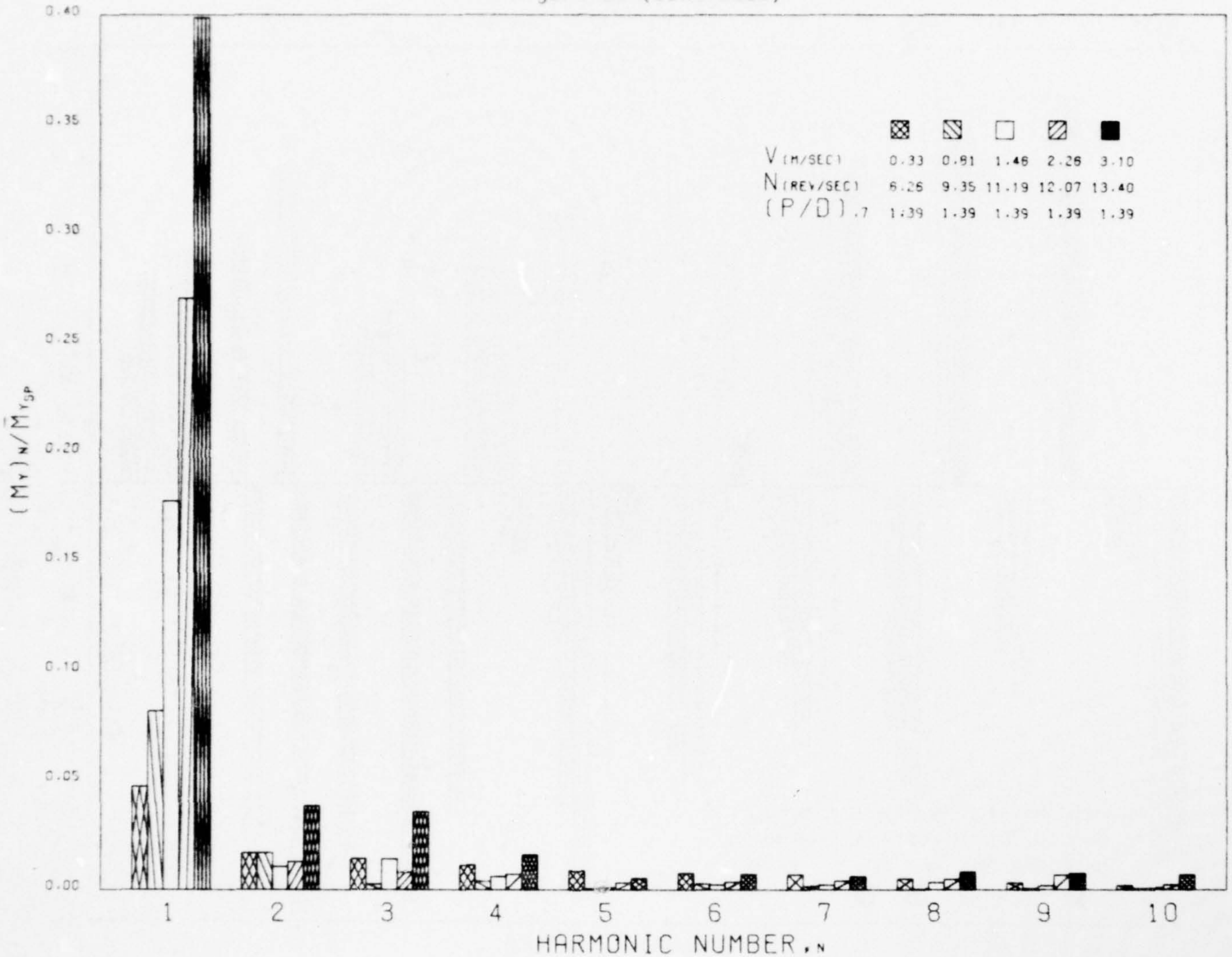

Figure 34 (Continued)

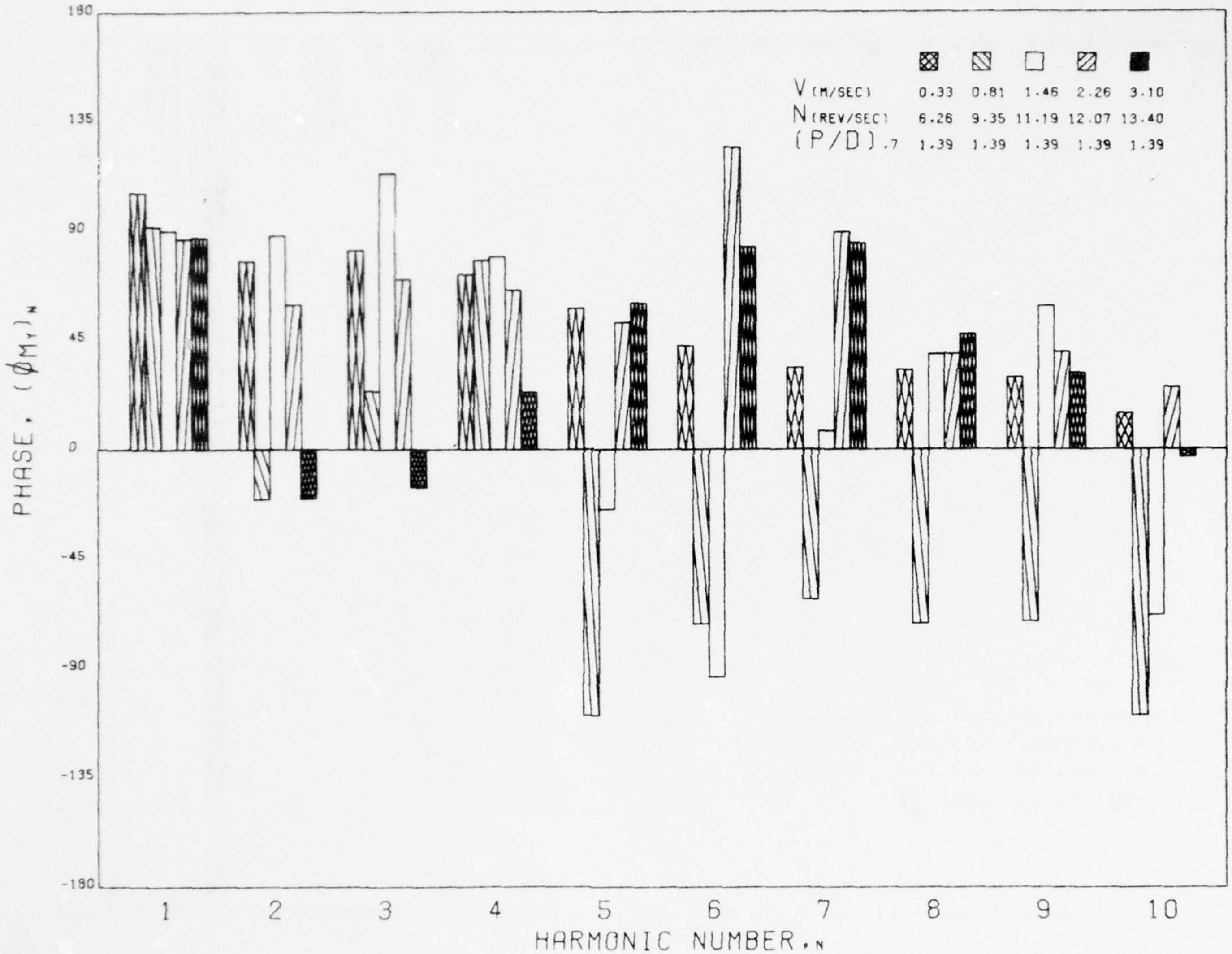

Figure 34 (Continued)

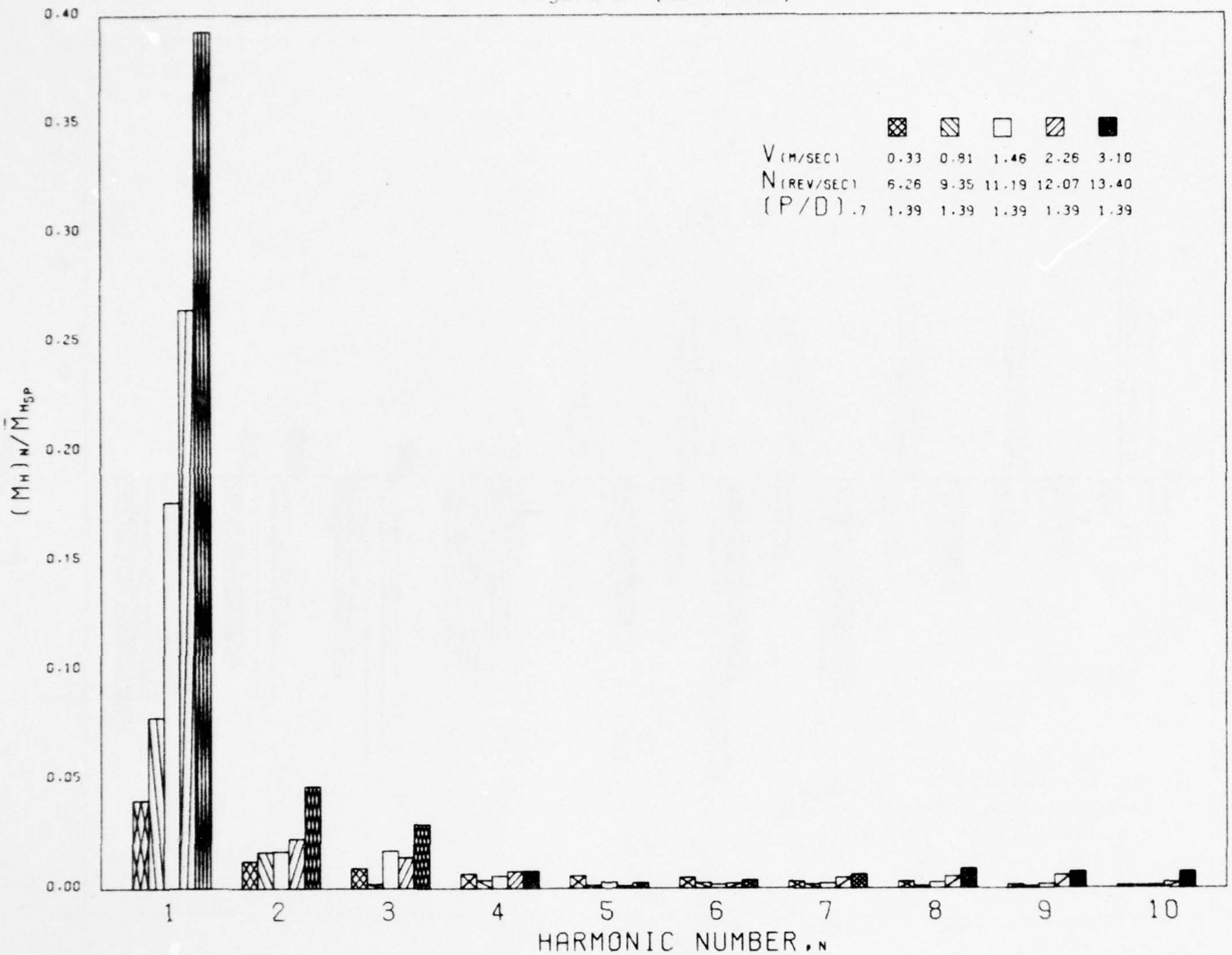

Figure 34 (Continued)

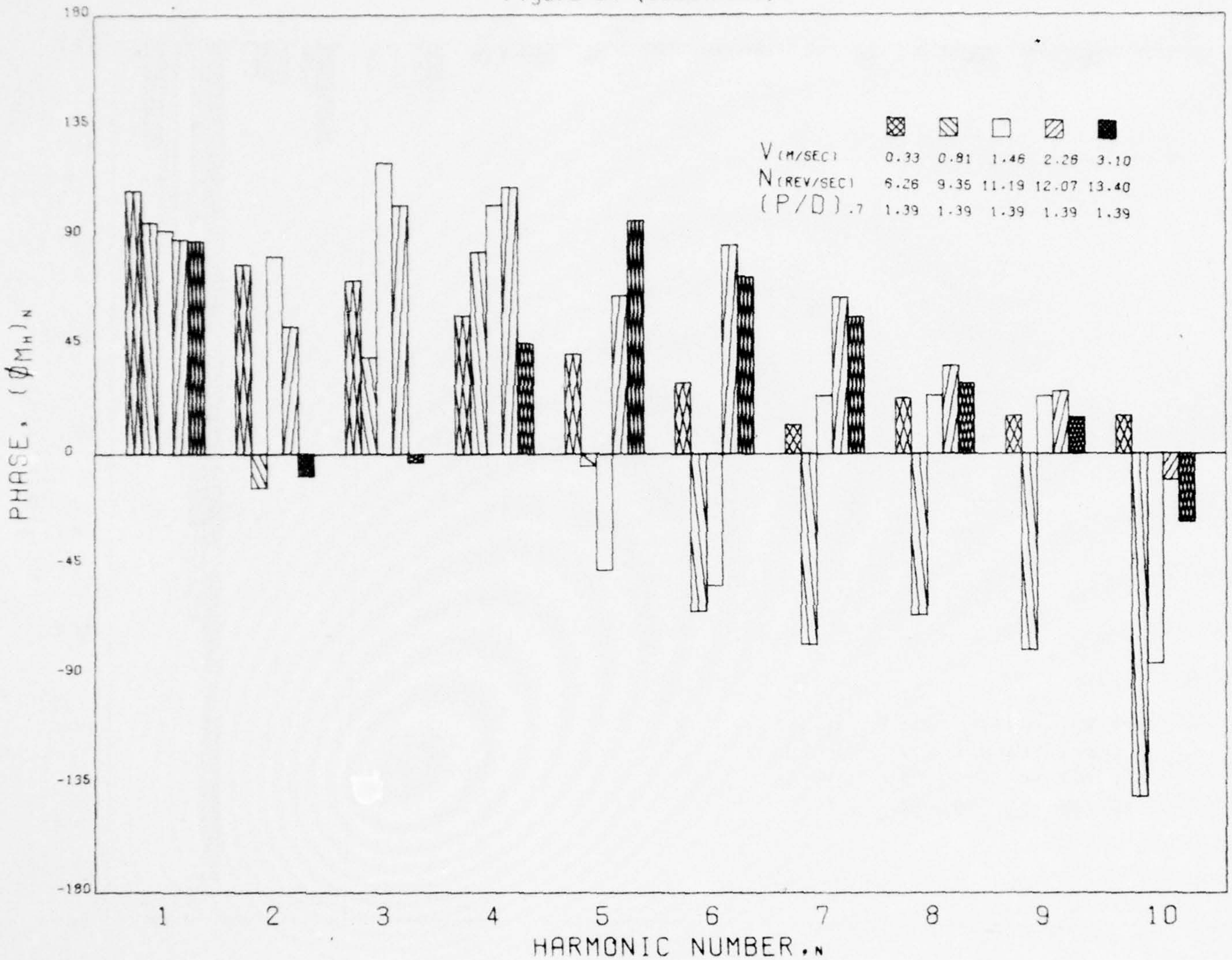

Figure 34 (Continued)

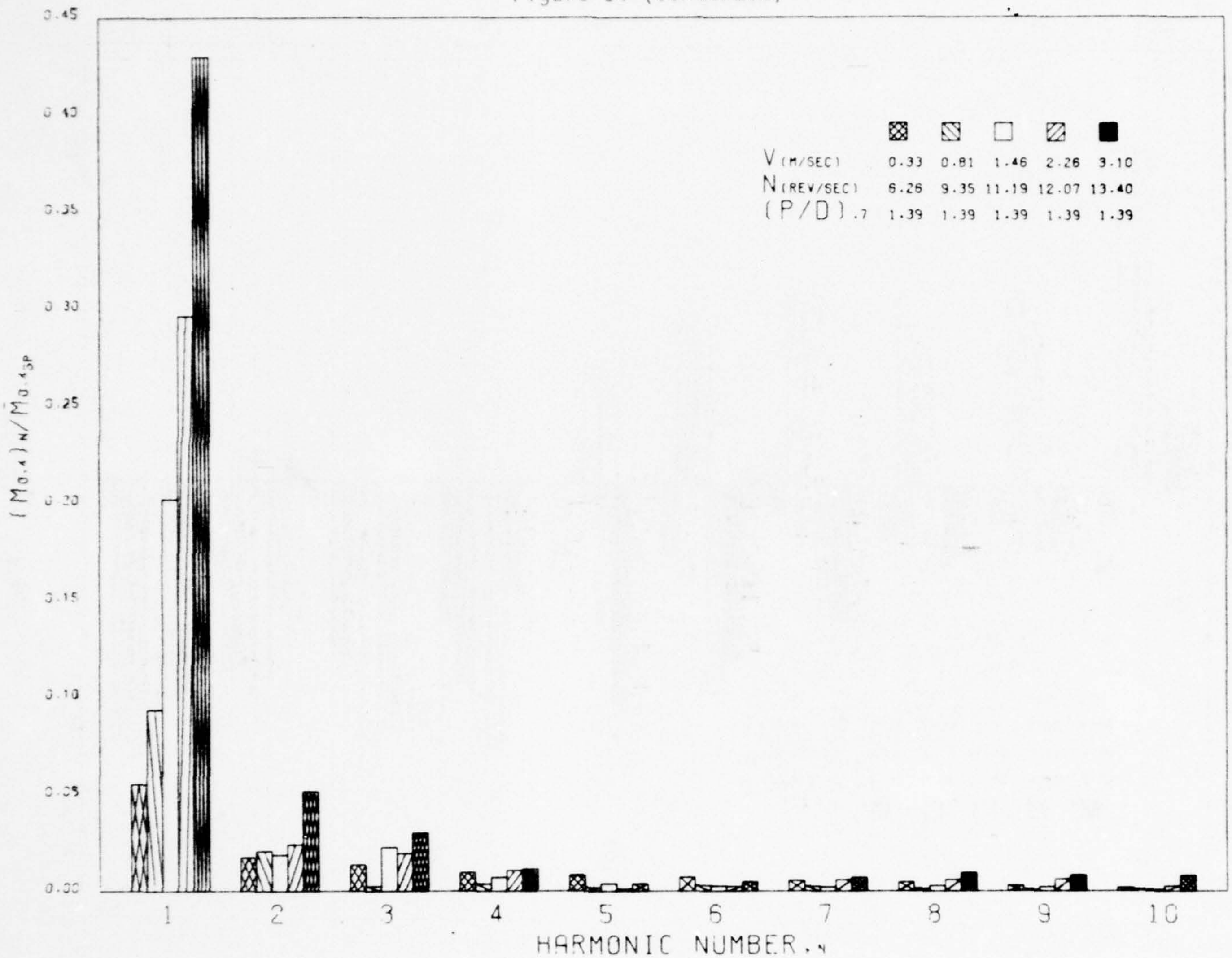

Figure 34 (Continued)

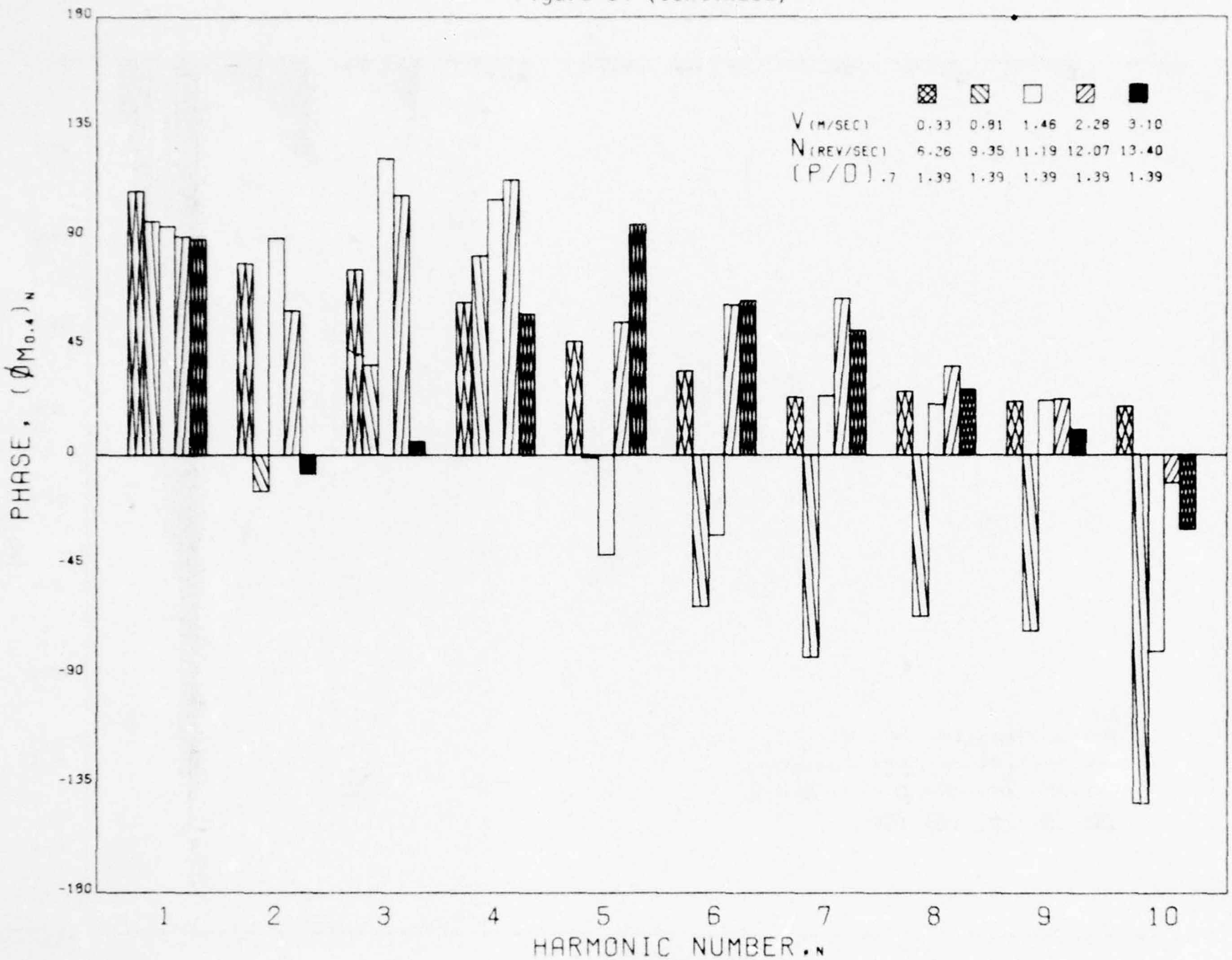

Figure 34 (Continued)

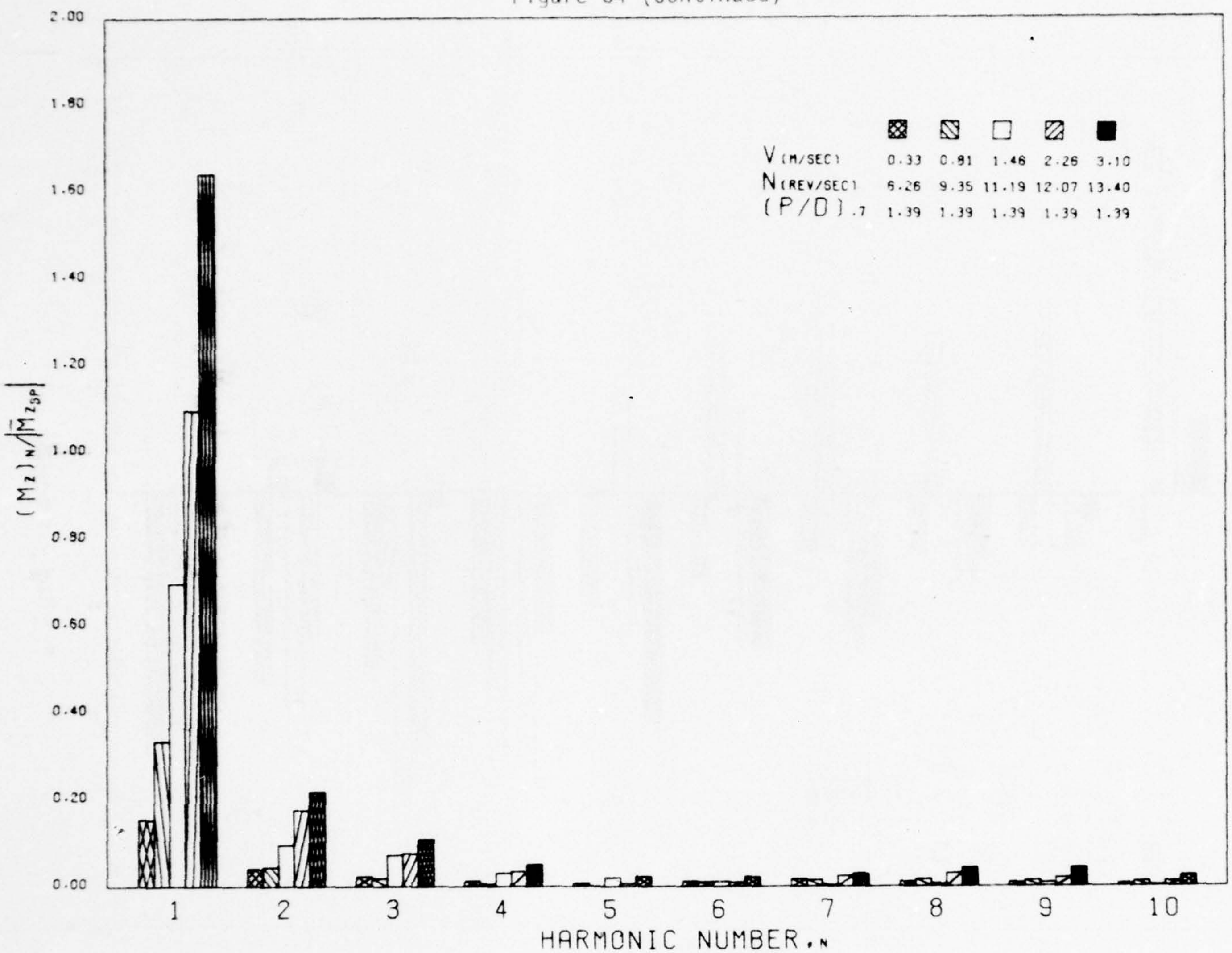

Figure 34 (Continued)

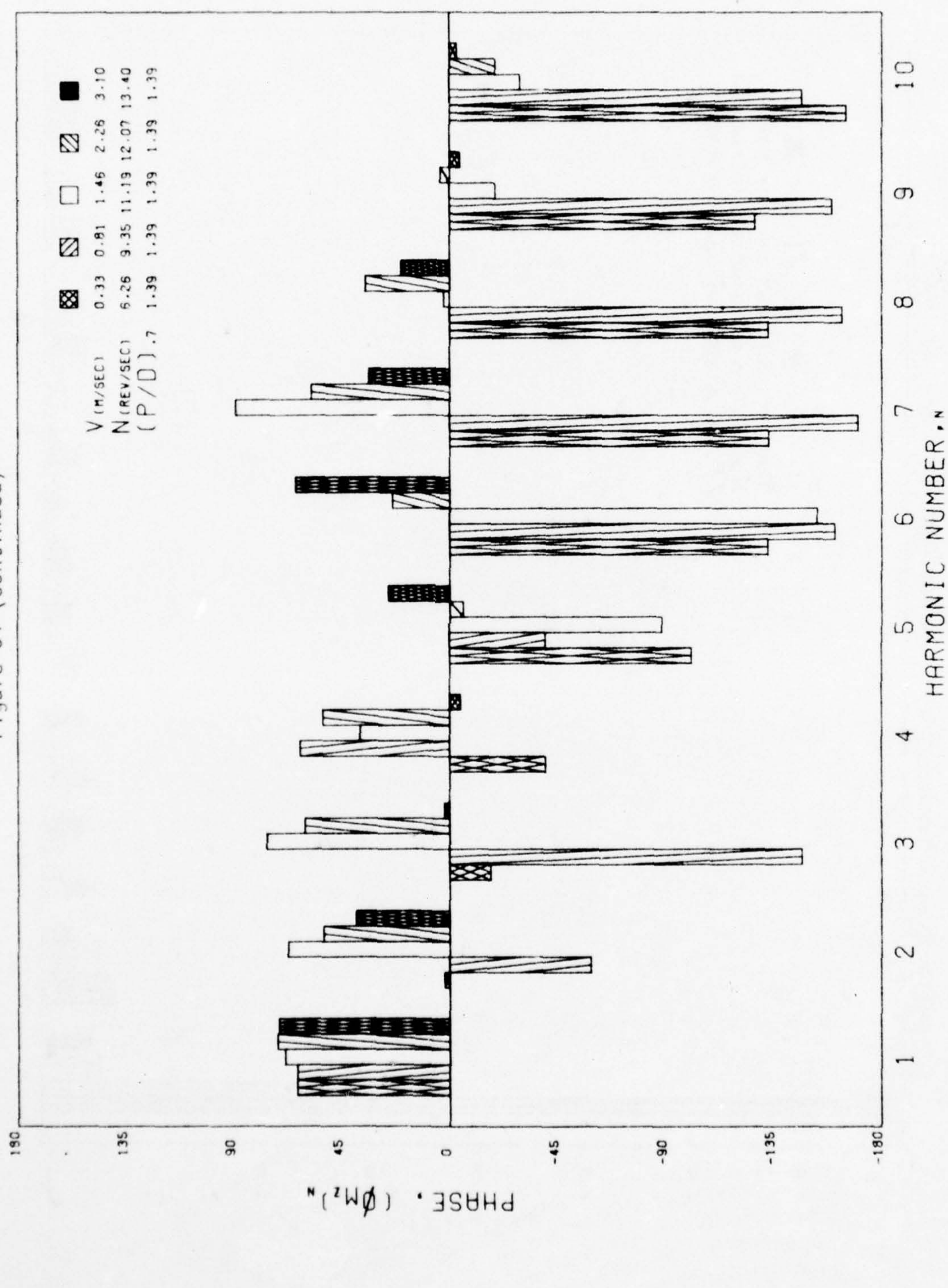

Figure 35 - Harmonics of Loads for Quasi-Steady Crash Astern

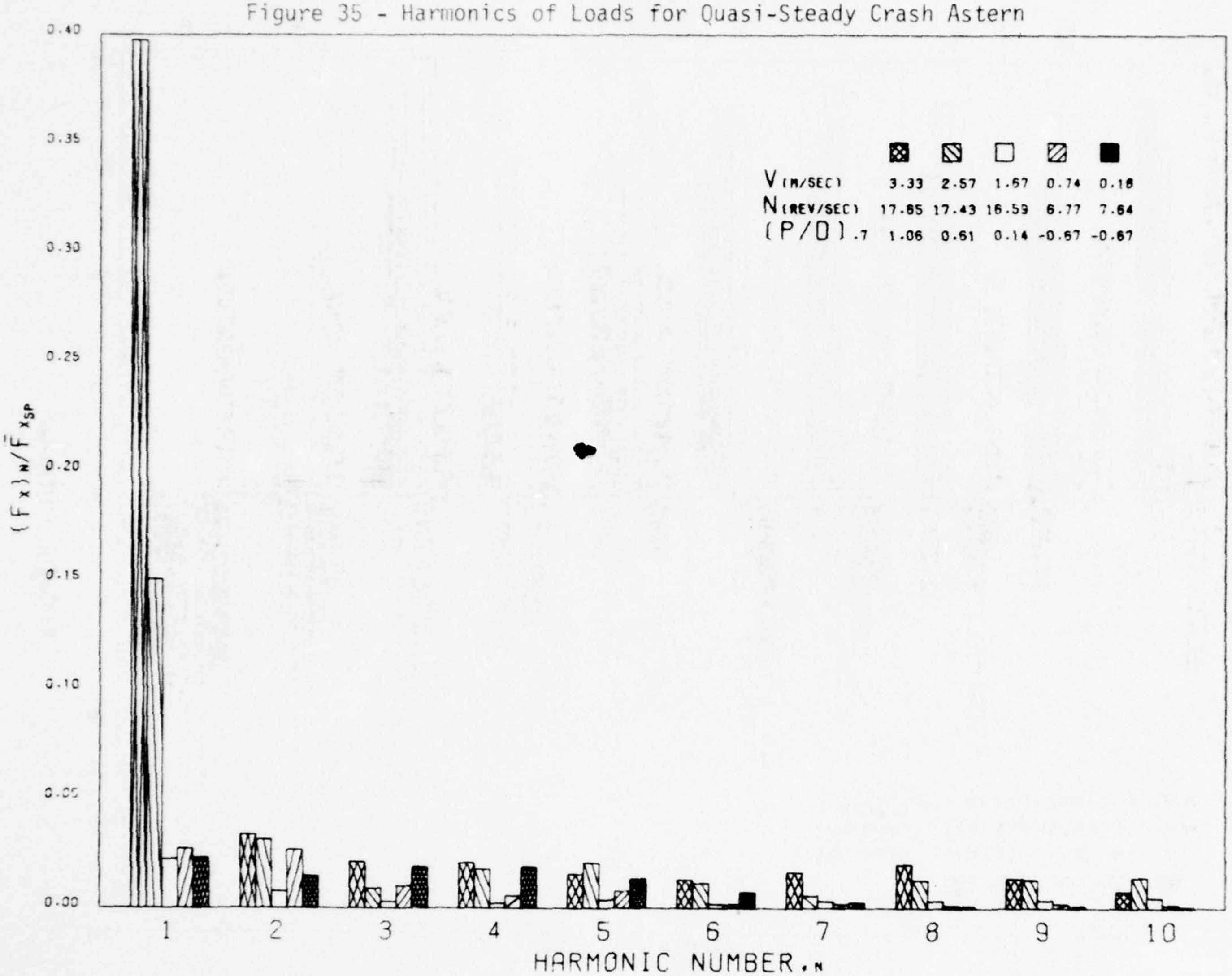

Figure 35 (Continued)

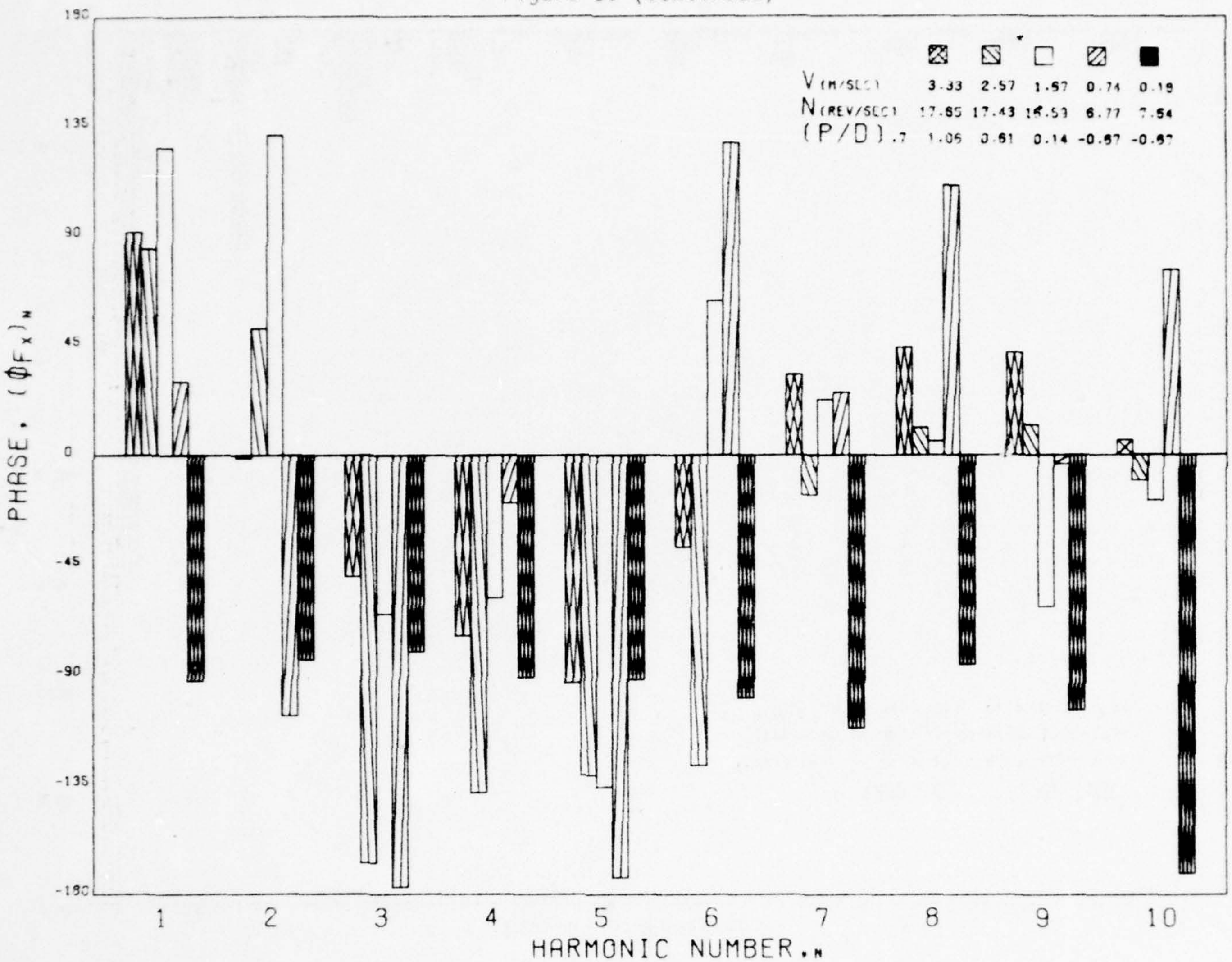

Figure 35 (Continued)

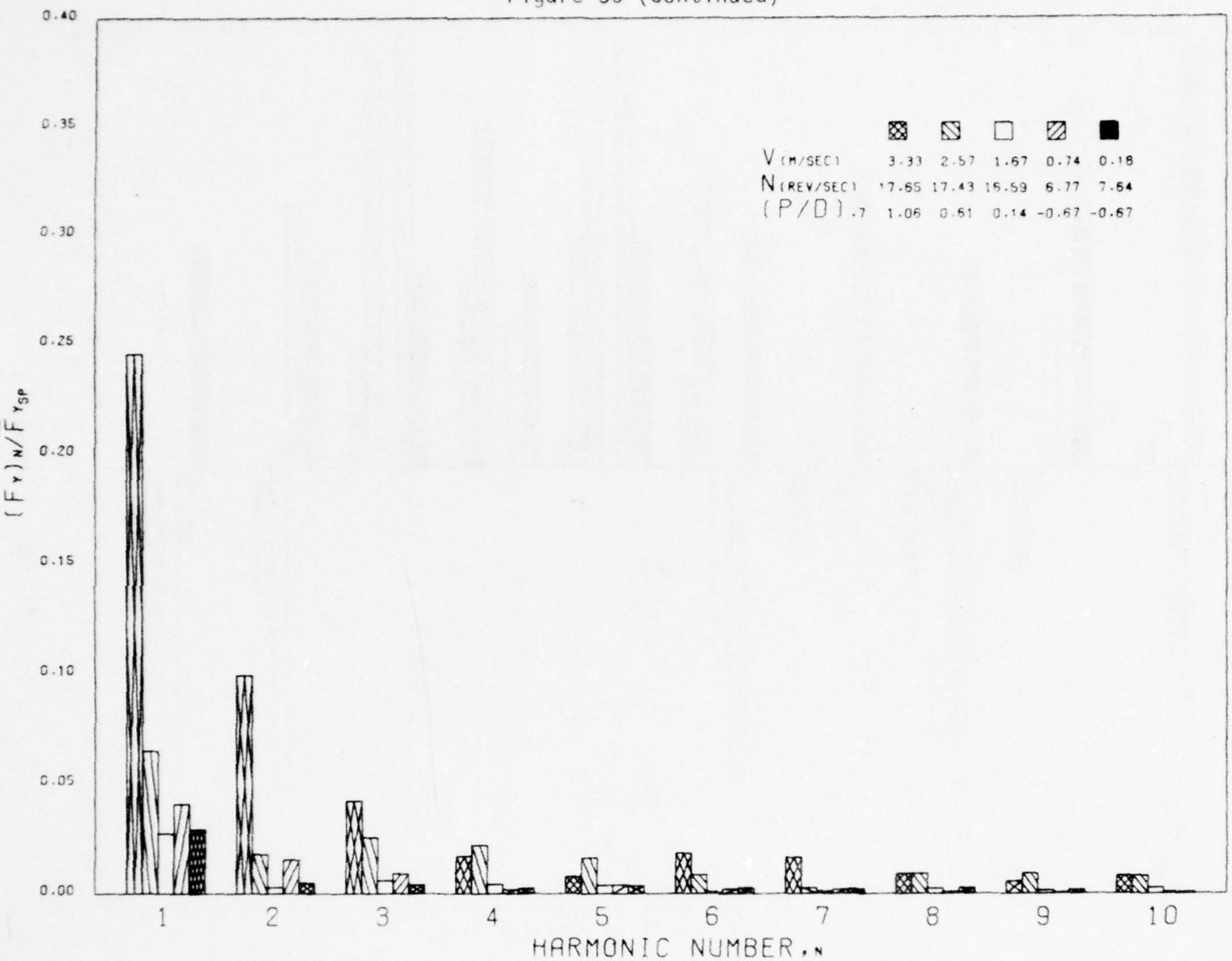

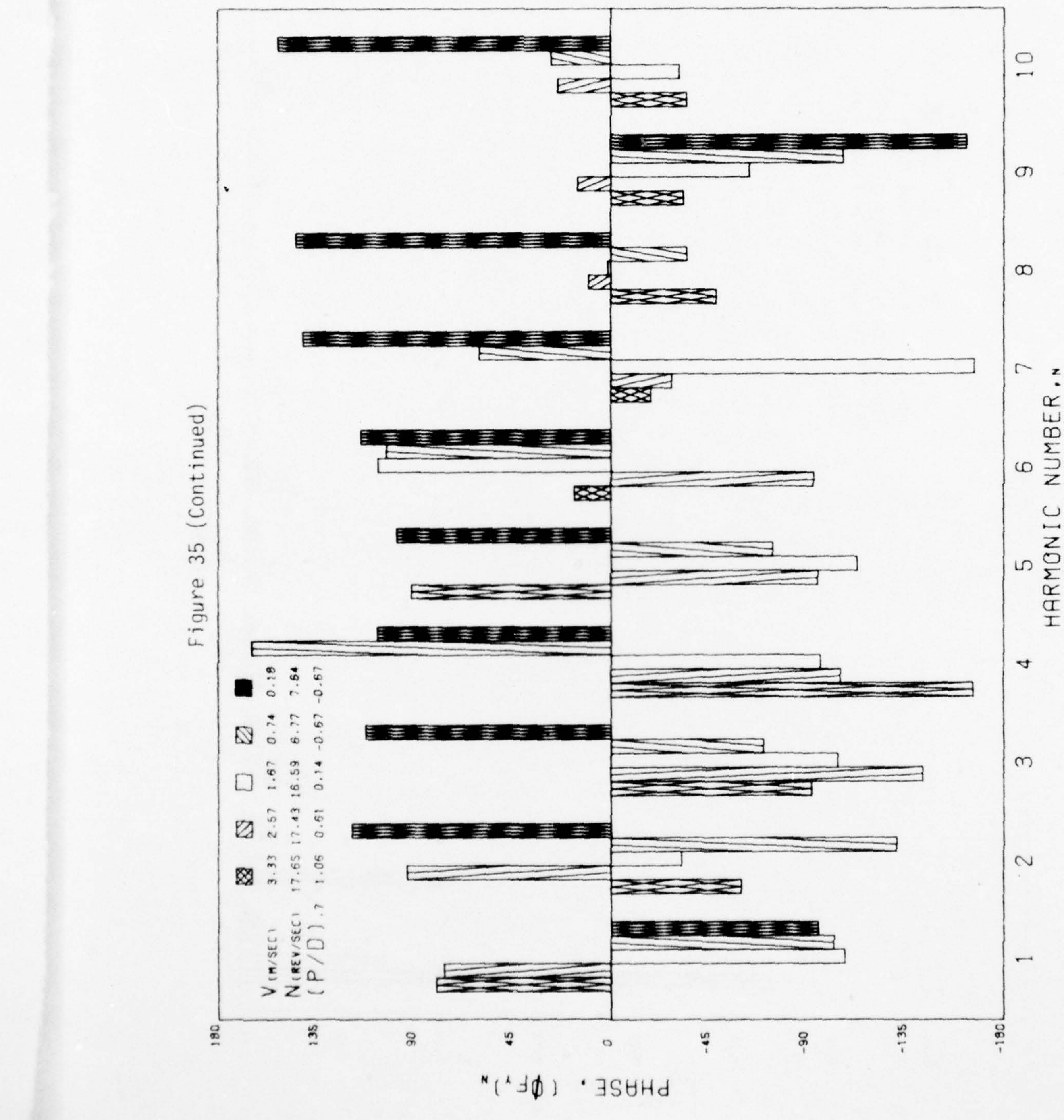

Figure 35 (Continued)

Figure 35 (Continued)

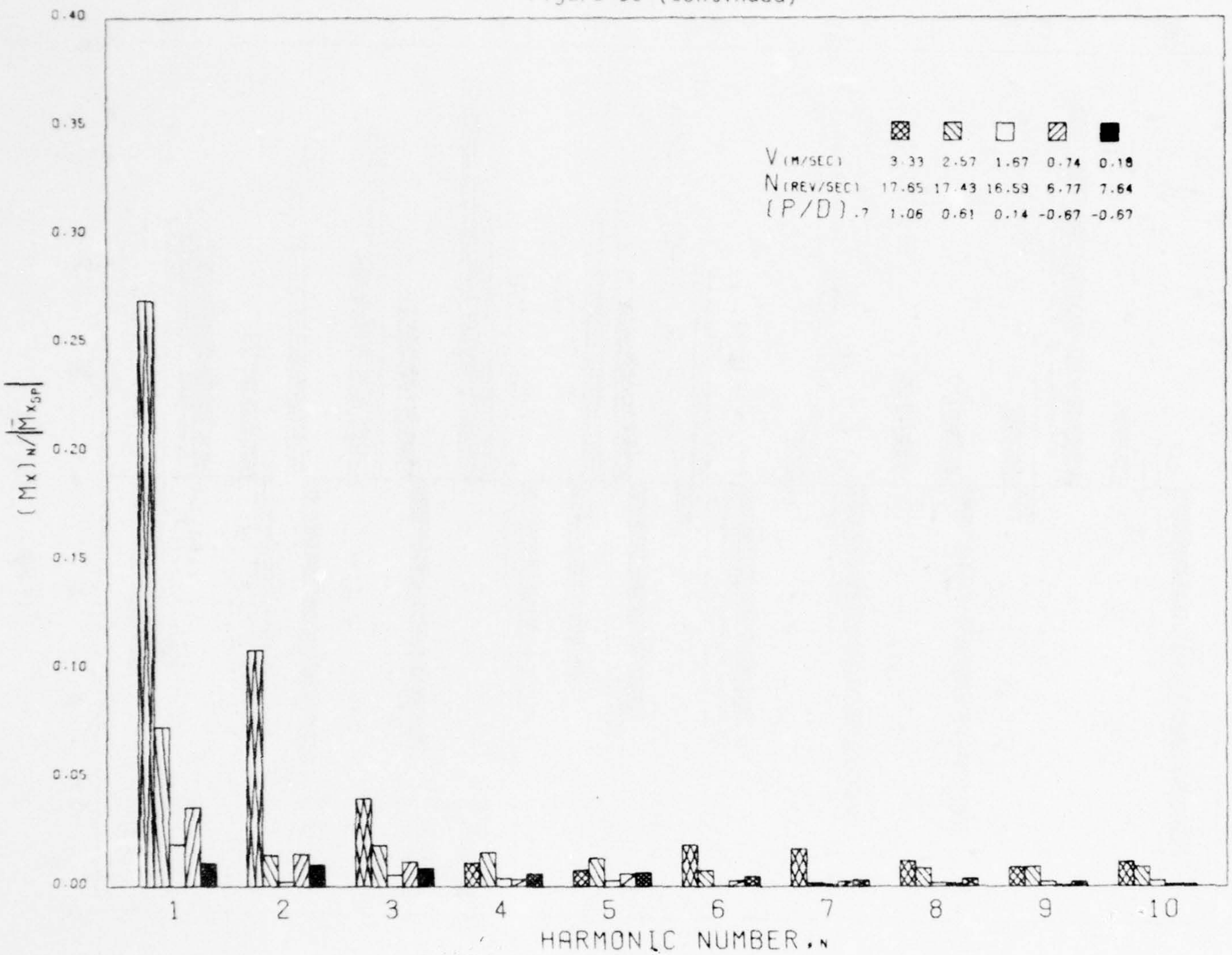

Figure 35 (Continued)

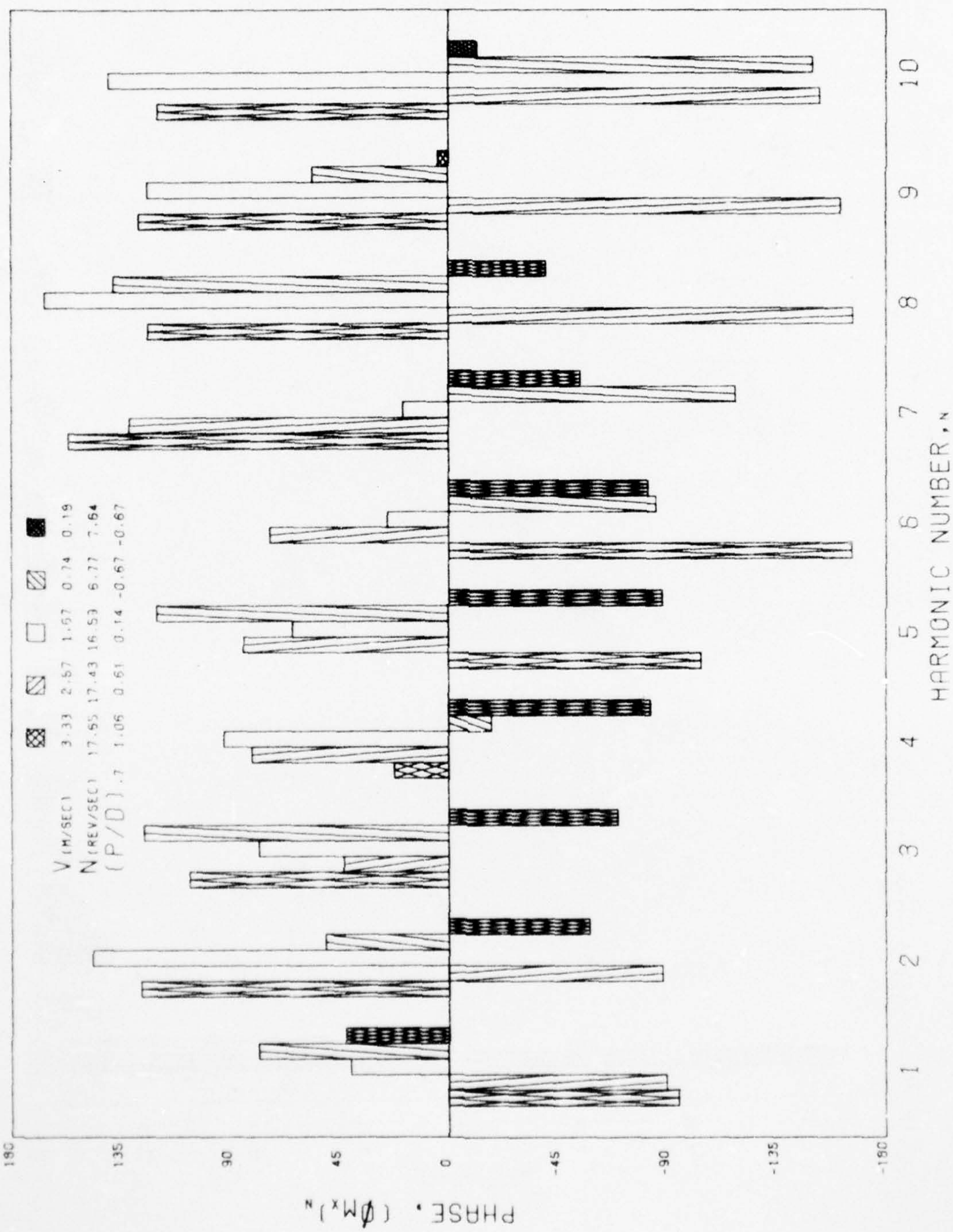

Figure 35 (Continued)

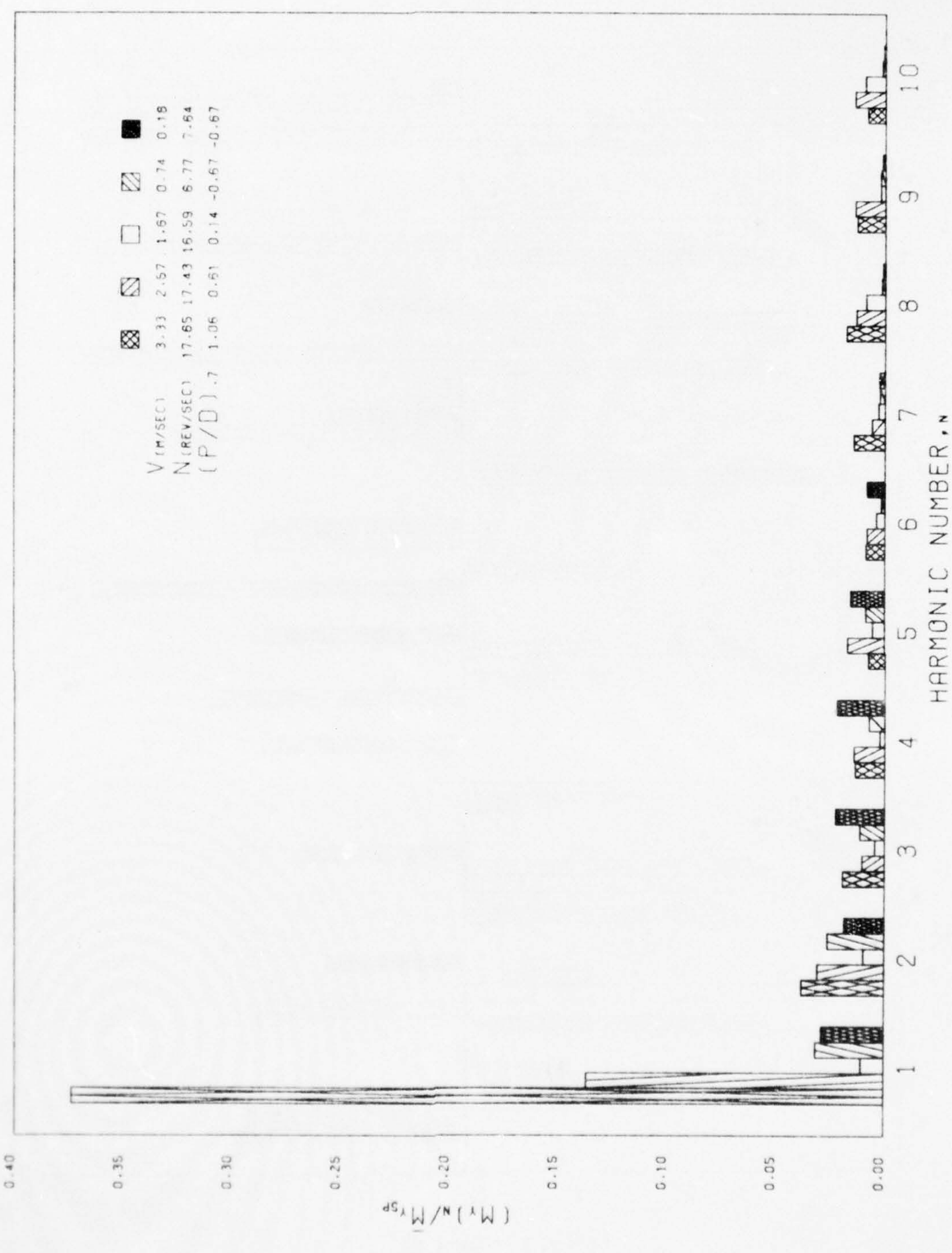

AD-A034 804 DAVID W TAYLOR NAVAL SHIP RESEARCH AND DEVELOPMENT CE--ETC F/G 13/10
EXPERIMENTAL UNSTEADY AND MEAN LOADS ON A CP PROPELLER BLADE ON--ETC(U)
OCT 76 R J BOSWELL, J J NELKA , S B DENNY

UNCLASSIFIED DTNSRDC-76-0125 NL

4 OF 4
AD
A034804

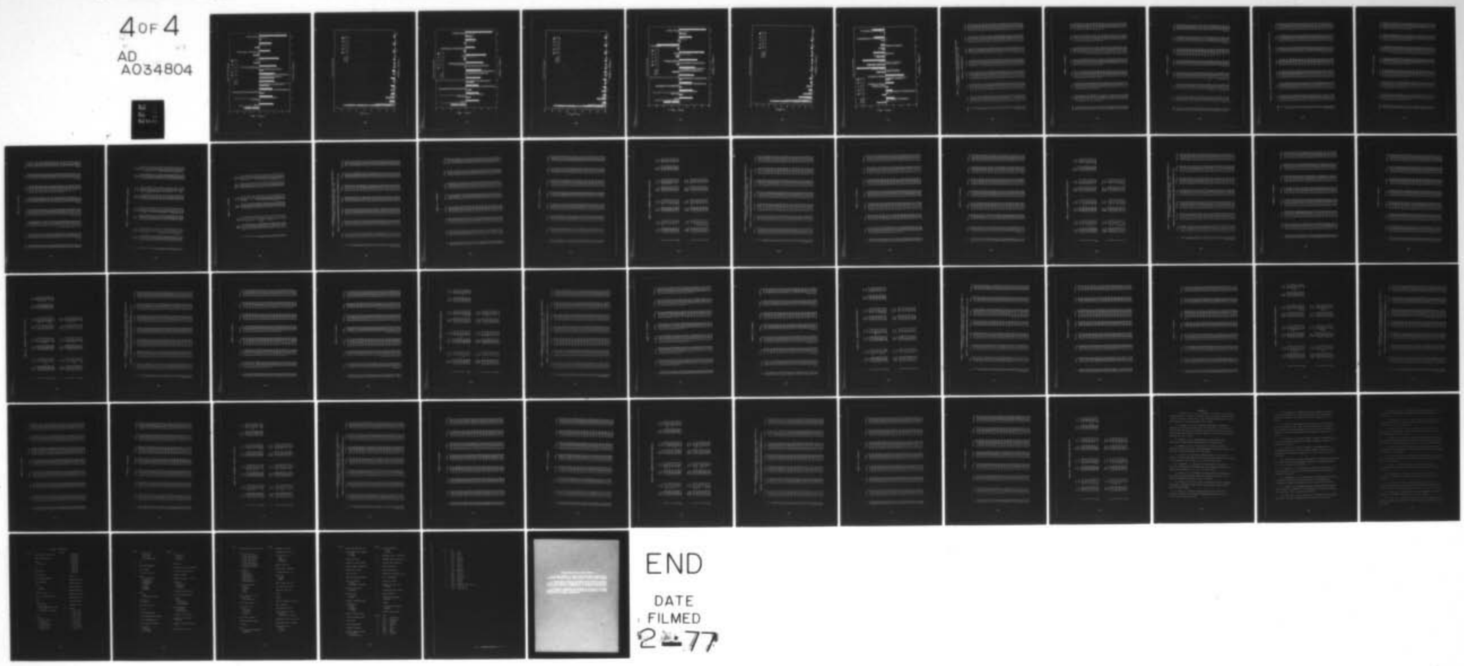

END
DATE
FILMED
2-77

Figure 35 (Continued)

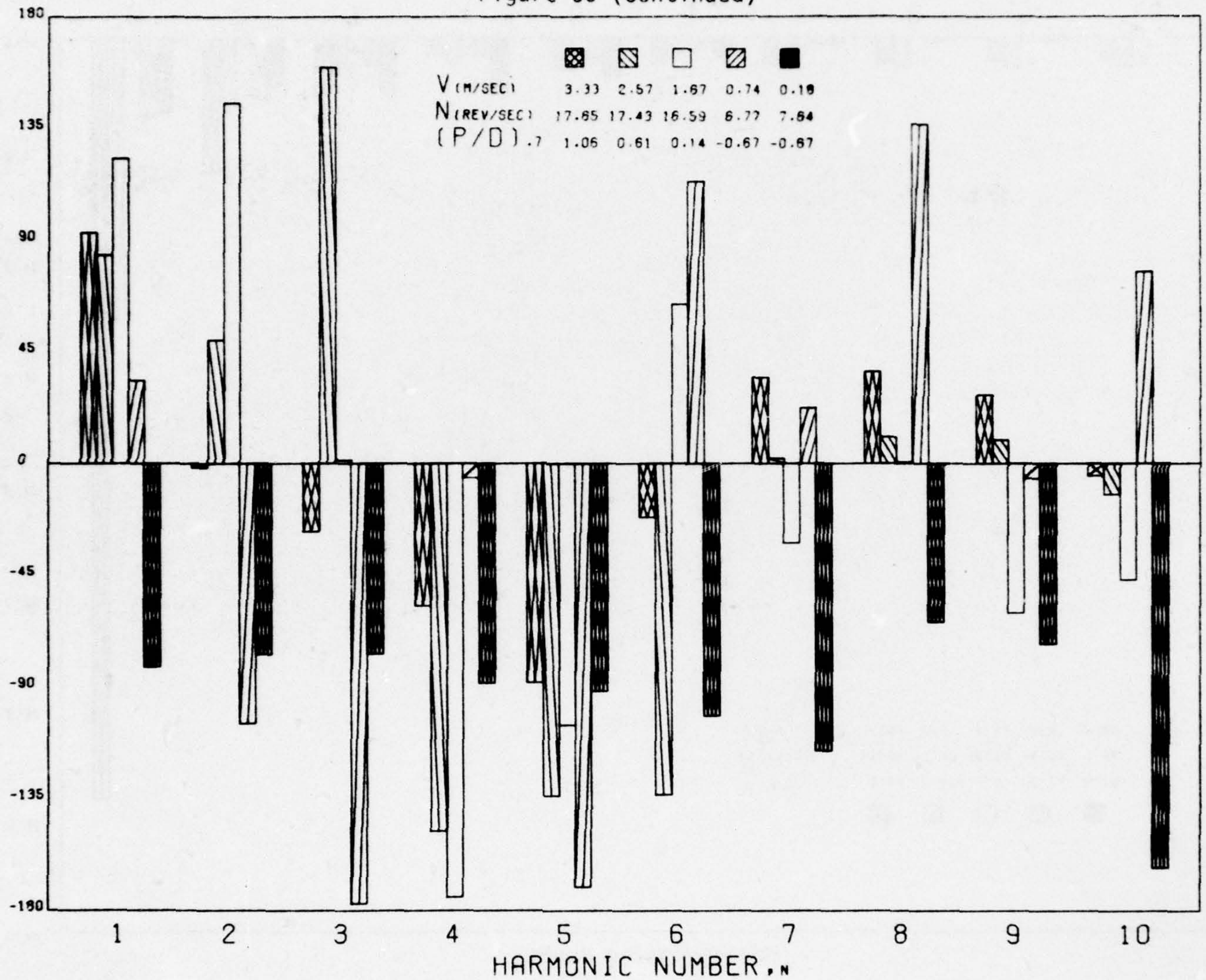

Figure 35 (Continued)

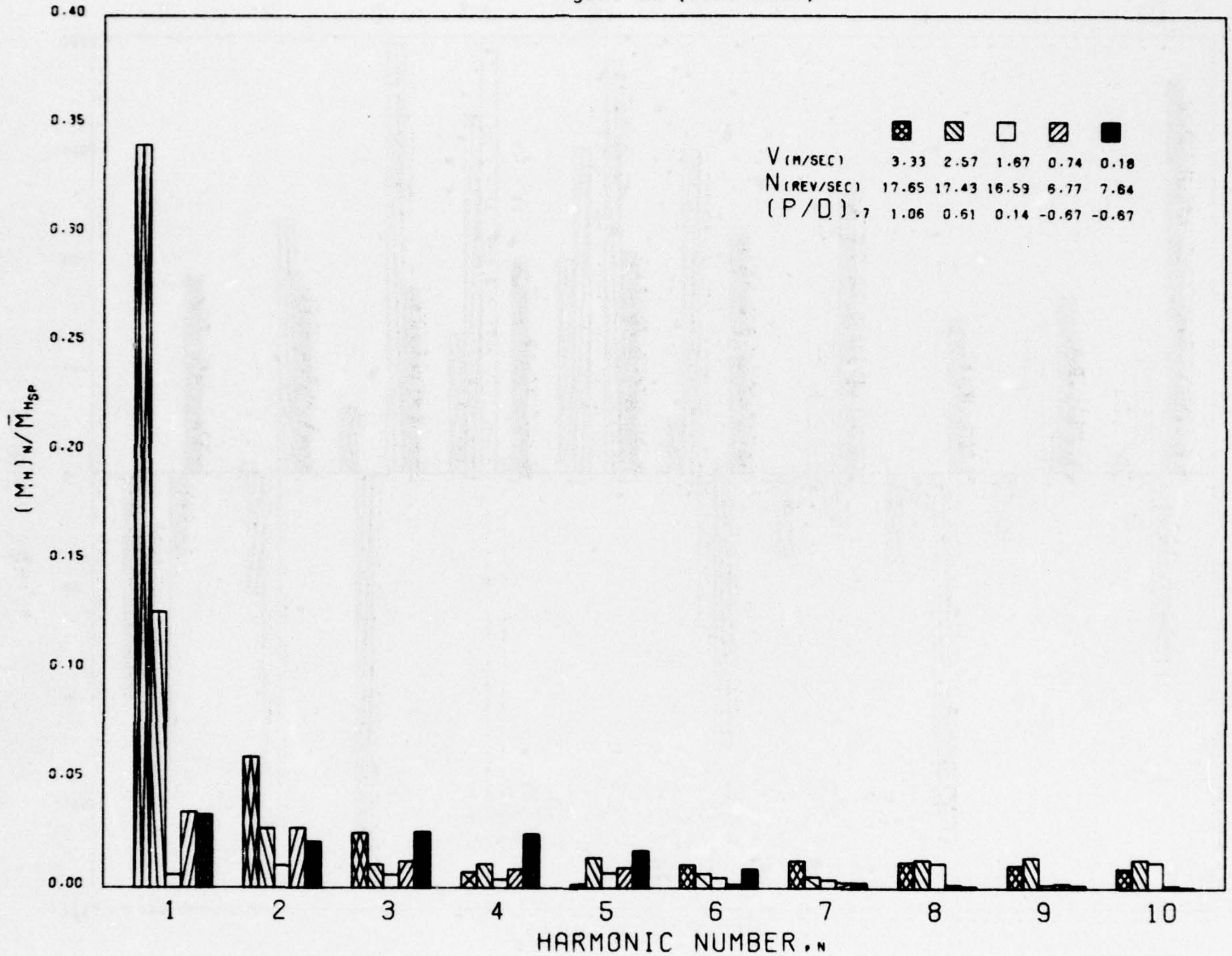

Figure 35 (Continued)

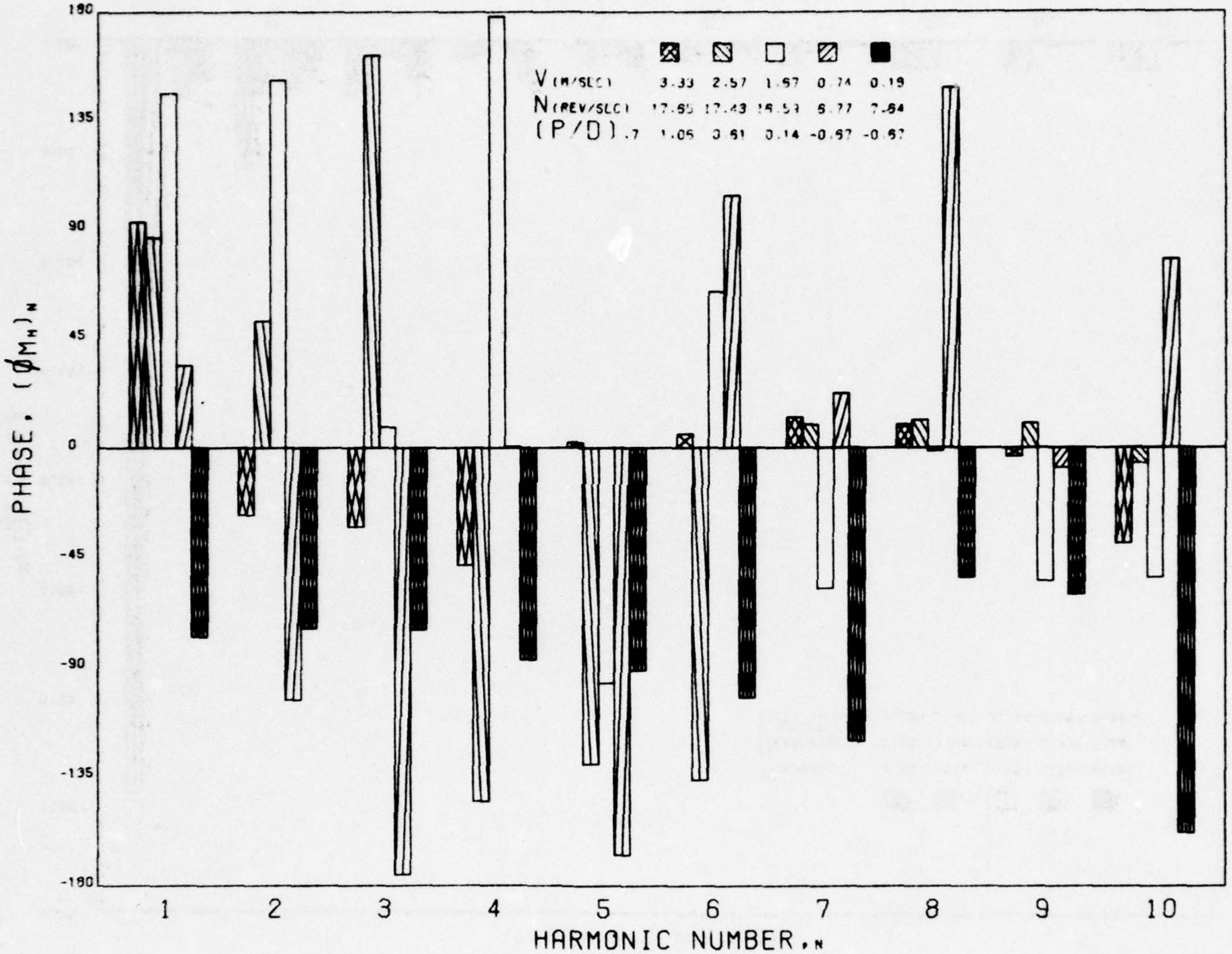

Figure 35 (Continued)

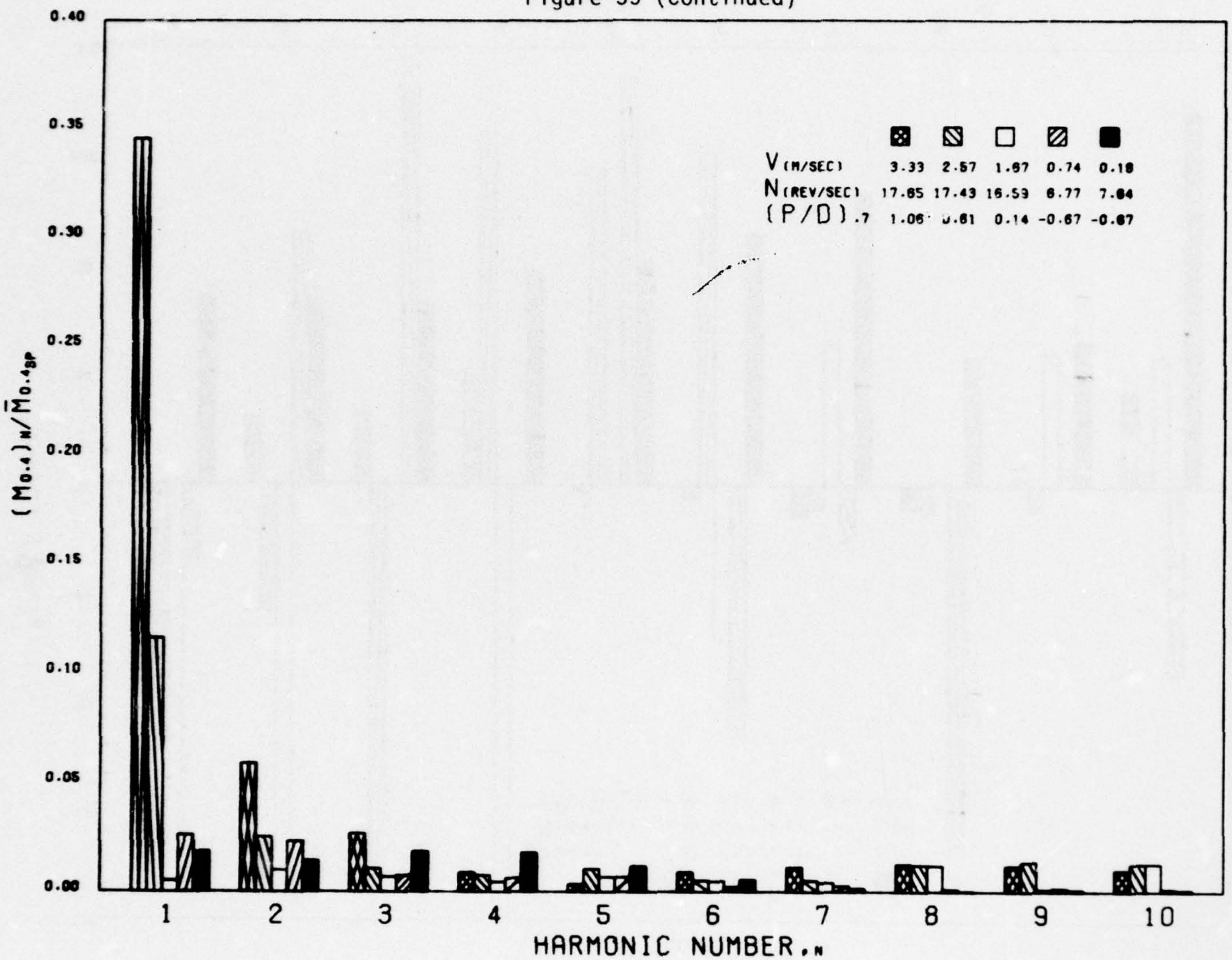

Figure 35 (Continued)

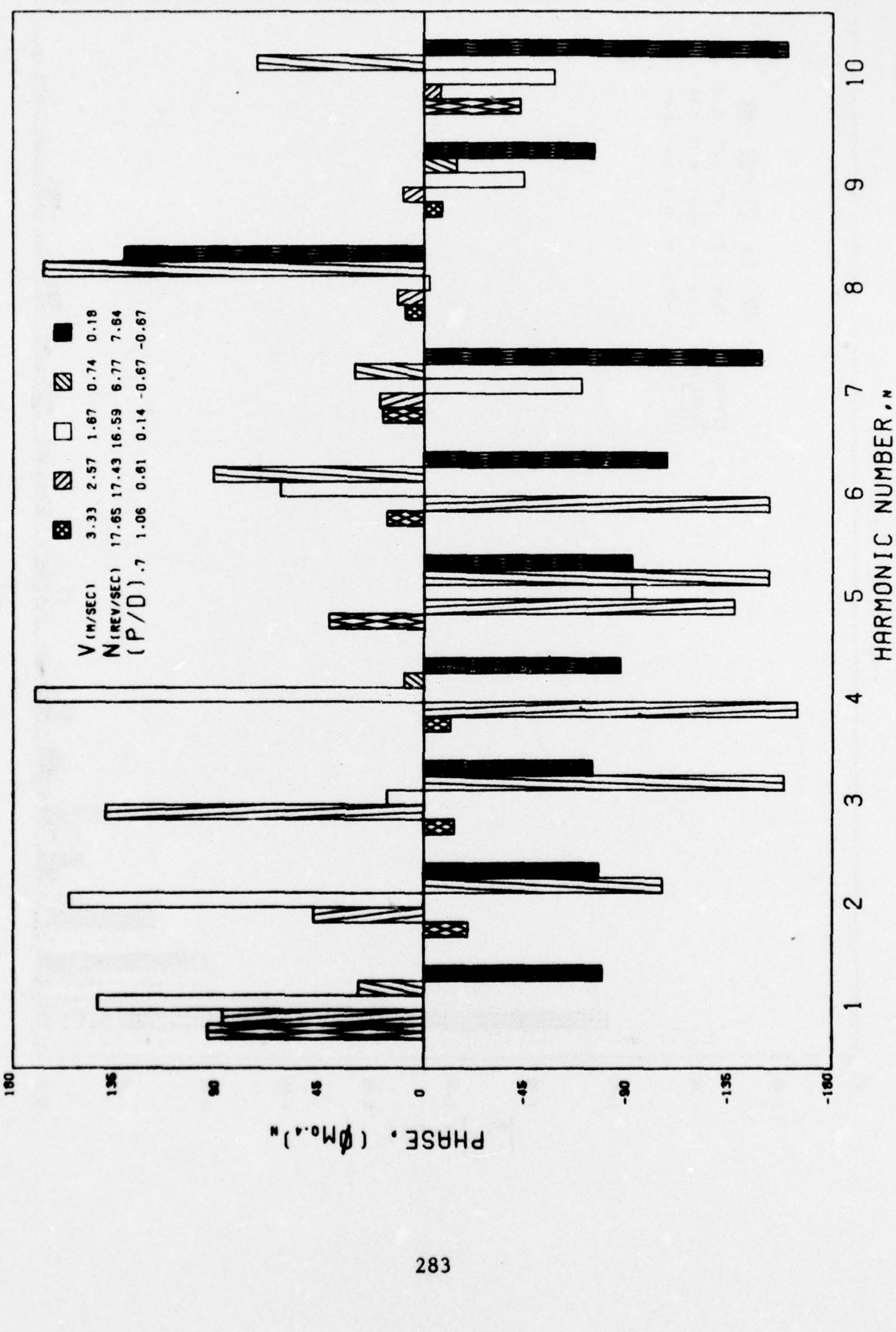

Figure 35 (Continued)

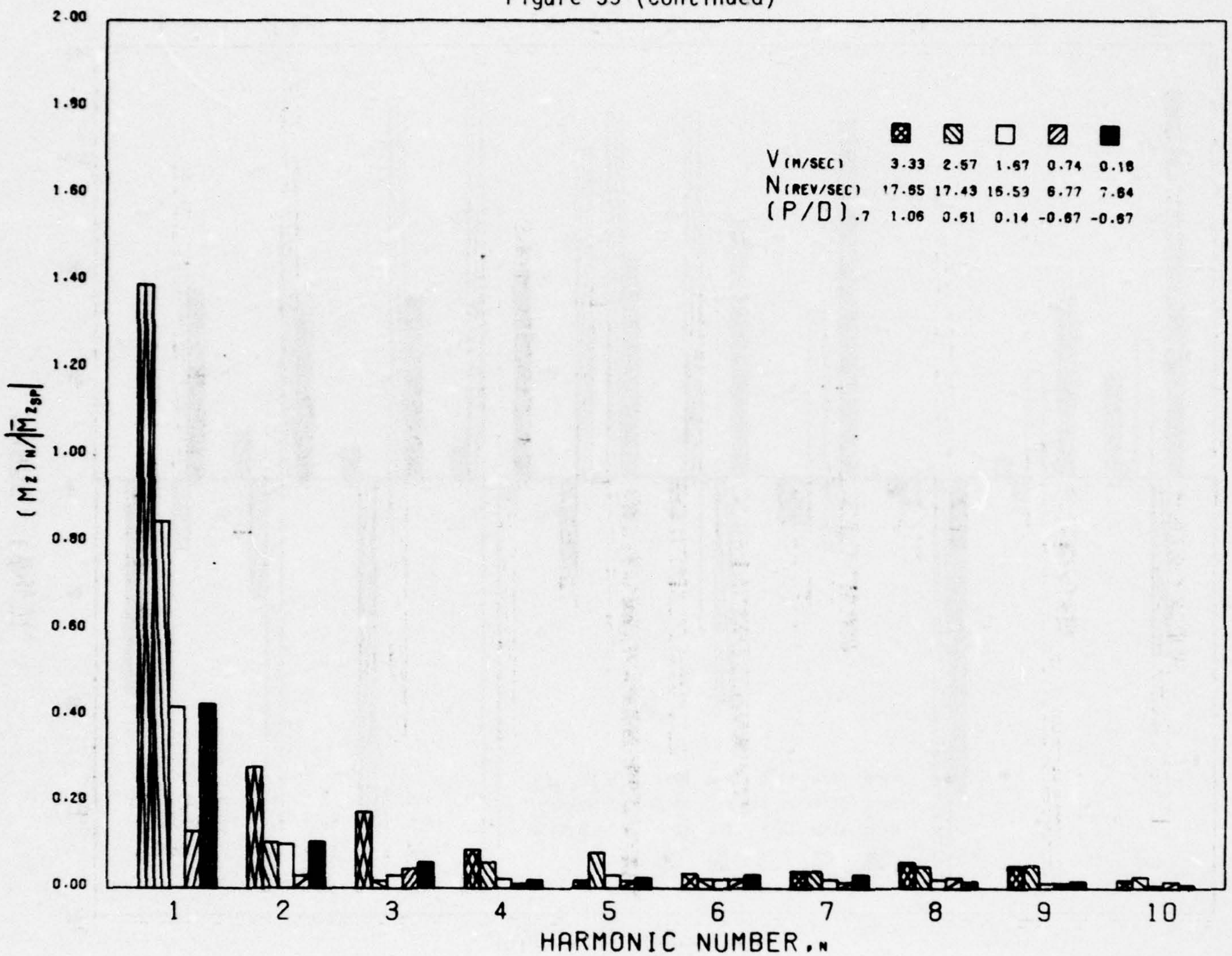

Figure 35 (Continued)

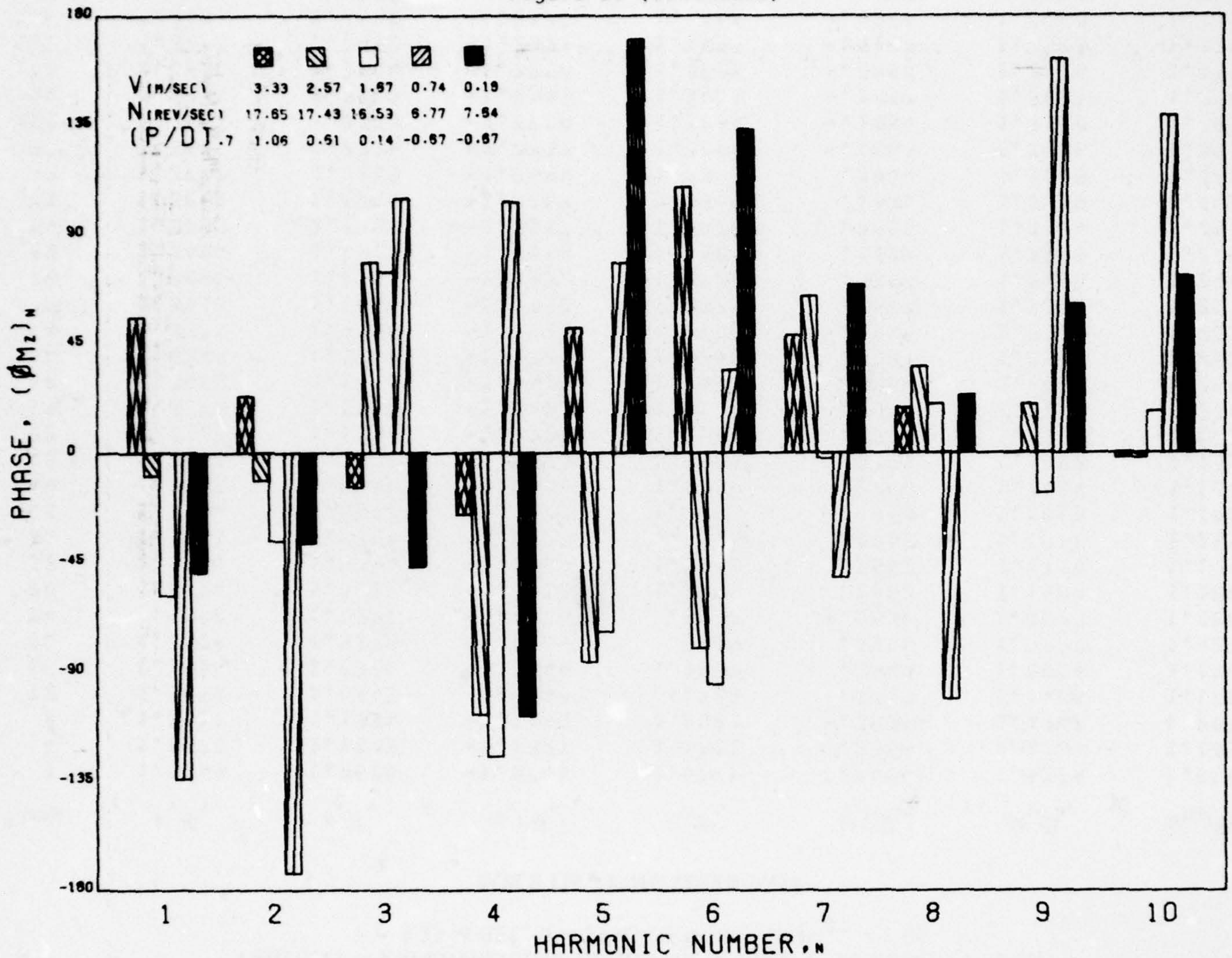

TABLE 11 – EXPERIMENTAL LOADS NEAR SELF PROPULSION POINT. $V = 3.33$ M/SEC, $n = 17.65$ REV/SEC, $(P/D)_{0.7} = 1.06$

TABLE 11a – UNFILTERED DATA

θ (deg)	$F_x/\bar{F}_x$	$F_y/\bar{F}_y$	$M_x/\lvert\bar{M}_x\rvert$	$M_y/\bar{M}_y$	$M_z/\lvert\bar{M}_z\rvert$	$M_h/\bar{M}_h$	$M_{0.4}/\bar{M}_{0.4}$
0	1.0249	1.0606	-1.0741	1.0051	.4454	1.0258	1.0157
4	1.0970	1.1075	-1.1327	1.1011	.2366	1.1264	1.1353
8	1.2017	1.1334	-1.1463	1.2023	-.3375	1.1942	1.2070
12	1.1653	1.0445	-1.0449	1.1768	-.1712	1.1466	1.1704
16	1.1004	1.0394	-1.0546	1.0959	.2740	1.0908	1.1001
20	1.0028	1.0239	-1.0465	.9979	.0101	1.0222	1.0235
24	.9902	1.0227	-1.0475	.9922	-.0631	1.0223	1.0268
28	1.0794	1.0612	-1.0912	1.0896	.2852	1.1088	1.1240
32	1.1311	1.0944	-1.1059	1.1945	.2662	1.1775	1.1949
36	1.2582	1.0768	-1.0727	1.2514	.0412	1.1974	1.2159
40	1.2594	1.0997	-1.1020	1.2323	-.0913	1.1860	1.1906
44	1.2510	1.0954	-1.0916	1.1989	.2060	1.1464	1.1348
48	1.2550	1.1022	-1.0933	1.2004	.2391	1.1452	1.1313
52	1.3167	1.1252	-1.1221	1.2541	.0205	1.1898	1.1756
56	1.3778	1.1456	-1.1421	1.3170	.0072	1.2404	1.2314
60	1.3980	1.1468	-1.1415	1.3446	.3207	1.2622	1.2595
64	1.3808	1.1700	-1.1721	1.3246	.1087	1.2586	1.2507
68	1.3271	1.1756	-1.1820	1.2775	-.1040	1.2331	1.2236
72	1.3010	1.1644	-1.1750	1.2571	.1875	1.2206	1.2134
76	1.3096	1.1798	-1.1926	1.2725	.3759	1.2403	1.2366
80	1.3404	1.1922	-1.2050	1.3101	.1178	1.2735	1.2759
84	1.3790	1.2036	-1.2117	1.3474	.0066	1.2994	1.3033
88	1.3860	1.2084	-1.2263	1.3518	.1831	1.3089	1.3124
92	1.3772	1.2215	-1.2494	1.3391	.0944	1.3085	1.3083
96	1.3687	1.2224	-1.2537	1.3294	-.1668	1.3036	1.3021
100	1.3664	1.2333	-1.2709	1.3284	-.1984	1.3108	1.3093
104	1.3734	1.2513	-1.2865	1.3409	-.1852	1.3260	1.3265
108	1.3620	1.2404	-1.2750	1.3525	-.2960	1.3316	1.3359
112	1.3773	1.2482	-1.2821	1.3496	-.4163	1.3323	1.3363
116	1.3606	1.2461	-1.2875	1.3348	-.4251	1.3269	1.3312
120	1.3386	1.2365	-1.2914	1.3119	-.4862	1.3099	1.3127

TABLE 11a – (Continued)

θ (deg)	$F_x/\bar{F}_x$	$F_y/\bar{F}_y$	$M_x/\lvert\bar{M}_x\rvert$	$M_y/\bar{M}_y$	$M_z/\lvert\bar{M}_z\rvert$	$M_h/\bar{M}_h$	$M_{0.4}/\bar{M}_{0.4}$
124	1.3167	1.2379	-1.2898	1.2950	-.6555	1.3052	1.3093
128	1.3035	1.2313	-1.2857	1.2877	-.7566	1.3023	1.3096
132	1.2940	1.2190	-1.2707	1.2813	-.7690	1.2937	1.3029
136	1.2801	1.2052	-1.2541	1.2693	-.8323	1.2803	1.2903
140	1.2628	1.1871	-1.2347	1.2522	-.9141	1.2621	1.2723
144	1.2415	1.1716	-1.2180	1.2310	-.9579	1.2419	1.2513
148	1.2155	1.1576	-1.2059	1.2065	-1.0363	1.2224	1.2317
152	1.1965	1.1418	-1.1924	1.1912	-1.1461	1.2039	1.2212
156	1.1815	1.1208	-1.1696	1.1789	-1.2233	1.1952	1.2088
160	1.1694	1.1033	-1.1492	1.1655	-1.2684	1.1782	1.1913
164	1.1463	1.0826	-1.1301	1.1445	-1.3476	1.1593	1.1735
168	1.1153	1.0596	-1.1044	1.1114	-1.4219	1.1266	1.1385
172	1.0863	1.0403	-1.0813	1.0827	-1.5111	1.0985	1.1092
176	1.0626	1.0224	-1.0568	1.0612	-1.5982	1.0749	1.0858
180	1.0441	1.0023	-1.0375	1.0441	-1.6427	1.0579	1.0598
184	1.0264	.9752	-1.0101	1.0306	-1.6912	1.0421	1.0576
188	.9926	.9615	-.9866	.9970	-1.7698	1.0084	1.0209
192	.9473	.9353	-.9617	.9517	-1.7971	.9696	.9803
196	.9074	.9003	-.9287	.9127	-1.8294	.9336	.9445
200	.8759	.8827	-.9059	.8847	-1.9314	.9070	.9181
204	.8648	.8666	-.8836	.8751	-2.0076	.8922	.9042
208	.8508	.8488	-.8617	.8625	-2.0301	.8760	.8889
212	.8254	.8282	-.8359	.8373	-2.0601	.8491	.8610
216	.7918	.7991	-.8065	.8025	-2.1085	.8153	.8260
220	.7558	.7656	-.7749	.7658	-2.1169	.7804	.7906
224	.7311	.7486	-.7556	.7428	-2.1462	.7585	.7688
228	.7164	.7341	-.7357	.7287	-2.1932	.7411	.7512
232	.7076	.7229	-.7192	.7227	-2.2422	.7314	.7428
236	.6923	.7111	-.7071	.7079	-2.2691	.7176	.7290
240	.6690	.6968	-.6932	.6813	-2.2686	.6935	.7021

TABLE 11a – (Continued)

θ (deg)	$F_x/\bar{F}_x$	$F_y/\bar{F}_y$	$M_x/\lvert\bar{M}_x\rvert$	$M_y/\bar{M}_y$	$M_z/\lvert\bar{M}_z\rvert$	$M_h/\bar{M}_h$	$M_{0.4}/\bar{M}_{0.4}$
244	.6418	.6821	-.6794	.6557	-2.2818	.6725	.6808
248	.6177	.6539	-.6584	.6313	-2.3297	.6480	.6553
252	.6061	.6677	-.6584	.6193	-2.3593	.6382	.6433
256	.6031	.6545	-.6355	.6187	-2.3282	.6289	.6356
260	.5974	.6454	-.6237	.6128	-2.2955	.6202	.6269
264	.5884	.6380	-.6167	.6023	-2.3218	.6102	.6158
268	.5731	.6192	-.5952	.5879	-2.3591	.5932	.5995
272	.5623	.6217	-.6004	.5766	-2.3309	.5875	.5924
276	.5590	.6302	-.6046	.5725	-2.3080	.5842	.5870
280	.5625	.6600	-.6272	.5791	-2.3327	.5946	.5958
284	.5737	.7036	-.6673	.5893	-2.3593	.6125	.6096
288	.5764	.7590	-.7176	.5916	-2.3092	.6272	.6181
292	.5706	.8042	-.7581	.5849	-2.2682	.6327	.6174
296	.5622	.8572	-.8115	.5751	-2.2822	.6415	.6190
300	.5649	.9096	-.8589	.5751	-2.2555	.6530	.6234
304	.5803	.9247	-.8756	.5932	-2.1857	.6724	.6446
308	.6055	.9574	-.9204	.6163	-2.0182	.7051	.6763
312	.6581	.9826	-.9344	.6676	-1.2101	.7409	.7132
316	.7331	1.0279	-1.0018	.7550	-.7547	.8350	.8199
320	.8519	1.1047	-1.0822	.8400	-1.6076	.9048	.8738
324	.8415	1.0274	-.9830	.8290	-1.6206	.8598	.8333
328	.8257	1.0257	-.9851	.7973	-.4287	.8324	.7952
332	.8055	.9973	-.9572	.7698	-.3668	.8016	.7609
336	.8171	.9871	-.9634	.7881	-1.1034	.8247	.7918
340	.8980	1.0307	-1.0346	.8801	-.7286	.9244	.9047
344	.9777	1.1091	-1.1289	.9621	.0401	1.0163	.9996
348	1.0236	1.1076	-1.1267	1.0102	-.1553	1.0500	1.0393
352	1.0174	1.1235	-1.1620	1.0009	-.4759	1.0591	1.0461
356	.9968	1.1496	-1.1842	.9706	.1446	1.0391	1.0151
360	1.0249	1.0606	-1.0741	1.0051	.4454	1.0258	1.0157

TABLE 11b – SIGNALS RECONSTRUCTED FROM FIRST TEN HARMONICS (Five for M_z)

θ (deg)	$F_x/\bar{F}_x$	$F_y/\bar{F}_y$	$M_x/\lvert M_x\rvert$	$M_y/\bar{M}_y$	$M_z/\lvert\bar{M}_z\rvert$	$M_h/\bar{M}_h$	$M_{0.4}/\bar{M}_{0.4}$
0	1.0978	1.1247	-1.1421	1.0967	.3050	1.1157	1.1139
4	1.1163	1.1073	-1.1181	1.1169	.3743	1.1211	1.1234
8	1.1156	1.0824	-1.0881	1.1186	.4200	1.1126	1.1184
12	1.1008	1.0576	-1.0615	1.1075	.4437	1.0979	1.1067
16	1.0615	1.0398	-1.0454	1.0926	.4479	1.0851	1.0967
20	1.0687	1.0331	-1.0423	1.0837	.4358	1.0809	1.0945
24	1.0715	1.0380	-1.0501	1.0880	.4113	1.0878	1.1024
28	1.0938	1.0514	-1.0634	1.1078	.3783	1.1046	1.1186
32	1.1342	1.0687	-1.0767	1.1409	.3408	1.1271	1.1386
36	1.1859	1.0851	-1.0860	1.1809	.3026	1.1503	1.1578
40	1.2399	1.0962	-1.0908	1.2206	.2665	1.1704	1.1726
44	1.2876	1.1076	-1.0933	1.2538	.2352	1.1857	1.1824
48	1.3228	1.1151	-1.0971	1.2772	.2099	1.1967	1.1887
52	1.3436	1.1231	-1.1054	1.2906	.1911	1.2054	1.1943
56	1.3513	1.1332	-1.1191	1.2964	.1783	1.2139	1.2017
60	1.3501	1.1456	-1.1366	1.2982	.1702	1.2233	1.2120
64	1.3449	1.1591	-1.1548	1.2991	.1649	1.2338	1.2247
68	1.3398	1.1715	-1.1706	1.3012	.1599	1.2444	1.2382
72	1.3375	1.1813	-1.1821	1.3055	.1526	1.2543	1.2510
76	1.3392	1.1881	-1.1899	1.3116	.1405	1.2631	1.2621
80	1.3446	1.1930	-1.1961	1.3190	.1211	1.2715	1.2719
84	1.3528	1.1978	-1.2037	1.3271	.0929	1.2804	1.2814
88	1.3622	1.2045	-1.2149	1.3355	.0546	1.2906	1.2916
92	1.3713	1.2139	-1.2297	1.3435	.0057	1.3019	1.3027
96	1.3787	1.2252	-1.2464	1.3504	-.0533	1.3134	1.3140
100	1.3829	1.2365	-1.2619	1.3553	-.1215	1.3231	1.3238
104	1.3827	1.2454	-1.2736	1.3567	-.1975	1.3293	1.3303
108	1.3776	1.2501	-1.2798	1.3541	-.2795	1.3310	1.3326
112	1.3679	1.2499	-1.2808	1.3473	-.3651	1.3281	1.3307
116	1.3545	1.2458	-1.2783	1.3369	-.4524	1.3220	1.3256
120	1.3389	1.2393	-1.2744	1.3244	-.5394	1.3143	1.3191

TABLE 11b – (Continued)

θ (deg)	$F_x/\bar{F}_x$	$F_y/\bar{F}_y$	$M_x/\lvert M_x \rvert$	$M_y/\bar{M}_y$	$M_z/\lvert \bar{M}_z \rvert$	$M_h/\bar{M}_h$	$M_{0.4}/\bar{M}_{0.4}$
124	1.3225	1.2319	-1.2703	1.3112	-.6247	1.3063	1.3123
128	1.3070	1.2245	-1.2661	1.2983	-.7070	1.2983	1.3054
132	1.2918	1.2165	-1.2604	1.2856	-.7858	1.2897	1.2978
136	1.2765	1.2069	-1.2513	1.2727	-.8609	1.2791	1.2881
140	1.2604	1.1943	-1.2375	1.2585	-.9327	1.2655	1.2752
144	1.2424	1.1760	-1.2190	1.2423	-1.0019	1.2486	1.2590
148	1.2226	1.1587	-1.1974	1.2238	-1.0692	1.2291	1.2400
152	1.2014	1.1377	-1.1752	1.2038	-1.1358	1.2085	1.2200
156	1.1796	1.1169	-1.1543	1.1833	-1.2026	1.1883	1.2004
160	1.1588	1.0977	-1.1357	1.1632	-1.2702	1.1693	1.1818
164	1.1386	1.0801	-1.1185	1.1438	-1.3392	1.1511	1.1639
168	1.1183	1.0633	-1.1009	1.1243	-1.4096	1.1322	1.1450
172	1.0968	1.0456	-1.0806	1.1035	-1.4812	1.1110	1.1237
176	1.0726	1.0256	-1.0564	1.0801	-1.5533	1.0854	1.0986
180	1.0445	1.0028	-1.0287	1.0533	-1.6252	1.0582	1.0701
184	1.0137	.9778	-.9993	1.0237	-1.6953	1.0278	1.0395
188	.9805	.9523	-.9707	.9925	-1.7638	.9972	1.0089
192	.9480	.9281	-.9448	.9618	-1.8283	.9682	.9801
196	.9171	.9063	-.9221	.9329	-1.8883	.9418	.9540
200	.8891	.8865	-.9012	.9066	-1.9431	.9176	.9298
204	.8637	.8674	-.8798	.8824	-1.9922	.8940	.9061
208	.8398	.8473	-.8557	.8591	-2.0356	.8694	.8811
212	.8160	.8248	-.8281	.8354	-2.0736	.8429	.8541
216	.7914	.7999	-.7980	.8108	-2.1067	.8150	.8257
220	.7662	.7741	-.7683	.7857	-2.1356	.7873	.7978
224	.7413	.7499	-.7421	.7614	-2.1613	.7620	.7725
228	.7182	.7297	-.7213	.7392	-2.1848	.7407	.7514
232	.6978	.7149	-.7077	.7198	-2.2070	.7236	.7345
236	.6803	.7049	-.6979	.7030	-2.2286	.7093	.7199
240	.6645	.6976	-.6891	.6876	-2.2503	.6955	.7053

TABLE 11b – (Continued)

θ (deg)	$F_x/\bar{F}_x$	$F_y/\bar{F}_y$	$M_x/\lvert M_x\rvert$	$M_y/\bar{M}_y$	$M_z/\lvert\bar{M}_z\rvert$	$M_h/\bar{M}_h$	$M_{0.4}/\bar{M}_{0.4}$
244	.6491	.6902	-.6779	.6719	-2.2723	.6799	.6834
248	.6327	.6802	-.6626	.6550	-2.2945	.6615	.6685
252	.6154	.6665	-.6436	.6372	-2.3166	.6413	.6472
256	.5984	.6505	-.6234	.6202	-2.3378	.6220	.6273
260	.5842	.6350	-.6058	.6064	-2.3569	.6065	.6121
264	.5747	.6238	-.5943	.5978	-2.3726	.5974	.6036
268	.5708	.6205	-.5913	.5949	-2.3832	.5949	.6017
272	.5714	.6270	-.5970	.5960	-2.3869	.5975	.6038
276	.5737	.6441	-.6110	.5981	-2.3817	.6020	.6064
280	.5743	.6710	-.6321	.5977	-2.3655	.6058	.6064
284	.5709	.7061	-.6600	.5931	-2.3365	.6081	.6033
288	.5639	.7478	-.6949	.5852	-2.2929	.6104	.5994
292	.5567	.7944	-.7371	.5778	-2.2331	.6165	.5995
296	.5550	.8442	-.7862	.5768	-2.1558	.6307	.6088
300	.5647	.8945	-.8392	.5877	-2.0604	.6557	.6306
304	.5898	.9420	-.8912	.6133	-1.9465	.6910	.6644
308	.6299	,9825	-.9360	.6523	-1.8145	.7326	.7056
312	.6805	1.0122	-.9678	.6992	-1.6655	.7739	.7470
316	.7340	1.0289	-.9839	.7461	-1.5013	.8084	.7812
320	.7818	1.0333	-.9860	.7853	-1.3242	.8319	.8038
324	.8181	1.0289	-.9802	.8125	-1.1375	.8447	.8151
328	.8415	1.0219	-.9754	.8281	-.9447	.8513	.8203
332	.8560	1.0190	-.9799	.8375	-.7502	.8594	.8278
336	.8688	1.0255	-.9990	.8488	-.5587	.8766	.8459
340	.8862	1.0429	-1.0323	.8699	-.3736	.9073	.8793
344	.9193	1.0685	-1.0736	.9050	-.2006	.9511	.9276
348	.9625	1.0963	-1.1133	.9529	-.0431	1.0025	.9845
352	1.0129	1.1186	-1.1415	1.0072	.0952	1.0527	1.0405
356	1.0611	1.1290	-1.1515	1.0582	.2118	1.0924	1.0858
360	1.0978	1.1247	-1.1421	1.0967	.3050	1.1157	1.1139

TABLE 11c – HARMONIC CONTENT OF SIGNALS

n	$\frac{(F_x)_n}{\bar{F}_x}$	$(\phi_x)_n$ (deg)	$\frac{(F_y)_n}{\bar{F}_y}$	$(\phi_y)_n$ (deg)	$\frac{(M_x)_n}{\lvert\bar{M}_x\rvert}$	$(\phi_x)_n$ (deg)	$\frac{(M_y)_n}{\bar{M}_y}$	$(\phi_y)_n$ (deg)
1	.3974	91.4	.2453	80.0	.2697	-94.8	.3737	92.8
2	.0336	-1.2	.0992	-59.7	.1038	126.8	.0380	-1.7
3	.0210	-49.6	.0421	-92.0	.0403	106.7	.0192	-27.4
4	.0206	-73.9	.0168	-166.1	.0108	22.4	.0133	-57.3
5	.0153	-93.3	.0076	91.2	.0074	-104.0	.0077	-88.2
6	.0128	-37.7	.0182	16.8	.0189	-165.9	.0086	-21.6
7	.0162	32.8	.0162	-18.3	.0170	156.5	.0141	34.5
8	.0199	43.9	.0091	-48.3	.0116	123.7	.0175	36.8
9	.0134	41.7	.0055	-33.2	.0087	127.4	.0127	27.4
10	.0075	6.1	.0079	-34.7	.0110	119.7	.0079	-5.0
11	.0029	-54.1	.0067	-54.7	.0095	113.1	.0027	-64.2
12	.0020	115.7	.0042	-96.9	.0046	66.5	.0034	125.6
13	.0163	138.7	.0070	-175.1	.0079	11.2	.0188	135.4
14	.0274	135.7	.0078	138.0	.0072	-37.0	.0304	131.1
15	.0208	172.1	.0072	152.4	.0079	-47.1	.0230	167.9
16	.0145	168.0	.0064	137.5	.0067	-59.0	.0155	164.6
17	.0055	174.9	.0036	95.8	.0043	-90.8	.0060	171.1
18	.0021	139.5	.0019	121.8	.0023	-84.0	.0026	145.4
19	.0007	-58.3	.0006	-148.1	.0005	81.6	.0006	-95.5
20	.0014	-79.2	.0026	-129.3	.0024	46.2	.0012	-104.1
21	.0017	-103.8	.0021	-143.9	.0030	34.2	.0018	-118.9
22	.0017	-139.9	.0021	-171.5	.0030	7.3	.0017	-151.9
23	.0015	165.7	.0023	145.7	.0030	-16.9	.0015	160.0
24	.0012	141.4	.0010	175.8	.0013	-19.1	.0012	137.0
25	.0010	80.6	.0005	-154.4	.0009	8.8	.0008	72.9

TABLE 11c – (Continued)

n	$\frac{(M_z)_n}{\lvert\overline{M}_z\rvert}$	$(\phi_z)_n$ (deg)	$\frac{(M_h)_n}{\overline{M}_h}$	$(\phi_h)_n$ (deg)	$\frac{(M_{0.4})_n}{\overline{M}_{0.4}}$	$(\phi_{0.4})_n$ (deg)
1	1.3923	55.8	.3403	92.8	.3451	94.8
2	.2917	23.4	.0599	-27.6	.0538	-19.3
3	.1771	-14.0	.0251	-32.5	.0267	-13.3
4	.0899	-25.2	.0071	-48.2	.0097	-11.6
5	.0180	31.3	.0018	2.1	.0035	41.3
6	.0345	109.3	.0105	5.6	.0089	16.1
7	.0394	49.1	.0123	12.4	.0112	17.9
8	.0597	18.5	.0118	9.6	.0125	8.3
9	.0514	-.2	.0103	-3.5	.0117	-8.0
10	.0194	-2.2	.0090	-39.2	.0097	-42.2
11	.0199	-111.5	.0056	-73.1	.0055	-78.7
12	.0208	-102.4	.0031	159.5	.0043	148.6
13	.0303	-10.9	.0154	142.8	.0178	138.9
14	.0496	-2.3	.0245	130.3	.0283	128.1
15	.0824	-7.9	.0190	159.1	.0218	158.1
16	.0721	-15.1	.0127	154.1	.0142	154.1
17	.0478	-29.1	.0048	150.1	.0055	153.8
18	.0256	-32.9	.0025	128.3	.0028	132.1
19	.0163	58.7	.0006	-100.6	.0007	-110.1
20	.0570	64.6	.0015	-129.6	.0014	-139.4
21	.0352	46.8	.0026	-136.5	.0027	-139.2
22	.1286	24.2	.0023	-166.4	.0024	-169.1
23	.1622	14.2	.0022	165.7	.0022	167.0
24	.1850	18.3	.0014	141.0	.0015	136.2
25	.1222	32.3	.0005	119.8	.0004	113.7

TABLE 12 – EXPERIMENTAL LOADS DURING QUASI-STEADY CRASH FORWARD AT
$V = 0.33$ M/SEC, $n = 6.26$ REV/SEC, $(P/D)_{0.7} = 1.39$

TABLE 12a – SIGNALS RECONSTRUCTED FROM FIRST TEN HARMONICS (Five for M_z)

θ	$F_x/\bar{F}_{x_{SP}}$	$F_y/\bar{F}_{y_{SP}}$	$M_x/\lvert\bar{M}_{x_{SP}}\rvert$	$M_y/\bar{M}_{y_{SP}}$	$M_z/\lvert\bar{M}_{z_{SP}}\rvert$	$M_h/\bar{M}_{h_{SP}}$	$M_{0.4}/M_{0.4_{SP}}$
0	.5046	.4523	-.5590	.5700	2.0758	.5937	.6856
4	.5177	.4500	-.5539	.5869	2.0785	.6028	.7093
8	.5249	.4477	-.5502	.5959	2.0791	.6072	.7077
12	.5265	.4459	-.5485	.5974	2.0791	.6076	.7086
16	.5240	.4448	-.5488	.5936	2.0762	.6054	.7052
20	.5198	.4445	-.5507	.5876	2.0737	.6025	.7002
24	.5159	.4448	-.5532	.5823	2.0712	.6003	.6963
28	.5135	.4454	-.5556	.5795	2.0688	.5999	.6950
32	.5134	.4460	-.5575	.5797	2.0668	.6012	.6365
36	.5149	.4462	-.5586	.5821	2.0653	.6038	.7001
40	.5172	.4459	-.5591	.5855	2.0642	.6067	.7043
44	.5192	.4451	-.5593	.5883	2.0633	.6091	.7078
48	.5202	.4439	-.5594	.5895	2.0627	.6105	.7098
52	.5200	.4425	-.5597	.5890	2.0621	.6108	.7100
56	.5188	.4412	-.5604	.5872	2.0614	.6103	.7092
60	.5171	.4402	-.5613	.5849	2.0605	.6097	.7079
64	.5154	.4397	-.5626	.5828	2.0593	.6093	.7070
68	.5141	.4399	-.5640	.5814	2.0578	.6094	.7068
72	.5133	.4406	-.5656	.5808	2.0561	.6100	.7073
76	.5171	.4416	-.5672	.5808	2.0542	.6108	.7082
80	.5134	.4426	-.5686	.5811	2.0521	.6116	.7089
84	.5140	.4433	-.5696	.5815	2.0500	.6121	.7093
88	.5143	.4434	-.5699	.5819	2.0478	.6123	.7092
92	.5160	.4428	-.5694	.5823	2.0455	.6122	.7090
96	.5171	.4415	-.5681	.5830	2.0431	.6120	.7088
100	.5181	.4398	-.5662	.5837	2.0405	.6117	.7088
104	.5186	.4381	-.5643	.5844	2.0375	.6115	.7090
108	.5185	.4368	-.5628	.5848	2.0341	.6113	.7093
112	.5180	.4363	-.5620	.5848	2.0300	.6111	.7095
116	.5169	.4366	-.5622	.5842	2.0253	.6110	.7095
120	.5154	.4378	-.5632	.5832	2.0197	.6108	.7092

TABLE 12a – (Continued)

θ	$F_x/\bar{F}_{x_{SP}}$	$F_y/\bar{F}_{y_{SP}}$	$M_x/\lvert\bar{M}_{x_{SP}}\rvert$	$M_y/\bar{M}_{y_{SP}}$	$M_z/\lvert\bar{M}_{z_{SP}}\rvert$	$M_h/\bar{M}_{h_{SP}}$	$M_{0.4}/M_{0.4_{SP}}$
124	.5141	.4396	-.5648	.5822	2.0132	.6108	.7089
128	.5130	.4416	-.5664	.5813	2.0060	.6108	.7086
132	.5124	.4434	-.5677	.5808	1.9980	.6108	.7083
136	.5119	.4448	-.5684	.5806	1.9896	.6107	.7081
140	.5114	.4456	-.5681	.5804	1.9807	.6102	.7076
144	.5107	.4458	-.5672	.5799	1.9717	.6093	.7066
148	.5096	.4456	-.5657	.5790	1.9627	.6078	.7050
152	.5080	.4452	-.5639	.5775	1.9540	.6059	.7028
156	.5063	.4448	-.5623	.5756	1.9455	.6037	.7002
160	.5045	.4448	-.5610	.5737	1.9374	.6016	.6976
164	.5030	.4453	-.5604	.5718	1.9297	.5997	.6951
168	.5015	.4464	-.5604	.5702	1.9222	.5983	.6931
172	.5001	.4481	-.5611	.5686	1.9148	.5971	.6913
176	.4985	.4503	-.5623	.5669	1.9073	.5961	.6895
180	.4966	.4527	-.5637	.5649	1.8997	.5949	.6875
184	.4943	.4551	-.5650	.5623	1.8916	.5933	.6850
188	.4917	.4570	-.5657	.5595	1.8830	.5912	.6818
192	.4891	.4583	-.5656	.5565	1.8739	.5887	.6783
196	.4867	.4589	-.5645	.5537	1.8643	.5859	.6746
200	.4846	.4588	-.5623	.5512	1.8543	.5831	.6710
204	.4827	.4584	-.5608	.5489	1.8442	.5804	.6677
208	.4808	.4579	-.5591	.5467	1.8342	.5780	.6647
212	.4787	.4578	-.5582	.5442	1.8246	.5757	.6617
216	.4761	.4582	-.5583	.5412	1.8157	.5737	.6588
220	.4732	.4594	-.5594	.5378	1.8077	.5718	.6558
224	.4701	.4611	-.5611	.5342	1.8009	.5699	.6528
228	.4672	.4629	-.5626	.5308	1.7957	.5681	.6497
232	.4648	.4645	-.5636	.5280	1.7909	.5663	.6469
236	.4629	.4654	-.5635	.5258	1.7877	.5644	.6443
240	.4615	.4656	-.5623	.5242	1.7854	.5625	.6418

TABLE 12a – (Continued)

θ	$F_x/\bar{F}_{x_{SP}}$	$F_y/\bar{F}_{y_{SP}}$	$M_x/\lvert\bar{M}_{x_{SP}}\rvert$	$M_y/\bar{M}_{y_{SP}}$	$M_z/\lvert\bar{M}_{z_{SP}}\rvert$	$M_h/\bar{M}_{h_{SP}}$	$M_{0.4}/M_{0.4_{SP}}$
244	.4603	.4650	-.5602	.5227	1.7839	.5603	.6392
248	.4590	.4638	-.5578	.5209	1.7825	.5578	.6363
252	.4573	.4624	-.5555	.5188	1.7812	.5552	.6331
256	.4555	.4610	-.5537	.5162	1.7798	.5526	.6297
260	.4536	.4600	-.5525	.5135	1.7780	.5502	.6264
264	.4521	.4594	-.5517	.5111	1.7756	.5481	.6235
268	.4511	.4591	-.5511	.5094	1.7734	.5465	.6212
272	.4503	.4590	-.5505	.5084	1.7709	.5453	.6196
276	.4501	.4588	-.5497	.5077	1.7688	.5443	.6183
280	.4495	.4585	-.5488	.5070	1.7676	.5432	.6170
284	.4487	.4580	-.5479	.5057	1.7679	.5419	.6152
288	.4474	.4572	-.5470	.5039	1.7702	.5403	.6130
292	.4460	.4560	-.5462	.5017	1.7751	.5385	.6106
296	.4449	.4546	-.5451	.4998	1.7830	.5367	.6082
300	.4446	.4528	-.5434	.4986	1.7942	.5352	.6062
304	.4443	.4507	-.5410	.4982	1.8089	.5339	.6047
308	.4454	.4483	-.5382	.4982	1.8269	.5325	.6032
312	.4451	.4459	-.5353	.4972	1.8478	.5306	.6011
316	.4432	.4437	-.5334	.4942	1.8712	.5277	.5973
320	.4389	.4422	-.5334	.4882	1.8963	.5240	.5917
324	.4326	.4418	-.5353	.4795	1.9223	.5197	.5846
328	.4255	.4425	-.5410	.4698	1.9483	.5160	.5775
332	.4196	.4445	-.5482	.4615	1.9734	.5144	.5728
336	.4176	.4472	-.5561	.4580	1.9968	.5162	.5730
340	.4209	.4502	-.5632	.4619	2.0178	.5225	.5801
344	.4309	.4528	-.5680	.4743	2.0359	.5334	.5946
348	.4467	.4545	-.5697	.4946	2.0506	.5480	.6154
352	.4663	.4549	-.5682	.5201	2.0623	.5645	.6400
356	.4867	.4541	-.5642	.5466	2.0706	.5805	.6646
360	.5046	.4523	-.5590	.5700	2.0758	.5937	.6856

TABLE 12b – HARMONIC CONTENT OF SIGNALS

n	$\frac{(F_x)_n}{\bar{F}_{x_{SP}}}$	$(\phi_x)_n$ (deg)	$\frac{(F_y)_n}{\bar{F}_{y_{SP}}}$	$(\phi_y)_n$ (deg)	$\frac{(M_x)_n}{\lvert\bar{M}_{x_{SP}}\rvert}$	$(\phi_x)_n$ (deg)	$\frac{(M_y)_n}{\bar{M}_{y_{SP}}}$	$(\phi_y)_n$ (deg)
1	.0398	101.0	.0098	-107.7	.0094	-52.3	.0471	105.5
2	.0122	74.6	.0042	84.5	.0030	-102.6	.0165	77.5
3	.0105	79.3	.0016	22.5	.0035	158.3	.0140	81.7
4	.0089	71.4	.0015	-6.8	.0036	134.4	.0110	71.7
5	.0064	60.1	.0015	-18.1	.0031	132.0	.0086	57.7
6	.0055	41.7	.0007	-37.9	.0022	107.6	.0075	42.3
7	.0054	33.8	.0028	-96.7	.0045	72.2	.0069	33.4
8	.0038	34.2	.0006	-11.2	.0010	96.0	.0050	32.5
9	.0022	29.7	.0004	-61.2	.0013	64.8	.0032	29.4
10	.0014	6.6	.0003	-146.7	.0009	24.4	.0019	14.7

n	$\frac{(M_z)_n}{\lvert\bar{M}_{z_{SP}}\rvert}$	$(\phi_z)_n$ (deg)	$\frac{(M_h)_n}{\bar{M}_{h_{SP}}}$	$(\phi_h)_n$ (deg)	$\frac{(M_{0.4})_n}{\bar{M}_{0.4_{SP}}}$	$(\phi_{0.4})_n$ (deg)
1	.1537	63.6	.0404	107.9	.0555	108.3
2	.0392	2.1	.0123	77.8	.0174	78.6
3	.0221	-17.0	.0091	71.1	.0136	76.2
4	.0122	-39.9	.0065	56.6	.0097	62.6
5	.0070	-100.8	.0055	40.8	.0083	46.4
6	.0115	-132.4	.0048	29.1	.0072	34.4
7	.0164	-132.9	.0032	11.9	.0054	23.5
8	.0111	-132.7	.0030	22.8	.0046	25.8
9	.0084	-127.3	.0016	15.4	.0028	21.9
10	.0050	-165.1	.0009	15.5	.0016	19.5

TABLE 13 – EXPERIMENTAL LOADS DURING QUASI-STEADY CRASH FORWARD AT $V = 0.81$ M/SEC, $n = 9.35$ REV/SEC, $(P/D)_{0.7} = 1.39$

TABLE 13a – SIGNALS RECONSTRUCTED FROM FIRST TEN HARMONICS (Five for M_z)

θ	$F_x/\bar{F}_{x_{SP}}$	$F_y/\bar{F}_{y_{SP}}$	$M_x/\lvert\bar{M}_{x_{SP}}\rvert$	$M_y/\bar{M}_{y_{SP}}$	$M_z/\lvert\bar{M}_{z_{SP}}\rvert$	$M_h/\bar{M}_{h_{SP}}$	$M_{0.4}/M_{0.4_{SP}}$
0	1.0295	.9561	-1.1672	1.1540	4.1808	1.2091	1.3853
4	1.0333	.9577	-1.1699	1.1571	4.1950	1.2120	1.3882
8	1.0370	.9594	-1.1728	1.1600	4.2084	1.2149	1.3910
12	1.0410	.9611	-1.1761	1.1633	4.2210	1.2183	1.3945
16	1.0453	.9631	-1.1798	1.1672	4.2330	1.2223	1.3989
20	1.0497	.9651	-1.1836	1.1716	4.2444	1.2268	1.4040
24	1.0539	.9672	-1.1871	1.1760	4.2551	1.2313	1.4093
28	1.0575	.9691	-1.1902	1.1801	4.2653	1.2354	1.4142
32	1.0605	.9706	-1.1925	1.1836	4.2749	1.2388	1.4184
36	1.0625	.9717	-1.1942	1.1861	4.2839	1.2412	1.4214
40	1.0639	.9722	-1.1952	1.1876	4.2923	1.2427	1.4233
44	1.0647	.9724	-1.1958	1.1884	4.3001	1.2435	1.4242
48	1.0650	.9721	-1.1959	1.1885	4.3071	1.2438	1.4244
52	1.0651	.9714	-1.1958	1.1883	4.3132	1.2437	1.4242
56	1.0649	.9705	-1.1954	1.1880	4.3184	1.2435	1.4240
60	1.0643	.9693	-1.1949	1.1876	4.3224	1.2433	1.4240
64	1.0639	.9682	-1.1945	1.1874	4.3253	1.2435	1.4245
68	1.0635	.9673	-1.1944	1.1876	4.3269	1.2441	1.4257
72	1.0636	.9667	-1.1948	1.1885	4.3271	1.2454	1.4277
76	1.0646	.9665	-1.1957	1.1901	4.3258	1.2474	1.4304
80	1.0667	.9669	-1.1972	1.1927	4.3230	1.2499	1.4336
84	1.0701	.9677	-1.1990	1.1960	4.3186	1.2529	1.4371
88	1.0745	.9687	-1.2009	1.1998	4.3127	1.2559	1.4405
92	1.0794	.9696	-1.2024	1.2038	4.3053	1.2587	1.4434
96	1.0840	.9703	-1.2035	1.2074	4.2963	1.2610	1.4458
100	1.0877	.9706	-1.2042	1.2102	4.2858	1.2627	1.4476
104	1.0895	.9706	-1.2044	1.2120	4.2740	1.2639	1.4489
105	1.0903	.9703	-1.2044	1.2128	4.2608	1.2646	1.4500
112	1.0891	.9699	-1.2044	1.2126	4.2464	1.2650	1.4509
116	1.0867	.9694	-1.2045	1.2116	4.2309	1.2651	1.4518
120	1.0835	.9690	-1.2044	1.2101	4.2144	1.2650	1.4524

TABLE 13a – (Continued)

θ	$F_x/\bar{F}_{x_{SP}}$	$F_y/\bar{F}_{y_{SP}}$	$M_x/\lvert\bar{M}_{x_{SP}}\rvert$	$M_y/\bar{M}_{y_{SP}}$	$M_z/\lvert\bar{M}_{z_{SP}}\rvert$	$M_h/\bar{M}_{h_{SP}}$	$M_{0.4}/M_{0.4_{SP}}$
124	1.0798	.9685	-1.2042	1.2081	4.1970	1.2645	1.4525
128	1.0762	.9678	-1.2037	1.2058	4.1789	1.2635	1.4519
132	1.0726	.9670	-1.2026	1.2032	4.1601	1.2618	1.4504
136	1.0692	.9659	-1.2011	1.2004	4.1407	1.2596	1.4481
140	1.0658	.9646	-1.1991	1.1973	4.1210	1.2570	1.4452
144	1.0625	.9631	-1.1969	1.1940	4.1009	1.2541	1.4418
148	1.0591	.9616	-1.1947	1.1906	4.0805	1.2510	1.4382
152	1.0557	.9602	-1.1924	1.1871	4.0600	1.2478	1.4345
156	1.0521	.9588	-1.1900	1.1834	4.0393	1.2444	1.4304
160	1.0483	.9574	-1.1875	1.1794	4.0185	1.2406	1.4259
164	1.0443	.9561	-1.1849	1.1750	3.9975	1.2364	1.4207
168	1.0398	.9547	-1.1820	1.1701	3.9762	1.2318	1.4150
172	1.0350	.9534	-1.1790	1.1647	3.9547	1.2267	1.4086
176	1.0296	.9521	-1.1760	1.1588	3.9328	1.2213	1.4019
180	1.0242	.9510	-1.1730	1.1528	3.9106	1.2158	1.3950
184	1.0184	.9499	-1.1701	1.1466	3.8879	1.2103	1.3881
188	1.0124	.9488	-1.1671	1.1403	3.8647	1.2047	1.3812
192	1.0063	.9475	-1.1638	1.1338	3.8412	1.1988	1.3740
196	1.0001	.9458	-1.1599	1.1272	3.8174	1.1926	1.3604
200	.9936	.9435	-1.1554	1.1202	3.7934	1.1858	1.3582
204	.9869	.9405	-1.1502	1.1128	3.7695	1.1786	1.3495
208	.9800	.9367	-1.1445	1.1052	3.7461	1.1711	1.3406
212	.9730	.9326	-1.1387	1.0975	3.7234	1.1636	1.3317
216	.9662	.9282	-1.1331	1.0899	3.7019	1.1565	1.3232
220	.9598	.9239	-1.1277	1.0828	3.6820	1.1498	1.3152
224	.9538	.9199	-1.1226	1.0763	3.6642	1.1435	1.3078
228	.9485	.9164	-1.1177	1.0703	3.6488	1.1375	1.3007
232	.9438	.9131	-1.1128	1.0647	3.6364	1.1315	1.2935
236	.9394	.9103	-1.1078	1.0593	3.6273	1.1254	1.2861
240	.9355	.9077	-1.1028	1.0541	3.6216	1.1193	1.2785

TABLE 13a – (Continued)

θ	$F_x/\bar{F}_{x_{SP}}$	$F_y/\bar{F}_{y_{SP}}$	$M_x/\lvert\bar{M}_{x_{SP}}\rvert$	$M_y/\bar{M}_{y_{SP}}$	$M_z/\lvert\bar{M}_{z_{SP}}\rvert$	$M_h/\bar{M}_{h_{SP}}$	$M_{0.4}/M_{0.4_{SP}}$
244	.9315	.9054	-1.0981	1.0491	3.6197	1.1133	1.2710
248	.9287	.9036	-1.0940	1.0447	3.6215	1.1080	1.2643
252	.9261	.9024	-1.0911	1.0410	3.6270	1.1037	1.2588
256	.9245	.9020	-1.0894	1.0385	3.6361	1.1009	1.2551
260	.9239	.9022	-1.0890	1.0374	3.6486	1.0997	1.2532
264	.9247	.9031	-1.0895	1.0377	3.6641	1.0998	1.2531
268	.9256	.9045	-1.0907	1.0390	3.6823	1.1010	1.2544
272	.9276	.9061	-1.0922	1.0412	3.7028	1.1028	1.2566
276	.9299	.9077	-1.0938	1.0439	3.7250	1.1051	1.2594
280	.9323	.9094	-1.0956	1.0468	3.7487	1.1076	1.2625
284	.9348	.9110	-1.0976	1.0498	3.7733	1.1105	1.2561
288	.9373	.9128	-1.1001	1.0529	3.7986	1.1137	1.2701
292	.9401	.9147	-1.1030	1.0563	3.8241	1.1173	1.2745
296	.9432	.9167	-1.1061	1.0599	3.8497	1.1211	1.2790
300	.9467	.9189	-1.1091	1.0637	3.8750	1.1248	1.2834
304	.9503	.9209	-1.1115	1.0676	3.9000	1.1281	1.2872
308	.9545	.9227	-1.1131	1.0714	3.9245	1.1308	1.2903
312	.9587	.9241	-1.1141	1.0751	3.9485	1.1330	1.2927
316	.9630	.9253	-1.1148	1.0789	3.9718	1.1352	1.2952
320	.9675	.9265	-1.1160	1.0832	3.9945	1.1380	1.2985
324	.9727	.9280	-1.1182	1.0884	4.0166	1.1422	1.3036
328	.9784	.9301	-1.1220	1.0948	4.0379	1.1483	1.3111
332	.9850	.9330	-1.1275	1.1027	4.0585	1.1563	1.3211
336	.9922	.9365	-1.1343	1.1116	4.0784	1.1658	1.3329
340	.9998	.9405	-1.1417	1.1210	4.0975	1.1759	1.3455
344	1.0073	.9445	-1.1489	1.1302	4.1158	1.1856	1.3575
348	1.0142	.9483	-1.1552	1.1384	4.1333	1.1940	1.3678
352	1.0202	.9515	-1.1602	1.1451	4.1500	1.2007	1.3759
356	1.0253	.9540	-1.1641	1.1502	4.1658	1.2056	1.3815
360	1.0295	.9561	-1.1672	1.1540	4.1808	1.2091	1.3853

TABLE 13b – HARMONIC CONTENT OF SIGNALS

n	$\frac{(F_x)_n}{\bar{F}_{x_{SP}}}$	$(\phi_x)_n$ (deg)	$\frac{(F_y)_n}{\bar{F}_{y_{SP}}}$	$(\phi_y)_n$ (deg)	$\frac{(M_x)_n}{\lvert\bar{M}_{x_{SP}}\rvert}$	$(\phi_x)_n$ (deg)	$\frac{(M_y)_n}{\bar{M}_{y_{SP}}}$	$(\phi_y)_n$ (deg)
1	.0757	89.1	.0323	85.3	.0555	-85.9	.0816	91.6
2	.0132	-24.2	.0083	-.9	.0119	177.7	.0167	-20.5
3	.0024	20.6	.0012	-175.3	.0009	-63.0	.0024	24.0
4	.0042	76.3	.0032	92.5	.0033	-89.9	.0038	77.6
5	.0018	-162.8	.0009	-67.5	.0011	170.7	.0005	-109.2
6	.0024	-78.6	.0005	-84.8	.0013	118.1	.0026	-71.9
7	.0010	-25.0	.0010	-48.2	.0015	106.3	.0015	-61.6
8	.0003	127.6	.0003	-30.7	.0007	121.5	.0004	-71.5
9	.0005	-96.4	.0003	-56.2	.0007	85.3	.0006	-70.7
10	.0006	-89.0	.0004	-126.2	.0008	28.3	.0006	-109.2

n	$\frac{(M_z)_n}{\lvert\bar{M}_{z_{SP}}\rvert}$	$(\phi_z)_n$ (deg)	$\frac{(M_h)_n}{\bar{M}_{h_{SP}}}$	$(\phi_h)_n$ (deg)	$\frac{(M_{0.4})_n}{\bar{M}_{0.4_{SP}}}$	$(\phi_{0.4})_n$ (deg)
1	.3346	63.5	.0783	94.7	.0937	95.7
2	.0436	-59.0	.0165	-13.9	.0208	-14.8
3	.0181	-147.0	.0019	39.5	.0025	36.6
4	.0051	62.2	.0036	82.7	.0037	81.7
5	.0013	-39.9	.0011	-5.0	.0019	-1.0
6	.0094	-160.6	.0024	-64.4	.0030	-62.3
7	.0139	-170.2	.0019	-78.0	.0025	-83.1
8	.0152	-163.7	.0009	-66.8	.0013	-66.4
9	.0125	-159.3	.0008	-80.3	.0009	-72.3
10	.0103	-146.8	.0008	-140.5	.0009	-143.0

TABLE 14 – EXPERIMENTAL LOADS DURING QUASI-STEADY CRASH FORWARD AT $V = 1.46$ M/SEC, $n = 11.19$ REV/SEC, $(P/D)_{0.7} = 1.39$

TABLE 14a – SIGNALS RECONSTRUCTED FROM FIRST TEN HARMONICS (Five for M_z)

θ	$F_x/\bar{F}_{x_{SP}}$	$F_y/\bar{F}_{y_{SP}}$	$M_x/\lvert\bar{M}_{x_{SP}}\rvert$	$M_y/\bar{M}_{y_{SP}}$	$M_z/\lvert\bar{M}_{z_{SP}}\rvert$	$M_h/\bar{M}_{h_{SP}}$	$M_{0.4}/M_{0.4_{SP}}$
0	1.2304	1.2363	-1.4527	1.3415	5.1659	1.4139	1.5824
4	1.2464	1.2482	-1.4682	1.3594	5.2337	1.4318	1.6034
8	1.2607	1.2582	-1.4820	1.3752	5.2964	1.4479	1.6222
12	1.2733	1.2667	-1.4946	1.3893	5.3536	1.4627	1.6397
16	1.2844	1.2744	-1.5070	1.4022	5.4049	1.4770	1.6565
20	1.2946	1.2822	-1.5195	1.4147	5.4501	1.4913	1.6736
24	1.3049	1.2904	-1.5326	1.4275	5.4892	1.5061	1.6915
28	1.3153	1.2994	-1.5460	1.4409	5.5218	1.5214	1.7101
32	1.3260	1.3087	-1.5592	1.4547	5.5479	1.5368	1.7288
36	1.3365	1.3177	-1.5716	1.4683	5.5675	1.5515	1.7468
40	1.3463	1.3256	-1.5823	1.4807	5.5804	1.5646	1.7629
44	1.3545	1.3316	-1.5903	1.4910	5.5868	1.5753	1.7761
48	1.3604	1.3352	-1.5965	1.4985	5.5869	1.5831	1.7858
52	1.3636	1.3361	-1.5993	1.5028	5.5811	1.5878	1.7919
56	1.3643	1.3345	-1.5994	1.5042	5.5700	1.5895	1.7945
60	1.3632	1.3311	-1.5972	1.5034	5.5544	1.5888	1.7944
64	1.3614	1.3264	-1.5932	1.5015	5.5350	1.5865	1.7923
68	1.3601	1.3215	-1.5883	1.4996	5.5130	1.5835	1.7892
72	1.3605	1.3169	-1.5831	1.4986	5.4892	1.5805	1.7858
76	1.3632	1.3131	-1.5783	1.4992	5.4647	1.5781	1.7827
80	1.3679	1.3102	-1.5741	1.5011	5.4402	1.5763	1.7802
84	1.3735	1.3079	-1.5706	1.5039	5.4165	1.5752	1.7781
88	1.3796	1.3058	-1.5675	1.5066	5.3938	1.5743	1.7762
92	1.3836	1.3034	-1.5645	1.5082	5.3722	1.5732	1.7744
96	1.3849	1.3002	-1.5614	1.5080	5.3516	1.5715	1.7723
100	1.3826	1.2963	-1.5581	1.5057	5.3316	1.5692	1.7700
104	1.3771	1.2919	-1.5546	1.5014	5.3113	1.5662	1.7676
108	1.3692	1.2871	-1.5510	1.4959	5.2902	1.5630	1.7652
112	1.3601	1.2826	-1.5476	1.4897	5.2674	1.5597	1.7630
116	1.3510	1.2784	-1.5444	1.4837	5.2422	1.5565	1.7610
120	1.3429	1.2746	-1.5411	1.4782	5.2140	1.5533	1.7587

TABLE 14a – (Continued)

θ	$F_x/\bar{F}_{x_{SP}}$	$F_y/\bar{F}_{y_{SP}}$	$M_x/\lvert\bar{M}_{x_{SP}}\rvert$	$M_y/\bar{M}_{y_{SP}}$	$M_z/\lvert\bar{M}_{z_{SP}}\rvert$	$M_h/\bar{M}_{h_{SP}}$	$M_{0.4}/M_{0.4_{SP}}$
124	1.3361	1.2710	-1.5375	1.4732	5.1825	1.5498	1.7557
128	1.3302	1.2673	-1.5333	1.4683	5.1476	1.5456	1.7516
132	1.3246	1.2633	-1.5283	1.4630	5.1096	1.5405	1.7460
136	1.3186	1.2588	-1.5225	1.4566	5.0688	1.5342	1.7388
140	1.3116	1.2540	-1.5163	1.4492	5.0260	1.5268	1.7303
144	1.3035	1.2492	-1.5099	1.4406	4.9820	1.5189	1.7209
148	1.2944	1.2444	-1.5035	1.4312	4.9376	1.5103	1.7111
152	1.2846	1.2398	-1.4974	1.4214	4.8937	1.5016	1.7012
156	1.2746	1.2350	-1.4911	1.4115	4.8509	1.4932	1.6913
160	1.2645	1.2298	-1.4842	1.4016	4.8096	1.4844	1.6812
164	1.2544	1.2236	-1.4763	1.3914	4.7701	1.4750	1.6706
168	1.2439	1.2163	-1.4672	1.3807	4.7321	1.4648	1.6591
172	1.2329	1.2080	-1.4569	1.3693	4.6955	1.4536	1.6465
176	1.2212	1.1992	-1.4459	1.3571	4.6596	1.4416	1.6329
180	1.2089	1.1907	-1.4352	1.3442	4.6238	1.4292	1.6188
184	1.1961	1.1832	-1.4252	1.3310	4.5876	1.4169	1.6045
188	1.1835	1.1772	-1.4165	1.3179	4.5504	1.4049	1.5904
192	1.1714	1.1724	-1.4089	1.3053	4.5119	1.3935	1.5768
196	1.1599	1.1684	-1.4018	1.2932	4.4720	1.3824	1.5634
200	1.1491	1.1643	-1.3943	1.2815	4.4311	1.3714	1.5501
204	1.1387	1.1591	-1.3858	1.2700	4.3898	1.3600	1.5363
208	1.1286	1.1522	-1.3758	1.2584	4.3490	1.3480	1.5220
212	1.1165	1.1436	-1.3645	1.2467	4.3100	1.3355	1.5074
216	1.1085	1.1339	-1.3523	1.2350	4.2739	1.3229	1.4928
220	1.0988	1.1239	-1.3402	1.2237	4.2421	1.3107	1.4787
224	1.0895	1.1144	-1.3290	1.2131	4.2157	1.2993	1.4657
228	1.0811	1.1064	-1.3190	1.2036	4.1956	1.2892	1.4542
232	1.0735	1.0999	-1.3105	1.1953	4.1823	1.2803	1.4439
236	1.0671	1.0948	-1.3031	1.1882	4.1758	1.2724	1.4349
240	1.0616	1.0908	-1.2966	1.1821	4.1759	1.2655	1.4269

TABLE 14a – (Continued)

θ	$F_x/\bar{F}_{x_{SP}}$	$F_y/\bar{F}_{y_{SP}}$	$M_x/\lvert\bar{M}_{x_{SP}}\rvert$	$M_y/\bar{M}_{y_{SP}}$	$M_z/\lvert\bar{M}_{z_{SP}}\rvert$	$M_h/\bar{M}_{h_{SP}}$	$M_{0.4}/M_{0.4_{SP}}$
244	1.0571	1.0875	-1.2909	1.1769	4.1816	1.2594	1.4199
248	1.0535	1.0848	-1.2861	1.1728	4.1918	1.2544	1.4140
252	1.0511	1.0826	-1.2825	1.1699	4.2050	1.2507	1.4097
256	1.0501	1.0812	-1.2804	1.1686	4.2196	1.2488	1.4075
260	1.0504	1.0810	-1.2800	1.1690	4.2340	1.2488	1.4077
264	1.0521	1.0817	-1.2809	1.1710	4.2470	1.2506	1.4099
268	1.0546	1.0831	-1.2824	1.1742	4.2573	1.2533	1.4135
272	1.0574	1.0846	-1.2836	1.1779	4.2644	1.2562	1.4174
276	1.0593	1.0853	-1.2838	1.1811	4.2683	1.2584	1.4205
280	1.0614	1.0851	-1.2827	1.1832	4.2692	1.2591	1.4220
284	1.0619	1.0840	-1.2805	1.1838	4.2682	1.2585	1.4216
288	1.0616	1.0827	-1.2783	1.1833	4.2667	1.2569	1.4198
292	1.0617	1.0822	-1.2773	1.1821	4.2662	1.2553	1.4174
296	1.0625	1.0836	-1.2785	1.1814	4.2686	1.2546	1.4156
300	1.0650	1.0875	-1.2825	1.1819	4.2757	1.2555	1.4150
304	1.0693	1.0941	-1.2890	1.1842	4.2892	1.2582	1.4160
308	1.0759	1.1026	-1.2972	1.1883	4.3105	1.2622	1.4184
312	1.0839	1.1120	-1.3056	1.1937	4.3405	1.2670	1.4215
316	1.0926	1.1211	-1.3135	1.1998	4.3798	1.2719	1.4249
320	1.1014	1.1291	-1.3201	1.2061	4.4282	1.2764	1.4281
324	1.1099	1.1359	-1.3259	1.2124	4.4853	1.2809	1.4317
328	1.1183	1.1419	-1.3318	1.2190	4.5502	1.2861	1.4364
332	1.1270	1.1481	-1.3391	1.2267	4.6214	1.2932	1.4436
336	1.1369	1.1557	-1.3491	1.2363	4.6975	1.3032	1.4544
340	1.1485	1.1655	-1.3623	1.2487	4.7763	1.3166	1.4694
344	1.1623	1.1777	-1.3786	1.2641	4.8575	1.3333	1.4887
348	1.1781	1.1920	-1.3971	1.2821	4.9382	1.3527	1.5111
352	1.1953	1.2073	-1.4165	1.3018	5.0172	1.3735	1.5352
356	1.2131	1.2224	-1.4353	1.3221	5.0934	1.3943	1.5595
360	1.2304	1.2363	-1.4527	1.3415	5.1658	1.4139	1.5824

TABLE 14b – HARMONIC CONTENT OF SIGNALS

n	$\frac{(F_x)_n}{\overline{F}_{x_{SP}}}$	$(\phi_x)_n$ (deg)	$\frac{(F_y)_n}{\overline{F}_{y_{SP}}}$	$(\phi_y)_n$ (deg)	$\frac{(M_x)_n}{\lvert\overline{M}_{x_{SP}}\rvert}$	$(\phi_x)_n$ (deg)	$\frac{(M_y)_n}{\overline{M}_{y_{SP}}}$	$(\phi_y)_n$ (deg)
1	.1686	36.6	.1213	80.3	.1571	-93.2	.1777	89.9
2	.0067	72.6	.0202	57.3	.0237	-115.1	.0104	87.9
3	.0078	93.2	.0073	115.5	.0127	-61.2	.0138	113.4
4	.0056	58.9	.0020	122.0	.0037	-53.3	.0059	79.0
5	.0015	134.7	.0022	-77.0	.0029	110.3	.0009	-24.6
6	.0032	-125.6	.0015	-159.8	.0006	69.3	.0021	-93.7
7	.0023	2.2	.0035	28.5	.0035	-147.9	.0020	7.4
8	.0037	45.5	.0019	27.4	.0021	-166.9	.0032	38.8
9	.0014	86.0	.0022	32.2	.0021	-170.3	.0017	58.5
10	.0007	-75.2	.0010	-86.0	.0012	82.1	.0008	-68.2

n	$\frac{(M_z)_n}{\lvert\overline{M}_{z_{SP}}\rvert}$	$(\phi_z)_n$ (deg)	$\frac{(M_h)_n}{\overline{M}_{h_{SP}}}$	$(\phi_h)_n$ (deg)	$\frac{(M_{0.4})_n}{\overline{M}_{0.4_{SP}}}$	$(\phi_{0.4})_n$ (deg)
1	.5971	58.7	.1765	91.5	.2023	93.7
2	.0946	57.4	.0168	81.0	.0187	89.0
3	.0713	76.2	.0171	119.3	.0227	121.7
4	.0295	37.2	.0055	102.0	.0071	104.7
5	.0194	-88.3	.0026	-47.4	.0039	-40.9
6	.0110	-153.1	.0016	-53.9	.0025	-33.1
7	.0035	89.0	.0022	23.8	.0021	24.0
8	.0050	2.3	.0025	23.9	.0027	20.6
9	.0072	-19.1	.0017	23.6	.0021	22.1
10	.0017	-29.5	.0009	-86.1	.0009	-80.6

TABLE 15 – EXPERIMENTAL LOADS DURING QUASI-STEADY CRASH FORWARD AT $V = 2.26$ M/SEC, $n = 12.07$ REV/SEC, $(P/D)_{0.7} = 1.39$

TABLE 15a – SIGNALS RECONSTRUCTED FROM FIRST TEN HARMONICS (Five for M_z)

θ	$F_x/\bar{F}_{x_{SP}}$	$F_y/\bar{F}_{y_{SP}}$	$M_x/\lvert\bar{M}_{x_{SP}}\rvert$	$M_y/\bar{M}_{y_{SP}}$	$M_z/\lvert\bar{M}_{z_{SP}}\rvert$	$M_h/\bar{M}_{h_{SP}}$	$M_{0.4}/M_{0.4_{SP}}$
0	1.1145	1.2095	-1.3664	1.1811	4.5820	1.2496	1.3632
4	1.1417	1.2310	-1.3922	1.2110	4.6909	1.2788	1.3972
8	1.1627	1.2466	-1.4119	1.2346	4.7905	1.3021	1.4246
12	1.1772	1.2572	-1.4270	1.2517	4.8793	1.3201	1.4462
16	1.1866	1.2652	-1.4402	1.2642	4.9565	1.3351	1.4644
20	1.1936	1.2733	-1.4539	1.2747	5.0217	1.3494	1.4819
24	1.2008	1.2831	-1.4697	1.2858	5.0749	1.3650	1.5007
28	1.2101	1.2952	-1.4875	1.2989	5.1165	1.3824	1.5215
32	1.2216	1.3086	-1.5060	1.3140	5.1470	1.4008	1.5433
36	1.2343	1.3216	-1.5231	1.3297	5.1675	1.4187	1.5643
40	1.2465	1.3322	-1.5369	1.3441	5.1791	1.4340	1.5824
44	1.2564	1.3391	-1.5461	1.3555	5.1829	1.4453	1.5960
48	1.2635	1.3419	-1.5506	1.3633	5.1801	1.4524	1.6046
52	1.2683	1.3413	-1.5511	1.3681	5.1719	1.4558	1.6090
56	1.2728	1.3386	-1.5488	1.3712	5.1592	1.4567	1.6103
60	1.2782	1.3348	-1.5449	1.3747	5.1430	1.4566	1.6101
64	1.2866	1.3310	-1.5403	1.3796	5.1240	1.4564	1.6095
68	1.2978	1.3275	-1.5353	1.3865	5.1028	1.4567	1.6091
72	1.3109	1.3243	-1.5301	1.3945	5.0797	1.4572	1.6087
76	1.3235	1.3210	-1.5248	1.4022	5.0552	1.4575	1.6081
80	1.3333	1.3174	-1.5196	1.4079	5.0292	1.4571	1.6068
84	1.3384	1.3136	-1.5149	1.4103	5.0018	1.4556	1.6047
88	1.3381	1.3097	-1.5110	1.4091	4.9730	1.4532	1.6022
92	1.3327	1.3060	-1.5081	1.4048	4.9427	1.4504	1.5996
96	1.3239	1.3026	-1.5060	1.3985	4.9107	1.4473	1.5973
100	1.3134	1.2995	-1.5042	1.3916	4.8768	1.4443	1.5954
104	1.3030	1.2963	-1.5021	1.3849	4.8409	1.4414	1.5937
108	1.2937	1.2929	-1.4993	1.3789	4.8028	1.4384	1.5918
112	1.2856	1.2888	-1.4954	1.3733	4.7623	1.4347	1.5890
116	1.2776	1.2841	-1.4905	1.3673	4.7194	1.4301	1.5849
120	1.2695	1.2787	-1.4848	1.3602	4.6740	1.4242	1.5790

TABLE 15a – (Continued)

θ	$F_x/\bar{F}_{x_{SP}}$	$F_y/\bar{F}_{y_{SP}}$	$M_x/\lvert\bar{M}_{x_{SP}}\rvert$	$M_y/\bar{M}_{y_{SP}}$	$M_z/\lvert\bar{M}_{z_{SP}}\rvert$	$M_h/\bar{M}_{h_{SP}}$	$M_{0.4}/M_{0.4_{SP}}$
124	1.2597	1.2727	-1.4785	1.3512	4.6262	1.4169	1.5712
128	1.2479	1.2662	-1.4717	1.3402	4.5758	1.4092	1.5615
132	1.2342	1.2589	-1.4642	1.3272	4.5233	1.3981	1.5502
136	1.2190	1.2510	-1.4558	1.3126	4.4686	1.3867	1.5376
140	1.2029	1.2421	-1.4462	1.2975	4.4120	1.3743	1.5238
144	1.1867	1.2324	-1.4354	1.2819	4.3539	1.3611	1.5091
148	1.1706	1.2221	-1.4236	1.2663	4.2946	1.3474	1.4939
152	1.1548	1.2116	-1.4113	1.2507	4.2343	1.3334	1.4783
156	1.1390	1.2010	-1.3989	1.2350	4.1736	1.3191	1.4624
160	1.1229	1.1904	-1.3864	1.2190	4.1125	1.3047	1.4462
164	1.1062	1.1796	-1.3737	1.2023	4.0515	1.2897	1.4293
168	1.0888	1.1683	-1.3603	1.1849	3.9907	1.2739	1.4115
172	1.0708	1.1561	-1.3458	1.1667	3.9302	1.2572	1.3926
176	1.0523	1.1430	-1.3301	1.1478	3.8702	1.2394	1.3727
180	1.0335	1.1293	-1.3134	1.1288	3.8106	1.2211	1.3520
184	1.0158	1.1156	-1.2964	1.1100	3.7515	1.2026	1.3311
188	.9985	1.1027	-1.2799	1.0921	3.6927	1.1847	1.3107
192	.9830	1.0910	-1.2644	1.0752	3.6344	1.1676	1.2912
196	.9683	1.0805	-1.2501	1.0594	3.5765	1.1515	1.2727
200	.9544	1.0705	-1.2364	1.0444	3.5191	1.1360	1.2548
204	.9408	1.0601	-1.2222	1.0295	3.4626	1.1205	1.2369
208	.9269	1.0482	-1.2067	1.0143	3.4071	1.1044	1.2185
212	.9124	1.0343	-1.1895	.9984	3.3531	1.0873	1.1993
216	.8973	1.0185	-1.1709	.9819	3.3012	1.0696	1.1795
220	.8820	1.0021	-1.1519	.9652	3.2518	1.0518	1.1598
224	.8671	.9862	-1.1338	.9492	3.2057	1.0348	1.1411
228	.8535	.9724	-1.1179	.9345	3.1635	1.0195	1.1240
232	.8418	.9614	-1.1047	.9217	3.1257	1.0062	1.1090
236	.8321	.9530	-1.0939	.9109	3.0927	.9947	1.0958
240	.8241	.9465	-1.0846	.9017	3.0649	.9846	1.0841

TABLE 15a – (Continued)

θ	$F_x/\bar{F}_{x_{SP}}$	$F_y/\bar{F}_{y_{SP}}$	$M_x/\lvert\bar{M}_{x_{SP}}\rvert$	$M_y/\bar{M}_{y_{SP}}$	$M_z/\lvert\bar{M}_{z_{SP}}\rvert$	$M_h/\bar{M}_{h_{SP}}$	$M_{0.4}/M_{0.4_{SP}}$
244	.8175	.9407	-1.0758	.8938	3.0423	.9754	1.0732
248	.8116	.9349	-1.0671	.8867	3.0249	.9667	1.0631
252	.8063	.9287	-1.0586	.8805	3.0126	.9589	1.0543
256	.8020	.9229	-1.0512	.8756	3.0050	.9527	1.0476
260	.7991	.9186	-1.0462	.8728	3.0015	.9491	1.0440
264	.7983	.9167	-1.0444	.8725	3.0017	.9486	1.0440
268	.7998	.9174	-1.0456	.8749	3.0050	.9509	1.0472
272	.8034	.9201	-1.0488	.8792	3.0112	.9550	1.0522
276	.8079	.9235	-1.0522	.8841	3.0199	.9593	1.0572
280	.8121	.9261	-1.0543	.8881	3.0311	.9622	1.0604
284	.8148	.9269	-1.0544	.8901	3.0451	.9630	1.0611
288	.8157	.9265	-1.0533	.8901	3.0623	.9620	1.0597
292	.8157	.9264	-1.0531	.8892	3.0836	.9610	1.0579
296	.8166	.9292	-1.0564	.8895	3.1099	.9622	1.0585
300	.8207	.9371	-1.0655	.8933	3.1422	.9678	1.0636
304	.8300	.9513	-1.0811	.9023	3.1819	.9788	1.0744
308	.8453	.9712	-1.1022	.9169	3.2299	.9947	1.0902
312	.8657	.9944	-1.1256	.9358	3.2874	1.0134	1.1087
316	.8891	1.0175	-1.1478	.9564	3.3550	1.0319	1.1266
320	.9122	1.0372	-1.1657	.9758	3.4331	1.0475	1.1413
324	.9325	1.0514	-1.1777	.9918	3.5218	1.0587	1.1512
328	.9485	1.0604	-1.1851	1.0036	3.6205	1.0661	1.1573
332	.9607	1.0665	-1.1910	1.0126	3.7283	1.0722	1.1625
336	.9714	1.0732	-1.1993	1.0217	3.8438	1.0804	1.1708
340	.9837	1.0841	-1.2137	1.0342	3.9653	1.0942	1.1859
344	1.0005	1.1013	-1.2361	1.0531	4.0905	1.1156	1.2100
348	1.0234	1.1251	-1.2659	1.0792	4.2173	1.1447	1.2430
352	1.0519	1.1534	-1.3001	1.1114	4.3430	1.1791	1.2824
356	1.0834	1.1828	-1.3349	1.1467	4.4653	1.2154	1.3239
360	1.1145	1.2095	-1.3664	1.1811	4.5820	1.2496	1.3632

TABLE 15b – HARMONIC CONTENT OF SIGNALS

n	$\frac{(F_x)_n}{\bar{F}_{x_{SP}}}$	$(\phi_x)_n$ (deg)	$\frac{(F_y)_n}{\bar{F}_{y_{SP}}}$	$(\phi_y)_n$ (deg)	$\frac{(M_x)_n}{\lvert\bar{M}_{x_{SP}}\rvert}$	$(\phi_x)_n$ (deg)	$\frac{(M_y)_n}{\bar{M}_{y_{SP}}}$	$(\phi_y)_n$ (deg)
1	.2627	84.2	.2073	80.9	.2490	-95.1	.2704	86.5
2	.0078	48.2	.0317	33.9	.0357	-140.4	.0126	59.4
3	.0080	-1.4	.0070	84.1	.0132	-75.5	.0079	69.7
4	.0080	25.0	.0038	137.0	.0070	-41.7	.0069	65.4
5	.0043	55.7	.0020	-128.1	.0021	39.1	.0032	51.8
6	.0053	140.7	.0027	116.6	.0020	-95.6	.0036	123.9
7	.0031	113.7	.0054	55.4	.0060	-130.3	.0040	89.1
8	.0042	38.1	.0047	39.9	.0055	-145.4	.0047	39.0
9	.0058	47.5	.0056	30.4	.0056	-160.9	.0065	39.8
10	.0023	42.9	.0031	-15.7	.0035	152.6	.0022	25.4

n	$\frac{(M_z)_n}{\lvert\bar{M}_{z_{SP}}\rvert}$	$(\phi_z)_n$ (deg)	$\frac{(M_h)_n}{\bar{M}_{h_{SP}}}$	$(\phi_h)_n$ (deg)	$\frac{(M_{0.4})_n}{\bar{M}_{0.4_{SP}}}$	$(\phi_{0.4})_n$ (deg)
1	1.0961	71.8	.2646	87.9	.2963	89.6
2	.1756	52.6	.0227	52.1	.0241	59.0
3	.0756	60.3	.0140	101.9	.0195	106.5
4	.0333	52.7	.0076	109.3	.0106	112.7
5	.0064	-5.7	.0009	64.8	.0011	54.3
6	.0091	23.8	.0022	85.4	.0025	61.5
7	.0233	57.6	.0049	64.0	.0058	64.1
8	.0295	34.9	.0052	35.8	.0058	36.3
9	.0191	3.8	.0056	25.6	.0061	22.7
10	.0105	-19.0	.0024	-10.9	.0026	-11.5

TABLE 16 – EXPERIMENTAL LOADS DURING QUASI-STEADY CRASH FORWARD AT $V = 3.10$ M/SEC, $n = 13.40$ REV/SEC, $(P/D)_{0.7} = 1.39$

TABLE 16a – SIGNALS RECONSTRUCTED FROM FIRST TEN HARMONICS (Five for M_z)

θ	$F_x/\bar{F}_{x_{SP}}$	$F_y/\bar{F}_{y_{SP}}$	$M_x/\lvert\bar{M}_{x_{SP}}\rvert$	$M_y/\bar{M}_{y_{SP}}$	$M_z/\lvert\bar{M}_{z_{SP}}\rvert$	$M_h/\bar{M}_{h_{SP}}$	$M_{0.4}/M_{0.4_{SP}}$
0	1.0983	1.1372	-1.2406	1.1494	+.1858	1.1636	1.2701
4	1.1279	1.1623	-1.2636	1.1816	4.3076	1.1910	1.3019
8	1.1452	1.1759	-1.2759	1.2011	4.4117	1.2073	1.3214
12	1.1515	1.1801	-1.2818	1.2097	+.4981	1.2159	1.3325
16	1.1505	1.1792	-1.2864	1.2114	+.5679	1.2215	1.3403
20	1.1471	1.1777	-1.2940	1.2112	4.6225	1.2284	1.3494
24	1.1457	1.1794	-1.3066	1.2128	4.6644	1.2386	1.3618
28	1.1479	1.1860	-1.3236	1.2178	4.6959	1.2521	1.3773
32	1.1542	1.1968	-1.3424	1.2261	+.7197	1.2668	1.3936
36	1.1632	1.2100	-1.3597	1.2358	4.7384	1.2803	1.4077
40	1.1730	1.2229	-1.3733	1.2452	4.7541	1.2906	1.4180
44	1.1825	1.2336	-1.3822	1.2536	4.7683	1.2974	1.4241
48	1.1931	1.2411	-1.3870	1.2614	4.7823	1.3018	1.4277
52	1.2052	1.2456	-1.3894	1.2703	4.7963	1.3059	1.4310
56	1.2210	1.2480	-1.3908	1.2819	4.8100	1.3115	1.4361
60	1.2410	1.2495	-1.3923	1.2971	4.8226	1.3194	1.4442
64	1.2645	1.2509	-1.3943	1.3157	+.8329	1.3295	1.4547
68	1.2903	1.2529	-1.3967	1.3360	4.8393	1.3406	1.4666
72	1.3147	1.2559	-1.3993	1.3558	4.8403	1.3516	1.4785
76	1.3355	1.2600	-1.4025	1.3731	4.8344	1.3615	1.4893
80	1.3511	1.2652	-1.4068	1.3870	4.8203	1.3704	1.4992
84	1.3613	1.2716	-1.4130	1.3973	+.7972	1.3786	1.5036
88	1.3671	1.2786	-1.4210	1.4047	4.7646	1.3867	1.5182
92	1.3695	1.2854	-1.4299	1.4101	4.7228	1.3947	1.5280
96	1.3705	1.2906	-1.4380	1.4139	4.6721	1.4019	1.5371
100	1.3694	1.2930	-1.4432	1.4159	4.6134	1.4071	1.5440
104	1.3661	1.2918	-1.4441	1.4152	4.5480	1.4087	1.5473
108	1.3597	1.2867	-1.4401	1.4111	4.4770	1.4062	1.5460
112	1.3495	1.2785	-1.4322	1.4030	4.4016	1.3996	1.5401
116	1.3356	1.2684	-1.4219	1.3912	+.3232	1.3898	1.5306
120	1.3187	1.2577	-1.4110	1.3767	+.2424	1.3783	1.5189

TABLE 16a – (Continued)

θ	$F_x/\bar{F}_{x_{SP}}$	$F_y/\bar{F}_{y_{SP}}$	$M_x/\lvert\bar{M}_{x_{SP}}\rvert$	$M_y/\bar{M}_{y_{SP}}$	$M_z/\lvert\bar{M}_{z_{SP}}\rvert$	$M_h/\bar{M}_{h_{SP}}$	$M_{0.4}/M_{0.4_{SP}}$
124	1.2993	1.2469	-1.4005	1.3604	4.1602	1.3659	1.5061
128	1.2801	1.2359	-1.3900	1.3429	4.0767	1.3530	1.4926
132	1.2595	1.2235	-1.3780	1.3243	3.9921	1.3387	1.4775
136	1.2376	1.2083	-1.3627	1.3041	3.9063	1.3219	1.4596
140	1.2137	1.1893	-1.3428	1.2813	3.8191	1.3016	1.4380
144	1.1870	1.1666	-1.3183	1.2555	3.7301	1.2776	1.4124
148	1.1575	1.1412	-1.2905	1.2271	3.6391	1.2508	1.3838
152	1.1267	1.1150	-1.2618	1.1973	3.5459	1.2227	1.3540
156	1.0959	1.0899	-1.2343	1.1678	3.4507	1.1954	1.3249
160	1.0670	1.0670	-1.2092	1.1401	3.3536	1.1700	1.2977
164	1.0411	1.0460	-1.1861	1.1149	3.2552	1.1466	1.2725
168	1.0160	1.0257	-1.1633	1.0917	3.1562	1.1241	1.2480
172	.9965	1.0043	-1.1387	1.0692	3.0574	1.1008	1.2225
176	.9748	.9803	-1.1107	1.0458	2.9596	1.0753	1.1944
180	.9513	.9535	-1.0793	1.0203	2.8636	1.0469	1.1637
184	.9253	.9251	-1.0461	.9924	2.7704	1.0165	1.1300
188	.8974	.8973	-1.0137	.9629	2.6804	.9858	1.0962
192	.8688	.8724	-.9847	.9335	2.5941	.9566	1.0638
196	.8412	.8521	-.9606	.9055	2.5116	.9301	1.0342
200	.8157	.8363	-.9409	.8796	2.4330	.9064	1.0072
204	.7923	.8235	-.9236	.8556	2.3581	.8842	.9816
208	.7703	.8115	-.9061	.8325	2.2866	.8620	.9556
212	.7483	.7978	-.8861	.8089	2.2181	.8383	.9280
216	.7254	.7812	-.8629	.7844	2.1524	.8127	.8987
220	.7016	.7618	-.8373	.7591	2.0893	.7862	.8687
224	.6779	.7409	-.8114	.7343	2.0286	.7603	.8400
228	.6558	.7206	-.7874	.7115	1.9704	.7370	.8144
232	.6367	.7024	-.7665	.6919	1.9150	.7171	.7927
236	.6212	.6866	-.7487	.6757	1.8627	.7004	.7744
240	.6086	.6727	-.7325	.6619	1.8143	.6854	.7579

TABLE 16a – (Continued)

θ	$F_x/\bar{F}_{x_{SP}}$	$F_y/\bar{F}_{y_{SP}}$	$M_x/\lvert\bar{M}_{x_{SP}}\rvert$	$M_y/\bar{M}_{y_{SP}}$	$M_z/\lvert\bar{M}_{z_{SP}}\rvert$	$M_h/\bar{M}_{h_{SP}}$	$M_{0.4}/M_{0.4_{SP}}$
244	.5973	.6593	-.7163	.6491	1.7702	.6706	.7413
248	.5863	.6454	-.6991	.6359	1.7310	.6549	.7236
252	.5742	.6310	-.6814	.6218	1.6976	.6387	.7053
256	.5617	.6172	-.6651	.6080	1.6702	.6234	.6884
260	.5504	.6059	-.6526	.5963	1.6495	.6116	.6755
264	.5427	.5990	-.6458	.5889	1.6361	.6050	.6685
268	.5393	.5970	-.6449	.5868	1.6300	.6042	.6680
272	.5423	.5992	-.6481	.5898	1.6318	.6076	.6721
276	.5483	.6034	-.6526	.5958	1.6418	.6128	.6779
280	.5553	.6072	-.6554	.6021	1.6605	.6170	.6823
284	.5600	.6091	-.6556	.6065	1.6885	.6187	.6839
288	.5640	.6097	-.6547	.6087	1.7265	.6187	.6838
292	.5660	.6120	-.6567	.6105	1.7755	.6203	.6853
296	.5703	.6201	-.6667	.6156	1.8363	.6277	.6931
300	.5811	.6382	-.6888	.6281	1.9101	.6447	.7113
304	.6020	.6684	-.7242	.6508	1.9977	.6728	.7410
308	.6341	.7095	-.7702	.6839	2.0997	.7102	.7801
312	.6753	.7573	-.8212	.7244	2.2167	.7524	.8236
316	.7209	.8055	-.8699	.7670	2.3484	.7934	.8650
320	.7649	.8481	-.9106	.8064	2.4943	.8282	.8992
324	.8028	.8810	-.9407	.8386	2.6531	.8545	.9242
328	.8323	.9039	-.9619	.8630	2.8226	.8737	.9422
332	.8551	.9201	-.9794	.8824	3.0005	.8904	.9587
336	.8755	.9351	-.9997	.9020	3.1835	.9106	.9804
340	.8989	.9546	-1.0281	.9273	3.3680	.9392	1.0128
344	.9294	.9825	-1.0664	.9619	3.5503	.9782	1.0575
348	.9682	1.0189	-1.1126	1.0060	3.7265	1.0257	1.1121
352	1.0129	1.0605	-1.1613	1.0560	3.8932	1.0767	1.1705
356	1.0583	1.1020	-1.2057	1.1059	4.0471	1.1245	1.2253
360	1.0983	1.1372	-1.2406	1.1494	4.1858	1.1636	1.2701

TABLE 16b – HARMONIC CONTENT OF SIGNALS

n	$\frac{(F_x)_n}{\bar{F}_{x_{SP}}}$	$(\phi_x)_n$ (deg)	$\frac{(F_y)_n}{\bar{F}_{y_{SP}}}$	$(\phi_y)_n$ (deg)	$\frac{(M_x)_n}{\lvert\bar{M}_{x_{SP}}\rvert}$	$(\phi_x)_n$ (deg)	$\frac{(M_y)_n}{\bar{M}_{y_{SP}}}$	$(\phi_y)_n$ (deg)
1	.3943	85.8	.3408	81.3	.3933	-95.9	.3986	87.0
2	.0335	-31.1	.0478	-5.9	.0558	176.0	.0383	-20.1
3	.0411	-27.2	.0338	-14.7	.0307	172.9	.0355	-15.6
4	.0187	6.7	.0034	-105.0	.0032	27.9	.0157	23.5
5	.0050	39.8	.0012	173.7	.0028	24.8	.0052	59.8
6	.0075	94.4	.0017	112.5	.0003	-22.0	.0078	82.9
7	.0057	105.0	.0093	67.1	.0085	-128.9	.0059	84.6
8	.0072	56.1	.0107	40.6	.0107	-154.4	.0080	47.0
9	.0070	38.9	.0073	46.1	.0072	-160.3	.0073	31.1
10	.0070	8.0	.0063	-20.9	.0083	142.9	.0067	-3.3

n	$\frac{(M_z)_n}{\lvert\bar{M}_{z_{SP}}\rvert}$	$(\phi_z)_n$ (deg)	$\frac{(M_h)_n}{\bar{M}_{h_{SP}}}$	$(\phi_h)_n$ (deg)	$\frac{(M_{0.4})_n}{\bar{M}_{0.4_{SP}}}$	$(\phi_{0.4})_n$ (deg)
1	1.6405	71.0	.3924	87.2	.4299	88.5
2	.2166	38.9	.0465	-9.1	.0515	-7.7
3	.1078	2.1	.0292	-3.4	.0302	5.4
4	.0497	-4.5	.0078	45.1	.0113	57.7
5	.0228	25.6	.0024	95.6	.0039	94.4
6	.0210	64.2	.0037	72.4	.0049	63.2
7	.0280	33.5	.0063	55.9	.0070	50.8
8	.0409	20.1	.0087	28.8	.0094	26.7
9	.0409	-4.3	.0072	14.7	.0081	10.1
10	.0232	-3.1	.0073	-27.9	.0080	-30.5

TABLE 17 – EXPERIMENTAL LOADS DURING QUASI-STEADY CRASH ASTERN AT $V = 2.57$ M/SEC, $n = 17.43$ REV/SEC, $(P/D)_{0.7} = 0.61$

TABLE 17a – SIGNALS RECONSTRUCTED FROM FIRST TEN HARMONICS (Five for M_z)

θ	$F_x/\bar{F}_{x_{SP}}$	$F_y/\bar{F}_{y_{SP}}$	$M_x/\lvert\bar{M}_{x_{SP}}\rvert$	$M_y/\bar{M}_{y_{SP}}$	$M_z/\lvert\bar{M}_{z_{SP}}\rvert$	$M_h/\bar{M}_{h_{SP}}$	$M_{0.4}/M_{0.4_{SP}}$
0	.4045	.4896	-.4200	.3748	-8.8959	.3790	.3192
4	.4002	.4781	-.4136	.3739	-8.9514	.3797	.3230
8	.3875	.4603	-.4002	.3633	-9.0079	.3699	.3161
12	.3753	.4415	-.3845	.3516	-9.0613	.3575	.3057
16	.3728	.4288	-.3732	.3482	-9.1083	.3518	.3006
20	.3867	.4284	-.3724	.3599	-9.1469	.3600	.3077
24	.4182	.4432	-.3854	.3881	-9.1767	.3843	.3288
28	.4622	.4720	-.4110	.4282	-9.1986	.4207	.3605
32	.5095	.5092	-.4441	.4711	-9.2149	.4609	.3952
36	.5497	.5471	-.4776	.5070	-9.2289	.4953	.4242
40	.5751	.5784	-.5044	.5285	-9.2445	.5165	.4407
44	.5825	.5984	-.5202	.5330	-9.2658	.5215	.4425
48	.5748	.6062	-.5248	.5233	-9.2966	.5127	.4321
52	.5577	.6044	-.5212	.5054	-9.3399	.4962	.4154
56	.5384	.5978	-.5145	.4862	-9.3974	.4788	.3987
60	.5225	.5910	-.5095	.4710	-9.4694	.4658	.3872
64	.5122	.5866	-.5087	.4617	-9.5547	.4593	.3822
68	.5069	.5850	-.5119	.4570	-9.6509	.4580	.3824
72	.5033	.5841	-.5166	.4542	-9.7543	.4585	.3842
76	.5006	.5812	-.5193	.4506	-9.8603	.4575	.3845
80	.4958	.5741	-.5175	.4450	-9.9643	.4534	.3815
84	.4900	.5624	-.5103	.4380	-10.0614	.4464	.3757
88	.4846	.5475	-.4993	.4315	-10.1479	.4387	.3692
92	.4817	.5321	-.4871	.4274	-10.2207	.4327	.3643
96	.4810	.5188	-.4765	.4263	-10.2781	.4296	.3623
100	.4815	.5091	-.4691	.4271	-10.3199	.4292	.3629
104	.4812	.5030	-.4650	.4277	-10.3472	.4298	.3646
108	.4780	.4993	-.4627	.4262	-10.3623	.4292	.3652
112	.4713	.4962	-.4603	.4216	-10.3685	.4261	.3634
116	.4622	.4923	-.4566	.4146	-10.3694	.4206	.3592
120	.4530	.4874	-.4514	.4074	-10.3688	.4143	.3540

TABLE 17a – (Continued)

θ	$F_x/\bar{F}_{x_{SP}}$	$F_y/\bar{F}_{y_{SP}}$	$M_x/\lvert\bar{M}_{x_{SP}}\rvert$	$M_y/\bar{M}_{y_{SP}}$	$M_z/\lvert\bar{M}_{z_{SP}}\rvert$	$M_h/\bar{M}_{h_{SP}}$	$M_{0.4}/M_{0.4_{SP}}$
124	.4462	.4822	-.4457	.4020	-10.3702	.4091	.3498
128	.4430	.4780	-.4410	.3999	-10.3761	.4065	.3478
132	.4430	.4758	-.4385	.4005	-10.3883	.4067	.3482
136	.4441	.4759	-.4384	.4020	-10.4074	.4081	.3497
140	.4435	.4775	-.4397	.4019	-10.4328	.4085	.3502
144	.4391	.4792	-.4408	.3984	-10.4630	.4061	.3481
148	.4308	.4799	-.4405	.3910	-10.4956	.4003	.3427
152	.4194	.4790	-.4381	.3813	-10.5281	.3921	.3350
156	.4085	.4770	-.4342	.3718	-10.5577	.3835	.3270
160	.4004	.4750	-.4303	.3649	-10.5820	.3769	.3207
164	.3963	.4743	-.4279	.3614	-10.5992	.3734	.3173
168	.3952	.4753	-.4277	.3605	-10.6081	.3724	.3161
172	.3947	.4777	-.4295	.3598	-10.6088	.3720	.3154
176	.3913	.4801	-.4317	.3566	-10.6018	.3697	.3129
180	.3846	.4810	-.4324	.3493	-10.5886	.3637	.3069
184	.3730	.4793	-.4302	.3380	-10.5711	.3539	.2974
188	.3592	.4749	-.4249	.3248	-10.5514	.3418	.2860
192	.3460	.4687	-.4175	.3126	-10.5314	.3300	.2749
196	.3361	.4623	-.4097	.3035	-10.5126	.3206	.2661
200	.3303	.4573	-.4034	.2982	-10.4959	.3146	.2605
204	.3271	.4543	-.3995	.2951	-10.4813	.3109	.2568
208	.3237	.4530	-.3976	.2914	-10.4682	.3071	.2529
212	.3171	.4523	-.3964	.2843	-10.4552	.3006	.2463
216	.3057	.4505	-.3939	.2726	-10.4402	.2899	.2357
220	.2901	.4467	-.3891	.2571	-10.4211	.2757	.2219
224	.2729	.4408	-.3817	.2406	-10.3957	.2602	.2070
228	.2578	.4336	-.3728	.2265	-10.3624	.2465	.1941
232	.2474	.4265	-.3640	.2173	-10.3201	.2370	.1853
236	.2423	.4207	-.3569	.2135	-10.2685	.2323	.1813
240	.2409	.4167	-.3521	.2130	-10.2083	.2310	.1804

TABLE 17a – (Continued)

θ	$F_x/\bar{F}_{x_{SP}}$	$F_y/\bar{F}_{y_{SP}}$	$M_x/\lvert\bar{M}_{x_{SP}}\rvert$	$M_y/\bar{M}_{y_{SP}}$	$M_z/\lvert\bar{M}_{z_{SP}}\rvert$	$M_h/\bar{M}_{h_{SP}}$	$M_{0.4}/M_{0.4_{SP}}$
244	.2400	.4142	-.3493	.2128	-10.1411	.2304	.1802
248	.2360	.4124	-.3474	.2099	-10.0693	.2278	.1780
252	.2289	.4105	-.3453	.2033	-9.9956	.2222	.1730
256	.2185	.4083	-.3425	.1942	-9.9232	.2146	.1660
260	.2084	.4064	-.3396	.1857	-9.8547	.2075	.1598
264	.2018	.4056	-.3376	.1811	-9.7924	.2039	.1570
268	.2007	.4068	-.3376	.1819	-9.7377	.2053	.1588
272	.2041	.4097	-.3397	.1869	-9.6911	.2105	.1542
276	.2087	.4131	-.3428	.1923	-9.6518	.2161	.1599
280	.2100	.4150	-.3447	.1938	-9.6182	.2180	.1717
284	.2048	.4137	-.3435	.1883	-9.5876	.2129	.1667
288	.1929	.4086	-.3379	.1760	-9.5571	.2010	.1551
292	.1783	.4009	-.3290	.1612	-9.5234	.1862	.1406
296	.1677	.3940	-.3199	.1507	-9.4836	.1748	.1295
300	.1681	.3915	-.3145	.1515	-9.4356	.1736	.1279
304	.1837	.3966	-.3166	.1674	-9.3779	.1865	.1396
308	.2141	.4102	-.3277	.1971	-9.3108	.2127	.1637
312	.2535	.4307	-.3465	.2344	-9.2355	.2466	.1946
316	.2928	.4537	-.3690	.2701	-9.1547	.2795	.2238
320	.3233	.4740	-.3896	.2953	-9.0720	.3028	.2434
324	.3392	.4875	-.4040	.3052	-8.9917	.3115	.2488
328	.3407	.4923	-.4096	.3006	-8.9184	.3062	.2410
332	.3330	.4900	-.4076	.2880	-8.8565	.2928	.2260
336	.3247	.4843	-.4017	.2767	-8.8098	.2804	.2128
340	.3236	.4796	-.3967	.2750	-8.7809	.2773	.2097
344	.3338	.4792	-.3965	.2868	-8.7710	.2880	.2208
348	.3536	.4832	-.4019	.3103	-8.7799	.3109	.2447
352	.3774	.4892	-.4106	.3385	-8.8058	.3394	.2748
356	.3964	.4927	-.4182	.3623	-8.8458	.3646	.3021
360	.4043	.4896	-.4200	.3748	-8.8959	.3790	.3192

TABLE 17b – HARMONIC CONTENT OF SIGNALS

n	$\frac{(F_x)_n}{\bar{F}_{x_{SP}}}$	$(\phi_x)_n$ (deg)	$\frac{(F_y)_n}{\bar{F}_{y_{SP}}}$	$(\phi_y)_n$ (deg)	$\frac{(M_x)_n}{\lvert\bar{M}_{x_{SP}}\rvert}$	$(\phi_x)_n$ (deg)	$\frac{(M_y)_n}{\bar{M}_{y_{SP}}}$	$(\phi_y)_n$ (deg)
1	.1503	34.6	.0648	76.5	.0733	-89.7	.1369	83.9
2	.0310	51.9	.0177	93.4	.0142	-88.0	.0306	49.7
3	.0088	-167.2	.0255	-142.8	.0189	43.1	.0102	159.5
4	.0175	-138.2	.0219	-105.1	.0156	81.0	.0140	-148.0
5	.0204	-131.1	.0162	-94.8	.0128	84.3	.0166	-133.7
6	.0112	-127.2	.0033	-92.8	.0072	73.5	.0080	-133.2
7	.0055	-16.3	.0024	-27.7	.0014	131.4	.0058	1.9
8	.0127	11.3	.0089	10.2	.0083	-166.5	.0131	10.6
9	.0128	12.4	.0090	15.2	.0088	-161.4	.0136	9.5
10	.0139	-10.5	.0079	24.3	.0087	-152.9	.0137	-12.5

n	$\frac{(M_z)_n}{\lvert\bar{M}_{z_{SP}}\rvert}$	$(\phi_z)_n$ (deg)	$\frac{(M_h)_n}{\bar{M}_{h_{SP}}}$	$(\phi_h)_n$ (deg)	$\frac{(M_{0.4})_n}{\bar{M}_{0.4_{SP}}}$	$(\phi_{0.4})_n$ (deg)
1	.0486	-9.3	.1263	86.4	.1162	88.2
2	.1058	-11.4	.0271	51.9	.0251	48.3
3	.0172	78.5	.0106	161.9	.0105	139.4
4	.0603	-107.6	.0108	-145.2	.0074	-164.5
5	.0819	-86.0	.0136	-130.0	.0105	-136.4
6	.0218	-80.2	.0066	-135.7	.0050	-151.9
7	.0391	64.3	.0051	9.5	.0050	19.1
8	.0499	35.3	.0129	11.3	.0121	11.5
9	.0528	19.7	.0138	10.1	.0134	9.2
10	.0255	-2.0	.0131	-6.5	.0125	-7.4

TABLE 18 – EXPERIMENTAL LOADS DURING QUASI-STEADY CRASH ASTERN AT $V = 1.67$ M/SEC, $n = 16.59$ REV/SEC, $(P/D)_{0.7} = 0.14$

TABLE 18a – SIGNALS RECONSTRUCTED FROM FIRST TEN HARMONICS (Five for M_z)

θ	$F_x/\bar{F}_{x_{SP}}$	$F_y/\bar{F}_{y_{SP}}$	$M_x/\lvert\bar{M}_{x_{SP}}\rvert$	$M_y/\bar{M}_{y_{SP}}$	$M_z/\lvert\bar{M}_{z_{SP}}\rvert$	$M_h/\bar{M}_{h_{SP}}$	$M_{0.4}/M_{0.4_{SP}}$
0	-.2686	.2400	-.2185	-.4534	-9.2938	-.5012	-.5061
4	-.2719	.2324	-.2116	-.4616	-9.3373	-.5129	-.5183
8	-.2775	.2246	-.2048	-.4724	-9.3823	-.5272	-.5328
12	-.2827	.2183	-.1999	-.4814	-9.4272	-.5385	-.5438
16	-.2850	.2144	-.1973	-.4850	-9.4707	-.5426	-.5474
20	-.2831	.2134	-.1987	-.4818	-9.5118	-.5384	-.5424
24	-.2774	.2149	-.2013	-.4733	-9.5499	-.5278	-.5315
28	-.2695	.2175	-.2058	-.4626	-9.5851	-.5151	-.5187
32	-.2616	.2199	-.2090	-.4532	-9.6177	-.5046	-.5086
36	-.2563	.2212	-.2106	-.4476	-9.6485	-.4990	-.5035
40	-.2537	.2211	-.2104	-.4463	-9.6785	-.4935	-.5036
44	-.2534	.2200	-.2093	-.4478	-9.7090	-.5012	-.5069
48	-.2538	.2188	-.2084	-.4500	-9.7408	-.5045	-.5104
52	-.2533	.2184	-.2086	-.4509	-9.7748	-.5060	-.5121
56	-.2509	.2191	-.2104	-.4499	-9.8115	-.5053	-.5116
60	-.2468	.2209	-.2135	-.4476	-9.8507	-.5035	-.5102
64	-.2423	.2230	-.2170	-.4457	-9.8918	-.5024	-.5097
68	-.2389	.2244	-.2199	-.4457	-9.9339	-.5036	-.5116
72	-.2378	.2247	-.2213	-.4479	-9.9754	-.5071	-.5155
76	-.2392	.2236	-.2212	-.4514	-10.0146	-.5116	-.5200
80	-.2422	.2216	-.2199	-.4545	-10.0496	-.5147	-.5224
84	-.2449	.2196	-.2185	-.4553	-10.0786	-.5144	-.5212
88	-.2459	.2181	-.2176	-.4530	-10.1002	-.5104	-.5162
92	-.2442	.2178	-.2178	-.4484	-10.1132	-.5041	-.5094
96	-.2403	.2184	-.2189	-.4434	-10.1170	-.4994	-.5037
100	-.2356	.2194	-.2206	-.4403	-10.1117	-.4960	-.5021
104	-.2322	.2205	-.2222	-.4407	-10.0979	-.4983	-.5054
108	-.2315	.2211	-.2231	-.4444	-10.0768	-.5041	-.5122
112	-.2333	.2213	-.2234	-.4495	-10.0501	-.5105	-.5187
116	-.2387	.2217	-.2235	-.4533	-10.0197	-.5136	-.5210
120	-.2442	.2228	-.2239	-.4535	-9.9877	-.5106	-.5164

TABLE 18a – (Continued)

θ	$F_x/\bar{F}_{x_{SP}}$	$F_y/\bar{F}_{y_{SP}}$	$M_x/\lvert\bar{M}_{x_{SP}}\rvert$	$M_y/\bar{M}_{y_{SP}}$	$M_z/\lvert\bar{M}_{z_{SP}}\rvert$	$M_h/\bar{M}_{h_{SP}}$	$M_{0.4}/M_{0.4_{SP}}$
124	-.2484	.2249	-.2251	-.4492	-9.9559	-.5015	-.5052
128	-.2504	.2281	-.2271	-.4419	-9.9260	-.4890	-.4908
132	-.2500	.2317	-.2296	-.4348	-9.8995	-.4781	-.4789
136	-.2483	.2349	-.2320	-.4316	-9.8771	-.4739	-.4747
140	-.2469	.2369	-.2337	-.4347	-9.8590	-.4793	-.4814
144	-.2472	.2374	-.2343	-.4445	-9.8452	-.4940	-.4980
148	-.2497	.2368	-.2342	-.4587	-9.8349	-.5142	-.5202
152	-.2533	.2358	-.2339	-.4731	-9.8273	-.5339	-.5412
156	-.2563	.2358	-.2341	-.4836	-9.8211	-.5471	-.5552
160	-.2612	.2374	-.2356	-.4872	-9.8152	-.5508	-.5586
164	-.2616	.2412	-.2385	-.4837	-9.8086	-.5448	-.5519
168	-.2593	.2466	-.2424	-.4752	-9.8003	-.5327	-.5392
172	-.2554	.2527	-.2465	-.4654	-9.7900	-.5196	-.5260
176	-.2513	.2582	-.2499	-.4579	-9.7773	-.5103	-.5172
180	-.2485	.2623	-.2521	-.4549	-9.7625	-.5073	-.5150
184	-.2481	.2644	-.2529	-.4563	-9.7453	-.5099	-.5186
188	-.2498	.2649	-.2525	-.4604	-9.7281	-.5154	-.5246
192	-.2527	.2644	-.2517	-.4644	-9.7099	-.5200	-.5291
196	-.2557	.2639	-.2509	-.4659	-9.6917	-.5208	-.5293
200	-.2577	.2639	-.2505	-.4643	-9.6742	-.5172	-.5249
204	-.2584	.2646	-.2505	-.4604	-9.6576	-.5110	-.5178
208	-.2583	.2659	-.2507	-.4563	-9.6419	-.5048	-.5112
212	-.2580	.2673	-.2508	-.4538	-9.6267	-.5015	-.5078
216	-.2585	.2684	-.2506	-.4542	-9.6117	-.5020	-.5087
220	-.2599	.2689	-.2501	-.4566	-9.5962	-.5054	-.5125
224	-.2621	.2690	-.2496	-.4600	-9.5794	-.5093	-.5165
228	-.2644	.2689	-.2491	-.4620	-9.5606	-.5111	-.5181
232	-.2660	.2689	-.2488	-.4614	-9.5394	-.5094	-.5157
236	-.2665	.2691	-.2486	-.4583	-9.5155	-.5044	-.5101
240	-.2658	.2694	-.2482	-.4579	-9.4888	-.4982	-.5034

TABLE 18a – (Continued)

θ	$F_x/\bar{F}_{x_{SP}}$	$F_y/\bar{F}_{y_{SP}}$	$M_x/\lvert\bar{M}_{x_{SP}}\rvert$	$M_y/\bar{M}_{y_{SP}}$	$M_z/\lvert\bar{M}_{z_{SP}}\rvert$	$M_h/\bar{M}_{h_{SP}}$	$M_{0.4}/M_{0.4_{SP}}$
244	-.2647	.2696	-.2473	-.4501	-9.4599	-.4935	-.4987
248	-.2637	.2694	-.2458	-.4484	-9.4293	-.4920	-.4977
252	-.2635	.2690	-.2440	-.4497	-9.3979	-.4941	-.5005
256	-.2645	.2683	-.2421	-.4520	-9.3570	-.4983	-.5054
260	-.2663	.2678	-.2408	-.4551	-9.3374	-.5022	-.5096
264	-.2686	.2675	-.2402	-.4571	-9.3103	-.5041	-.5112
268	-.2713	.2674	-.2401	-.4577	-9.2865	-.5034	-.5097
272	-.2743	.2672	-.2401	-.4577	-9.2665	-.5017	-.5069
276	-.2781	.2664	-.2394	-.4590	-9.2503	-.5015	-.5056
280	-.2829	.2645	-.2375	-.4630	-9.2379	-.5051	-.5085
284	-.2886	.2616	-.2343	-.4702	-9.2285	-.5133	-.5164
288	-.2944	.2581	-.2304	-.4792	-9.2214	-.5245	-.5276
292	-.2992	.2550	-.2268	-.4874	-9.2157	-.5350	-.5395
296	-.3014	.2533	-.2246	-.4918	-9.2101	-.5408	-.5447
300	-.3001	.2537	-.2247	-.4903	-9.2040	-.5394	-.5435
304	-.2954	.2563	-.2269	-.4831	-9.1966	-.5308	-.5351
308	-.2886	.2605	-.2307	-.4727	-9.1878	-.5183	-.5228
312	-.2819	.2652	-.2348	-.4631	-9.1775	-.5069	-.5118
316	-.2775	.2687	-.2373	-.4582	-9.1664	-.5016	-.5072
320	-.2770	.2702	-.2387	-.4604	-9.1554	-.5051	-.5114
324	-.2805	.2692	-.2376	-.4690	-9.1457	-.5165	-.5235
328	-.2866	.2663	-.2350	-.4810	-9.1388	-.5316	-.5389
332	-.2929	.2624	-.2321	-.4914	-9.1361	-.5443	-.5514
336	-.2963	.2588	-.2300	-.4961	-9.1388	-.5495	-.5560
340	-.2956	.2561	-.2291	-.4929	-9.1479	-.5449	-.5504
344	-.2904	.2543	-.2291	-.4828	-9.1641	-.5321	-.5366
348	-.2825	.2528	-.2290	-.4693	-9.1874	-.5159	-.5198
352	-.2746	.2504	-.2277	-.4576	-9.2174	-.5026	-.5064
356	-.2695	.2462	-.2242	-.4517	-9.2533	-.4971	-.5013
360	-.2685	.2400	-.2185	-.4534	-9.2938	-.5012	-.5061

TABLE 18b – HARMONIC CONTENT OF SIGNALS

n	$\frac{(F_x)_n}{\bar{F}_{x_{SP}}}$	$(\phi_x)_n$ (deg)	$\frac{(F_y)_n}{\bar{F}_{y_{SP}}}$	$(\phi_y)_n$ (deg)	$\frac{(M_x)_n}{\lvert\bar{M}_{x_{SP}}\rvert}$	$(\phi_x)_n$ (deg)	$\frac{(M_y)_n}{\bar{M}_{y_{SP}}}$	$(\phi_y)_n$ (deg)
1	.0222	125.9	.0272	-107.1	.0193	40.2	.0105	122.8
2	.0076	131.1	.0028	-32.4	.0019	146.7	.0095	145.3
3	.0028	-65.0	.0059	-104.0	.0051	78.2	.0043	1.3
4	.0019	-58.5	.0042	-95.8	.0036	92.4	.0021	-174.7
5	.0036	-135.9	.0036	-112.8	.0028	64.2	.0053	-105.2
6	.0017	63.1	.0006	106.7	.0002	25.1	.0038	64.0
7	.0030	22.6	.0009	-166.6	.0010	18.6	.0029	-32.0
8	.0033	5.6	.0023	1.3	.0016	166.2	.0085	.4
9	.0035	-62.0	.0014	-63.4	.0020	123.9	.0020	-60.1
10	.0047	-18.6	.0025	-31.2	.0025	139.7	.0090	-46.8

n	$\frac{(M_z)_n}{\lvert\bar{M}_{z_{SP}}\rvert}$	$(\phi_z)_n$ (deg)	$\frac{(M_h)_n}{\bar{M}_{h_{SP}}}$	$(\phi_h)_n$ (deg)	$\frac{(M_{0.4})_n}{\bar{M}_{0.4_{SP}}}$	$(\phi_{0.4})_n$ (deg)
1	.4201	-58.7	.0058	146.3	.0051	142.9
2	.1015	-36.3	.0100	151.6	.0098	155.6
3	.0295	74.6	.0059	8.5	.0067	16.2
4	.0212	-124.9	.0037	178.0	.0044	170.2
5	.0296	-73.5	.0067	-96.6	.0067	-91.1
6	.0212	-95.3	.0047	63.8	.0047	62.9
7	.0203	-2.3	.0037	-57.8	.0042	-68.9
8	.0201	20.0	.0113	-1.3	.0117	-2.5
9	.0117	-16.8	.0014	-54.6	.0009	-43.7
10	.0063	16.9	.0119	-53.2	.0126	-57.0

TABLE 19 – EXPERIMENTAL LOADS DURING QUASI-STEADY CRASH ASTERN AT V = 0.74 M/SEC, n = 6.77 REV/SEC, $(P/D)_{0.7}$ = −0.67

TABLE 19a – SIGNALS RECONSTRUCTED FROM FIRST TEN HARMONICS (Five for M_z)

θ	$F_x/\bar{F}_{x_{SP}}$	$F_y/\bar{F}_{y_{SP}}$	$M_x/\lvert\bar{M}_{x_{SP}}\rvert$	$M_y/\bar{M}_{y_{SP}}$	$M_z/\lvert\bar{M}_{z_{SP}}\rvert$	$M_h/\bar{M}_{h_{SP}}$	$M_{0.4}/M_{0.4_{SP}}$
0	-.4030	.1609	-.3022	-.4459	-2.6159	-.4736	-.2636
4	-.4041	.1547	-.2958	-.4467	-2.6044	-.4745	-.2654
8	-.4058	.1483	-.2888	-.4480	-2.5929	-.4759	-.2677
12	-.4080	.1418	-.2815	-.4498	-2.5826	-.4778	-.2706
16	-.4102	.1358	-.2745	-.4516	-2.5745	-.4797	-.2736
20	-.4117	.1307	-.2684	-.4528	-2.5692	-.4811	-.2760
24	-.4116	.1266	-.2635	-.4529	-2.5670	-.4813	-.2774
28	-.4103	.1237	-.2600	-.4516	-2.5679	-.4802	-.2776
32	-.4075	.1221	-.2580	-.4491	-2.5716	-.4781	-.2766
36	-.4041	.1215	-.2572	-.4463	-2.5773	-.4754	-.2750
40	-.4012	.1218	-.2576	-.4438	-2.5843	-.4731	-.2733
44	-.3993	.1230	-.2590	-.4421	-2.5918	-.4715	-.2719
48	-.3987	.1249	-.2613	-.4416	-2.5988	-.4709	-.2708
52	-.3991	.1274	-.2642	-.4418	-2.6047	-.4708	-.2700
56	-.3995	.1305	-.2677	-.4421	-2.6089	-.4708	-.2691
60	-.3996	.1337	-.2713	-.4418	-2.6111	-.4702	-.2677
64	-.3984	.1369	-.2747	-.4405	-2.6112	-.4687	-.2658
68	-.3960	.1397	-.2776	-.4383	-2.6093	-.4664	-.2635
72	-.3929	.1417	-.2797	-.4355	-2.6056	-.4637	-.2613
76	-.3897	.1432	-.2808	-.4327	-2.6010	-.4610	-.2593
80	-.3871	.1441	-.2814	-.4305	-2.5954	-.4589	-.2579
84	-.3853	.1450	-.2819	-.4289	-2.5893	-.4575	-.2570
88	-.3843	.1462	-.2828	-.4279	-2.5832	-.4564	-.2562
92	-.3837	.1481	-.2845	-.4271	-2.5772	-.4553	-.2550
96	-.3831	.1508	-.2874	-.4261	-2.5712	-.4539	-.2533
100	-.3823	.1542	-.2913	-.4249	-2.5652	-.4523	-.2510
104	-.3815	.1580	-.2959	-.4240	-2.5588	-.4511	-.2488
108	-.3815	.1616	-.3006	-.4242	-2.5516	-.4511	-.2475
112	-.3831	.1646	-.3049	-.4262	-2.5434	-.4533	-.2480
116	-.3865	.1668	-.3084	-.4305	-2.5337	-.4581	-.2509
120	-.3918	.1681	-.3107	-.4369	-2.5224	-.4654	-.2561

TABLE 19a – (Continued)

θ	$F_x/\bar{F}_{x_{SP}}$	$F_y/\bar{F}_{y_{SP}}$	$M_x/\|\bar{M}_{x_{SP}}\|$	$M_y/\bar{M}_{y_{SP}}$	$M_z/\|\bar{M}_{z_{SP}}\|$	$M_h/\bar{M}_{h_{SP}}$	$M_{0.4}/M_{0.4_{SP}}$
124	-.3982	.1686	-.3119	-.4446	-2.5095	-.4742	-.2630
128	-.4045	.1685	-.3120	-.4523	-2.4952	-.4831	-.2702
132	-.4095	.1678	-.3110	-.4585	-2.4798	-.4904	-.2767
136	-.4125	.1668	-.3090	-.4623	-2.4639	-.4949	-.2814
140	-.4130	.1654	-.3060	-.4632	-2.4483	-.4963	-.2840
144	-.4115	.1635	-.3023	-.4618	-2.4336	-.4950	-.2845
148	-.4093	.1614	-.2981	-.4591	-2.4210	-.4922	-.2839
152	-.4073	.1592	-.2938	-.4564	-2.4107	-.4893	-.2831
156	-.4067	.1574	-.2900	-.4549	-2.4034	-.4874	-.2829
160	-.4077	.1562	-.2872	-.4551	-2.3992	-.4871	-.2836
164	-.4101	.1562	-.2860	-.4568	-2.3982	-.4885	-.2851
168	-.4133	.1575	-.2865	-.4594	-2.4001	-.4909	-.2870
172	-.4165	.1601	-.2887	-.4623	-2.4043	-.4935	-.2888
176	-.4196	.1639	-.2922	-.4650	-2.4100	-.4960	-.2901
180	-.4223	.1684	-.2968	-.4675	-2.4164	-.4983	-.2909
184	-.4252	.1732	-.3020	-.4703	-2.4226	-.5009	-.2918
188	-.4290	.1783	-.3076	-.4740	-2.4277	-.5045	-.2933
192	-.4343	.1832	-.3134	-.4794	-2.4310	-.5099	-.2961
196	-.4413	.1881	-.3194	-.4868	-2.4320	-.5176	-.3006
200	-.4496	.1928	-.3255	-.4960	-2.4304	-.5273	-.3068
204	-.4586	.1971	-.3314	-.5062	-2.4262	-.5385	-.3143
208	-.4672	.2009	-.3366	-.5164	-2.4197	-.5499	-.3222
212	-.4743	.2039	-.3407	-.5254	-2.4113	-.5603	-.3298
216	-.4792	.2057	-.3431	-.5322	-2.4018	-.5684	-.3362
220	-.4815	.2064	-.3437	-.5361	-2.3917	-.5735	-.3407
224	-.4811	.2062	-.3427	-.5368	-2.3817	-.5750	-.3429
228	-.4784	.2054	-.3407	-.5345	-2.3724	-.5730	-.3425
232	-.4736	.2046	-.3384	-.5295	-2.3643	-.5679	-.3396
236	-.4672	.2045	-.3369	-.5225	-2.3576	-.5603	-.3344
240	-.4595	.2055	-.3367	-.5139	-2.3524	-.5508	-.3273

TABLE 19a – (Continued)

θ	$F_x/\bar{F}_{x_{SP}}$	$F_y/\bar{F}_{y_{SP}}$	$M_x/\lvert\bar{M}_{x_{SP}}\rvert$	$M_y/\bar{M}_{y_{SP}}$	$M_z/\lvert\bar{M}_{z_{SP}}\rvert$	$M_h/\bar{M}_{h_{SP}}$	$M_{0.4}/M_{0.4_{SP}}$
244	-.4513	.2077	-.3381	-.5046	-2.3486	-.5404	-.3189
248	-.4429	.2108	-.3410	-.4951	-2.3453	-.5298	-.3100
252	-.4345	.2143	-.3445	-.4860	-2.3438	-.5197	-.3012
256	-.4269	.2177	-.3481	-.4778	-2.3423	-.5107	-.2933
260	-.4204	.2203	-.3507	-.4708	-2.3410	-.5031	-.2867
264	-.4149	.2217	-.3520	-.4650	-2.3398	-.4968	-.2816
268	-.4105	.2219	-.3518	-.4603	-2.3388	-.4918	-.2778
272	-.4068	.2210	-.3503	-.4565	-2.3382	-.4877	-.2751
276	-.4037	.2194	-.3481	-.4531	-2.3385	-.4842	-.2730
280	-.4009	.2176	-.3457	-.4499	-2.3403	-.4808	-.2709
284	-.3981	.2159	-.3437	-.4468	-2.3443	-.4775	-.2687
288	-.3952	.2147	-.3426	-.4436	-2.3511	-.4740	-.2660
292	-.3921	.2142	-.3423	-.4402	-2.3614	-.4703	-.2629
296	-.3887	.2142	-.3429	-.4365	-2.3756	-.4662	-.2593
300	-.3847	.2148	-.3441	-.4324	-2.3938	-.4618	-.2553
304	-.3802	.2155	-.3454	-.4279	-2.4159	-.4570	-.2511
308	-.3753	.2160	-.3464	-.4231	-2.4413	-.4521	-.2469
312	-.3705	.2160	-.3468	-.4184	-2.4692	-.4473	-.2430
316	-.3664	.2151	-.3462	-.4145	-2.4985	-.4433	-.2400
320	-.3639	.2130	-.3445	-.4121	-2.5279	-.4409	-.2382
324	-.3637	.2097	-.3418	-.4118	-2.5560	-.4406	-.2381
328	-.3663	.2053	-.3381	-.4139	-2.5814	-.4426	-.2397
332	-.3713	.2001	-.3339	-.4182	-2.6031	-.4468	-.2429
336	-.3779	.1944	-.3295	-.4241	-2.6199	-.4525	-.2470
340	-.3852	.1887	-.3252	-.4305	-2.6314	-.4586	-.2515
344	-.3917	.1831	-.3210	-.4363	-2.6374	-.4642	-.2554
348	-.3968	.1776	-.3169	-.4407	-2.6380	-.4685	-.2585
352	-.4001	.1723	-.3126	-.4435	-2.6340	-.4712	-.2607
356	-.4019	.1668	-.3078	-.4450	-2.6262	-.4727	-.2622
360	-.4030	.1609	-.3022	-.4459	-2.6159	-.4736	-.2636

TABLE 19b – HARMONIC CONTENT OF SIGNALS

n	$\frac{(F_x)_n}{\bar{F}_{x_{SP}}}$	$(\phi_x)_n$ (deg)	$\frac{(F_y)_n}{\bar{F}_{y_{SP}}}$	$(\phi_y)_n$ (deg)	$\frac{(M_x)_n}{\lvert\bar{M}_{x_{SP}}\rvert}$	$(\phi_x)_n$ (deg)	$\frac{(M_y)_n}{\bar{M}_{y_{SP}}}$	$(\phi_y)_n$ (deg)
1	.0271	30.1	.0406	-102.4	.0363	78.1	.0314	33.4
2	.0265	-106.6	.0152	-130.7	.0147	50.8	.0261	-104.6
3	.0100	-177.1	.0089	-69.8	.0113	125.4	.0112	-177.2
4	.0055	-19.5	.0018	164.6	.0032	-17.6	.0071	-5.7
5	.0076	-173.3	.0041	-74.0	.0058	120.0	.0094	-170.6
6	.0016	128.0	.0021	102.6	.0025	-85.3	.0016	113.6
7	.0019	25.6	.0019	60.2	.0023	-118.1	.0022	22.4
8	.0012	110.4	.0006	-34.9	.0013	137.9	.0014	136.4
9	.0020	-3.7	.0005	-106.5	.0006	55.7	.0020	-6.1
10	.0015	75.8	.0006	27.4	.0007	-149.8	.0014	77.2

n	$\frac{(M_z)_n}{\lvert\bar{M}_{z_{SP}}\rvert}$	$(\phi_z)_n$ (deg)	$\frac{(M_h)_n}{\bar{M}_{h_{SP}}}$	$(\phi_h)_n$ (deg)	$\frac{(M_{0.4})_n}{\bar{M}_{0.4_{SP}}}$	$(\phi_{0.4})_n$ (deg)
1	.1316	-134.3	.0346	33.8	.0260	28.7
2	.0286	-173.0	.0273	-103.7	.0231	-104.7
3	.0457	104.7	.0120	-175.5	.0075	-158.5
4	.0104	103.2	.0084	.5	.0062	8.7
5	.0179	78.2	.0092	-167.5	.0067	-151.9
6	.0206	33.8	.0018	103.5	.0021	92.0
7	.0135	-51.2	.0026	22.3	.0027	30.2
8	.0247	-101.3	.0017	148.5	.0011	166.8
9	.0106	161.9	.0021	-8.3	.0015	-14.4
10	.0153	138.4	.0014	77.4	.0011	72.9

TABLE 20 – EXPERIMENTAL LOADS DURING QUASI-STEADY CRASH ASTERN AT
$V = 0.17$ M/SEC, $n = 7.64$ REV/SEC, $(P/D)_{0.7} = -0.67$

TABLE 20a – SIGNALS RECONSTRUCTED FROM FIRST TEN HARMONICS (Five for M_z)

θ	$F_x/\bar{F}_{x_{SP}}$	$F_y/\bar{F}_{y_{SP}}$	$M_x/\lvert\bar{M}_{x_{SP}}\rvert$	$M_y/\bar{M}_{y_{SP}}$	$M_z/\lvert\bar{M}_{z_{SP}}\rvert$	$M_h/\bar{M}_{h_{SP}}$	$M_{0.4}/M_{0.4_{SP}}$
0	-.4106	.2155	-.3991	-.5068	-4.4683	-.5667	-.3215
4	-.4323	.2199	-.4106	-.5324	-4.5131	-.5952	-.3397
8	-.4511	.2256	-.4230	-.5553	-4.5587	-.6208	-.3558
12	-.4654	.2309	-.4342	-.5734	-4.6044	-.6414	-.3686
16	-.4745	.2345	-.4420	-.5857	-4.6501	-.6558	-.3777
20	-.4784	.2354	-.4452	-.5918	-4.6958	-.6634	-.3829
24	-.4777	.2331	-.4435	-.5924	-4.7415	-.6649	-.3846
28	-.4733	.2283	-.4380	-.5885	-4.7872	-.6614	-.3834
32	-.4665	.2221	-.4304	-.5815	-4.8330	-.6543	-.3799
36	-.4582	.2157	-.4228	-.5728	-4.8788	-.6454	-.3746
40	-.4493	.2105	-.4172	-.5637	-4.9242	-.6358	-.3681
44	-.4415	.2072	-.4144	-.5551	-4.9687	-.6268	-.3612
48	-.4345	.2059	-.4145	-.5479	-5.0115	-.6192	-.3545
52	-.4290	.2062	-.4167	-.5424	-5.0518	-.6132	-.3486
56	-.4257	.2073	-.4198	-.5386	-5.0888	-.6091	-.3439
60	-.4233	.2083	-.4223	-.5365	-5.1216	-.6066	-.3407
64	-.4225	.2085	-.4235	-.5356	-5.1496	-.6055	-.3391
68	-.4231	.2078	-.4232	-.5357	-5.1723	-.6053	-.3387
72	-.4240	.2062	-.4216	-.5363	-5.1896	-.6058	-.3391
76	-.4252	.2041	-.4195	-.5372	-5.2017	-.6066	-.3400
80	-.4261	.2022	-.4176	-.5381	-5.2090	-.6075	-.3410
84	-.4265	.2008	-.4164	-.5388	-5.2124	-.6085	-.3419
88	-.4271	.2000	-.4160	-.5395	-5.2129	-.6093	-.3426
92	-.4271	.2000	-.4163	-.5399	-5.2115	-.6100	-.3430
96	-.4269	.2003	-.4169	-.5400	-5.2093	-.6103	-.3432
100	-.4264	.2008	-.4174	-.5397	-5.2072	-.6102	-.3432
104	-.4255	.2012	-.4173	-.5391	-5.2061	-.6096	-.3430
108	-.4246	.2012	-.4168	-.5380	-5.2063	-.6085	-.3424
112	-.4234	.2011	-.4159	-.5366	-5.2079	-.6070	-.3417
116	-.4221	.2009	-.4149	-.5351	-5.2107	-.6053	-.3409
120	-.4209	.2010	-.4142	-.5337	-5.2143	-.6038	-.3401

TABLE 20a – (Continued)

θ	$F_x/\bar{F}_{x_{SP}}$	$F_y/\bar{F}_{y_{SP}}$	$M_x/\lvert\bar{M}_{x_{SP}}\rvert$	$M_y/\bar{M}_{y_{SP}}$	$M_z/\lvert\bar{M}_{z_{SP}}\rvert$	$M_h/\bar{M}_{h_{SP}}$	$M_{0.4}/M_{0.4_{SP}}$
124	-.4193	.2016	-.4141	-.5325	-5.2179	-.6025	-.3395
128	-.4190	.2030	-.4148	-.5317	-5.2206	-.6017	-.3391
132	-.4184	.2052	-.4162	-.5312	-5.2217	-.6012	-.3389
136	-.4179	.2080	-.4180	-.5308	-5.2204	-.6008	-.3388
140	-.4174	.2111	-.4201	-.5303	-5.2161	-.6002	-.3385
144	-.4167	.2141	-.4220	-.5296	-5.2086	-.5994	-.3381
148	-.4160	.2167	-.4235	-.5286	-5.1978	-.5984	-.3375
152	-.4152	.2186	-.4244	-.5276	-5.1840	-.5972	-.3369
156	-.4145	.2201	-.4247	-.5267	-5.1678	-.5960	-.3364
160	-.4139	.2211	-.4247	-.5259	-5.1498	-.5952	-.3361
164	-.4136	.2222	-.4245	-.5254	-5.1310	-.5946	-.3363
168	-.4133	.2236	-.4247	-.5251	-5.1120	-.5943	-.3366
172	-.4130	.2256	-.4253	-.5248	-5.0934	-.5940	-.3369
176	-.4124	.2291	-.4265	-.5242	-5.0758	-.5934	-.3369
180	-.4115	.2310	-.4281	-.5232	-5.0593	-.5923	-.3363
184	-.4104	.2338	-.4298	-.5218	-5.0439	-.5907	-.3353
188	-.4091	.2364	-.4313	-.5202	-5.0290	-.5887	-.3339
192	-.4075	.2383	-.4323	-.5185	-5.0142	-.5867	-.3325
196	-.4065	.2398	-.4326	-.5169	-4.9987	-.5848	-.3314
200	-.4055	.2409	-.4324	-.5155	-4.9819	-.5832	-.3306
204	-.4045	.2421	-.4321	-.5142	-4.9631	-.5818	-.3302
208	-.4032	.2436	-.4320	-.5127	-4.9419	-.5802	-.3298
212	-.4016	.2457	-.4324	-.5110	-4.9180	-.5784	-.3290
216	-.3997	.2484	-.4336	-.5088	-4.8918	-.5760	-.3276
220	-.3976	.2514	-.4353	-.5064	-4.8637	-.5732	-.3257
224	-.3958	.2544	-.4372	-.5040	-4.8344	-.5704	-.3234
228	-.3944	.2568	-.4390	-.5021	-4.8052	-.5680	-.3214
232	-.3939	.2587	-.4404	-.5011	-4.7770	-.5665	-.3200
236	-.3942	.2598	-.4412	-.5009	-4.7510	-.5661	-.3195
240	-.3950	.2605	-.4414	-.5015	-4.7282	-.5665	-.3199

TABLE 20a – (Continued)

θ	$F_x/\bar{F}_{x_{SP}}$	$F_y/\bar{F}_{y_{SP}}$	$M_x/\lvert\bar{M}_{x_{SP}}\rvert$	$M_y/\bar{M}_{y_{SP}}$	$M_z/\lvert\bar{M}_{z_{SP}}\rvert$	$M_h/\bar{M}_{h_{SP}}$	$M_{0.4}/M_{0.4_{SP}}$
244	-.3959	.2609	-.4412	-.5023	-4.7093	-.5673	-.3209
248	-.3963	.2613	-.4407	-.5028	-4.6946	-.5679	-.3218
252	-.3961	.2618	-.4403	-.5025	-4.6839	-.5677	-.3222
256	-.3953	.2624	-.4398	-.5015	-4.6766	-.5665	-.3218
260	-.3941	.2627	-.4393	-.4999	-4.6717	-.5647	-.3207
264	-.3932	.2628	-.4387	-.4985	-4.6678	-.5623	-.3195
268	-.3932	.2625	-.4380	-.4979	-4.6633	-.5619	-.3188
272	-.3945	.2619	-.4373	-.4987	-4.6567	-.5626	-.3193
276	-.3970	.2613	-.4368	-.5013	-4.6464	-.5652	-.3214
280	-.4004	.2607	-.4366	-.5052	-4.6311	-.5696	-.3248
284	-.4041	.2603	-.4367	-.5097	-4.6102	-.5748	-.3290
288	-.4073	.2600	-.4368	-.5139	-4.5837	-.5799	-.3331
292	-.4093	.2595	-.4366	-.5169	-4.5508	-.5835	-.3362
296	-.4099	.2585	-.4355	-.5177	-4.5136	-.5845	-.3373
300	-.4086	.2567	-.4334	-.5158	-4.4731	-.5824	-.3359
304	-.4055	.2541	-.4301	-.5112	-4.4310	-.5767	-.3318
308	-.4005	.2510	-.4258	-.5039	-4.3896	-.5678	-.3252
312	-.3935	.2476	-.4210	-.4940	-4.3510	-.5559	-.3163
316	-.3848	.2444	-.4161	-.4821	-4.3173	-.5417	-.3056
320	-.3744	.2416	-.4116	-.4687	-4.2903	-.5260	-.2938
324	-.3630	.2392	-.4075	-.4547	-4.2715	-.5100	-.2818
328	-.3517	.2368	-.4036	-.4414	-4.2618	-.4950	-.2707
332	-.3421	.2340	-.3994	-.4302	-4.2616	-.4827	-.2619
336	-.3358	.2303	-.3950	-.4230	-4.2708	-.4749	-.2566
340	-.3345	.2258	-.3905	-.4215	-4.2888	-.4732	-.2560
344	-.3393	.2210	-.3867	-.4266	-4.3144	-.4789	-.2606
348	-.3503	.2167	-.3846	-.4389	-4.3466	-.4922	-.2706
352	-.3674	.2138	-.3857	-.4575	-4.3839	-.5126	-.2851
356	-.3881	.2133	-.3905	-.4810	-4.4248	-.5383	-.3026
360	-.4105	.2155	-.3991	-.5068	-4.4683	-.5667	-.3215

TABLE 20b – HARMONIC CONTENT OF SIGNALS

n	$\frac{(F_x)_n}{\overline{F}_{x_{SP}}}$	$(\phi_x)_n$ (deg)	$\frac{(F_y)_n}{\overline{F}_{y_{SP}}}$	$(\phi_y)_n$ (deg)	$\frac{(M_x)_n}{\lvert\overline{M}_{x_{SP}}\rvert}$	$(\phi_x)_n$ (deg)	$\frac{(M_y)_n}{\overline{M}_{y_{SP}}}$	$(\phi_y)_n$ (deg)
1	.0228	-92.5	.0292	-94.9	.0105	42.3	.0287	-81.8
2	.0145	-63.7	.0049	118.8	.0099	-58.2	.0193	-76.8
3	.0185	-80.4	.0040	112.4	.0080	-69.5	.0224	-76.5
4	.0185	-91.1	.0023	107.0	.0059	-83.0	.0218	-88.4
5	.0133	-92.1	.0034	98.1	.0063	-87.8	.0154	-91.6
6	.0072	-99.6	.0025	114.5	.0043	-82.1	.0080	-101.4
7	.0024	-111.9	.0020	141.0	.0028	-54.1	.0025	-115.6
8	.0009	-85.8	.0025	144.2	.0036	-40.1	.0010	-63.8
9	.0011	-104.4	.0017	-163.2	.0021	4.4	.0011	-72.5
10	.0007	-171.4	.0006	152.1	.0008	-11.9	.0007	-162.7

n	$\frac{(M_z)_n}{\lvert\overline{M}_{z_{SP}}\rvert}$	$(\phi_z)_n$ (deg)	$\frac{(M_h)_n}{\overline{M}_{h_{SP}}}$	$(\phi_h)_n$ (deg)	$\frac{(M_{0.4})_n}{\overline{M}_{0.4_{SP}}}$	$(\phi_{0.4})_n$ (deg)
1	.4272	-49.2	.0333	-77.7	.0183	-78.0
2	.1081	-37.0	.0211	-74.1	.0141	-76.5
3	.0592	-46.7	.0255	-74.7	.0181	-73.9
4	.0191	-108.1	.0245	-87.0	.0176	-85.9
5	.0245	170.1	.0170	-91.4	.0115	-91.1
6	.0305	133.0	.0087	-102.7	.0054	-106.5
7	.0315	69.0	.0026	-120.4	.0016	-148.6
8	.0157	23.5	.0009	-53.2	.0004	131.2
9	.0159	60.9	.0013	-60.3	.0008	-74.6
10	.0077	72.2	.0007	-158.2	.0008	-160.3

REFERENCES

1. Boswell, R.J. et al., "Experimental Determination of Mean and Unsteady Loads on a Model CP Propeller Blade for Various Simulated Modes of Ship Operation," Transactions of the Eleventh ONR Symposium on Naval Hydrodynamics, Government Printing Office (1976).

2. Schwanecke, H. and R. Wereldsma, "Strength of Propellers Considering Steady and Unsteady Shaft and Blade Forces, Stationary and Nonstationary Environmental Conditions," Proceedings of the Thirteenth International Towing Tank Conference, Report of the Propeller Committee, Appendix 2b, Vol. 2 (1972).

3. Rusetskiy, A.A., "Hydrodynamics of Controllable Pitch Propellers," Shipbuilding Publishing House, Leningrad (1968).

4. Hawdon, L. et al., "The Analysis of Controllable-Pitch Propeller Characteristics at Off-Design Conditions," Transactions of the Institute of Marine Engineers, Vol. 88 (1976).

5. van Gent, W., "Unsteady Lifting Surface Theory for Ship Screws: Deviation and Numerical Treament of Integral Equations," Journal of Ship Research, Vol. 19, No. 4, pp. 243--253 (Dec 1975).

6. Schwanecke, H., "Comparative Calculations on Unsteady Propeller Blade Forces," Proceedings of the Fourteenth International Towing Tank Conference, Vol. 3, pp. 357--397 (1975).

7. Breslin, J.P., "Propeller Excitation Theory," Proceedings of the Fourteenth International Towing Tank Conference, Report of the Propeller Committee, Appendix 2c, Vol. 2 (1972).

8. Boswell, R.J. and M.L. Miller, "Unsteady Propeller Loading-Measurement, Correlation with Theory, and Parametric Study," NSRDC Report 2625 (Oct 1968).

9. Meyne, K., "Propeller Manufacture-Propeller Materials-Propeller Strength," International Shipbuilding Progress, Vol. 22, No. 247, pp. 77--102 (Mar 1975).

10. Wereldsma, R., "Comparative Tests on Vibratory Propeller Forces," Proceedings of the Thirteenth International Towing Tank Conference, Report of the Propeller Committee, Appendix 2a, Vol. 2 (1972).

11. Huse, E., "An Experimental Investigation of the Dynamic Forces and Moments on One Blade of a Ship Propeller," Proceedings of the Symposium on Testing Techniques in Ship Cavitation Research, The Norwegian Ship Model Experimental Tank, Trondheim, Norway (May-Jun 1967).

12. Blaurock, J., "Propeller Blade Loading in Nonuniform Flow," The Society of Naval Architects and Marine Engineers, Propellers 75 Symposium (Jul 1975).

13. Albrecht, K. and K.R. Suhrbier, "Investigation of the Fluctuating Blade Forces of a Cavitating Propeller in Oblique Flow," International Shipbuilding Progress, Vol. 22, No. 248, pp. 132--147 (Apr 1975).

14. Bednarzik, R., "Untersuchung uber die Belastungs-schwankungen am Einzelflugel schrag angestromter Propeller," Schiffbauforschung, Vol. 8, No. 1/2, pp. 57--80 (1969).

15. Dobay, G.F., "Time-Dependent Blade-Load Measurements on a Screw-Propeller," Presented to the Sixteenth American Towing Tank Conference (Aug 1971).

16. Wereldsma, R., "Last Remarks on the Comparative Model Tests on Vibratory Propeller Forces," Proceedings of the Fourteenth International Towing Tank Conference, Vol. 3, pp. 421--426 (1975).

17. Tasaki, R., "Propulsion Factors and Fluctuating Propeller Loads in Waves," Proceedings of the Fourteenth International Towing Tank Conference, Vol. 4, pp. 224--236 (1975).

18. Keil, H.G. et al., "Stresses in the Blades of a Cargo Ship Propeller," Journal of Hydronautics, Vol. 6, No. 1 (Jan 1972).

19. Watanabe, K. et al., "Propeller Stress Measurements on the Container Ship HAKONE MARU," Shipbuilding Research Association of Japan (1973).

20. Tsakonas, S. et al., "An Exact Linear Lifting Surface Theory for Marine Propeller in a Nonuniform Flow Field," Journal of Ship Research, Vol. 17, No. 4 (Dec 1974).

21. McCarthy, J.H., "On the Calculation of Thrust and Torque Fluctuations of Propellers in Nonuniform Wake Flow," David W. Taylor Model Basin Report 1533 (Oct 1961).

22. Brandau, J.H., "Static and Dynamic Calibration of Propeller Model Fluctuating Force Balances," David Taylor Model Basin Report 2350 (Mar 1967); see also Technologia Naval, Vol. 1, pp. 48--74 (Jan 1968).

23. Boswell, R.J., "A Method of Calculating the Spindle Torque of a Controllable-Pitch Propeller at Design Conditions," David Taylor Model Basin Report 1529 (Aug 1961).

24. Boswell, R.J. et al., "Experimental Spindle Torque and Open-Water Performance of Two Skewed Controllable-Pitch Propellers," DTNSRDC Report 4753 (Dec 1975).

25. Denny, S.B. and H.G. Stephens, "Blade Spindle Moment on Controllable-Pitch Propellers," NSRDC Departmental Report SPD-011-14 (Jul 1974).

26. Wereldsma, R., "Tendencies of Marine Propeller Shaft Excitations," International Shipbuilding Progress, Vol. 19, No. 218 (Oct 1972).

27. Tsakonas, S. et al., "Correlation and Application of an Unsteady Flow Theory for Propeller Forces," Transactions of the Society of Naval Architects and Marine Engineers, Vol. 75, pp. 158--193 (1967).

28. Gutsche, F., "Untersuchung von Schiffsschrauben in schrager Anstromung," Schiffbauforschung, Vol. 3, No. 3/4 (1964).

29. Cheng, H.M., "Analysis of Wake Survey of Ship Models-Computer Program AML Problem No. 840--219F," David Taylor Model Basin Report 1804 (Mar 1964).

INITIAL DISTRIBUTION

Copies	
1	ARMY CHIEF OF RES & DEV
1	ARMY ENGR R&D LAB
2	CHONR 1 Code 438
1	NRL
4	ONR BOSTON
4	ONR CHICAGO
4	ONR LONDON, ENGLAND
4	ONR PASADENA
2	USNA 1 LIB 1 JOHNSON
1	NAVPGSCOL LIB
1	NROTC & NAVADMINU, MIT
1	NADC
4	NAVUSEACEN 1 1311 LIB 1 6005/FABULA, SAN DIEGO 1 13111 LIB 1 2501/HOYT, PASADENA
1	NWC
41	NAVSEA 2 NAVSEA 09G32 20 NAVSEA 033 1 NAVSEA 034 1 NAVSEA 03412 1 NAVSEA 037 1 NAVSEA 037Z 1 NAVSEA 08 1 PMS-378 1 PMS-380 1 PMS-381 1 PMS-383 1 PMS-389 1 PMS-391 1 PMS-392 1 PMS-393 1 PMS-397 1 PMS-399

Copies	
1	FAC 032C
1	NAVSHIPYD/PTSMH
1	NAVSHIPYD/PHILA
1	NAVSHIPYD/NORVA
1	NAVSHIPYD/CHASN
1	NAVSHIPYD/LBEACH
1	NAVSHIPYD/MARE
1	NAVSHIPYD/BREM
1	NAVSHIPD/PEARL
18	NAVSEC 2 SEC 6334B 1 SEC 6100 1 SEC 6101A 1 SEC 6101D 1 SEC 6110 1 SEC 6114H 1 SEC 6120 1 SEC 6136 1 SEC 6140 1 SEC 6140B 2 SEC 6144

Copies	
	1 SEC 6144G
	1 SEC 6145B
	2 SEC 6148
	1 SEC 6600 NORVA
12	DDC
1	BUSTAND/KLEBANOFF
1	HQS COGARD
1	LC/SCI & TECH DIV
7	MARAD
	1 DIV SHIP DES
	1 COORD RES
	1 NACHTSHEIM
	1 SCHUBERT
	1 FALLS
	1 DASHNAW
	1 HAMMER
2	MMA
	1 LIB
	1 MARITIME RES CEN
2	NASA STIF
	1 DIR RES
1	NSF ENGR DIV LIB
1	DOT LIB
1	U BRIDGEPORT/URAM
1	U CAL BERKELEY/DEPT NAME
1	U CAL NAME/WEHAUSEN
1	U CAL SAN DIEGO/ELLIS
2	UC SCRIPPS
	1 POLLACK
	1 SILVERMAN

Copies	
4	CIT
	1 AERO LIB
	1 ACOSTA
	1 PLESSET
	1 WU
1	CATHOLIC U
1	COLORADO STATE U/ALBERTSON
1	U CONNECTICUT/SCOTTRON
1	CORNELL U/SEARS
1	FLORIDA ATLANTIC U OE LIB
3	HARVARD U
	1 MCKAY LIB
	1 BIRKHOFF
	1 CARRIER
2	U HAWAII/BRETSCHNEIDER
1	U ILLINOIS/ROBERTSON
3	U IOWA
	1 ROUSE
	1 IHR/KENNEDY
	1 IHR/LANDWEBER
2	JOHNS HOPKINS U
	1 PHILLIPS
	1 INST COOP RES
1	U KANSAS CIV ENGR LIB
1	KANSAS ST U ENGR EXP/ NESMITH
1	LEHIGH U FRITZ ENGR LAB LIB
1	LONG ISLAND U/PRICE

Copies	
1	U MARYLAND/GLEN MARTIN INST
8	MIT
	1 OCEAN ENGR/LIB
	1 OCEAN ENGR/KERWIN
	1 OCEAN ENGR/LEEHEY
	1 OCEAN ENGR/LEWIS
	1 OCEAN ENGR/LYON
	1 OCEAN ENGR/MANDEL
	1 OCEAN ENGR/NEWMAN
	1 PARSONS LAB/IPPEN
6	U MICHIGAN
	1 NAME LIB
	1 NAME/COUCH
	1 NAME/HAMMITT
	1 NAME/OGILVIE
	1 NAME/NOWACKI
	1 WILLOW RUN LABS
4	U MINNESOTA SAFHL
	1 KILLEN
	1 SCHIEBE
	1 SONG
	1 WETZEL
2	STATE U MARITIME COLL
	1 ENGR DEPT
	1 INST MATH SCI
1	NOTRE DAME ENGR LIB
4	PENN STATE U ARL
	1 LIB
	1 HENDERSON
	1 TSUCHIMA
	1 PARKIN
1	PRINCETON U/MELLOR
1	RENSSELAER/DEPT MATH
1	ST JOHNS U
2	SWRI
	1 APPLIED MECH REVIEW
	1 ABRAMSON

Copies	
1	STANFORD U/ASHLEY
1	STANFORD RES INST LIB
3	SIT DAVIDSON LAB
	1 LIB
	1 BRESLIN
	1 TSAKONAS
1	TEXAS U ARL LIB
1	UTAH STATE U/JEPPSON
1	U WASHINGTON APL LIB
2	WEBB INST
	1 LEWIS
	1 WARD
1	WHOI OCEAN ENGR DEPT
1	WPI ALDEN HYDR LAB LIB
1	ASME/RES COMM INFO
1	ASNE
1	SNAME
1	AERO JET-GENERAL/BECKWITH
1	AVCO LYCOMING
1	BAKER MANUFACTURING
2	BATH IRON WORKS CORP
	1 HANSEN
	1 FFG PROJECT OFFICE
1	BETHLEHEM STEEL NY/DE LUCE
1	BETHLEHEM STEEL SPARROWS
2	BIRD-JOHNSON CO
	1 CASE
	1 RIDLEY

Copies	
1	BOEING ADV MAR SYS DIV
2	BOLT BERANEK AND NEWMAN 1 BROWN 1 JACKSON
1	BREWER ENGR LAB
1	CAMBRIDGE ACOUS/JUNGER
1	CORNELL AERO LAB/RITTER
1	EASTERN RES GROUP
1	ESSO DES DIV
1	FRIEDE & GOLDMAN/MICHEL
2	GEN DYN CONVAIR 1 PARKIN 1 ASW-MARINE SCIENCES
1	GEN DYN ELEC BOAT/ BOATWRIGHT
2	GIBBS & COX 1 TECH LIB 1 OLSON
1	GRUMMAN AEROSPACE/CARL
3	HYDRONAUTICS 1 DUNNE 1 SCHERER 1 LIBRARY
1	INGALLS SHIPBUILDING
1	INST FOR DEFENSE ANAL
1	ITEK VIDYA
1	LITTON INDUSTRIES
1	LOCKHEED M&S/WAID
2	MARINE VIBRATION ASSOC 1 BRADSHOW 1 VASSILOPOULIS

Copies	
2	DOUGLAS AIRCRAFT 1 HESS 1 SMITH
1	NATIONAL STEEL & SHIPBLDG
1	NEWPORT NEWS SHIPBLDG LIB
1	NIELSEN ENGR/SPANGLER
1	OCEANICS/KAPLAN
1	NAR SPACE/UJIHARA
1	PROPULSION DYNAMICS, INC
1	K.E. SCHOENHERR
1	GEORGE G. SHARP
1	SPERRY SYS MGMT LIB/ SHAPIRO
1	SUN SHIPBUILDING/PAVLIK
1	ROBERT TAGGART
1	TETRA TECH PASADENA/ CHAPKIS
1	TRACOR
1	UA HAMILTON STANDARD/ CORNELL

CENTER DISTRIBUTION

Copies	Code	
1	11	Ellsworth
1	1102.1	Nakonechny
1	15	Cummins
1	1509	Pollard
1	152	Wermter
1	1524	Lin
1	1524	Hecker
1	1524	Day
1	1524	Remmers
1	1524	Gordon

Copies	Code	
1	1524	Roddy
1	1532	Dobay
10	1532L	Denny
1	154	Morgan
1	1544	Cumming
30	1544	Boswell
1	156	Hagen
1	1556	Santore
10	1556	Nelka
1	172	Krenzke
1	1720.6	Rockwell
1	19	Sevik
1	1962	Zaloumis
1	1962	Noonan
1	1962	Antonides
1	2723	Spargo
1	2731	Moken
1	2814	Czyryca
30	5214.1	Reports Distribution
1	5221	Library (C)
1	5222	Library (A)

 *U.S. GOVERNMENT PRINTING OFFICE:1976 240-524/70 1-3

DTNSRDC ISSUES THREE TYPES OF REPORTS

(1) DTNSRDC REPORTS, A FORMAL SERIES PUBLISHING INFORMATION OF PERMANENT TECHNICAL VALUE, DESIGNATED BY A SERIAL REPORT NUMBER.

(2) DEPARTMENTAL REPORTS, A SEMIFORMAL SERIES, RECORDING INFORMATION OF A PRELIMINARY OR TEMPORARY NATURE, OR OF LIMITED INTEREST OR SIGNIFICANCE, CARRYING A DEPARTMENTAL ALPHANUMERIC IDENTIFICATION.

(3) TECHNICAL MEMORANDA, AN INFORMAL SERIES, USUALLY INTERNAL WORKING PAPERS OR DIRECT REPORTS TO SPONSORS, NUMBERED AS TM SERIES REPORTS; NOT FOR GENERAL DISTRIBUTION.